Regulation of transcription by SRF and MRTF

Tea Toteva

University College London

and

The Francis Crick Institute

PhD Supervisor: Richard Treisman

A thesis submitted for the degree of

Doctor of Philosophy

University College London

February 2021

Declaration

I Tea Toteva confirm that the work presented in this thesis is my own. Where information has been derived from other sources, I confirm that this has been indicated in the thesis.

Abstract

The serum response factor (SRF) is a transcription factor involved in the regulation of cell proliferation and migration. At cytoskeletal genes, SRF acts cooperatively with the actin-regulated myocardin-related transcription factors MRTF-A and MRTF-B. In addition to regulating MRTFs' subcellular localization, G-actin also controls their nuclear activities. Previous work showed that nuclear accumulation of MRTF-A in the absence of an activating signal is sufficient for its association with genomic loci but not for target gene activation, demonstrating a repressive effect of nuclear actin on MRTF activity. However, the exact mechanism is unclear. The data presented below demonstrates that G-actin interferes with ternary complex formation between SRF and MRTF on DNA. In response to G-actin depletion, MRTF is recruited to target gene promoters and activates gene expression, whereas increasing the concentration of G-actin inhibits MRTF recruitment to target promoters. We used inhibition of the Crm1 nuclear export receptor and reconstitution of MRTF-A/MRTF-B null cells with a constitutively nuclear MRTF-NLS to induce MRTF nuclear accumulation in the absence of an activating signal. Under resting G-actin levels, nuclear MRTF is recruited to target promoters, albeit at reduced levels, and induces non-productive transcription. TTseq and RNAseq experiments demonstrate that while RNA Polymerase II is engaged in elongation, no pre-mRNA accumulates. This inhibited transcriptional state correlates with aberrant Pol II CTD phosphorylation, Mtr4 recruitment and degradation of the nascent transcripts by the nuclear exosome. Inhibition of phosphorylation at Ser7 of the Pol II CTD is sufficient to induce Mtr4-mediated degradation of MRTF-dependent transcripts under induced conditions.

Impact Statement

The serum response factor (SRF) is a transcription factor involved in the regulation of cell proliferation and migration. At cytoskeletal genes, SRF acts cooperatively with the actin-regulated myocardin-related transcription factors MRTF-A and MRTF-B (Miralles et al., 2003). The data presented below demonstrates that in addition to regulating MRTF subcellular localization, G-actin regulates MRTF activity in the nucleus. While G-actin depletion is required for productive RNA synthesis, under resting G-actin levels, nuclear MRTF is recruited to target promoters and induces non-productive transcription. Under this condition, RNA Polymerase II is engaged in elongation, but no pre-mRNA accumulates.

MRTF-SRF signalling is required for various actin-based processes in the cell including adhesion, chemotaxis and migration (Alberti et al., 2005; Costello et al., 2015; Gau et al., 2017; Knöll et al., 2006). In addition, MRTF/SRF signalling is also involved in invasion and metastasis of cancer cells (Haak et al., 2017; Medjkane et al., 2009; Mokalled et al., 2010).

MRTF is constitutively localized in the nucleus in cancer-associated fibroblasts (CAFs) and MDA-MB-231 breast cancer cells. Nevertheless, these cells are still responsive to changes in G-actin concentration (Foster et al., 2017; Medjkane et al., 2009), suggesting that specific cell types might employ actin-dependent mechanisms to control MRTF activity in the nucleus. Understanding the nuclear regulation of MRTF could potentially contribute to modulating the contractile and pro-invasive behaviour of CAFs and breast cancer cells.

We found that the non-productive transcriptional state at MRTF target genes correlates with aberrant Pol II CTD phosphorylation, Mtr4 recruitment and degradation of the nascent transcripts by the nuclear exosome. Moreover, inhibition of phosphorylation at serine 7 of the Pol II CTD was sufficient to induce Mtr4-mediated degradation of MRTF-dependent transcripts under induced conditions.

Phosphorylation is the best characterized modification of the Pol II CTD. Distinct phospho-marks serve to regulate different stages of the transcription cycle and couple transcription and processing of the newly-synthesised transcript. Hence, understanding the role of CTD phosphorylations is essential to understanding the mechanisms that control gene expression.

While phosphorylation of Ser5 and Ser2 of the Pol II CTD have been extensively studied, little is known about phosphorylation of Ser7 (Gomes et al., 2006; Kim & Sharp, 2001; Kim et al., 2002; Komarnitsky et al., 2000; Schroeder et al., 2000). Phospho-serine 7 is present at all actively transcribed genes. However, apart from its role in transcription and RNA processing at snRNA genes, its function is unknown (Egloff et al., 2007). Our findings suggest that it might be involved in protecting MRTF-dependent transcripts from being targeted for degradation by Mtr4 and the nuclear exosome.

Mtr4 is essential for all functions of the nuclear exosome. It is required for recruiting the exosome to its targets, through facilitating access of multiple exosome adapter complexes to the core exosome, and threading the RNA substrate into the exosome (Ogami et al., 2017; Weick et al., 2018). In addition to its well-characterized role in regulating the turn-over of non-coding RNAs, our data suggests that Mtr4 is also involved in the regulation of specific protein-coding transcripts, consistent with recent publications (Fan et al., 2017; J. Wang et al., 2019; Yu et al., 2020). Regulation by Mtr4 provides an additional layer of regulation on gene expression, which might be particularly important in response to stress or during development, when the RNA pool needs to be tightly regulated.

Acknowledgement

I thank Richard for the opportunity to work in his lab and all his help and support during my PhD.

I thank Francesco Gualdrini for the analysis of the genomic data in the thesis, as well as Philip East and Aengus Stewart for their contribution, Ana Vidakovic for the Rpb1 and Rpb1-S7A plasmids and her help generating cell lines, both Ana and Lea Gregersen for their help with the TTseq experiments, Dora Sideri and Radhika Warrier for their help with the RIP experiments, Patrick Costello for his help with generating cell lines, Charlie Foster for his help with gel contraction assays, Roman Fedoryshchak for his help with microscopy, the staff at the Advanced sequencing and the FACS STPs in the Crick.

I am grateful to Jesper Svejstrup, Caroline Hill and Tariq Enver for the guidance, helpful suggestions and discussions and all members of the Svejstrup and the van Werven labs for their help with reagents, protocols, experiments and ideas.

Thank you to everyone in the lab, Patrick, Diane, Maria, Julie, Jessica, Roman and Lucy for their support and encouragement. Thank you to Fabien Moretto and Naomi Chambers for all their help and a special thank you to Fernandez.

Table of Contents

Abstract **3**
Impact Statement **4**
Acknowledgement **6**
Table of Contents **7**
Table of figures **11**
Abbreviations **17**
Chapter 1.Introduction **22**
1.1 The MRTF/SRF signalling pathway **22**
The Serum Response Factor 22
SRF integrates ERK and Rho Signalling 23
The MRTFs are G-actin binding RPEL proteins 24
MRTFs and TCFs regulate distinct target genes 25
The role of TCFs and MRTFs in the cell 27
MRTF regulation 29
Regulation of MRTF activity in the nucleus 31
1.2 RNA Polymerase II **32**
The RNA Polymerase II CTD code 33
CTD kinases 38
CTD phosphatases 41
1.3 The transcription cycle **42**
Initiation 42
Promoter-proximal pausing 44
Pause-release 46
Elongation 47
Co-transcriptional chromatin remodeling 48
Termination 51
1.4 Co-transcriptional RNA processing **54**
Capping 54
Splicing 56
3’ end processing 56
1.5 The nuclear exosome **58**
Core nuclear exosome 58
Exosome adapter complexes 59
The role of the CBC in exosome recruitment 61
Chapter 2.Materials & Methods **63**
2.1 Cell culture and growth curves **63**
2.2 Drug treatments **63**
2.3 Immunofluorescence **64**
2.4 siRNA and transient transfection **64**
2.5 Cell fractionation **65**
2.6 Western blot **65**
2.7 Contractility assay **66**
2.8 RNA extraction, cDNA synthesis and qPCR **66**
2.9 Chromatin Immunoprecipitation (ChIP) **67**
2.10 TT_{chem}-seq **68**

2.11 Library preparation and sequencing 70
2.12 Data analysis 71
RNAseq and TTseq 71
ChIPseq 81
2.13 Immunoprecipitation (IP) 90
2.14 UV-RIP 90
2.15 Plasmids and molecular cloning 91
2.16 List of plasmids 94
2.17 Stable cell line generation 109
2.18 Genotyping 110
2.19 List of primers 110
2.20 List of siRNA 114
2.21 List of antibodies 115
Chapter 3. Nuclear MRTF induces non-productive RNA synthesis 117
3.1 Nuclear MRTF does not activate target gene expression 119
3.2 G-actin inhibits MRTF recruitment to target genes 123
3.3 Nuclear MRTF induces transcription but not productive RNA synthesis 128
The transcriptional response to CD 129
The transcriptional response to LMB 134
Chapter 4. Constitutively nuclear MRTF does not induce productive RNA synthesis 142
4.1 Characterization of cells with constitutively nuclear MRTF 142
4.2 Constitutively nuclear MRTF is recruited to target gene promoters 150
4.3 Constitutively nuclear MRTF induces non-productive transcription 152
Defining a stringent CD-induced gene set in dKO^{MRTF} and dKO$^{MRTF\text{-}NLS}$ cells 152
MRTF-NLS induces non-productive transcription 158
Chapter 5. The nuclear exosome regulates transcription at MRTF target genes 164
5.1 Inactivating the nuclear exosome rescues non-productive transcription in LMB-treated cells 164 165
5.2 Genome-wide expression analysis in Mtr4-depleted cells 172
CD- and LMB-induced changes in gene expression in Mtr4-depleted cells 172
Mtr4 depletion restores productive RNA synthesis at LMB-induced genes 178
Effect of Mtr4 depletion in resting cells 182
5.3 Mtr4 is recruited to transcripts of MRTF target genes 184
5.4 Nrde2 depletion inhibits activation of MRTF target genes 186
Chapter 6. Evidence that the nuclear exosome regulates transcription in dKO$^{MRTF\text{-}NLS}$ cells 190
6.1 Inactivating the nuclear exosome rescues the pre-mRNA synthesis defect in dKO$^{MRTF\text{-}NLS}$ cells 190

6.2 Genome-wide expression analysis in dKO$^{MRTF\text{-}NLS}$ cells depleted of Mtr4 194
6.3 Appendix 201
Chapter 7. Recruitment of the exosome correlates with aberrant phosphorylation of the Pol II CTD at MRTF target genes 207
7.1 Chromatin remodeling is not defective in LMB-treated cells 207
7.2 Pol II pause-release occurs in LMB-treated cells 210
7.3 The non-productive transcriptional state in LMB-treated cells correlates with aberrant phosphorylation of the Pol II CTD 212
7.4 Mtr4 and Nrde2 depletion does not affect Pol II recruitment at MRTF target genes 222
7.5 The non-productive transcriptional state in dKO$^{MRTF\text{-}NLS}$ cells correlates with aberrant phosphorylation of the Pol II CTD 225
Chapter 8. Phospho-Ser7 of the Pol II CTD is required for productive RNA synthesis at MRTF target genes 233
8.1 The effect of CDK inhibitors on MRTF target gene expression 233
8.2 Generation of NIH3T3 cells expressing Rpb1-S7A mutant 241
8.3 Inhibition of phosphorylation at Ser7 of the Pol II CTD perturbs MRTF target gene activation 243
8.4 Depletion of Mtr4 restores productive RNA synthesis at MRTF target genes in Ser7P-depleted cells 250
8.5 Depletion of Nrde2 does not exacerbate the transcriptional defect in Ser7P-depleted cells 253
Chapter 9. Discussion 256
9.1 Regulation of MRTF activity in the nucleus 256
G-actin inhibits ternary complex formation between MRTF and SRF on DNA 256
Under resting G-actin levels, nuclear MRTF is recruited to target genes at reduced levels 259
Does LMB induce an unstable MRTF-SRF-DNA complex? 260
Biological significance of regulated MRTF-SRF interaction 261
9.2 Nuclear MRTF induces non-productive transcription 262
The transcriptional response to CD 262
The non-productive transcriptional state at MRTF target genes 262
9.3 Mtr4 regulates MRTF target gene expression 263
Inactivation of the NEXT and CBCA complexes restores productive transcription at MRTF target genes 263
Is the NEXT or the PAXT complex involved in MRTF target gene regulation? 264
Mtr4 is recruited to transcripts of MRTF target genes 265
Depletion of Mtr4 rescues the defect in the non-productive transcriptional state 266
Mtr4 regulates DNA repair and cell cycle genes 267
How is the exosome recruited to its substrates? 267
9.4 Pol II CTD phosphorylation and transcription at MRTF target genes 270
The inhibited transcriptional state at MRTF target genes correlates with aberrant Pol II CTD phosphorylation 270

Chromatin remodeling at MRTF target genes is not impaired in the inhibited state 271
Pol II pause-release into elongation is not defective in the inhibited transcriptional state 271
The inhibited transcriptional state does not reflect defective activity of CDK7 or CDK9 272
Pol II lacking Ser2P displays a normal transcriptional profile 273
Ser2P and transcription termination 274
Ser7P of the Pol II CTD is required for productive transcription at MRTF target genes 275
How might defective Ser7P arise in the non-productive transcriptional state? 276
9.5 A model for the non-productive transcriptional state 278
Transition into productive elongation might involve exchange of Mtr4 for the RNA export machinery 278
Phosphorylation of Ser7 of the Pol II CTD protects MRTF-dependent transcripts from degradation 279
Chapter 10.Appendix 283
Chapter 11.Reference List....329

Table of figures

Figure 1 SRF integrates Rho and Ras signalling 24
Figure 2 MRTF-A regulation. 26
Figure 3 Sequence of the Rpb1 CTD 34
Figure 4 RNA Pol II CTD modifications 37
Figure 5 CTD kinases and phosphatases 40
Figure 6 The transcription cycle. 44
Figure 7 Histone remodeling on actively transcribed genes. 49
Figure 8 Pre-mRNA processing 55
Figure 9 Exosome adapter complexes 60
Figure 10 Mutually exclusive CBCA containing complexes. 62
Figure 11 Principal component analysis (PCA) of RNAseq samples in NIH3T3 cells 73
Figure 12 Heatmap of Poisson distance of RNAseq samples in NIH3T3 cells 74
Figure 13 Principal component analysis (PCA) of TTseq samples in NIH3T3 cells 75
Figure 14 Heatmap of Poisson distance of TTseq samples in NIH3T3 cells 76
Figure 15 Principal component analysis (PCA) of RNAseq samples in dKO^{MRTF} and dKO$^{MRTF-NLS}$ cells 77
Figure 16 Heatmap of Poisson distance of RNAseq samples in dKO^{MRTF} and dKO$^{MRTF-NLS}$ cells 78
Figure 17 Principal component analysis (PCA) of TTseq samples in dKO^{MRTF} and dKO$^{MRTF-NLS}$ cells 79
Figure 18 Heatmap of Poisson distance of TTseq samples in dKO^{MRTF} and dKO$^{MRTF-NLS}$ cells 80
Figure 19 Principal component analysis (PCA) of Ser5P ChIPseq samples in NIH3T3 cells 82
Figure 20 Heatmap of Poisson distance of Ser5P ChIPseq samples in NIH3T3 cells 83
Figure 21 Principal component analysis (PCA) of Ser2P ChIPseq samples in NIH3T3 cells 84
Figure 22 Heatmap of Poisson distance of Ser2P ChIPseq samples in NIH3T3 cells 85

Figure 23 Principal component analysis (PCA) of Ser7P ChIPseq samples in NIH3T3 cells 86
Figure 24 Heatmap of Poisson distance of Ser7P ChIPseq samples in NIH3T3 cells 87
Figure 25 Principal component analysis (PCA) of total Pol II ChIPseq samples in NIH3T3 cells 88
Figure 26 Heatmap of Poisson distance of total Pol II ChIPseq samples in NIH3T3 cells 89
Figure 27 MRTF subcellular localization 122
Figure 28 Nuclear MRTF does not activate target genes 122
Figure 29 MRTF recruitment to target gene promoters in response to stimulation 124
Figure 30 SRF recruitment to target gene promoters in response to stimulation 125
Figure 31 G-actin inhibits MRTF target gene activation 127
Figure 32 G-actin inhibits SRF/MRTF recruitment to target genes 128
Figure 33 The response to CD stimulation by RNAseq 130
Figure 34 The response to CD stimulation by TTseq 131
Figure 35 Defining a stringent CD-induced gene set 132
Figure 36 LMB stimulation does not induce gene activation 135
Figure 37 LMB induces nascent RNA synthesis 136
Figure 38 Nuclear MRTF induces non-productive RNA synthesis 139
Figure 39 The transcriptional response to LMB and CD 141
Figure 40 Reconstitution of MRTF-A/B null cells 145
Figure 41 MRTF subcellular localization 147
Figure 42 Nuclear MRTF does not activate target genes 149
Figure 43 Nuclear MRTF is recruited to target gene promoters 151
Figure 44 dKO^{MRTF} RNAseq 153
Figure 45 dKO$^{MRTF\text{-}NLS}$ RNAseq 155
Figure 46 Defining a stringent CD-induced gene set 157
Figure 47 dKO^{MRTF} TTseq 159
Figure 48 dKO$^{MRTF\text{-}NLS}$ TTseq 160
Figure 49 Constitutively nuclear MRTF induces non-productive transcription 163
Figure 50 Inactivation of the nuclear exosome restores pre-mRNA accumulation in LMB-treated cells 165

Figure 51 Inactivation of Dis3, the NEXT or CBCA complexes restores pre-mRNA accumulation in LMB-treated cells 169
Figure 52 Inactivation of the NEXT but not the PAXT complex rescues pre-mRNA accumulation in LMB-treated cells 172
Figure 53 CD- and LMB- induced gene expression changes in Mtr4-depleted cells 174
Figure 54 Mtr4 depletion restores productive RNA synthesis at MRTF target genes in LMB-treated cells 175
Figure 55 Mtr4 depletion supresses CD induction at MRTF target genes 177
Figure 56 Mtr4 depletion restores productive transcription at a subset of LMB-inducible genes 181
Figure 57 Transcriptional changes induced by Mtr4 depletion 183
Figure 58 Mtr4 is recruited to MRTF-dependent transcripts in response to LMB 186
Figure 59 Nrde2 depletion inhibits MRTF target gene expression in response to stimulation 188
Figure 60 Inactivating the nuclear exosome restores pre-mRNA accumulation at MRTF target genes in dKO$^{MRTF\text{-}NLS}$ cells 193
Figure 61 The transcriptional response to CD and LatB in Mtr4-depleted dKO$^{MRTF\text{-}NLS}$ cells 195
Figure 62 Gene expression changes, relative to LatB-treated cells, in Mtr4-depleted dKO$^{MRTF\text{-}NLS}$ cells 198
Figure 63 Defining a Mtr4-controlled MRTF target gene set in dKO$^{MRTF\text{-}NLS}$ cells 200
Figure 64 Gene expression analysis at the 180 stringent CD-induced gene set in Mtr4-depleted dKO$^{MRTF\text{-}NLS}$ cells 202
Figure 65 Gene expression analysis at the 312 stringent CD-induced gene set from NIH3T3 cells in Mtr4-depleted dKO$^{MRTF\text{-}NLS}$ cells 204
Figure 66 Gene expression analysis at the 455 LMB-induced Mtr4-controlled gene set from NIH3T3 cells in Mtr4-depleted dKO$^{MRTF\text{-}NLS}$ cells 206
Figure 67 Chromatin remodeling in LMB-treated cells 209
Figure 68 Pol II undergoes pause-release in LMB-treated cells 212
Figure 69 Inhibition of Crm1 does not affect Pol II CTD phosphorylation globally 214
Figure 70 Pol II recruitment and CTD phosphorylation at the *Acta2* gene 215
Figure 71 Pol II ChIPseq at the stringent 312 CD-inducible gene set 220
Figure 72 Pol II ChIPseq at constitutively expressed genes 221

Figure 73 Depletion of Mtr4 and Nrde2 does not affect Pol II recruitment 224
Figure 74 Pol II recruitment and phosphorylation at MRTF target genes in dKO^{MRTF} cells 228
Figure 75 Pol II recruitment and phosphorylation at MRTF target genes in dKO$^{MRTF\text{-}NLS}$ cells 230
Figure 76 Pol II recruitment and phosphorylation at MRTF target genes in dKO$^{MRTF\text{-}XXX}$ cells 232
Figure 77 The effect of CDK inhibitors on MRTF target gene expression 234
Figure 78 THZ1 inhibits Pol II recruitment at MRTF target genes 236
Figure 79 FP inhibits Pol II elongation at MRTF target genes 237
Figure 80 THZ531 does not affect Pol II elongation at MRTF target genes 238
Figure 81 GW843682X does not affect Pol II elongation MRTF target genes 240
Figure 82 Generation of WT-ON and S7A-ON cells 242
Figure 83 MRTF target gene expression in WT-ON and S7A-ON cells 244
Figure 84 MRTF target gene expression in WT-off and S7A-off cells 245
Figure 85 Ser7P inhibition alters the Pol II profile at MRTF target genes 249
Figure 86 Mtr4 depletion restores MRTF target gene expression in S7A-ON cells 251
Figure 87 Mtr4 depletion does not affect MRTF target gene expression in WT-off and S7A-off cells 252
Figure 88 Nrde2 depletion does not affect MRTF target gene expression in S7A-ON cells 254
Figure 89 G-actin inhibits the interaction between MRTF and SRF on DNA..... 258
Figure 90 Kinetic competition between the exosome and the export machinery . 269
Figure 91 Regulation of transcription at MRTF target genes..... 282
Figure 92 Gene ontology analysis of genes upregulated in response to CD in NIH3T3 cells by RNAseq 285
Figure 93 Gene ontology analysis of genes downregulated in response to CD in NIH3T3 cells by RNAseq 287
Figure 94 Gene ontology analysis of genes upregulated in response to CD in NIH3T3 cells by TTseq 289
Figure 95 Gene ontology analysis of genes downregulated in response to CD in NIH3T3 cells by TTseq 291

Figure 96 Gene ontology analysis of genes upregulated in response to LMB in NIH3T3 cells by TTseq 293
Figure 97 Gene ontology analysis of genes downregulated in response to LMB treatment in NIH3T3 cells by TTseq 295
Figure 98 Gene ontology analysis of genes upregulated in response to CD treatment in dKO^{MRTF} cells by RNAseq..... 297
Figure 99 Gene ontology analysis of genes downregulated in response to CD treatment in dKO^{MRTF} cells by RNAseq..... 299
Figure 100 Gene ontology analysis of genes upregulated in response to CD in dKO$^{MRTF-NLS}$ cells by RNAseq..... 301
Figure 101 Gene ontology analysis of genes downregulated in response to CD in dKO$^{MRTF-NLS}$ cells by RNAseq..... 303
Figure 102 Gene ontology analysis of genes upregulated in response to CD in dKO^{MRTF} cells by TTseq..... 305
Figure 103 Gene ontology analysis of genes downregulated in response to CD in dKO^{MRTF} cells by TTseq..... 307
Figure 104 Gene ontology analysis of genes upregulated in response to CD in dKO$^{MRTF-NLS}$ cells by TTseq 309
Figure 105 Gene ontology analysis of genes downregulated in response to CD in dKO$^{MRTF-NLS}$ cells by TTseq 311
Figure 106 Gene ontology analysis of genes upregulated in response to CD in Mtr4-depeted NIH3T3 cells by RNAseq 313
Figure 107 Gene ontology analysis of genes downregulated in response to CD in Mtr4-depeted NIH3T3 cells by RNAseq 315
Figure 108 Gene ontology analysis of genes upregulated in response to LMB in Mtr4-depeted NIH3T3 cells by RNAseq 317
Figure 109 Gene ontology analysis of genes downregulated in response to LMB in Mtr4-depeted NIH3T3 cells by RNAseq 319
Figure 110 Gene ontology analysis of genes upregulated by Mtr4 depletion..... 321
Figure 111 Gene ontology analysis of genes upregulated in response to CD, relative to LatB-treated cells, in Mtr4-depleted dKO$^{MRTF-NLS}$ cells 323
Figure 112 Gene ontology analysis of genes active in untreated cells, relative to LatB-treated cells, in Mtr4-depleted dKO$^{MRTF-NLS}$ cells..... 325

Figure 113 Gene ontology analysis of the 55 Mtr4-controlled MRTF-NLS-induced genes 327
Figure 114 Correlation plots of full datasets 328

Abbreviations

4SU-4-thiouridine

4TU-4-thiouracil

Abl1-Abelson murine leukemia viral oncogene homolog 1

Abl2-ABL proto-oncogene 2 non-receptor tyrosine kinase

AF9-ALL fused gene from chromosome 9

AFF1-AF4/FMR2 Family Member 1

ATP-adenosine triphosphate

Brd4- bromodomain-containing protein 4

CBC-cap-binding complex

CBCA-CBC and Ars2

CBP-CREB-binding protein

CD-cytochalasin D

CDK12-cyclin-dependent kinase 12

CDK13-cyclin-dependent kinase 13

CDK7-cyclin-dependent kinase 7

CDK8-cyclin-dependent kinase 8

CDK9-cyclin-dependent kinase 9

Chd1-chromodomain helicase DNA binding protein 1

ChIP-chromatin immunoprecipitation

Cobl- Cordon-bleu protein

CoTC-co-transcriptional cleavage

CPA-cleavage and polyadenylation complex

CPSF-cleavage and polyadenylation specificity factor

Crm1-chromosomal region maintenance 1

CstF-cleavage stimulation factor

CTD-carboxy-terminal domain

Ctdp1-CTD phosphatase subunit 1

DAPI-4′,6-diamidino-2-phenylindole

DMEM-Dulbecco’s modified eagle medium

DNAPK- DNA-dependent protein kinase

DSIF- DRB sensitivity-inducing factor

ECL-enhanced chemiluminescence

EDTA-ethylenediaminetetraacetic acid

EGTA-ethylene glycol tetraacetic acid

ELL-eleven-nineteen lysine-rich leukemia

ENL-eleven-nineteen leukemia

ERK-extracellular-signal-regulated kinase

eRNA-enhancer RNA

Ets-erythroblast transformation specific

F-actin-filamentous actin

FACT-facilitates chromatin transcription

FBS-fetal bovine serum

FP-flavopiridol

G-actin-globular actin

GSK-3 beta- Glycogen synthase kinase-3 beta

GTPase-guanosine triphosphate hydrolase

H2Bub-histone H2B monoubiquitinated at lysine 120

H3-histone 3

H3K122Ac-histone H3 acetylated at lysine 122

H3K14Ac-histone H3 acetylated at lysine 14

H3K16Ac-histone H3 acetylated at lysine 16

H3K27Ac-histone H3 acetylated at lysine 27

H3K36me3-histone H3 trimethylated at lysine 36

H3K4me3-histone H3 trimethylated at lysine 4

H3K56Ac-histone H3 acetylated at lysine 56

H3K79me3-histone H3 trimethylated at lysine 79

H3K9Ac-histone H3 acetylated at lysine 9

H4-histone 4

HEPES-4-(2-hydroxyethyl)-1-piperazineethanesulfonic acid

HEXIM1- hexamethylene bisacetamide (HMBA) inducible protein 1

HP1-heterochromatin protein

HRP-horseradish peroxidase

IEG-immediate-early gene

IF-immunofluorescence

IP-immunoprecipitation

LatB-latrunculin B

LIMK-LIM kinase

LINC complex- linker of nucleoskeleton and cytoskeleton complex

lincRNA-long intergenic non-coding RNA

LMB-leptomycin B

MAPK-mitogen-activated protein kinase

MDA-MB-231-human triple-negative breast cancer (TNBC) cell line

mDia1-mammalian diaphanous

MEF-mouse embryonic fibroblast

MICAL2- molecule interacting with CasL

MLL-mixed lineage leukaemia

MOPS-3-(N-morpholino) propanesulfonic acid

mRNA-messenger RNA

MRTF myocardin-related transcription factor

MTSEA- 2-((Biotinoyl) amino) ethyl methanethiosulfonate

N-WASP- Neural Wiskott-Aldrich Syndrome Protein

Ncbp-nuclear cap binding protein

ncRNA-non-coding RNA

NELF-negative elongation factor

NES-nuclear export sequence

NEXT-nuclear exosome targeting complex

NF-kB- nuclear factor kappa-light-chain-enhancer of activated B cells

NIH3T3-mouse fibroblast 3-day transfer, inoculum 3×10^5 cells

NLS-nuclear localization sequence

Npl3-nucleolar protein 3

NRDE2-nuclear exosome regulator 2

PAF-polymerase-associated factor

PAP-the poly(A) polymerase

PARP-poly (ADP-ribose) polymerase

PAS-polyadenylation site

PAXT-poly(A) exosome targeting complex

PBS-phosphate-buffered saline

PBST-PBS Tween-20

PHAX-phosphorylated adapter RNA export protein

PIC-pre-initiation complex

Pin1- Peptidyl-prolyl cis-trans isomerase NIMA-interacting 1

Plk3-polo-like kinase 3

PNUTS- phosphatase 1 Nuclear Targeting Subunit

Pol II-RNA polymerase II

Poly(A)-polyadenylation

PP1-protein phosphatase 1

PRC-polycomb repressive complex

PROMPT-promoter upstream transcripts

pTEF-b- positive transcription elongation factor

RIP-RNA immunoprecipitation

ROCK-Rho-associated protein kinase

RPAP- RNA polymerase II-associated protein 1

RPRD-regulation of nuclear pre-mRNA domain containing protein

rRNA-ribosomal RNA

SCP- Sterol Carrier Protein

SDS-sodium dodecyl sulfate

SEC-super elongating complex

Ser2P- RNA polymerase II C-terminal domain phosphorylated at serine 2

Ser5P-RNA polymerase II C-terminal domain phosphorylated at serine 5

Ser7P- RNA polymerase II C-terminal domain phosphorylated at serine 7

siRNA-small interfering RNA

SKIP-SKI-interacting protein

SLBP-stem-loop binding protein

snoRNA-small nucleolar RNAs

snRNA-small nuclear RNA

SRE-serum response element

SRF-serum response factor

SRSF2-serine/arginine-rich splicing factor 2

SWI/SNF-SWItch/Sucrose Non-Fermentable

TBP-TATA-binding protein

TCF-ternary complex factor

TFIIA- transcription factor IIA

TFIIB-transcription factor II B

TFIID-transcription factor II D

TFIIE-transcription factor II E

TFIIF-transcription factor II F

TFIIH-transcription factor II human

Thr4P- RNA polymerase II C-terminal domain phosphorylated at threonine 4

TOP1-DNA topoisomerase 1

TPA-12-o-tetradecanoylphorbol-13-acetate

TRAMP-Trf4/Air2/Mtr4p Polyadenylation complex

TREX-transcription export complex

TSS-transcription start site

TSSa-RNA- transcription start site associated RNA

Tyr1P- RNA polymerase II C-terminal domain phosphorylated at tyrosine 1

WAVE2- WASP-family verprolin- homologous protein 2

WB-western blot

XPB-xeroderma pigmentosum type B

XPD-xeroderma pigmentosum group D

YAP1- yes-associated protein 1

YPD-yeast extract peptone dextrose

Chapter 1. Introduction

1.1 The MRTF/SRF signalling pathway

The complicated interplay among a limited number of signalling molecules is responsible for the diversity of cellular responses to physiological and environmental cues. The transcription factor SRF integrates signalling through two distinct antagonistic pathways, the Ras-ERK and the Rho-actin signalling cascades, to control the balance between cell proliferative and migratory phenotypes (Figure 1).

The Serum Response Factor

The serum response factor (SRF) was first identified as a transcriptional regulator of the growth factor-inducible gene *c-Fos* (Treisman, 1986). It is a conserved, ubiquitously expressed protein which belongs to the MADS-box family of transcription factors (Norman et al., 1988; Shore & Sharrocks, 1995). SRF mediates signal-stimulated transcriptional activation of immediate-early genes (IEGs), as well as cytoskeletal and cell type-specific genes. Thus, it is an important regulator of cell proliferation, migration and differentiation and plays a key role in muscle-specific and neuronal gene expression (Greenberg et al., 1987; Mohun et al., 1987; Norman et al., 1988; Treisman, 1986, 1990).

At target genes, SRF associates with the serum response element (SRE), a 5' flanking sequence of the gene that is required for its efficient transcriptional activation (Gilman et al., 1986; Greenberg et al., 1987; Norman et al., 1988; Treisman, 1985). More specifically, it binds to the consensus sequence CC(A/T)6GG, named the CArG-box (Pellegrini et al., 1995; Pollock & Treisman, 1991; Treisman, 1985).

Despite its constitutively nuclear localization, SRF appears to have little activity on its own. Instead, target gene activation is promoted by ternary complex formation with two families of ubiquitous signal-regulated co-factors, the Ternary complex factor (TCF) family of Ets-proteins ELK-1, NET and SAP-1 (ELK1, ELK3, and ELK4) and the myocardin-related transcription factors (MRTF-A and MRTF-B), as

well as myocardin itself, which is constitutively active and muscle-specific (Olson & Nordheim, 2010; Posern & Treisman, 2006). The TCFs and MRTFs compete for binding to the SRF MADS-box domain and thus allow coupling of SRF to distinct signalling pathways (Gineitis & Treisman, 2001; Gualdrini et al., 2016; Hill et al., 1994; Miralles et al., 2003; Shaw et al., 1989; Wang & Olson, 2004; Zaromytidou et al., 2006).

SRF integrates ERK and Rho Signalling

At IEGs such as *c-Fos* and *Egr-1*, SRF co-operates with the TCFs (Figure 1). They respond to Ras-ERK signaling to control cell growth, proliferation and survival (Kortenjann et al., 1994; Marais et al., 1993; Treisman, 1994). In the ternary complex, the TCF interacts with both SRF and an Ets-binding motif adjacent to the SRF DNA-binding site (Dalton & Treisman, 1992; Hassler & Richmond, 2001; Hipskind et al., 1991; Shaw et al., 1989). TCF activity is regulated through phosphorylation of their C-terminal transcriptional activation domains by MAP kinases. While this phosphorylation does not regulate DNA binding, it potentiates their transcriptional activation function (Marais et al., 1993; Price et al., 1996; Raingeaud et al., 1996; Treisman, 1994). The TCFs are partially functionally redundant and are also able to function independently of SRF (Boros et al., 2009; Buchwalter et al., 2005; Costello et al., 2010; Weinl et al., 2014).

However, some SRE-containing promoters also respond to stimulation in the absence of the TCFs (Graham & Gilman, 1991; Hill et al., 1993; Hill et al., 1995; Olson & Nordheim, 2010). At cytoskeletal genes, SRF co-operates with the MRTFs (Figure 1). As discussed in the following sections, MRTF-A and MRTF-B are regulated similarly and appear to be mostly functionally redundant. The MRTFs respond to signaling through Rho-family GTPases and are involved in the control of cell morphology, adhesion and migration (Miralles et al., 2003; Olson & Nordheim, 2010; Schratt et al., 2002; Wang et al., 2002).

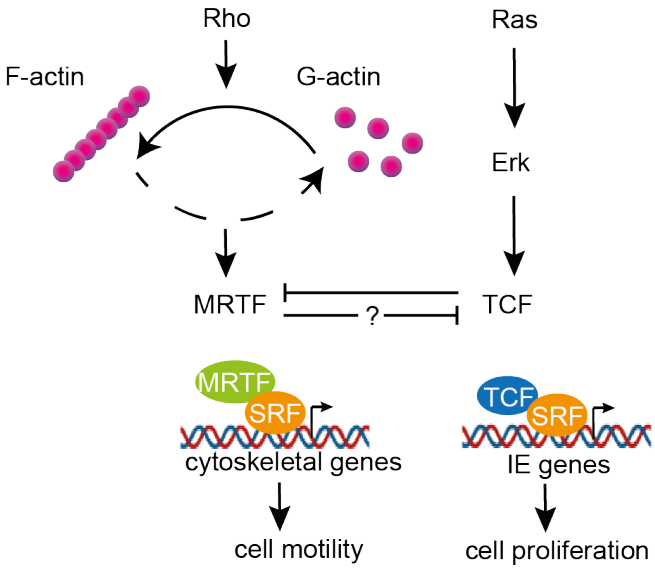

Figure 1 SRF integrates Rho and Ras signalling

Two co-factor families, the MRTFs, which respond to Rho activation and subsequent changes in actin dynamics, and the TCFs, which respond to Ras activation, compete for binding to SRF. SRF cooperates with the MRTFs at cytoskeletal genes and thus MRTF-SRF signalling is involved in the regulation of cell morphology and motility. At immediate early genes, SRF cooperates with the TCFs, and TCF-SRF signalling is involved in the control of cell growth and proliferation.

The MRTFs are G-actin binding RPEL proteins

The MRTFs belong to the RPEL family of proteins which act as G-actin sensors. They contain RPEL motifs, sequences that bind G-actin (Mouilleron et al., 2008), and it is generally thought that their activity is regulated by competition between G-actin and additional regulatory proteins. For instance, G-actin competes with the protein phosphatase 1 (PP1) for binding to Phactrs, which regulate cytoplasmic cytoskeletal dynamics, and with Rac1 for binding to ArhGAPs, which regulate actin-dependent cell surface structures (Diring et al., 2019; Huet et al., 2013; Wiezlak et al., 2012). Similarly, importin α/β binding to MRTF is inhibited by G-actin (Hirano & Matsuura, 2011; Panayiotou et al., 2016).

The MRTFs can interact with up to five monomeric G-actin molecules through an RPEL domain located at the N-terminus of the protein (Figure 2A). Each of the three RPEL motif and the two intervening spacer sequences can bind a single G-actin molecule (Mouilleron et al., 2008; Mouilleron et al., 2011). Embedded within the RPEL domain, is an extended bipartite nuclear localization signal (NLS), composed of two basic elements B2 and B3, which is required for importin α/β - mediated nuclear import of MRTF. In addition, a hydrophobic region, called the Q-box, also affects MRTF nuclear localization (Guettler et al., 2008; Miralles et al., 2003; Panayiotou et al., 2016). Furthermore, the Q-box promotes interactions with SRF. However, the element required for the formation of ternary complex with MRTF, SRF and DNA is the B1 box (Miralles et al., 2003; Zaromytidou et al., 2006).

MRTFs and TCFs regulate distinct target genes

SRF responds to signalling from both the mitogen-activated ERK cascade and the Rho signalling pathway. Because the TCFs and MRTFs compete for a common surface of SRF, they interact with SRF in a mutually exclusive manner, thus potentially providing target gene specificity (Esnault et al., 2014; Gineitis & Treisman, 2001; Gualdrini et al., 2016; Miralles et al., 2003; Sotiropoulos et al., 1999; Wang & Olson, 2004; Zaromytidou et al., 2006).

Nevertheless, the basis for differential recruitment of the TCFs and MRTFs remains unclear. Unlike the TCFs, the MRTFs do not have a defined sequence-specific DNA binding motif (Esnault et al., 2014). Nevertheless, they contact DNA directly, provided that the DNA is appropriately bent at a 72° angle by SRF binding (Pellegrini et al., 1995; Zaromytidou et al., 2006).

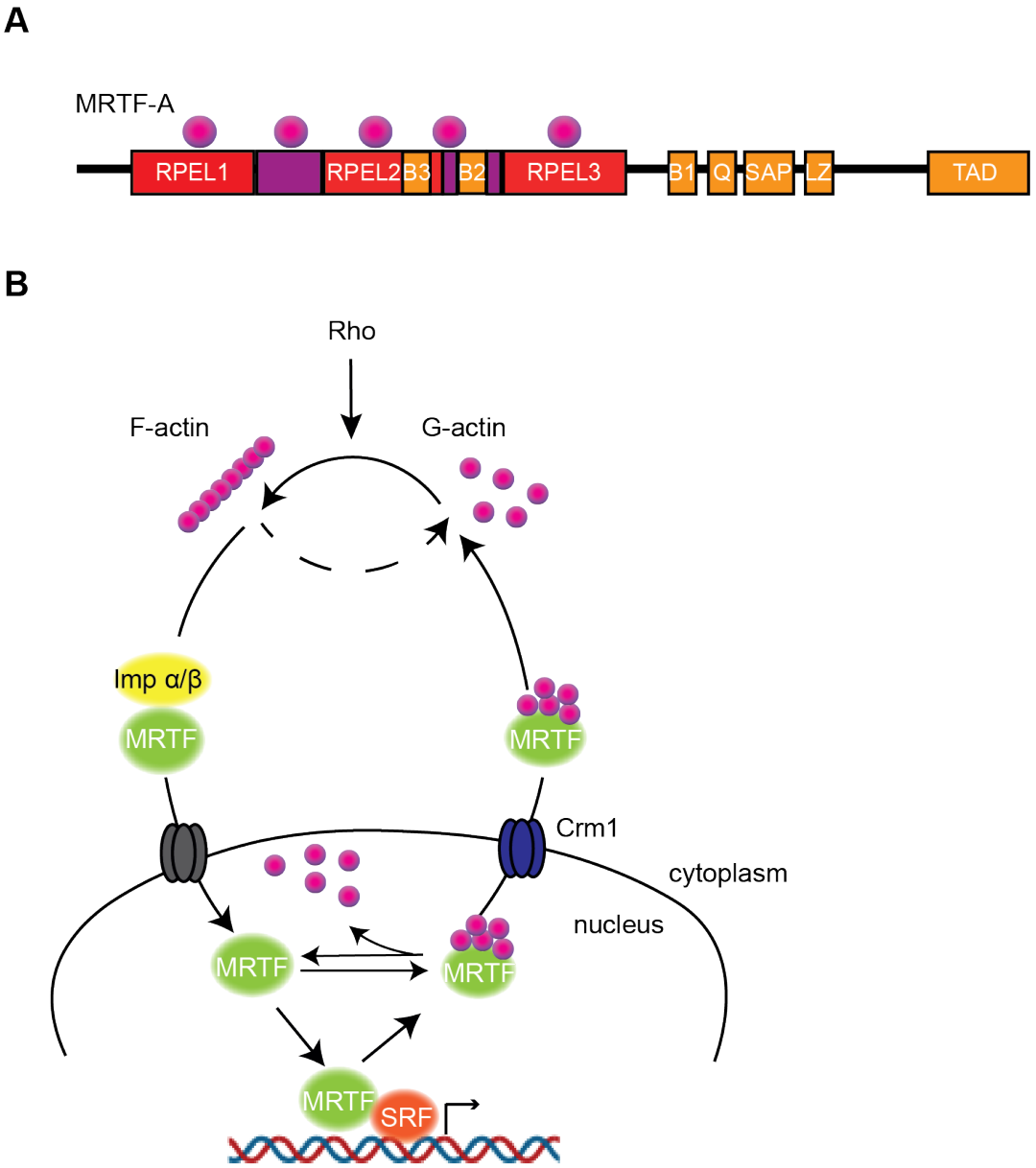

Figure 2 MRTF-A regulation. (A) Schematic representation of MRTF-A. Located at the N-terminus, three RPEL motifs (in red), separated by spacer regions (in purple) are involved in actin binding. Each RPEL motif and each spacer region can be bound by one molecule of actin (pink circles), forming a pentavalent complex. A basic region comprising B3 and B2 contains a bipartite nuclear localization sequence. Another basic region B1 is involved in SRF binding. Glutamine-rich Q domain promotes nuclear export and regulates interaction with SRF. SAP domain-a putative DNA binding motif; LZ - leucine zipper domain required for dimerization; TAD - transactivation domain. (B) MRTF regulation. Importin α/β and monomeric G-actin compete for binding to MRTF-A. A decrease in the cellular pool of monomeric G-actin, such as due to activation of Rho GTPases and subsequent actin polymerization, allows for importin α/β -mediated nuclear import of MRTF-A, its interaction with SRF and target gene activation. G-actin binding to MRTF-A promotes its export into the cytoplasm through the Crm1 nuclear export receptor.

SRF binding *in vivo* occurs both at perfectly conserved and slightly degenerated CArG motifs and it appears that the quality of the consensus reflects the binding co-operation with SRF co-transcriptional activators (Esnault et al., 2014). Conserved consensus sequence better correlates with co-activators with no DNA preferences such as the MRTFs. On the other hand, degenerated consensus correlates with loci at which SRF co-operates with the TCFs, which have DNA sequence specificity.

In addition, SRF binding sites could be classified as constitutive, which are mainly associated with TCF activity, and inducible, at which SRF binding is potentiated by complex formation with the MRTFs. The majority of SRF binding events are inducible and exhibit a better match to the CArG box than constitutive sites.

Thus, SRF target genes are coupled predominantly to one pathway or the other (Gineitis & Treisman, 2001; Sotiropoulos et al., 1999), with MRTF-SRF signaling regulating cytoskeletal genes and the TCF-SRF pathway controlling genes involved in cell proliferation and survival (Esnault et al., 2014; Medjkane et al., 2009; Olson & Nordheim, 2010).

Nevertheless, at some target genes, both co-factor families can variably access SRF, depending on cellular context. Genomic studies of TCF knock-out cells suggest that the TCFs acts as general inhibitors of MRTF recruitment at target genes (Gualdrini et al., 2016). Similarly, a fraction of MRTF-SRF target genes such as *Cyr61* and *Ctgf* are also regulated by the mechanosensitive transcription factor YAP (Esnault et al., 2014; Foster et al., 2017).

The role of TCFs and MRTFs in the cell

TCF-SRF signalling is involved in thymocyte positive selection (Costello et al., 2010; Costello et al., 2004) and T cell differentiation (Maurice et al., 2018), whereas MRTF-SRF signaling is required for various actin-based processes in the cell, including adhesion, chemotaxis and migration, as well as invasion and metastasis of cancer cells (Haak et al., 2017; Medjkane et al., 2009; Mokalled et al., 2010).

Co-ablation of MRTF-A and MRTF-B largely phenocopies SRF deletion *in vivo*. For instance, deletion of SRF in the brain results in impaired neuronal cell migration and neurite outgrowth (Alberti et al., 2005; Knöll et al., 2006). While mice lacking a single MRTF isoform exhibit normal brain development, co-ablation of MRTF-A and MRTF-B causes abnormalities that phenocopy the defect in SRF null mice, suggesting that MRTF-A and MRTF-B act redundantly to support normal brain development (Mokalled et al., 2010). Similarly, animals lacking both MRTFs recapitulate the defect in bone colonization of hematopoietic stem cells observed in SRF knock-out mice (Costello et al., 2015). Inactivation of SRF or both MRTF-A and MRTF-B leads to impaired angiogenesis and filopodia formation in endothelial cells (Franco et al., 2013), defects in retinal vascularization (Weinl et al., 2013) and plasma membrane blebbing and entotic invasion (Hinojosa et al., 2017). That developmental defects in mice caused by conditional deletion of SRF can be reproduced only when both MRTFs are ablated suggests that MRTF-A and MRTF-B act redundantly and is consistent with structural similarities between the two isoforms and studies demonstrating that inactivation of both MRTFs is required for a complete inhibition of serum- and RhoA-mediated activation of reporter genes (Cen et al., 2003).

Nevertheless, there is a unique requirement for MRTF-A and MRTF-B in specific contexts. MRTF-B is indispensable for the development of a subset of neural crest-derived vascular smooth muscle cells (Li et al., 2005; Oh et al., 2005), while MRTF-A is essential for myofibroblast differentiation (Li et al., 2006; Sun et al., 2006). MRTF-B deletion results in embryonic lethality at E13.5 and E14.5. Mutant mice display defects in differentiation of neural-crest-derived smooth muscle cells and anatomical abnormalities in branchial arch arteries and the cardiac outflow tract (Li et al., 2005; Oh et al., 2005). In contrast, MRTF-A mice are viable and fertile but exhibit defects in differentiation of myoepithelial cells of the mammary gland during pregnancy and lactation (Li et al., 2006; Sun et al., 2006). While this could reflect a unique function of MRTF-A and MRTF-B in mammary myoepithelial cells and neural crest-derived vascular smooth muscle cells, respectively, it could also suggest that in specific contexts loss of one MRTF isoform reduces the level of MRTF family members below a threshold required to support extensive proliferation and differentiation.

MRTF regulation

In fibroblasts, MRTF constantly shuttles between the nucleus and the cytoplasm and its subcellular localization is controlled by free monomeric G-actin (Figure 2B) (Vartiainen et al., 2007). Since the RPEL domain of MRTF overlaps with its NLS sequences, G-actin competes with importin α/β for MRTF binding (Hirano & Matsuura, 2011; Mouilleron et al., 2008; Mouilleron et al., 2011; Pawłowski et al., 2010). In addition, an actin-independent mechanism of MRTF nuclear import has been described, which depends on the Ddx19 RNA helicase. Ddx19 facilitates the interaction between MRTF and importin α/β through mediating a conformational change in the MRTF protein (Rajakylä et al., 2015).

Actin also regulates the export of MRTF from the nucleus. MRTF harbors several Crm1-dependent nuclear export sequences (NES) and G-actin binding to MRTF is required for its export through the Crm1 nuclear receptor (Panayiotou et al., 2016; Vartiainen et al., 2007). In fact, it appears that MRTF localization is mainly regulated through export rather than import and it is the high basal MRTF export rate that maintains its cytoplasmic localization in unstimulated cells (Vartiainen et al., 2007).

While under resting conditions MRTF is predominantly in the cytoplasm, activation of Rho by mitogenic stimuli or mechanical cues and subsequent actin polymerization results in MRTF nuclear accumulation. Depletion of the free monomeric G-actin pool upon Rho activation promotes MRTF-importin interaction and nuclear import, allowing complex formation with SRF and activation of gene expression (Cen et al., 2003; Du et al., 2004; Miralles et al., 2003; Vartiainen et al., 2007). Downstream of Rho, two effector pathways mediate actin polymerization: the formin mDia1 pathway which nucleates actin filaments and the ROCK-LIMK-cofilin pathway which de-stabilizes F-actin (Copeland & Treisman, 2002; Geneste et al., 2002; Sotiropoulos et al., 1999; Tominaga et al., 2000). However, Rho signaling is not essential for the activation of SRF-MRTF signaling. Depletion of the G-actin pool is both required and sufficient for the transcriptional response at MRTF target genes.

Monomeric G-actin and polymerized F-actin inhibits and activates SRF-MRTF signalling, respectively (Miralles et al., 2003; Posern et al., 2004; Posern et al., 2002; Stern et al., 2009). Increased G-actin levels by overexpression of wild-type β-actin or ectopic expression of the non-polymerizable actin mutants R62D, G13R and actin-VP16 inhibits MRTF nuclear accumulation and SRF activation by directly binding to MRTF (Miralles et al., 2003; Posern et al., 2002). On the other hand, expression of actins S14C, V159N and G15S, which stabilize F-actin, promotes MRTF nuclear accumulation and SRF target gene activation (Posern et al., 2004). Moreover, overexpression of WH2-domain containing proteins, such as the actin nucleation factors N-WASP, WAVE2, Spire and Cobl, promote MRTF activation through competition for G-actin binding (Weissbach et al., 2016).

Chemicals which interfere with the actin treadmilling cycle can also influence MRTF activity. Latrunculin B (LatB) prevents actin polymerization by sequestering monomeric G-actin. It blocks the G-actin ATP binding cleft and inhibts its addition to growing filaments, thus increasing the concentration of G-actin and inhibiting MRTF (Morton et al., 2000; Spector et al., 1989; Spector et al., 1983). On the other hand, serum-induced actin polymerization, or disruption of the MRTF-actin complex by treatment with Jasplakinolide, Swinholide A or Cytochalasin D (CD) promotes MRTF nuclear accumulation (Cen et al., 2003; Miralles et al., 2003; Posern et al., 2004; Sotiropoulos et al., 1999; Vartiainen et al., 2007). Similarly to LatB, CD also disrupts actin filaments. Its mode of action is however different. CD promotes ATP hydrolysis and directly binds to G-actin, at the cleft contacted by MRTF's RPEL motifs, thus preventing MRTF/G-actin binding and activating MRTF (Brenner & Korn, 1980; Tellam & Frieden, 1982).

Even though it does not affect the actin treadmilling cycle, Leptomycin B (LMB) can be used to modulate MRTF activity since it targets the Crm1 nuclear export receptor, through which MRTF export from the nucleus is mediated (Vartiainen et al., 2007). LMB blocks Crm1 by covalently binding to the sulfhydryl group of Cys529 of Crm1 (Kudo et al., 1999). LMB-induced nuclear MRTF does not activate transcription at target genes (Vartiainen et al., 2007).

An additional layer of MRTF regulation is added by post-translational modifications. With 26 phosphorylation sites mapped, some of which ERK-dependent, it was shown that phosphorylation acts both positively and negatively on MRTF activity. ERK-mediated phosphorylation of S98 within the RPEL domain activates MRTF by reducing its affinity for G-actin, while S33 phosphorylation of one of the six Crm1-dependent NESs promotes MRTF nuclear export (Panayiotou et al., 2016). Similarly, S545 phosphorylation has also been reported to promote MRTF export from the nucleus (Muehlich et al., 2008). Additionally, MRTF protein levels are regulated through GSK-3β-mediated phosphorylation, which promotes MRTF ubiquitination and proteasomal degradation (Charbonney et al., 2011).

Regulation of MRTF activity in the nucleus

In addition to regulating MRTF subcellular localization, G-actin also regulates the nuclear activity of MRTF. In NIH3T3 mouse fibroblasts, MRTF stays predominantly nuclear for several hours after stimulation, even though transcriptional activation is transient (Gineitis & Treisman, 2001; Miralles et al., 2003; Vartiainen et al., 2007). Moreover, nuclear accumulation of MRTF in the absence of an activating signal is not sufficient for target gene activation. Fusing MRTF with an additional NLS or blocking Crm1-mediated nuclear export with LMB does not elicit a transcriptional response (Posern et al., 2002; Vartiainen et al., 2007). In contrast, MRTF mutant protein harbouring point mutations in its RPEL motifs (MRTF-XXX), which cannot bind G-actin, is not only constitutively nuclear, but also constitutively transcriptionally active (Miralles et al., 2003; Vartiainen et al., 2007).

Several studies provide direct evidence for regulation of MRTF by actin in the nucleus. First, FRET studies demonstrate that MRTF-actin interaction occurs in the nucleus (Vartiainen et al., 2007). MRTF activity is promoted by NLS-tagged mutant actins G15S and S14C, which promote F-actin formation, while over-expression of NLS-actin inhibits MRTF target genes (Sharili et al., 2016). Similarly, formins and nucleoskeletal proteins such as the LINC complex, which mediate actin polymerization in the nucleus, stimulate MRTF activity (Baarlink et al., 2013; Plessner et al., 2015), and so does the monooxygenase MICAL2, which causes nuclear G-actin depletion (Lundquist et al., 2014). These data demonstrate a

repressive effect of nuclear actin on MRTF activity, however the exact mechanism is unclear.

1.2 RNA Polymerase II

The essential function of sequence-specific transcription factors such as SRF and MRTF is to direct RNA Polymerase to target gene promoters and promote transcription. As discussed below, Pol II is recruited via the interaction between sequence-specific transcription factors and the Mediator complex, which serves as a scaffold in the assembly of the pre-initiation complex (PIC) (Allen & Taatjes, 2015; Malik & Roeder, 2010; Taatjes, 2010). Mediator facilitates PIC formation through its interactions with general transcription factors, Pol II itself and cohesin, which maintains enhancer-promoter looping (Kagey et al., 2010). In addition, transcription factors promote open chromatin structure, through recruiting histone modifiers such as p300 and Brd4 (Barboric et al., 2001; Col et al., 2017; Huang et al., 2009; Wu et al., 2015), and can stimulate transcription elongation through recruitment of pTEFb, which regulates the transition from initiation into elongation (Hargreaves et al., 2009; Rahl et al., 2010).

While the general principles of transcription are conserved, the transcriptional machinery in eukaryotes is more complex than that in prokaryotes. In bacteria, there is only one RNA polymerase enzyme, whereas in eukaryotic organisms, the RNA Polymerase I, II and III are responsible for the transcription of different RNA classes (Roeder, 2019).

The most abundant RNAs in the cell are the ribososmal RNAs (rRNA), the majority of which is produced by RNA polymerase I. 5S rRNA and tRNA are transcribed by RNA polymerase III, while all messenger RNA (mRNA) and most regulatory RNA, including miRNA, snRNA and snoRNA, are made by RNA polymerase II (Pol II). Pol II is highly conserved among species and consists of 12 subunits, Rpb1-12. The largest subunit Rpb1 and Rpb2 form the catalytic centre of the Pol II (Carter & Drouin, 2009; Cramer et al., 2008; Cramer et al., 2001; Jasiak et al., 2006; Kuhn et al., 2007; Osman & Cramer, 2020b).

The RNA Polymerase II CTD code

Mammalian cells contain two forms of Pol II, hypo-phosphorylated (Pol IIA) and hyper-phosphorylated (Pol II0), the latter being associated with active transcription (Cadena & Dahmus, 1987; Kim & Dahmus, 1986; Payne et al., 1989). The majority of phosphorylation events occur within the carboxy-terminal domain (CTD) of the Rpb1 subunit of Pol II.

The length and the complexity of the Pol II CTD increases with the complexity of the organism (Eick & Geyer, 2013). The CTD consists of 52 heptad repeats of the sequence $Y^1S^2P^3T^4S^5P^6S^7$ in mammalian cells and 26 repeats in yeast (Allison et al., 1988; Bartolomei et al., 1988; Corden et al., 1985). In addition to being longer, the CTD in mammalian cells deviates from the consensus in its distal part (Figure 3). The last 31 heptad repeats are non-consensus, with substitutions at positions 2, 4 ,5 and 7 (Corden et al., 1985). While deletion of the Pol II CTD is lethal, cells expressing Rpb1 consisting of approximately half the number of CTD repeats are viable. At least 8 or 26 repeats are required for viability in yeast and mouse, respectively (West & Corden, 1995).

Human Rpb1 CTD		*Saccharomyces cerevisiae* Rpb1 CTD
1 YSPTSPA	27 YTPTSPN	1 FSPTSPT
2 YEPRSPGG	28 YSPTSPS	2 YSPTSPA
3 YTPQSPS	29 YSPTSPS	3 YSPTSPS
4 YSPTSPS	30 YSPTSPS	4 YSPTSPS
5 YSPTSPS	31 YSPSSPR	5 YSPTSPS
6 YSPTSPN	32 YTPQSPT	6 YSPTSPS
7 YSPTSPS	33 YTPSSPS	7 YSPTSPS
8 YSPTSPS	34 YSPSSPS	8 YSPTSPS
9 YSPTSPS	35 YSPTSPK	9 YSPTSPS
10 YSPTSPS	36 YTPTSPS	10 YSPTSPS
11 YSPTSPS	37 YSPSSPE	11 YSPTSPS
12 YSPTSPS	38 YTPTSPK	12 YSPTSPS
13 YSPTSPS	39 YSPTSPK	13 YSPTSPS
14 YSPTSPS	40 YSPTSPK	14 YSPTSPS
15 YSPTSPS	41 YSPTSPT	15 YSPTSPS
16 YSPTSPS	42 YSPTTPK	16 YSPTSPS
17 YSPTSPS	43 YSPTSPT	17 YSPTSPA
18 YSPTSPS	44 YSPTSPV	18 YSPTSPS
19 YSPTSPS	45 YTPTSPK	19 YSPTSPS
20 YSPTSPS	46 YSPTSPT	20 YSPTSPS
21 YSPTSPS	47 YSPTSPK	21 YSPTSPS
22 YSPTSPN	48 YSPTSPT	22 YSPTSPN
23 YSPTSPN	49 YSPTSPKGST	23 YSPTSPS
24 YTPTSPS	50 YSPTSPG	24 YSPTSPG
25 YSPTSPS	51 YSPTSPT	25 YSPGSPA
26 YSPTSPN	52 YSLTSPAISPDDSDEEN	26 YSPKQDEQKHNENENSR

Figure 3 Sequence of the Rpb1 CTD

Comparison of the Rpb1 CTDs of human and yeast. Divergence from the consensus heptad repeat is shown in red.

Each of the residues within the Pol II CTD are subject to post-translational modification and distinct modifications correlate with different stages of the transcription cycle (Figure 4) (Zaborowska et al., 2016). The stages of the transcription cycle and the factors involved are discussed below (see 1.3 The transcription cycle).

Phosphorylation is the best characterized CTD modification. Serine 5 (Ser5) is phosphorylated early in the transcription cycle and is associated with initiation of transcription (Hengartner et al., 1998; Komarnitsky et al., 2000; Lu et al., 1992; Schroeder et al., 2000), chromatin de-condensation (Ng, Robert, et al., 2003) and 5' end processing of the nascent RNA (Komarnitsky et al., 2000). Consistently, Pol II is phosphorylated on Ser5 along the gene, with a distinct peak at the transcription start site (TSS). In contrast, phospho-serine 2 (Ser2P) starts accumulating in the gene body and peaks towards the 3' region of the gene. It plays a key role during transcriptional elongation and termination (Gomes et al., 2006; Kim et al., 2002; Komarnitsky et al., 2000). Phospho-serine 7 (Ser7P) distribution along the gene is similar to that of Ser5P (Akhtar et al., 2009; Chapman et al., 2007). In contrast to lack of Ser5P and Ser2P, ablation of phospho-Ser7 does not reduce mRNA levels globally (Egloff et al., 2007). However, it is essential for transcription and RNA processing at snRNA genes, specifically (Egloff et al., 2007).

One of the less characterized modifications of the Pol II CTD is tyrosine 1 (Tyr1) phosphorylation (Baskaran et al., 1993). Tyr1P is predominantly found at promoters and it is involved in the control of bidirectional and anti-sense transcription (Descostes et al., 2014; Hsin, Li, et al., 2014). Lack of Tyr1P results in a readthrough phenotype in the anti-sense direction at 5' ends of genes and the sense direction at 3' ends. Tyr1P is thus required for the inhibition of pervasive transcription. It also plays a role in transcription termination and it is required for Pol II stability (Descostes et al., 2014; Mayer et al., 2012).

In addition, the Pol II CTD is phosphorylated on threonine 4 (Thr4) (Zhang & Corden, 1991). Thr4P is found predominately at the 3′ ends of genes (Heidemann et al., 2013; Hintermair et al., 2012). Similarly to Ser2P, Thr4P plays a role in elongation and termination (Hintermair et al., 2012; Nemec et al., 2017; Schlackow

et al., 2017). Furthermore, it is required for transcription and 3′ end formation at histone genes (Hsin et al., 2011) and during M-phase progression (Hintermair et al., 2016).

Isomerization of prolines 3 and 6 by the peptidyl-prolyl isomerase Pin1 (Morris et al., 1999; Wu et al., 2000) impacts on the overall phosphorylation status of the Pol II by regulating the binding of CTD modifying enzymes (Bataille et al., 2012; Krishnamurthy et al., 2009; Xu et al., 2003; Xu & Manley, 2007). In addition, the Pol II CTD can be glycosylated. This occurs prior to Pol II recruitment to genes. It is thought that glycosylation sterically blocks CTD phosphorylation and its removal regulates transcription initiation (Ranuncolo et al., 2012).

Residues within the non-consensus CTD repeats can also be modified. Methylation of arginine 7 has been implicated in transcription termination and in regulation of snRNA and snoRNA genes, while lysine 7 methylation is thought to play a role in early stages of transcription (Dias et al., 2015; Sims et al., 2011). Because of its enrichment at TSSs, Lys7 acetylation is believed to be involved in initiation of transcription (Voss et al., 2015). In addition, it is required for the expression of the *Egr1* and *c-Fos* genes (Schröder et al., 2013). Lys7 can also be ubiquitinated, which leads to Rpb1 degradation by the proteasome (H. Li et al., 2007).

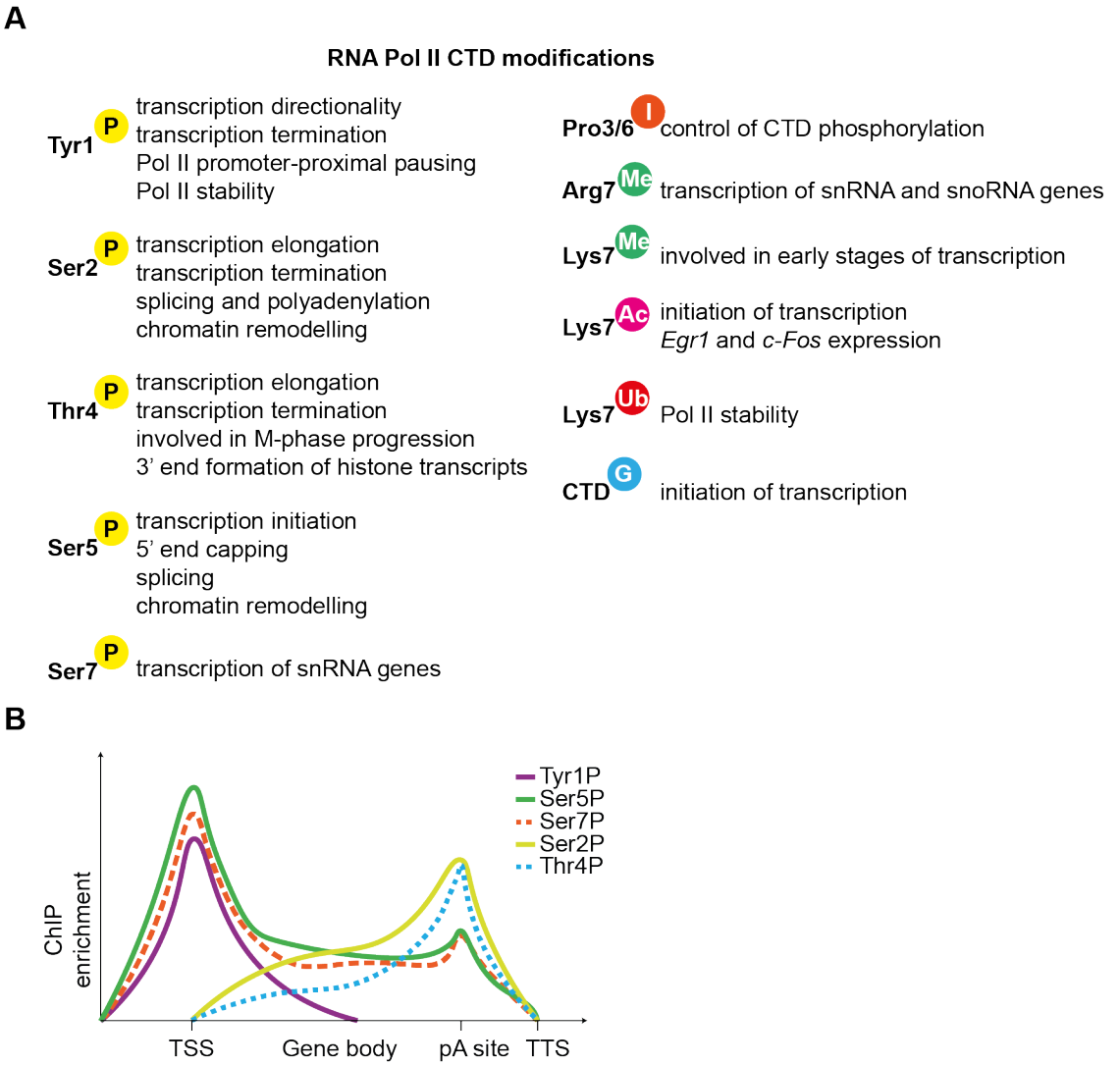

Figure 4 RNA Pol II CTD modifications

(A) Modifications the Pol II CTD and their functions. In the figure phosphorylation is indicated by (P), isomerization (I), methylation (Me), acetylation (Ac), ubiquitination (Ub) and glycosylation (G). (B) Pol II CTD phosphorylations. Phospho-serine 5 (Ser5P) peaks at the transcription start site (TSS) and stays on along the gene body, with a small peak at the 3' end of the gene. Phospho-serine 7 (Ser7P) has a similar profile. Phospho-tyrosine 1 (Tyr1P) is present at the 5'end of the gene, with a peak at the TSS. Phospho-serine 2 (Ser2P) and phospho-threonine 4 (Thr4P) have a similar profile. These marks start accumulating in the gene body and peak at the 3' end of the gene.

Mass spectrometry analyses show that all five phospho-marks are found along the entire length of the Pol II CTD, with Ser5P and Ser2P being the most abundant ones (Schüller et al., 2016; Suh et al., 2016). In cells, the majority of heptad repeats are phosphorylated on only one residue and Ser5P and Ser2P predominate in mono-phosphorylated repeats. These two phosphorylation events appear to be distinct, separated spatially on the CTD, as well as temporally during the transcriptional cycle (Czudnochowski et al., 2012; Schüller et al., 2016). Even though more rarely, all possible double-phosphorylations are detected within the same heptad (Schüller et al., 2016; Suh et al., 2016). Thr4P frequently co-occurs with Ser2P, while Tyr1P is often found on Ser5P containing repeats (Schüller et al., 2016). However, triple phosphorylations within the same heptads are not detected (Schüller et al., 2016).

CTD phospho-marks appear to be placed in succession, with some of the modifications being preferentially deposited on pre-phosphorylated heptad repeats. Thus, Ser5P precedes Ser7P (Boeing et al., 2010) and Ser2 phosphorylation (Komarnitsky et al., 2000). Ser7 phosphorylation, which is dependent on pre-phosphorylation of Ser5 (Akhtar et al., 2009; Boeing et al., 2010; Chapman et al., 2007), primes Ser2 phosphorylation (Akhtar et al., 2009; Boeing et al., 2010; Bösken et al., 2014; Chapman et al., 2007). Inhibition of Ser2P decreases levels of Thr4P, while it does not affect Ser5P or Ser7P levels (Krajewska et al., 2019). Furthermore, Thr4P is strictly associated with the occurrence of the Ser2P mark, suggesting that phosphorylation of Ser2 precedes that of Thr4 (Hintermair et al., 2012).

CTD kinases

The CTD modifications are dynamic and various kinases act during the transcriptional cycle to ensure appropriate regulation of the Pol II. The phosphorylation state of the CTD orchestrates the temporal and spatial recruitment of various factors that mediate transcription and RNA processing throughout the transcriptional cycle. Therefore, changes in CTD phosphorylation by site-specific kinases and phosphatases are critical for the accurate transmission of information during transcription.

Ser5 is phosphorylated by the cyclin-dependent kinase 7 (CDK7) (Komarnitsky et al., 2000; Lu et al., 1992; Ramanathan et al., 2001; Schroeder et al., 2000; Schwartz et al., 2003). In addition to Ser5, CDK7 also phosphorylates Ser7 of the Pol II CTD (Akhtar et al., 2009; Boeing et al., 2010; Glover-Cutter et al., 2009). However, since inhibition of CDK7 does not completely abolish Ser7P, there appear to be additional unidentified Ser7 kinases (Boeing et al., 2010; Tietjen et al., 2010).

There are three kinases responsible for phosphorylation of Ser2, the positive transcription elongation factor (pTEF-b), which comprises the catalytically active cyclin-dependent kinase 9 (CDK9) and its regulator cyclin T (Marshall et al., 1996; Ramanathan et al., 2001; Shim et al., 2002), and CDK12/13 (Bartkowiak et al., 2010; Blazek et al., 2011; Bowman et al., 2013; Zhang et al., 2016). CDK9 and CDK12 have distinct distribution along the gene. While both kinases are found along the gene body, CDK12 is not observed near transcription start sites (Bartkowiak et al., 2010; Gomes et al., 2006). Furthermore, unlike inhibition of CDK9 which affects transcription globally, in the absence of CDK12/13 only a subset of genes involved in DNA replication, recombination and repair are affected (Blazek et al., 2011; Liang et al., 2015; Zhang et al., 2016).

Apart from CDK7, CDK9 and CDK12, CDK8 can also phosphorylate the Pol II CTD, both at Ser2 and Ser5, with a preference for the latter (Liao et al., 1995; Ramanathan et al., 2001; Rickert et al., 1999; Sun et al., 1998). In addition, the MAP Kinases ERK1 and ERK2 are capable of phosphorylating Ser5 (Trigon et al., 1998), while Serines 7 and 2 can be phosphorylated by the DNA-dependent Protein Kinase (DNAPK) (Egloff et al., 2010; Trigon et al., 1998). It has been proposed that DYRK1A is a gene-specific kinase that controls Ser5 and Ser2 phosphorylation (Di Vona et al., 2015). Finally, Brd4 can phosphorylate Ser2 of the Pol II CTD upon CDK9 inactivation (Devaiah et al., 2012).

In cells, the majority of Thr4 phosphorylation is mediated by the polo-like kinase 3 (Plk3) (Heidemann et al., 2013; Hintermair et al., 2012). However, CDK9 is also able to phosphorylate Thr4 *in vitro* (Hsin et al., 2011).

The only known Tyr1 kinases are the Abl1/2 kinases (Baskaran et al., 1993). Nevertheless, the Pol II CTD is phosphorylated on Tyr1 in c-Abl knock-out mouse cells so, as is the case with Ser7 phosphorylation, there must be additional unidentified Tyr1 kinases (Baskaran et al., 1993).

Defining the specificity of CDKs for a particular residue within the Pol II CTD and their distinct role in the transcription cycle has proven challenging. Due to structural similarities among CDKs, chemical inhibitors often have dose-dependent off-target effects. Furthermore, kinase specificity *in vitro* does not always correlate with *in vivo* data (Galbraith et al., 2019; Whittaker et al., 2017).

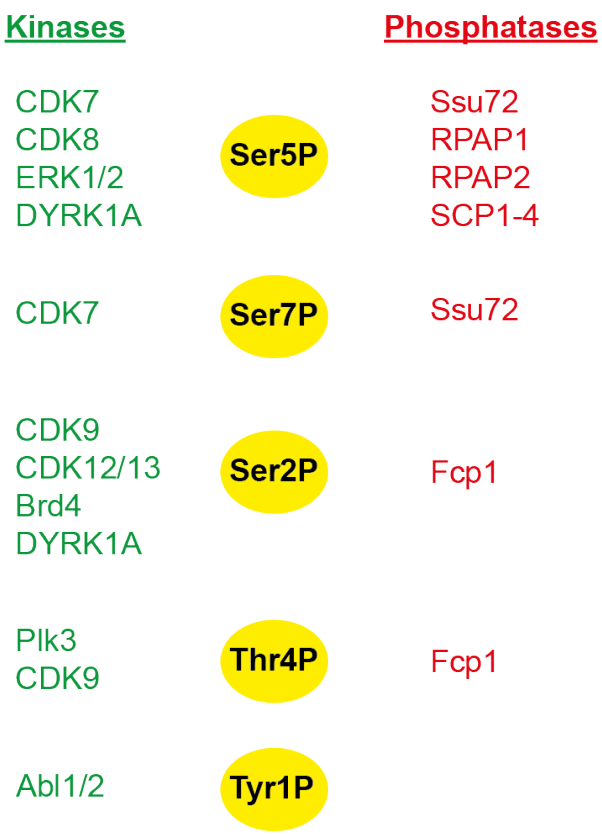

Figure 5 CTD kinases and phosphatases

Kinases and phosphatases shown to target Ser5, Ser7, Ser2, Thr4 and Tyr1 of the Pol II CTD.

CTD phosphatases

The first phosphorylation event in the transcription cycle occurs at Ser5 of the CTD. Ser5P peaks at the TSS, with its levels gradually reducing along the gene to allow for additional modifications of the CTD to occur as the Pol II transitions into elongation. Ser5 dephosphorylation occurs during elongation, accompanying phosphorylation of Ser2 (Cho et al., 2001). A family of small CTD phosphatases SCP1-3 preferentially dephosphorylate Ser5P (Kamenski et al., 2004; Krishnamurthy et al., 2004; Mosley et al., 2009; Yeo et al., 2003). In addition, S5P is a target of RPAP1 and RPAP2 phosphatases (Egloff et al., 2012; Mosley et al., 2009). RPAP2 directly interacts with Ser7 phosphorylated Pol II CTD and plays a role in snRNA gene expression (Egloff et al., 2012), while RPAP1 acts as a Ser5 phosphatase at developmental genes, specifically (Lynch et al., 2018). Three additional RNA Pol II interacting proteins RPRD1A, RPRD1B and RPRD2 target Ser5P and stimulate its dephosphorylation by RPAP2 (Ni et al., 2011; Ni et al., 2014).

Ssu72 is another CTD phosphatase which targets both Ser5P (Krishnamurthy et al., 2004; Mosley et al., 2009; Wani et al., 2014; Yeo et al., 2003) and Ser7P (Bataille et al., 2012; Wani et al., 2014; Zhang et al., 2012). Nevertheless, it exhibits a strong preference for Ser5 (Xiang et al., 2012).

Fcp1/Ctdp1 is known to dephosphorylate Ser2P at 3' end of genes (Cho et al., 2001; Ghosh et al., 2008; Hausmann & Shuman, 2002). However, it seems to be a promiscuous phosphatase which exhibits a preference for Ser2P but is also capable of acting on additional phospho-residues within the CTD. Lack of Fcp1 results in an increase of Ser2 phosphorylation and frequency of triply phosphorylated CTD heptad repeats (Suh et al., 2016), as well as increased Thr4P levels (Hsin, Xiang, et al., 2014). It is also involved in the recycling of Pol II at the end of the transcriptional cycle (Bataille et al., 2012; Cho et al., 2001; Cho et al., 1999; Lin et al., 2002).

1.3 The transcription cycle

Pol II catalyses RNA synthesis, however it is unable to transcribe on its own (Weil et al., 1979). The transcription cycle consists of a series of rate-limiting steps, during which transcription factors and co-activators enhance transcription rate by lowering the energy barriers that these steps represent.

Initially, Pol II needs to gain access to the promoter. Promoter remodeling and the factors involved are discussed below (see Co-transcriptional chromatin remodeling). Pol II is recruited by the Mediator complex and general transcription factors, which form the pre-initiation complex (PIC). Mediator contributes to stabilization of the PIC and promotes CDK7-dependent Pol II phosphorylation. Phosphorylation at Ser5 of the Pol II CTD facilitates the transition into initiation. The next regulatory step is promoter-proximal pausing, during which 5' end RNA processing occurs and the Pol II CTD gets further phosphorylated at Ser7. Pol II pause-release into elongation requires the recruitment of CDK9 and phosphorylation at Ser2 of the Pol II CTD. During elongation, numerous factors which increase Pol II processivity through the chromatin template are recruited. Termination is the final regulatory step in the transcription cycle. Pol II dissociates from the DNA template and its CTD is de-phosphorylated. At certain genes, the terminating Pol II is recycled for subsequent rounds of transcription via DNA looping between promoter and termination regions (Cramer, 2019; Eick & Geyer, 2013; Osman & Cramer, 2020a; Srivastava & Ahn, 2015).

Initiation

The first step of the transcription cycle is the formation of the pre-initiation complex (PIC) at the gene promoter (Sainsbury et al., 2015). PIC assembly and Pol II recruitment is promoted by the Mediator complex. Mediator is recruited by TFs bound to enhancer regions. In addition, it also interacts with most components of the PIC and it is thus required for enhancer-promoter looping (Allen & Taatjes, 2015; Jeronimo & Robert, 2017; Pokholok et al., 2002; Wong et al., 2014). Promoter-enhancer interactions are maintained by cohesin, which also physically interacts with the Mediator complex (Kagey et al., 2010; Phillips-Cremins et al., 2013; Rollins et al., 2004).

The PIC consists of Pol II and general transcription factors TFIIA, TFIIB, TFIID, TFIIE, TFIIF and TFIIH (Pokholok et al., 2002). The TATA-binding protein (TBP) subunit of TFIID is involved in the recognition of core promoter elements (Nakajima et al., 1988; Parker & Topol, 1984). TFIIB promotes Pol II recruitment, while TFIIF stabilizes the Pol II-containing complex. Finally, TFIIE and TFIIH are recruited. TFIIH is the largest GTF and its activity is stimulated by TFIIE. TFIIH contains three catalytically active subunits, CDK7 and two DNA helicases (XPB and XPD), which are responsible for DNA unwinding at the transcription start site (TSS) and the formation of the open promoter complex. (Goodrich & Tjian, 1994; Kim et al., 2000). Pol II enters the pre-initiation complex in a hypo-phosphorylated form and its transition into initiation is dependent on CDK7-mediated phosphorylation of Ser5 of the Pol II CTD (Figure 6A) (Hengartner et al., 1998; Lu et al., 1992).

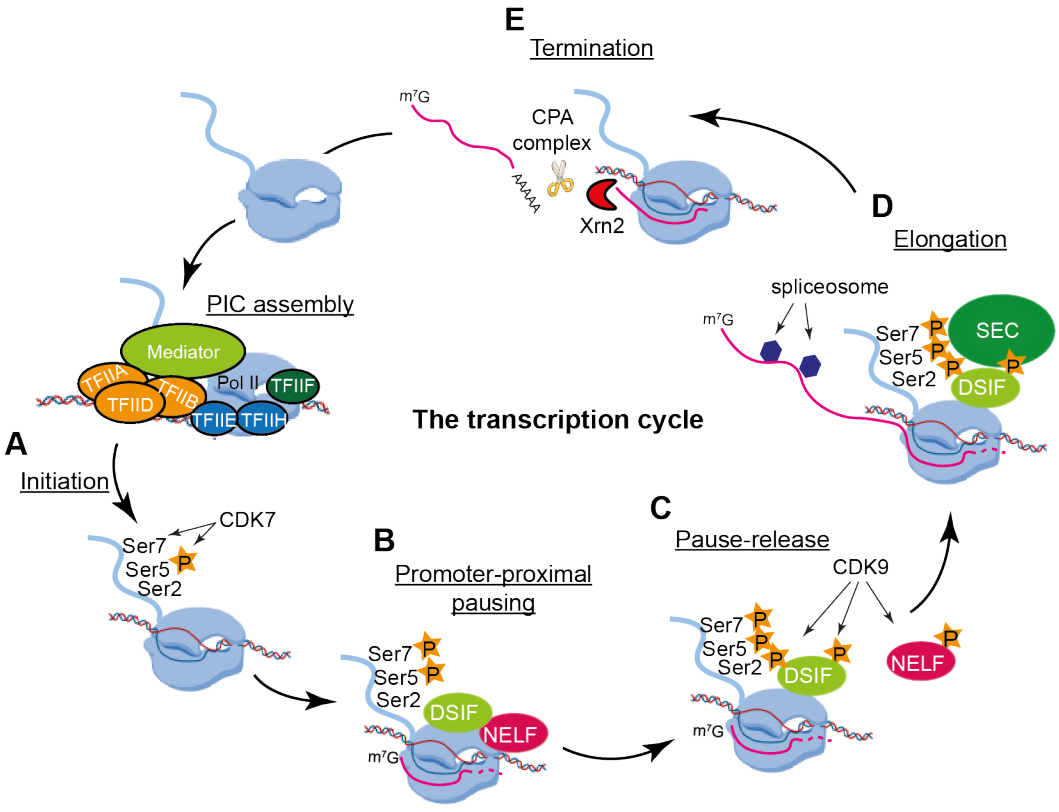

Figure 6 The transcription cycle. (A) The first step of the transcription cycle is the formation of the pre-initiation complex (PIC) at the gene promoter. The PIC consists of Pol II and general transcription factors TFIIA, TFIIB, TFIID, TFIIE, TFIIF and TFIIH. The TATA-binding protein (TBP) subunit of TFIID is involved in the recognition of core promoter elements. TFIIB promotes Pol II recruitment, while TFIIF stabilizes the Pol II-containing complex. Finally, TFIIE and TFIIH are recruited. TFIIH is the largest GTF and its activity is stimulated by TFIIE. TFIIH contains three catalytically active subunits, CDK7 and two DNA helicases (XPB and XPD), which are responsible for DNA unwinding at the transcription start site (TSS) and the formation of the open promoter complex. Although TFs do not directly bind Pol II, one mechanism by which they can promote its recruitment is by binding to the Mediator complex. Mediator enables Pol II recruitment via interaction with the C-terminal domain (CTD) of the Rpb1 subunit of the Pol II. Mediator promotes stable PIC formation by directly interacting with multiple PIC factors. Pol II enters the pre-initiation complex in a hypo-phosphorylated form and during transcription initiation, the Pol II CTD is phosphorylated at Serine 5 by the CDK7 subunit of the general transcription factor TFIIH. (B) Slightly downstream of the transcription start site Pol II pauses. Promoter-proximal pausing is mediated by the negative elongation factor (NELF) and the DRB sensitivity-inducing factor (DSIF). The CTD of the paused Pol II is phosphorylated at Ser5 and Ser7. The nascent RNA gets capped. (C) Pause-release is dependent on CDK9. CDK9 phosphorylates NELF which causes its release from Pol II, DSIF and Serine 2 of the Pol II CTD, allowing Pol II to transition into elongation. (D) During elongation Pol II is in its hyper-phosphorylated form. It is bound by the super elongating complex (SEC) which promotes Pol II processivity. Co-transcriptional splicing is carried out by the spliceosome complex. (E) After transcribing the polyadenylation signal, the cleavage and polyadenylation complex (CPA) is recruited. Following cleavage of the transcript, the Xrn2 exonuclease degrades the uncapped RNA, eventually catching up with Pol II and causing its release from the DNA template. The Pol II CTD is dephosphorylated and Pol II gets recycled for subsequent rounds of transcription.

Promoter-proximal pausing

At many eukaryotic genes, Pol II is present at a disproportionally high amount at the TSS of the gene, as compared to the gene body (Core & Adelman, 2019). Pol II pauses 20-120 nucleotides downstream of the TSS (Plet et al., 1995; Schwartz et al., 2003). Promoter-proximal pausing was first described at heat-shock inducible genes in Drosophila (Rougvie & Lis, 1988) and the growth factor inducible genes c-myc and c-fos in mammalian cells (Albert et al., 1997; Brown et al., 1996; Cheng & Sharp, 2003; Krumm et al., 1992; Plet et al., 1995). However, it is now known that

pausing occurs at most metazoan genes and that Pol II promoter-proximal pausing is the first regulatory step after transcription initiation (Core et al., 2008; Guenther et al., 2007; Muse et al., 2007; Zeitlinger et al., 2007). Nevertheless, the duration and stability of the promoter-proximal pausing is variable. Some promoter-proximally stalled polymerases are stably associated with genes and have a slow turnover rate (Buckley et al., 2014; Chen et al., 2015; Jonkers et al., 2014; Ni et al., 2008), while others undergo multiple cycles of initiation and pre-mature termination (Brannan et al., 2012; Plet et al., 1995; Wagschal et al., 2012).

The significance of Pol II pausing has remained unclear. One possibility is that promoter-proximal pausing could facilitate further rounds of transcription by maintaining an open chromatin structure (Guenther et al., 2007; Muse et al., 2007; Zeitlinger et al., 2007). Thus, it could provide a way for rapid activation of gene expression on inducible genes (Core & Lis, 2008), as well as facilitate coordinated patterns of activation amongst groups of cells (Chen et al., 2008; Lagha et al., 2013). Alternatively, paused polymerase might reduce inappropriate transcription initiation by sterically inhibiting the binding of additional Pol II complexes (Chopra et al., 2009; Lagha et al., 2013). Furthermore, pausing potentially represents a transcriptional checkpoint to ensure that Pol II is competent for productive elongation.

The paused Pol II is phosphorylated at Ser5 (Plet et al., 1995; Schwartz et al., 2003) and Ser7 (Glover-Cutter et al., 2009) and it is bound by the negative elongation factor (NELF) (Yamaguchi, Takagi, et al., 1999; Yamaguchi, Wada, et al., 1999). In addition, the DRB sensitivity-inducing factor (DSIF), which consists of Spt4 and Spt5, is also associated with the paused polymerase (Hartzog et al., 1998; Wada et al., 1998; Yamaguchi, Wada, et al., 1999). NELF and DSIF function cooperatively to inhibit Pol II elongation (Figure 6B) (Muse et al., 2007). However, while NELF is restricted to the TSS of the gene, Spt5 has a profile identical to the one of the elongating polymerase (Gomes et al., 2006). Furthermore, Spt5 is a key elongation factor in yeast (Mason & Struhl, 2005). In mammalian cells, its positive effect on elongation is conserved and it is dependent on its phosphorylation by the CDK9 subunit of p-TEFb (Yamada et al., 2006).

Pause-release

p-TEFb regulates the transition of the paused polymerase into elongation (Barboric et al., 2001; Chen et al., 2018; Eberhardy & Farnham, 2002; Lis et al., 2000). It is recruited to promoter regions of target genes where it phosphorylates the Pol II CTD in response to various stimuli (Barboric et al., 2001; Eberhardy & Farnham, 2002; Lis et al., 2000). In addition to Ser2 of the Pol II CTD (Andrulis et al., 2000; Kim & Sharp, 2001), CDK9 phosphorylates NELF (Boehm et al., 2003; Ivanov et al., 2000; Wu et al., 2003) and Spt5 (Andrulis et al., 2000; Ivanov et al., 2000; Kim & Sharp, 2001) (Figure 6C). This phosphorylation releases NELF from the polymerase (Fujinaga et al., 2004), while phosphorylated DSIF functions as a positive elongation factor associated with the travelling Pol II as the nascent RNA is being synthesized (Ping & Rana, 2001; Pokholok et al., 2002; Yamada et al., 2006).

p-TEFb activity is controlled by sequestering it in an inactive complex with the RNA binding protein HEXIM1/2 and the 7SK small nuclear RNA (Michels et al., 2004; Nguyen et al., 2001; Yang et al., 2001; Yik et al., 2003) and its release from this complex is dependent on stress signalling (Biglione et al., 2007; Yang et al., 2001; Yik et al., 2003). Thus, the balance between active and inactive p-TEFb in cells can be regulated by external stimuli such as UV and transcriptional inhibitors, as well as post-translational modifications of CDK9 (Chen et al., 2008).

Sequence-specific transcription factors can contribute to regulating Pol II release into elongation by stimulating p-TEFb recruitment. p-TEFb is recruited to promoters by transcription factors including NF-kB (Barboric et al., 2001) and c-Myc or by chromatin remodelers such as Brd4 (Hargreaves et al., 2009) which directly interact with p-TEFb and recruit it to the promoter regions of their target genes (Eberhardy & Farnham, 2001). Furthermore, the transition into elongation is facilitated by the Mediator complex which interacts with pTEF-b, elongation factors and histone modifying complexes (Donner et al., 2010; Takahashi et al., 2011).

Elongation

A number of factors associate with Pol II during the elongation phase which have specific functions in promoting speed, processivity and resolving stalling of Pol II along the gene (Chen et al., 2018). Phosphorylated Spt5 remains associated with Pol II throughout the transcription cycle and it is required for productive elongation (Henriques et al., 2018; Shetty et al., 2017). Spt5 controls the rate of Pol II elongation (Baluapuri et al., 2019), which influences not only overall levels of mRNA (Danko et al., 2013), but also splicing (de la Mata et al., 2003; Howe et al., 2003; Shukla & Oberdoerffer, 2012) and 3' end processing of the transcript (Lee et al., 2007; Nag et al., 2007). In addition, dephosphorylation of Spt5 by PNUTS-PP1, which causes a decrease in the speed of Pol II, is involved in the release of Pol II from the DNA template during transcriptional termination (Cortazar et al., 2019; Hazelbaker et al., 2013). Apart from influencing the speed of the elongating Pol II, Spt5 enhances its processivity by binding to the DNA exit region of Pol II, facilitating re-winding of upstream DNA and preventing aberrant backtracking of Pol II (Bernecky et al., 2017; Ehara et al., 2017; Fitz et al., 2018).

Occasionally, Pol II may stall during elongation due to pause sites within the gene body. TFIIS facilitates Pol II backtracking at such pause sites (Kettenberger et al., 2004). It stimulates cleavage and re-alignment of the nascent transcript with the active site of Pol II which allows for elongation to resume (Adelman et al., 2005; Conaway et al., 1993; Fish & Kane, 2002; Reines et al., 1989). In addition to TFIIS, Elongin and members of the ELL protein family (eleven-nineteen lysine-rich leukemia) such as ELL1 are also involved in alleviation of transient Pol II pausing along the gene (Luo et al., 2012). ELL1 interacts with the elongating Pol II as a part of a multiprotein complex called the super elongating complex (SEC) (Figure 6D). SEC consists of AFF1 and AFF4 (AF4/FMR2 family members 1 and 4), ENL (eleven-nineteen leukemia) or AF9 (ALL fused gene from chromosome 9), ELL1 or ELL2 and pTEF-b (Lin et al., 2010; Luo et al., 2012).

Phospho-serine 2 is required for Pol II elongation (Dengl et al., 2009; Kizer et al., 2005; Li et al., 2003). Pol II CTD phosphorylated at Ser2 is a prerequisite for the recruitment of additional elongation factors, which promote Pol II processivity

through chromatin, such as the PAF and FACT complexes and the histone chaperone Spt6 (Adelman et al., 2006; Ardehali & Lis, 2009; Belotserkovskaya et al., 2003; Bortvin & Winston, 1996; Pokholok et al., 2002; Reinberg & Sims, 2006; Saunders et al., 2003; Sun et al., 2010; Yoh et al., 2007; Zhu, Mandal, et al., 2005).

The polymerase associated factor (PAF) complex has an intrinsic ability to stimulate transcription from a chromatin template and it is involved in histone ubiquitination (Chu et al., 2007; Krogan et al., 2003; Laribee et al., 2005; Ng, Robert, et al., 2003; Wood et al., 2005). It also serves as a platform for the recruitment of additional chromatin remodelers such as the histone chaperone complex FACT (facilitates chromatin transcription) and the Set2 methyltransferase (He et al., 2011). Additionally, PAF also plays a role in RNA metabolism by recruiting pre-mRNA processing factors (Zhu, Mandal, et al., 2005).

Furthermore, the elongating Pol II interacts with topoisomerases such as TOP1, which resolve DNA supercoiling accumulating ahead and behind the travelling Pol II (Liu & Wang, 1987; Ljungman & Hanawalt, 1996; Solier et al., 2013); helicases, which prevent the formation of RNA:DNA hybrids during elongation, thereby ensuring efficient transcription of long genes and preventing deleterious DNA recombination (Huertas & Aguilera, 2003; Ljungman & Hanawalt, 1996) and poly(ADP-ribose) polymerase (PARP), which not only targets NELF (Gibson et al., 2016), thus promoting pause-release, but also chromatin remodelers and histones (Hottiger, 2015; Wright et al., 2016).

Co-transcriptional chromatin remodeling

A large proportion of the factors associated with the elongating Pol II are involved in chromatin remodeling. Dense nucleosome occupancy obstructs the elongating polymerase and inversely correlates with transcription rates (Bernstein et al., 2004; Lee et al., 2004). Modifications of histones alter the physical and chemical properties of chromatin and influence its compaction and accessibility. Thus, actively transcribed and transcriptionally silenced regions of the genome have distinct chromatin signatures (B. Li et al., 2007) (Figure 7). Nevertheless, it is not

clear to what extent chromatin signatures are a cause or a consequence of transcriptional activity.

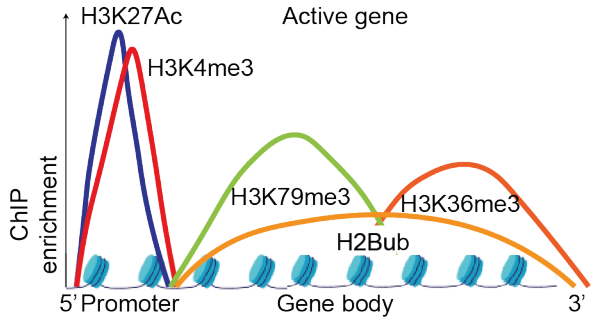

Figure 7 Histone remodeling on actively transcribed genes. Active gene promoters are characterized by acetylation of histone 3 lysine 27 (H3K27Ac) and trimethylation of histone 3 lysine 4 (H3K4me3). Within gene bodies, histone 2 is modified by monoubiquitylation (H2Bub), while histone 3 lysine 79 tri-methylation (H3K79me3) and histone 3 lysine 36 tri-methylation (H3K36me3) are found at the 5' and 3' end of actively transcribed genes, respectively.

Initially, pioneer factors, a class of transcription factors, which appear to be able to access their binding sites even in closed chromatin, facilitate the recruitment of other transcription factors. The chromatin remodeling SWI/SNF complex disrupts the first nucleosomes following the pause site (Brown & Kingston, 1997), while other histone remodelers such as Chd1 (Simic et al., 2003), Ino80 (Kobor et al., 2004; Papamichos-Chronakis et al., 2011) and SWR (Mizuguchi et al., 2004) are involved in histone variant exchange. Histone variants H3.3 (Daury et al., 2006; Mito et al., 2005; Talbert & Henikoff, 2010; Wirbelauer et al., 2005) and H2A.Z (Jin et al., 2009; Meneghini et al., 2003), whose incorporation within the nucleosome reduces its stability, are commonly found within actively transcribed genes.

H3 and H4 histone tails also interfere with transcription and their acetylation supresses this effect (Lee et al., 1993; Protacio et al., 2000; Wasylyk & Chambon,

1979). Histones H3 and H4 at active gene promoters are commonly acetylated at histone H3 lysine 9, 14, 16 and 27 (H3K9Ac, H3K14Ac, H3K16Ac and H3K27Ac) (Bernstein et al., 2005; Gelbart et al., 2009; Liang et al., 2004; Pokholok et al., 2005; Tie et al., 2009; Wang et al., 2008; Zippo et al., 2009) by histone acetyltransferases such as Gcn5, TAF1 and p300/CBP (Sterner & Berger, 2000; Strahl & Allis, 2000). In addition, trimethylation of H3K4 (H3K4me3) at TSSs by MLL1, MLL2 and Set1 histone methyltransferases strongly correlates with transcriptional activity (Bernstein et al., 2005; Liang et al., 2004; Milne et al., 2002; Nakamura et al., 2002; Pokholok et al., 2005; Santos-Rosa et al., 2002; Vakoc et al., 2006). These promoter-associated chromatin modifications are dependent on Ser5P of the Pol II CTD, which serves as a docking site for acetyltransferases and methyltransferases (Ng, Robert, et al., 2003).

Similarly, Ser2P of the CTD is required for the recruitment of enzymes associated with chromatin remodeling downstream of promoters. H3K36me3 (Pokholok et al., 2005; Rando & Chang, 2009; Vakoc et al., 2006) and H2B monoubiquitylated at K120 (Fuchs et al., 2014; Kao et al., 2004; J. Kim et al., 2009; Pavri et al., 2006; Xiao et al., 2005; Zhu, Zheng, et al., 2005) are present within the gene bodies of actively transcribed genes. These modifications are deposited by Set2 methyltransferase (Li et al., 2003; Strahl et al., 2002; Xiao et al., 2003) and the PAF complex (Laribee et al., 2005; Pavri et al., 2006; Wood et al., 2005), respectively, which are recruited through Ser2P of the Pol II CTD (Kizer et al., 2005; Li et al., 2003; Xiao et al., 2003).

Apart from histone tails, modifications within the globular domain of histones also impact on transcription. For example, acetylation at H3K56 (Schneider et al., 2006; Williams et al., 2008; Xu et al., 2005) and H3K122 are associated with actively transcribed genes (Tropberger et al., 2013). H3K122Ac co-localizes with H3K4me3 and histone variants H2A.Z and H3.3 and promotes H3K27Ac and nucleosome eviction, thus facilitating access of the transcriptional machinery (Tropberger et al., 2013). In a similar way, H3K56Ac is involved in the disassembly of H3/H4 at promoter regions of active genes (Williams et al., 2008). Active transcription also correlates with H3K79me3 within gene bodies (Pokholok et al., 2005; Schübeler et al., 2004; Steger et al., 2008). In contrast to H3K36me3 which is enriched towards

the 3' end of genes, H3K79me3 occupies the 5' region of the gene body (Vakoc et al., 2006). It is catalysed by Dot1L (Feng et al., 2002; Ng, Ciccone, et al., 2003; Steger et al., 2008), which interacts with AF9 and ENL components of the SEC complex (Krogan et al., 2003; Mohan et al., 2010).

Histone modifications also play a role in pre-mRNA processing events. H3K36me3 promotes co-transcriptional splicing (Guo et al., 2014; Jelinic et al., 2011; Kumar et al., 2012; Luco et al., 2010).Similarly, H2Bub is involved in regulating splicing (Lee et al., 2012), 3' end formation (Pirngruber et al., 2009) and RNA nuclear export (Vitaliano-Prunier et al., 2012).

Histone modifications are often interdependent and facilitate further chromatin remodeling. H3K79me3 co-occurs with H3 and H4 acetylation and H3K4me3 (Schübeler et al., 2004), while monoubiquitylation of H2B is required for correct H3K4 and H3K79 methylation. (Dover et al., 2002; Lee et al., 2007; Ng, Robert, et al., 2003; Sun & Allis, 2002). Furthermore, MLL1 (H3K4 methyltransferase) and MOF (H4K16 acetyltransferase) physically interact and are both required for efficient activation of a target genes (Dou et al., 2005). Conversely, certain modifications can inhibit others. For example, H3S10P inhibits H3K9me3 and H3K27me3, which are abundant at silenced heterochromatin loci and are associated with the heterochromatin protein 1 (HP1) and the polycomb repressive complex (PRC) (Bannister et al., 2001; Kuzmichev et al., 2002; Lachner et al., 2001; Margueron & Reinberg, 2011; Pengelly et al., 2013; Rea et al., 2000).

Global histone acetylases, deacetylases and methylases restore chromatin structure at the end of the transcription cycle (Katan-Khaykovich & Struhl, 2002; Vogelauer et al., 2000).

Termination

Termination is the last step in the regulation of the transcription cycle (Figure 6E). Aberrant termination could lead to readthrough transcription and inhibit expression of downstream genes through transcriptional interference (Greger et al., 1998; Greger & Proudfoot, 1998; Shearwin et al., 2005), collision with polymerases

transcribing opposite strands of the DNA or with DNA replication forks, leading to DNA damage and genome instability (Hobson et al., 2012; Prescott & Proudfoot, 2002).

Termination of transcription is tightly coupled to 3′ end processing of the nascent transcript (see 3' end processing). Pol II becomes competent for termination after transcribing the polyadenylation (poly(A)) signal, which is then recognised and bound by the 3' processing machinery. Pcf11, a component of the cleavage and polyadenylation complex (CPA), is involved not only in 3′ processing (Amrani et al., 1997; de Vries et al., 2000; Gross & Moore, 2001) and mRNA export (Johnson et al., 2009; Volanakis et al., 2017), but also in transcription termination (West & Proudfoot, 2008; Zhang et al., 2005; Zhang & Gilmour, 2006). Pcf11 directly interacts with Ser2P of the Pol II CTD (Meinhart & Cramer, 2004), and is required for poly(A) site recognition (Kamieniarz-Gdula et al., 2019; West & Proudfoot, 2008).

Two complementary mechanisms leading to transcription termination have been proposed, which involve a conformational change in the elongating Pol II and the collision of the Xrn2 exonuclease with Pol II, respectively. In the allosteric model, passage through the poly(A) site and subsequent recruitment of the cleavage and polyadenylation complex (CPA) at the CTD causes a conformational change within the Pol II active site, resulting in Pol II release from DNA (Logan et al., 1987; Zhang et al., 2015). This allosteric change is dependent on the dephosphorylation of the Pol II associated elongation factor Spt5 (Cortazar et al., 2019).

In the torpedo model, the nuclear 5'->3' Xrn2 exonuclease is recruited at poly(A) sites and following cleavage of the transcript progressively degrades the uncapped 5' end of the nascent RNA. Thus, termination is dependent on kinetic competition between degradation of the nascent RNA by Xrn2 and its extension by Pol II (Fong et al., 2015). When Xrn2 catches up with Pol II, it induces the release of Pol II from DNA and transcription termination (Connelly & Manley, 1988; Fong et al., 2015; Kim et al., 2004; West et al., 2004). According to this model the termination site would be determined by the relative rates of Xrn2-mediated degradation and Pol II elongation. Thus, the speed of the elongating Pol II influences termination. Fast

transcription prolongs the competition between Xrn2 and Pol II, resulting in a more distant termination, while slowing down of Pol II causes a more proximal termination (Fong et al., 2015).

The collision of Xrn2 with the elongating Pol II is promoted by transcription pause sites near the poly(A) site which slow down Pol II, causing its accumulation at the 3' end of genes (Anamika et al., 2012; Coudreuse et al., 2010; Glover-Cutter et al., 2008; Gromak et al., 2006). The Pol II speed is affected by at least two factors. First, transcription pause sites downstream of the poly(A) site which decrease its processivity; second, PNUTS-PP1 mediated Spt5 dephosphorylation which also slows down the Pol II elongation rate. An allosteric change in Pol II, mediated by poly(A) site-dependent Spt5 dephosphorylation, slows down elongation, allowing Xrn2 to catch up with Pol II and dislodge it (Cortazar et al., 2019).

A subset of coding genes use an alternative of poly(A) site-dependent termination, for which an AU-rich sequence acts to mediate co-transcriptional cleavage (CoTC). It is again dependent on rapid 5'->3' degradation of the transcript for Pol II release (Nojima et al., 2013; White et al., 2013).

Pol II dissociation from the DNA template and CTD dephosphorylation marks the end of the transcription cycle. At certain genes, the terminating Pol II is recycled for subsequent rounds of transcription via DNA looping between promoter and termination regions. Gene looping occurs as a result of the physical interaction between initiation and termination factors. It is established in a TFIIB-dependent manner. Not only is TFIIB part of the PIC at promoter regions, but it also physically interacts with cleavage and polyadenylation factors at the 3'end of genes (O'Reilly & Greaves, 2007; Tan-Wong et al., 2008; Wang et al., 2010). Gene-looping contributes to transcriptional memory and stimulates re-initiation of transcription (Ansari & Hampsey, 2005; Tan-Wong et al., 2009). Furthermore, it represses pervasive antisense transcription by establishing promoter directionality and bringing in termination factors in promoter-proximal regions (Tan-Wong et al., 2012).

1.4 Co-transcriptional RNA processing

Pre-mRNA processing occurs concomitantly with transcription, reflecting the association of processing factors with the Pol II CTD at different stages during the transcription cycle (Hirose & Manley, 1998; Hirose et al., 1999; Rodriguez et al., 2000). The three major pre-mRNA processing events are 5' capping, intron splicing, 3' end cleavage and polyadenylation, all independently stimulated by the Pol II CTD (Fong & Bentley, 2001).

Capping

The 5' cap is added on the transcript immediately after it emerges from the Pol II exit channel (Jove & Manley, 1984; Rasmussen & Lis, 1993) and it functions to protect the nascent transcript from degradation by 5′->3′ exonucleases (Ramanathan et al., 2016) (Figure 8A).

Capping of the nascent RNA is a promoter-proximal event (Glover-Cutter et al., 2008; Jove & Manley, 1984) and correctly capped nascent RNA is a prerequisite for pause-release (Pei et al., 2003). Ser5P of the Pol II CTD is required for the recruitment of the capping enzyme and it promotes its activity (Cho et al., 1997; Ho & Shuman, 1999; Lu et al., 1991; McCracken et al., 1997; Rodriguez et al., 2000; Yue et al., 1997).

Apart from protecting the nascent RNA from exonucleases, the 5' cap is required for subsequent RNA processing events. The 5' cap promotes pre-mRNA splicing (Fresco & Buratowski, 1996; Inoue et al., 1989; Izaurralde et al., 1994; Konarska et al., 1984; Ohno et al., 1987; Pabis et al., 2013), 3' end processing and polyadenylation (Flaherty et al., 1997; Glover-Cutter et al., 2008; Narita et al., 2007; Topisirovic et al., 2011), intranuclear transport (Boulon et al., 2004) and nonsense-mediated decay (Hosoda et al., 2005). In addition, it is involved in RNA surveillance by the nuclear exosome (Andersen et al., 2013), nuclear export (Chen et al., 2006; Cheng et al., 2006; Jarmolowski et al., 1994) and efficient initiation of translation (K. M. Kim et al., 2009; Muthukrishnan et al., 1975; Shatkin & Manley, 2000).

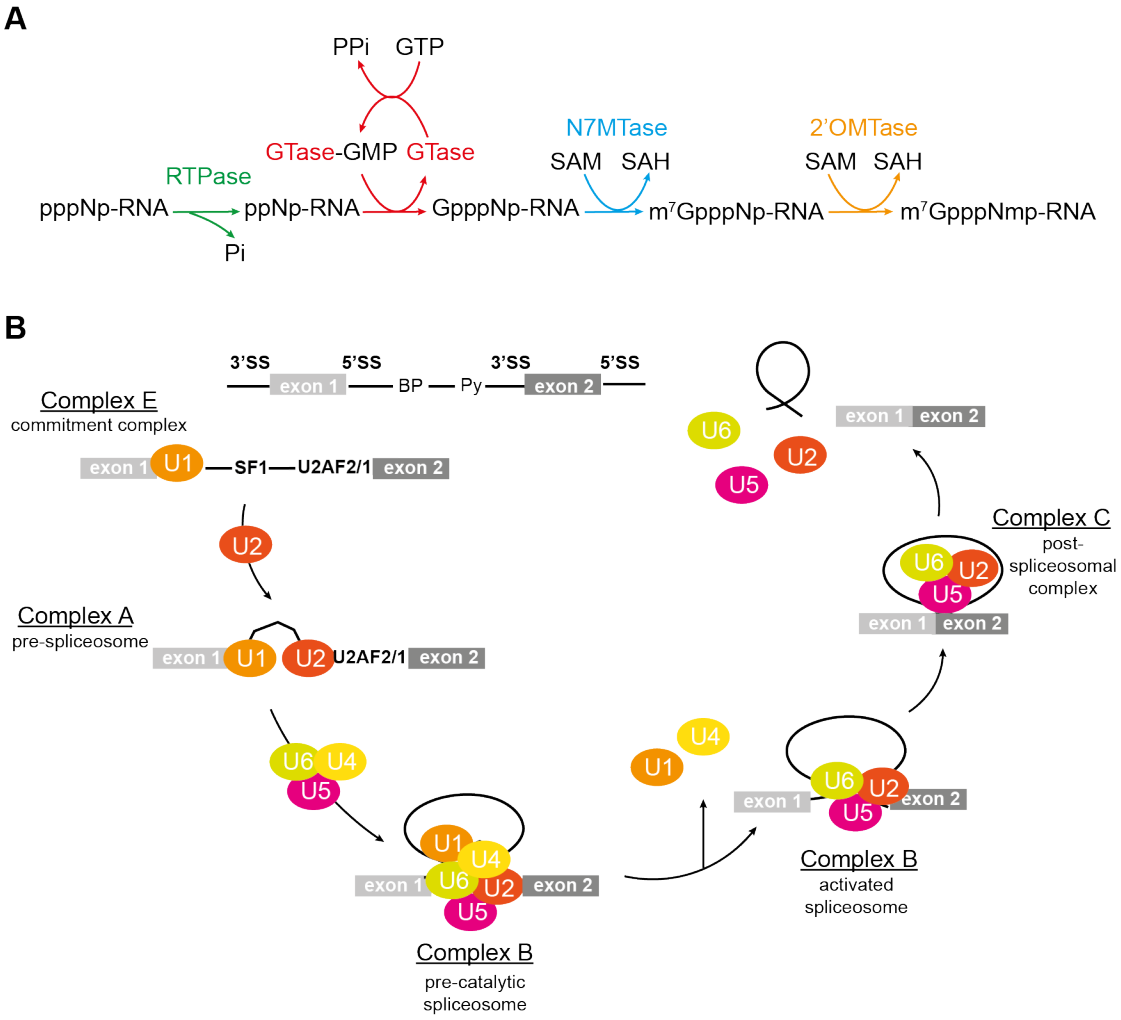

Figure 8 Pre-mRNA processing

(A) Pre-mRNA capping. RNA triphosphatase (RTPase) removes the γ-phosphate from the 5' end of the nascent RNA to generate 5' diphosphate and inorganic phosphate. The guanyltransferase (GTase) transfers a GMP from GTP to the 5' diphosphate through a lysine-GMP covalent intermediate. The guanine-N7 MTase (N7MTase) adds a methyl group N7 amine of the guanine cap. The m7G-specific 2'O methyltransferase (2'OMTase) methylates the ribonucleotide at the 2'O position of the ribose to generate the complete cap structure. (B) pre-mRNA splicing. Initially, the 5' splice site of the intron (5'SS) is bound by the U1 snRNP and the splicing factors SF1, U2AF2 and U2AF1 recognise the branch point sequence (BP), the polypyrimidine tract (Py) and the 3'end splice site (3'SS), respectively, to form the commitment complex (Complex E). Next, the U2 snRNP displaces SF1 and the pre-spliceosome is assembled (Complex A). Then, the U4/U5/U6 snRNP trimer is recruited to form the pre-catalytic spliceosome (Complex B). The activated spliceosome (Complex C) is formed after rearrangements that detach U1 and U4. U6 binds at the 5'SS and to U2 and U5 binds the intron. The 5' end of the intron is ligated to the BP, U5 binds at the 3'SS and the 5'SS is cleaved. The intron is excised and removed as a lariat RNA and the two exons are ligated. The lariat is degraded and the U2, U5, and U6 snRNPs are recycled for subsequent rounds of splicing.

Splicing

Most mammalian genes contain multiple introns and accurate splicing is critical for the assembly of the coding sequence in the mRNA. Splicing defects lead to exon skipping, intron retention or alternative splice forms of the transcript, all of which affect the functionality and stability of the mRNA.

The spliceosome is composed of five U snRNPs (U1, U2, U4, U5, and U6), each containing a small stable RNA bound by several RBPs (Figure 8B)(Herzel et al., 2017; Saldi et al., 2016). The majority of splicing is carried out co-transcriptionally during Pol II elongation (Alpert et al., 2017; Brugiolo et al., 2013; Khodor et al., 2011). Ser2 phosphorylation of the Pol II CTD is required for the recruitment of splicing factors to the nascent RNA and efficient splicing (Ahn et al., 2004; Gu et al., 2013; Ni et al., 2004). The spliceosome and the exon junction complex interact with the Ser2 kinase CDK12 (Bartkowiak et al., 2010; Eifler et al., 2015; Liang et al., 2015) and CDK12 inhibition leads to splicing defects (Chen et al., 2006; Chen et al., 2007; Greenleaf, 2019). Specifically, Ser2P is essential for the recruitment of U2 snRNA and U2AF2, while it is dispensable for the early spliceosome assembly, such as recruitment of U1 snRNA (Gu et al., 2013). Early spliceosome recruitment is dependent on Ser5P instead (Harlen et al., 2016).

In the same way that promoter-proximal pausing stimulates 5’ cap formation, transient pausing at intron-exon junctions contributes to recognition of splicing sites and improves splicing accuracy (Khodor et al., 2011; Kwak et al., 2013). Moreover, splicing factors SKIP (Brès et al., 2005), Npl3 (Dermody et al., 2008) and SRSF2 (Lin et al., 2008) have stimulatory effects on transcription elongation, while their depletion causes increased Pol II pausing within gene bodies and defective elongation (Lin et al., 2008).

3’ end processing

3’ end cleavage and polyadenylation of transcripts is necessary for successful transcription termination (Nojima et al., 2015) and regulates transcript stability, nuclear export and efficiency of translation (Colgan & Manley, 1997; Zhao et al., 1999).

In mammalian cells, pre-mRNA 3′ processing is carried out by cleavage and polyadenylation specificity factor (CPSF) and cleavage stimulation factor (CstF), which are involved in the recognition of the poly(A) site (PAS) on the pre-mRNA (Hirose & Manley, 2000), cleavage factors CF I and CF II, which have endonuclease activity (Mandel et al., 2006) and the poly(A) polymerase (PAP) (Colgan & Manley, 1997; Takagaki et al., 1989; Zhao et al., 1999). The 3' end processing machinery co-transcriptionally monitors nascent transcripts for specific sequences and, upon recognition of the PAS, endonucleolytic cleavage of the nascent mRNA 3' end followed by poly(A) tail synthesis takes place (Cho et al., 1999). The poly(A) tail serves to protect the mRNA from degradation and promotes translation after mRNA export (Colgan & Manley, 1997; Proudfoot, 1996).

3' end cleavage and polyadenylation factors are recruited in a Ser2P-dependent manner and directly interact with the Ser2 kinase CDK12 (Bartkowiak et al., 2010; Eifler et al., 2015; Liang et al., 2015). Lack of Ser2P impairs 3' cleavage (Gu et al., 2013) and polyadenylation (Ahn et al., 2004; Ni et al., 2004; Skaar & Greenleaf, 2002). Thus, Ser2P is required for efficient 3' end processing (Ahn et al., 2004; Barillà et al., 2001; Fong & Bentley, 2001; Gomes et al., 2006; Kim et al., 2010; Komarnitsky et al., 2000; Licatalosi et al., 2002). The efficiency of 3' end processing is further stimulated by appropriate co-transcriptional splicing (Licatalosi et al., 2002) and the two RNA processing events are coupled through interactions between CPSF and a component of the U2 snRNP (Kyburz et al., 2006).

Not all Pol II transcripts are polyadenylated and alternative processing mechanisms have been defined for histone and snRNA genes. Histone genes end with a 3' stem-loop sequence, which is recognized by stem-loop binding protein (SLBP) and U7 snRNP, and 3' end formation is mediated by a cleavage complex containing CPSF73, CPSF100, and Symplekin (Marzluff et al., 2008). At histone genes, Thr4P is involved in 3′ end processing and mutations in Thr4 inhibit recruitment of CPSF and cause failure to generate 3' ends (Hintermair et al., 2012; Hsin et al., 2011). At snRNA genes, 3′ end formation is dependent on the "3′ box", located just downstream of the snRNA-encoding region (Egloff et al., 2008). This sequence is

recognized, cleaved and processed by the Integrator complex, which is recruited in a Ser7P-dependent manner (Egloff et al., 2007; Egloff et al., 2010).

1.5 The nuclear exosome

Pol II can initiate transcription non-specifically and bidirectionally on nucleosome-depleted chromatin (Core & Lis, 2008; Preker et al., 2008; Seila et al., 2008). Such promiscuous transcription generates non-coding RNAs (ncRNAs). Some ncRNAs play a role in regulating transcription, for instance through recruiting regulatory factors to chromatin (Chu et al., 2015; McHugh et al., 2015), sequestering of transcriptional regulators (Holz-Schietinger et al., 2012; Sigova et al., 2015), transcriptional interference (Latos et al., 2012) and genome organization (Dowen et al., 2014; Kagey et al., 2010). However, the majority of ncRNAs are unstable and rapidly degraded by the nuclear exosome (Neil et al., 2009; Xu et al., 2009). These include transcription start site associated RNA (TSSa-RNA) (Seila et al., 2008; Valen et al., 2011), products of anti-sense transcription (Tan-Wong et al., 2012), enhancer RNAs (eRNAs) (Sigova et al., 2013) and promoter upstream transcripts (PROMPTs) (Flynn et al., 2011; Preker et al., 2011; Preker et al., 2008).

The nuclear exosome also functions in the processing of many stable RNAs, ribosomal RNA (rRNA), small nuclear RNAs (snRNAs), and small nucleolar RNAs (snoRNAs), as well as rapidly degrading mis-spliced pre-mRNAs (Bousquet-Antonelli et al., 2000) and pre-mRNAs with aberrant poly(A) tails (Hilleren et al., 2001). The factors that determine the fate of the transcript and how the exosome recognizes its substrates remain poorly understood.

Core nuclear exosome

The RNA exosome is an evolutionary conserved RNA degradation complex composed of a catalytically inactive barrel-shaped core of nine subunits: CsL4, Rrp4, Rrp40, Rrp41, Rrp46, Mtr3, Rrp42, Rrp43 and Rrp45 (Exosc1-9) (Anderson et al., 2006; Greimann & Lima, 2008; Kilchert et al., 2016). The catalytic activity of the exosome is achieved through its association with non-core subunits Rrp6 (Exosc10), which is an exonuclease localized mainly in the nucleolus (Chlebowski et al., 2010; Mitchell et al., 1997; Schneider et al., 2009; Tomecki et al., 2010), or

Dis3 family proteins. Both Dis3L and Dis3L2 are cytoplasmic exonucleases (Lubas et al., 2013; Staals et al., 2010; Tomecki et al., 2010), while Dis3 is exclusively nuclear, with nucleolar exclusion, and possesses both exo- and endonuclease activity (Greimann & Lima, 2008; Lebreton et al., 2008; Schaeffer et al., 2009).

Exosome adapter complexes

The nuclear exosome associates with a variety of co-factors to achieve its function, among which the Mtr4 ATP-dependent RNA helicase. Mtr4 is essential for exosomal degradation *in vivo*. It is involved in the unwinding of the RNA substrate and mediating its access to the core exosome (Gerlach et al., 2018; Johnson & Jackson, 2013; Schneider & Tollervey, 2014; Weick et al., 2018). Mtr4 is negatively regulated by NRDE2, which binds to Mtr4, inhibits its recruitment to RNA and prevents its interaction with Rrp6 and Dis3 (J. Wang et al., 2019).

In mammalian cells, three nuclear exosome adapter complexes have been characterized and Mtr4 is part of all of them (Figure 9)(Ogami et al., 2018). In the nucleoli, Mtr4 associates with the RNA binding protein Zcchc7 (Air1/2 in yeast) and the poly(A) polymerase Papd5 (Trf4/5 in yeast), forming the TRAMP complex (Trf4/Air2/Mtr4p Polyadenylation complex). It is required for the 3' end processing and decay of rRNA via the addition of an unstructured oligo(A) tail at 3' ends of its RNA substrates (LaCava et al., 2005; Lubas et al., 2011; Shcherbik et al., 2010; Vanácová et al., 2005; Wyers et al., 2005). In the nucleoplasm, the PAXT (poly(A) exosome targeting) and NEXT (nuclear exosome targeting) complexes are found. In the PAXT complex, Zfc3h1 protein mediates the interaction between Mtr4 and the poly(A)-binding protein Pabpn1. While PAXT substrates are mature, polyadenylated RNAs (Giacometti et al., 2017; Meola et al., 2016; Silla et al., 2018), the NEXT complex is involved in the degradation of newly synthesised, unstable transcripts. Its substrates include PROMPTs, eRNAs and lincRNAs, as well as aberrantly processed snRNA, snoRNA and histone RNA (Giacometti et al., 2017; Lubas et al., 2015; Lubas et al., 2011). In the NEXT complex, the adapter protein Zcchc8 mediates the interaction between Mtr4 and the RNA binding protein Rmb7 (Falk et al., 2016; Lubas et al., 2011). It is recruited to RNA via the cap-

binding complex (CBC) in association with Ars2 and Zc3h18 co-factors (Andersen et al., 2013; Hallais et al., 2013; Lubas et al., 2015).

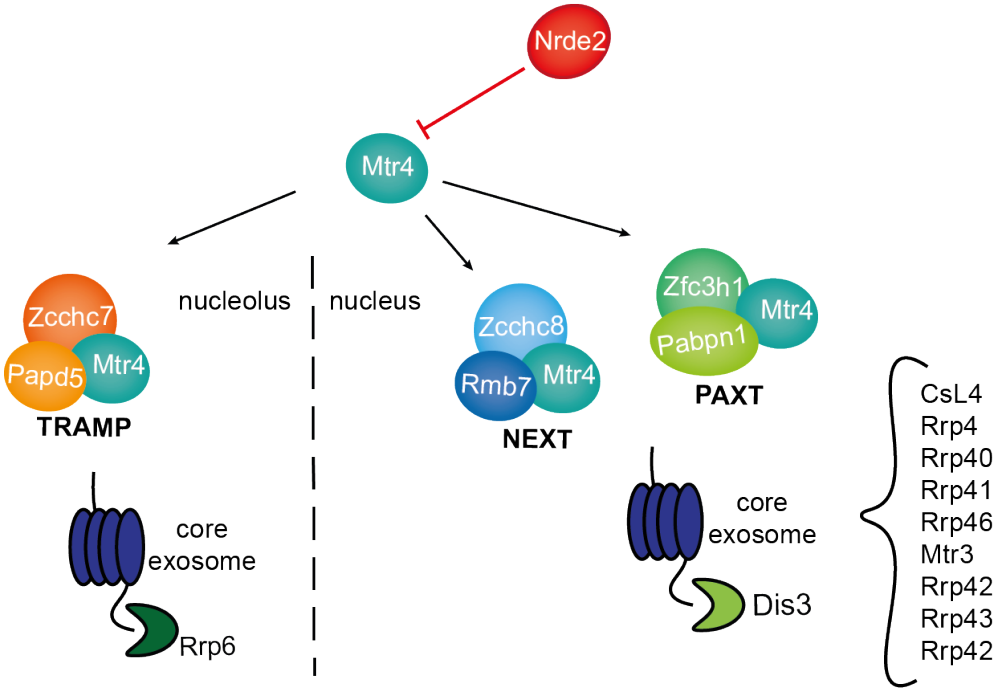

Figure 9 Exosome adapter complexes

The RNA helicase Mtr4 is part of all three nuclear exosome adapter complexes. The TRAMP complex, which is restricted to the nucleolus, consists of the RNA binding protein Papd5, the adapter protein Zcchc7 and Mtr4. Both the NEXT and the PAXT complexes are nuclear. In the NEXT complex, Mtr4 interacts with the RNA binding protein Rmb7 and the adapter protein Zcchc8. The PAXT complex is composed of the RNA binding protein Pabpn1, the adapter protein Zfc3h1 and Mtr4. Mtr4 directly interacts with the exosome and it is responsible for threading the RNA through the core exosome to its catalytic subunit Rrp6 (Exosc10) in the nucleolus or Dis3 in the nucleus. Mtr4 activity is inhibited by Nrde2, which binds to Mtr4 and prevents its association with RNA and the exosome.

The role of the CBC in exosome recruitment

The 5' cap of the nascent RNA is bound by nuclear cap-binding proteins Ncbp1 and Ncbp2, which form the CBC (Izaurralde et al., 1994). In addition to protecting the nascent transcript from de-capping and subsequent 5'->3' degradation, distinct CBC-containing complexes target RNAs either for export into the cytoplasm or for exosomal degradation. The CBC interacts with the Ars2 adapter protein, forming the CBCA complex (Giacometti et al., 2017; Gruber et al., 2009; Schulze et al., 2018). Subsequently, the CBCA forms higher order complexes with distinct RNA processing factors (Figure 10) (Schulze et al., 2018). The competition between RNA export factors and the exosome co-factors is important for the sorting of RNAs into the export or degradation pathways (Fan et al., 2017; Giacometti et al., 2017; Silla et al., 2018).

Ars2-dependent recruitment of the DROSHA complex targets RNAs to the miRNA processing pathway (Gruber et al., 2009; O'Sullivan et al., 2015), whereas at snRNA and snoRNA, CBCA recruits the PHAX complex. PHAX is involved in 3' end processing and export of the RNA through mediating the interaction between the CBC and the Crm1 nuclear export receptor (Boulon et al., 2004; Hallais et al., 2013; Ohno et al., 2000). Similarly, Ars2 mediates binding of the FLASH complex to CBC, which is involved in 3' end processing and export of histone mRNAs (Kiriyama et al., 2009; Yang et al., 2009), while the exosome adapter complexes NEXT and PAXT are recruited to their target RNAs through Zc3h18 bound CBCA complex (Andersen et al., 2013; Falk et al., 2016; Hrossova et al., 2015; Meola et al., 2016).

The mRNA nuclear export complex (TREX), PHAX and Zc3h18 compete for binding to the CBCA complex. Furthermore, Mtr4-containing complexes TRAMP, PAXT and NEXT interact with Zfc3h18 in a mutually exclusive manner (Fan et al., 2017; Giacometti et al., 2017; Meola et al., 2016; Schulze et al., 2018; Strässer & Hurt, 2000). Such differential recruitment of distinct RNA processing complexes at the 5' cap of the nascent transcript is thought to provide specificity and play an important role in determining the fate of the transcript. However, the mechanism

through which the RNA substrate is recognized by these RNA processing complexes is not well understood.

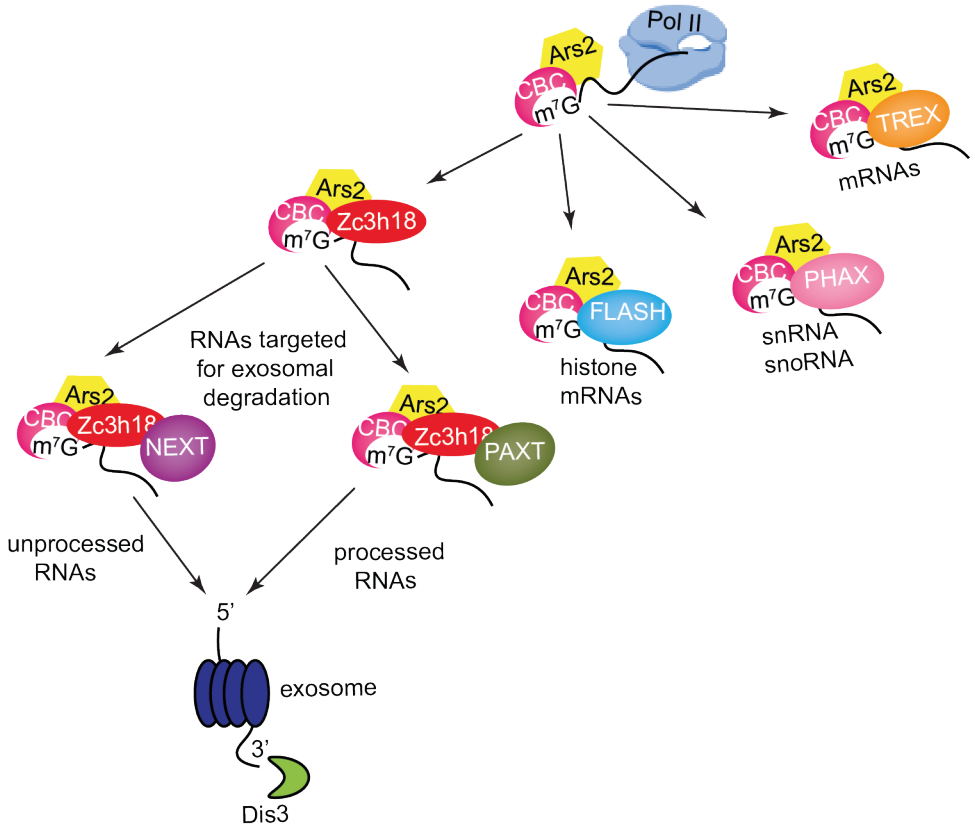

Figure 10 Mutually exclusive CBCA containing complexes. The m7G cap of the nascent RNA is bound by the cap binding complex (CBC). The CBC interacts with the Ars2 protein to form the CBCA complex through which additional co-factors are recruited. For mRNAs, the CBCA recruits TREX which mediates nuclear export. At snRNAs/snoRNAs and histone mRNAs, the CBCA recruits the PHAX and FLASH RNA processing complexes, respectively. RNAs are targeted for exosomal degradation through recruitment of Zc3h18 to the CBCA complex. Through Zc3h18, the PAXT and the NEXT exosome adapter complexes are recruited which then thread the RNA through the exosome to facilitate its degradation by the Dis3 catalytic subunit of the nuclear exosome. While the NEXT complex associates with nascent, unprocessed RNAs, the PAXT complex binds to processed, polyadenylated RNAs.

Chapter 2. Materials & Methods

2.1 Cell culture and growth curves

NIH3T3 and MEF cell lines were cultured in DMEM (Dulbecco's Modified Eagle Medium, 41966-029, Sigma) supplemented with 10% FBS (Fetal Bovine Serum, 10270106, Thermo Fisher Scientific) and penicillin-streptomycin (P4333, Sigma) at 37^0C 10% CO_2. Phoenix cells were grown at 37^0C 5% CO_2. Cells were passaged every 3rd day. Growth medium was aspirated, plates were washed with PBS (phosphate-buffered saline) and incubated in trypsin EDTA (R001100, Thermo Fisher Scientific) in a tissue culture incubator for 3 min. Trypsin was inactivated by addition of growth medium, cells were spun down at 300g for 5 min, resuspended in growth medium and plated in tissue culture dishes, as needed. For growth curves, cells were counted using Neubauer cell counting chamber.

2.2 Drug treatments

For antibiotic selection, zeocin (ant-zn-1, InvivoGen) was used at 100 µg/ml; blasticidin (ant-bl-1, InvivoGen) at 3 µg/ml; hygromycin (10687-010, Thermo Fisher Scientific) at 100 µg/ml. Tamoxifen (H6278, Sigma) was used at a final concentration of 1µM. Doxycycline (D9891, Sigma) was used at 2 µg/ml. For serum shock, cells were starved overnight in DMEM supplemented with 0.3% FBS and subsequently stimulated with 15% FBS for 30 minutes. Cells were treated with CD (Cytochalasin D, 250255, Merck) at 3µM for 30 min; LMB (Leptomycin B, 9676, Cell Signalling) at 50nM for 30 min (*Note on LMB: LMB was diluted 1/500 in EtOH in a glass vial before adding to the growth media); LatB (Latrunculin B, 428020, VWR International) at 0.5µM for 30 min; TPA (12-o-tetradecanoylphorbol-13-acetate, P8139 , Sigma) was used at 50 ng/ml; FP (Flavopiridol, 10009197, Cambridge Bioscience) at 0.5µM for 1h; THZ1 (A8882, Generon) at 0.5µM for 1h; THZ531 (HY-103618, Generon) at 1µM for 1h; GW843682X (G2171, Sigma) at 10µM for 1h.

2.3 Immunofluorescence

Cells, seeded on glass coverslips and treated as indicated in the figures, were fixed with 4% paraformaldehyde (199431LT, VWR International) for 10 min at room temperature, washed twice in PBS (phosphate-buffered saline), permeabilized in 0.2% Triton X-100 (X100-100ML, Sigma) for 20 min at room temperature and incubated in blocking solution (10% FBS, 0.5% fish skin gelatine (G7765, Sigma) in PBS) for 1h at room temperature. Coverslips were then incubated with primary antibody for 1h at room temperature in blocking solution, washed three times in 0.1% Triton X-100 and incubated with secondary antibody and DAPI stain (4′,6-diamidino-2-phenylindole, D9542, Sigma) for 1h at room temperature in blocking buffer. Following three washes with 0.1% Triton X-100, three washes with PBS and one wash with dH_20, coverslips were mounted on glass slides using Mowiol medium (475904, Calbiochem). Imaging was done using Leica SP8 confocal microscope. Images were processed using ImageJ.

2.4 siRNA and transient transfection

Cells were transfected with siRNA oligonucleotides using Lipofectamine RNAiMAX transfection reagent (13778-150, Invitrogen), according to the manufacturer's instructions. Cells were diluted in DMEM, supplemented with 10% FBS, so that they reach confluence 48h post-seeding. siRNA duplex to a final concentration of 10 nM and lipofectamine RNAiMAX reagent were mixed in OptiMEM (31985-047, Sigma), incubated for 30 min at room temperature and added to the cell suspension. Cells were then plated and efficiency of the knock-down was assessed by Western blot or qPCR 48h post-transfection.

For transient transfection, cells were seeded at 25% confluence in 10 cm dishes in DMEM, supplemented with 10% FBS. The following day, 3 µg plasmid DNA and 1:200 Fugene transfection reagent (E2311, Promega) were mixed in OptiMEM, incubated at room temperature for 30 min, added directly to the cell medium and incubated overnight at 37^0C 10% CO_2.

2.5 Cell fractionation

Cells were trypsinized and spun down at 300g for 5 min. Cell pellets were resuspended in 2PCV of hypotonic buffer (10 mM HEPES-KOH pH 7.5, 10 mM KCl, 1.5 mM $MgCl_2$, protease inhibitors (11873580001, Roche), phosphatase inhibitors (A32961, Thermo Fisher Scientific) and incubated on ice for 20 min to achieve cell swelling. Cells were lysed by pipetting up and down 20 times. Nuclei were pelleted by centrifugation at 3000g for 15 min at 4^0C. The cytoplasmic fraction in the supernatant was removed and pelleted nuclei were washed twice in hypotonic buffer and then resuspended in 2PCV nucleoplasmic extraction buffer (20 mM HEPES-KOH pH 7.5, 1.5 mM $MgCl_2$, 10% glycerol, 150 mM potassium acetate, 0.05% NP-40, protease inhibitors (11873580001, Roche), phosphatase inhibitors (A32961, Thermo Fisher Scientific)) and incubated for 20 min at 4^0C shaking. Nucleoplasm (supernatant) was recovered through centrifugation at 20000g for 20 min 4^0C and EDTA to 1 mM was added. Pellets were resuspended in 1PCV chromatin digestion buffer (20 mM HEPES-KOH pH 7.5, 1.5 mM $MgCl_2$, 10% glycerol, 150 mM NaCl, 0.05% NP-40, protease inhibitors (11873580001, Roche), phosphatase inhibitors (A32961, Thermo Fisher Scientific)), 125 units/ml benzonase (70664-3, Merck) was added and samples were incubated for 30 min on ice. Low salt chromatin was recovered through centrifugation at 20000g for 20 min at 4^0C and EDTA to 3 mM was added. Pellets were resuspended in 1PCV of 500 mM NaCl buffer (20 mM HEPES-KOH pH 7.5, 3 mM EDTA, 1.5 mM $MgCl_2$, 10% glycerol, 500 mM NaCl, 0.05% NP-40, protease inhibitors (11873580001, Roche), phosphatase inhibitors (A32961, Thermo Fisher Scientific)) and incubated for 30 min on ice. 2.3V of salt dilution buffer (20 mM HEPES-KOH pH 7.5, 3 mM EDTA, 1.5 mM $MgCl_2$, 10% glycerol, 0.05% NP-40, protease inhibitors (11873580001, Roche), phosphatase inhibitors (A32961, Thermo Fisher Scientific)) was added and samples were cleared by centrifugation at 20000g for 20 min. Low and high salt chromatin fractions were pooled and used for Western blot analysis.

2.6 Western blot

Cells were trypsinized and spun down at 300g for 5 min. Cell pellets were resuspended and lysed in RIPA buffer (1% Nonidet P-40, 1% Na deoxycholate,

0.1% SDS, 150 mM NaCl, 0.01 M sodium phosphate pH 7.2, 2 mM EDTA, protease inhibitor (11873580001, Roche)) for 1h at 4^0C shaking and lysates were then pre-cleared by centrifugation at 12000g for 10min. Protein concentration was measured using Bradford reagent (500-0006, Biorad). 10-20 µg total protein was used for blotting. Lysates were mixed with laemmli buffer (2% SDS, 10% glycerol, 60 mM Tris-HCl pH 6.8, 0.02% bromophenol blue) and incubated at 100^0C for 10 min, prior to loading on a 4-12% Bis Tris protein gel (NP0323BOX, Life Technologies). Gels were run at 180V for 1h in MOPS buffer (NP0001, Life Technologies), transferred using wet transfer to a nitrocellulose membrane (10600003, VWR International) at 300mA for 1.5h in transfer buffer (25 mM Tris-HCl, 192 mM Glycine, 10% Methanol). Membranes were blocked in 5% semi-skimmed milk in PBST (0.1% Tween-20 in PBS) for 1h at room temperature and then incubated with primary antibody in blocking buffer overnight at 4^0C. The following day, membranes were washed three times in PBST (0.1% Tween-20 in PBS), incubated with secondary-HRP conjugated antibody for 1h at room temperature in blocking buffer, washed three times with PBST and signal was visualized using ECL reagent (RPN2106, VWR International) on a film (28906837, VWR International). SeeBlue pre-stained protein standard (LC5925, Thermo Fisher Scientific) was used as reference.

2.7 Contractility assay

50 000 cells were embedded in collagen I/Matrigel mixture (20mM Hepes pH 7.5, 0.4% $NaHCO_3$, 4.6 mg/ml collagen (354249, Thermo Fisher Scientific), 2.2 mg/ml Matrigel (354234, Thermo Fisher Scientific), 10% FCS in DMEM) and seeded on a 24 well glass-bottom MatTek dish (P24G-1.5-13-F, MatTek). Gels were left to set for 30 min in a tissue culture incubator, after which tissue culture medium was added. Original gel size, as seen at 3h post-seeding, was compared to gel size 48h post-seeding. Gel sizes were obtained using ImageJ software and gel contraction values represent percentage of the original gel size.

2.8 RNA extraction, cDNA synthesis and qPCR

Total RNA was purified using Genelute mammalian total RNA extraction kit (RTN350-1KT, Sigma), according to the manufacturer's instructions. 200 ng RNA

was used for cDNA synthesis, performed using Transcriptor First Strand cDNA Synthesis Kit (04897030001, Roche). Samples were treated with 1 U DNase I (AM2224, Ambion) in 1X DNase I buffer (AM8170G, Ambion) for 15 min at 37^0C. DNase I was inactivated with 5mM EDTA at 72^0C for 10 min. Random hexamer primers (60µM) were annealed at 65^0C for 10 min. Finally, the reverse transcription reaction was carried out as follows: 10 units reverse transcriptase, 1mM dNTPs, 20 units protector RNase inhibitor and 8mM $MgCl_2$ were added to the samples in a total volume of 20 ul and the samples were incubated at 25^0C for 10 min, 55^0C for 30 min, followed by inactivation of the reverse transcriptase at 85^0C for 5 min. cDNA was diluted 10 times in TE buffer (10 mM Tris-HCl pH 8, 1 mM EDTA) and qPCR reactions were set up as follows: 2 µl cDNA, 0.2 µM primer mix (10µM of each primer) and 5 µl PowerUp SYBR Green Master Mix (A25742, Life Technologies) in a total volume of 10 µl. Initial denaturation was carried out at 95^0C for 10 min, followed by 40 cycles of denaturation at 95^0C for 10 sec and annealing, extension and read fluorescence at 60^0C for 25 sec. qPCRs were done using QuantStudio 3 Real-Time PCR system. Standard curve was generated using genomic DNA or cDNA dilutions. Samples were normalized to *Gapdh*.

2.9 Chromatin Immunoprecipitation (ChIP)

The ChIP protocol was adapted from (Schmidt et al., 2009). Cells were fixed in 1% formaldehyde (F/1501/PB17, Thermo Fisher Scientific) in PBS at room temperature. After 10 min, the reaction was quenched using 0.25 M Glycine, cells were washed twice with PBS, scraped in ice-cold PBS, supplemented with protease inhibitor (5056489001, Roche), pelleted at 2000g for 5 min and frozen at -80^0C. Cell pellets were defrosted, resuspended and lysed in 7ml LB1 buffer (50 mM Hepes-KOH, pH 7.5; 140 mM NaCl; 1mM EDTA; 10% Glycerol; 0.5% NP-40 or Igepal CA-630; 0.25% Triton X-100, protease inhibitor (11873580001, Roche)) for 15 min at 4^0C with rotation and pelleted at 2000g for 5min. Cell pellets were resuspended in 7ml LB2 buffer (10 mM Tris-HCL, pH8.0; 200 mM NaCl; 1 mM EDTA; 0.5 mM EGTA, protease inhibitor (11873580001, Roche)), pelleted by centrifugation at 2000g for 5 min and resuspended in 300 µl LB3 buffer (10 mM Tris-HCl, pH 8; 100 mM NaCl; 1 mM EDTA; 0.5 mM EGTA; 0.1% Na-Deoxycholate; 0.5% N-lauroylsarcosine, protease inhibitor (11873580001, Roche)).

Shearing of chromatin was performed using Bioruptor sonicator (Diagenode). For NIH3T3 and MEF cells, $20x10^6$ cells were sonicated for 10 min (30" ON/30" OFF) at high energy, for MDA-MB-231 $20x10^6$ cells were sonicated for 8 min at high energy. 1:5 input sample was reverse-crosslinked in FA/SDS-like buffer (50 mM Hepes KOH pH 7.5, 150 mM NaCl, 1% Triton X-100, 0.1% Na deoxycholate) and 20 µg proteinase K (19133, Qiagen) overnight at 65^0C. Chromatin was pre-cleared with 25ul dynabeads (10009D, Thermo Fisher Scientific), previously blocked in 0.1% BSA (bovine serum albumin), for 1h at 4^0C. 50 µl dynabeads were coupled to 10 µg antibody for 1h at 4^0C in 0.1% BSA. Pre-cleared chromatin and antibody-coupled dynabeads were incubated overnight at 4^0C shaking. The following day, the IPs were washed 5 times with RIPA buffer (50 mM Hepes-KOH, pH 7.5; 500 mM LiCl; 1mM EDTA; 1% NP-40 or Igepal CA-630; 0.7% Na-Deoxycholate) and once with TBS (20 mM Tris-HCl, pH 7.6; 150 mM NaCl) on a magnetic rack and chromatin was eluted in 130µl elution buffer (25 mM Tris-HCl pH 7.5, 5 mM EDTA, 0.5% SDS) at 65^0C for 30 min. For reverse-crosslinking, the elution was incubated with 20 µg proteinase K at 65^0C overnight. The DNA was extracted using PCR purification kit (28106, Qiagen). Efficiency of sonication was evaluated on a 2% agarose gel, stained with ethidium bromide, and integrity of the target protein was checked by Western blot. Samples were used for qPCR, as described above, and normalized to input.

2.10 TT_{chem}-seq

TT_{chem}- seq was performed as described in (Gregersen et al., 2020). Nascent RNA was pulse-labelled with 4-thiouridine (4SU). 1mM 4SU (GN6085, Glentham Life Sciences) was added directly to the tissue culture medium for 15 min, after which cells were lysed in 1ml TRIzol (15596018, Thermo Fisher Scientific). 200 ul chloroform (43685, Thermo Fisher Scientific) was added, samples were mixed and spun down at 12000g for 15 min at 4^0C. The aqueous phase was combined with an equal volume of chloroform/isoamyl alcohol (24:1) (C0549, Sigma-Aldrich), mixed and spun down at 12000g for 10 min at 4^0C. 1.1 volume of isopropanol (P/7500/PC17, Thermo Fisher Scientific) was added to the aqueous phase. Samples were mixed, incubated for 20 min at room temperature and spun down at 12000g for 30 min. RNA pellets were washed with 80% ethanol, air-dried and

resuspended in 50-100 µl RNase-free water. RNA concentration was measured using Qubit RNA BR Assay Kit (Q10210, Thermo Fisher Scientific) and RNA integrity was checked on a 2100 Bioanalyzer, using an Agilent RNA 6000 Nano Kit (5067-1511, Agilent), according to the manufacturer's instruction.

A 50 ml mid-log phase *S. cerevisiae* BY4741 culture in YPD medium supplemented with 2% glucose was labelled with 5mM 4TU (4-thiouracil, 440736, Sigma) for 5 min at 30^0C. Cells were spun down at 5000g for 5 min. Pellets were resuspended in 1 ml TES buffer (10 mM Tris HCl pH 7.5, 10 mM EDTA, 0.5% SDS). 1 ml acid phenol (AM9720, Thermo Fisher Scientific) was added, samples were incubated at 65^0C for 45 min at 1400rpm shaking and spun down at 12000g for 10 min at 4^0C. The aqueous phase was mixed with 1 ml 100% ethanol and 3M NaAc and incubated overnight at 4^0C. Samples were then spun down at 12000g for 30 min, RNA pellets were washed with 80% ethanol, air-dried and resuspended in RNase-free water. RNA concentration was measured using Qubit RNA BR Assay Kit.

For each sample, 100 µg of 4SU-labeled mammalian RNA and 1 µg of *S. cerevisiae* 4TU-labeled RNA were mixed in a total volume of 100 µl. To fragment the RNA, 160mM NaOH was used for 20 min on ice. The reaction was quenched with 400mM Tris pH 6.8 and the fragmented RNA was purified using Micro Bio-Gel spin columns (732-6223, Biorad), according to manufacturer's instructions. To biotinylate the fragmented RNA, 3 µl biotin buffer (833 mM Tris-HCl, pH 7.4, and 83.3 mM EDTA) and 5 ug MTSEA biotin-XX linker (BT90066, Biotium) was added to the 200 µl RNA. Samples were mixed and incubated at room temperature for 30 min, protected from light. Excess free biotin was removed by mixing the samples with an equal volume of phenol/chloroform/isoamyl alcohol (15593031, Thermo Fisher Scientific), centrifugation at 12000g for 10 min and precipitation of the RNA in the aqueous phase with isopropanol. RNA pellets were reconstituted in 50 µl RNase-free water.

Efficiency of 4SU and 4TU incorporation was assessed by dot blot. 10 µg of mammalian RNA or 1 µg of yeast RNA was spotted on a Hybond-N membrane (RPN203N, GE Healthcare). The membrane was UV-crosslinked at 0.2 J/cm2 (254 nm) in a Stratalinker, blocked in blocking buffer (10% SDS, 1 mM EDTA in PBS) for

30 min at room temperature and probed with 1/50000 of 1 mg/ml HRP-conjugated streptavidin (N100, Thermo Fisher Scientific) in blocking buffer for 30 min at room temperature. The membrane was then washed three times in wash buffer 1 (1% SDS in PBS) and three times in wash buffer 2 (0.1% SDS in PBS), with each wash lasting 10 min at room temperature. The signal of the biotin-bound HRP-conjugated streptavidin was visualized using ECL reagent (RPN2106, VWR International) on film (28906837, VWR International).

In order to purify the biotinylated RNA, the RNA was denatured at 65^0C for 10 min and incubated with 200 µl µMACS streptavidin MicroBeads (130-074-101, Miltenyi) on a rotating wheel for 30 min at room temperature. Samples were placed on a µMACS magnetic separator, washed twice with pull-out wash buffer (100 mM Tris-HCl pH 7.4, 10 mM EDTA, 1 M NaCl and 0.1% Tween 20), pre-warmed at 55^0C, and eluted in 200 µl 100 mM DTT. Nascent RNA was purified using RNeasy MinElute Cleanup Kit (74204, Qiagen). RNA concentration was measured using Qubit RNA Assay Kit and the size of the purified 4SU-RNA on a Bioanalyzer, using Agilent RNA 6000 Pico Kit, according to the manufacturer's instructions.

2.11 Library preparation and sequencing

For TT_{chem}- seq, 100 ng of 4SU RNA was used to prepare libraries for sequencing using KAPA RNA HyperPrep Kit (08098107702, Roche) together with the KAPA Dual-Indexed Adapter Kit (08278555702, Roche), according to manufacturer's instructions. Samples were sequenced in single-end mode at 50 million reads per sample on a HiSeq platform.

ChIP-seq libraries were prepared from 1 ng ChIP sample using NEBNext Ultra II DNA Library Prep Kit for Illumina (E7645L), according to manufacturer's instructions. Samples were sequenced in single-end mode at 25 million reads per sample on a HiSeq platform.

cDNA libraries for RNA-seq were prepared from 100 ng total RNA, extracted with Genelute mammalian total RNA extraction kit (RTN350-1KT, Sigma), using KAPA RNA HyperPrep Kit with RiboErase (Roche). Samples were sequenced in single-

end mode at 30 million reads per sample on a HiSeq platform. Sequencing was performed by the Sequencing STP.

2.12 Data analysis

RNAseq and TTseq

RNAseq and TTseq data analysis was performed by Francesco Gualdrini. For QC and reproducibility of RNAseq biological replicates in NIH3T3 cells see Figure 11 and Figure 12. For QC and reproducibility of RNAseq biological replicates in dKO^{MRTF} and $dKO^{MRTF\text{-}NLS}$ cells see Figure 15 and Figure 16. One replicate of untreated and LatB-treated sample in dKO^{MRTF} , $dKO^{MRTF\text{-}NLS}$ and Mtr4-depleted $dKO^{MRTF\text{-}NLS}$ cells was excluded due to possible sample swap. For QC and reproducibility of TTseq biological replicates in NIH3T3 cells see Figure 13 and Figure 14. For QC and reproducibility of RNAseq biological replicates in dKO^{MRTF} and $dKO^{MRTF\text{-}NLS}$ cells see Figure 17 and Figure 18. One replicate of untreated and LatB-treated sample in $dKO^{MRTF\text{-}NLS}$ cells and one replicate of CD-treated sample in $dKO^{MRTF\text{-}NLS}$ cells was excluded from the analysis. Adapter and quality trimming of RNAseq and TTseq reads was performed with Trim Galore. rRNA removal was done using SortMeRNA. RNAseq reads were aligned to the mm10 mouse genome using STAR (default settings). Reads were counted into transcript gene features using functions part of the GRanges library (Bioconductor) in R using the summarizeOverlaps function. For RNAseq, reads strictly falling within exons were defined as exonic reads per gene/transcript and reads containing intronic features were defined as intronic reads per gene/transcript. Normalization was done against a set of invariant genes across samples, assuming a quasi-normal distribution of gene read counts, as described in (Gualdrini et al., 2016). Frequency distribution of invariant genes across conditions follow a log-normal distribution. Gene counts falling within one standard deviation of the theoretical log-normal were considered to scale samples. Differential gene expression analysis was performed with Deseq2 (comparing each condition to untreated cells; adjusted p value (padj) ≤ 0.01; minimum fold change of 1). Volcano plots were generated using Prism by plotting $\log_2$(fold change) vs $\log_{10}$(padj value). Venn diagrams were plotted in

Illustrator. Linear regression analyses and Spearman's rank order correlation analyses of log_2(fold change) expression between conditions were performed using Prism. Slope, 95% confidence lines and Spearman's correlation coefficient (r) are shown in figures. TTseq read coverage profiles genome alignment BAM files were merged across biological replicates and visualized using Integrative Genomic Viewer (IGV). Heatmaps and violin plots were generated in Prism. Z-scores were calculated using the formula $z = (x-\mu)/\sigma$, where x is the raw value, μ is the population mean, and σ is the population standard deviation. For plots showing distance to SRF binding site, previously published SRF binding coordinates as assessed by ChIPseq in NIH3T3 cells in response to stimulation were used (Esnault et al., 2014). Genes were separated into associated with direct SRF binding (their TSS is found within 5kb of the nearest SRF binding site), near (their TSS is found between 5kb and 70kb of the nearest SRF binding site) and far (their TSS is found beyond 70kb of the nearest SRF binding site). In figures genes associated with direct, near and far SRF binding are shown as % of genes identified in the analysis. For plots showing FCS-inducible LatB-sensitive genes, previously published RNAseq dataset in NIH3T3 cells was used (Esnault et al., 2014). In figures FCS-inducible LatB-sensitive genes are shown as % of genes identified in the analysis. Gene ontology analysis and transcription factor binding motif search were performed using the Molecular Signatures Database (MSigDB) (Liberzon et al., 2011; Subramanian et al., 2005).

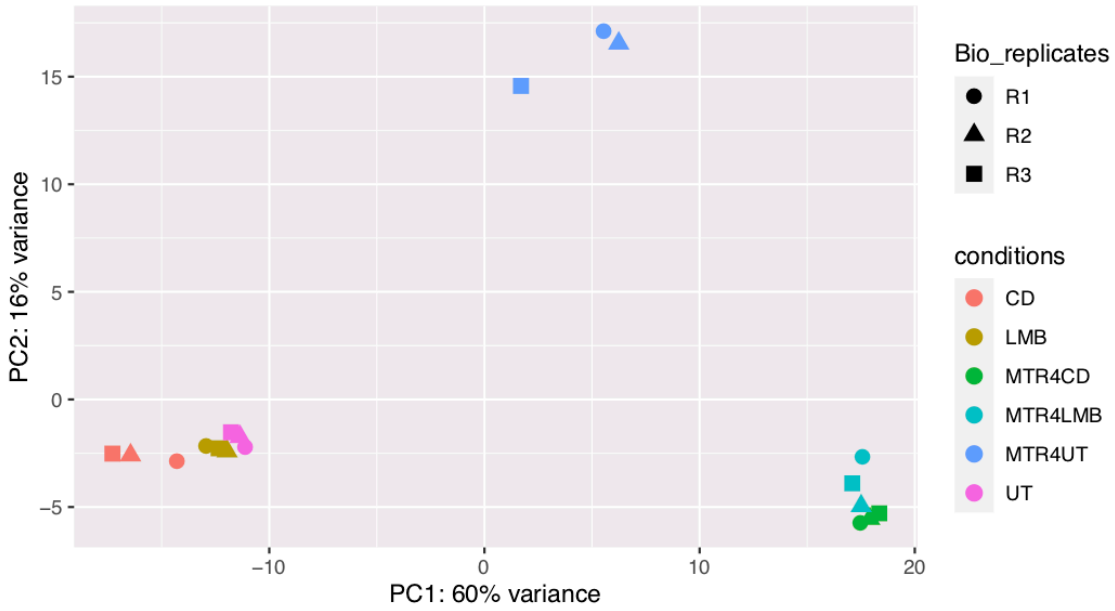

Figure 11 Principal component analysis (PCA) of RNAseq samples in NIH3T3 cells

Shown is the clustering of three biological replicates (R1, R2, R3) for individual treatments. CD (3μM Cytochalasin D, 30 min); LMB (50nM Leptomycin B, 30 min); UT (untreated); MTR4CD (siMtr4 for 48h, 3μM Cytochalasin D for 30 min); MTR4LMB (siMtr4 for 48h, Leptomycin B for 30 min); MTR4UT (siMtr4 for 48h). Samples clustering closely have similar gene expression profiles, whereas distant samples show distinct expression profiles. RNAseq data analysis was performed by Francesco Gualdrini.

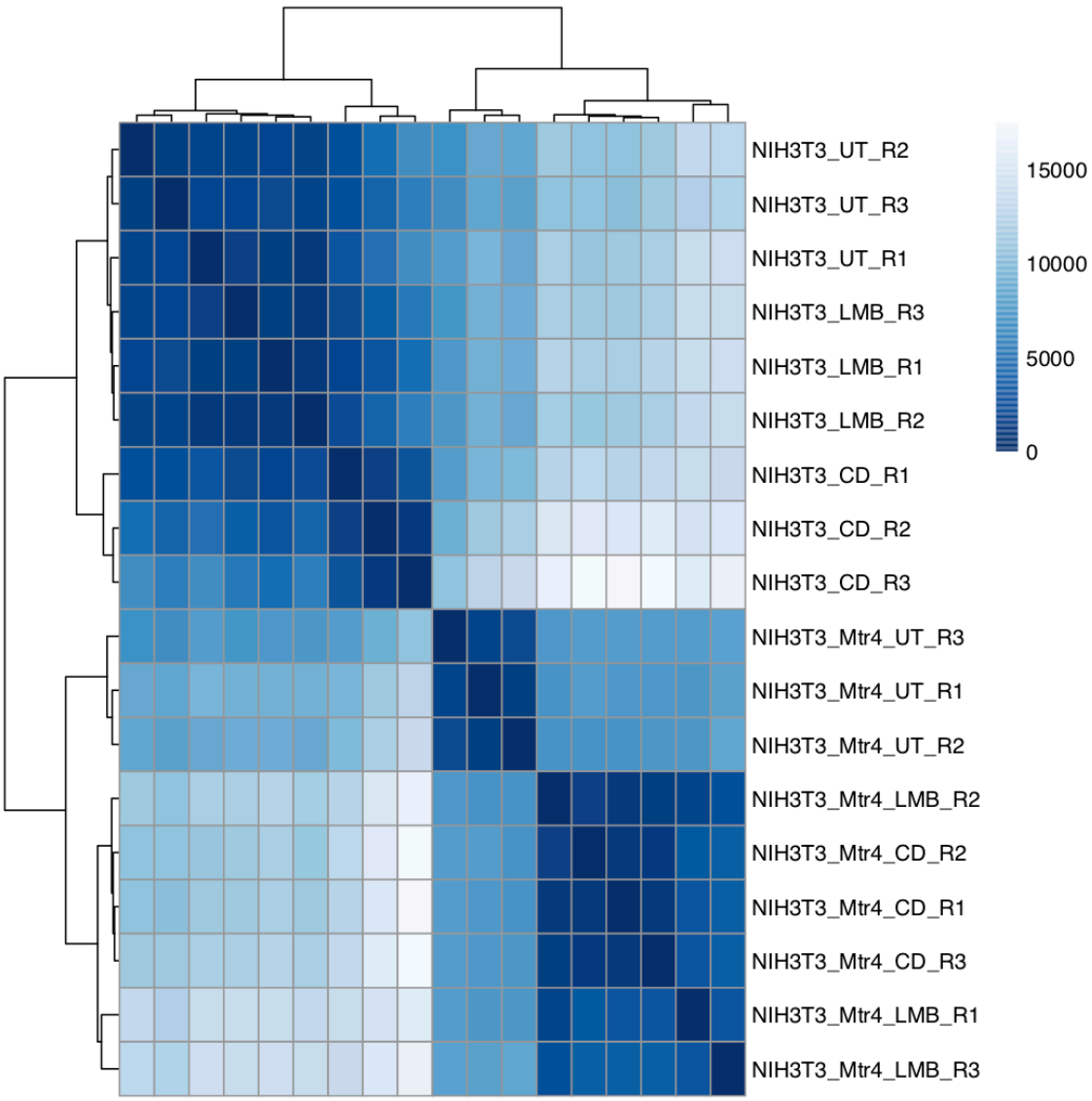

Figure 12 Heatmap of Poisson distance of RNAseq samples in NIH3T3 cells

A hierarchical clustering heatmap showing differences in the transcriptional profile between three biological replicates (R1, R2, R3) in different treatments. CD (3μM Cytochalasin D, 30 min); LMB (50nM Leptomycin B, 30 min); UT (untreated); MTR4CD (siMtr4 for 48h, 3μM Cytochalasin D for 30 min); MTR4LMB (siMtr4 for 48h, Leptomycin B for 30 min); MTR4UT (siMtr4 for 48h). Poisson distances are shown from low to high, indicated by darker to lighter blue shading. Samples clustering closely have similar gene expression profiles, whereas distant samples show distinct expression profiles. RNAseq data analysis was performed by Francesco Gualdrini.

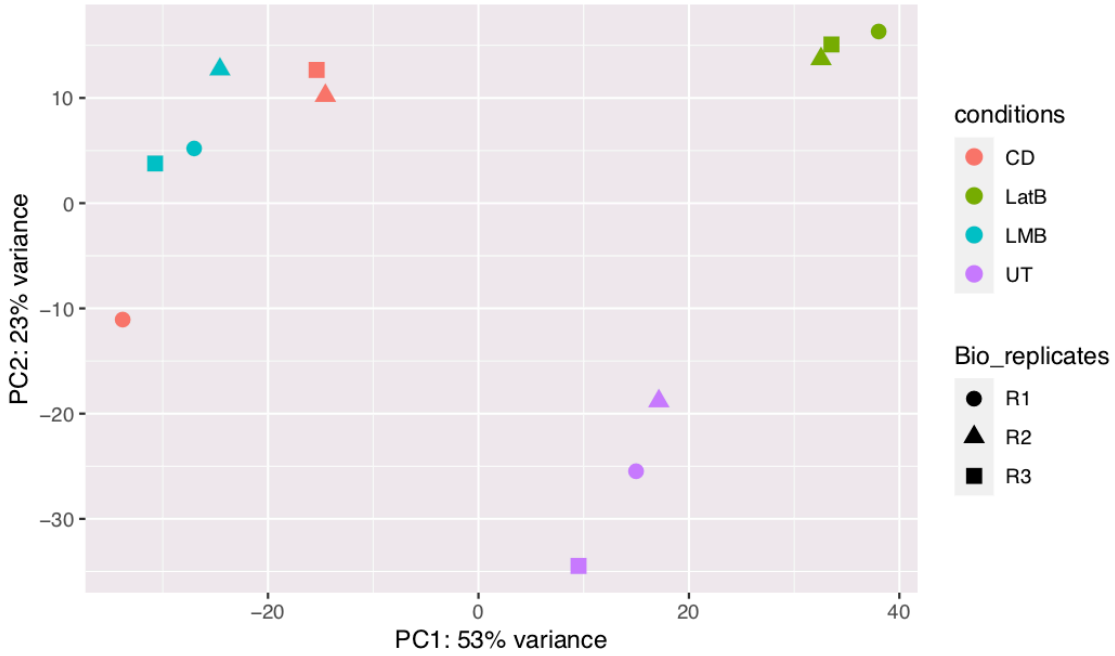

Figure 13 Principal component analysis (PCA) of TTseq samples in NIH3T3 cells

Shown is the clustering of three biological replicates (R1, R2, R3) for individual treatments. CD (3µM Cytochalasin D, 30 min); LatB (0.5 µM Latrunculin B, 30 min); LMB (50nM Leptomycin B, 30 min); UT (untreated). Samples clustering closely have similar gene expression profiles, whereas distant samples show distinct expression profiles. TTseq data analysis was performed by Francesco Gualdrini.

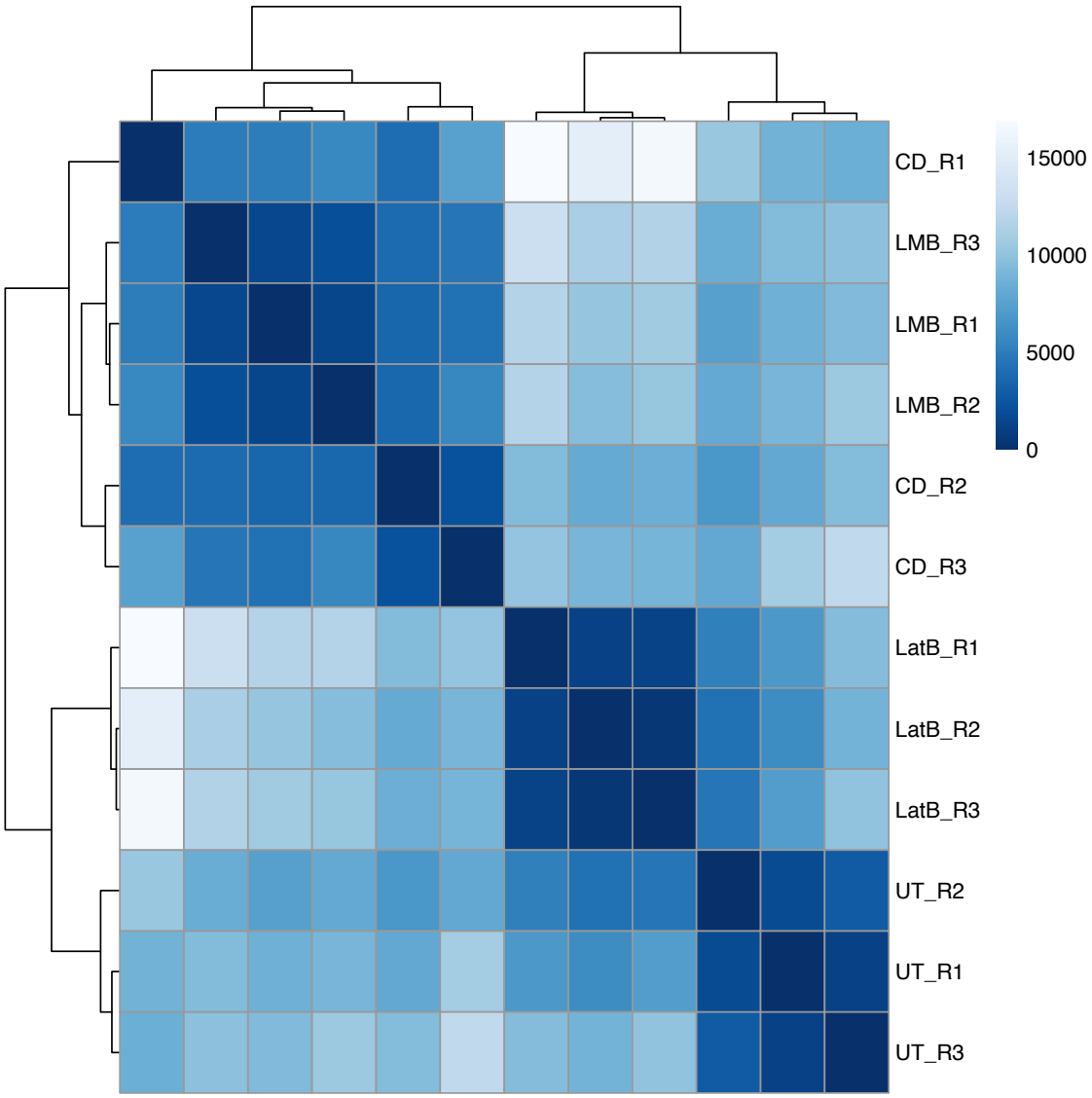

Figure 14 Heatmap of Poisson distance of TTseq samples in NIH3T3 cells

A hierarchical clustering heatmap showing differences in the transcriptional profile between three biological replicates (R1, R2, R3) in different treatments. CD (3μM Cytochalasin D, 30 min); LatB (0.5 μM Latrunculin B, 30 min); LMB (50nM Leptomycin B, 30 min); UT (untreated). Poisson distances are shown from low to high, indicated by darker to lighter blue shading. Samples clustering closely have similar gene expression profiles, whereas distant samples show distinct expression profiles. TTseq data analysis was performed by Francesco Gualdrini.

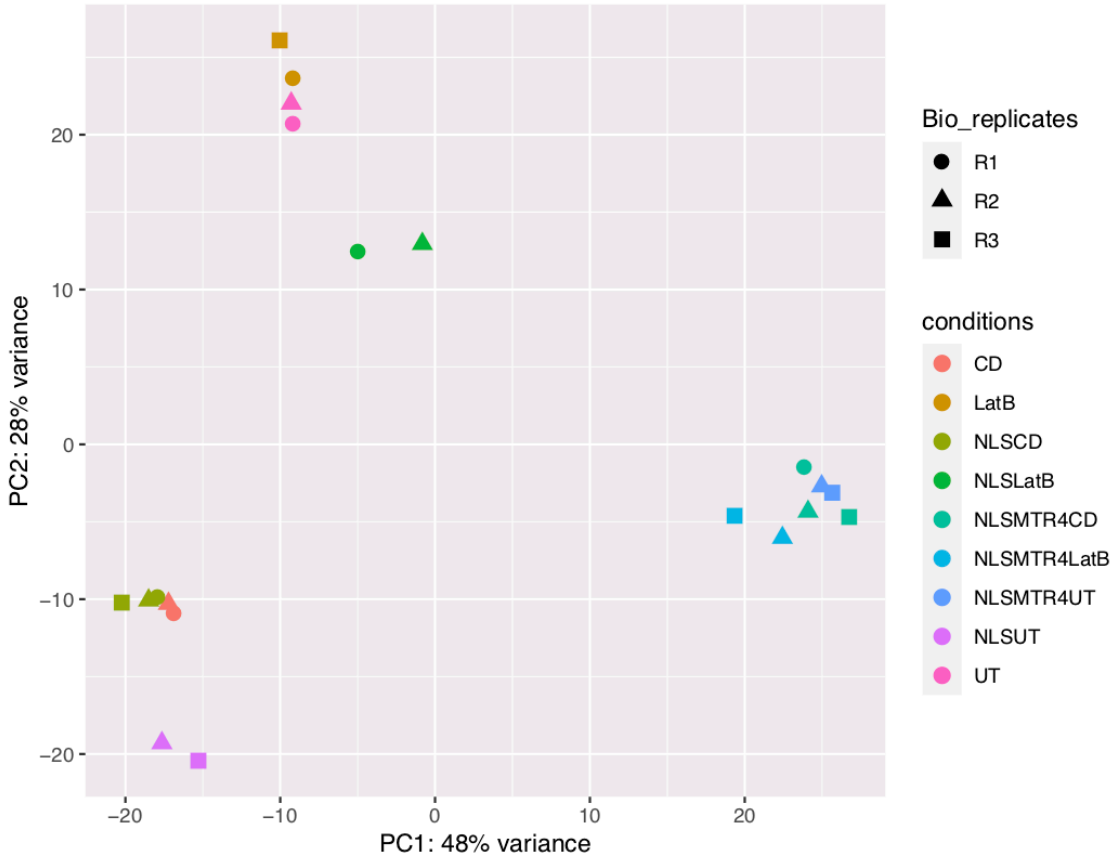

Figure 15 Principal component analysis (PCA) of RNAseq samples in dKO^{MRTF} and dKO$^{MRTF\text{-}NLS}$ cells

Shown is the clustering of three biological replicates (R1, R2, R3) for individual treatments. CD (3μM Cytochalasin D, 30 min); LatB (0.5 μM Latrunculin B, 30 min); UT (untreated) in dKO^{MRTF} cells. NLSCD (3μM Cytochalasin D, 30 min); NLSLatB (0.5 μM Latrunculin B, 30 min); NLSUT (untreated); NLSMTR4CD (siMtr4 for 48h, 3μM Cytochalasin D, 30 min); NLSMTR4LatB (siMtr4 for 48h, 0.5 μM Latrunculin B for 30 min); NLSMTR4UT (siMtr4 for 48h) in dKO$^{MRTF\text{-}NLS}$ cells. Samples clustering closely have similar gene expression profiles, whereas distant samples show distinct expression profiles. RNAseq data analysis was performed by Francesco Gualdrini.

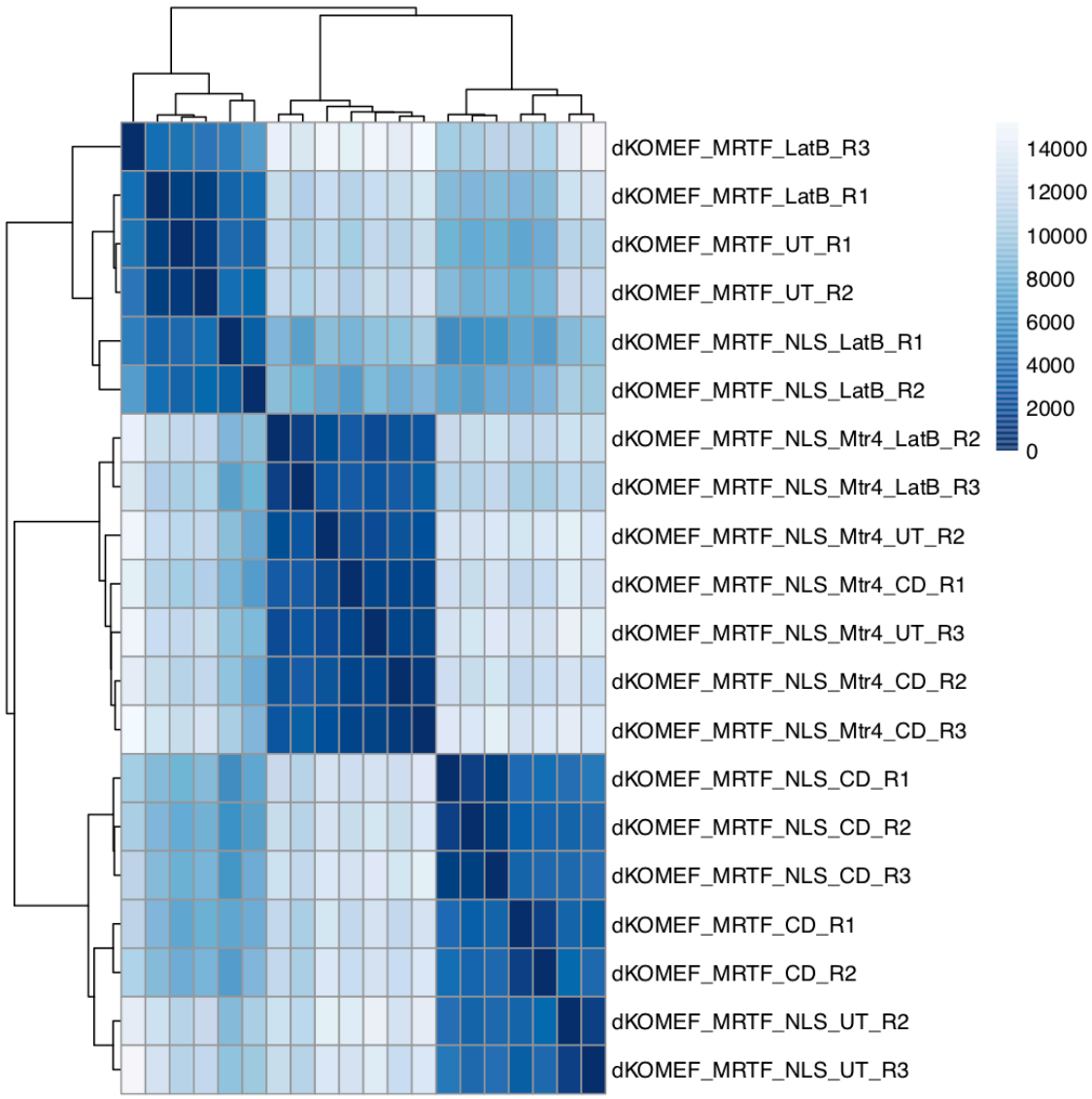

Figure 16 Heatmap of Poisson distance of RNAseq samples in dKO^{MRTF} and dKO$^{MRTF\text{-}NLS}$ cells

A hierarchical clustering heatmap showing differences in the transcriptional profile between three biological replicates (R1, R2, R3) in different treatments. dKOMEF_MRTF_CD (3μM Cytochalasin D, 30 min); dKOMEF_MRTF_LatB (0.5 μM Latrunculin B, 30 min); dKOMEF_MRTF_UT (untreated) in dKO^{MRTF} cells. dKOMEF_MRTF_NLS_CD (3μM Cytochalasin D, 30 min); dKOMEF_MRTF_NLS_LatB (0.5 μM Latrunculin B, 30 min); dKOMEF_MRTF_NLS_UT (untreated); dKOMEF_MRTF_NLS_MTR4_CD (siMtr4 for 48h, 3μM Cytochalasin D, 30 min); dKOMEF_MRTF_NLS_MTR4_LatB (siMtr4 for 48h, 0.5 μM Latrunculin B for 30 min); dKOMEF_MRTF_NLS_MTR4_UT (siMtr4 for 48h) in dKO$^{MRTF\text{-}NLS}$ cells. Poisson distances are shown from low to high, indicated by darker to lighter blue shading. Samples clustering closely have similar gene expression profiles, whereas distant samples show distinct expression profiles. RNAseq data analysis was performed by Francesco Gualdrini.

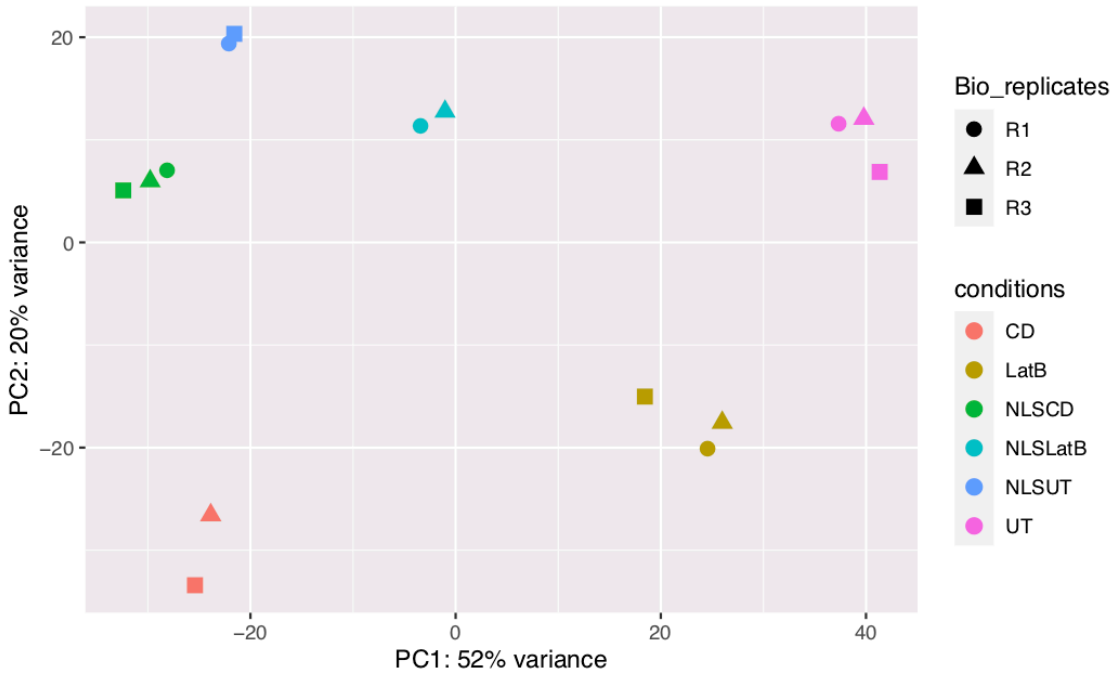

Figure 17 Principal component analysis (PCA) of TTseq samples in dKO^{MRTF} and dKO$^{MRTF-NLS}$ cells

Shown is the clustering of three biological replicates (R1, R2, R3) for individual treatments. CD (3µM Cytochalasin D, 30 min); LatB (0.5 µM Latrunculin B, 30 min); UT (untreated) in dKO^{MRTF} cells. NLSCD (3µM Cytochalasin D, 30 min); NLSLatB (0.5 µM Latrunculin B, 30 min); NLSUT (untreated) in dKO$^{MRTF-NLS}$ cells. Samples clustering closely have similar gene expression profiles, whereas distant samples show distinct expression profiles. TTseq data analysis was performed by Francesco Gualdrini.

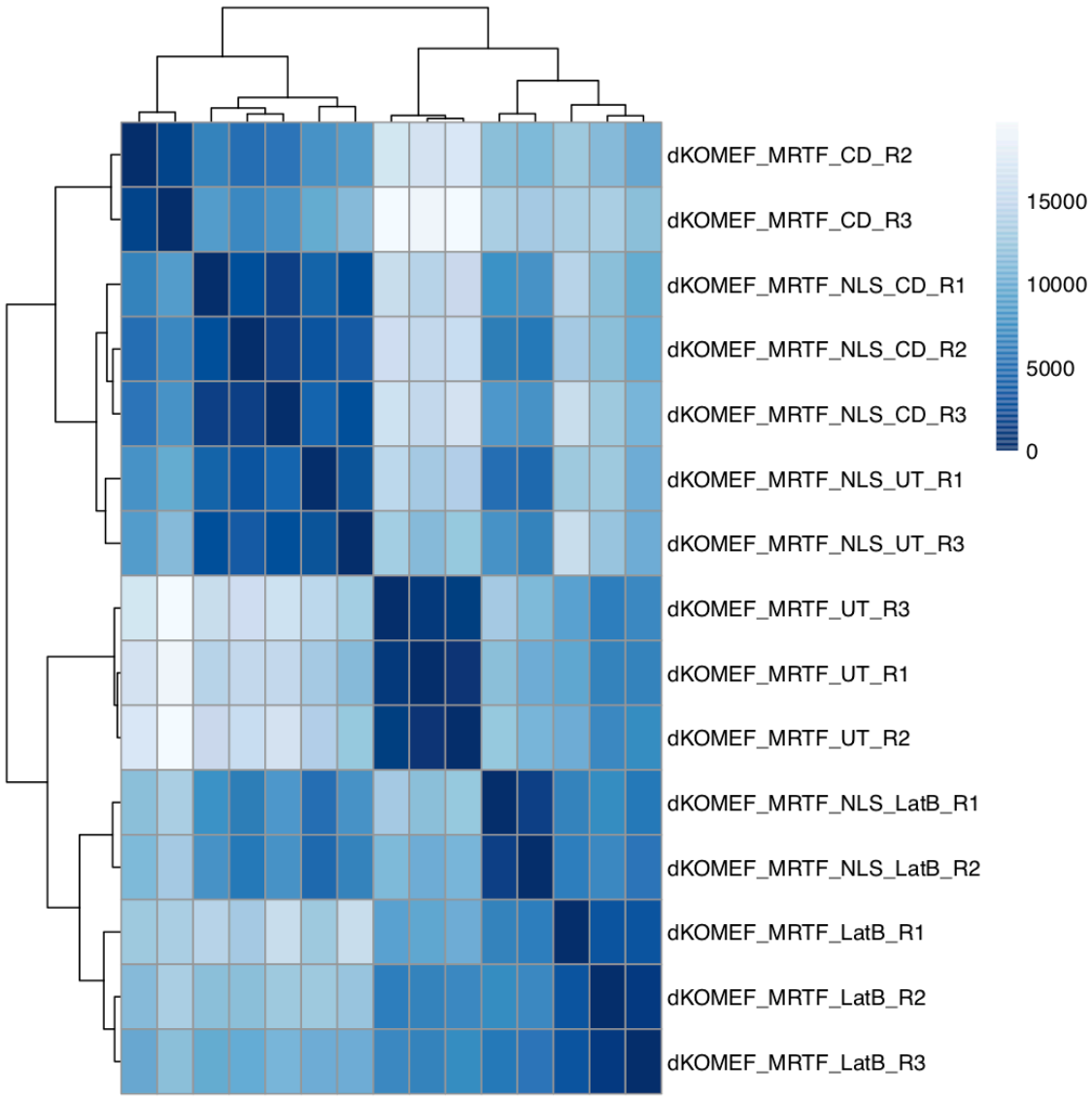

Figure 18 Heatmap of Poisson distance of TTseq samples in dKO^{MRTF} and dKO$^{MRTF\text{-}NLS}$ cells

A hierarchical clustering heatmap showing differences in the transcriptional profile between three biological replicates (R1, R2, R3) in different treatments. dKOMEF_MRTF_CD (3μM Cytochalasin D, 30 min); dKOMEF_MRTF_LatB (0.5 μM Latrunculin B, 30 min); dKOMEF_MRTF_UT (untreated) in dKO^{MRTF} cells. dKOMEF_MRTF_NLS_CD (3μM Cytochalasin D, 30 min); dKOMEF_MRTF_NLS_LatB (0.5 μM Latrunculin B, 30 min); dKOMEF_MRTF_NLS_UT (untreated) in dKO$^{MRTF\text{-}NLS}$ cells. Poisson distances are shown from low to high, indicated by darker to lighter blue shading. Samples clustering closely have similar gene expression profiles, whereas distant samples show distinct expression profiles. TTseq data analysis was performed by Francesco Gualdrini.

ChIPseq

ChIPseq data analysis was performed by Francesco Gualdrini. For QC and reproducibility of biological replicates see Figure 19 and Figure 20 for Ser5P ChIPseq samples, Figure 21 and Figure 22 for Ser2P ChIPseq samples, Figure 23 and Figure 24 for Ser7P ChIPseq samples and Figure 25 and Figure 26 for total Pol II ChIPseq samples. Adapter and quality trimming of ChIPseq reads was performed with Trim Galore. Reads were aligned to the mm10 mouse genome using BWA MEM (default settings). Duplicated reads were marked with Picard. Reads were filtered to remove blacklist regions from the Encode database, unmapped reads, low quality reads, multimappers, reads with insert size > 2kb, pairs mapping to different chromosomes. ChIPseq reads were counted at TSS (-150bp + 500 bp); Gene body (+150bp from TSS and -500 from the TES); TES (-500bp +7000bp) using CountOverlap function part of the GRanges library in Bioconductor/R. Normalization was performed as for RNAseq and TTseq using whole reads (TSS+gene body+TES) for total Pol II and Ser5P and TES only for Ser2P and Ser7P. Metaprofiles where generated using functionalities of the genomation library in Bioconductor/R. For ChIP metaprofiles the TSS was defined as the region spanning 500bp upstream to 500bp downstream of the TSS. The gene body was defined as the region 500bp downstream of the TSS to 500bp upstream of the TTS and shown in figures as normalized to 100%. The TTS was defined as the region 500bp upstream of the TTS to 7000bp downstream of the TTS.

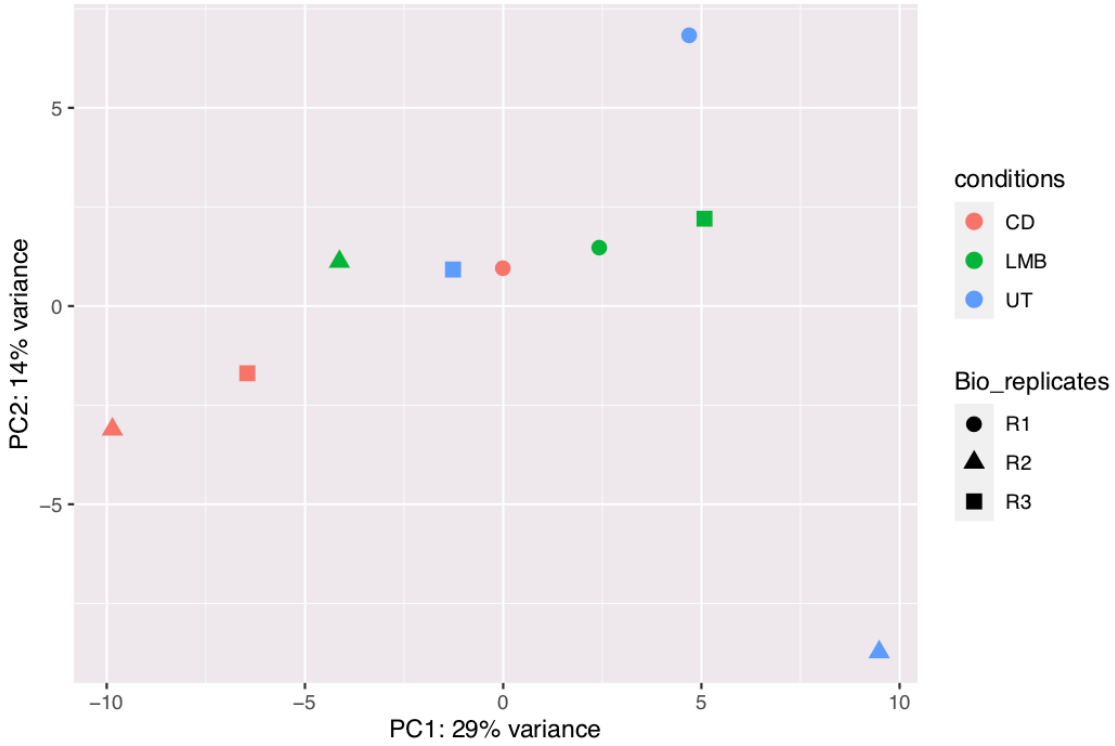

Figure 19 Principal component analysis (PCA) of Ser5P ChIPseq samples in NIH3T3 cells

Shown is the clustering of biological replicates (R1, R2, R3, R4, R5) for individual treatments. CD (3μM Cytochalasin D, 30 min); LMB (50nM Leptomycin B, 30 min); UT (untreated) in NIH3T3 cells. Samples clustering closely have similar read profiles, whereas distant samples show distinct profiles. ChIPseq data analysis was performed by Francesco Gualdrini.

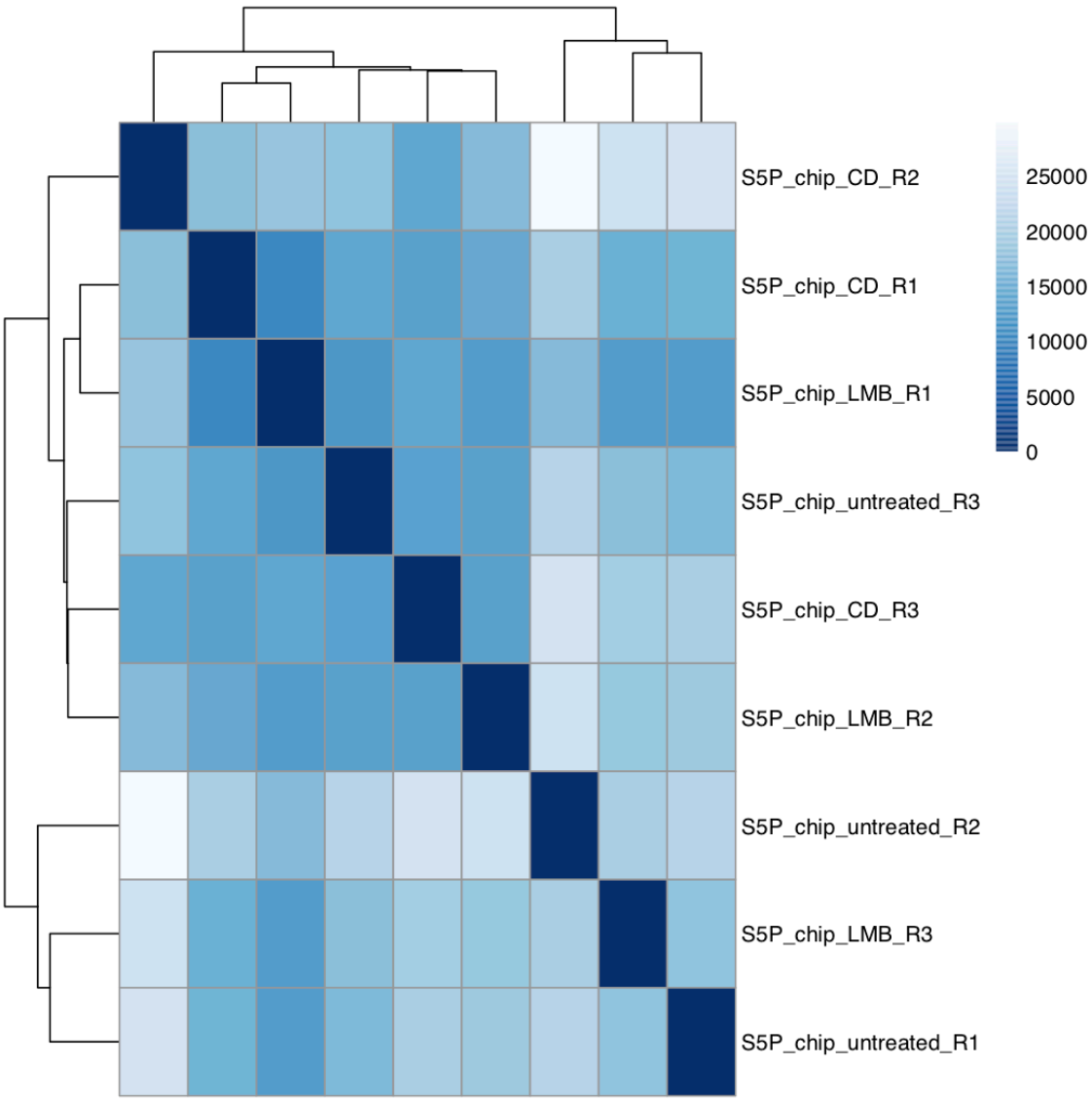

Figure 20 Heatmap of Poisson distance of Ser5P ChIPseq samples in NIH3T3 cells

A hierarchical clustering heatmap showing differences in the transcriptional profile between biological replicates (R1, R2, R3) in different treatments. CD (3μM Cytochalasin D, 30 min); LMB (50nM Leptomycin B, 30 min); UT (untreated). Poisson distances are shown from low to high, indicated by darker to lighter blue shading. Samples clustering closely have similar read profiles, whereas distant samples show distinct profiles. ChIPseq data analysis was performed by Francesco Gualdrini.

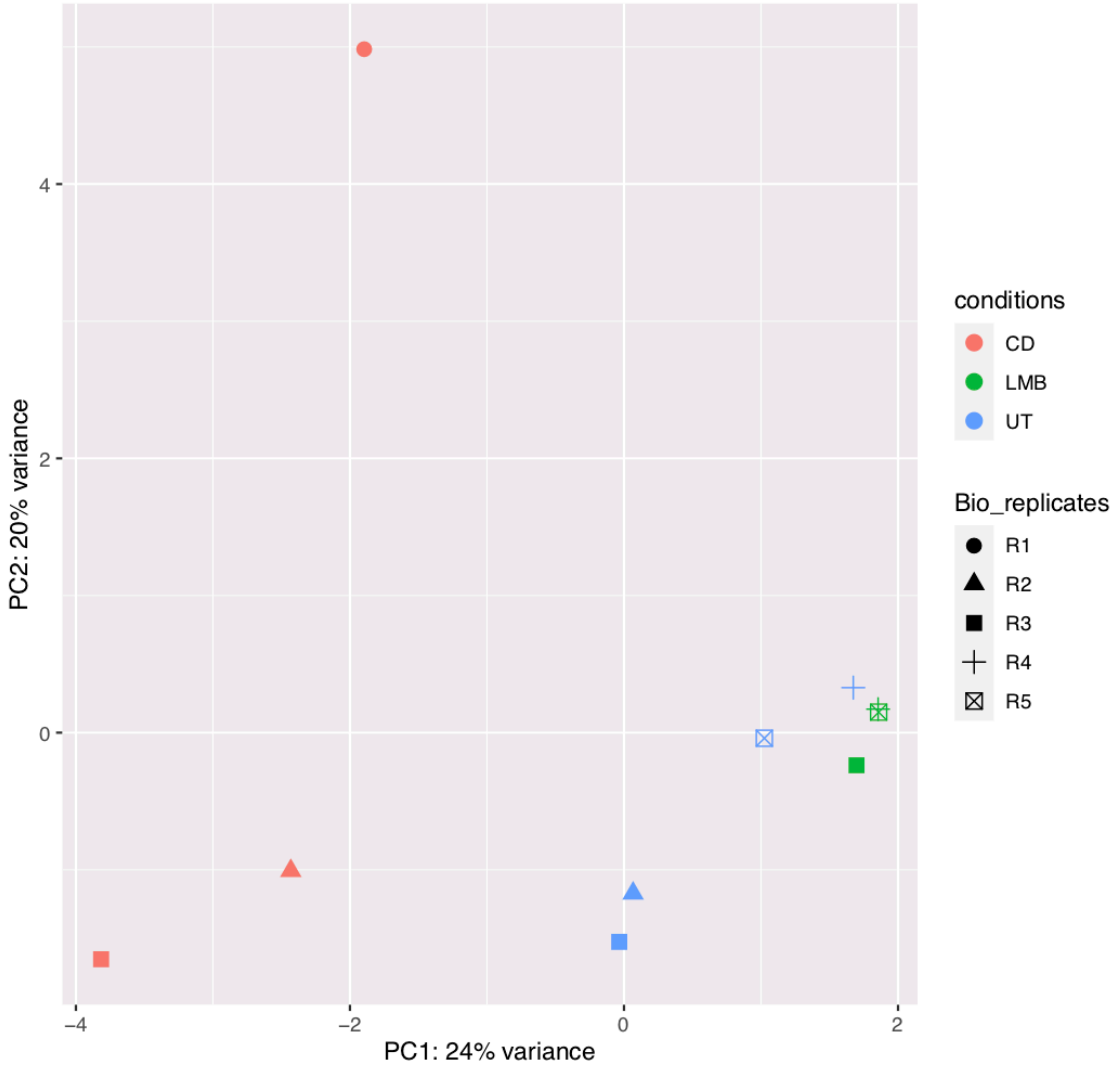

Figure 21 Principal component analysis (PCA) of Ser2P ChIPseq samples in NIH3T3 cells

Shown is the clustering of biological replicates (R1, R2, R3, R4, R5) for individual treatments. CD (3μM Cytochalasin D, 30 min); LMB (50nM Leptomycin B, 30 min); UT (untreated) in NIH3T3 cells. Samples clustering closely have similar read profiles, whereas distant samples show distinct profiles. ChIPseq data analysis was performed by Francesco Gualdrini.

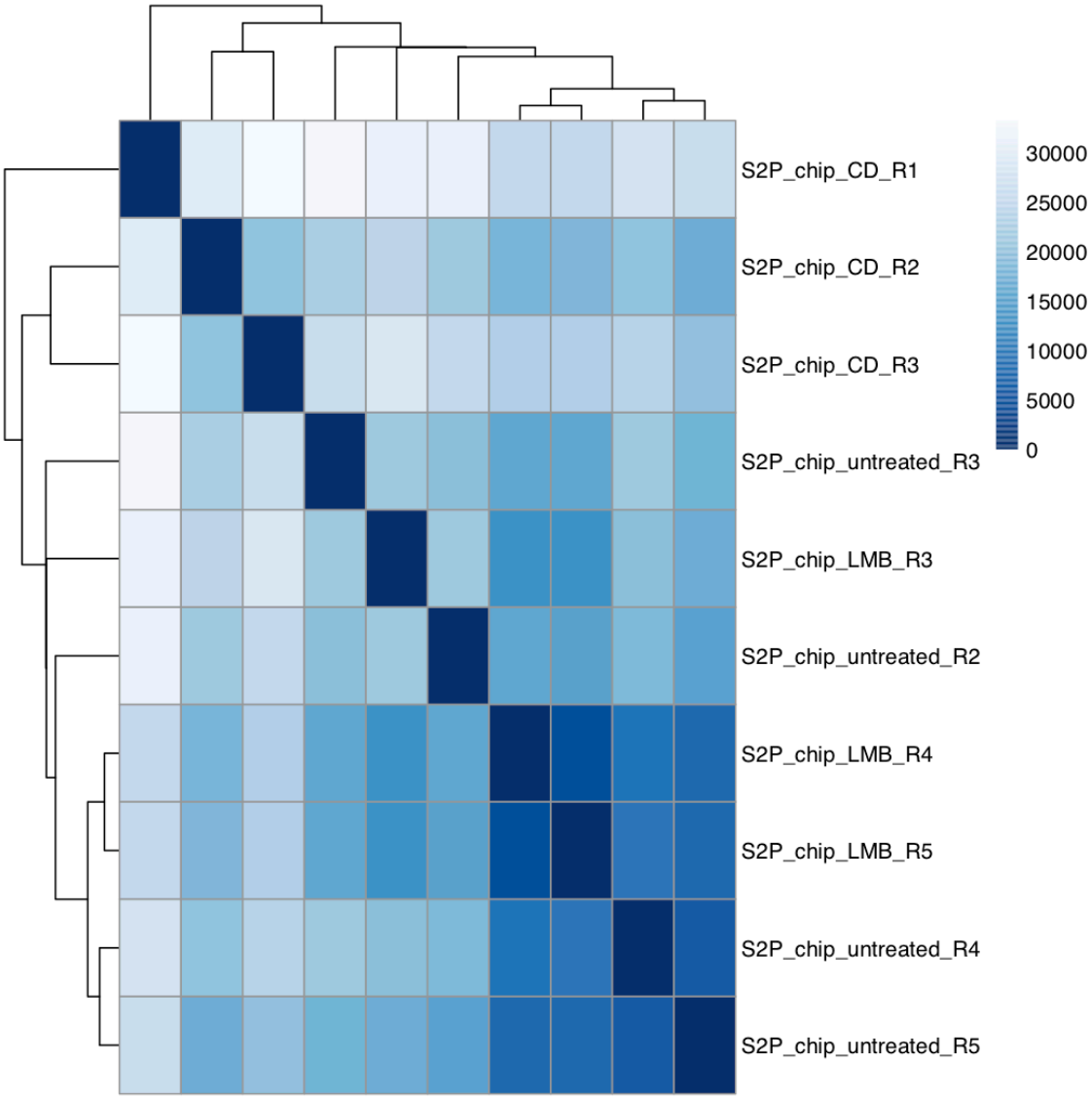

Figure 22 Heatmap of Poisson distance of Ser2P ChIPseq samples in NIH3T3 cells

A hierarchical clustering heatmap showing differences in the transcriptional profile between biological replicates (R1, R2, R3, R4, R5) in different treatments. CD (3μM Cytochalasin D, 30 min); LMB (50nM Leptomycin B, 30 min); UT (untreated). Poisson distances are shown from low to high, indicated by darker to lighter blue shading. Samples clustering closely have similar read profiles, whereas distant samples show distinct profiles. ChIPseq data analysis was performed by Francesco Gualdrini.

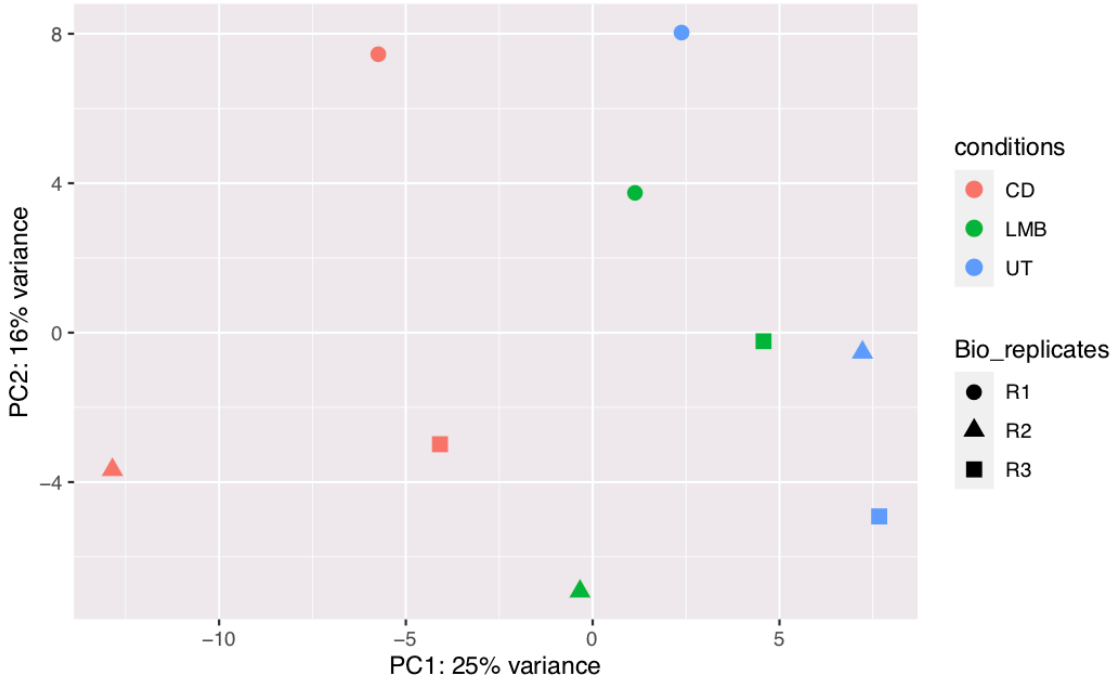

Figure 23 Principal component analysis (PCA) of Ser7P ChIPseq samples in NIH3T3 cells

Shown is the clustering of biological replicates (R1, R2, R3, R4, R5) for individual treatments. CD (3μM Cytochalasin D, 30 min); LMB (50nM Leptomycin B, 30 min); UT (untreated) in NIH3T3 cells. Samples clustering closely have similar read profiles, whereas distant samples show distinct profiles. ChIPseq data analysis was performed by Francesco Gualdrini.

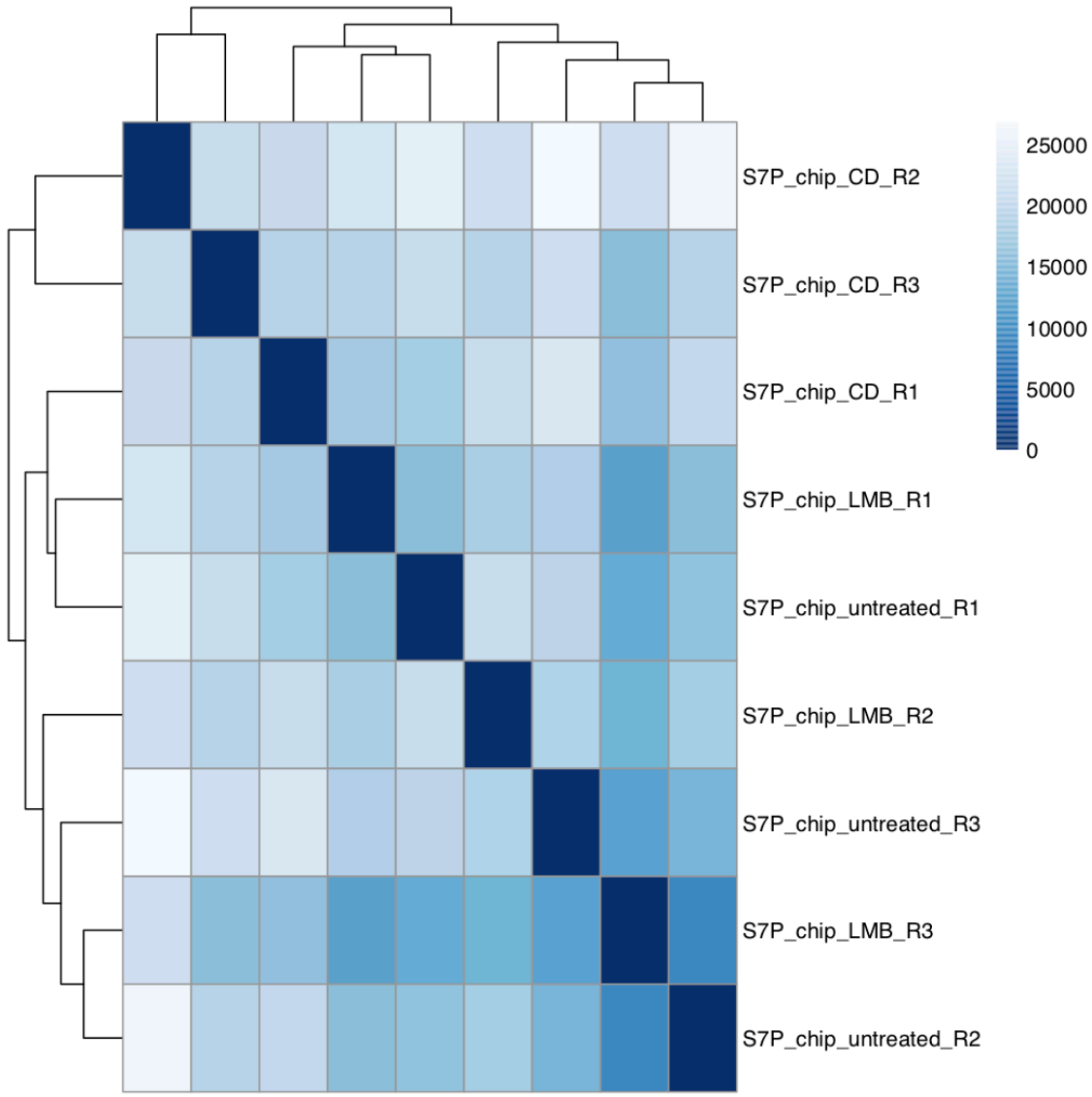

Figure 24 Heatmap of Poisson distance of Ser7P ChIPseq samples in NIH3T3 cells

A hierarchical clustering heatmap showing differences in the transcriptional profile between biological replicates (R1, R2, R3) in different treatments. CD (3μM Cytochalasin D, 30 min); LMB (50nM Leptomycin B, 30 min); UT (untreated). Poisson distances are shown from low to high, indicated by darker to lighter blue shading. Samples clustering closely have similar read profiles, whereas distant samples show distinct profiles. ChIPseq data analysis was performed by Francesco Gualdrini.

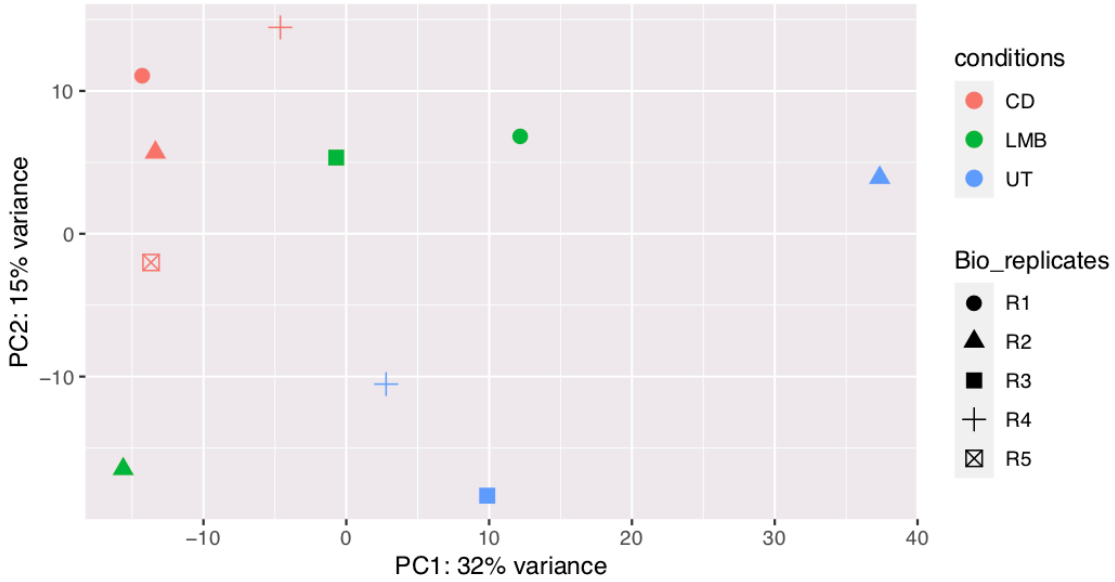

Figure 25 Principal component analysis (PCA) of total Pol II ChIPseq samples in NIH3T3 cells

Shown is the clustering of biological replicates (R1, R2, R3, R4, R5) for individual treatments. CD (3μM Cytochalasin D, 30 min); LMB (50nM Leptomycin B, 30 min); UT (untreated) in NIH3T3 cells. Samples clustering closely have similar read profiles, whereas distant samples show distinct profiles. ChIPseq data analysis was performed by Francesco Gualdrini.

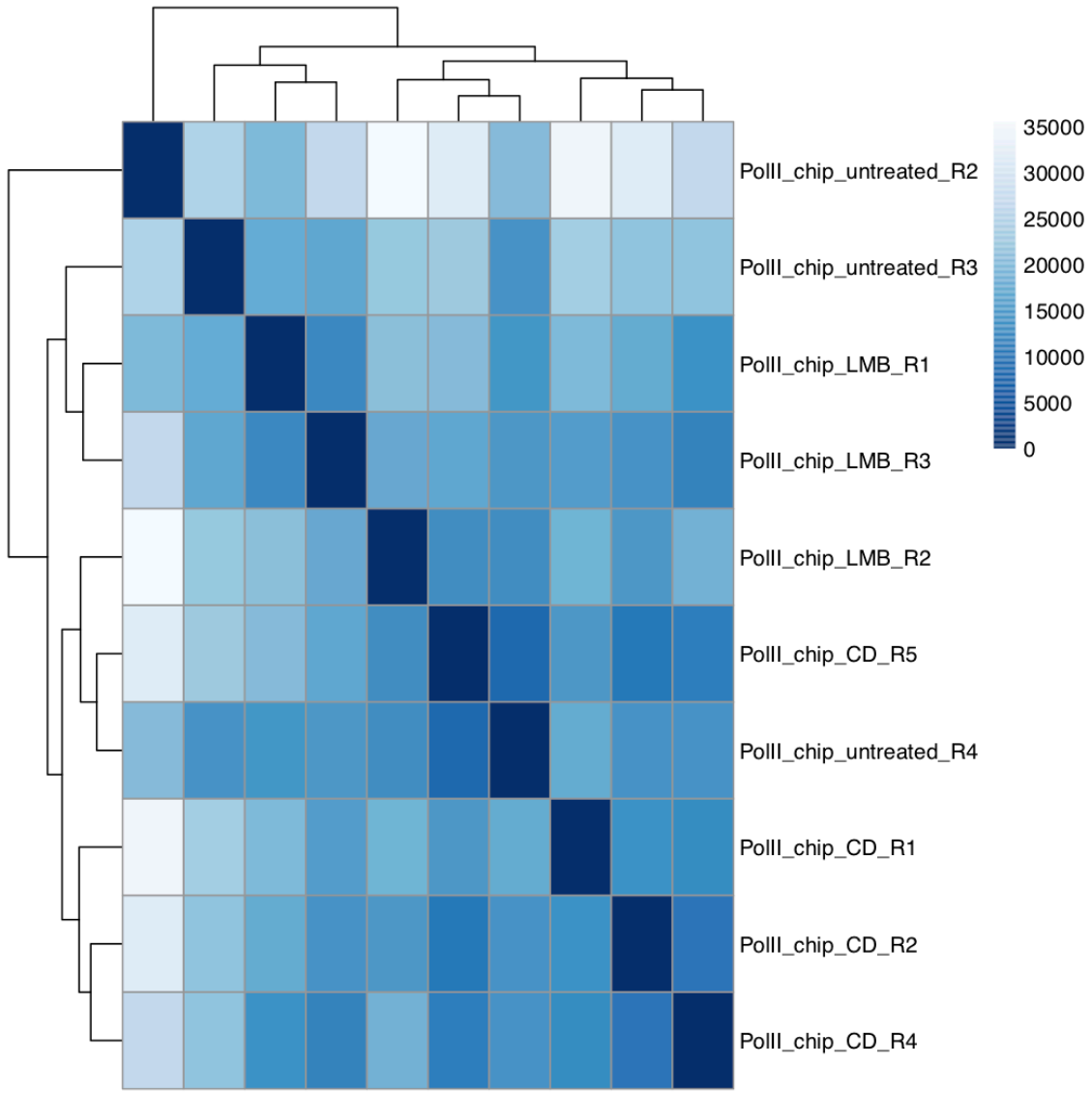

Figure 26 Heatmap of Poisson distance of total Pol II ChIPseq samples in NIH3T3 cells

A hierarchical clustering heatmap showing differences in the transcriptional profile between biological replicates (R1, R2, R3, R4, R5) in different treatments. CD (3μM Cytochalasin D, 30 min); LMB (50nM Leptomycin B, 30 min); UT (untreated). Poisson distances are shown from low to high, indicated by darker to lighter blue shading. Samples clustering closely have similar read profiles, whereas distant samples show distinct profiles. ChIPseq data analysis was performed by Francesco Gualdrini.

2.13 Immunoprecipitation (IP)

For co-IPs, 50 µl dynabeads (10009D, Thermo Fisher Scientific) were blocked in 0.1% BSA in PBS and coupled to 10 µg antibody for 1h at 4^0C with shaking. Cells were trypsinized, pelleted by centrifugation at 300g for 5min, resuspended and lysed in RIPA buffer (50 mM Hepes-KOH, pH 7.5; 500 mM LiCl; 1mM EDTA; 1% NP-40 or Igepal CA-630; 0.7% Na-Deoxycholate, protease inhibitors (11873580001, Roche)) for 1h at 4^0C shaking. Lysates were cleared by centrifugation at 13000g for 15 min at 4^0C and protein concentration was measured using Bradford reagent (500-0006, Biorad). 1 mg total protein was used per IP. Samples were pre-cleared by incubation with 25 µl dynabeads, previously blocked in 0.1% BSA, for 1h at 4^0C. Pre-cleared samples were incubated with antibody-coupled dynabeads overnight at 4^0C with shaking. The following day, IPs were washed 3 times with RIPA buffer (50 mM Hepes-KOH, pH 7.5; 500 mM LiCl; 1mM EDTA; 1% NP-40 or Igepal CA-630; 0.7% Na-Deoxycholate) and once with TBS (20 mM Tris-HCl, pH 7.6; 150 mM NaCl) on a magnetic rack and elution was performed in 100 µl elution buffer (25 mM Tris-HCl pH 7.5, 5 mM EDTA, 0.5% SDS) at 65^0C for 30 min. Samples were then used for Western blotting. IgG IP was used as a control.

2.14 UV-RIP

The UV-RIP protocol was adapted from (Ule et al., 2005). For Mtr4 RNA IP, cells were UV-crosslinked at 254nm 150mJ/cm^2 and scraped in ice-cold PBS, supplemented with protease inhibitors (11873580001, Roche) and RNase inhibitors. Pellets were resuspended and lysed in lysis buffer (50 mM Tris-HCl pH 7.4, 100 mM NaCl, 1% NP-40, 0.1% SDS, 0.5% Na deoxycholate) for 15 min at 4^0C and sonicated for 8 min (30”ON/30”OFF) at low energy using Bioruptor sonicator (Diagenode). Lysates were pre-cleared and incubated with antibody, as described in section 2.9. IPs were washed twice with High-salt buffer (50 mM Tris-HCl pH 7.4, 1M NaCl, 1 mM EDTA, 1% NP-40, 0.1% SDS, 0.5% Na deoxycholate) and twice in PNK buffer (20 mM Tris-HCl pH 7.4, 10 mM $MgCl_2$, 0.2% Tween-20) and eluted in elution buffer (25 mM Tris-HCl pH 7.5, 5 mM EDTA, 0.5% SDS) with

20µg proteinase K (19133, Qiagen) for 1h at 55^0C. RNA was purified using RNeasy MinElute Cleanup Kit (74204, Qiagen).

2.15 Plasmids and molecular cloning

MRTF-A siRAR cDNA sequence (Pawłowski et al., 2010):

RPEL1

RPEL2

RPEL3

ATGCCCCCTTCCGTCATTGCTGTGAATGGGCTGGACGGAGGAGGGGCTGGC
GAAAATGACGACGAGCCAGTGCTCCTGTCTCTGTCTGCGGCCCCCAGCCCCC
AGAGCGAAGCTGTTGCCAATGAACTGCAGGAGCTGTCCCTGCAGCCCGAGCT
GACTCTAGGCCTCCATCCTGGGAGGAACCCCAATTTACCTCCACTTAGTGAGC
GGAAGAATGTGCTGCAGTTGAAGCTCCAGCAGCGGCGGACCCGGGAGGAAC
TGGTGAGCCAAGGGATCATGCCGCCTTTGAAAAGCCCCGCTGCATTTCATGA
GCAGAGAAGAAGCCTGGAGCGGGCCAGGACCGAGGACTATTTGAAACGGAA
GATCCGTTCCCGGCCCGAGAGAGCAGAGCTGGTCAGGATGCACATTCTGGAA
GAGACCTCGGCTGAGCCTTCGCTCCAGGCCAAGCAGCTGAAGCTGAAGAGA
GCCAGGCTGGCTGATGACCTCAATGAAAAGATTGCACAGAGGCCTGGCCCCA
TGGAACTAGTAGAAAAGAATATCCTGCCTGTGGAGTCCAGCCTGAAGGAGGC
TATCATTGTGGGCCAGGTAAATTACCCAAAGGTAGCAGACAGTTCCTCCTTCG
ACGAGGACAGCAGCGATGCCCTGTCTCCTGAGCAGCCTGCCAGCCATGAGTC
CCAGGGTTCAGTGCCATCACCCTTGGAGTCCCGAGTCAGTGATCCACTGCCC
AGTGCCACCTCCATATCACCCACTCAGGTTCTTTCTCAACTCCCAATGGCTCC
GGATCCTGGAGAGACGCTTTTTCTGGCAGAGCAGCCTCCTCTGCCTCCCGCA
CCTCTGCTGCCCCCAAGCCTAGCCAATGGAAGCATCGTCCCCACTGCCAAGC
CTGCTCCCACACTCATCAAGCAAAGCCAACCCAAGTCTGCCAGCGAGAAATC
ACAGCGCAGCAAGAAGGCCAAGGAGCTGAAGCCAAAGGTGAAGAAGCTCAA
GTACCACCAGTACATCCCCCCGGACCAGAAGCAGGACAAGGGGGCGCCCGC
CATGGACTCCTCCTATGCCAAGATCCTGCAGCAGCAGCAGCTCTTCCTGCAG
CTGCAGATCCTCAACCAGCAGCAGCAGCAGCAGCAGCAACAGCACTACAACT
ACCAGGCCATCCTGCCTGCCCCTCCCAAGCCCTCGGCTGAGACTCCTGGAAG
CAGTGCCCCTACCCCATCACGCAGCCTCTCCACCAGTAGCAGCCCCAGCTCA
GGCACCCCAGGGCCCAGCGGGCTGGCACGCCAGAGCAGCACCGCACTAGCT

GCCAAACCAGGAGCCCTGCCAGCCAACCTGGATGACATGAAGGTGGCAGAG
CTGAAGCAAGAACTGAAGTTGCGGTCCCTTCCCGTCTCAGGCACCAAGACAG
AGCTGATAGAACGCCTGCGTGCCTACCAAGACCAAGTCAGCCCAGCTCCAGG
AGCCCCCAAGGCCCCTGCCACCACCTCTGTGCTGTCCAAGGCTGGTGAGGTA
GTGGTCGCCTTCCCTGCGGCCCTGCTAAGCACAGGGTCAGCTCTTGTAACAG
CAGGCCTTGCACCAGCTGAGATGGTGGTGGCCACAGTAACCAGCAATGGCAT
GGTGAAGTTTGGCAGCACAGGCTCCACACCCCCCGTGTCTCCCACCCCTTCA
GAGCGCTCACTGCTCAGCACGGGTGATGAGAATTCCACACCTGGGGATGCCT
TTGGTGAAATGGTGACATCGCCGCTGACACAGCTCACCCTGCAGGCCTCCCC
ACTGCAGATCGTGAAGGAGGAGGGTGCCCGTGCTGCGTCCTGCTGTCTAAGC
CCTGGTGCTCGGGCTGAGCTGGAGGGACTGGACAAGGACCAGATGCTGCAG
GAGAAGGACAAGCAGATTGAGGAGCTGACCCGAATGCTCCAACAGAAGCAGC
AGCTGGTTGAGCTGCTGCGGCTACAGCTGGAGCAGCAGAAGCGGGCCCAGC
AGCCAGCCCCAGCCAGCAGCCCTGTGAAGAGGGAAAGTGGTTTCTCCAGTTG
CCAGCTGAGCTGCCAGCCCCAGGGCTCTGCCCATGCTTTTGGCTCTGGCCTA
GTGGTTCCCACTACCAACCATGGAGACACTCAGGCCCCAGCGCCAGAGTCCC
CACCTGTGGTGGTGAAGCAGGAAGCTGGGCCACCTGAGCCAGATCTGGCCC
CCAGCTCCCAGCTGCTCTTGGGCTCCCAGGGCACCAGCTTCCTCAAGAGGGT
CAGCCCTCCTACCCTGGTCACTGACTCTACAGGGACTCACCTCATCCTCACTG
TGACCAATAAGAGTGCTGATGGCCCTGGCTTGCCTGCAGGGAGCCCCCAGCA
GCCCTTGTCCCAGCCTGGTTCTCCAGCCCCTGGTCCACCTGCCCAGATGGAC
CTGGAGCACCCACCTCAGCCTCCGTTTGCAACCCCCACATCTCTGCTGAAGA
AGGAGCCCCCTGGTTATGAAGAGACTGTGACCCAGCAGCCTAAGCAGCAGGA
AAATGGCTCCTCCAGTCAGCACATGGATGATCTGTTTGATATTCTTATTCAGAG
TGGAGAGATTTCAGCAGATTTCAAAGAGCCACCATCCCTACCAGGCAAGGAAA
AGTCACCTCCAGCAGCAGCAGCGTATGGGCCTCCATTGACACCACAACCCTC
GCCTTTGAGTGAACTCCCCCAAGCTGCTCCTCCACCAGGCTCCCCCACCCTC
CCAGGGCGCCTTGAAGACTTCCTGGAGAGCAGCACAGGGCTGCCCCTGCTG
ACAAGTGGGCACGAGGGACCAGAACCCCTTTCCCTCATTGATGACCTCCACA
GCCAGATGCTGAGCAGCTCCGCCATCCTGGACCACCCCCCATCACCCATGGA
CACCTCTGAATTGCACTTTGCTCCTGAGCCCAGCAGTGGTATGGGCCTGGAC
CTGGCTGTTGGCCACCTGGACAGCATGGACTGGCTGGAGCTGTCGTCTGGTG
GCCCTGTGCTCAGCCTGGCTCCCCTCAGCACTGCAGCCCCCAGCCTCTTCTC

GATGGACTTCCTGGATGGACACGACTTGCAGCTCCACTGGGATTCCTGCTTGT
AA

MRTF-XXX contains three point-mutations Arginine to Alanine, one in each RPEL motif: RPEL1 (RRTREEL->ARTREEL), RPEL2 (RPERAEL-> APERAEL), RPEL3 (RPGPMEL-> APGPMEL).

SV40 NLS sequence:
CCTAAGAAAAAGCGGAAGGTG

HA-tag sequence:
TACCCATACGATGTTCCTGACTATGCG

MRTF-A and MRTF-XXX siRAR cDNA, SV40 NLS and HA tag sequences were obtained from Treisman lab plasmids generated by Francesco Gualdrini by PCR using KOD DNA polymerase (71086-3, Millipore) and inserted between XhoI and NotI restriction enzyme sites in the pMY-IRES-GFP vector (RTV-021, Cell Biolabs) using In-fusion cloning system (639647, Takara), according to the manufacturer's protocol.

Stbl3 competent *E.coli* cells (C737303, Thermo Fisher Scientific) were thawed on ice, mixed with DNA and incubated on ice for 30 min. Cells were heat-shocked at 42^0C for 45 sec, followed by a 2 min incubation on ice. 250 ul SOC medium (2% tryptone, 0.5% yeast extract, 10 mM NaCl, 2.5 mM KCl, 10 mM MgCl2, 10 mM MgSO4, and 20 mM glucose) was added and cells were incubated at 37^0C shaking for 1h, before plating on agar plates (1% w/v Bacto-tryptone, 0.5% w/v Bacto-yeast extract, 1% w/v NaCl, 1.5% w/v Bacto-agar), supplemented with 100 ug/ml ampicillin (A0166-25G, Sigma), and incubated at 37^0C overnight. Bacterial colonies were picked and grown in LB medium (1% w/v Bacto-tryptone, 0.5% w/v Bacto-yeast extract, 1% w/v NaCl), supplemented with 100 ug/ml ampicillin overnight at 37^0C shaking. Plasmid mini-preps were done using QIAprep Spin Miniprep Kit (27106, Qiagen) and plasmids were sequenced by the Genomics Equipment park STP.

2.16 List of plasmids

pMY-IRES-GFP lentiviral expression vector (RTV-021, Cell Biolabs) was used to constitutively express MRTF, MRTF-NLS and MRTF-XXX in dKO MEF cells. It expresses the Ampicillin resistance gene for selection in bacteria and EGFP for selection in mammalian cells.

pcDNA6/TR vector (V102520, Thermo Fisher Scientific) was used to generate the Flp-in 3T3 TR cell line. It constitutively expresses the tetracycline repressor protein under a strong CMV promoter, the Ampicillin resistance gene for selection in bacteria and the Blasticidin resistance gene for selection in mammalian cells.

pOG44 plasmid (V6005-20, Thermo Fisher Scientific) expresses the Flp recombinase under a CMV promoter and the Ampicillin resistance gene for selection in bacteria. When co-transfected with pFRT plasmid, containing a gene of interest, into mammalian Flp-in host cell line, it mediates integration of the pFRT vector into the genome via Flp recombination target sites. It was used in combination with pFRT-TO-RPB1 and pFRT-TO-RPB1-S7A plasmids to generate NIH3T3 cells expressing wild-type Rpb1 and Rpb1-S7A mutant.

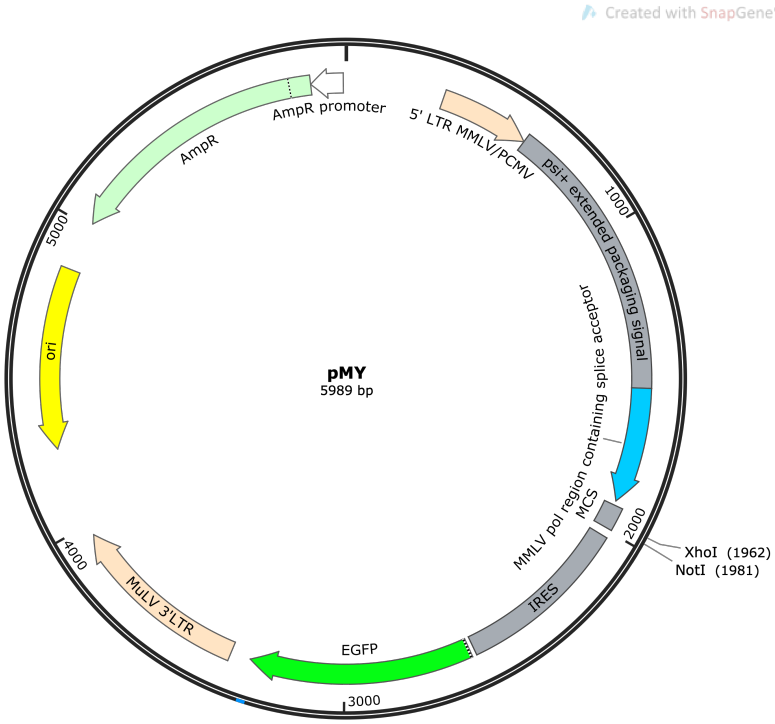
Created with SnapGene®
AmpR promoter
5' LTR MMLV/PCMV
psi+ extended packaging signal
1000
AmpR
5000
ori
pMY
5989 bp
MMLV pol region containing splice acceptor
MCS
2000
XhoI (1962)
NotI (1981)
4000
MuLV 3'LTR
IRES
EGFP
3000

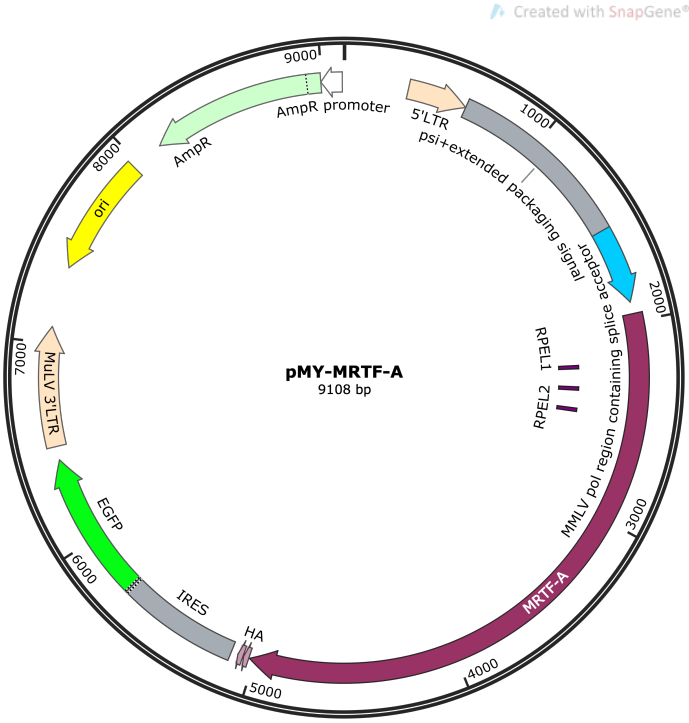
Created with SnapGene®
9000
AmpR promoter
5'LTR
1000
psi+extended packaging signal
AmpR
8000
ori
2000
RPEL1
RPEL2
pMY-MRTF-A
9108 bp
MMLV pol region containing splice acceptor
7000
MuLV 3'LTR
3000
EGFP
MRTF-A
6000
IRES
HA
4000
5000

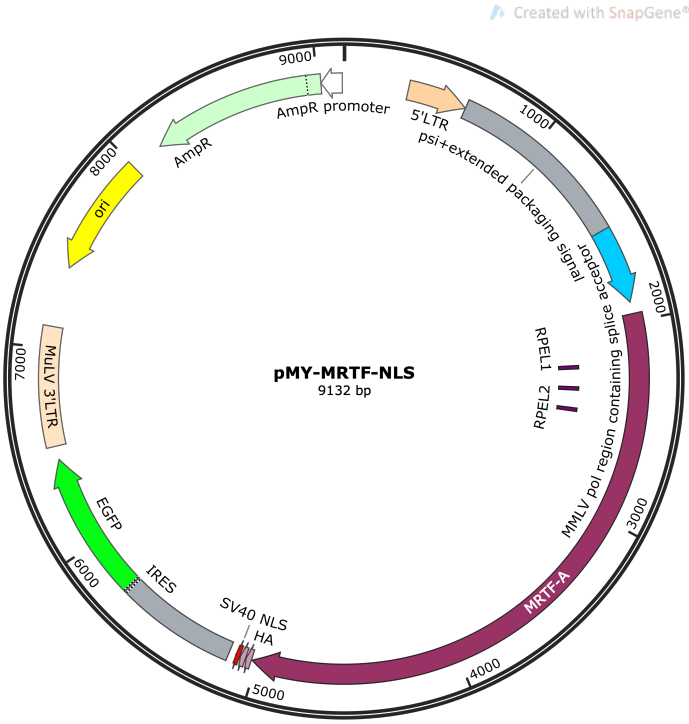
Created with SnapGene®
pMY-MRTF-NLS
9132 bp
9000
AmpR promoter
AmpR
8000
ori
1000
5'LTR
psi+extended packaging signal
acceptor
2000
RPEL1
RPEL2
MMLV pol region containing splice
3000
MRTF-A
4000
5000
SV40 NLS
HA
IRES
6000
EGFP
7000
MuLV 3'LTR

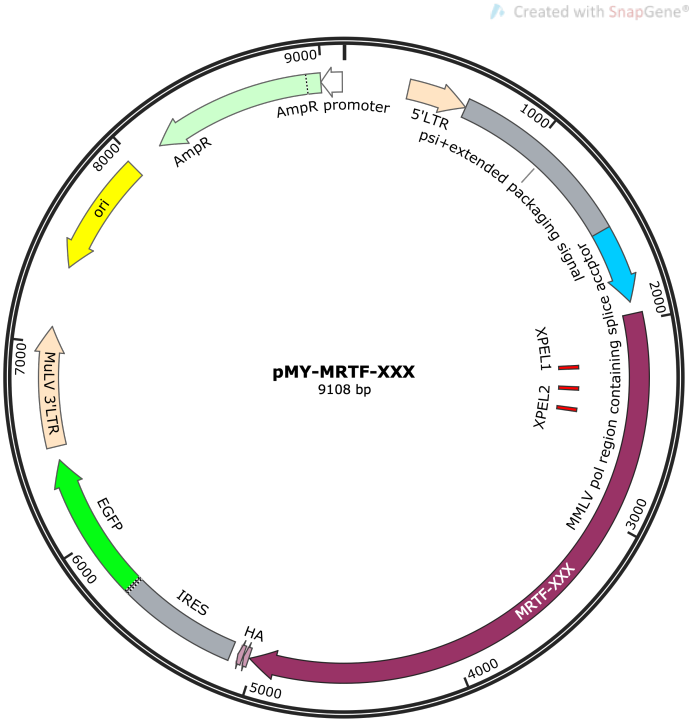
Created with SnapGene®
pMY-MRTF-XXX
9108 bp
9000
AmpR promoter
AmpR
8000
ori
1000
5'LTR
psi+extended packaging signal
acceptor
2000
XPEL1
XPEL2
MMLV pol region containing splice
3000
MRTF-XXX
4000
5000
HA
IRES
6000
EGFP
7000
MuLV 3'LTR

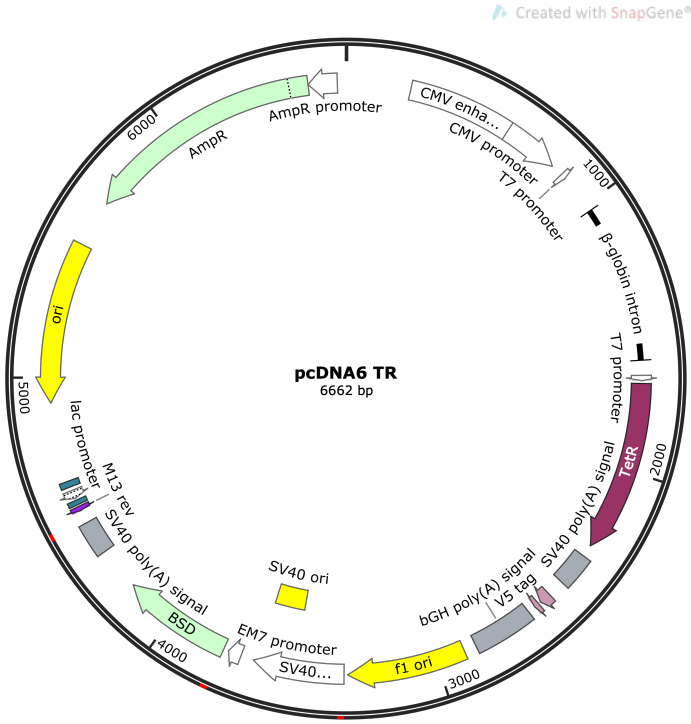
Created with SnapGene®
pcDNA6 TR
6662 bp
AmpR promoter
AmpR
CMV enha...
CMV promoter
T7 promoter
β-globin intron
T7 promoter
TetR
SV40 poly(A) signal
V5 tag
bGH poly(A) signal
f1 ori
SV40...
EM7 promoter
BSD
SV40 poly(A) signal
SV40 ori
M13 rev
lac promoter
ori
1000
2000
3000
4000
5000
6000

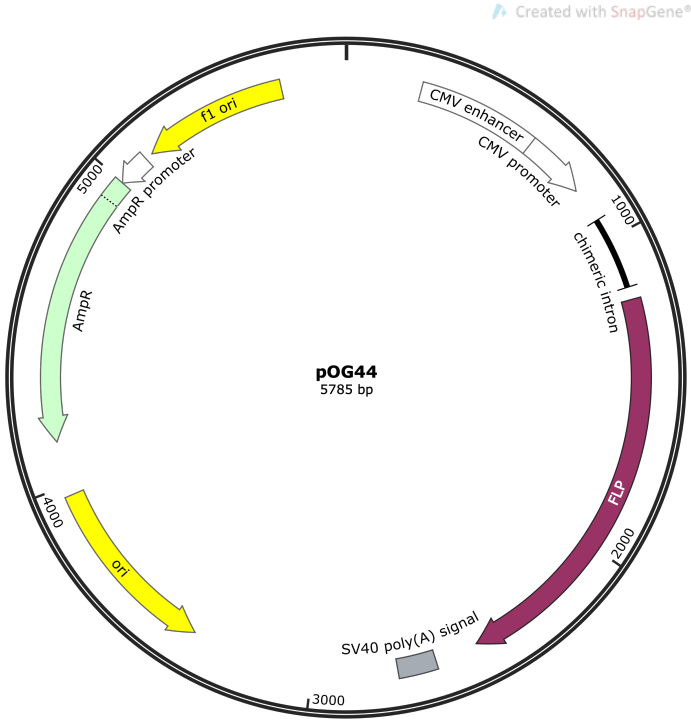
Created with SnapGene®
pOG44
5785 bp
f1 ori
CMV enhancer
CMV promoter
chimeric intron
FLP
SV40 poly(A) signal
ori
AmpR promoter
AmpR
1000
2000
3000
4000
5000

pFRT-TO-RPB1 and pFRT-TO-RPB1-S7A plasmids express a wild-type Rpb1 and a mutant Rbp1 in which Ser7 is mutated to alanine in all 26 Ser7-containing repeats of the Rpb1 CTD, respectively, under the control of a doxycycline-inducible CMV promoter. In addition, they contain point mutations making them resistant to siRNAs (GTGACGAAATGAATCTTCA and TTATCGAAGTGATTGAAAA). These plasmids were generated by Ana Tufegdzic Vidakovic.

Wild-type Rpb1 cDNA sequence:

CTD repeats are numbered and Ser7-containing repeats are highlighted in yellow.

GCATGCACGGGGGTGGCCCCCCCTCGGGGGACAGCGCATGCCCGCTGCGC
ACCATCAAGAGAGTCCAGTTCGGAGTCCTGAGTCCGGATGAACTGAAGCGAA
TGTCTGTGACGGAGGGTGGCATCAAATACCCAGAGACGACTGAGGGAGGCC
GCCCCAAGCTTGGGGGGCTGATGGACCCGAGGCAGGGGGTGATTGAGCGGA
CTGGCCGCTGCCAAACATGTGCAGGAAACATGACAGAGTGTCCTGGCCACTT
TGGCCACATTGAACTGGCCAAGCCTGTGTTTCACGTGGGCTTCCTGGTGAAG
ACAATGAAAGTTTTGCGCTGTGTCTGCTTCTTCTGCTCCAAACTGCTTGTGGA
CTCTAACAACCCAAAGATCAAGGATATCCTGGCTAAGTCCAAGGGACAGCCCA
AGAAGCGGCTCACACATGTCTACGACCTTTGCAAGGGCAAAAACATATGCGA
GGGTGGGGAGGAGATGGACAACAAGTTCGGTGTGGAACAACCTGAGGGTGA
CGAGGATCTGACCAAAGAAAAGGGCCATGGTGGCTGTGGGCGGTACCAGCC
CAGGATCCGGCGTTCTGGCCTAGAGCTGTATGCGGAATGGAAGCACGTTAAT
GAGGACTCTCAGGAGAAGAAGATCCTGCTGAGTCCAGAGCGAGTGCATGAGA
TCTTCAAACGCATCTCAGATGAGGAGTGTTTTGTGCTGGGCATGGAGCCCCG
CTATGCACGGCCAGAGTGGATGATTGTCACAGTGCTGCCTGTGCCCCCGCTC
TCCGTGCGGCCTGCTGTTGTGATGCAGGGCTCTGCCCGTAACCAGGATGACC
TGACTCACAAACTGGCTGACATCGTGAAGATCAACAATCAGCTGCGGCGCAAT
GAGCAGAACGGCGCAGCGGCCCATGTCATTGCAGAGGATGTGAAGCTCCTC
CAGTTCCATGTGGCCACCATGGTGGACAATGAGCTGCCTGGCTTGCCCCGTG
CCATGCAGAAGTCTGGGCGTCCCCTCAAGTCCCTGAAGCAGCGGTTGAAGGG
CAAGGAAGGCCGGGTGCGAGGGAACCTGATGGGCAAAAGAGTGGACTTCTC
GGCCCGTACTGTCATCACCCCCGACCCCAACCTCTCCATTGACCAGGTTGGC
GTGCCCCGCTCCATTGCTGCCAACATGACCTTTGCGGAGATTGTCACCCCCTT

CAACATTGACAGACTTCAAGAACTAGTGCGCAGGGGGAACAGCCAGTACCCA
GGCGCCAAGTACATCATCCGAGACAATGGTGATCGCATTGACTTGCGTTTCCA
CCCCAAGCCCAGTGACCTTCACCTGCAGACCGGCTATAAGGTGGAACGGCAC
ATGTGTGATGGGGACATTGTTATCTTCAACCGGCAGCCAACTCTGCACAAAAT
GTCCATGATGGGGCATCGGGTCCGCATTCTCCCATGGTCTACCTTTCGCTTGA
ATCTTAGTGTGACAACTCCGTACAATGCAGACTTTGACGGTGACGAAATGAAT
CTTCACCTGCCACAGTCTCTGGAGACGCGAGCAGAGATCCAGGAGCTGGCCA
TGGTTCCTCGCATGATTGTCACCCCCCAGAGCAATCGGCCTGTCATGGGTATT
GTGCAGGACACACTCACAGCAGTGCGCAAATTCACCAAGAGAGACGTCTTCC
TGGAGCGGGGTGAAGTGATGAACCTCCTGATGTTCCTGTCGACGTGGGATGG
GAAGGTCCCACAGCCGGCCATCCTAAAGCCCCGGCCCCTGTGGACAGGCAA
GCAAATCTTCTCCCTCATCATACCTGGTCACATCAATTGTATCCGTACCCACAG
CACCCATCCCGATGATGAAGACAGTGGCCCTTACAAGCACATCTCTCCTGGG
GACACCAAGGTGGTGGTGGAGAATGGGGAGCTGATCATGGGCATCCTGTGTA
AGAAGTCTCTGGGCACGTCAGCTGGCTCCCTGGTCCACATCTCCTACCTAGA
GATGGGTCATGACATCACTCGCCTCTTCTACTCCAACATTCAGACTGTCATTAA
CAACTGGCTCCTCATCGAGGGTCATACTATTGGCATTGGGGACTCCATTGCTG
ATTCTAAGACTTACCAGGACATTCAGAACACTATTAAGAAGGCCAAGCAGGAC
GTTATCGAAGTGATTGAAAAGGCACACAACAATGAGCTGGAGCCCACCCCAG
GGAACACTCTGCGGCAGACGTTTGAGAATCAGGTGAACCGCATTCTTAACGAT
GCCCGAGACAAGACTGGCTCCTCTGCTCAGAAATCCCTGTCTGAATACAACAA
CTTCAAGTCTATGGTCGTGTCCGGAGCTAAAGGTTCCAAGATTAACATCTCCC
AGGTCATTGCTGTCGTTGGACAGCAGAACGTCGAGGGCAAGCGGATTCCATT
TGGCTTCAAGCACCGGACTCTGCCTCACTTCATCAAGGATGACTACGGGCCT
GAGAGCCGTGGCTTTGTGGAGAACTCCTACCTAGCCGGCCTCACACCCACTG
AGTTCTTTTTCCACGCCATGGGGGGTCGTGAGGGGCTCATTGACACGGCTGT
CAAGACTGCTGAGACTGGATACATCCAGCGGCGGCTGATCAAGTCCATGGAG
TCAGTGATGGTGAAGTACGACGCGACTGTGCGGAACTCCATCAACCAGGTGG
TGCAGCTGCGCTACGGCGAAGACGGCCTGGCAGGCGAGAGCGTTGAGTTCC
AGAACCTGGCTACGCTTAAGCCTTCCAACAAGGCTTTTGAGAAGAAGTTCCGC
TTTGATTATACCAATGAGAGGGCCCTGCGGCGCACTCTGCAGGAGGACCTGG
TGAAGGACGTGCTGAGCAACGCACACATCCAGAACGAGTTGGAGCGGGAATT
TGAGCGGATGCGGGAGGATCGGGAGGTGCTCAGGGTCATCTTCCCAACTGG
AGACAGCAAGGTCGTCCTCCCCTGTAACCTGCTGCGGATGATCTGGAATGCT

CAGAAAATCTTCCACATCAACCCACGCCTTCCCTCCGACCTGCACCCCATCAA
AGTGGTGGAGGGAGTCAAGGAATTGAGCAAGAAGCTGGTGATTGTGAATGGG
GATGACCCACTAAGTCGACAGGCCCAGGAAAATGCCACGCTGCTCTTCAACA
TCCACCTGCGGTCCACGTTGTGTTCCCGCCGCATGGCAGAGGAGTTTCGGCT
CAGTGGGGAGGCCTTCGACTGGCTGCTTGGGGAGATTGAGTCCAAGTTCAAC
CAAGCCATTGCGCATCCCGGGGAAATGGTGGGGGCTCTGGCTGCGCAGTCC
CTTGGAGAACCTGCCACCCAGATGACCTTGAATACCTTCCACTATGCTGGTGT
GTCTGCCAAGAATGTGACGCTGGGTGTGCCCCGACTTAAGGAGCTCATCAAC
ATTTCCAAGAAGCCAAAGACTCCTTCGCTTACTGTCTTCCTGTTGGGCCAGTC
CGCTCGTGATGCTGAGAGAGCCAAGGATATTCTGTGCCGTCTGGAGCATACA
ACGTTGAGGAAGGTGACTGCCAACACAGCCATCTACTATGACCCCAACCCCC
AGAGCACGGTGGTGGCAGAGGATCAGGAATGGGTGAATGTCTACTATGAAAT
GCCTGACTTTGATGTGGCCCGAATCTCCCCCTGGCTGTTGCGGGTGGAGCTG
GATCGGAAGCACATGACTGACCGGAAGCTCACCATGGAGCAGATTGCTGAAA
AGATCAATGCTGGTTTTGGTGACGACTTGAACTGCATCTTTAATGATGACAATG
CAGAGAAGCTGGTGCTCCGTATTCGCATCATGAACAGTGATGAGAACAAGAT
GCAAGAAGAGGAAGAGGTGGTGGACAAGATGGATGATGATGTCTTCCTGCGC
TGCATCGAGTCCAACATGCTGACAGATATGACCCTGCAGGGCATCGAGCAGA
TCAGCAAGGTGTACATGCACTTGCCACAGACAGACAACAAGAAGAAGATCATC
ATCACGGAGGATGGGGAATTCAAGGCCCTGCAGGAGTGGATCCTGGAGACG
GACGGCGTGAGCTTGATGCGGGTGCTGTCAGAGAAAGACGTGGATCCAGTAC
GCACAACGTCGAATGACATTGTGGAGATCTTCACGGTGCTGGGCATTGAAGC
CGTGCGGAAGGCCCTGGAGCGGGAGCTGTACCACGTCATCTCCTTTGATGGC
TCCTATGTCAATTACCGACACTTGGCTCTCTTGTGTGATACCATGACCTGTCGT
GGCCACTTGATGGCCATCACCCGACACGGAGTCAACCGCCAGGACACAGGA
CCACTCATGAAGTGTTCCTTTGAGGAAACGGTGGACGTGCTTATGGAAGCAG
CCGCACACGGTGAGAGTGACCCCATGAAGGGGGTCTCTGAGAATATCATGCT
GGGCCAGCTGGCTCCGGCCGGCACTGGCTGCTTTGACCTCCTGCTTGATGCA
GAGAAGTGCAAGTATGGCATGGAGATCCCCACCAATATCCCCGGCCTGGGGG
CTGCTGGACCCACCGGCATGTTCTTTGGTTCAGCACCCAGTCCCATGGGTGG
AATCTCTCCTGCCATGACACCTTGGAACCAGGGTGCAACCCCTGCCTATGGC
GCCTGGTCCCCCAGTGTTGGGAGTGGAATGACCCCAGGGGCAGCCGGCTTC
TCTCCCAGTGCTGCGTCAGATGCCAGCGGCTTCAGCCCAGGTTACTCCCCTG

CCTGGTCTCCCACACCGGGCTCCCCGGGGTCCCCAGGTCCCTCAAGCCCCT
ACATCCCTTCACCAGGTGGTGCCATGTCTCCCAGC
1 TACTCGCCAACGTCACCTGCC
2 TACGAGCCCCGCTCTCCTGGGGGC
3 TACACACCCCAGAGTCCCTCT
4 TATTCCCCCACTTCACCCTCC
5 TACTCCCCTACCTCTCCATCC
6 TATTCTCCAACCAGTCCCAAC
7 TATAGTCCCACATCACCCAGC
8 TATTCGCCAACGTCACCCAGC
9 TACTCACCGACCTCTCCCAGC
10 TACTCACCCACCTCTCCCAGC
11 TACTCGCCCACCTCTCCCAGC
12 TACTCGCCCACCTCTCCCAGC
13 TACTCACCCACTTCCCCAGCC
14 TACTCGCCCACTTCCCCTAGC
15 TACTCGCCAACGTCTCCCAGC
16 TACTCGCCGACATCTCCCAGC
17 TACTCGCCAACTTCACCCAGC
18 TATTCTCCCACTTCTCCCAGC
19 TACTCACCTACCTCTCCAAGC
20 TATTCACCCACCTCCCCCAGC
21 TACTCACCCACTTCCCCAAGT
22 TACTCACCCACCAGCCCGAAC
23 TATTCTCCAACCAGTCCCAAT
24 TACACCCCAACATCACCCAGC
25 TACAGCCCGACATCACCCAGC
26 TATTCACCTACTAGTCCCAAC
27 TACACACCTACCAGCCCTAAC
28 TACAGCCCAACCTCTCCAAGC
29 TACTCTCCAACATCACCCAGC
30 TATTCCCCGACCTCACCAAGT
31 TACTCCCCTTCCAGCCCACGA
32 TACACACCACAGTCTCCAACC

33 TATACCCCAAGCTCACCCAGC

34 TACAGCCCCAGCTCGCCCAGC

35 TACAGCCCAACCTCACCCAAG

36 TACACCCCAACCAGTCCTTCT

37 TACAGTCCCAGCTCCCCAGAG

38 TATACCCCAACCTCTCCCAAG

39 TACTCACCTACCAGTCCCAAA

40 TATTCACCCACCTCTCCCAAG

41 TACTCGCCTACCAGTCCCACC

42 TATTCACCCACCACCCCAAAA

43 TACTCCCCAACATCTCCTACT

44 TATTCCCCAACCTCTCCAGTC

45 TACACCCCAACCTCTCCCAAG

46 TACTCACCTACTAGCCCCACT

47 TACTCGCCCACTTCCCCCAAG

48 TACTCGCCCACCAGCCCCACC

49 TACTCGCCCACCTCCCCCAAAGGCTCAACC

50 TACTCTCCCACTTCCCCTGGT

51 TACTCGCCCACCAGCCCCACC

52TACAGTCTCACAAGCCCGGCTATCAGCCCGGATGACAGTGACGAGGAGAA
CTGA

S7A-Rpb1 cDNA sequence:

CTD repeats are numbered and Ser7-containing repeats are highlighted in yellow. Ser7 to Ala mutations are in red.

GCATGCACGGGGGTGGCCCCCCCTCGGGGGACAGCGCATGCCCGCTGCGC
ACCATCAAGAGAGTCCAGTTCGGAGTCCTGAGTCCGGATGAACTGAAGCGAA
TGTCTGTGACGGAGGGTGGCATCAAATACCCAGAGACGACTGAGGGAGGCC
GCCCCAAGCTTGGGGGGCTGATGGACCCGAGGCAGGGGGTGATTGAGCGGA
CTGGCCGCTGCCAAACATGTGCAGGAAACATGACAGAGTGTCCTGGCCACTT
TGGCCACATTGAACTGGCCAAGCCTGTGTTTCACGTGGGCTTCCTGGTGAAG
ACAATGAAAGTTTTGCGCTGTGTCTGCTTCTTCTGCTCCAAACTGCTTGTGGA

CTCTAACAACCCAAAGATCAAGGATATCCTGGCTAAGTCCAAGGGACAGCCCA
AGAAGCGGCTCACACATGTCTACGACCTTTGCAAGGGCAAAAACATATGCGA
GGGTGGGGAGGAGATGGACAACAAGTTCGGTGTGGAACAACCTGAGGGTGA
CGAGGATCTGACCAAAGAAAAGGGCCATGGTGGCTGTGGGCGGTACCAGCC
CAGGATCCGGCGTTCTGGCCTAGAGCTGTATGCGGAATGGAAGCACGTTAAT
GAGGACTCTCAGGAGAAGAAGATCCTGCTGAGTCCAGAGCGAGTGCATGAGA
TCTTCAAACGCATCTCAGATGAGGAGTGTTTTGTGCTGGGCATGGAGCCCCG
CTATGCACGGCCAGAGTGGATGATTGTCACAGTGCTGCCTGTGCCCCCGCTC
TCCGTGCGGCCTGCTGTTGTGATGCAGGGCTCTGCCCGTAACCAGGATGACC
TGACTCACAAACTGGCTGACATCGTGAAGATCAACAATCAGCTGCGGCGCAAT
GAGCAGAACGGCGCAGCGGCCCATGTCATTGCAGAGGATGTGAAGCTCCTC
CAGTTCCATGTGGCCACCATGGTGGACAATGAGCTGCCTGGCTTGCCCCGTG
CCATGCAGAAGTCTGGGCGTCCCCTCAAGTCCCTGAAGCAGCGGTTGAAGGG
CAAGGAAGGCCGGGTGCGAGGGAACCTGATGGGCAAAAGAGTGGACTTCTC
GGCCCGTACTGTCATCACCCCCGACCCCAACCTCTCCATTGACCAGGTTGGC
GTGCCCCGCTCCATTGCTGCCAACATGACCTTTGCGGAGATTGTCACCCCCTT
CAACATTGACAGACTTCAAGAACTAGTGCGCAGGGGGAACAGCCAGTACCCA
GGCGCCAAGTACATCATCCGAGACAATGGTGATCGCATTGACTTGCGTTTCCA
CCCCAAGCCCAGTGACCTTCACCTGCAGACCGGCTATAAGGTGGAACGGCAC
ATGTGTGATGGGGACATTGTTATCTTCAACCGGCAGCCAACTCTGCACAAAAT
GTCCATGATGGGGCATCGGGTCCGCATTCTCCCATGGTCTACCTTTCGCTTGA
ATCTTAGTGTGACAACTCCGTACAATGCAGACTTTGACGGTGACGAAATGAAT
CTTCACCTGCCACAGTCTCTGGAGACGCGAGCAGAGATCCAGGAGCTGGCCA
TGGTTCCTCGCATGATTGTCACCCCCCAGAGCAATCGGCCTGTCATGGGTATT
GTGCAGGACACACTCACAGCAGTGCGCAAATTCACCAAGAGAGACGTCTTCC
TGGAGCGGGGTGAAGTGATGAACCTCCTGATGTTCCTGTCGACGTGGGATGG
GAAGGTCCCACAGCCGGCCATCCTAAAGCCCCGGCCCCTGTGGACAGGCAA
GCAAATCTTCTCCCTCATCATACCTGGTCACATCAATTGTATCCGTACCCACAG
CACCCATCCCGATGATGAAGACAGTGGCCCTTACAAGCACATCTCTCCTGGG
GACACCAAGGTGGTGGTGGAGAATGGGGAGCTGATCATGGGCATCCTGTGTA
AGAAGTCTCTGGGCACGTCAGCTGGCTCCCTGGTCCACATCTCCTACCTAGA
GATGGGTCATGACATCACTCGCCTCTTCTACTCCAACATTCAGACTGTCATTAA
CAACTGGCTCCTCATCGAGGGTCATACTATTGGCATTGGGGACTCCATTGCTG
ATTCTAAGACTTACCAGGACATTCAGAACACTATTAAGAAGGCCAAGCAGGAC

GTTATCGAAGTGATTGAAAAGGCACACAACAATGAGCTGGAGCCCACCCCAG
GGAACACTCTGCGGCAGACGTTTGAGAATCAGGTGAACCGCATTCTTAACGAT
GCCCGAGACAAGACTGGCTCCTCTGCTCAGAAATCCCTGTCTGAATACAACAA
CTTCAAGTCTATGGTCGTGTCCGGAGCTAAAGGTTCCAAGATTAACATCTCCC
AGGTCATTGCTGTCGTTGGACAGCAGAACGTCGAGGGCAAGCGGATTCCATT
TGGCTTCAAGCACCGGACTCTGCCTCACTTCATCAAGGATGACTACGGGCCT
GAGAGCCGTGGCTTTGTGGAGAACTCCTACCTAGCCGGCCTCACACCCACTG
AGTTCTTTTTCCACGCCATGGGGGGTCGTGAGGGGCTCATTGACACGGCTGT
CAAGACTGCTGAGACTGGATACATCCAGCGGCGGCTGATCAAGTCCATGGAG
TCAGTGATGGTGAAGTACGACGCGACTGTGCGGAACTCCATCAACCAGGTGG
TGCAGCTGCGCTACGGCGAAGACGGCCTGGCAGGCGAGAGCGTTGAGTTCC
AGAACCTGGCTACGCTTAAGCCTTCCAACAAGGCTTTTGAGAAGAAGTTCCGC
TTTGATTATACCAATGAGAGGGCCCTGCGGCGCACTCTGCAGGAGGACCTGG
TGAAGGACGTGCTGAGCAACGCACACATCCAGAACGAGTTGGAGCGGGAATT
TGAGCGGATGCGGGAGGATCGGGAGGTGCTCAGGGTCATCTTCCCAACTGG
AGACAGCAAGGTCGTCCTCCCCTGTAACCTGCTGCGGATGATCTGGAATGCT
CAGAAAATCTTCCACATCAACCCACGCCTTCCCTCCGACCTGCACCCCATCAA
AGTGGTGGAGGGAGTCAAGGAATTGAGCAAGAAGCTGGTGATTGTGAATGGG
GATGACCCACTAAGTCGACAGGCCCAGGAAAATGCCACGCTGCTCTTCAACA
TCCACCTGCGGTCCACGTTGTGTTCCCGCCGCATGGCAGAGGAGTTTCGGCT
CAGTGGGGAGGCCTTCGACTGGCTGCTTGGGGAGATTGAGTCCAAGTTCAAC
CAAGCCATTGCGCATCCCGGGGAAATGGTGGGGGCTCTGGCTGCGCAGTCC
CTTGGAGAACCTGCCACCCAGATGACCTTGAATACCTTCCACTATGCTGGTGT
GTCTGCCAAGAATGTGACGCTGGGTGTGCCCCGACTTAAGGAGCTCATCAAC
ATTTCCAAGAAGCCAAAGACTCCTTCGCTTACTGTCTTCCTGTTGGGCCAGTC
CGCTCGTGATGCTGAGAGAGCCAAGGATATTCTGTGCCGTCTGGAGCATACA
ACGTTGAGGAAGGTGACTGCCAACACAGCCATCTACTATGACCCCAACCCCC
AGAGCACGGTGGTGGCAGAGGATCAGGAATGGGTGAATGTCTACTATGAAAT
GCCTGACTTTGATGTGGCCCGAATCTCCCCCTGGCTGTTGCGGGTGGAGCTG
GATCGGAAGCACATGACTGACCGGAAGCTCACCATGGAGCAGATTGCTGAAA
AGATCAATGCTGGTTTTGGTGACGACTTGAACTGCATCTTTAATGATGACAATG
CAGAGAAGCTGGTGCTCCGTATTCGCATCATGAACAGTGATGAGAACAAGAT
GCAAGAAGAGGAAGAGGTGGTGGACAAGATGGATGATGATGTCTTCCTGCGC
TGCATCGAGTCCAACATGCTGACAGATATGACCCTGCAGGGCATCGAGCAGA

TCAGCAAGGTGTACATGCACTTGCCACAGACAGACAACAAGAAGAAGATCATC
ATCACGGAGGATGGGGAATTCAAGGCCCTGCAGGAGTGGATCCTGGAGACG
GACGGCGTGAGCTTGATGCGGGTGCTGTCAGAGAAAGACGTGGATCCAGTAC
GCACAACGTCGAATGACATTGTGGAGATCTTCACGGTGCTGGGCATTGAAGC
CGTGCGGAAGGCCCTGGAGCGGGAGCTGTACCACGTCATCTCCTTTGATGGC
TCCTATGTCAATTACCGACACTTGGCTCTCTTGTGTGATACCATGACCTGTCGT
GGCCACTTGATGGCCATCACCCGACACGGAGTCAACCGCCAGGACACAGGA
CCACTCATGAAGTGTTCCTTTGAGGAAACGGTGGACGTGCTTATGGAAGCAG
CCGCACACGGTGAGAGTGACCCCATGAAGGGGGTCTCTGAGAATATCATGCT
GGGCCAGCTGGCTCCGGCCGGCACTGGCTGCTTTGACCTCCTGCTTGATGCA
GAGAAGTGCAAGTATGGCATGGAGATCCCCACCAATATCCCCGGCCTGGGGG
CTGCTGGACCCACCGGCATGTTCTTTGGTTCAGCACCCAGTCCCATGGGTGG
AATCTCTCCTGCCATGACACCTTGGAACCAGGGTGCAACCCCTGCCTATGGC
GCCTGGTCCCCCAGTGTTGGGAGTGGAATGACCCCAGGGGCAGCCGGCTTC
TCTCCCAGTGCTGCGTCAGATGCCAGCGGCTTCAGCCCAGGTTACTCCCCTG
CCTGGTCTCCCACACCGGGCTCCCCGGGGTCCCCAGGTCCCTCAAGCCCCT
ACATCCCTTCACCAGGTGGTGCCATGTCTCCCAGC
1 TACTCGCCAACGTCACCTGCC
2 TACGAGCCCCGCTCTCCTGGGGGC
3 TACACACCCCAGAGTCCCGCT
4 TATTCCCCCACTTCACCCGCC
5 TACTCCCCTACCTCTCCAGCC
6 TATTCTCCAACCAGTCCCAAC
7 TATAGTCCCACATCACCCGCC
8 TATTCGCCAACGTCACCCGCC
9 TACTCACCGACCTCTCCCGCC
10 TACTCACCCACCTCTCCCGCC
11 TACTCGCCCACCTCTCCCGCC
12 TACTCGCCCACCTCTCCCGCC
13 TACTCACCCACTTCCCCAGCC
14 TACTCGCCCACTTCCCCTAGC
15 TACTCGCCAACGTCTCCCAGC
16 TACTCGCCGACATCTCCCGCC
17 TACTCGCCAACTTCACCCGCC

18 TATTCTCCCACTTCTCCCGCC
19 TACTCACCTACCTCTCCAGCC
20 TATTCACCCACCTCCCCCGCC
21 TACTCACCCACTTCCCCAGCA
22 TACTCACCCACCAGCCCGAAC
23 TATTCTCCAACCAGTCCCAAT
24 TACACCCCAACATCACCCGCC
25 TACAGCCCGACATCACCCGCC
26 TATTCACCTACTAGTCCCAAC
27 TACACACCTACCAGCCCTAAC
28 TACAGCCCAACCTCTCCAGCC
29 TACTCTCCAACATCACCCGCC
30 TATTCCCCGACCTCACCAGCA
31 TACTCCCCTTCCAGCCCACGA
32 TACACACCACAGTCTCCAACC
33 TATACCCCAAGCTCACCCGCC
34 TACAGCCCCAGCTCGCCCGCC
35 TACAGCCCAACCTCACCCAAG
36 TACACCCCAACCAGTCCTGCT
37 TACAGTCCCAGCTCCCCAGAG
38 TATACCCCAACCTCTCCCAAG
39 TACTCACCTACCAGTCCCAAA
40 TATTCACCCACCTCTCCCAAG
41 TACTCGCCTACCAGTCCCACC
42 TATTCACCCACCACCCCAAAA
43 TACTCCCCAACATCTCCTACT
44 TATTCCCCAACCTCTCCAGTC
45 TACACCCCAACCTCTCCCAAG
46 TACTCACCTACTAGCCCCACT
47 TACTCGCCCACTTCCCCCAAG
48 TACTCGCCCACCAGCCCCACC
49 TACTCGCCCACCTCCCCCAAAGGCTCAACC
50 TACTCTCCCACTTCCCCTGGT
51 TACTCGCCCACCAGCCCCACC

52TACAGTCTCACAAGCCCGGCTATCAGCCCGGATGACAGTGACGAGGAGAA
CTGA

For lentivirus production in Phoenix cells, pCMV-VSV-G and psPAX2 plasmids were used. pCMV-VSV-G plasmid (631530, Clonetech) expresses the G glycoprotein of the vesicular stomatitis virus (VSV-G), which mediates fusion of viral and cellular membranes, under the control of the CMV promoter. It expresses the Ampicillin resistance gene for selection in bacteria. psPAX2 (12260, Addgene) is a lentiviral packaging plasmid. It expresses the Ampicillin resistance gene for selection in bacteria.

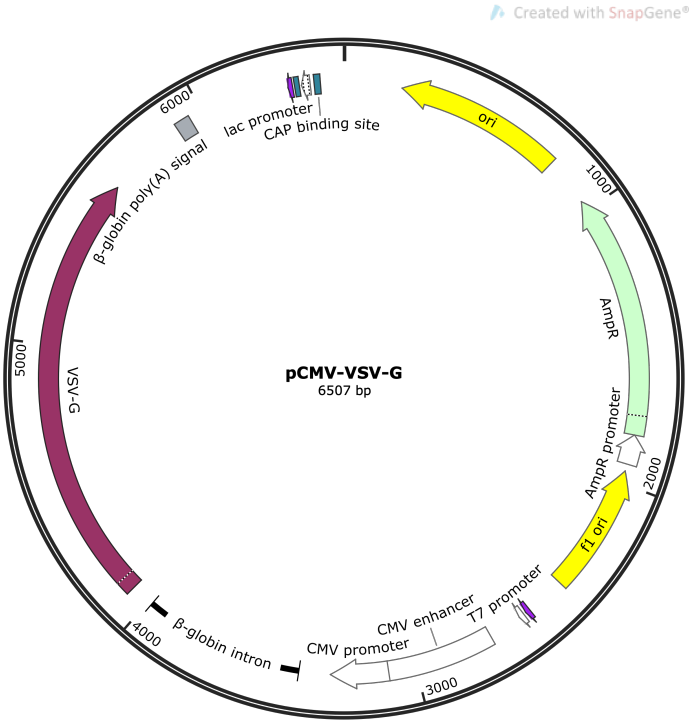
Created with SnapGene®
pCMV-VSV-G
6507 bp
lac promoter
CAP binding site
ori
AmpR
AmpR promoter
f1 ori
T7 promoter
CMV enhancer
CMV promoter
β-globin intron
VSV-G
β-globin poly(A) signal
1000
2000
3000
4000
5000
6000

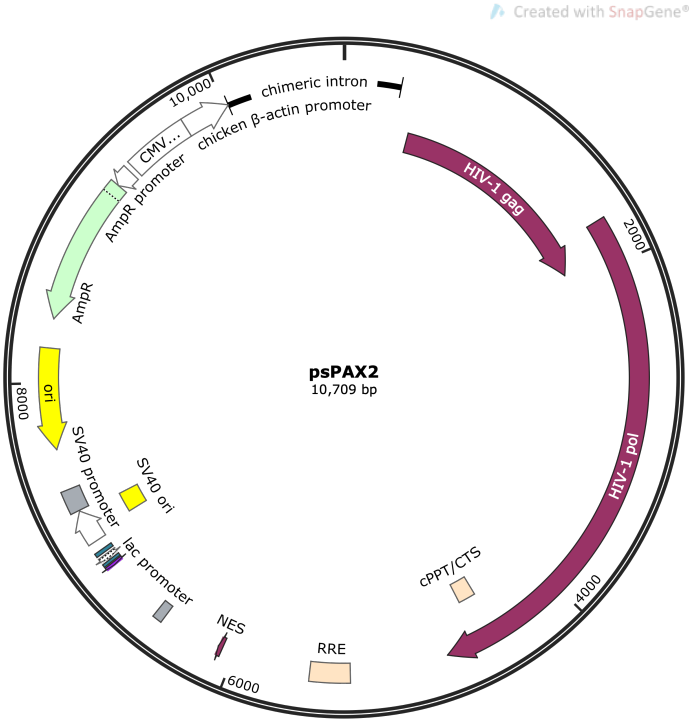
Created with SnapGene®
psPAX2
10,709 bp
chimeric intron
chicken β-actin promoter
CMV...
AmpR promoter
AmpR
ori
SV40 promoter
SV40 ori
lac promoter
NES
RRE
cPPT/CTS
HIV-1 pol
HIV-1 gag
2000
4000
6000
8000
10,000

2.17 Stable cell line generation

MRTF-A/MRTF-B knock-out MEF cells reconstituted with wild-type MRTF-A (dKO^{MRTF}), MRTF fused to an additional NLS ($dKO^{MRTF\text{-}NLS}$) or MRTF harbouring point mutations in its RPEL domain ($dKO^{MRTF\text{-}XXX}$) were generated through lentiviral infection. MEF cells with the genotype MRTF-$A^{-/-}$, MRTF-B $^{fl/fl}$, 6-Gt(Rosa)26$Sor^{tm9(cre/ESR1)Arte}$ were seeded at 25% confluence and treated with 1 μM tamoxifen to achieve MRTF-B knock-out and simultaneously infected with virus, containing MRTF-A-expressing plasmids.

Phoenix cells were transfected with 0.6 μg pCMV-VSV-G plasmid, 3 μg psPAX2 plasmid and 6 μg pMY-MRTF, pMY-MRTF-NLS, pMY-MRTF-XXX or pMY plasmid, using Fugene transfection reagent (E2311, Promega), as described in section 2.4. Transfected cells were incubated overnight at 37^0C, 5% CO_2. 24h post-transfection, media was aspirated and replaced with fresh DMEM, supplemented with 10% FBS. Virus was harvested 48h post-transfection. Viral supernatant was centrifuged at 500g for 5 min, filtered through a 0.45 um PES filter, diluted 1:4 in DMEM, mixed with polybrene at 10 μg/ml and used to infect MEF cells. Three consecutive infections 24h apart were carried out. Cells were expanded, genotyped to confirm MRTF-B knock-out and FACS sorted to select GFP-positive cells. MRTF protein levels were assessed by Western blot. Cell sorting by FACS was performed by the staff at the FACS STP.

Flp-in NIH3T3 cells (R76107, Invitrogen) were transfected with 3 μg pCDNA6/TR plasmid using Fugene, as described in section 2.4. Cells expressing the Tet repressor were selected using blasticidin at 3 μg/ml and zeocin at 100 μg/ml to generate Flp-in TR cells. Flp-in TR cells were co-transfected with 4.5 μg pOG44 and 500 ng pFRT-Rpb1-TO or pFRT-S7A-TO plasmids using Fugene, as described in section 2.4. Transfected cells were selected using 100 μg/ml hygromycin and 3 μg/ml blasticidin. Clonal Flp-in TR-Rbp1 and Flp-in-TR-S7A lines were generated by expanding colonies from single cells in a 96-well plate. Cells sensitivity to zeocin was tested and inducibility of expression of the Rpb1 or S7A-Rbp1 was tested by Western blot.

2.18 Genotyping

Genomic DNA extraction was performed using DNeasy Blood and Tissue Kit (69506, Qiagen), according to the manufacturer's instructions. Genotyping PCR reactions were set up using BIOTAQ DNA polymerase (BIO-21040, Bioline) as follows: 100 ng genomic DNA, 0.2 µM primer, 5 units BIOTAQ polymerase, 1X BIOTAQ buffer, 200 µM dNTPs, 3 mM $MgCl_2$ in a total volume of 50 ul. For MRTF-A genotyping, primers GT5, GT6 and lacZ3-Q8 were used with following cycling conditions: 94^0C 5 min - 30x (94^0C 30 sec – 57^0C 30 sec – 72^0C 1 min) – 72^0C 10 min – 4^0C. For a wild-type MRTF-A allele a fragment of 600 bp is generated by primers GT5 and GT6, while a fragment of 350 bp is generated by primers GT5 and lacZ3-Q8 for the knock-out allele. For MRTF-B primers LAF, EXR and SAR were used with the following cycling conditions: 94^0C 5 min - 30x (94^0C 30 sec – 70^0C 30 sec – 72^0C 1 min) – 72^0C 10 min – 4^0C. For a wild-type MRTF-B allele, a fragment of 460 bp is generated by primers LAF and EXR, a fragment of 570 bp is generated by primers LAF and EXR for the loxP allele and a fragment of 360 bp is generated by primers LAF and SAR for the knock-out allele.

2.19 List of primers

Genotyping primers	Sequence
GT5	GTTGCTCAGTCATGTGACACCTGTACAG
GT6	GGCTTCAGTACCTTCCTAAGCTCTGCAG
lacZ3-Q8	CATGGTGGATCCTGAGACTGGCGAATTC
EXR	GGCTTAGACAAGATGGTTGGTCTGGCACTGC
LAF	CCAGTGGTGTCCAGTCTTACTGAACAGCTCACTCAG
SAR	CATGGCGACTTCCTTCTCCTCTTCTCAAGGCTG

ChIP primers	Sequence
Acta2(-1kb) FP	CCTGCAAGCCAAGGTTCTGA
Acta2(-1kb) RP	GCACTCCCAGAATCCATCCA
Acta2(-0.3kb) FP	GAGGCCTGGGTCTCTTCCA
Acta2(-0.3kb) RP	GCTGAGCTGCCTCCTGTTTC
Acta2(TSS) FP	CATTCAGATTCCCACAGACAATG
Acta2(TSS) RP	TCGAGTTTTCCCAGGCTCTTT
Acta2(2.8kb) FP	CCCACGATGGATGGGAAA
Acta2(2.8kb) RP	CGGCTTCGCTGGTGATG
Acta2(6.6kb) FP	AGAGGAGCGTGGTAATCTGTTCTT
Acta2(6.6kb) RP	GAACATCCCTGTCCCTTTCCA
Acta2(12.3kb) FP	ACTGGACCCCTGAGTTTCACA
Acta2(12.3kb) RP	GGCAAGCCTCAATTCTCCAA
Acta2(14.1kb) FP	ATACGCAAGGCTTGATGCAA
Acta2(14.1kb) RP	AAGCATACACACGTGCATGGA
Acta2(16.3kb) FP	CCGTATTTGAATCTGCAACATTCT
Acta2(16.3) RP	TATAACACAAGAGCAAATGGCTGAA
Actb (-1kb) FP	TCCCCCTCACCTAAGTACCAG
Actb (-1kb) RP	CTGACCCCGTGTGTAGCTC
Actb FP	GCCGCCGGGTTTTATAGG
Actb RP	CGTTCCGAAAGTTGCCTTTTA
Actb (TSS) FP	AGGAGCTGCAAAGAAGCTGT
Actb (TSS) RP	CCGCTGTGGCGTCCTATAAA
Actb (1Kb) FP	GGCTTTGCACATGCCGGA
Actb (1Kb) RP	CTTTTGTGTCTTGATAGTTCGCCA
Actb (2Kb) FP	CGGAGTCCATCACAATGCCT
Actb (2Kb) RP	GCCATGTACGTAGCCATCCA
Actb (3.1kb) FP	GCCTTCACCGTTCCAGTTTT
Actb (3.1kb) RP	TGAGCTGCGTTTTACACCCT
Actb (4.1kb) FP	GTCCAAGGATCACGACTGACA
Actb (4.1kb) RP	CATCCTGGAAATCAGCCCCT
Actg1 FP	AACGCGGTGCACGAGAAG
Actg1 RP	TCACACTGCCCAGTTGCAA
Col1a1 FP	CCAGGAGGGCATATGGAAGA
Col1a1 RP	GTCCTCAGCCCCTTATTTGGT
Mir145-143 FP	CCTTGCCCGTGGCTCTCT
Mir145-143 RP	AGGCTCGTTTCTTCAGCTCATATAA
FilaminA FP	TGAGCTCAGCGCTCTGTGAA
FilaminA RP	GCTCTGGAGGTGAGCCCTACT
Zfp37 FP	CCAGCAATGTGTGACTTGGATC

Zfp37 RP	TATTTCGAGCGCTGTGGCA
Vcl (-1kb) FP	CGAGGTCCCCTCTCTCTGG
Vcl (-1kb) RP	TCCGCAGGATCACCTCAGTA
Vcl (TSS) FP	GAGGGAAGCCCGGACTCTA
Vcl (TSS) RP	AAAACTGGGATCCGTAGGGC
Vcl (40kb) FP	AGGTGCTACCAGGTTTCACTAA
Vcl (40kb) RP	ACCATTCACTGGCTTCGAGT
Vcl (104kb) FP	CGTGAACACTAGCCGGAAGC
Vcl (104kb) RP	AAAGGGAGTTGGTGAACCGT
Vcl (106kb) FP	ATTCCGAGGTTAGGCTTGGC
Vcl (106kb) RP	TTGGGCTTAGCCAGGAACTT

Expression primers	Sequence
Gadph FP	TCTTGTGCAGTGCCAGCCT
Gadph RP	CAATATGGCCAAATCCGTTCA
Ctgf Intron FP	GCTCCTCGCTCTCTGCAC
Ctgf Intron RP	TGTGATCGCAGCTCACTCTG
Ctgf Exon FP	GGAGGAAAACATTAAGAAGGGCAA
Ctgf Exon RP	AACTTGACAGGCTTGGCGAT
Vcl Intron FP	CGTCACTTGCGTTGAGTACC
Vcl Intron RP	GAAACCACCCACAGGTTGGA
Vcl Exon FP	ACGGCTCTAGGGGAATCCTT
Vcl Exon RP	TTACGAACCTCAGCCTCATCG
Srf Intron FP	TCAAGGCAGCAGCAGTTTCT
Srf Intron RP	CAGGCAGGGTTAGGAACCAG
Srf Exon FP	TGAAGAAGGCCTATGAGCTGTC
Srf Exon RP	ACACATGGCCTGTCTCACTG
Acta2 Intron FP	CCAGAAGCAATGCGTCCACT
Acta2 Intron RP	TGAGGTAGTTGCCTGCTCTC
Acta2 Exon FP	CTGTCAGGAACCCTGAGACGC
Acta2 Exon RP	GGCTGTGCTGTCTTCCTCTT
Cyr61 Intron FP	CGTAAACTGCCCTGAGCCTA
Cyr61 Intron RP	GACGCGATCGAGACACTTCT
Cyr61 Exon FP	ATCGCAATTGGAAAAGGCAGC
Cyr61 Exon RP	GGTGCCAAAGACAGGAAGCCT
Actb Intron FP	CGTAGCGTCTGGTTCCCAAT

Actb Intron RP	GTGTGGGCATTTGATGAGCC
Actb Exon FP	CGCCACCAGTTCGCCAT
Actb Exon RP	CTTTGCACATGCCGGAGC
Egr1 Intron FP	TGATGTCTCCGCTGCAGATC
Egr1 Intron RP	GGTGGGTGAGTGAGGAAAGG
Egr1 Exon FP	ATTGATGTCTCCGCTGCAGATC
Egr1 Exon RP	TCAGCAGCATCATCTCCTCCA
Fos Intron FP	GCATGGGCTCTCCTGTCAA
Fos Intron RP	GACCTGGCGGCTACACAAA
Fos Exon FP	TTCCTACTACCATTCCCCAGCC
Fos Exon RP	GATCTGCGCAAAAGTCCTGTG
B2m Intron FP	TGGGCTGGAACAGAGAAACC
B2m Intron RP	CCTCAGGTGGCAGGTGTTAG
Pbgd Intron FP	CTGGCCAAGGAGGTTCTGAG
Pbgd Intron RP	ATCATTTTGCCCACCTGGCT
Hprt Intron FP	TTCAGCAGTAAGACGCAGCA
Hprt Intron RP	GCTACAAGAGGGTATGTAGAGCA
Rps16 Intron FP	CCCCGGGATGATAGGGAGTT
Rps16 Intron RP	GCCCAGGTTAAGGTCTACCG
Mtr4 Exon FP	GAAATGGAAGGGGCCACCAG
Mtr4 Exon RP	GTATCCAGTCGTTTCCCGGC
Ars2 Exon FP	CATCTTGGGCTATGGAGTCCC
Ars2 Exon RP	AGCATCATAGTTCCCACGGC
Dis3 Exon FP	GCACCAGATTGATGTCCTCG
Dis3 Exon RP	CGCTCCGGTTTCTCACTTCT
Zcchc8 Exon FP	CGCGCCGAGAATCAAGAACT
Zcchc8 Exon RP	ACCACTGGGTCTTGTCAGAA
Rmb7 Exon FP	CGGCAAGCAGTGATGAACAG
Rmb7 Exon RP	GATCCGCATGTGGAGAACCA
Ncbp1 Exon FP	GCTAGCAACTCAGATCGGCT
Ncbp1 Exon RP	TGTGAGGTTGTCCACCATCG
Zc3h18 Exon FP	TGAGGAGCGAAAAGGCTGAG
Zc3h18 Exon RP	CCCACAGATCTCAACGCGAA
Nrde2 Exon FP	CACCACCGCCAAGGAGTC
Nrde2 Exon RP	TCGCTAGTGTTGCTCTCACC
Zfc3h1 Exon FP	CAGTTCTCCAGCGCCTTCA
Zfc3h1 Exon RP	GCTGGTGGAGGCAAAGAAAC
Pabpn1 Exon FP	CCATCCCAAAGGGTTTGCAT
Pabpn1 Exon RP	GGGACGTCCTCACTGACTCT

2.20 List of siRNA

Target	Catalogue Number
Dis3	L-048884-01-0005
Dis3l	L-054584-01-0005
Dis3l2	L-054755-01-0005
Eri1	L-059530-02-0005
Eri2	L-059795-01-0005
Eri3	L-049763-01-0005
Exosc1	L-064024-01-0005
Exosc2	L-064407-01-0005
Exosc3	L-064537-01-0005
Exosc4	L-063925-01-0005
Exosc5	L-064420-01-0005
Exosc6	L-064503-01-0005
Exosc7	L-062387-00-0005
Exosc8	L-064119-01-0005
Exosc9	L-040354-01-0005
Exosc10	L-049286-00-0005
Xrn1	L-046621-01-0005
Xrn2	L-046490-01-0005
Nrd1	L-061245-01-0005
Setx	L-066634-00-0005
Smg6	L-066166-01-0005
Dcp1a	L-065144-01-0005
Dcp1b	L-056964-00-0005
Dcp2	L-040353-01-0005
Dcps	L-046656-01-0005
Nudt16	L-048777-01-0005
Zcchc7	L-056810-02-0005
Papd5	L-061333-01-0005
Mtr4	L-058707-01-0005
Zcchc8	L-057599-01-0005
Rmb7	L-055957-01-0005
Dom3z	L-050491-01-0005
Ncbp1	L-160309-00-0005
Ars2	L-045428-02-0005
Zc3h18	L-066066-01-0005
Srf	L-050116-01-0005

Scrambled	D-001810-10
Swt1	L-050799-01-0005
Zfc3h1	L-063190-01-0005
Pabpn1	L-045150-01-0005
Nrde2	L-066291-01-0005
Rpb1	D-011186-03-0020
Rpb1	D-011186-05-0020

2.21 List of antibodies

ChIP and IP antibodies	Catalogue Number	Concentration
MRTF-A	sc-21558, Santa Cruz	5 ug
SRF	16821-1-AP, Proteintech	3 ug
Rpb1	14958S, Cell Signalling	10 ug
phospho-Ser5 CTD	61085, Active Motif	10 ug
phospho-Ser2 CTD	61083, Active Motif	10 ug
phospho-Ser7 CTD	61087, Active Motif	10 ug
phospho-Thr4 CTD	61361, Active Motif	10 ug
phospho-Tyr1 CTD	61383, Active Motif	10 ug
CDK9	2316, Cell Signalling	10 ug
Spt5	sc-28678, Santa Cruz	10 ug
NELF-E	10705-1-AP, Proteintech	10 ug
Total H3	ab1791, Abcam	3 ug
H3K4me3	ab8580, Abcam	3 ug
H3K27Ac	ab4729, Abcam	3 ug
H3K36me3	ab9050, Abcam	3 ug
H3K79me3	ab2621, Abcam	3 ug
HA	11867431001, Roche	5 ug
IgG	ab6703, Abcam	3 ug
Mtr4	nb100-1574, Novus	10 ug

IF antibodies and dyes	Catalogue Number	Concentration
HA	MMS-101R-500, Cambridge Bioscience	1/1000
Phalloidin	T7471, Life technologies	1/40
MRTF	sc-21558, Santa Cruz	1/50

WB antibodies	Catalogue Number	Concentration
HA	11867431001, Roche	1/1000
MRTF	sc-21558, Santa Cruz	1/1000
tubulin	T5162, Sigma	1/10000
Rpb1	14958S, Cell Signalling	1/1000
phospho-Ser5 CTD	Dirk Eick laboratory	1/5000
phospho-Ser2 CTD	Dirk Eick laboratory	1/5000
phospho-Ser7 CTD	Dirk Eick laboratory	1/2000
phospho-Thr4 CTD	Dirk Eick laboratory	1/500
phospho-Tyr1 CTD	Dirk Eick laboratory	1/500
SRF	16821-1-AP, Proteintech	1/1000
Mtr4	nb100-1574, Novus	1/1000
Gapdh	sc-25778, Santa Cruz	1/1000
α-actin	sc-56499, Santa Cruz	1/1000
β-actin	sc-47778, Santa Cruz	1/1000

Chapter 3. Nuclear MRTF induces non-productive RNA synthesis

MRTF responds to changes in actin dynamics to regulate cytoskeletal genes. In NIH3T3 fibroblasts, the majority of MRTF binding sites are bound by MRTF-A and MRTF-B homodimers or heterodimers, recruited in association with SRF. Even though at some loci SRF is constitutively bound, these are predominantly TCF-associated, whereas inducible SRF binding reflects MRTF recruitment. 683 SRF/MRTF target genes were identified as induced by serum, bound by SRF and MRTF and sensitive to CD or LatB treatment. These include the *Acta2*, *Actb* and *Actg1* genes, genes associated with F-actin, actomyocin, focal adhesion and extracellular matrix (Esnault et al., 2014).

MRTF directly interacts with monomeric G-actin through an RPEL domain located at the N-terminus of the protein and this interaction controls the localization of MRTF in the cell (Guettler et al., 2008; Hirano & Matsuura, 2011; Miralles et al., 2003; Mouilleron et al., 2011; Pawłowski et al., 2010; Vartiainen et al., 2007). While depletion of the G-actin pool promotes MRTF-importin interaction and nuclear import, G-actin binding to MRTF promotes its export through the Crm1 nuclear export receptor (Hirano & Matsuura, 2011; Mouilleron et al., 2008; Mouilleron et al., 2011; Panayiotou et al., 2016; Pawłowski et al., 2010; Vartiainen et al., 2007).

In addition to controlling MRTF subcellular localization, G-actin also regulates its nuclear activity. MRTF directly interacts with actin in the nucleus (Vartiainen et al., 2007) and MRTF activity is promoted by NLS-tagged mutant actins G15S and S14C, which promote F-actin formation, while over-expression of NLS-actin inhibits MRTF target genes (Kokai et al., 2014; Posern et al., 2004; Sharili et al., 2016). Similarly, the mDia formin and nucleoskeletal proteins such as the LINC complex, which mediate actin polymerization in the nucleus, stimulate MRTF activity (Baarlink et al., 2013; Plessner et al., 2015), and so does the monooxygenase MICAL2, which causes nuclear G-actin depletion (Lundquist et al., 2014).

In NIH3T3 mouse fibroblasts, even though the transcriptional activation following serum stimulation is transient, MRTF remains in the nucleus for hours (Vartiainen et al., 2007). Thus, nuclear accumulation of MRTF in the absence of an activating signal is not sufficient for target gene activation. Fusing MRTF with an additional NLS or blocking Crm1-mediated nuclear export by LMB does not elicit a transcriptional response. Nevertheless, nuclear MRTF is recruited to target genes (Vartiainen et al., 2007). In contrast, MRTF mutant protein harbouring point mutations in its RPEL motifs (MRTF-XXX), making it insensitive to G-actin, is not only constitutively nuclear, but also constitutively transcriptionally active (Miralles et al., 2003; Vartiainen et al., 2007).

This data demonstrates a repressive effect of nuclear actin on MRTF activity, however the exact mechanism is unclear. In this chapter, to investigate the nuclear regulation of MRTF, Crm1 inhibition by LMB was used to induce nuclear accumulation of MRTF in the absence of an activating signal.

3.1 Nuclear MRTF does not activate target gene expression

To study the inhibitory role of G-actin in the MRTF-mediated transcriptional response, recruitment of nuclear MRTF to target genes and its ability to activate transcription was examined in cells treated with the Crm1 inhibitor LMB.

First, the effect of actin-binding agents on MRTF subcellular localization was assessed by immunofluorescence in NIH3T3 cells. Cells were treated with serum, which activates Rho signaling and actin polymerization; CD, which directly disrupts the MRTF/G-actin interaction; LatB, which increases the cellular concentration of G-actin; or LMB, which does not affect the actin treadmilling cycle but prevents MRTF export from the nucleus. Following treatment, cells were fixed and an MRTF antibody was used to visualize the transcription factor. In addition, cells were stained with Phalloidin, to examine the effect of the treatment on F-actin, and DAPI, to visualize the nucleus. Results are shown in Figure 27.

In unstimulated cells, MRTF was found predominantly in the cytoplasm, whereas serum shock caused MRTF nuclear accumulation, consistent with previous studies (Miralles et al., 2003; Vartiainen et al., 2007). Both CD and LatB disrupted actin filaments, as visualized by Phalloidin staining, but had opposing effects on MRTF localization. While CD treatment caused nuclear translocation of MRTF, MRTF remained cytoplasmic upon LatB treatment. Following LMB treatment, MRTF was found predominantly in the nucleus. Subsequent stimulation of LMB-treated cells with FCS, CD or LatB did not alter MRTF subcellular localization.

As previously reported, inhibition of Crm1 causes nuclear accumulation of MRTF, without disrupting actin filaments (Vartiainen et al., 2007). Furthermore, subsequent stimulation of LMB pre-treated cells with CD or LatB disrupts actin filaments, without affecting MRTF localization, which would allow us to study the role of G-actin in regulation of MRTF activity in the nucleus.

Next, MRTF target gene expression was examined in the same conditions. To assess the relative transcription rate at endogenous MRTF-SRF target genes,

qPCR probes targeting the first intron of the gene were used to measure pre-mRNA levels. The specificity of the treatments for MRTF target genes was tested by examining pre-mRNA levels at the *Egr1* gene. Although serum-inducible, *Egr1* is activated by ERK signalling to the TCF family of SRF co-factors (Esnault et al., 2014). Results are shown in Figure 28.

As previously reported, MRTF target genes were not expressed in untreated cells or in response to LatB treatment (Miralles et al., 2003; Vartiainen et al., 2007). Stimulation with serum or CD, which interfere with MRTF/G-actin interaction, either by directly disrupting it or by promoting F-actin assembly, induced gene expression. In LMB-treated cells, nuclear MRTF did not activate target genes. Nevertheless, treatment with LMB slightly increased baseline expression at MRTF target genes, as compared to this in untreated cells.

To test whether nuclear MRTF was responsive to changes in G-actin concentration, cells pre-treated with LMB were re-stimulated with FCS, CD or LatB. Subsequent stimulation of LMB-treated cells with CD or FCS induced gene expression, whereas subsequent LatB treatment reversed the increased baseline expression in cells treated with LMB alone. The *Egr1* gene was insensitive to LMB or CD treatment. It was only activated in response to serum stimulation (Figure 28B).

Taken together these results confirm that although LMB treatment induces MRTF nuclear accumulation, under this condition MRTF target genes remain inactive. Nuclear MRTF is nevertheless responsive to changes in G-actin concentration, since subsequent stimulation of LMB pre-treated cells with FCS or CD results in gene activation.

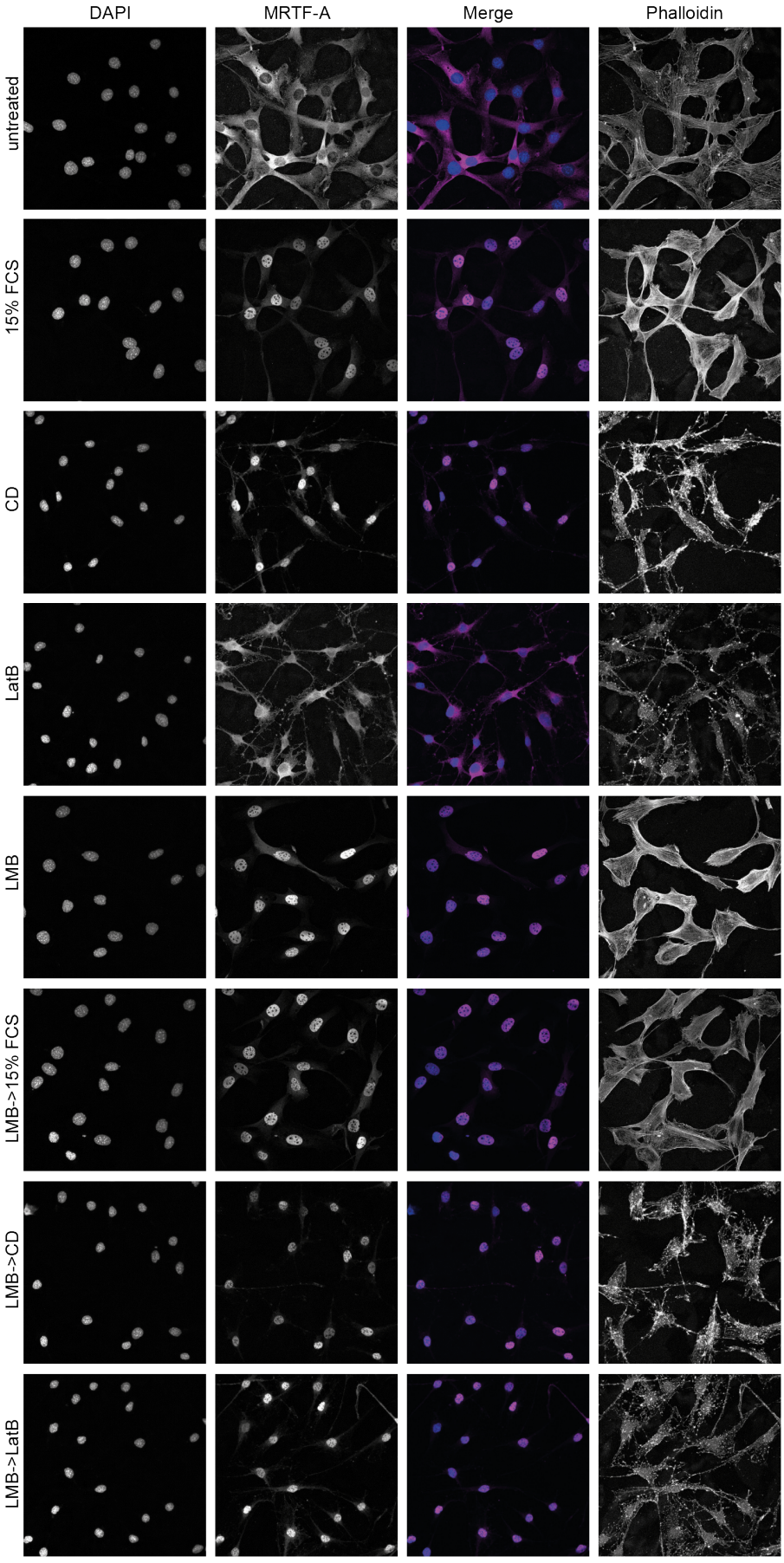
DAPI
MRTF-A
Merge
Phalloidin
untreated
15% FCS
CD
LatB
LMB
LMB->15% FCS
LMB->CD
LMB->LatB

Figure 27 MRTF subcellular localization

Immunofluorescence microscopy of MRTF-A in NIH3T3 fibroblasts. Cells were serum-starved overnight and stimulated for 30 min with 3µM CD (Cytochalasin D); 50nM LMB (Leptomycin B); 15% FCS; 0.5µM LatB (Latrunculin B); LMB->CD (30 min LMB followed by 30 min CD); LMB->LatB (30 min LMB followed by 30 min LatB); LMB->15% FCS (30 min LMB followed by 30 min 15%FCS). Phalloidin was used to stain actin filaments and DAPI to stain the nucleus. In the merged images, MRTF (sc-21558) is shown in magenta and DAPI in blue.

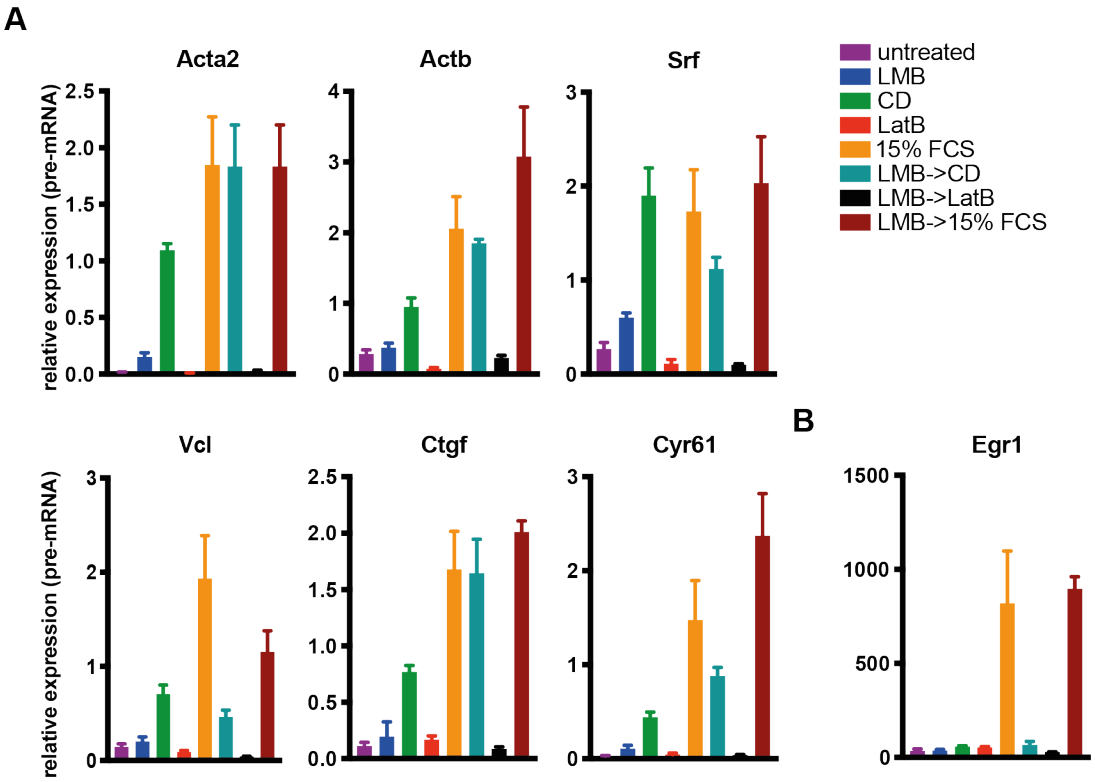

Figure 28 Nuclear MRTF does not activate target genes

Pre-mRNA accumulation in response to stimulation at MRTF target genes (A) and the TCF target gene *Egr1* (B). NIH3T3 fibroblasts were serum-starved overnight and stimulated for 30 min with 3µM CD (Cytochalasin D); 50nM LMB (Leptomycin B); 15% FCS; 0.5µM LatB (Latrunculin B); LMB->CD (30 min LMB followed by 30 min CD); LMB->LatB (30 min LMB followed by 30 min LatB); LMB->15% FCS (30 min LMB followed by 30 min 15% FCS). qPCR probes are located within the first intron of each gene. Signal was normalized to *Gapdh*. Data is shown as mean ± SEM and is representative of three independent experiments.

3.2 G-actin inhibits MRTF recruitment to target genes

To investigate how G-actin interferes with MRTF-dependent gene expression, MRTF and SRF recruitment to target gene promoters in response to stimulation was examined by ChIP-qPCR.

As shown in Figure 29A, MRTF was bound to target gene promoters in response to stimulation with CD and serum and absent in untreated and LatB-treated cells. As previously described even though LMB treatment did not activate MRTF target genes, in this condition MRTF was recruited to target promoters, while it was not detectable at the *Zfp37* control gene (Figure 29B)(Vartiainen et al., 2007). However, DNA binding was reduced as compared to this in CD-stimulated cells.

To test whether the LMB-induced recruitment of MRTF was subject to regulation by G-actin, ChIP assays in LMB pre-treated cells subsequently stimulated with CD, FCS or LatB were performed. Strikingly, while CD and FCS re-stimulation increased ChIP signal in LMB treated cells, treatment with LatB reduced it.

In addition, SRF recruitment to target gene promoters was examined by ChIP-qPCR under the same conditions. Results are shown in Figure 30.

Like MRTF, SRF was bound to target gene promoters in response to serum stimulation and in CD-treated cells, while it was not recruited in untreated and LatB-treated cells. In response to LMB, SRF was recruited to target genes, albeit at reduced levels, relative to these in CD-stimulated cells. SRF was not detected at the *Zfp37* control gene in response to any of the treatments (Figure 30B).

As for MRTF, SRF recruitment upon LMB treatment was subject to regulation by G-actin. Re-stimulation of LMB pre-treated cells with CD or serum, which disrupt the interaction between MRTF and G-actin, increased SRF ChIP signal. In contrast, LatB addition, which increases the concentration of free G-actin, disrupted SRF recruitment to target gene promoters.

Despite the low enrichment of MRTF-A in the ChIP assay (see Figure 29), MRTF ChIP levels were sensitive to treatement with LMB, CD, FCS and LatB at MRTF target genes specifically and not at the *Zfp37* control gene, which is not under the regulation of MRTF. Furthermore, the same pattern of recruitment to DNA was observed for SRF (see Figure 30). The low enrichment in MRTF-A ChIP could reflect efficiency of the MRTF-A antibody, low abundance of MRTF-A on DNA or less stable recruitment of the protein to DNA. Using an alternative ChIP protocol (Tian et al., 2012) did not increase the quality of the MRTF ChIP assay, as it increased background due to inefficient sonication and degradation of the protein.

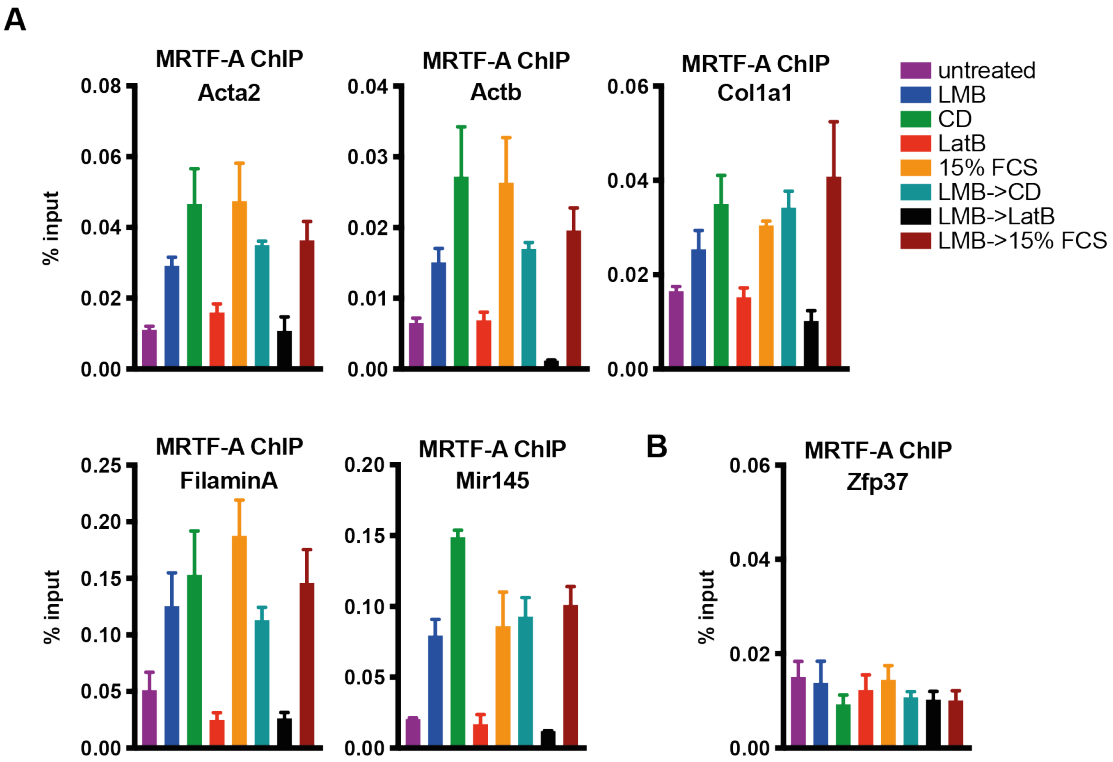

Figure 29 MRTF recruitment to target gene promoters in response to stimulation

MRTF-A (sc-21558) ChIP at MRTF target gene promoters (A) and at the *Zfp37* promoter (B). NIH3T3 fibroblasts were serum-starved overnight and stimulated for 30 min with 3µM CD (Cytochalasin D); 50nM LMB (Leptomycin B); 15% FCS; 0.5µM LatB (Latrunculin B); LMB->CD (30 min LMB followed by 30 min CD); LMB->LatB (30 min LMB followed by 30 min LatB); LMB->15% FCS (30 min LMB followed by 30 min 15% FCS). Signal was normalized to input. Data is shown as mean ± SEM and is representative of three independent experiments.

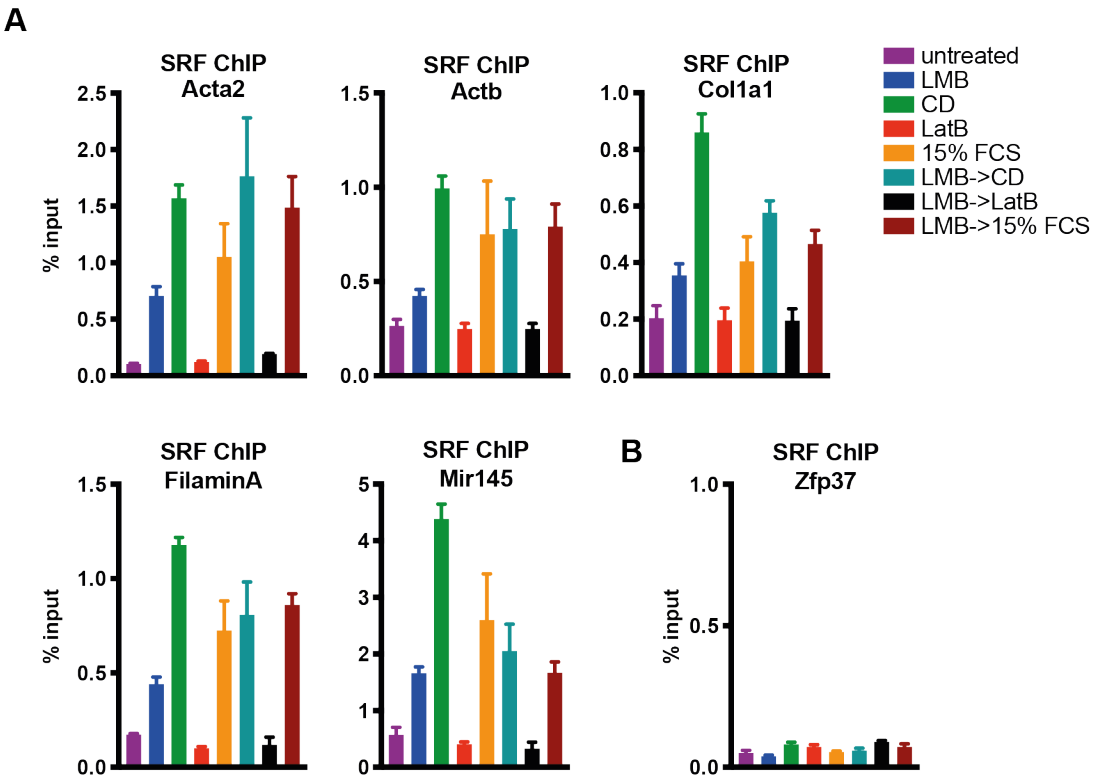

Figure 30 SRF recruitment to target gene promoters in response to stimulation

SRF (16821-1-AP) ChIP at MRTF target gene promoters (A) and at the *Zfp37* promoter (B). NIH3T3 fibroblasts were serum-starved overnight and stimulated for 30 min with 3µM CD (Cytochalasin D); 50nM LMB (Leptomycin B); 15% FCS; 0.5µM LatB (Latrunculin B); LMB->CD (30 min LMB followed by 30 min CD); LMB->LatB (30 min LMB followed by 30 min LatB); LMB->15% FCS (30 min LMB followed by 30 min 15% FCS). Signal was normalized to input. Data is shown as mean ± SEM and is representative of three independent experiments.

The results presented above are consistent with a model in which G-actin interferes with ternary complex formation between SRF and MRTF on DNA. To exclude the possibility that the reduction in SRF and MRTF recruitment to target gene promoters observed upon LMB treatment reflects slower binding kinetics, SRF/MRTF recruitment and activation of the model gene *Acta2* was examined in a time-course over 90 min following stimulation with CD, FCS or LMB.

First, we used qPCR probes targeting the first intron of the *Acta2* gene to measure pre-mRNA levels, as an indication of the relative transcription rate. As shown in Figure 31A, prolonged treatment with LMB did not activate the *Acta2* gene. In response to CD or serum, precursor RNA started accumulating 15 min following stimulation and reached maximum at 30 min. The response to serum-shock was transient and pre-mRNA levels started decreasing 30 min after treatment, whereas the response to CD lasted throughout the time-course. Addition of LatB to cells pre-stimulated with CD or FCS for 30 min inhibited Acta2 pre-mRNA synthesis. Precursor RNA production stopped within 5-10 min following addition of LatB and was completely abolished by 30 min.

In addition, exonic qPCR probes, targeting sequences flanking intron 2, were used to measure mature RNA levels at the *Acta2* gene in response to stimulation. Results are shown in Figure 31B.

mRNA started accumulating 60 min following CD or FCS stimulation. Consistent with the inhibitory effect of LatB on pre-mRNA synthesis, addition of LatB to cells pre-stimulated with CD or FCS for 30 min prevented mRNA accumulation.

Next, SRF recruitment to the *Acta2* promoter was examined by ChIP at different time points following stimulation with CD or LMB. As shown in Figure 32, despite the lack of precursor RNA in LMB-treated cells, SRF bound to the *Acta2* promoter in response to LMB treatment. SRF recruitment was observed 15 min following LMB addition. ChIP levels did not increase with time. SRF recruitment to the *Acta2* promoter was sensitive to an increase in G-actin concentration. Addition of LatB to LMB-treated cells abolished DNA binding within 5 min. Similarly, SRF bound to DNA 15 min following stimulation with CD. Consistent with the observed reduction in pre-mRNA levels following LatB addition to cells pre-stimulated with CD (Figure 31A), SRF binding was reduced within 5 min after LatB addition and was completely abolished within 30 min (Figure 32).

As shown in Figure 32, SRF ChIP levels in cells treated with CD or LMB were comparable at 15 min following addition of the drug, a time point at which precursor

RNA was observed only in cells treated with CD and not in cells treated with LMB (see Figure 31A).

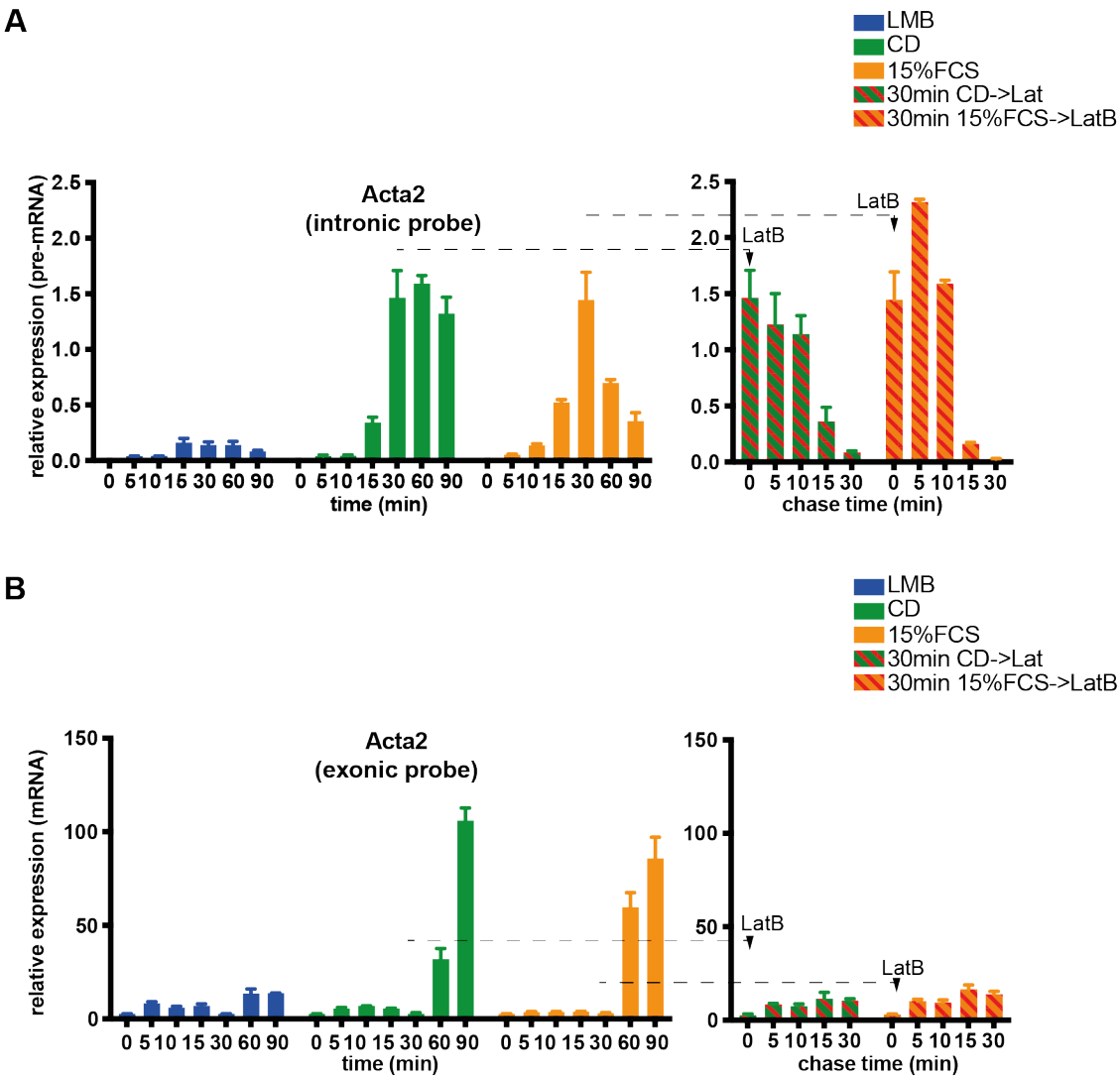

Figure 31 G-actin inhibits MRTF target gene activation

Pre-mRNA (A) and mRNA (B) accumulation at the inducible MRTF model gene *Acta2* in response to stimulation over the timeframe of 90 min. NIH3T3 fibroblasts were serum-starved overnight and stimulated for 30 min with 3µM CD (Cytochalasin D); 50nM LMB (Leptomycin B); 15% FCS; CD->LatB (30 min CD followed by 30 min LatB); 15% FCS->LatB (30 min 15% FCS followed by 30 min LatB). To measure pre-mRNA qPCR probes targeting the first intron of the gene were used. To measure mRNA exonic qPCR probes targeting sequences flanking intron 2 of the gene were used. Signal was normalized to *Gapdh*. Data is shown as mean ± SEM and is representative of three independent experiments.

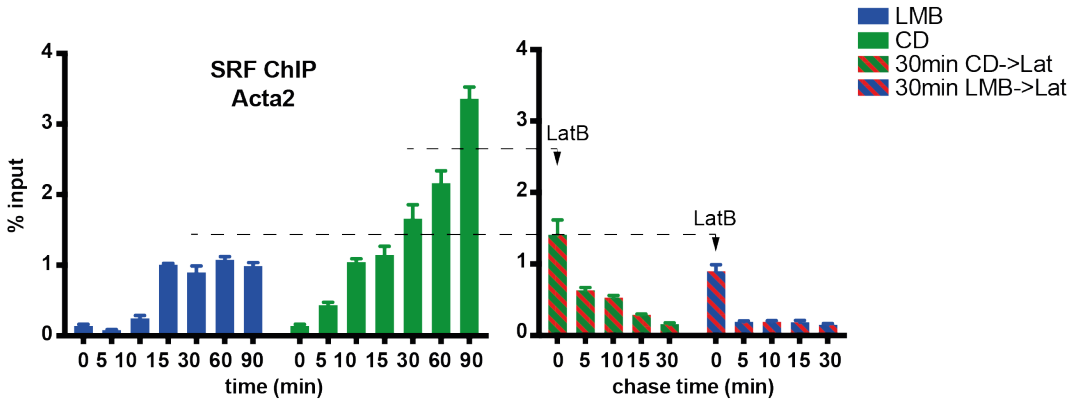

Figure 32 G-actin inhibits SRF/MRTF recruitment to target genes

SRF (16821-1-AP) ChIP in at the promoter of the MRTF model gene *Acta2* in response to stimulation over the timeframe of 90 min. NIH3T3 fibroblasts were serum-starved overnight and stimulated for 30 min with 3µM CD (Cytochalasin D); 50nM LMB (Leptomycin B); CD->LatB (30 min CD followed by 30 min LatB); LMB->LatB (30 min LMB followed by 30 min LatB). Signal was normalized to input. Data is shown as mean ± SEM and is representative of three independent experiments.

In LMB-treated cells, SRF binding levels at the *Acta2* promoter rapidly reach maximum and persist over time. This is consistent with less efficient binding, rather than slower recruitment of the transcription factor. Furthermore, SRF/MRTF recruitment at early timepoints is broadly comparable between LMB and CD stimulated cells, whereas only CD induces a transcriptional response, suggesting that reduced transcription factor recruitment alone does not cause the defective pre-mRNA accumulation in LMB-treated cells.

3.3 Nuclear MRTF induces transcription but not productive RNA synthesis

In the absence of G-actin depletion, nuclear MRTF is recruited to target gene promoters but does not induce pre-mRNA synthesis. This could potentially occur because Pol II fails to be recruited at target genes or due to increased stalling at the TSS. Alternatively, under this condition transcripts could be co-transcriptionally degraded.

To characterize the transcriptional response to LMB and CD, both RNAseq and transient transcriptome sequencing (TTseq), a method that employs metabolic labelling of RNA with 4-thiouridine (4SU) to measure nascent Pol II-associated transcripts were performed (Gregersen et al., 2020; Gregersen et al., 2019; Schwalb et al., 2016; Tufegdžić Vidaković et al., 2020).

The transcriptional response to CD

For RNAseq, sequencing libraries were prepared from total RNA purified from NIH3T3 cells treated with CD for 30 min. Bioinformatic analysis of RNAseq data was performed by Francesco Gualdrini. To increase sensitivity, read count within introns only (intronic reads) or exons only (exonic reads) were analysed. Differential gene expression analysis was performed, comparing each stimulus to untreated cells (for discussion of the processing analysis strategy see Chapter 2.12). Results are shown in Figure 33.

CD stimulation resulted in detectable upregulation of 2116 genes in intronic reads and 679 genes, as assessed by exonic reads. These were enriched in genes involved in cytoskeleton organization and actin-based processes, gene categories which are also significantly overrepresented in MRTF-SRF target genes (Esnault et al., 2014). For full list of significantly overrepresented GO terms see Figure 92. Genes downregulated in response to CD treatment were not enriched in gene categories associated with MRTF-SRF signalling (see Figure 93). This result is consistent with MRTF being the only transcription factor known to be directly activated by CD.

To examine nascent transcription, NIH3T3 cells were stimulated with CD for 30 min and, guided by the findings in Figure 31A, newly-synthesised RNA was pulse-labelled with 4SU for the last 15 min. The 4SU-labelled RNA was then purified and sequenced. Bioinformatic analysis of TTseq data was performed by Francesco Gualdrini. As before, differential gene expression analysis was performed, comparing each stimulus to untreated cells. Results are shown in Figure 34.

A

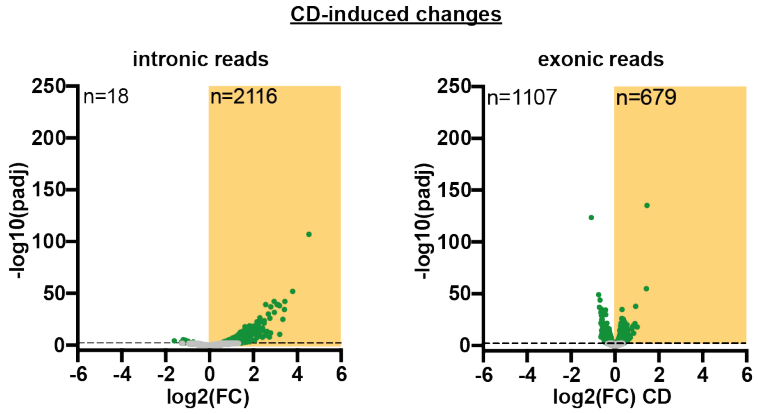

B

GO BIOLOGICAL PROCESS	# Genes	p-value	FDR q-value
CYTOSKELETON ORGANIZATION	247	2.14E-74	1.62E-70
CELL PROJECTION ORGANIZATION	256	1.54E-68	5.82E-65
POSITIVE REGULATION OF NUCLEOBASE CONTAINING COMPOUND METABOLIC PROCESS	278	2.96E-67	7.47E-64
CELL MORPHOGENESIS	200	4.19E-66	7.93E-63
ACTIN FILAMENT BASED PROCESS	173	1.01E-64	1.54E-61
NEUROGENESIS	256	8.58E-64	1.05E-60
POSITIVE REGULATION OF CELLULAR BIOSYNTHETIC PROCESS	281	9.67E-64	1.05E-60
REGULATION OF INTRACELLULAR SIGNAL TRANSDUCTION	268	3.05E-61	2.89E-58
POSITIVE REGULATION OF MOLECULAR FUNCTION	263	2.35E-60	1.98E-57
CELLULAR MACROMOLECULE LOCALIZATION	275	2.56E-59	1.94E-56

Figure 33 The response to CD stimulation by RNAseq

(A) Volcano plots representing CD-induced changes in gene expression, as compared to untreated cells, by RNAseq. NIH3T3 cells were serum-starved overnight and subsequently stimulated with 3μM CD for 30 min. Significant changes (fold change>1 and pvalue>0.01) are marked in green. Significantly upregulated genes are shown in the yellow boxes. (B) Gene ontology analysis of genes upregulated by CD treatement. Shown are the top 10 GO categories. FDR<0.05. Bioinformatic analysis of RNAseq data was performed by Francesco Gualdrini.

A

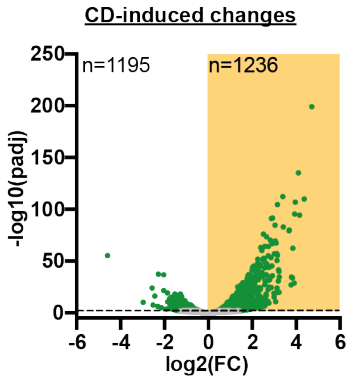

B

GO BIOLOGICAL PROCESS	# Genes	p-value	FDR q-value
ACTIN FILAMENT BASED PROCESS	114	3.39E-56	2.56E-52
CYTOSKELETON ORGANIZATION	145	3.73E-54	1.41E-50
CELL MOTILITY	153	1.68E-45	4.24E-42
BIOLOGICAL ADHESION	134	3.78E-43	7.16E-40
APOPTOTIC PROCESS	156	1.65E-42	2.17E-39
SUPRAMOLECULAR FIBER ORGANIZATION	93	1.72E-42	2.17E-39
REGULATION OF INTRACELLULAR SIGNAL TRANSDUCTION	150	2.90E-42	3.14E-39
REGULATION OF CELL DEATH	140	3.47E-39	3.28E-36
REGULATION OF CELL DIFFERENTIATION	147	3.02E-38	2.54E-35
REGULATION OF CELLULAR COMPONENT MOVEMENT	109	4.20E-37	3.18E-34

Figure 34 The response to CD stimulation by TTseq

(A) Volcano plots representing CD-induced changes in gene expression, as compared to untreated cells, by TTseq. NIH3T3 cells were serum-starved overnight and subsequently stimulated with 3μM CD for 30 min. Significant changes (fold change>1 and pvalue>0.01) are marked in green. Significantly upregulated genes are shown in the yellow boxes. (B) Gene ontology analysis of genes upregulated by CD treatement. Shown are the top 10 GO categories. FDR<0.05. Bioinformatic analysis of TTseq data was performed by Francesco Gualdrini.

As in the RNAseq experiment, by TTseq CD stimulation induced the expression of genes associated with actin-based processes. In addition, genes involved in apoptosis and cell differentiation were overrepresented (Figure 34B). For full list of significantly overrepresented GO terms see Figure 94. Genes downregulated in response to CD treatment were not enriched in gene categories associated with MRTF-SRF signalling. Genes involved in cell cycle control were overrepresented (see Figure 95).

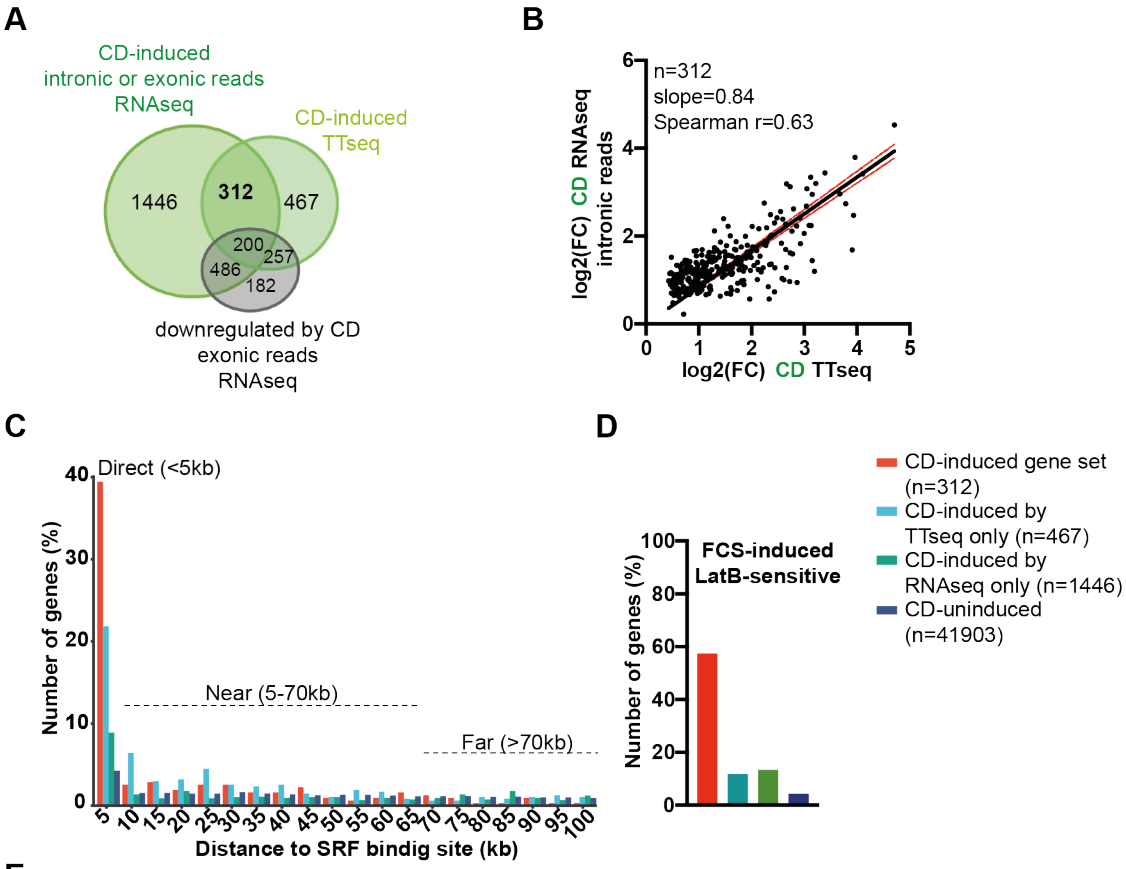

E

GO BIOLOGICAL PROCESS	# Genes	p-value	FDR q-value
ACTIN FILAMENT BASED PROCESS	61	1.21E-26	9.19E-23
CELL MOTILITY	40	4.86E-24	1.84E-20
CYTOSKELETON ORGANIZATION	47	1.47E-22	3.70E-19
BIOLOGICAL ADHESION	49	1.13E-20	2.13E-17
REGULATION OF INTRACELLULAR SIGNAL TRANSDUCTION	47	2.08E-20	3.15E-17
SUPRAMOLECULAR FIBER ORGANIZATION	39	2.22E-19	2.80E-16
ANATOMICAL STRUCTURE FORMATION INVOLVED IN MORPHOGENESIS	39	2.37E-18	2.56E-15
ACTIN FILAMENT ORGANIZATION	26	3.02E-18	2.86E-15
REGULATION OF CELLULAR COMPONENT MOVEMENT	38	1.84E-17	1.55E-14
CELL SUBSTRATE ADHESION	31	7.07E-17	5.35E-14

Figure 35 Defining a stringent CD-induced gene set

(A) Venn diagram representing the overlap between CD-induced genes in NIH3T3 cells by RNAseq and TTseq. Note that some genes where intronic reads were increased by CD stimulation, nevertheless showed a decrease on the exonic level (shown in black). (B) Scatter plot comparing fold change expression by RNAseq and TTseq at the stringent CD-induced gene set (n=312). The red lines represent the 95% confidence bands of the best-fit line (black). (C) Distance to the closest SRF binding site within CD-induced genes. Coordinates of SRF binding sites published in (Esnault et al., 2014) were used. (D) Proportion of genes overlapping with FCS-inducible LatB sensitive genes (n=1022), as defined in (Esnault et al., 2014). (E) Gene ontology analysis of the stringent CD-induced gene set (n=312). Shown are the top 10 GO categories. FDR<0.05. Bioinformatic analysis of RNAseq and TTseq data was performed by Francesco Gualdrini.

Next, to define a stringent set of CD-responsive genes, the overlap between CD-induced genes by TTseq and RNAseq in intronic or exonic reads was used. Results are shown in Figure 35.

512 genes were detectably induced by CD in both assays (Figure 35A). However, 200 of those were downregulated on the exonic level in CD-treated cells, probably reflecting indirect effects of the CD treatment on RNA stability. These genes were therefore excluded. Using this approach, 312 genes were identified as induced by CD both by RNAseq and TTseq and not downregulated in CD-treated cells in exonic reads. As presented in Figure 35B, expression of the stringent 312 gene set strongly correlated between the RNAseq and TTseq experiments. There was a weak correlation between expression changes in CD-treated cells in the RNAseq and TTseq experiments in the full dataset (see Figure 114A).

Next, a previously published dataset of SRF ChIP in NIH3T3 cells was used to examine the association of CD activated genes with SRF binding (Esnault, Stewart et al. 2014). It has been proposed that the maximum distance at which an SRF binding site influences transcription is 70kb (Esnault, Stewart et al. 2014). Therefore, SRF binding sites were classified into direct (within 5kb of the TSS of the nearest gene), near (between 5 and 70 kb away from the TSS of the nearest gene) and far (beyond 70kb of the TSS of the nearest gene).

Genes in the stringent CD-activated set were associated with direct SRF binding (Figure 35C). Using previously published coordinates of SRF binding sites, an SRF binding site was found within 5 kb of the TSS of 40% of the stringent CD-induced set (Esnault, Stewart et al. 2014). In contrast, less than 5% of inactive genes in CD-treated cells were located in close proximity to an SRF binding site. Genes upregulated in response to CD by TTseq only (n=467) were also associated with direct SRF binding: approximately 20% of these were with an SRF binding site within 5kb of their TSS (Figure 35C).

Furthermore, as shown in Figure 35D, the stringent CD-induced gene set was heavily enriched in previously defined FCS-inducible LatB-sensitive genes (Esnault et al., 2014). Whereas only approximately 10% of other CD-activated genes and

less than 5% of genes inactive in CD-stimulated cells were present in the FCS-inducible LatB-sensitive gene set.

Finally, gene ontology analysis was performed on the stringent CD-induced gene set (Figure 35E). CD-activated genes were functionally related to MRTF-SRF targets. These were enriched in genes involved in actin-based processes, cell morphology, migration and adhesion, showing an overlap with signatures of MRTF-SRF target genes.

Overall, the stringent CD-induced gene set is enriched in serum-inducible genes, whose expression is sensitive to an increase in G-actin concentration by LatB, physically associated with SRF and functionally related to MRTF-SRF target genes. This is consistent with the transcriptional response to CD being MRTF-dependent.

The transcriptional response to LMB

The same approach was used to characterize the transcriptional response to LMB. As before, for RNAseq, sequencing libraries were prepared from total RNA purified from NIH3T3 cells treated with LMB for 30 min. Bioinformatic analysis of RNAseq data was performed by Francesco Gualdrini. To increase sensitivity, read count within introns only (intronic reads) or exons only (exonic reads) were analysed. Differential gene expression analysis was performed, comparing each stimulus to untreated cells. Results are shown in Figure 36.

Consistent with previous studies and data presented above, no transcriptional response was detected by RNAseq following treatment with LMB (Vartiainen et al., 2007).

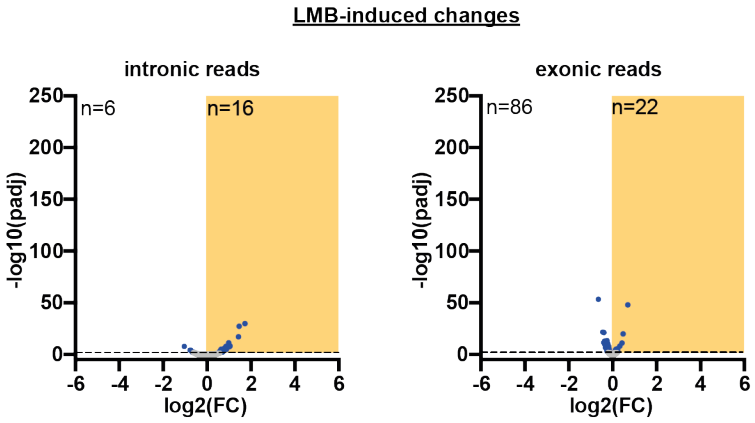

Figure 36 LMB stimulation does not induce gene activation

Volcano plots representing LMB-induced changes in gene expression, as compared to untreated cells, by RNAseq. NIH3T3 cells were serum-starved overnight and subsequently stimulated with 50nM LMB for 30 min. Significant changes (fold change>1 and pvalue>0.01) are marked in blue. Significantly upregulated genes are shown in the yellow boxes. Bioinformatic analysis of RNAseq data was performed by Francesco Gualdrini.

A

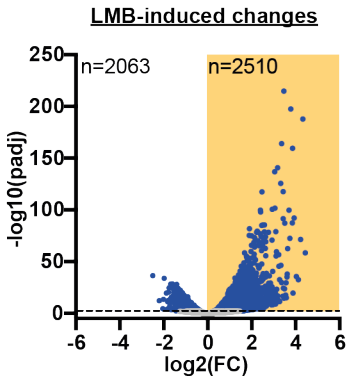

B

	GO BIOLOGICAL PROCESS	# Genes	p-value	FDR q-value
*	CYTOSKELETON ORGANIZATION	203	7.16E-62	5.42E-58
*	ACTIN FILAMENT BASED PROCESS	146	1.57E-56	5.94E-53
*	BIOLOGICAL ADHESION	201	2.95E-56	7.45E-53
*	CELL MOTILITY	225	6.15E-56	1.16E-52
*	REGULATION OF INTRACELLULAR SIGNAL TRANSDUCTION	223	6.69E-53	1.01E-49
*	APOPTOTIC PROCESS	229	2.89E-51	3.65E-48
*	REGULATION OF CELL DEATH	205	3.29E-47	3.55E-44
*	ANATOMICAL STRUCTURE FORMATION INVOLVED IN MORPHOGENESIS	164	4.93E-46	4.67E-43
*	CELL MORPHOGENESIS	151	1.15E-45	9.69E-43
*	SUPRAMOLECULAR FIBER ORGANIZATION	123	6.43E-45	4.87E-42

Figure 37 LMB induces nascent RNA synthesis

(A) Volcano plots representing LMB-induced changes in gene expression, as compared to untreated cells, by TTseq. NIH3T3 cells were serum-starved overnight and subsequently stimulated with 50nM LMB. Significant changes (fold change>1 and pvalue>0.01) are marked in blue. Significantly upregulated genes are shown in the yellow boxes. (B) Gene ontology analysis of genes upregulated by LMB treatement. Shown are the top 10 GO categories. FDR<0.05. GO categories also enriched in CD-induced genes by RNAseq or TTseq are marked with *. Bioinformatic analysis of TTseq data was performed by Francesco Gualdrini.

Next, to examine nascent transcription, NIH3T3 cells were stimulated with LMB for 30 min and newly-synthesised RNA was pulse-labelled with 4SU for the last 15 min. The 4SU-labelled RNA was then purified and sequenced. Bioinformatic analysis of TTseq data was performed by Francesco Gualdrini. As before, differential gene expression analysis was performed, comparing each stimulus to untreated cells. Results are shown in Figure 37.

Strikingly, although no transcriptional response to LMB treatment was detected by RNAseq, by TTseq LMB upregulated the expression of genes enriched in the same

GO categories as MRTF-SRF targets and CD-induced genes-cell morphology, migration and adhesion. As in CD-stimulated cells, genes associated with cell death and apoptosis were also upregulated (Figure 34B and Figure 37B). For full list of significantly overrepresented GO terms see Figure 96. Genes downregulated in response to LMB treatment were not enriched in gene categories associated with MRTF-SRF signalling (see Figure 97).

This data demonstrates that LMB treatment induces transcription but under this condition pre-mRNA accumulation is defective. The LMB-induced gene set is functionally related to MRTF-SRF target genes, suggesting that the transcriptional response to LMB is mediated by MRTF.

Even though no gene activation was detected in response to LMB by RNAseq, more than 90% of the stringent CD-induced gene set was activated on the nascent RNA level, as assessed by TTseq (Figure 38A). Moreover, as shown in Figure 38B, induction levels of these genes in response to LMB strongly correlated with those following CD stimulation, not only in the TTseq, but also in the RNAseq experiment.

At the 312 stringent CD-induced gene set, while no gene activation was detected in response to LMB by RNAseq, as assessed by TTseq gene expression was upregulated to levels comparable to these following CD stimulation (Figure 38C and D). Furthermore, as shown in Figure 38E, the TTseq read profiles at MRTF-SRF target genes in response to CD and LMB were very similar. No differences in Pol II processivity and elongation speed or termination were apparent.

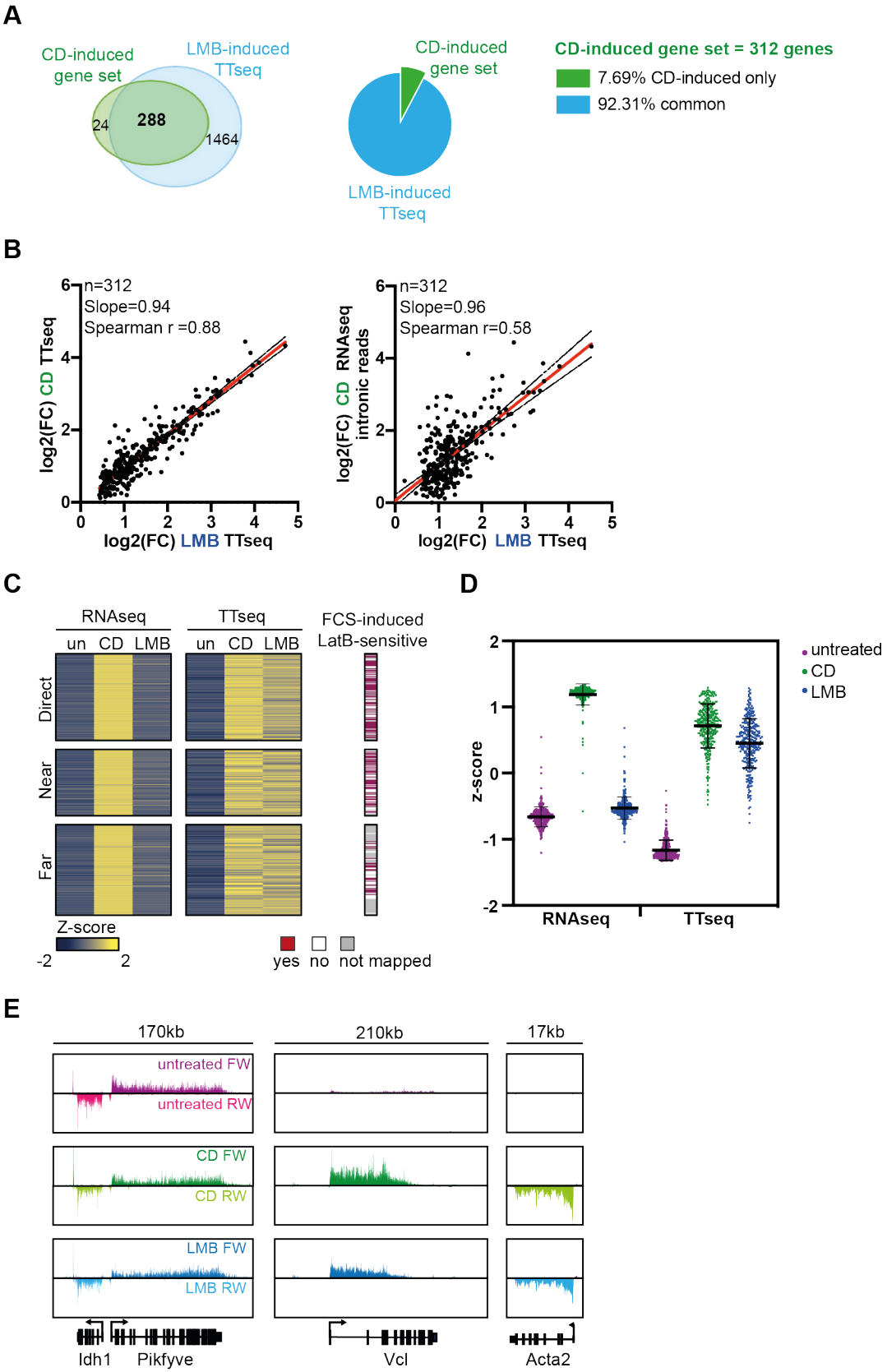
A
CD-induced gene set
LMB-induced TTseq
24
288
1464
CD-induced gene set
LMB-induced TTseq
CD-induced gene set = 312 genes
7.69% CD-induced only
92.31% common
B
n=312
Slope=0.94
Spearman r =0.88
log2(FC) CD TTseq
log2(FC) LMB TTseq
n=312
Slope=0.96
Spearman r=0.58
log2(FC) CD RNAseq intronic reads
log2(FC) LMB TTseq
C
RNAseq
TTseq
un CD LMB
un CD LMB
FCS-induced LatB-sensitive
Direct
Near
Far
Z-score
-2
2
yes no not mapped
D
z-score
RNAseq
TTseq
untreated
CD
LMB
E
170kb
210kb
17kb
untreated FW
untreated RW
CD FW
CD RW
LMB FW
LMB RW
Idh1
Pikfyve
Vcl
Acta2

Figure 38 Nuclear MRTF induces non-productive RNA synthesis

(A) Venn diagram representing the overlap between the stringent CD-induced gene set (n=312) and LMB-induced genes by TTseq. Pie chart representing percentage of CD-induced genes also upregulated by LMB on the nascent RNA level. (B) Scatter plots comparing fold change expression by CD TTseq and LMB TTseq and CD RNAseq and LMB TTseq at the stringent CD-induced gene set (n=312). The black lines represent the 95% confidence bands of the best-fit line (red). (C) Heatmap representing gene expression changes at the 312 genes in the stringent CD-induced gene set in untreated, LMB-stimulated and CD-stimulated cells by RNAseq and TTseq. Genes are separated by distance to their nearest SRF binding site, direct (within 5kb); near (within 70kb); far (>70kb). Overlap with FCS-induced LatB-sensitive genes (n=1022), as published in (Esnault et al., 2014), is shown. The red lines represent FCS-induced LatB-sensitive genes, the white lines represent genes not present in the FCS-induced LatB-sensitive gene set and the grey lines represent genes not identified in the analysis. (D) Violin plot representing gene expression changes at the 312 genes in the stringent CD-induced gene set in untreated, LMB-stimulated and CD-stimulated cells by RNAseq and TTseq. (E) TTseq plots in untreated, CD-stimulated and LMB-treated cells at the constitutive *Idh1* and *Pikfyve* genes and the CD-inducible MRTF-SRF target genes *Vcl* and *Acta2*. Bioinformatic analysis of RNAseq and TTseq data was performed by Francesco Gualdrini.

These results suggest that in response to LMB, nuclear MRTF induces non-productive transcription at target genes.

Finally, CD- and LMB-induced genes that were not present in the stringent CD-induced set were examined. As shown in Figure 39A, 592 genes were upregulated in response to CD and LMB stimulation as assessed by TTseq but were not detectably induced following CD-stimulation by RNAseq. To determine whether these were physically and functionally linked to SRF, as before, distance to the nearest SRF binding site, overlap with published FCS-controlled genes and gene ontology analyses were performed.

Approximately 20% of the 592 gene set was associated with direct SRF binding and present in the published FCS-controlled gene set (Figure 39B and C). Out of the 132 genes upregulated in response to CD but not LMB, approximately 20% were associated with direct SRF binding, induced by serum stimulation and

sensitive to LatB treatment. In contrast, there was little enrichment for direct SRF binding sites in genes insensitive to CD. Approximately 10% of genes upregulated only by LMB were physically linked to SRF or present in the published FCS-controlled LatB-sensitive gene set.

The 592 gene set was mainly enriched in genes involved in apoptosis and cell differentiation. Nevertheless, cytoskeletal genes and genes associated with cell motility were also overrepresented (Figure 39D).

It appears that some SRF-controlled CD-inducible genes are detected by TTseq and not by RNAseq. This could be due to higher basal expression in untreated cells, lower inducibility by CD, impaired RNA stability or increased sensitivity of the TTseq method.

In conclusion, the transcriptional response to CD and LMB appears to be mediated by MRTF. While CD, which disrupts the MRTF/G-actin interaction, induces productive RNA synthesis, LMB-induced nuclear MRTF induces non-productive transcription. In response to LMB, Pol II is recruited and although it engages in elongation, no pre-mRNA accumulates, suggesting that under this condition, nascent transcripts might be co-transcriptionally degraded.

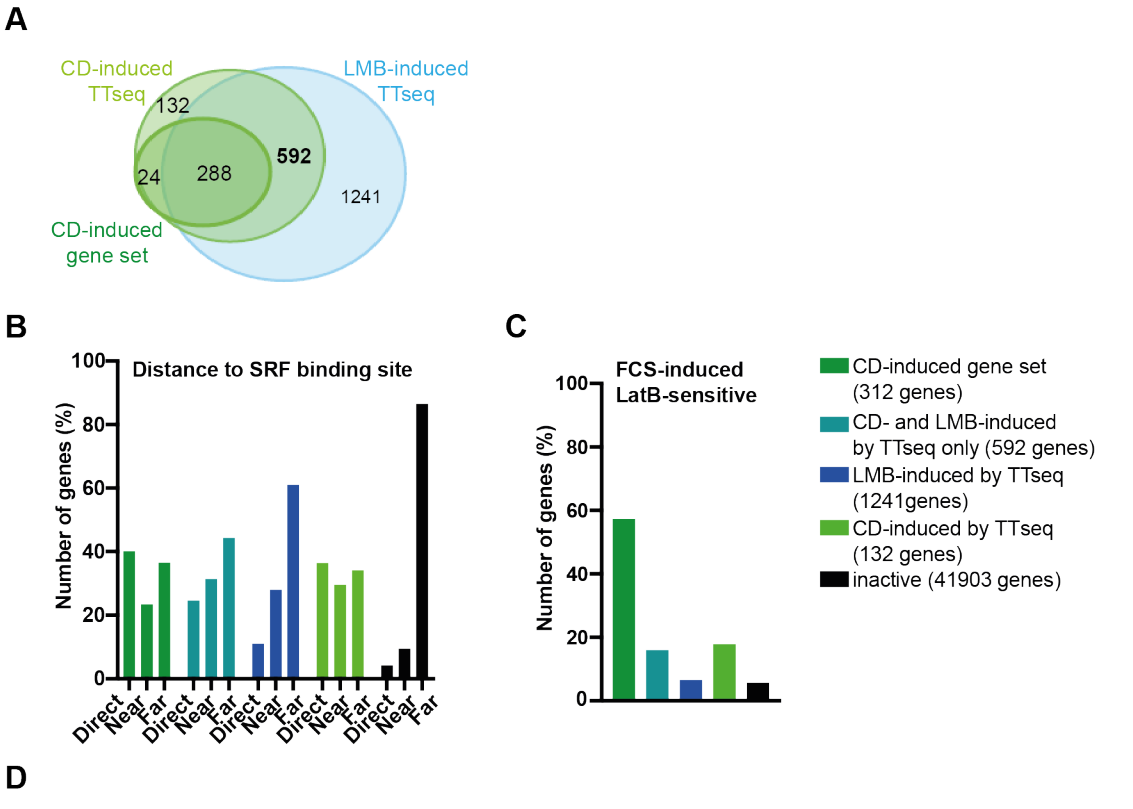

D

	GO BIOLOGICAL PROCESS	# Genes	p-value	FDR q-value
	REGULATION OF TRANSPORT	55	4.23E-15	2.20E-11
*	APOPTOTIC PROCESS	57	5.82E-15	2.20E-11
*	REGULATION OF CELL DIFFERENTIATION	54	1.07E-13	2.71E-10
*	REGULATION OF CELL DEATH	50	3.14E-13	5.94E-10
*	CYTOSKELETON ORGANIZATION	44	4.00E-13	6.05E-10
*	POSITIVE REGULATION OF RNA BIOSYNTHETIC PROCESS	47	7.33E-13	9.25E-10
*	POSITIVE REGULATION OF NUCLEOBASE CONTAINING COMPOUND METABOLIC PROCESS	51	9.21E-13	9.96E-10
*	CELL MOTILITY	50	1.42E-12	1.26E-09
	ION TRANSPORT	48	1.50E-12	1.26E-09
	CELL CELL SIGNALING	49	4.12E-12	3.12E-09

Figure 39 The transcriptional response to LMB and CD

(A) Venn diagram representing the overlap between CD- and LMB-induced genes by TTseq only. (B) Distance to the closest SRF binding site. Coordinates of SRF binding sites published in (Esnault et al., 2014) were used. (C) Proportion of FCS-inducible LatB-sensitive genes (n=1022), as defined in (Esnault et al., 2014). (D) Gene ontology analysis of the 592 genes upregulated by CD and LMB treatment by TTseq, but not present in the stringent CD-induced gene set. Shown are the top 10 GO categories. FDR<0.05. GO categories also enriched in CD-induced genes by RNAseq or TTseq are marked with *. Bioinformatic analysis of RNAseq data was performed by Francesco Gualdrini.

Chapter 4. Constitutively nuclear MRTF does not induce productive RNA synthesis

The preceding results show that in LMB-treated NIH3T3 cells, unless the interaction between MRTF and G-actin is disrupted, nuclear accumulation of MRTF is not sufficient for productive RNA synthesis. Nevertheless, under this condition, MRTF is recruited at target promoters and induces transcription. To exclude the possibility that this transcriptional defect is a result of Crm1 inhibition by LMB, MRTF-A/MRTF-B null cells were reconstituted with an NLS-tagged MRTF and used to study the properties of nuclear MRTF in the absence of LMB. In this chapter, the recruitment of the constitutively nuclear MRTF to target genes, as well as its ability to induce transcription in the absence of stimulation were assessed.

4.1 Characterization of cells with constitutively nuclear MRTF

Even though MRTF isoforms are mostly redundant, in specific contexts they may have a unique function. While deletion of MRTF-A does not affect viability, it causes defects myofibroblast differentiation (Lei et al., 2015; Li et al., 2006; Sun et al., 2006). On the other hand, deletion of MRTF-B causes embryonic lethality due to defects in neural crest development (Li et al., 2005; Oh et al., 2005). Previous work in the laboratory has shown that MRTF-A $^{-/-}$ MRTF-B $^{flox/flox}$ MEF cells are viable, whereas following tamoxifen-induced deletion of MRTF-B, MRTF-A $^{-/-}$ MRTF-B $^{-/-}$ MEF cells (dKO) enter senescence (Bellamy S. (2019) MRTF-SRF signalling in migration, PhD thesis; Nielsen J., unpublished). This observation was exploited to generate cells expressing wild-type or mutant MRTF derivatives at levels sufficient to restore proliferation.

To generate MEF cells with constitutively nuclear MRTF, MRTF-A fused to an additional NLS (MRTF-NLS) was introduced in MRTF-A $^{-/-}$,MRTF-B $^{flox/flox}$ MEF cells, which were simultaneously treated with tamoxifen to delete MRTF-B. Since dKO MEFs are senescent, cells expressing MRTF-NLS at a level sufficient for normal growth were selected, generating dKO$^{MRTF-NLS}$ cells (Figure 40A). In addition, cells reconstituted with a wild-type MRTF-A (dKO^{MRTF}) and an MRTF

RPEL domain mutant ($dKO^{MRTF\text{-}XXX}$) were generated in the same way. MRTF-XXX harbours a single amino acid substitution of arginine to alanine in each of the three RPEL motifs which prevent it from interacting with G-actin and make it constitutively active (Guettler et al., 2008; Miralles et al., 2003; Vartiainen et al., 2007). All ectopically expressed MRTFs were fused to a C-terminal HA tag.

We were unable to generate clonal cell lines from dKO^{MRTF} , $dKO^{MRTF\text{-}NLS}$ or $dKO^{MRTF\text{-}XXX}$ cells by single cell sorting. In addition, we attempted to generate pools of cells expressing MRTF at low/medium/high levels by FACS. However, MRTF protein levels fluctuated after sorting and over time returned to levels observed prior to sorting, suggesting that rescuing senescence of dKO cells selects for a particular level of MRTF activity. Consistent with levels of MRTF protein in the cell being tightly regulated, we were unable to over-express wild-type MRTF, MRTF-NLS or MRTF-XXX in NIH3T3 cells using the doxycycline-inducible pTRIPZ vector.

To characterize the reconstituted cell lines, their proliferation following MRTF re-expression was assessed. Results are shown in Figure 40B. Consistent with dKO MEF cells entering senescence, dKO MEFs stopped proliferating a week following treatment with tamoxifen. In contrast, re-expression of wild-type MRTF, the constitutively nuclear MRTF-NLS or the constitutively active MRTF-XXX prevented dKO MEFs from entering senescence. All the reconstituted cell lines proliferated at rates comparable to wild-type MEF cells.

As shown in Figure 40C, PCR on genomic DNA confirmed knock-out of the endogenous MRTF-A and MRTF-B in the reconstituted cell lines. As presented in Figure 40D, in the reconstituted cell lines, MRTF-NLS was expressed at a level comparable to that in cells reconstituted with the wild-type protein and wild-type MEF cells, whereas the constitutively active MRTF-XXX was present at a much lower level.

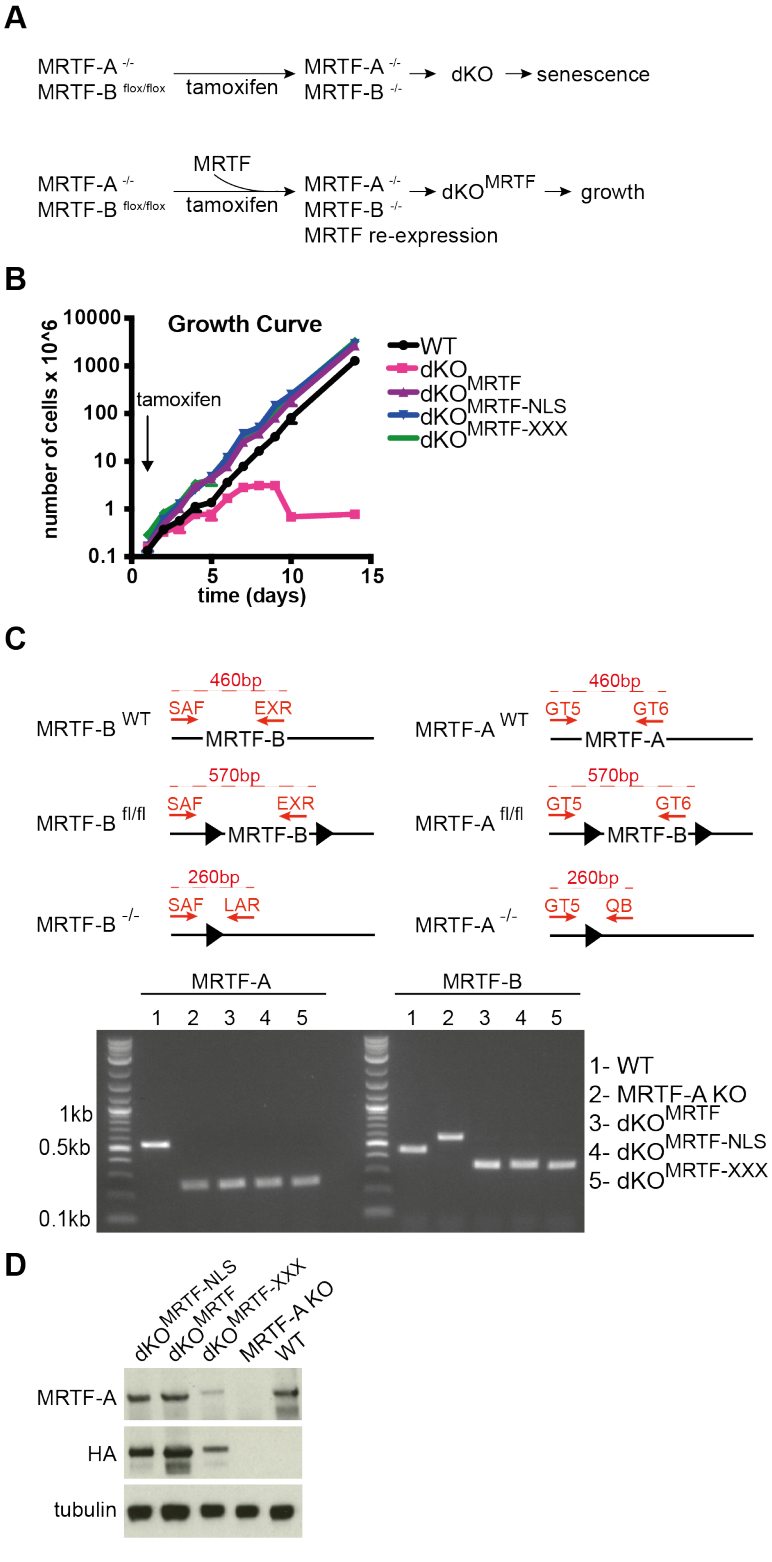
A
MRTF-A -/-
MRTF-B flox/flox
tamoxifen
MRTF-A -/-
MRTF-B -/-
dKO
senescence
MRTF-A -/-
MRTF-B flox/flox
MRTF
tamoxifen
MRTF-A -/-
MRTF-B -/-
MRTF re-expression
dKO MRTF
growth
B
Growth Curve
number of cells x 10^6
10000
1000
100
10
1
0.1
tamoxifen
0
5
10
15
time (days)
WT
dKO MRTF
dKO MRTF-NLS
dKO MRTF-XXX
C
MRTF-B WT
460bp
SAF
EXR
MRTF-B
MRTF-A WT
460bp
GT5
GT6
MRTF-A
MRTF-B fl/fl
570bp
SAF
EXR
MRTF-B
MRTF-A fl/fl
570bp
GT5
GT6
MRTF-B
MRTF-B -/-
260bp
SAF
LAR
MRTF-A -/-
260bp
GT5
QB
MRTF-A
MRTF-B
1 2 3 4 5
1 2 3 4 5
1kb
0.5kb
0.1kb
1- WT
2- MRTF-A KO
3- dKO MRTF
4- dKO MRTF-NLS
5- dKO MRTF-XXX
D
dKO MRTF-NLS
dKO MRTF
dKO MRTF-XXX
MRTF-A KO
WT
MRTF-A
HA
tubulin

Figure 40 Reconstitution of MRTF-A/B null cells

(A) Stable cell line generation. MRTF-A $^{-/-}$ MRTF-B $^{flox/flox}$ MEF cells were treated with tamoxifen to generate MRTF-A/B null cells (dKO) and simultaneously infected with lentivirus expressing pMY-MRTF-A/MRTF-NLS/MRTF-XXX-IRES-GFP or vector alone. MRTF-A/B null cells enter senescence, while ectopic expression of MRTF prevents cells from entry into senescence. (B) Growth curves. Cells were counted daily (in triplicate) after addition of tamoxifen over the period of 14 days. Data is shown as mean ± SEM. (C) Genotyping. PCRs were set up with genomic DNA isolated from WT MEF, MRTF-A KO MEF, dKO^{MRTF}, dKO$^{MRTF-NLS}$ and dKO$^{MRTF-XXX}$ cells and primers SAF, EXR and LAR or GT5, GT6 and QB to test MRTF-A and MRTF-B knock-out, respectively. Expected PCR product size for the wild-type, the floxed and the knock-out alleles are indicated in red in the schematic. (D) Western blot. Protein lysates from WT MEF, MRTF-A KO MEF, dKO^{MRTF}, dKO$^{MRTF-NLS}$ and dKO$^{MRTF-XXX}$ cells were probed with antibodies against MRTF-A (sc-21558) or HA (11867431001). Tubulin (T5162) was used as a loading control.

Taken together these results suggest that rescuing senescence of dKO cells selects for a particular level of MRTF activity. The observation that MRTF-XXX expression is low indicates that regulation by G-actin is maintained in dKO^{MRTF} and dKO$^{MRTF-NLS}$ cells, which express higher levels of MRTF.

dKO^{MRTF}, dKO$^{MRTF-NLS}$ and dKO$^{MRTF-XXX}$ were unresponsive to stimulation with FCS or CD following serum starvation, which presumably reflects changes arising during the selection process. Nevertheless, cells cultured in 10%FCS remained responsive to CD stimulation and were used to examine MRTF regulation.

First, MRTF subcellular localization in the reconstituted cell lines was examined. To test whether the ectopically expressed MRTF was responsive to changes in G-actin concentration, cells were treated with CD, which directly disrupts the MRTF/G-actin interaction, or LatB, which increases the concentration of G-actin. Following treatment, cells were fixed and an HA antibody was used to visualize MRTF. In addition, cells were stained with Phalloidin, to examine the effect of the treatment on F-actin, and DAPI, to visualize the nucleus. Results are shown in Figure 41.

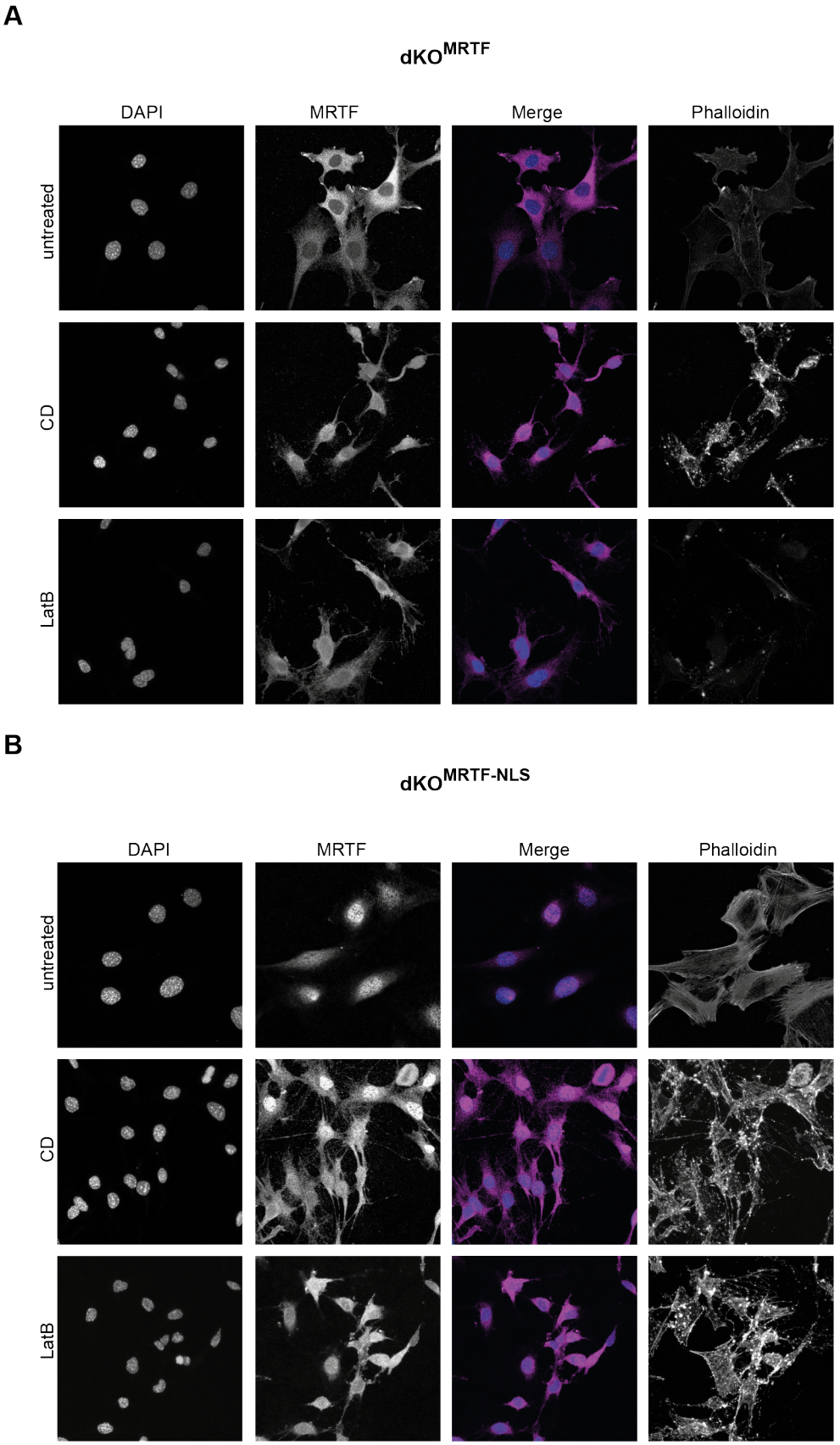
A
dKO^MRTF
DAPI
MRTF
Merge
Phalloidin
untreated
CD
LatB
B
dKO^MRTF-NLS
DAPI
MRTF
Merge
Phalloidin
untreated
CD
LatB

C

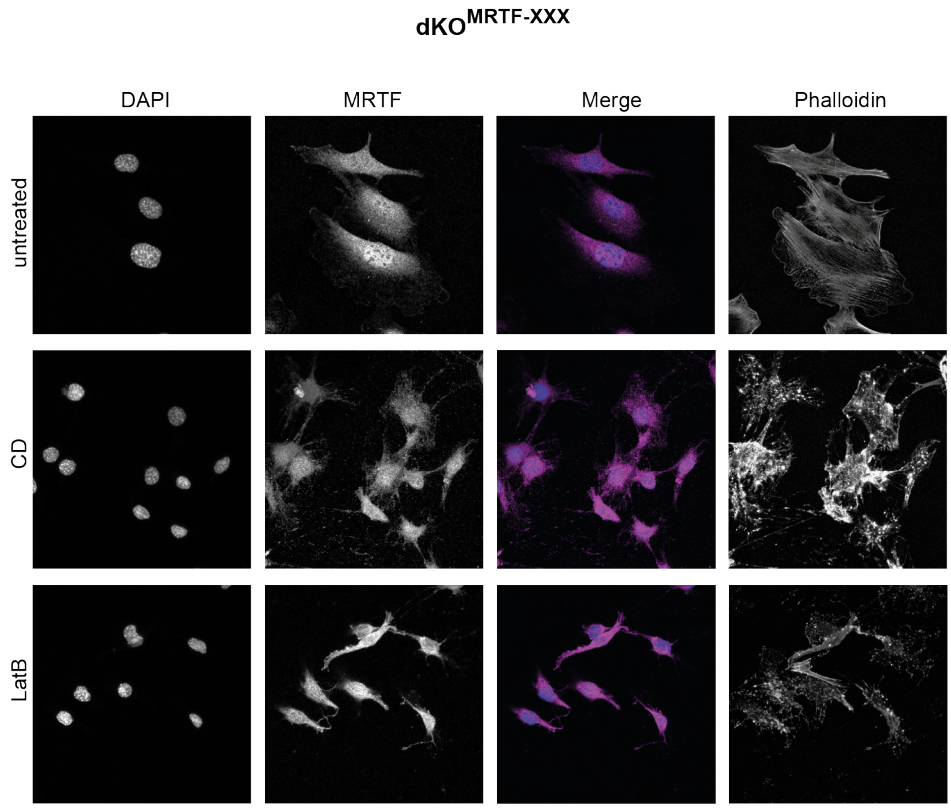

Figure 41 MRTF subcellular localization

Immunofluorescence microscopy of MRTF-A in dKO^{MRTF} cells (A), dKO$^{MRTF-NLS}$ cells (B), dKO$^{MRTF-XXX}$ cells (C). Cells were stimulated for 30 min with 3µM CD (Cytochalasin D); 0.5µM LatB (Latrunculin B) or left untreated. Phalloidin was used to stain actin filaments and DAPI to stain the nucleus. In the merged images, MRTF (MMS-101R-500) is shown in magenta and DAPI in blue.

In cells reconstituted with wild-type protein (dKO^{MRTF}), MRTF was found predominantly in the cytoplasm in untreated cells and LatB-treated cells and translocated into the nucleus following stimulation with CD. In contrast, in dKO$^{MRTF-NLS}$ and dKO$^{MRTF-XXX}$ cells, MRTF was predominantly nuclear in untreated cells and its localization was not affected by treatment with LatB or CD. Nevertheless, CD and LatB disrupted F-actin, as visualized by Phalloidin staining.

As in wild-type fibroblasts, MRTF subcellular localization in dKO^{MRTF} cells is controlled by G-actin. In contrast, MRTF-NLS and MRTF-XXX remain nuclear despite CD or LatB treatment, allowing us to study the effect of changes in G-actin concentration on MRTF activity in the nucleus.

Next, MRTF transcriptional activity in the reconstituted cell lines was assessed by qPCR at endogenous MRTF-SRF target genes under resting and stimulated conditions. As before, as an indication of relative transcription rates, qPCR probes targeting the first intron of the gene were used to measure pre-mRNA levels. Results are shown in Figure 42A.

As in wild-type fibroblasts, in dKO^{MRTF} cells, MRTF target genes were inactive in untreated cells, remained uninduced in LatB-treated cells and were activated in response to stimulation with CD. In untreated dKO$^{MRTF\text{-}NLS}$ cells, even though MRTF was found in the nucleus, target genes were inactive. While target genes remained inactive in response to LatB, treatment with CD induced MRTF target gene expression. In dKO$^{MRTF\text{-}XXX}$ cells, MRTF target genes were constitutively induced. Consistent with the inability of MRTF-XXX to interact with G-actin, MRTF target gene expression was not altered by CD or LatB treatment.

In addition, a gel contraction assay was used as a readout of MRTF activity. MRTF regulates the expression of contractility markers such as the αSMA (*Acta2*) and MLC2 (*Myl9*) genes and has been shown to control cell contractility and pro-invasive behaviour of fibroblasts (Foster et al., 2017; Gualdrini et al., 2016). Wild-type MEF, dKO^{MRTF}, dKO$^{MRTF\text{-}NLS}$ and dKO$^{MRTF\text{-}XXX}$ cells were seeded in collagen gels. Two days later, gel area was measured and compared to its original size. As shown in Figure 42B, wild-type MEF cells did not contract collagen gels. Consistent with the gene expression data presented above, neither did dKO^{MRTF} or dKO$^{MRTF\text{-}NLS}$ cells. In contrast, dKO$^{MRTF\text{-}XXX}$ cells reduced their gel area to approximately half its original size.

The results presented above corroborate findings in LMB-treated NIH3T3 cells. Since both MRTF-NLS and MRTF-XXX are constitutively nuclear, these results demonstrate that that G-actin regulates MRTF activity in the nucleus.

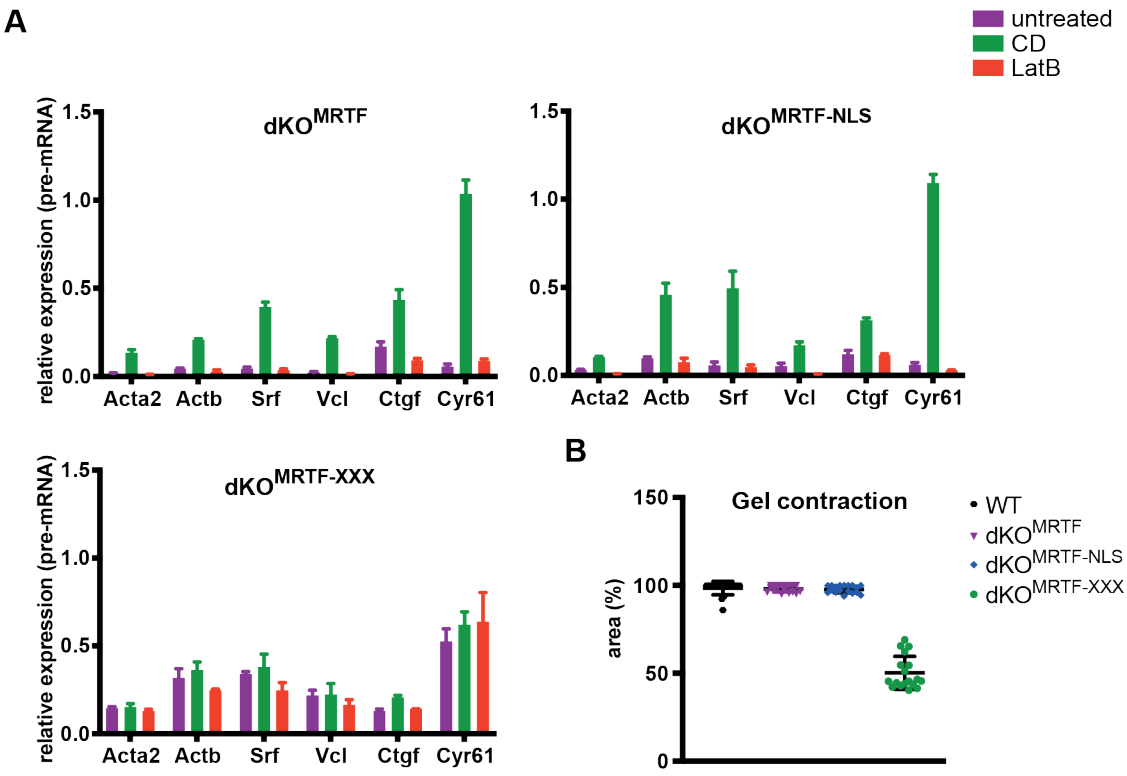

Figure 42 Nuclear MRTF does not activate target genes

(A) Pre-mRNA accumulation at MRTF target genes in dKO^{MRTF} cells, dKO$^{MRTF-NLS}$ cells and dKO$^{MRTF-XXX}$ cells. Cells were stimulated for 30 min with 3µM CD (Cytochalasin D); 0.5µM LatB (Latrunculin B); or left untreated. qPCR probes targeting the first intron of the gene were used to measure pre-mRNA levels. Signal was normalized to *Gapdh*. Data is shown as mean ± SEM and is representative of three independent experiments. (D) Gel contraction assay. Cells were seeded in collagen gels and gel contraction was measured after 48h, expressed as percentage of the original gel area. Data is shown as mean ± SEM and is representative of three independent experiments.

4.2 Constitutively nuclear MRTF is recruited to target gene promoters

In dKO$^{MRTF\text{-}NLS}$ cells, the constitutively nuclear MRTF does not induce target genes in the absence of G-actin depletion. To test whether the MRTF-NLS is nevertheless recruited to target gene promoters, MRTF and SRF ChIP assays were performed. Results are shown in Figure 43.

In dKO^{MRTF} cells, MRTF and SRF did not bind to target gene promoters in untreated or LatB-treated cells but were recruited in response to CD stimulation. In dKO$^{MRTF\text{-}NLS}$ cells, under resting conditions, MRTF and SRF were bound to target gene promoters, but were not detected at the *Zfp37* control gene. CD stimulation only slightly increased ChIP signal at MRTF target genes. In contrast, addition of LatB reduced ChIP signal to background levels. Finally, in dKO$^{MRTF\text{-}XXX}$ cells, MRTF and SRF were constitutively bound to target promoters and their recruitment was not altered by CD or LatB treatments.

As in LMB-treated NIH3T3 cells, in dKO$^{MRTF\text{-}NLS}$ cells MRTF is recruited at target gene promoters, but it is unable to activate gene expression, unless its interaction with G-actin has been disrupted. As observed before, MRTF and SRF recruitment to target promoters is sensitive to an increase in G-actin concentration. The data presented above corroborates findings in NIH3T3 cells and is consistent with a model in which G-actin interferes with ternary complex formation between SRF and MRTF on DNA.

As was the case for MRTF ChIP (see Figure 29), despite the low enrichment of HA ChIP, ChIP levels were sensitive to treatement with CD and LatB at MRTF target genes specifically and not at the *Zfp37* control gene, which is not under the regulation of MRTF (Figure 43A). Furthermore, the same pattern of recruitment to DNA was observed for SRF (Figure 43B). The low enrichment in the HA ChIP assay could reflect efficiency of the HA antibody, low abundance of MRTF-A on DNA or less stable recruitment of the protein to DNA.

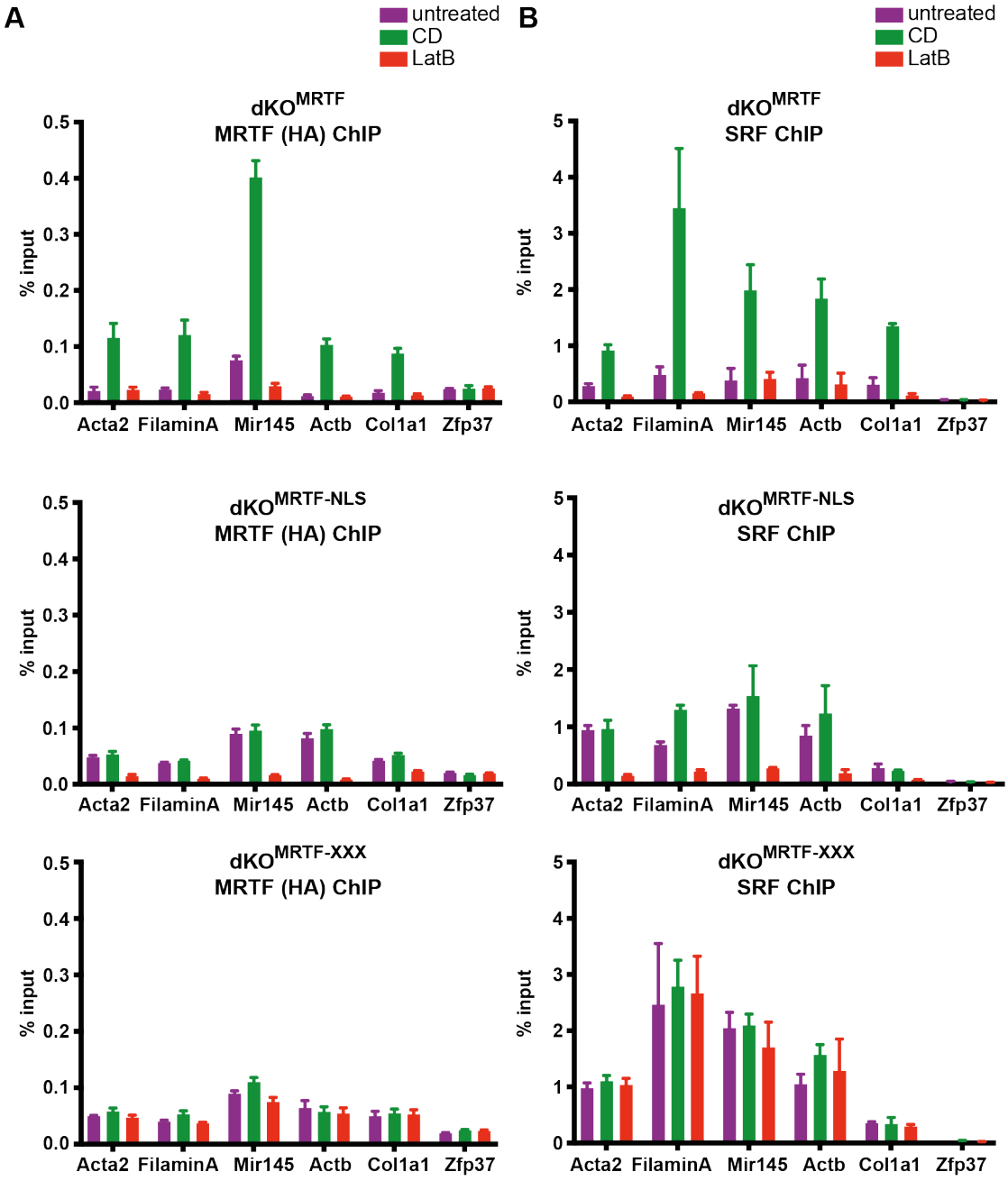

Figure 43 Nuclear MRTF is recruited to target gene promoters

HA (11867431001) ChIP (A) and SRF (16821-1-AP) ChIP (B) in dKO^{MRTF}, dKO$^{MRTF-NLS}$ and dKO$^{MRTF-XXX}$ cells at the MRTF-SRF target genes *Acta2*, *FilaminA, Mir145, Actb*, *Col1a1* and the *Zfp37* gene, which is not an MRTF-SRF target. Cells were stimulated for 30 min with 3μM CD (Cytochalasin D); 0.5μM LatB (Latrunculin B) or left untreated. Signal was normalized to input. Data is shown as mean ± SEM and is representative of three independent experiments.

4.3 Constitutively nuclear MRTF induces non-productive transcription

Under resting conditions, MRTF-NLS is recruited at target promoters but does not induce productive RNA synthesis. To characterize the transcriptional response to the constitutively nuclear MRTF-NLS genome-wide, RNAseq and TTseq experiments were performed in the dKO^{MRTF} and dKO$^{MRTF\text{-}NLS}$ cell lines.

Defining a stringent CD-induced gene set in dKO^{MRTF} and dKO$^{MRTF\text{-}NLS}$ cells

For RNAseq, sequencing libraries were prepared from total RNA purified from cells treated with CD or LatB for 30 min. Bioinformatic analysis of RNAseq data was performed by Francesco Gualdrini. As in NIH3T3 cells, to increase sensitivity, read count within introns only (intronic reads) or exons only (exonic reads) were analysed. Differential gene expression analysis was performed, comparing each stimulus to untreated cells, and results were processed.

As presented in Figure 44, in dKO^{MRTF} cells, CD stimulation resulted in detectable upregulation of 334 genes in intronic reads and 2583 genes, as assessed by exonic reads. Gene ontology analysis showed that the CD-induced genes were enriched in genes involved in cytoskeleton organization and actin-based processes (Figure 44B). Consistent with MRTF being the only transcription factor known to be directly activated by CD, these gene categories are also significantly overrepresented in MRTF-SRF target genes in NIH3T3 cells (see Figure 35E and (Esnault et al., 2014)). For full list of significantly overrepresented GO terms see Figure 98. Genes downregulated in response to CD treatment also included gene categories associated with MRTF-SRF signalling, which could potentially reflect indirect effects of the CD treatment on RNA stability (see Figure 99). No transcriptional response was detected by RNAseq following treatment with LatB.

A

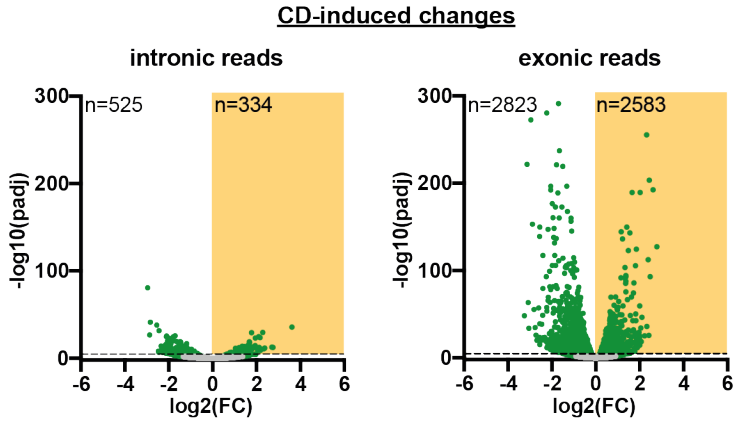

B

	GO BIOLOGICAL PROCESS	# Genes	p-value	FDR q-value
*	ACTIN FILAMENT BASED PROCESS	50	1.88E-30	1.42E-26
*	CYTOSKELETON ORGANIZATION	59	5.09E-27	1.93E-23
*	CELL MOTILITY	66	1.61E-26	4.07E-23
	RESPONSE TO CYTOKINE	54	1.39E-25	2.64E-22
*	ANATOMICAL STRUCTURE FORMATION INVOLVED IN MORPHOGENESIS	51	1.99E-23	3.02E-20
*	SUPRAMOLECULAR FIBER ORGANIZATION	40	1.03E-22	1.31E-19
*	APOPTOTIC PROCESS	62	2.00E-21	2.17E-18
*	REGULATION OF CELLULAR COMPONENT MOVEMENT	47	4.47E-21	4.23E-18
*	BIOLOGICAL ADHESION	53	5.49E-21	4.62E-18
	POSITIVE REGULATION OF MULTICELLULAR ORGANISMAL PROCESS	58	3.60E-20	2.72E-17

C

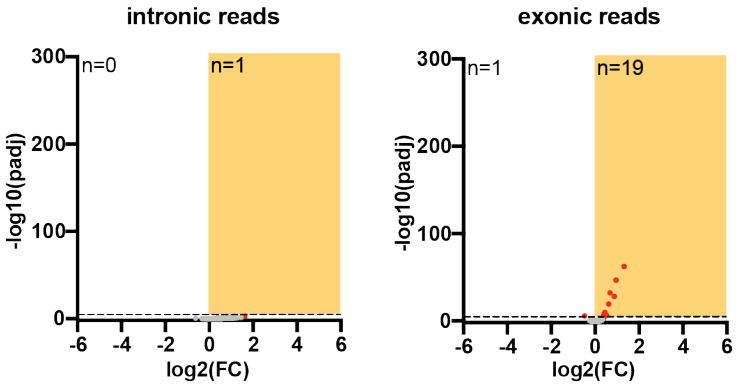

Figure 44 dKO^{MRTF} RNAseq

(A) Volcano plots representing CD-induced changes in gene expression, as compared to untreated cells, by RNAseq. dKO^{MRTF} cells were stimulated with 3μM CD for 30 min. Significant changes (fold change>1 and pvalue>0.01) are marked in green. Significantly upregulated genes are shown in the yellow boxes. (B) Gene ontology analysis of genes upregulated by CD treatement. Shown are the top 10 GO categories. FDR<0.05. GO categories also enriched in CD-induced genes by RNAseq or TTseq in NIH3T3 cells are marked with *. (C) Volcano plots representing LatB-induced changes in gene expression, as compared to untreated cells, by RNAseq. dKO^{MRTF} cells were treated with 0.5μM LatB for 30 min. Significant changes (fold change>1 and pvalue>0.01) are marked in red. Significantly upregulated genes are shown in the yellow boxes. Bioinformatic analysis of RNAseq data was performed by Francesco Gualdrini.

The same experiment was performed in dKO$^{MRTF\text{-}NLS}$ cells. Bioinformatic analysis of RNAseq data was performed by Francesco Gualdrini. Results are shown in Figure 45. CD stimulation resulted in fewer changes in intronic features than in dKO^{MRTF} cells (Figure 45A), perhaps reflecting higher basal transcription in dKO$^{MRTF\text{-}NLS}$ cells under resting conditions. Nevertheless, genes within the union of intronic and exonic features upregulated in response to CD were enriched in GO categories which were also overrepresented in CD-induced genes in NIH3T3 cells (Figure 45B). For full list of significantly overrepresented GO terms see Figure 100. Genes downregulated in response to CD treatment were not enriched in gene categories associated with MRTF-SRF signalling (see Figure 101).

A

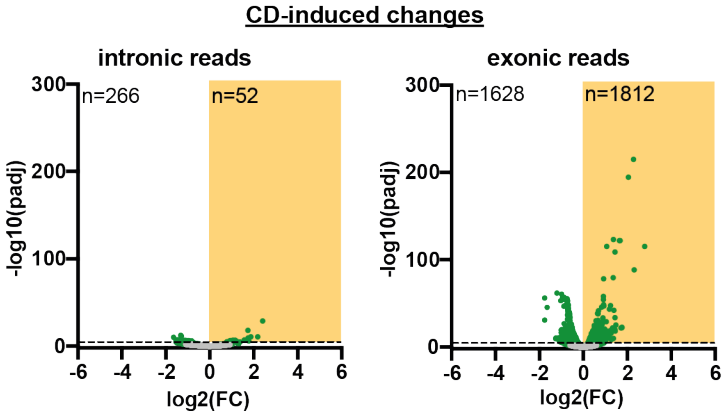

B

	GO BIOLOGOCAL PROCESS	# Genes	p-value	FDR q-value
*	REGULATION OF CELL DIFFERENTIATION	366	6.75E-134	5.11E-130
*	CYTOSKELETON ORGANIZATION	306	1.93E-129	7.32E-126
*	NEUROGENESIS	321	1.02E-118	2.56E-115
*	POSITIVE REGULATION OF NUCLEOBASE CONTAINING COMPOUND METABOLIC PROCESS	327	6.39E-110	1.21E-106
	POSITIVE REGULATION OF MULTICELLULAR ORGANISMAL PROCESS	321	5.06E-106	7.67E-103
	NEURON DIFFERENTIATION	277	1.44E-104	1.82E-101
	POSITIVE REGULATION OF DEVELOPMENTAL PROCESS	281	4.31E-103	4.66E-100
	POSITIVE REGULATION OF CELLULAR BIOSYNTHETIC PROCESS	325	1.31E-101	1.24E-98
	CELL CYCLE	317	2.67E-101	2.25E-98
*	CELL MOTILITY	311	5.92E-101	4.48E-98

C

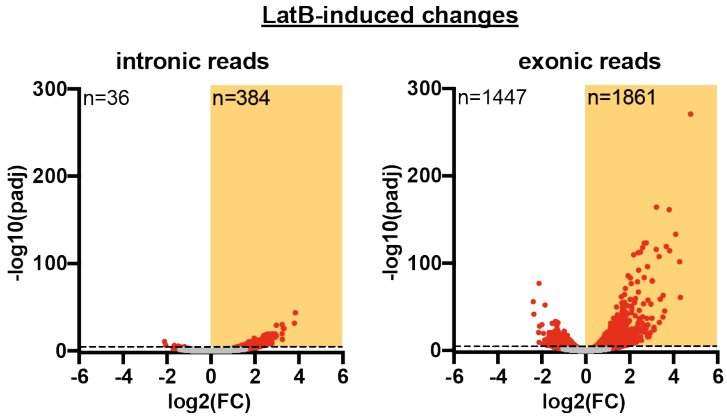

Figure 45 dKO$^{MRTF\text{-}NLS}$ RNAseq

(A) Volcano plots representing CD-induced changes in gene expression, as compared to untreated cells, by RNAseq. dKO$^{MRTF\text{-}NLS}$ cells were stimulated with 3μM CD for 30 min. Significant changes (fold change>1 and pvalue>0.01) are marked in green. Significantly upregulated genes are shown in the yellow boxes. (B) Gene ontology analysis of genes upregulated by CD treatement. Shown are the top 10 GO categories. FDR<0.05. GO categories also enriched in CD-induced genes by RNAseq or TTseq in NIH3T3 cells are marked with *. (C) Volcano plots representing LatB-induced changes in gene expression, as compared to untreated cells, by RNAseq. dKO$^{MRTF\text{-}NLS}$ cells were treated with 0.5μM LatB for 30 min. Significant changes (fold change>1 and pvalue>0.01) are marked in red. Significantly upregulated genes are shown in the yellow boxes. Bioinformatic analysis of RNAseq data was performed by Francesco Gualdrini.

To define a stringent set of CD-responsive genes, the overlap between CD-induced genes in dKO^{MRTF} and dKO$^{MRTF-NLS}$ cells in intronic or exonic reads was used. Results are shown in Figure 46.

As was the case in NIH3T3 cells, some of the CD-induced genes were downregulated on the exonic level in CD-treated cells. Again, this is likely due to indirect effects of the CD treatment on RNA stability. These genes were therefore excluded. 180 genes were induced by CD both in dKO^{MRTF} and dKO$^{MRTF-NLS}$ cells and not downregulated in CD-treated cells in exonic reads (Figure 46A). As shown in Figure 46B, induction in response to CD at the 180 gene set strongly correlated in dKO^{MRTF} and dKO$^{MRTF-NLS}$ cells. However, global expression changes in response to CD did not correlate in dKO^{MRTF} and dKO$^{MRTF-NLS}$ cells (see Figure 114B).

Next, to determine whether CD-induced genes were physically and functionally linked to SRF, gene ontology analysis, SRF binding and the overlap with published FCS-controlled genes were examined.

As presented in Figure 46C, CD-activated genes were functionally related to SRF-MRTF targets identified in NIH3T3 cells. The stringent CD-induced gene set was enriched in genes involved in cytoskeleton organization and cell migration, showing an overlap with signatures of MRTF-SRF target genes.

Because previously published SRF ChIPseq datasets do not include MRTF stimulus such as serum or CD stimulation, to assess whether CD-induced genes were associated with SRF recruitment, transcription factor binding motif search was performed. Genes within the stringent CD set were associated with SRF binding sites. These were enriched in genes with at least one SRF binding site found within 4kb of their TSS (Figure 46D).

A

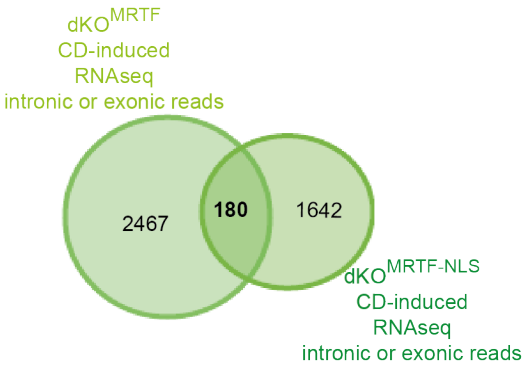

B

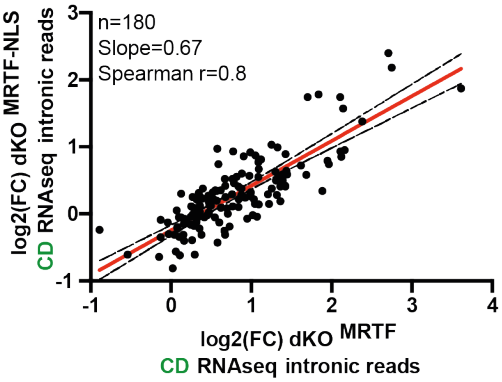

C

	GO BIOLOGICAL PROCESS	# Genes in	p-value	FDR q-value
*	REGULATION OF CELL DEATH	48	1.62E-28	1.23E-24
*	APOPTOTIC PROCESS	50	5.93E-28	2.25E-24
*	CELL MOTILITY	48	9.85E-28	2.49E-24
*	POSITIVE REGULATION OF NUCLEOBASE CONTAINING COMPOUND METABOLIC PROCESS	44	2.07E-23	3.91E-20
	POSITIVE REGULATION OF MULTICELLULAR ORGANISMAL PROCESS	43	1.51E-22	2.29E-19
	RESPONSE TO CYTOKINE	36	3.81E-22	4.81E-19
	RESPONSE TO ENDOGENOUS STIMULUS	40	1.71E-21	1.85E-18
	NEGATIVE REGULATION OF CELL DEATH	33	2.18E-21	2.06E-18
*	CYTOSKELETON ORGANIZATION	37	2.98E-21	2.51E-18
	VASCULATURE DEVELOPMENT	30	4.93E-21	3.73E-18

D

TF BINDING MOTIF	p-value	FDR q-value
SRF_Q5_01	5.75E-28	3.39E-25
SRF_C	7.33E-27	2.16E-24
SRF_Q4	1.23E-24	2.42E-22
SRF_Q6	1.98E-22	2.91E-20
TATAAA_TATA_01	4.06E-12	4.79E-10

E

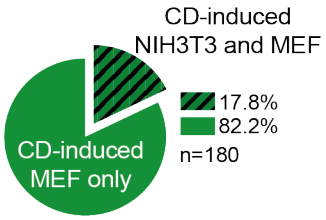

F

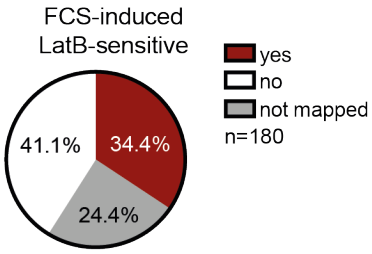

Figure 46 Defining a stringent CD-induced gene set

(A) Venn diagram representing the overlap between CD-induced genes by RNAseq in dKO^{MRTF} and dKO$^{MRTF\text{-}NLS}$ cells. (B) Scatter plot comparing fold change expression by RNAseq at the 180 genes in the CD-induced gene set. The black lines represent the 95% confidence bands of the best-fit line (red). (C) Gene ontology analysis of the CD-induced gene set. Shown are the top 10 GO categories. FDR<0.05. GO categories also enriched in CD-induced genes by RNAseq or TTseq in NIH3T3 cells are marked with *. (D) Transcription factor binding motif analysis of the CD-induced gene set. Shown are the top 5 transcription factor binding motifs. FDR<0.05. (E) Overlap of CD-induced genes in MEF and NIH3T3 cells (312 CD-induced gene set defined in Chapter 3.3). (F) Overlap of CD-induced genes in MEF and FCS-induced LatB-sensitive genes in NIH3T3 cells (n=1022), as defined in (Esnault et al., 2014). FCS-induced LatB-sensitive genes are shown in red, genes not present in the FCS-induced LatB-sensitive gene set are shown in white and genes not identified in the analysis are shown in grey. Bioinformatic analysis of RNAseq data was performed by Francesco Gualdrini.

Next, the overlap between CD-induced genes in MEF and NIH3T3 cells was examined. As shown in Figure 46E, less than 20% of the CD-induced genes in MEFs were present within the stringent CD-induced gene set in NIH3T3 cells. Nevertheless, the CD-induced gene set was enriched in previously published FCS-inducible LatB-sensitive genes (Figure 46F) (Esnault et al., 2014).

Overall, the stringent CD-induced gene set is enriched in serum-inducible genes, whose expression is sensitive to an increase in G-actin concentration by LatB, associated with SRF binding sites and functionally related to MRTF-SRF target genes. This data is consistent with the transcriptional response to CD being MRTF-dependent and corroborates results in NIH3T3 cells presented in Chapter 3.

MRTF-NLS induces non-productive transcription

To examine nascent transcription in dKO^{MRTF} and dKO$^{MRTF\text{-}NLS}$ cells, TTseq was performed. Cells were stimulated with CD or LatB for 30 min and during treatment, newly-synthesised RNA was pulse-labelled with 4SU for 15 min. The 4SU-labelled RNA was then purified and sequenced. Bioinformatic analysis of TTseq data was performed by Francesco Gualdrini. As before, differential gene expression analysis was performed, comparing each stimulus to untreated cells.

First, gene expression changes in dKO^{MRTF} cells were examined. Results are shown in Figure 47. 2996 genes were upregulated in response to CD. As in the RNAseq experiment, by TTseq CD stimulation induced the expression of genes associated with actin-based processes. In addition, genes involved in apoptosis and cell differentiation were overrepresented (Figure 47C). For full list of significantly overrepresented GO terms see Figure 102. Genes downregulated in response to CD treatment were not enriched in gene categories associated with MRTF-SRF signalling (see Figure 103).

A

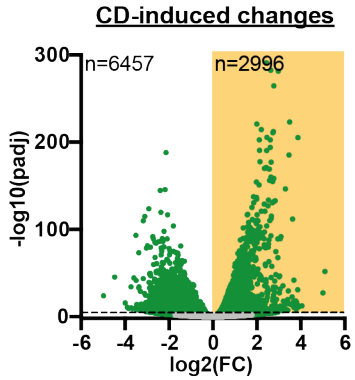

B

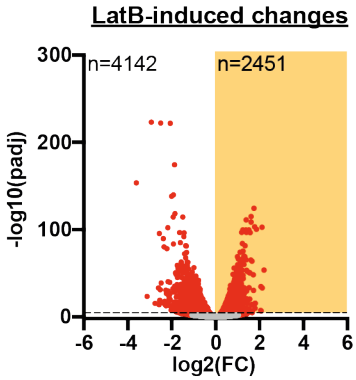

C

	GO BIOLOGICAL PROCESS	# Genes	p-value	FDR q-value
*	ACTIN FILAMENT BASED PROCESS	154	1.60E-65	1.21E-61
*	CYTOSKELETON ORGANIZATION	202	2.00E-64	7.56E-61
*	REGULATION OF INTRACELLULAR SIGNAL TRANSDUCTION	234	4.55E-63	1.15E-59
*	CELL MORPHOGENESIS	169	5.69E-61	1.08E-57
*	CELL MOTILITY	226	5.36E-60	8.12E-57
*	BIOLOGICAL ADHESION	199	4.46E-58	5.63E-55
*	CELLULAR MACROMOLECULE LOCALIZATION	234	8.07E-58	8.73E-55
*	REGULATION OF CELL DIFFERENTIATION	227	2.15E-55	2.04E-52
*	APOPTOTIC PROCESS	229	1.17E-54	9.84E-52
*	POSITIVE REGULATION OF MOLECULAR FUNCTION	216	1.05E-53	7.93E-51

Figure 47 dKO^{MRTF} TTseq

(A) Volcano plots representing CD-induced changes in gene expression, as compared to untreated cells, by TTseq. dKO^{MRTF} cells were stimulated with 3μM CD for 30 min. Significant changes (fold change>1 and pvalue>0.01) are marked in green. Significantly upregulated genes are shown in the yellow boxes. (B) Volcano plots representing LatB-induced changes in gene expression, as compared to untreated cells, by TTseq. dKO^{MRTF} cells were stimulated with 0.5μM LatB for 30 min. Significant changes (fold change>1 and pvalue>0.01) are marked in red. Significantly upregulated genes are shown in the yellow boxes. (C) Gene ontology analysis of genes upregulated by CD treatement. Shown are the top 10 GO categories. FDR<0.05. GO categories also enriched in CD-induced genes by RNAseq or TTseq in NIH3T3 cells are marked with *. Bioinformatic analysis of TTseq data was performed by Francesco Gualdrini.

A

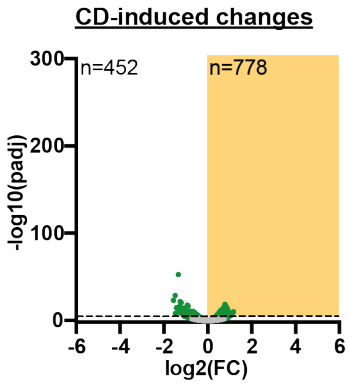

B

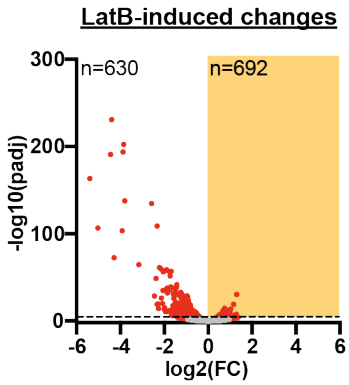

C

	GO BIOLOGICAL PROCESS	# Genes	p-value	FDR q-value
	MRNA METABOLIC PROCESS	143	1.48E-98	1.12E-94
	TRANSLATIONAL INITIATION	78	1.39E-87	5.28E-84
	CELLULAR MACROMOLECULE CATABOLIC PROCESS	145	4.09E-82	1.03E-78
	INTRACELLULAR TRANSPORT	170	7.44E-82	1.41E-78
	RNA CATABOLIC PROCESS	96	5.77E-81	8.74E-78
	COTRANSLATIONAL PROTEIN TARGETING TO MEMBRANE	61	7.93E-81	1.00E-77
	MACROMOLECULE CATABOLIC PROCESS	154	3.10E-80	3.35E-77
	NUCLEAR TRANSCRIBED MRNA C ATABOLIC PROCESS NONSENSE MEDIATED DECAY	62	4.68E-78	4.43E-75
*	CELLULAR MACROMOLECULE LOCALIZATION	175	6.39E-78	5.37E-75
	ESTABLISHMENT OF PROTEIN LOCALIZATION TO ENDOPLASMIC RETICULUM	62	9.46E-78	7.16E-75

Figure 48 dKO$^{MRTF\text{-}NLS}$ TTseq

(A) Volcano plots representing CD-induced changes in gene expression, as compared to untreated cells, by TTseq. dKO$^{MRTF\text{-}NLS}$ cells were stimulated with 3μM CD for 30 min. Significant changes (fold change>1 and pvalue>0.01) are marked in green. Significantly upregulated genes are shown in the yellow boxes. (B) Volcano plots representing LatB-induced changes in gene expression, as compared to untreated cells, by TTseq. dKO$^{MRTF\text{-}NLS}$ cells were stimulated with 0.5μM LatB for 30 min. Significant changes (fold change>1 and pvalue>0.01) are marked in red. Significantly upregulated genes are shown in the yellow boxes. (C) Gene ontology analysis of genes upregulated by CD treatement. Shown are the top 10 GO categories. FDR<0.05. GO categories also enriched in CD-induced genes by RNAseq or TTseq in NIH3T3 cells are marked with *. Bioinformatic analysis of TTseq data was performed by Francesco Gualdrini.

In contrast, as shown in Figure 48, CD-induced genes by TTseq in dKO$^{MRTF\text{-}NLS}$ cells were depleted of cytoskeletal genes. In dKO$^{MRTF\text{-}NLS}$ cells, CD stimulation caused fewer changes in gene expression than in dKO^{MRTF} cells (Figure 48A), perhaps reflecting higher basal transcription in dKO$^{MRTF\text{-}NLS}$ cells under resting conditions. CD stimulation resulted in upregulated expression of genes associated with RNA metabolism processes (Figure 48C). For full list of significantly

overrepresented GO terms see Figure 104. Genes downregulated in response to CD treatment were not enriched in gene categories associated with MRTF-SRF signalling either (see Figure 105).

Next, gene expression changes by TTseq were examined at the 180 stringent CD-induced gene set. Results are shown in Figure 49.

In dKO^{MRTF} cells, as in the RNAseq experiment, by TTseq genes within the stringent CD set were inactive in untreated cells, remained uninduced in LatB-treated cells and were activated in response to stimulation with CD.
In dKO$^{MRTF-NLS}$ cells, even though no gene activation was detected under resting conditions by RNAseq, genes within the stringent CD set were induced in the absence of an activating signal as assessed by TTseq. Furthermore, their expression was sensitive to treatement with LatB and subsequent increase in G-actin concentration.

As shown in Figure 49C, in dKO^{MRTF} cells, Pol II was engaged in elongation only in response to stimulation with CD and was not recruited at MRTF target genes under resting conditions and in LatB-treated cells. In contrast, in dKO$^{MRTF-NLS}$ cells, the TTseq profiles at MRTF-SRF target genes under resting conditions and in response to CD were very similar. Pol II was engaged in elongation in the absence of an activating signal and its recruitment was sensitive to LatB addition and subsequent increase in G-actin levels (Figure 49D).

Consistent with MRTF activity in the nucleus being under the regulation of G-actin, nuclear MRTF induces non-productive transcription at target genes, whereas disrupting the interaction between MRTF and G-actin is required for productive RNA synthesis. Under resting G-actin levels, despite the lack of pre-mRNA accumulation, Pol II is engaged in elongation at MRTF target genes, suggesting that nascent transcripts might be co-transcriptionally degraded. Even though MRTF-NLS differs from LMB-induced nuclear MRTF, in that the dKO$^{MRTF-NLS}$ cells are subjected to chronic stimulation, rather than an acute stimulus like the LMB treatment, this data corroborates findings in NIH3T3 cells.

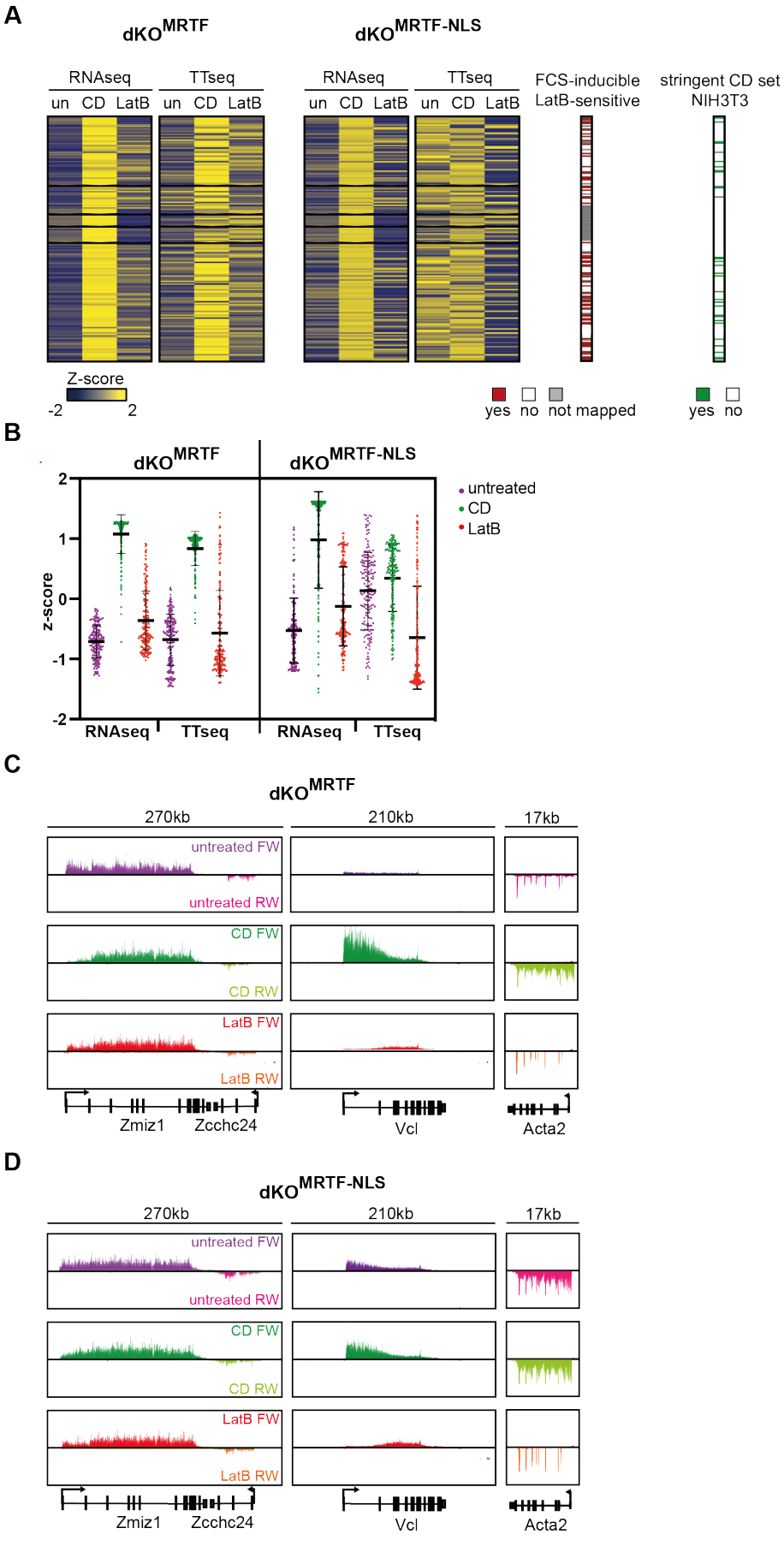
A
dKO^MRTF
dKO^MRTF-NLS
RNAseq
TTseq
un CD LatB
FCS-inducible LatB-sensitive
stringent CD set NIH3T3
Z-score
-2
2
yes no not mapped
yes no
B
dKO^MRTF
dKO^MRTF-NLS
untreated
CD
LatB
z-score
RNAseq
TTseq
C
dKO^MRTF
270kb
210kb
17kb
untreated FW
untreated RW
CD FW
CD RW
LatB FW
LatB RW
Zmiz1
Zcchc24
Vcl
Acta2
D
dKO^MRTF-NLS
270kb
210kb
17kb
untreated FW
untreated RW
CD FW
CD RW
LatB FW
LatB RW
Zmiz1
Zcchc24
Vcl
Acta2

Figure 49 Constitutively nuclear MRTF induces non-productive transcription

(A) Heatmap representing gene expression changes at the 180 genes in the CD-induced gene set in untreated, CD-stimulated and LatB-treated cells by RNAseq and TTseq in dKO^{MRTF} and dKO$^{MRTF\text{-}NLS}$ cells. Overlap with previously published FCS-induced LatB-sensitive genes (n=1022) is shown (Esnault et al., 2014). The red lines represent FCS-induced LatB-sensitive genes, the white lines represent genes not present in the FCS-induced LatB-sensitive gene set and the grey lines represent genes not identified in the analysis. Overlap with the 312 stringent CD-induced gene set in NIH3T3 cells is shown. The green lines represent CD-inducible genes, the white lines represent genes not present in the stringent CD-induced gene set in NIH3T3 cells. (B) Violin plot representing gene expression changes at the 180 genes in the CD-induced gene set in untreated, CD-stimulated and LatB-treated cells by RNAseq and TTseq in dKO^{MRTF} and dKO$^{MRTF\text{-}NLS}$ cells. (C) TTseq plots in untreated, CD-stimulated and LatB-treated dKO^{MRTF} cells at the constitutive *Zmiz1* and *Zcchc24* genes and the CD-inducible MRTF-SRF target genes *Vcl* and *Acta2*. (D) TTseq plots in untreated, CD-stimulated and LatB-treated dKO$^{MRTF\text{-}NLS}$ cells at the constitutive *Zmiz1* and *Zcchc24* genes and the CD-inducible MRTF-SRF target genes *Vcl* and *Acta2*. Bioinformatic analysis of RNAseq and TTseq data was performed by Francesco Gualdrini.

Chapter 5. The nuclear exosome regulates transcription at MRTF target genes

In the absence of G-actin depletion, nuclear MRTF is recruited to target gene promoters and induces transcription. Even though Pol II is actively transcribing MRTF target genes, pre-mRNA does not accumulate. These data suggest that under this condition, nascent MRTF-dependent transcripts might be co-transcriptionally degraded. In this chapter, the role of the nuclear exosome complex in regulating MRTF target gene expression was studied.

5.1 Inactivating the nuclear exosome rescues non-productive transcription in LMB-treated cells

In the nucleus, various complexes regulate co-transcriptional RNA processing and degradation (Schmid & Jensen, 2018). A small-scale RNAi screen was conducted in order to investigate the potential involvement of known RNA exonucleases and de-capping enzymes, the core nuclear exosome, its adapter complexes TRAMP, NEXT and PAXT and the CBCA complex, through which these are recruited to target RNAs.

Depletion of any protein involved should result in accumulation of MRTF target gene transcript in LMB-treated cells. Therefore, NIH3T3 cells were treated with siRNA for 48 hours and subsequently treated with LMB for 30 min. Pre-mRNA levels at the *Acta2* gene were measured by qPCR and compared to these in CD-stimulated cells. Depletion of SRF was used as a negative control. In addition, non-targeting scrambled siRNA control was used. Results are shown in Figure 50.

Depletion of Dis3l1 or Dis3l2 catalytic subunits of the cytoplasmic exosome, 5’ RNA exonucleases or de-capping enzymes did not affect precursor RNA levels at the *Acta2* gene. In contrast, depletion of the catalytic subunit of the nuclear exosome, Dis3, as well as components of the core exosome Exosc 2,3,7,9 and 10, upregulated pre-mRNA levels in LMB-treated cells.

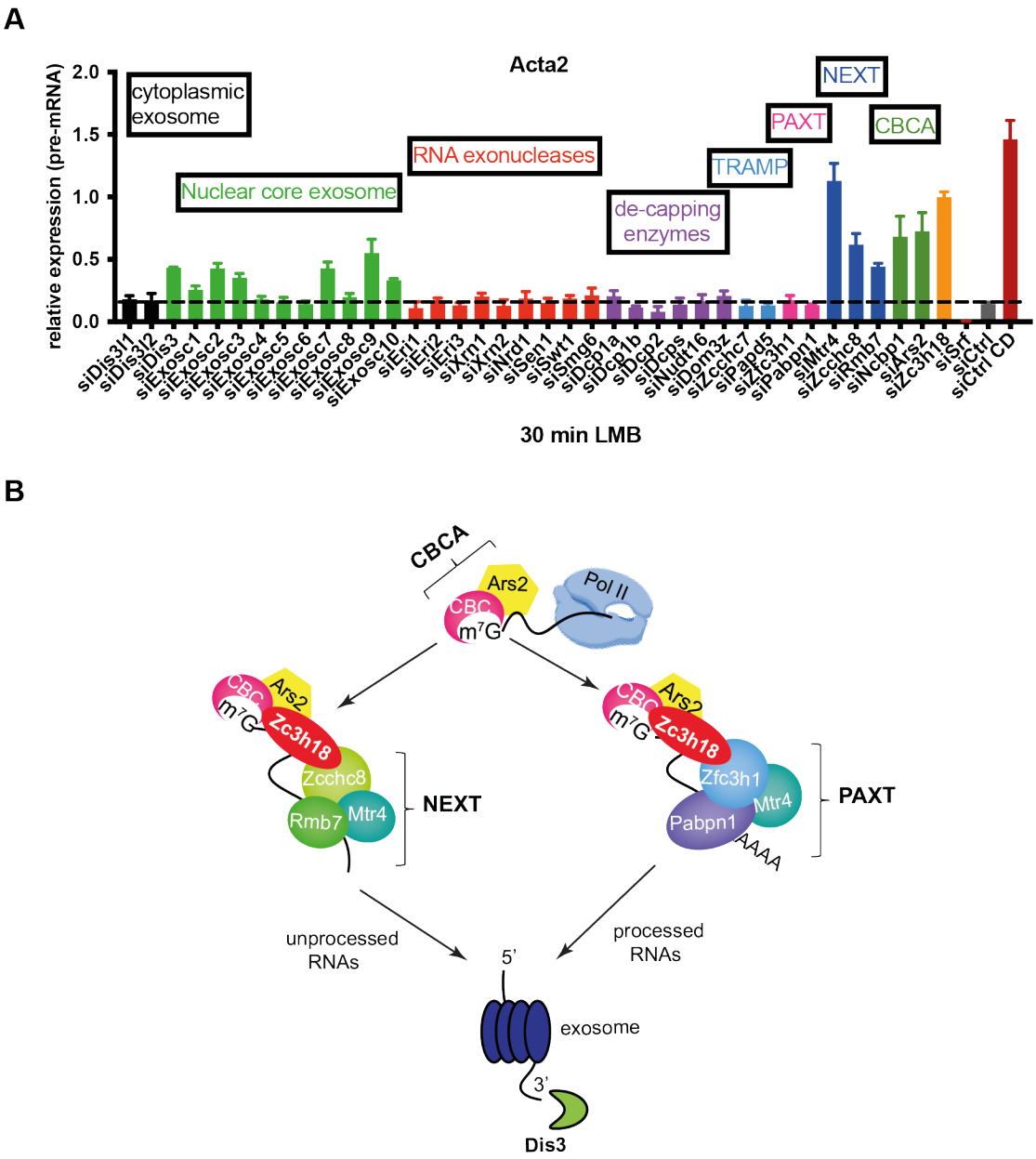

Figure 50 Inactivation of the nuclear exosome restores pre-mRNA accumulation in LMB-treated cells

(A) siRNA screen in NIH3T3 fibroblasts. Pre-mRNA at the MRTF model gene *Acta2* was measured using qPCR probes targeting the first intron of the gene. Cells were treated with siRNA for 48h, serum-starved overnight and stimulated for 30 min with 50nM LMB (Leptomycin B) or 3µM CD (Cytochalasin D) (dark red bar). Signal was normalized to *Gapdh*. Data is shown as mean ± SEM and is representative of three independent experiments. The black dotted line represents pre-mRNA levels in cells treated with scrambled siRNA (siCtrl) and LMB. (B) Nuclear exosome adapter complexes. The NEXT (Mtr4, Zcchc8, Rmb7) and PAXT (Mtr4, Zfc3h1, Pabpn1) complexes share the Mtr4 RNA helicase, which interacts with the core exosome. The NEXT and PAXT are both recruited to target RNAs through Zc3h18 and the CBCA (CBC and Ars2) complex.

Depletion of the Mtr4 RNA helicase, which is responsible for the unwinding of the RNA substrate and mediating its access to the core exosome, upregulated pre-mRNA levels at the *Acta2* gene in LMB-treated cells, to levels comparable to these in CD-stimulated cells. In addition, depletion of the Rmb7 RNA binding protein and the Zcchc8 protein, which together with Mtr4 form the NEXT complex, also increased precursor RNA levels. In contrast, depletion of Pabpn1 and Zfc3h1, components of the PAXT complex, or Papd5 and Zcchc7, components of the TRAMP complex, did not.

The NEXT complex is recruited to RNA via the cap-binding complex (CBC) in association with Ars2 and Zc3h18 co-factors (Figure 50B). Depletion of the nuclear cap binding protein (Ncbp1) and Ars2 (CBCA complex), as well as Zc3h18 also upregulated pre-mRNA levels at the *Acta2* gene in response to LMB treatment.

Overall, inactivating the nuclear exosome through depletion of individual components of the CBCA, NEXT or core exosome complexes rescues the *Acta2* pre-mRNA synthesis defect observed in LMB-treated NIH3T3 cells. To corroborate these findings, the involvement of these factors in the regulation of MRTF-dependent transcripts on additional MRTF target genes, including *Actb*, *Srf* and *Vcl*, was assessed (Figure 51).

As before, NIH3T3 cells were treated with siRNA for 48 hours and subsequently stimulated with LMB for 30 min. Baseline expression levels were assessed in untreated cells, when MRTF is in the cytoplasm and its target genes are inactive. As a control, non-targeting scrambled siRNA was used. To test whether the observed effects are MRTF-dependent, LMB-treated cells were subsequently stimulated with CD, which disrupts the MRTF/G-actin interaction and activates MRTF, or LatB, which increases the concentration of G-actin and inhibits MRTF-dependent transcription. In addition, the experiment was repeated in cells depleted of SRF, in which MRTF cannot be recruited to target genes. The specificity for MRTF target genes was tested by examining pre-mRNA levels at the *Egr1* gene, which is not under the regulation of MRTF. Although serum-inducible, *Egr1* is activated by ERK signalling to the TCF family of SRF co-factors (Esnault et al., 2014). Knock-down efficiency following siRNA treatment was assessed by

measuring target mRNA by qPCR using exonic probes and comparing their levels to these in cells treated with a non-targeting siCtrl. Results are presented in Figure 51.

Overall, depletion of Dis3, Zc3h18 and individual components of the NEXT (Zcchc8, Rmb7 and Mtr4) and CBCA (Ncbp1 and Ars2) complexes upregulated pre-mRNA levels in response to LMB treatment not only at the *Acta2* gene, but also at the *Actb*, *Vcl* and *Srf* genes, to variable degrees. The increased expression in response to LMB was MRTF-dependent, since it was inhibited by SRF depletion or LatB addition to LMB pre-treated cells, both of which prevent MRTF recruitment to targets.

Depletion of the Mtr4 helicase had a pronounced effect at MRTF-target genes in LMB-treated cells, in specific, without affecting pre-mRNA levels in untreated cells or expression of the *Egr1* gene. Despite having a milder effect, depletion of Dis3 and Rmb7 also specifically affected transcription at MRTF target genes in response to LMB.

In addition to its effect in LMB-treated cells, depletion of Zcchc8 also inhibited CD induction at MRTF target genes, as well as FCS stimulation at the *Egr1* gene. Similarly, depletion of Ncbp1 and Ars2 affected expression levels in response to CD and FCS stimulation at MRTF target genes and at the *Egr1* gene, respectively. Ars2 and Ncbp1 depletion also mildly upregulated *Egr1* pre-mRNA in LMB-treated cells.

Apart from increasing gene expression levels in response to LMB treatment, Zc3h18 depletion upregulated pre-mRNA levels in untreated and CD-stimulated cells at all MRTF target genes tested, except for the *Acta2* gene. Furthermore, its depletion also enhanced the expression of the *Egr1* gene in untreated cells, as well as in response to LMB and FCS stimulation.

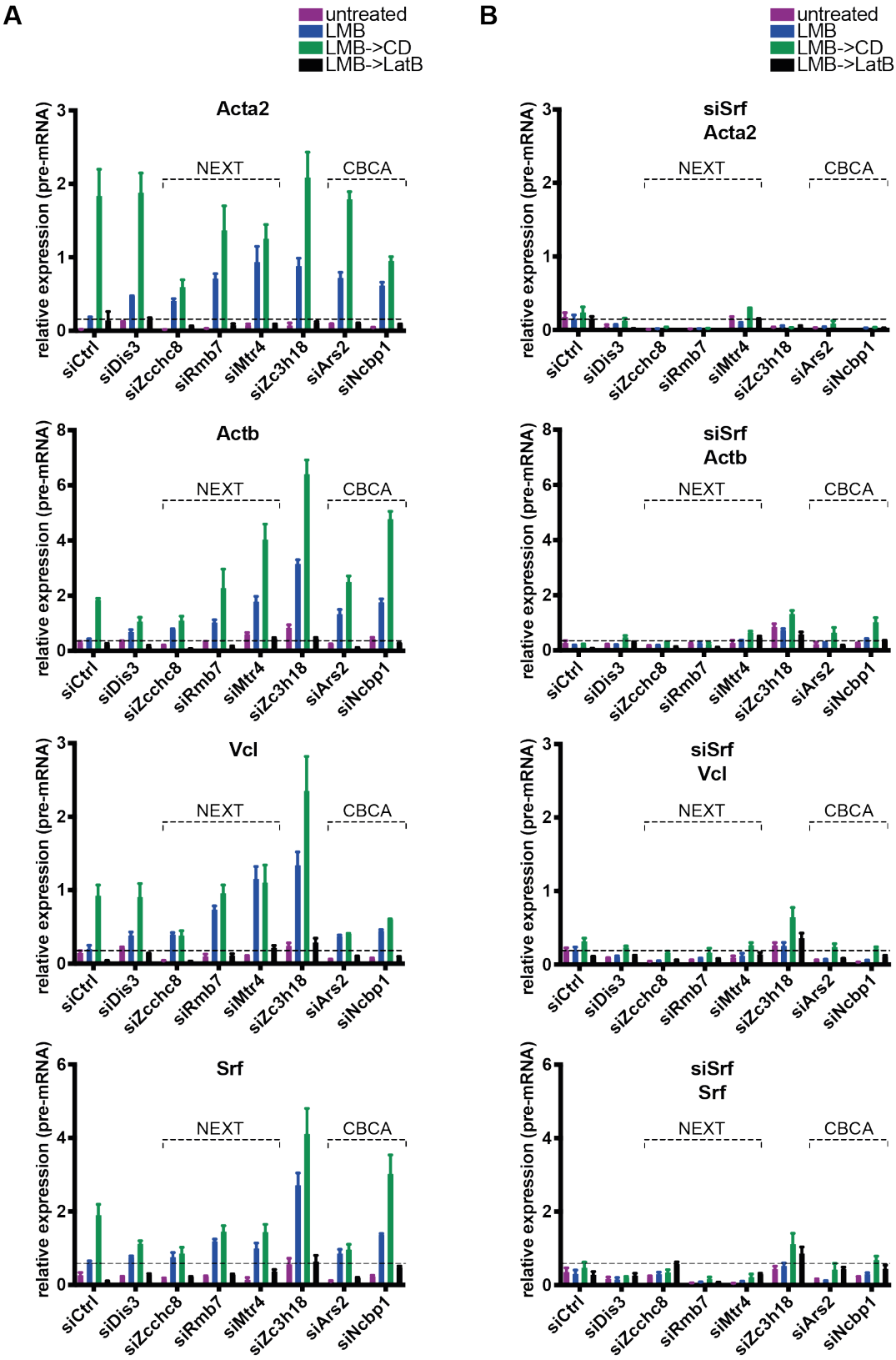
A
B
untreated
LMB
LMB->CD
LMB->LatB
Acta2
siSrf
Acta2
Actb
siSrf
Actb
Vcl
siSrf
Vcl
Srf
siSrf
Srf
relative expression (pre-mRNA)
NEXT
CBCA
siCtrl
siDis3
siZcchc8
siRmb7
siMtr4
siZc3h18
siArs2
siNcbp1

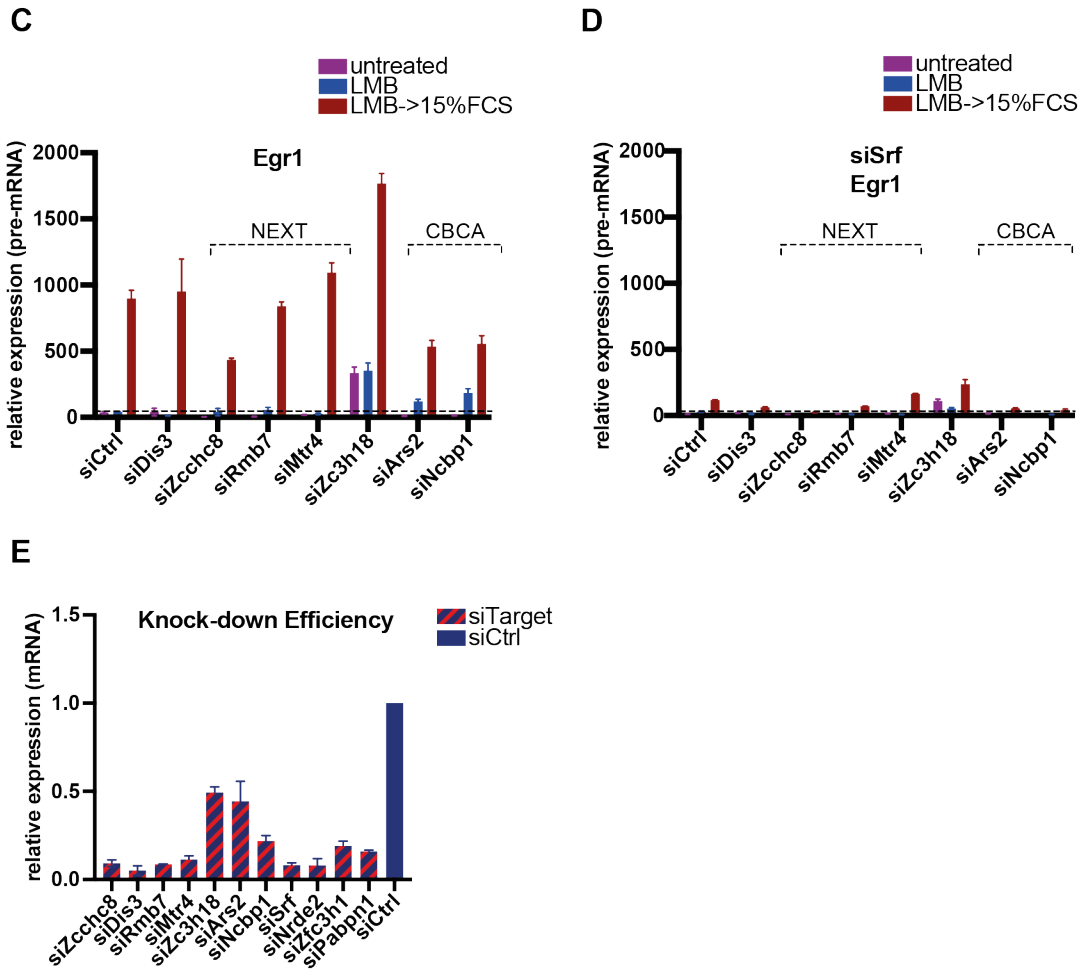

Figure 51 Inactivation of Dis3, the NEXT or CBCA complexes restores pre-mRNA accumulation in LMB-treated cells

Pre-mRNA accumulation at MRTF target genes in NIH3T3 fibroblasts (A) and SRF depleted NIH3T3 fibroblasts (B). Pre-mRNA accumulation at the TCF/SRF target gene *Egr1* in NIH3T3 fibroblasts (C) and SRF depleted NIH3T3 fibroblasts (D). Cells were treated with siRNA for 48h, serum-starved overnight and stimulated for 30 min with 50nM LMB (Leptomycin B), LMB->CD (30 min LMB followed by 30 min 3µM CD (Cytochalasin D)), LMB->LatB (30 min LMB followed by 30 min 0.5µM LatB (Latrunculin B)), LMB->15% FCS (30 min LMB followed by 30 min 15% FCS) or left untreated. Pre-mRNA was measured using qPCR probes targeting the first intron of the gene. Signal was normalized to *Gapdh*. Data is shown as mean ± SEM and is representative of three independent experiments. The black dotted lines represent pre-mRNA levels in cells treated with scrambled control siRNA and LMB. (E) siRNA efficiency. NIH3T3 cells were treated with siRNA for 48h. mRNA was measured using exonic qPCR probes. mRNA levels following siRNA treatment are shown, relative to these in cells treated with non-targeting scrambled siRNA control. Signal was normalized to *Gapdh*. Data is shown as mean ± SEM and is representative of three independent experiments.

Taken together these results indicate that in LMB-treated cells MRTF-dependent transcripts are targeted for degradation by the CBCA-dependent NEXT exosome complex. The strongest rescue of the pre-mRNA accumulation defect in LMB-treated cells was observed in cells depleted of Mtr4.

Since Mtr4 is shared between the NEXT and the PAXT exosome adapter complexes (Ogami et al., 2018), its depletion inactivates both. Although depletion of the PAXT-specific components Pabpn1 and Zfc3h1 did not affect *Acta2* transcription in LMB-treated cells, next the effect of simultaneous depletion of PAXT- and NEXT-specific components was determined. Results are presented in Figure 52.

As shown above, depletion of Mtr4, as well as depletion of Zcchc8 and Rmb7 of the NEXT complex restored pre-mRNA accumulation at MRTF target genes in LMB-treated cells, whereas depletion of Pabpn1 and Zfc3h1 of the PAXT complex did not. Co-depleting a component from the NEXT and the PAXT complex (Rmb7 and Pabpn1; Rmb7 and Zfc3h1; Zcchc8 and Pabpn1; Zcchc8 and Zfc3h1) did not enhance the effect of individual depletion of Rmb7 or Zcchc8 in LMB-treated cells. Nevertheless, inactivating both PAXT and NEXT complexes resulted in upregulation of *Acta2* and *Vcl* pre-mRNA in CD re-stimulated cells.

Since inactivating both the NEXT and the PAXT nuclear exosome adapter complexes does not increase pre-mRNA levels in LMB-treated cells, relative to these in cells depleted of Zcchc8 or Rmb7 alone, it appears unlikely that the PAXT complex is involved in regulating MRTF-dependent transcript levels in LMB treated cells.

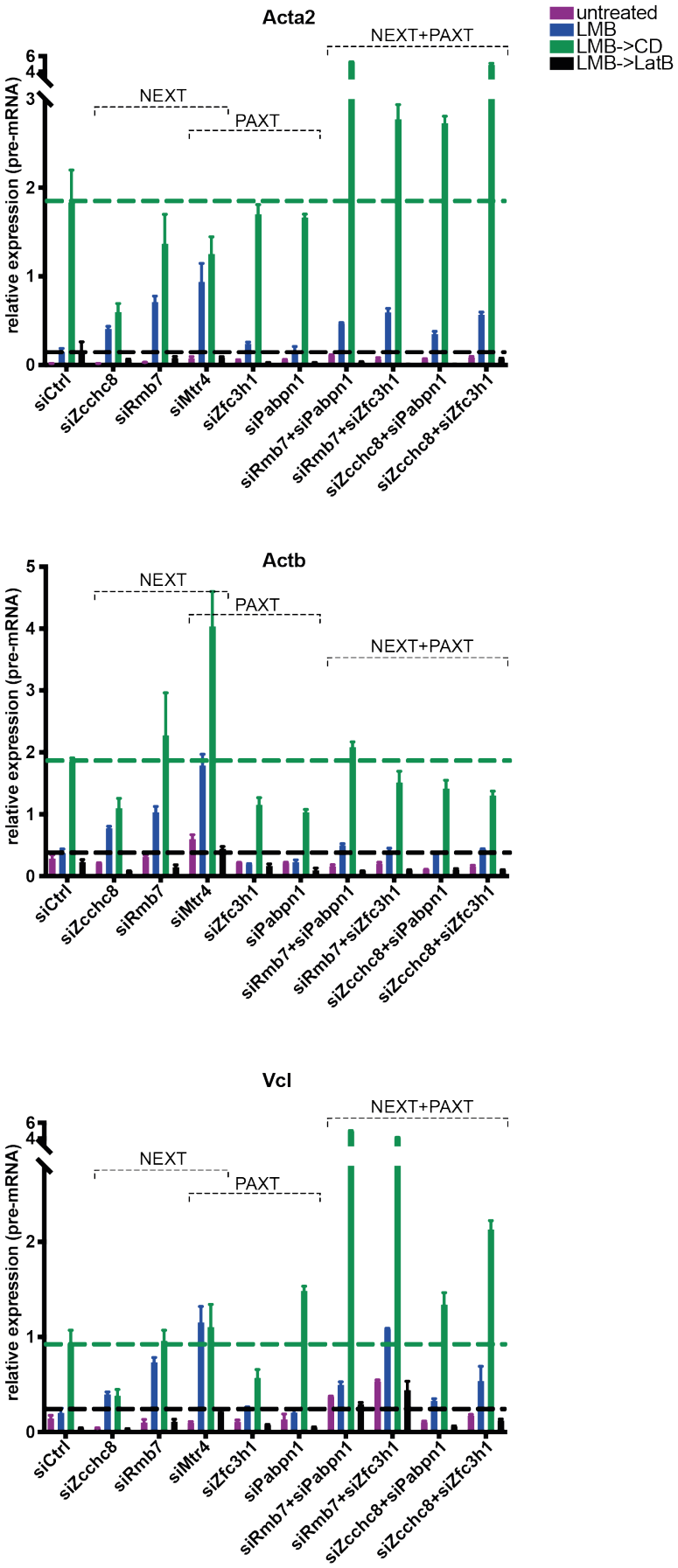
Acta2
Actb
Vcl
untreated
LMB
LMB->CD
LMB->LatB
NEXT
PAXT
NEXT+PAXT
relative expression (pre-mRNA)
siCtrl
siZcchc8
siRmb7
siMtr4
siZfc3h1
siPabpn1
siRmb7+siPabpn1
siRmb7+siZfc3h1
siZcchc8+siPabpn1
siZcchc8+siZfc3h1

Figure 52 Inactivation of the NEXT but not the PAXT complex rescues pre-mRNA accumulation in LMB-treated cells

Pre-mRNA accumulation at MRTF target genes in NIH3T3 fibroblasts. Cells were treated with siRNA for 48h, serum-starved overnight and stimulated for 30 min with 50nM LMB (Leptomycin B), LMB->CD (30 min LMB followed by 30 min 3μM CD (Cytochalasin D)), LMB->LatB (30 min LMB followed by 30 min 0.5μM LatB (Latrunculin B)) or left untreated. Pre-mRNA levels were measured using qPCR probes targeting the first intron of the gene. Signal was normalized to *Gapdh*. Data is shown as mean ± SEM and is representative of three independent experiments. The black and green dotted lines represent pre-mRNA levels in cells treated with scrambled control siRNA and LMB or CD, respectively.

5.2 Genome-wide expression analysis in Mtr4-depleted cells

The results presented above show that inactivation of the nuclear exosome rescues the non-productive transcriptional state in LMB-treated cells at individual MRTF target genes. The most potent effect is observed in cells depleted of Mtr4. To examine the effect of Mtr4 depletion across the whole genome, RNAseq was performed in cells depleted of Mtr4.

CD- and LMB-induced changes in gene expression in Mtr4-depleted cells

Sequencing libraries were prepared from total RNA purified from NIH3T3 cells treated with siMtr4 for 48 hours and subsequently stimulated with LMB or CD for 30 min. Bioinformatic analysis of RNAseq data was performed by Francesco Gualdrini. As before, to increase sensitivity, read count within introns only (intronic reads) or exons only (exonic reads) were analysed. Differential gene expression analysis was performed, comparing each stimulus to untreated cells. Results are shown in Figure 53.

A

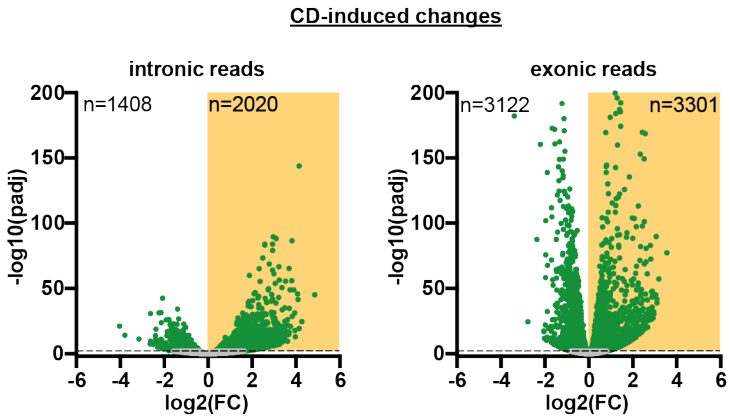

B

	GO BIOLOGICAL PROCESS	# Genes	p-value	FDR q-value
	CELL CYCLE	152	4.49E-32	3.40E-28
	CELL CYCLE PROCESS	120	5.72E-27	2.17E-23
	MITOTIC CELL CYCLE	96	4.23E-24	1.07E-20
	CELLULAR RESPONSE TO DNA DAMAGE STIMULUS	85	1.43E-23	2.71E-20
*	REGULATION OF INTRACELLULAR SIGNAL TRANSDUCTION	131	4.21E-22	6.37E-19
*	CYTOSKELETON ORGANIZATION	107	6.71E-21	8.47E-18
	PROTEIN CONTAINING COMPLEX SUBUNIT ORGANIZATION	130	1.80E-19	1.95E-16
*	CELLULAR MACROMOLECULE LOCALIZATION	128	1.94E-18	1.84E-15
	REGULATION OF CELL CYCLE	93	5.53E-18	4.66E-15
	REGULATION OF ORGANELLE ORGANIZATION	96	1.50E-17	1.14E-14

C

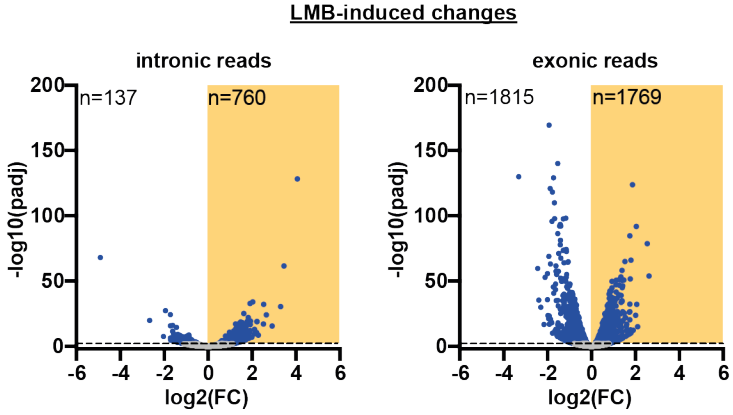

D

	GO BIOLOGICAL PROCESS	# Genes	p-value	FDR q-value	
*	ACTIN FILAMENT BASED PROCESS	85	3.13E-45	2.37E-41	*
*	CYTOSKELETON ORGANIZATION	105	4.22E-42	1.60E-38	*
*	BIOLOGICAL ADHESION	104	4.96E-39	1.25E-35	*
*	REGULATION OF INTRACELLULAR SIGNAL TRANSDUCTION	115	6.91E-38	1.31E-34	*
	REGULATION OF PHOSPHORUS METABOLIC PROCESS	114	4.19E-37	6.35E-34	
*	REGULATION OF CELL DIFFERENTIATION	115	3.74E-36	4.68E-33	
*	CELL MOTILITY	111	4.33E-36	4.68E-33	*
*	APOPTOTIC PROCESS	115	3.76E-35	3.56E-32	*
*	REGULATION OF CELL DEATH	105	1.53E-33	1.29E-30	*
	REGULATION OF PHOSPHORYLATION	102	3.66E-33	2.77E-30	

Figure 53 CD- and LMB- induced gene expression changes in Mtr4-depleted cells

(A) Volcano plots representing CD-induced changes in gene expression, as compared to untreated cells, by RNAseq. NIH3T3 cells were treated with siRNA against Mtr4 for 48h, serum-starved overnight and subsequently stimulated with 3μM CD for 30 min. Significant changes (fold change>1 and pvalue>0.01) are marked in green. Significantly upregulated genes are shown in the yellow boxes. (B) Gene ontology analysis of genes upregulated by CD treatement. Shown are the top 10 GO categories. FDR<0.05. GO categories also enriched in CD-induced genes by RNAseq or TTseq in NIH3T3 cells are marked with *. (C) Volcano plots representing LMB-induced changes in gene expression, as compared to untreated cells, by RNAseq. NIH3T3 cells were treated with siRNA against Mtr4 for 48h, serum-starved overnight and subsequently stimulated with 50nM LMB for 30 min. Significant changes (fold change>1 and pvalue>0.01) are marked in blue. Significantly upregulated genes are shown in the yellow boxes. (D) Gene ontology analysis of genes upregulated by LMB treatement. Shown are the top 10 GO categories. FDR<0.05. GO categories also enriched in CD-induced genes by RNAseq or TTseq in NIH3T3 cells are marked with *. GO categories also enriched in LMB-induced genes by TTseq in NIH3T3 cells are marked with *. Bioinformatic analysis of RNAseq data was performed by Francesco Gualdrini.

In Mtr4-depleted cells, CD stimulation resulted in detectable upregulation of 2020 genes in intronic reads and 3301 genes in exonic reads (Figure 53A). Mtr4 depletion appeared to alter the profile of CD-induced gene expression. CD-induced gene were enriched in genes involved mainly in cell cycle regulation. While genes associated with actin-based processes were also upregulated, these were not as enriched as in CD-stimulated wild-type NIH3T3 cells (Figure 53B). For full list of significantly overrepresented GO terms see Figure 106. Genes downregulated in response to CD treatment were not enriched in gene categories associated with MRTF-SRF signalling or cell cycle regulation (see Figure 107).

Whereas in wild-type NIH3T3 cells LMB treatment did not elicit a transcriptional response detectable by RNAseq (see Figure 36), in cells depleted of Mtr4, induction of 760 genes in intronic and 1769 genes in exonic reads was detected by RNAseq (Figure 53C). LMB-stimulation induced expression of genes associated with actin cytoskeleton, cell adhesion and motility (Figure 53D). For full list of significantly overrepresented GO terms see Figure 108.

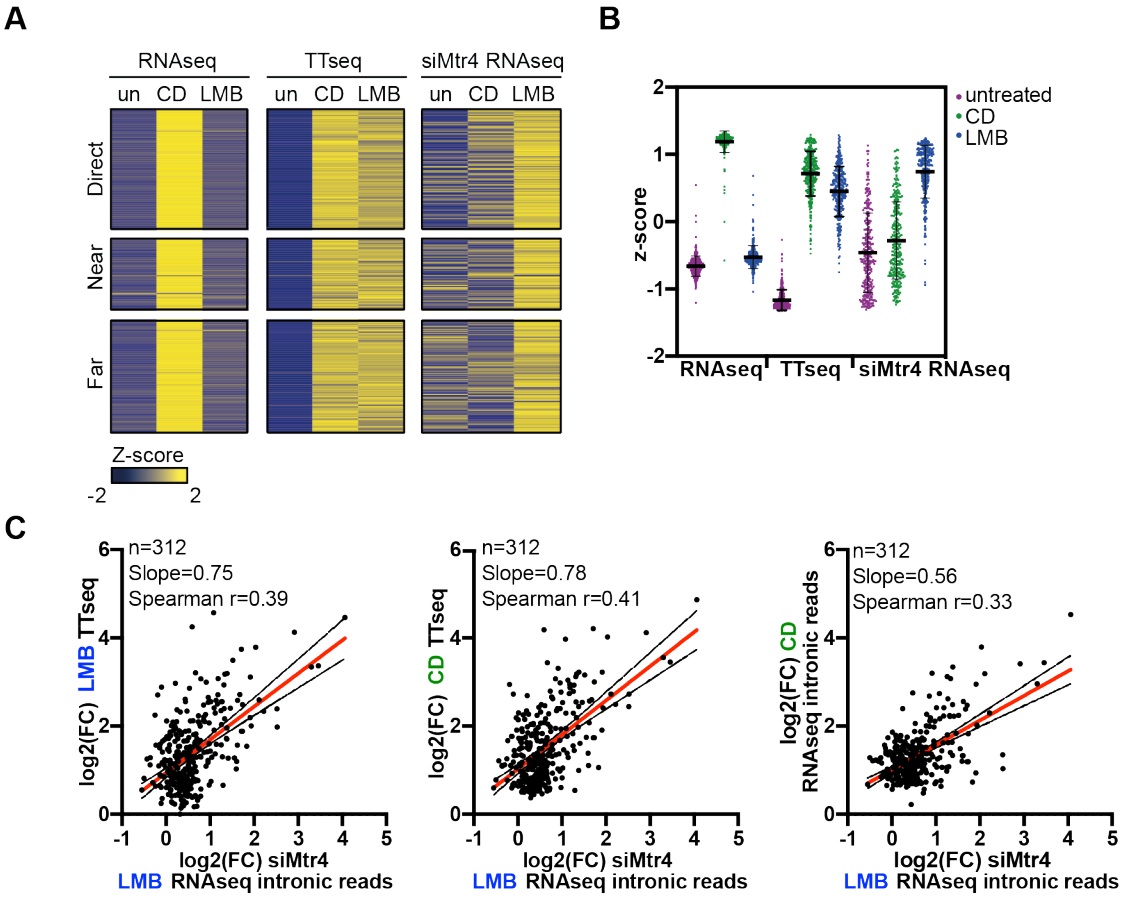

Figure 54 Mtr4 depletion restores productive RNA synthesis at MRTF target genes in LMB-treated cells

(A) Heatmap representing gene expression changes at the 312 stringent CD-induced gene set in untreated, LMB-stimulated and CD-stimulated cells by RNAseq and TTseq in wild-type NIH3T3 cells and by RNAseq in Mtr4-depleted NIH3T3 cells. Genes are separated by distance to their nearest SRF binding site, direct (within 5kb); near (within 70kb); far (>70kb). (B) Violin plot representing gene expression changes at the 312 stringent CD-induced gene set in untreated, LMB-stimulated and CD-stimulated cells by RNAseq and TTseq in wild-type NIH3T3 cells and by RNAseq in Mtr4-depleted NIH3T3 cells. (C) Scatter plots comparing fold change expression at the 312 stringent CD-induced gene set between conditions. The black lines represent the 95% confidence bands of the best-fit line (red). Bioinformatic analysis of RNAseq and TTseq data was performed by Francesco Gualdrini.

This gene signature overlapped with the one of MRTF-SRF target genes, CD-responsive genes (see Figure 33B and Figure 34B) and the LMB-induced gene set from the TTseq experiment (see Figure 37B), indicating that Mtr4 depletion restores productive transcription at MRTF target genes in response to LMB. Genes downregulated in response to LMB treatment were not enriched in gene categories associated with MRTF-SRF signalling (see Figure 109).

First, the effect of Mtr4 depletion on MRTF-regulated genes was assessed. The behaviour of the 312 stringent CD-induced gene set defined in Chapter 3.3 were examined. Results are shown in Figure 54.

At these genes Mtr4 depletion led to elevated basal expression in untreated cells, as compared to that in wild-type NIH3T3 cells, and inducibility in response to CD was attenuated. Nevertheless, LMB stimulation stimulated gene expression, with a magnitude of induction comparable to that observed by TTseq (Figure 54A and B). Fold induction in LMB-treated cells correlated with that observed in LMB-treated and CD-treated wild-type cells by TTseq. There was a weaker correlation between fold induction in LMB treated Mtr4-depleted cells and CD-stimulated wild-type NIH3T3 cells by RNAseq (Figure 54C). There was no correlation in gene expression changes globally between LMB-treated Mtr4-depletedcells and LMB-treated cells by TTseq, CD-treated cells by TTseq or CD-treated cells by RNAseq. For correlation plots between full datasets see Figure 114C.

These results suggest that Mtr4-depetion rescues the RNA synthesis defect observed in the LMB-induced non-productive transcriptional state at MRTF target genes.

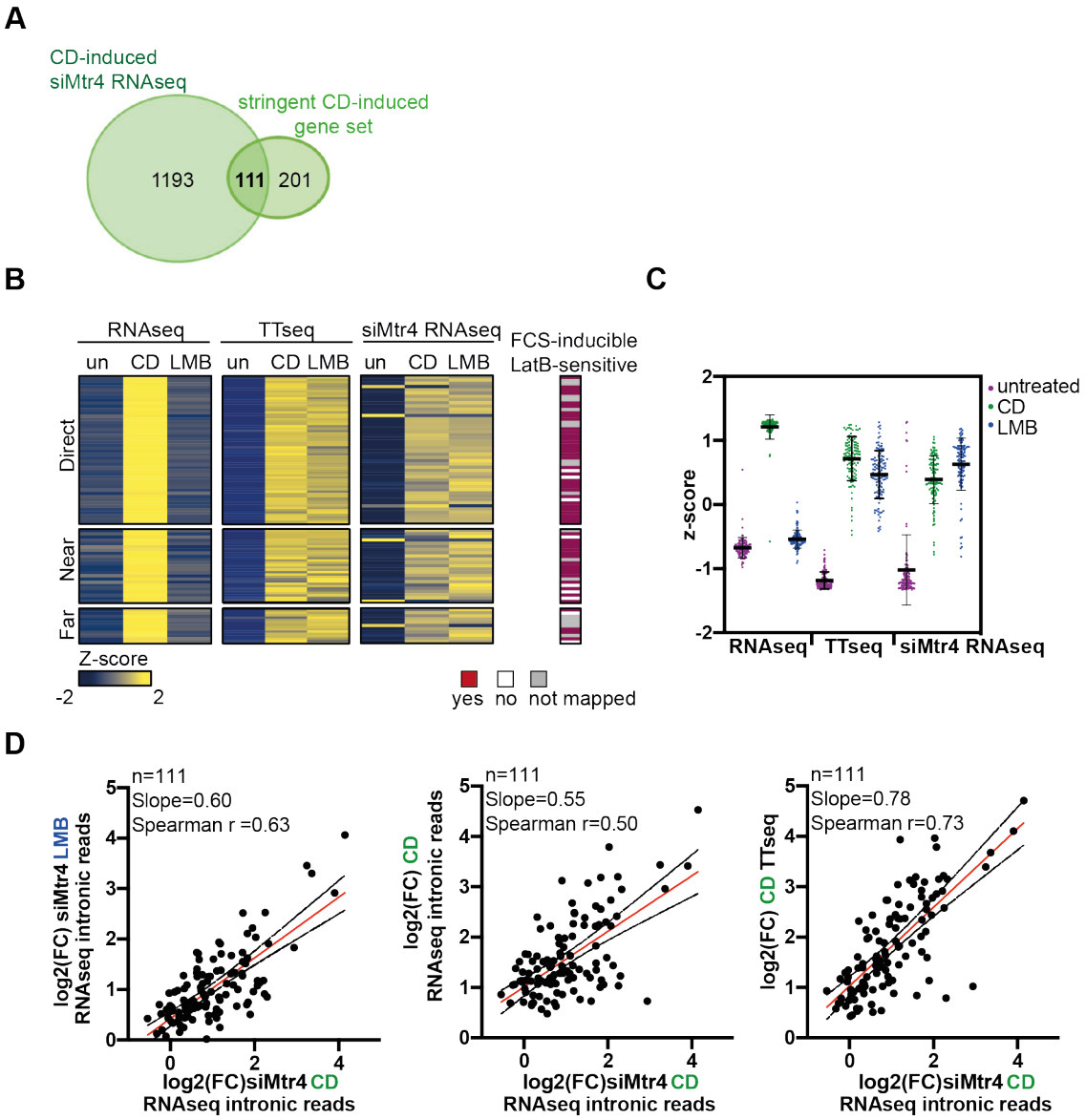

Figure 55 Mtr4 depletion supresses CD induction at MRTF target genes

(A) Venn diagram representing the subset of CD-induced genes which remain responsive to CD stimulation in the absence of Mtr4. (B) Heatmap representing gene expression changes at the subset of 111 CD-inducible genes in untreated, LMB-stimulated and CD-stimulated cells by RNAseq and TTseq in wild-type NIH3T3 cells and by RNAseq in Mtr4-depleted NIH3T3 cells. Genes are separated by distance to their nearest SRF binding site, direct (within 5kb); near (within 70kb); far (>70kb). Overlap with previously published FCS-induced LatB-sensitive genes (n=1022) is shown (Esnault et al., 2014). The red lines represent FCS-induced LatB-sensitive genes, the white lines represent genes not present in the FCS-induced LatB-sensitive gene set and the grey lines represent genes not identified in the analysis. (C) Violin plot representing gene expression changes at the subset of 111 CD-inducible genes in untreated, LMB-stimulated and CD-stimulated cells by RNAseq and TTseq in wild-type NIH3T3 cells and by RNAseq in Mtr4-depleted NIH3T3 cells. (D) Scatter plots comparing fold change induction at the subset of 111 CD-inducible genes between conditions. The black lines represent the 95% confidence bands of the best-fit line (red). Bioinformatic analysis of RNAseq and TTseq data was performed by Francesco Gualdrini.

CD stimulation is impaired in Mtr4 depleted cells, perhaps a result of the increased baseline expression in untreated cells. As shown in Figure 55A, 111 genes remained CD-inducible upon Mtr4 knock-down. These were heavily enriched in SRF direct target genes and FCS-inducible genes, sensitive to LatB treatment. Induction levels in response to CD in Mtr4-depleted cells strongly correlated with those in LMB-treated cells, as well as with those in CD-stimulated wild-type NIH3T3 cells (Figure 55C). There was no correlation in gene expression changes globally between CD-treated Mtr4-depleted cells and LMB-treated Mtr4-depleted cells by RNAseq, CD-treated cells by RNAseq or CD-treated cells by TTseq. For correlation plots between full datasets see Figure 114D.

Mtr4 depletion restores productive RNA synthesis at LMB-induced genes

As an alternative approach, the effect of Mtr4 depletion on LMB-induced transcripts, without pre-selecting for CD-inducibility, was examined. Results are shown in Figure 56.

Of the 2510 LMB-induced genes by TTseq, 455 were also detectably upregulated in Mtr4-depleted cells by RNAseq (Figure 56A). To determine whether these were physically and functionally linked to SRF, as before, distance to the nearest SRF binding site, overlap with published SRF-controlled genes and gene ontology analyses were performed.

More than 30% of the 455 LMB-induced Mtr4-controlled gene set was associated with direct SRF binding (Figure 56B). In contrast, approximately 5% of inactive genes and less than 10% of other LMB-responsive genes were located in close proximity to an SRF binding site. Furthermore, these were functionally related to MRTF-SRF targets. This gene set was heavily enriched in exactly the same gene classes as the stringent CD-induced gene set, genes involved in actin filament-based processes, cytoskeleton organization, biological adhesion, cell motility (Figure 56C). In addition, consistent with regulation by MRTF, these were strongly enriched in serum-inducible LatB-sensitive genes (Figure 56D).

Genes in the 455 gene set were inactive in untreated cells and expressed in response to CD in all experiments. Like at bona-fide MRTF target genes, in response to LMB, no gene activation was detectable by RNAseq, despite being upregulated by TTseq and in Mtr4-depleted cells (Figure 56D and E).

Fold induction in LMB-treated Mtr4-depleted cells strongly correlated with that in LMB-treated wild-type cells by TTseq. There was also a correlation with CD-induced fold change by TTseq and a weak correlation with CD-induction by RNAseq (Figure 56F).

The LMB-induced gene set regulated by Mtr4 is enriched in CD- and FCS-inducible genes, sensitive to an increase in G-actin concentration by LatB, physically associated with SRF and functionally related to MRTF-SRF target genes, strongly suggesting these are MRTF regulated.

A

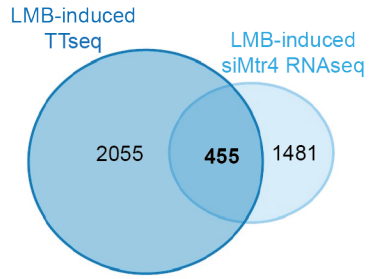

B

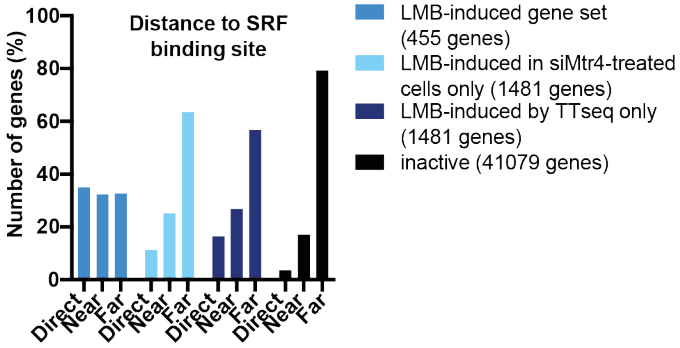

C

	GO BIOLOGICAL PROCESS	# Genes	p-value	FDR q-value
*	ACTIN FILAMENT BASED PROCESS	69	2.04E-46	1.54E-42
*	CYTOSKELETON ORGANIZATION	81	7.33E-42	2.77E-38
*	BIOLOGICAL ADHESION	75	1.09E-34	2.75E-31
*	SUPRAMOLECULAR FIBER ORGANIZATION	51	2.52E-30	4.77E-27
*	CELL MOTILITY	76	1.12E-29	1.70E-26
*	ANATOMICAL STRUCTURE FORMATION INVOLVED IN MORPHOGENESIS	60	2.52E-27	3.18E-24
*	ACTIN FILAMENT ORGANIZATION	39	4.16E-27	4.50E-24
*	REGULATION OF INTRACELLULAR SIGNAL TRANSDUCTION	72	5.09E-26	4.82E-23
*	REGULATION OF CELL DIFFERENTIATION	72	6.33E-25	5.33E-22
*	CELL SUBSTRATE ADHESION	34	1.84E-24	1.39E-21

D

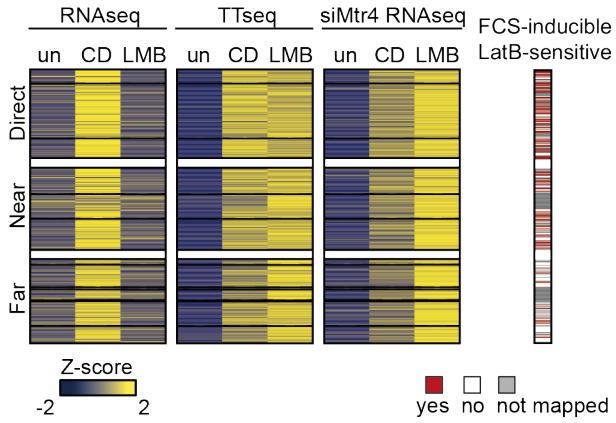

E

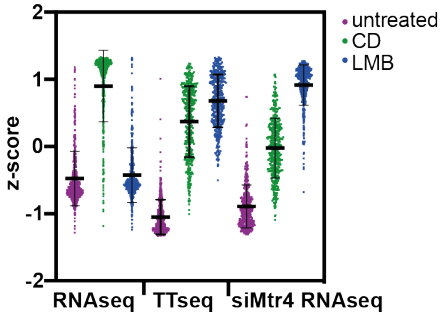

F

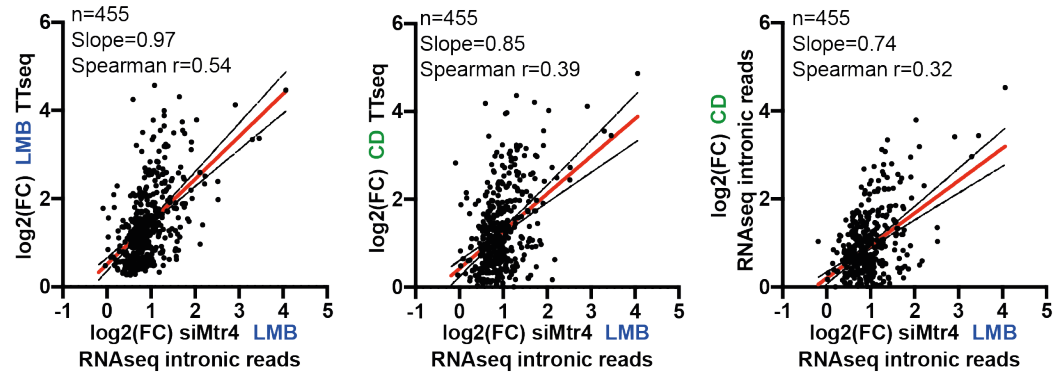

Figure 56 Mtr4 depletion restores productive transcription at a subset of LMB-inducible genes

(A) Venn diagram representing the subset of LMB-induced genes regulated by Mtr4. (B) Distance to SRF binding site. Coordinates of SRF binding sites published in (Esnault et al., 2014) were used. (C) GO analysis of LMB-induced genes regulated by Mtr4. Shown are the top 10 GO categories. FDR<0.05. GO categories also enriched in CD-induced genes by RNAseq or TTseq in NIH3T3 cells are marked with *. (D) Heatmap representing gene expression changes at LMB-induced genes regulated by Mtr4 in untreated, LMB-stimulated and CD-stimulated cells by RNAseq and TTseq in wild-type NIH3T3 cells and by RNAseq in Mtr4-depleted NIH3T3 cells. Genes are separated by distance to their nearest SRF binding site, direct (within 5kb); near (within 70kb); far (>70kb). Overlap with previously published FCS-induced LatB-sensitive genes (n=1022) is shown (Esnault et al., 2014). The red lines represent FCS-induced LatB-sensitive genes, the white lines represent genes not present in the FCS-induced LatB-sensitive gene set and the grey lines represent genes not identified in the analysis. (E) Violin plot representing gene expression changes at LMB-induced genes regulated by Mtr4 in untreated, LMB-stimulated and CD-stimulated cells by RNAseq and TTseq in wild-type NIH3T3 cells and by RNAseq in Mtr4-depleted NIH3T3 cells. (F) Scatter plots comparing fold change expression in response to CD and LMB between experiments. The black lines represent the 95% confidence bands of the best-fit line (red). Bioinformatic analysis of RNAseq and TTseq data was performed by Francesco Gualdrini.

Effect of Mtr4 depletion in resting cells

Finally, the effect of Mtr4 depletion on gene expression under resting conditions was examined. Differential gene expression analysis was performed comparing Mtr4-depleted untreated cells with wild-type untreated cells. Results are shown in Figure 57.

Mtr4 depletion resulted in a significant increase in RNA levels at 1894 genes in intronic reads and 2425 genes in exonic reads (Figure 57A). The Mtr4-sensitive genes were not associated with direct SRF binding or present in the FCS controlled set (Figure 57B). The majority of upregulated genes were protein-coding, enriched in genes involved in cell cycle control and the DNA damage repair response (Figure 57C and D). For full list of significantly overrepresented GO terms see Figure 110.

In addition to its characterized role in regulating non-coding transcripts, this data suggests that Mtr4 also controls the expression of specific subsets of protein-coding genes.

Overall, Mtr4 depletion restores productive RNA synthesis in response to LMB stimulation at MRTF controlled genes. This data is consistent with a model in which in the absence of G-actin depletion, LMB-induced recruitment of MRTF to target gene promoters induces production of nascent transcripts that are targeted for co-transcriptional degradation by Mtr4 and the nuclear exosome complex.

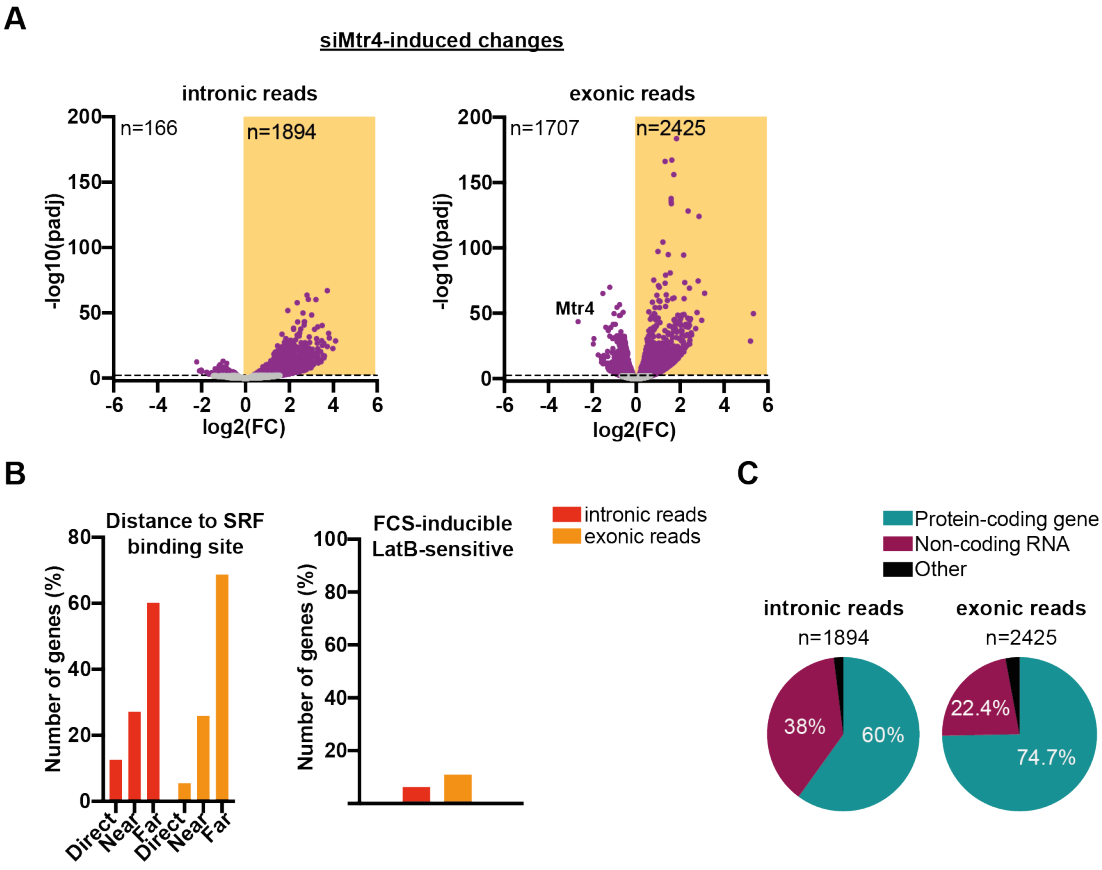

	GO BIOLOGICAL PROCESS	# Genes	p-value	FDR q-value
	CELL CYCLE	145	4.08E-30	3.09E-26
	CELLULAR RESPONSE TO DNA DAMAGE STIMULUS	88	1.63E-26	6.16E-23
	CELL CYCLE PROCESS	112	4.77E-24	1.20E-20
	CARBOHYDRATE DERIVATIVE METABOLIC PROCESS	94	5.01E-22	9.48E-19
	REGULATION OF CELL CYCLE	95	5.09E-20	7.72E-17
	DNA METABOLIC PROCESS	80	2.67E-19	3.37E-16
	MITOTIC CELL CYCLE	82	1.55E-17	1.68E-14
	DNA REPAIR	56	7.74E-17	7.33E-14
	CARBOHYDRATE DERIVATIVE BIOSYNTHETIC PROCESS	60	9.78E-16	7.99E-13
*	POSITIVE REGULATION OF NUCLEOBASE CONTAINING COMPOUND METABOLIC PROCESS	113	1.05E-15	7.99E-13

Figure 57 Transcriptional changes induced by Mtr4 depletion

(A) Volcano plots representing changes in gene expression induced by Mtr4 depletion in untreated cells. Significant changes (fold change>1 and pvalue>0.01) are marked in purple. Significantly upregulated genes are shown in the yellow boxes. (B) Distance to SRF binding sites. Coordinates of SRF binding sites published in (Esnault et al., 2014) were used. Overlap with previously published FCS-induced LatB-sensitive genes (n=1022) is shown (Esnault et al., 2014). (C) Fraction of protein-coding and non-coding transcripts upregulated in Mtr4-depleted cells. (D) Gene ontology analysis of genes upregulated by Mtr4 depletion. Shown are the top 10 GO categories. FDR<0.05. GO categories also enriched in CD-induced genes by RNAseq or TTseq in NIH3T3 cells are marked with *. Bioinformatic analysis of RNAseq data was performed by Francesco Gualdrini.

5.3 Mtr4 is recruited to transcripts of MRTF target genes

The results presented above show that Mtr4 depletion restores pre-mRNA accumulation at MRTF target genes in LMB-treated cells. To determine whether this effect reflects direct action of the nuclear exosome complex on MRTF-dependent transcripts, the association of Mtr4 with transcripts of MRTF target genes in response to stimulation was examined.

Following treatment, cells were UV-irradiated to induce RNA-protein cross-linking and Mtr4-associated RNA was recovered by immunoprecipitation (Ule et al., 2005). Recovered RNA was quantified by qPCR. Signal was normalized to IgG immunoprecipitates. To test the specificity for transcripts of MRTF target genes, the constitutively expressed *B2m* and *Rps16* genes, which are not SRF targets, and the serum-inducible TCF-SRF target gene *c-Fos* were used. Results are shown in Figure 58A.

In untreated cells, Mtr4 was not detectably associated with any of the transcripts tested. While CD and FCS stimulation had no effect on Mtr4 recruitment to *B2m*, *Rps16* or *c-Fos*, they caused a marginal increase in the association of Mtr4 with transcripts of MRTF target genes, which are strongly induced by CD and FCS. In contrast, LMB treatment, which does not induce transcript accumulation detectable by RNAseq, strongly induced Mtr4 association with MRTF-dependent transcripts.

Thus, the non-productive transcriptional state at MRTF targets in LMB-treated cells is associated with direct recruitment of Mtr4 to transcripts of MRTF target genes.

To determine whether the rescued transcripts in Mtr4-depleted LMB-treated cells generate functional RNA, mature RNA levels were assessed by qPCR using exonic probes. NIH3T3 cells were treated with a non-targeting scrambled siRNA or siRNA against Mtr4 for 48 hours and subsequently stimulated with LMB or CD for 1 hour. Results are presented in Figure 58B. Depletion of Mtr4 caused upregulation of *Acta2*, *Actb* and *Vcl* mRNA in response to LMB treatment, while it did not affect their levels in untreated cells.

To test whether the RNA rescued in Mtr4-depleted cells was competent for nuclear export and translation, α-actin and β-actin protein levels in cells depleted of Mtr4 were examined. NIH3T3 cells were treated with a non-targeting scrambled siRNA or siRNA against Mtr4 for 48 hours and subsequently stimulated with LMB or CD for 4 hours.

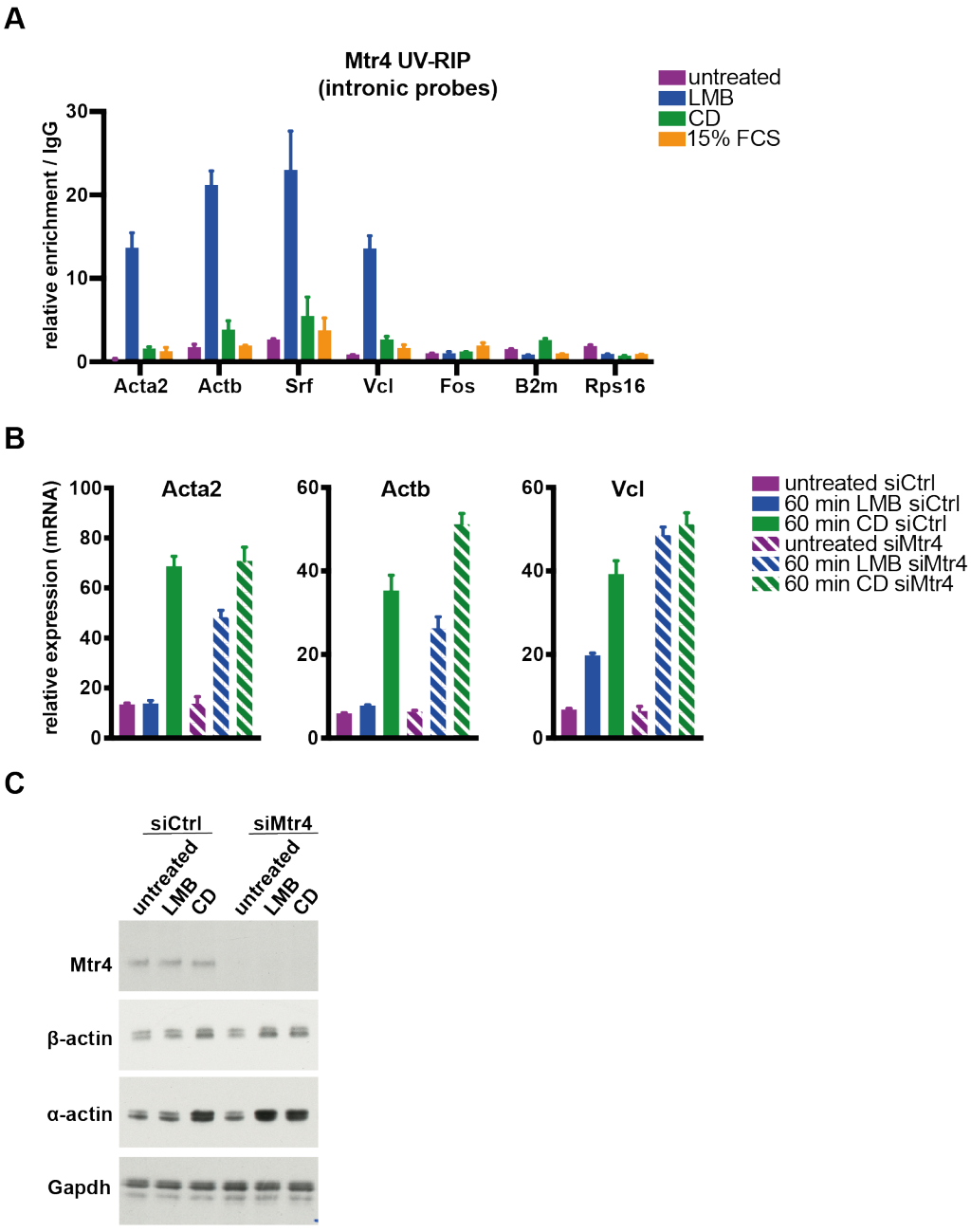

Figure 58 Mtr4 is recruited to MRTF-dependent transcripts in response to LMB

(A) Mtr4 UV-RIP. NIH3T3 fibroblasts were serum-starved overnight and stimulated for 30 min with 50nM LMB (Leptomycin B), 3μM CD (Cytochalasin D), 15% FCS or left untreated. Signal was normalized to IgG IP. Pre-mRNA levels were measured using qPCR probes targeting the first intron of the gene. Data is shown as mean ± SEM and is representative of three independent experiments. (B) mRNA accumulation at MRTF target genes. NIH3T3 fibroblasts were treated with siRNA for 48h, serum-starved overnight and stimulated for 60 min with 50nM LMB (Leptomycin B), 3μM CD (Cytochalasin D) or left untreated. mRNA levels were measured using exonic qPCR probes. Signal was normalized to *Gapdh*. Data is shown as mean ± SEM and is representative of three independent experiments. (C) Western blot. Cells were treated with siMtr4 or scrambled control siRNA for 48h, serum-starved overnight and stimulated for 4 hours with 50nM LMB (Leptomycin B), 3μM CD (Cytochalasin D) or left untreated. Protein lysates were probed with antibodies against Mtr4 (nb100-1574), α-actin (sc-56499), β-actin (sc-47778) and Gapdh (sc-25778).

In cells treated with control siRNA, CD stimulation upregulated α-actin and β-actin protein levels, as compared to these in untreated cells. Whereas LMB treatment did not affect α-actin and β-actin protein levels. In contrast, in cells depleted of Mtr4, α-actin and β-actin levels were upregulated not only in CD-stimulated cells but also in response to LMB treatment. The effect on α-actin protein level was more pronounced than the one on ß-actin. Depletion of Mtr4 did not affect protein levels in the absence of stimulation, and Gapdh levels remained unchanged across conditions.

Overall, Mtr4 directly interacts specifically with MRTF-dependent transcripts and its depletion is sufficient to restore productive transcription at MRTF target genes in LMB-treated cells.

5.4 Nrde2 depletion inhibits activation of MRTF target genes

Recent studies show that Mtr4 activity is negatively regulated by Nrde2, which binds to Mtr4, inhibits its recruitment to RNA, as well as its interaction with the Dis3 exosome subunit (J. Wang et al., 2019). Depletion of Nrde2 thus potentially provides a route to increasing Mtr4-dependent RNA processing. The crosslinking

data in Figure 58A suggests that Mtr4 might be weakly recruited to transcripts of MRTF targets under inducing conditions. Therefore, whether depletion of Nrde2 might potentiate Mtr4 activity to the point at which it would detectably inhibit productive transcription at MRTF target genes, even under inducing conditions, was tested.

As before, NIH3T3 cells were treated with siRNA for 48 hours and subsequently stimulated with CD or FCS, both of which activate MRTF, either by directly disrupting MRTF/G-actin interaction or by promoting F-actin assembly. Non-targeting scrambled siRNA was used as a control. Transcription at MRTF target genes was assessed by qPCR using probes targeting the first intron of the gene. Baseline expression levels were assessed in untreated cells, when MRTF is in the cytoplasm and its target genes are inactive. The specificity for MRTF target genes was tested by examining pre-mRNA levels at the *Egr1* and *c-Fos* genes. Although serum-inducible *Egr1* and *c-Fos* are activated by ERK signalling to the TCF family of SRF co-factors (Esnault et al., 2014). In addition, pre-mRNA levels at the constitutively active genes *B2m*, *Rps16*, *Pbgd* and *Hprt*, which are not SRF targets, were examined. To confirm that any potential effect of Nrde2 depletion reflects the activity of Mtr4, the experiment was repeated in cells depleted of Mtr4. Results are shown in Figure 59.

In cells treated with siCtrl, stimulation with CD induced expression of MRTF target genes and this was unaffected by depletion of Mtr4. In contrast, depletion of Nrde2 inhibited CD stimulation, while co-depletion of Nrde2 and Mtr4 restored pre-mRNA accumulation, to levels comparable to these in cells treated with siCtrl (Figure 59A). Pre-mRNA levels in untreated cells remained unaffected in all the conditions tested. In contrast, depletion of Nrde2 did not affect expression of the constitutively active *B2m*, *Rps16*, *Pbgd* and *Hprt* genes (Figure 59B).

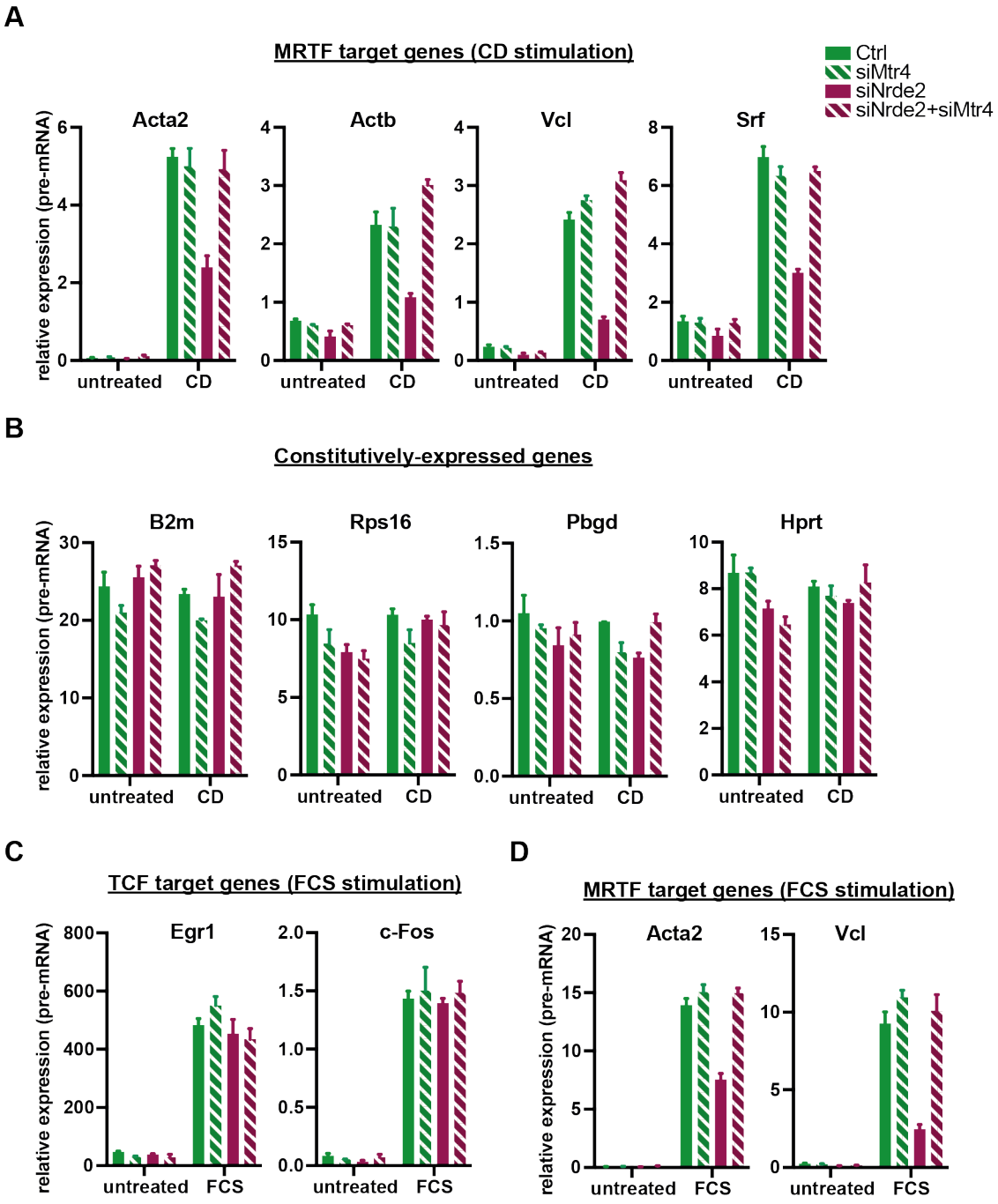

Figure 59 Nrde2 depletion inhibits MRTF target gene expression in response to stimulation

Pre-mRNA accumulation at MRTF target genes (A), constitutively expressed genes (B), TCF target genes in response to FCS stimulation (C) and MRTF target genes in response to serum stimulation (D). NIH3T3 fibroblasts were treated with siRNA for 48h, serum-starved overnight and stimulated for 30 min with 3µM CD (Cytochalasin D), 15% FCS or left untreated. qPCR probes targeting the first intron of the gene were used to measure ore-mRNA levels. Signal was normalized to *Gapdh*. Data is shown as mean ± SEM and is representative of three independent experiments.

Next, the effect of Nrde2 depletion on FCS stimulation was examined. Depletion of Nrde2 or Mtr4 had no effect on serum induction of *Egr1* and *c-Fos*, whose activation is dependent on Ras-ERK-TCF signalling (Figure 59C). However, Nrde2 depletion reduced FCS induction of the *Acta2* and *Vcl* genes, which are activated via the Rho-actin-MRTF pathway. In this case the effect of Nrde2 depletion was relieved by simultaneous Mtr4 depletion (Figure 59D).

The data presented above demonstrates that Nrde2 depletion inhibits gene activation in response to stimulation at MRTF target genes, in specific, and its effect reflects Mtr4 activity. These findings suggest that Mtr4 recruitment to MRTF target genes might be a feature of their normal regulation.

Chapter 6. Evidence that the nuclear exosome regulates transcription in dKO$^{MRTF\text{-}NLS}$ cells

Inactivating the nuclear exosome through depletion of individual components of the CBCA, NEXT and core exosome complexes rescues the pre-mRNA synthesis defect observed in LMB-treated NIH3T3 cells. To exclude the possibility that the rescue of RNA synthesis in LMB-treated cells reflects pleiotropic effects of Crm1 inhibition by LMB, the involvement of these factors in the regulation of MRTF-dependent transcripts in cells with constitutively nuclear MRTF was tested.

6.1 Inactivating the nuclear exosome rescues the pre-mRNA synthesis defect in dKO$^{MRTF\text{-}NLS}$ cells

As presented in Chapter 4.3, in dKO$^{MRTF\text{-}NLS}$ cells MRTF target genes exhibit elevated levels of transcription by TTseq that is not detectable by RNAseq. To test whether the defect in pre-mRNA accumulation reflects the activity of the nuclear exosome, siRNA depletions of exosome components were performed.

dKO$^{MRTF\text{-}NLS}$ cells were treated with siRNA for 48 hours and transcription at MRTF target genes was assessed by qPCR using probes targeting the first intron of the gene. Non-targeting scrambled siRNA was used as a control. To test whether the observed effects are MRTF-dependent, cells were stimulated with CD, which disrupts the MRTF/G-actin interaction and activates MRTF, or LatB, which increases the concentration of G-actin and inhibits MRTF-dependent transcription. In addition, the experiment was repeated in cells depleted of SRF, in which MRTF cannot be recruited to target genes. The specificity for MRTF target genes was tested by examining pre-mRNA levels at the *Egr1* gene, whose activation is dependent on Ras-ERK-TCF signalling. To induce the *Egr1* gene, cells were stimulated with 12-O-tetradecanoyl phorbol-13-acetate (TPA), which activates ERK and the TCFs, but not Rho-actin signalling (Griner and Kazanietz, 2007). Knock-down efficiency following siRNA treatment was assessed by measuring target

mRNA by qPCR using exonic probes and comparing their levels to these in cells treated with a non-targeting siCtrl. Results are presented in Figure 60.

Transcription at MRTF target genes was induced by CD stimulation in siCtrl treated cells. In cells depleted of Dis3, Zc3h18 and individual components of the NEXT (Zcchc8, Rmb7 and Mtr4) and CBCA (Ncbp1 and Ars2) complexes pre-mRNA levels in the absence of stimulation were upregulated, to levels comparable to these in CD-stimulated cells. The increased expression was MRTF-dependent, since it was inhibited by SRF depletion or LatB addition, both of which prevent MRTF recruitment to targets. In contrast, the TCF-SRF controlled gene *Egr1* showed no change in baseline expression upon depletion of Dis3, Mtr4, Rmb7 or Zcchc8.

However, as in NIH3T3 cells, depletion of Zcchc8 also impaired stimulation with CD at MRTF target genes, as well as TPA stimulation of the *Egr1* gene. Similarly, depletion of Ncbp1 and Ars2 affected expression levels in response to CD and TPA at MRTF target genes and at the *Egr1* gene, respectively.

Apart from increasing gene expression levels under resting conditions, Zc3h18 depletion upregulated pre-mRNA levels in CD-stimulated cells at MRTF target genes. Furthermore, its depletion also enhanced the expression of the *Egr1* gene in untreated cells, as well as in response to TPA stimulation.

The results presented above are consistent with findings in LMB-treated NIH3T3 cells and further support a model in which under resting G-actin levels, MRTF-dependent transcripts are targeted for degradation by the CBCA-dependent NEXT exosome complex.

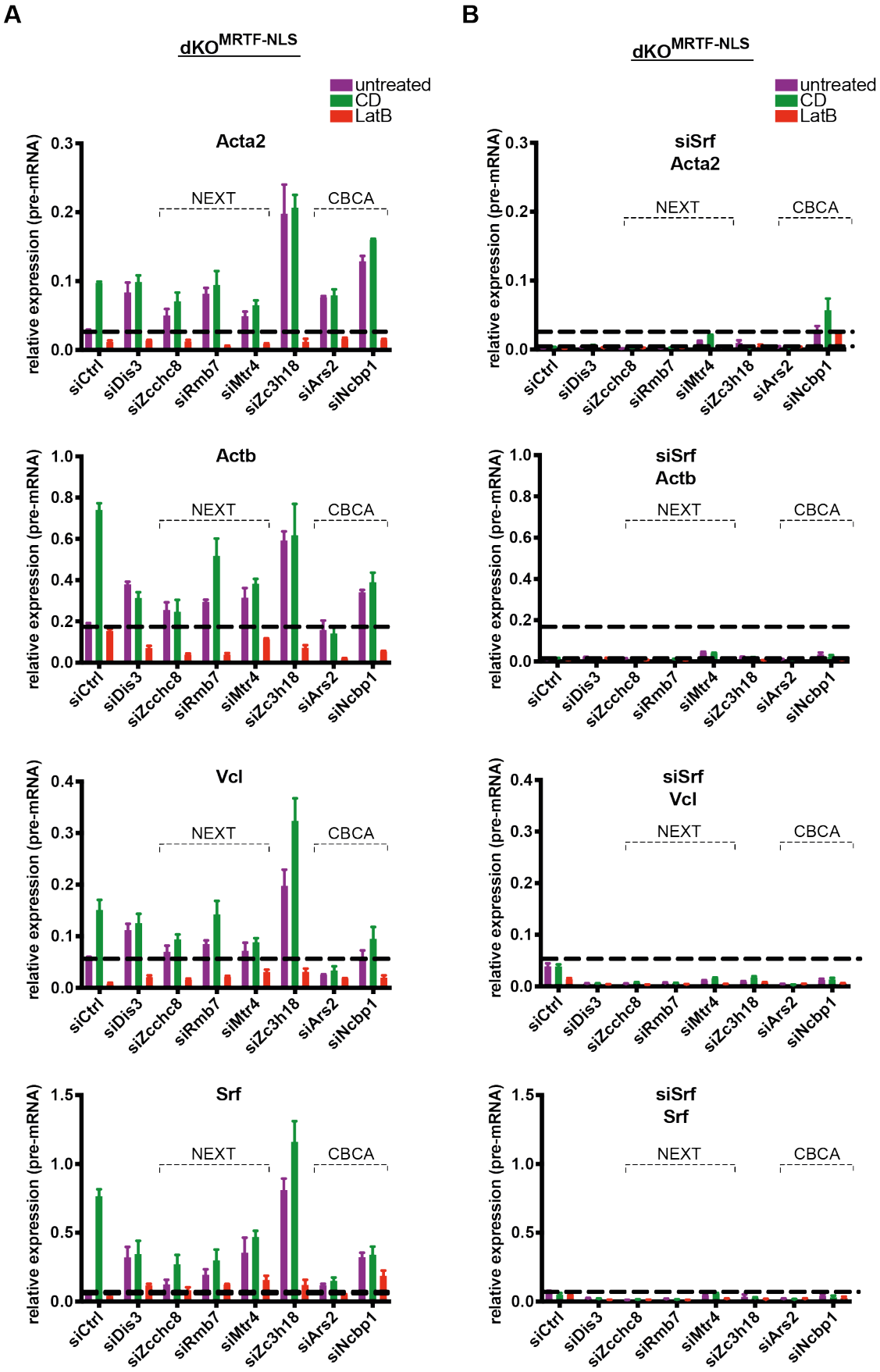
A
B
dKO MRTF-NLS
dKO MRTF-NLS
untreated
CD
LatB
Acta2
siSrf Acta2
Actb
siSrf Actb
Vcl
siSrf Vcl
Srf
siSrf Srf
relative expression (pre-mRNA)
NEXT
CBCA
siCtrl
siDis3
siZcchc8
siRmb7
siMtr4
siZc3h18
siArs2
siNcbp1

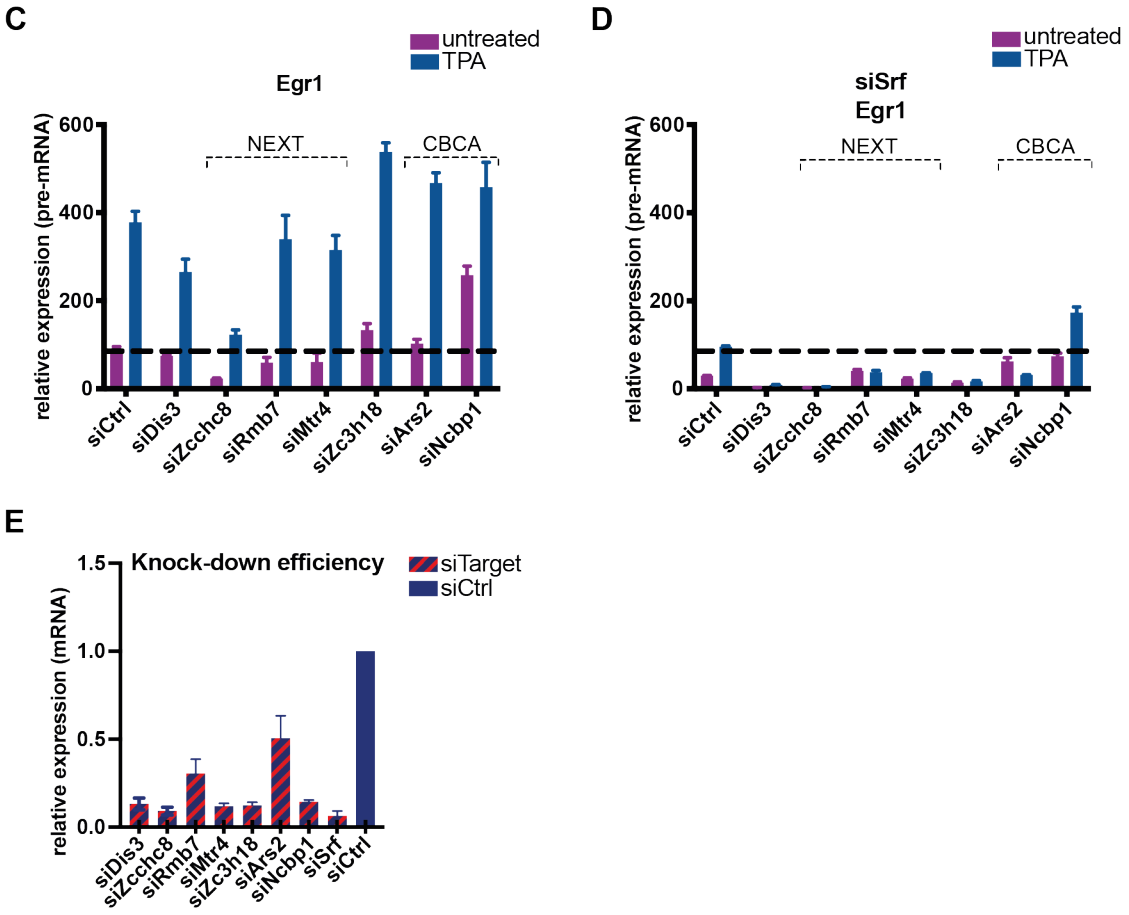

Figure 60 Inactivating the nuclear exosome restores pre-mRNA accumulation at MRTF target genes in dKO$^{MRTF\text{-}NLS}$ cells.

Pre-mRNA accumulation at MRTF target genes in dKO$^{MRTF\text{-}NLS}$ cells (A) and SRF depleted dKO$^{MRTF\text{-}NLS}$ cells (B). Pre-mRNA accumulation at the TCF target gene *Egr1* in dKO$^{MRTF\text{-}NLS}$ cells (C) and SRF depleted dKO$^{MRTF\text{-}NLS}$ cells (D). Cells were treated with siRNA for 48h, serum-starved overnight and stimulated for 30 min with 3µM CD (Cytochalasin D), 0.5µM LatB (Latrunculin B) or left untreated. Pre-mRNA levels were measured using qPCR probes targeting the first intron of the gene. Signal was normalized to *Gapdh*. Data is shown as mean ± SEM and is representative of three independent experiments. The black dotted lines represent pre-mRNA levels in cells treated with scrambled control siRNA. (E) siRNA efficiency. dKO$^{MRTF\text{-}NLS}$ cells were treated with siRNA for 48h. mRNA levels were measured using exonic qPCR probes. Signal was normalized to *Gapdh*. mRNA levels following siRNA treatment are shown, relative to these in cells treated with non-targeting scrambled siRNA control. Data is shown as mean ± SEM and is representative of three independent experiments.

6.2 Genome-wide expression analysis in dKO$^{MRTF\text{-}NLS}$ cells depleted of Mtr4

Results presented in Chapter 5 demonstrate that the non-productive transcriptional state in LMB-treated NIH3T3 cells correlates with Mtr4 recruitment to MRTF-dependent transcripts and that its depletion is sufficient to restore productive transcription. Moreover, Mtr4 depletion rescues productive RNA synthesis at individual MRTF target genes in untreated dKO$^{MRTF\text{-}NLS}$ cells, when nascent RNA synthesis is detected by TTseq. To generalize these findings, RNAseq in dKO$^{MRTF\text{-}NLS}$ cells depleted of Mtr4 was performed.

Sequencing libraries were prepared from total RNA purified from dKO$^{MRTF\text{-}NLS}$ cells treated with siMtr4 for 48 hours and subsequently stimulated with CD or LatB for 30 min. Bioinformatic analysis of RNAseq data was performed by Francesco Gualdrini. To increase sensitivity, read count within introns only (intronic reads) or exons only (exonic reads) were analysed. Differential gene expression analysis was performed, comparing each stimulus to untreated cells.

As shown in Figure 61, virtually no gene expression changes in response to CD or LatB were detected by RNAseq in Mtr4-depleted dKO$^{MRTF\text{-}NLS}$ cells. Nevertheless, the effect of Mtr4 depletion on the expression of the stringent CD-induced gene set defined in Chapter 4.3 was examined. Results are presented in the appendix at the end of this chapter.

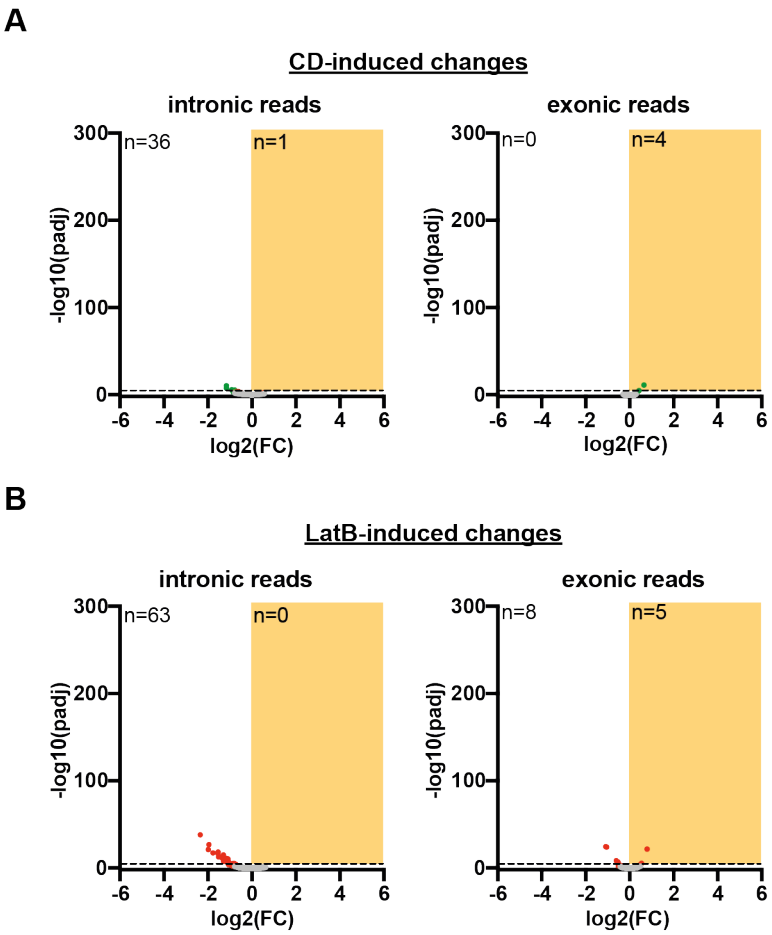

Figure 61 The transcriptional response to CD and LatB in Mtr4-depleted dKO$^{MRTF\text{-}NLS}$ cells

(A) Volcano plots representing CD-induced changes in gene expression, as compared to untreated cells, by RNAseq. dKO$^{MRTF\text{-}NLS}$ cells were treated with siRNA against Mtr4 for 48h and subsequently stimulated with 3μM CD for 30 min. Significant changes (fold change>1 and pvalue>0.01) are marked in green. Significantly upregulated genes are shown in the yellow boxes. (B) Volcano plots representing LatB-induced changes in gene expression, as compared to untreated cells, by RNAseq. dKO$^{MRTF\text{-}NLS}$ cells were treated with siRNA against Mtr4 for 48h and subsequently stimulated with 0.5μM LatB for 30 min. Significant changes (fold change>1 and pvalue>0.01) are marked in red. Significantly upregulated genes are shown in the yellow boxes. Bioinformatic analysis of RNAseq data was performed by Francesco Gualdrini.

dKO$^{MRTF\text{-}NLS}$ cells are subjected to chronic stimulation by the constitutively nuclear MRTF-NLS fusion. This in combination with the siRNA treatment might lead to elevated basal transcription and reduced sensitivity to signal. Therefore, we sought to identify genes regulated by MRTF using their sensitivity to LatB.

First, to identify genes whose expression under resting conditions in Mtr4-depleted cells was sensitive to LatB treatment, as an indication of MRTF activity, differential gene expression analysis was performed comparing expression levels in CD-stimulated and untreated cells to those in response to LatB. Results are shown in Figure 62.

In response to CD treatment 133 genes were upregulated in intronic reads and 253 in exonic reads, relative to LatB-treated cells (Figure 62A). Genes upregulated in response to CD were enriched in genes associated with cell proliferation and adhesion (Figure 62B). For full list of significantly overrepresented GO terms see Figure 111. 63 genes showed elevated expression in untreated cells, relative to LatB-treated cells, in intronic reads and 8 in exonic reads (Figure 62C). These were depleted of genes associated with MRTF-SRF signature (Figure 62D). For full list of significantly overrepresented GO terms see Figure 112.

Next, the same approach was applied to identify genes active in untreated dKO$^{MRTF\text{-}NLS}$ cells as assessed by TTseq, whose expression was sensitive to LatB and subsequent increase in G-actin levels, as an indication of regulation by MRTF. Differential gene expression analysis was performed comparing expression levels in untreated cells to those in response to LatB. As shown in Figure 63A, 630 genes were active under resting conditions in dKO$^{MRTF\text{-}NLS}$ cells and showed sensitivity to LatB treatment.

A

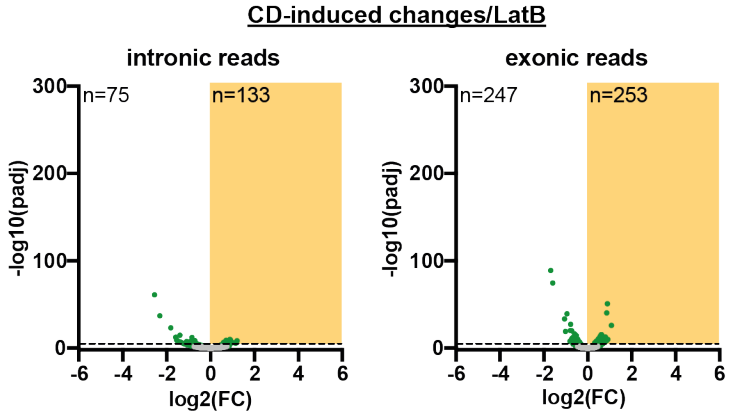

B

	GO BIOLOGICAL PROCESS	# Genes	p-value	FDR q-value
	REGULATION OF CELL POPULATION PROLIFERATION	65	1.56E-24	1.18E-20
	POSITIVE REGULATION OF CELL POPULATION PROLIFERATION	45	3.79E-24	1.44E-20
*	BIOLOGICAL ADHESION	55	1.14E-23	2.89E-20
*	RESPONSE TO CYTOKINE	47	1.43E-22	2.71E-19
*	POSITIVE REGULATION OF MULTICELLULAR ORGANISMAL PROCESS	47	5.68E-22	8.60E-19
	POSITIVE REGULATION OF DEVELOPMENTAL PROCESS	28	5.28E-20	6.66E-17
	POSITIVE REGULATION OF CELL ADHESION	53	3.58E-19	3.88E-16
	REGULATION OF PHOSPHORUS METABOLIC PROCESS	52	2.72E-18	2.57E-15
*	POSITIVE REGULATION OF MOLECULAR FUNCTION	34	4.47E-18	3.76E-15
	REGULATION OF PHOSPHORYLATION	46	1.18E-17	8.96E-15

C

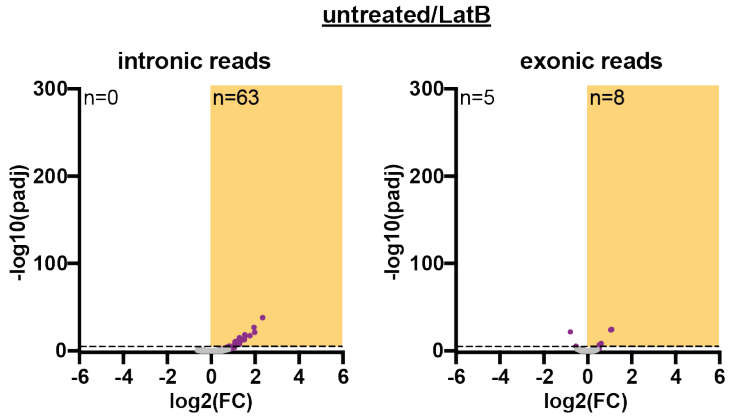

D

GO BIOLOGICAL PROCESS	# Genes	p-value	FDR q-value
REGULATION OF CELL DEATH	23	4.04E-17	3.02E-13
APOPTOTIC PROCESS	23	1.06E-15	2.76E-12
RESPONSE TO WOUNDING	16	1.10E-15	2.76E-12
LOCOMOTION	23	1.72E-15	3.22E-12
MUSCLE STRUCTURE DEVELOPMENT	15	8.47E-15	1.27E-11
CELL POPULATION PROLIFERATION	22	1.72E-14	2.14E-11
WOUND HEALING	14	3.42E-14	3.66E-11
PROTEIN PHOSPHORYLATION	20	6.41E-14	5.99E-11
POSITIVE REGULATION OF MOLECULAR FUNCTION	20	2.66E-13	2.21E-10
CIRCULATORY SYSTEM DEVELOPMENT	17	3.82E-13	2.67E-10

Figure 62 Gene expression changes, relative to LatB-treated cells, in Mtr4-depleted dKO$^{MRTF\text{-}NLS}$ cells

(A) Volcano plots representing CD-induced changes in gene expression, as compared to LatB-treated cells, by RNAseq. dKO$^{MRTF\text{-}NLS}$ cells were treated with siRNA against Mtr4 for 48h and subsequently stimulated with 3μM CD or 0.5μM LatB for 30 min for 30 min. Significant changes (fold change>1 and pvalue>0.01) are marked in green. Significantly upregulated genes are shown in the yellow boxes. (B) Gene ontology analysis of genes upregulated by CD treatement. Shown are the top 10 GO categories. FDR<0.05. GO categories also enriched in CD-induced genes by RNAseq or TTseq in dKO$^{MRTF\text{-}NLS}$ cells are marked with *. (C) Volcano plots representing upregulated and downregulated genes under resting conditions, as compared to LatB-treated cells, by RNAseq. dKO$^{MRTF\text{-}NLS}$ cells were treated with siMtr4 for 48h and subsequently stimulated with 0.5μM LatB for 30 min or left untreated. Significant changes (fold change>1 and pvalue>0.01) are marked in purple. Significantly upregulated genes are shown in the yellow boxes. (D) Gene ontology analysis of active genes under resting conditions. Shown are the top 10 GO categories. FDR<0.05. GO categories also enriched in CD-induced genes by RNAseq or TTseq in dKO$^{MRTF\text{-}NLS}$ cells are marked with *. Bioinformatic analysis of RNAseq data was performed by Francesco Gualdrini.

Of the 67 genes which were active under resting conditions and sensitive to LatB treatment in Mtr4-depleted dKO$^{MRTF\text{-}NLS}$ cells, 55 fulfilled the same criteria as assessed by TTseq in dKO$^{MRTF\text{-}NLS}$ cells (Figure 63B). In contrast, their expression under resting conditions was not detectable by RNAseq (Figure 63C and D). Nevertheless, these were induced in response to CD not only in the RNAseq experiment, but also by TTseq and in Mtr4-depleted cells. Finally, in dKO^{MRTF} cells these genes were inactive in untreated and LatB-treated cells and induced in response to CD in both the RNAseq and TTseq experiments. The same pattern of gene expression was observed at CD-inducible genes and is consistent with regulation by MRTF.

A

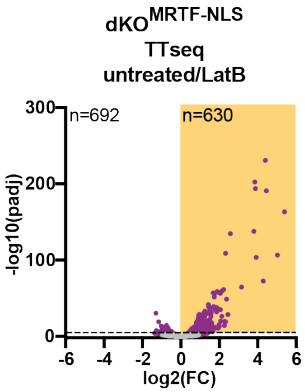

B

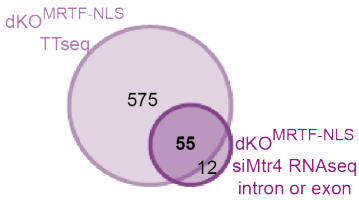

C

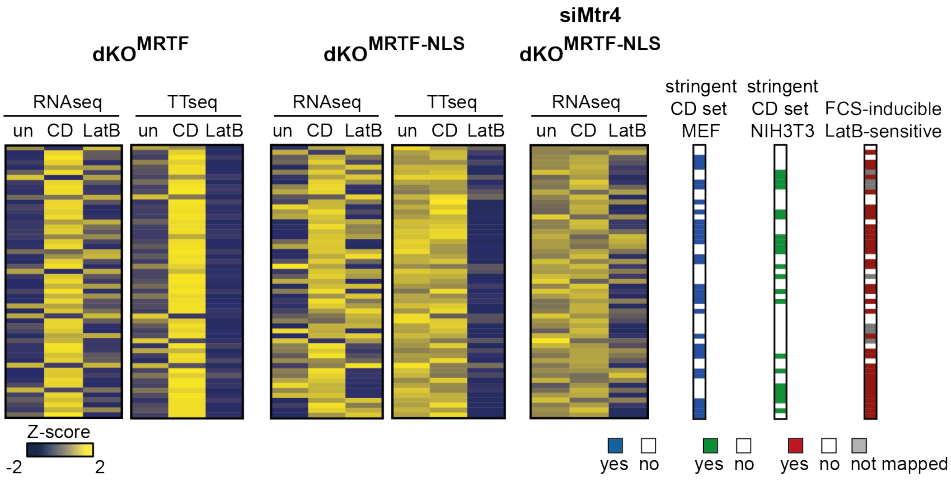

D

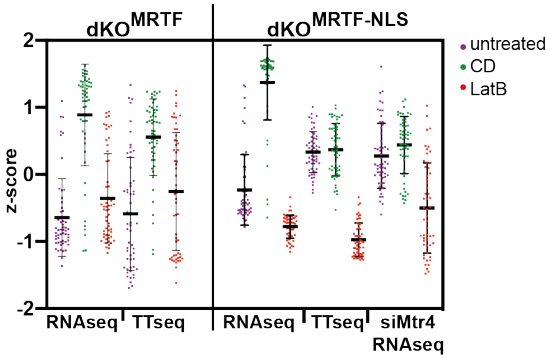

E

TF BINDING MOTIF	p-value	FDR q-value
SRF_Q5_01	7.02E-24	3.07E-21
SRF_Q4	1.01E-23	3.07E-21
SRF_C	2.13E-20	4.34E-18
SRF_01	8.15E-20	1.24E-17
SRF_Q6	2.48E-14	3.02E-12

F

	GO BIOLOGICAL PROCESS	# Genes	p-value	FDR q-value
	MUSCLE STRUCTURE DEVELOPMENT	15	4.16E-19	1.64E-15
*	REGULATION OF CELL DEATH	22	4.33E-19	1.64E-15
*	APOPTOTIC PROCESS	21	8.93E-18	2.26E-14
	REGULATION OF CELL POPULATION PROLIFERATION	20	1.63E-16	3.07E-13
	RESPONSE TO ENDOGENOUS STIMULUS	19	7.40E-16	1.12E-12
	RESPONSE TO HORMONE	15	1.35E-15	1.70E-12
*	CELL MOTILITY	17	4.40E-15	4.62E-12
	RESPONSE TO WOUNDING	16	4.88E-15	4.62E-12
	CIRCULATORY SYSTEM DEVELOPMENT	16	7.50E-15	6.19E-12
*	ANATOMICAL STRUCTURE FORMATION INVOLVED IN MORPHOGENESIS	16	8.17E-15	6.19E-12

Figure 63 Defining a Mtr4-controlled MRTF target gene set in dKO$^{MRTF\text{-}NLS}$ cells

(A) Volcano plot representing genes active under resting conditions in dKO$^{MRTF\text{-}NLS}$ cells, relative to LatB-treated cells, as assessed by TTseq. dKO$^{MRTF\text{-}NLS}$ cells were treated with 0.5μM LatB for 30 min or left untreated. Significant changes (fold change>1 and pvalue>0.01) are marked in purple. Significantly upregulated genes are shown in the yellow boxes. (B) Venn diagram representing the subset of genes active under resting conditions by TTseq in dKO$^{MRTF\text{-}NLS}$ cell and by RNAseq in Mtr4-depleted dKO$^{MRTF\text{-}NLS}$ cells. (C) Heatmap representing gene expression changes at the 55 Mtr4-controlled MRTF-NLS-induced genes in untreated, CD-stimulated and LatB-treated cells by RNAseq and TTseq in dKO^{MRTF} and dKO$^{MRTF\text{-}NLS}$ cells and by RNAseq in Mtr4-depleted dKO$^{MRTF\text{-}NLS}$ cells. Overlap with previously published FCS-induced LatB-sensitive genes (n=1022) is shown (Esnault et al., 2014). The red lines represent FCS-induced LatB-sensitive genes, the white lines represent genes not present in the FCS-induced LatB-sensitive gene set and the grey lines represent genes not identified in the analysis. Overlap with the 180 stringent CD-induced gene set in MEF is shown. The blue lines represent CD-induced genes, the white lines represent genes not present in the gene set. Overlap with the 312 stringent CD-induced gene set in NIH3T3 is shown. The green lines represent CD-induced genes, the white lines represent genes not present in the gene set. (D) Violin plot representing gene expression changes at the 55 Mtr4-controlled MRTF-NLS-induced genes in untreated, CD-stimulated and LatB-treated cells by RNAseq and TTseq in dKO^{MRTF} and dKO$^{MRTF\text{-}NLS}$ cells and by RNAseq in Mtr4-depleted dKO$^{MRTF\text{-}NLS}$ cells. (E) Transcription factor binding motif analysis of the 55 Mtr4-controlled MRTF-NLS-induced genes. Shown are the top 5 TF binding motifs. FDR<0.05. (F) Gene ontology analysis of the 55 Mtr4-controlled MRTF-NLS-induced genes. Shown are the top 10 GO categories. FDR<0.05. GO categories also enriched in CD-induced genes by RNAseq or TTseq in dKO$^{MRTF\text{-}NLS}$ cells are marked with *. Bioinformatic analysis of RNAseq and TTseq data was performed by Francesco Gualdrini.

29 out of the 55 MRTF-NLS-induced Mtr4-sensitive genes were present in the stringent CD-induced gene set defined in MEFs (n=180) and 21 were also CD-inducible in NIH3T3 cells. In addition, 34 of the 55 genes overlapped with previously published FCS-inducible LatB-sensitive genes (Esnault et al., 2014). The 55 MRTF-NLS-induced Mtr4-sensitive genes were enriched in genes associated with SRF binding sites (Figure 63E). Gene ontology analysis showed that genes associated with cell proliferation were overrepresented. In addition, genes associated with apoptotic processes, cell proliferation and cell motility were

enriched in that group (Figure 63F). For full list of significantly overrepresented GO terms see Figure 113.

Taken together, these results and qPCR data on bona-fide MRTF-SRF target genes are consistent with the observation in NIH3T3 cells that nuclear MRTF generates unstable nascent transcripts that are degraded in a Mtr4-dependent manner. However, the chronic state of the dKO$^{MRTF\text{-}NLS}$ cells in combination with the prolonged siRNA treatment complicated genome-wide analysis of transcriptional changes in Mtr4-depleted cells.

6.3 Appendix

Relative to untreated cells, no significant changes in gene expression were detected in response to CD or LatB in Mtr4-depleted cells (see Figure 61). Nevertheless, the effect of Mtr4 depletion on expression of genes in the stringent 180 CD-induced gene set defined in Chapter 4 was assessed (see Figure 46).

As described in Chapter 4.3, this gene set was expressed in response to stimulation with CD and inactive in untreated and LatB-treated dKO^{MRTF} cells by RNAseq and TTseq. In dKO$^{MRTF\text{-}NLS}$ cells, while under resting conditions no gene expression was detected by RNAseq, genes within the stringent CD set were induced by TTseq in the absence of an activating signal. Their expression was sensitive to treatement with LatB and subsequent increase in G-actin concentration (see Figure 49). In contrast, in Mtr4-depleted dKO$^{MRTF\text{-}NLS}$ cells, whereas these genes were induced in untreated cells, they were unresponsive to stimulation with CD and LatB (Figure 64).

This data suggests that Mtr4 depletion in dKO$^{MRTF\text{-}NLS}$ cells disrupts signal regulation of the CD-inducible set.

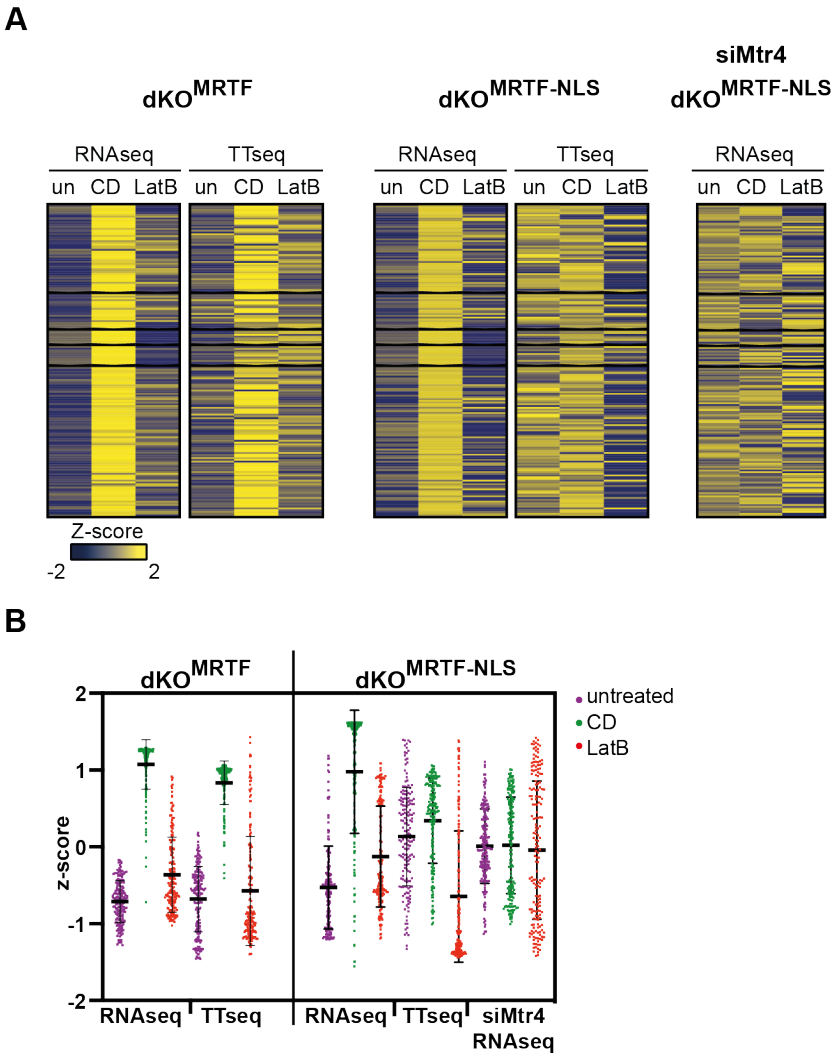

Figure 64 Gene expression analysis at the 180 stringent CD-induced gene set in Mtr4-depleted dKO$^{MRTF-NLS}$ cells

(A) Heatmap representing gene expression changes at the 180 genes in the stringent CD-induced gene set defined in Chapter 4.3 (see Figure 46) in untreated, CD-stimulated and LatB-treated cells by RNAseq and TTseq in dKO^{MRTF} and dKO$^{MRTF-NLS}$ cells and by RNAseq in Mtr4-depleted dKO$^{MRTF-NLS}$ cells. Data for dKO^{MRTF} and dKO$^{MRTF-NLS}$ RNAseq and TTseq is from Figure 49. (B) Violin plot representing gene expression changes at the 180 genes in the CD-induced gene set in untreated, CD-stimulated and LatB-treated cells by RNAseq and TTseq in dKO^{MRTF} and dKO$^{MRTF-NLS}$ cells and by RNAseq in Mtr4-depleted dKO$^{MRTF-NLS}$ cells. Data for dKO^{MRTF} and dKO$^{MRTF-NLS}$ RNAseq and TTseq is from Figure 49. Bioinformatic analysis of RNAseq and TTseq data was performed by Francesco Gualdrini.

Next, gene expression at the 312 stringent CD-induced gene set in NIH3T3 cells defined in Chapter 3 was examined (see Figure 35). As described in Chapter 3.3, genes within this set were induced by CD stimulation and inactive in untreated and LMB-treated NIH3T3 cells by RNAseq. Nevertheless, they were induced in response to LMB as assessed by TTseq and by RNAseq in Mtr4-depleted cells.

As expected from the small overlap between CD-induced genes in MEF and NIH3T3 cells (see Figure 46), these were only weakly induced by CD in dKO^{MRTF} cells (Figure 65A and B). Genes within this set exhibited lack of sensitivity to LatB treatment not only in Mtr4-depleted dKO$^{MRTF-NLS}$, but also in dKO^{MRTF} and dKO$^{MRTF-NLS}$ cells as assessed by RNAseq, further indicating their expression might not be MRTF-dependent. This might reflect differential regulation of these genes in NIH3T3 and MEF cells or changes arising during the generation of the reconstituted dKO^{MRTF} and dKO$^{MRTF-NLS}$ cell lines. Nevertheless, in the TTseq experiment genes within this set were significantly upregulated in response to CD stimulation and sensitive to LatB treatment both in dKO^{MRTF} and dKO$^{MRTF-NLS}$ cells, potentially due to higher sensitivity of the TTseq method.

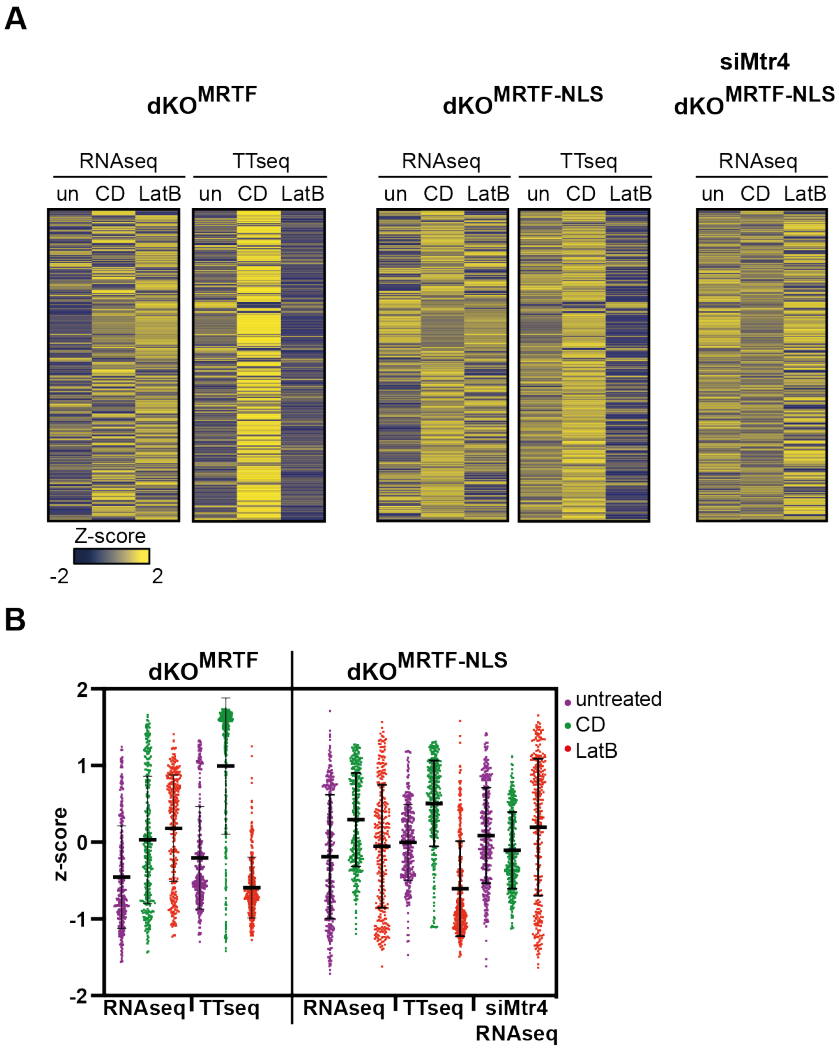

Figure 65 Gene expression analysis at the 312 stringent CD-induced gene set from NIH3T3 cells in Mtr4-depleted dKO$^{MRTF-NLS}$ cells

(A) Heatmap representing gene expression changes at the 312 genes in the CD-induced gene set in NIH3T3 cells defined in Chapter 3.3 in untreated, CD-stimulated and LatB-treated cells by RNAseq and TTseq in dKO^{MRTF} and dKO$^{MRTF-NLS}$ cells and by RNAseq in Mtr4-depleted dKO$^{MRTF-NLS}$ cells. (B) Violin plot representing gene expression changes at the 312 genes in the CD-induced gene set defined in NIH3T3 cells in untreated, CD-stimulated and LatB-treated cells by RNAseq and TTseq in dKO^{MRTF} and dKO$^{MRTF-NLS}$ cells and by RNAseq in Mtr4-depleted dKO$^{MRTF-NLS}$ cells. Bioinformatic analysis of RNAseq and TTseq data was performed by Francesco Gualdrini.

Finally, the expression of the 455 LMB-induced Mtr4-sensitive gene set in NIH3T3 cells defined in Chapter 5 was assessed. As described in Chapter 5.2, this gene set was inactive in untreated cells NIH3T3 cells and expressed in response to CD by TTseq and RNAseq. In response to LMB, no gene activation was detectable by RNAseq, despite being upregulated by TTseq and in Mtr4-depleted cells (see Figure 56).

The results from this analysis were similar to these at the 312 stringent CD-induced gene set. As presented in Figure 66, genes in the 455 LMB-induced Mtr4-controlled gene set exhibited elevated basal expression and lack of sensitivity to CD and LatB not only in Mtr4-depleted dKO$^{MRTF\text{-}NLS}$ cells, but also in dKO^{MRTF} and dKO$^{MRTF\text{-}NLS}$ cells as assessed by RNAseq, potentially reflecting differences arising during the reconstitution of MRTF-A/B null cells. In the TTseq experiment genes within this set were mostly sensitive to LatB treatment both in dKO^{MRTF} and dKO$^{MRTF\text{-}NLS}$ cells, which might potentially be due to higher sensitivity of the TTseq method.

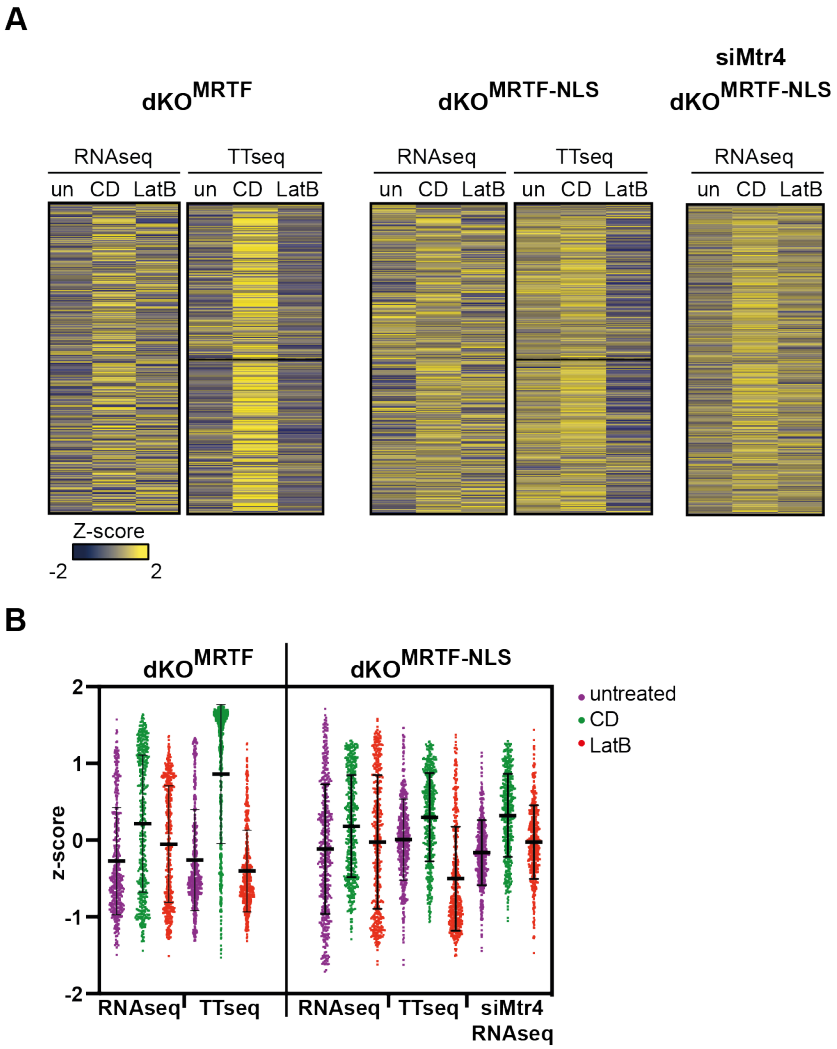

Figure 66 Gene expression analysis at the 455 LMB-induced Mtr4-controlled gene set from NIH3T3 cells in Mtr4-depleted dKO$^{MRTF-NLS}$ cells

(A) Heatmap representing gene expression changes at the 455 genes in the LMB-induced Mtr4-controlled gene set in NIH3T3 cells defined in Chapter 5.2 in untreated, CD-stimulated and LatB-treated cells by RNAseq and TTseq in dKO^{MRTF} and dKO$^{MRTF-NLS}$ cells and by RNAseq in Mtr4-depleted dKO$^{MRTF-NLS}$ cells. (B) Violin plot representing gene expression changes at the 455 genes in the LMB-induced Mtr4-controlled gene set defined in NIH3T3 cells in untreated, CD-stimulated and LatB-treated cells by RNAseq and TTseq in dKO^{MRTF} and dKO$^{MRTF-NLS}$ cells and by RNAseq in Mtr4-depleted dKO$^{MRTF-NLS}$ cells. Bioinformatic analysis of RNAseq and TTseq data was performed by Francesco Gualdrini.

Chapter 7. Recruitment of the exosome correlates with aberrant phosphorylation of the Pol II CTD at MRTF target genes

The data presented in the previous chapters demonstrates that in the absence of G-actin depletion, nuclear MRTF induces Pol II recruitment and nascent RNA synthesis but no pre-mRNA accumulates. In this setting, Mtr4 is recruited to transcripts of MRTF target genes and appears to target them for degradation by the nuclear exosome. In this chapter, to characterize the non-productive transcriptional state at MRTF-SRF targets in LMB-treated cells, chromatin remodeling, the recruitment of pausing and elongation factors, as well as the phosphorylation state of the Pol II CTD at MRTF target genes were examined.

7.1 Chromatin remodeling is not defective in LMB-treated cells

Dense nucleosome occupancy obstructs the elongating polymerase and inversely correlates with transcription rates (Gates et al., 2017). Various chromatin remodelers and histone modifiers associate with Pol II during elongation to promote its processivity though chromatin. Modifications of histones alter the physical and chemical properties of chromatin and influence its compaction and accessibility. Thus, actively transcribed and transcriptionally silenced regions of the genome have distinct chromatin signatures. H3K4me3 and H3K27Ac are canonical chromatin marks present at active gene promoters, whereas H3K36me3, H3K79me3 and H2Bub are found within gene bodies and associated with the elongating Pol II. Whether these chromatin marks are deposited normally at MRTF target genes in the non-productive transcriptional state was examined.

NIH3T3 cells were treated with CD, which activates MRTF target genes, or LMB, which induces non-productive transcription at MRTF targets. H3K4me3, H3K27Ac, H3K36me3 and H3K79me3 were examined by ChIP-qPCR. qPCR probes targeting regions along the length of the *Acta2* and *Actb* model genes were used. Results are shown in Figure 67.

A

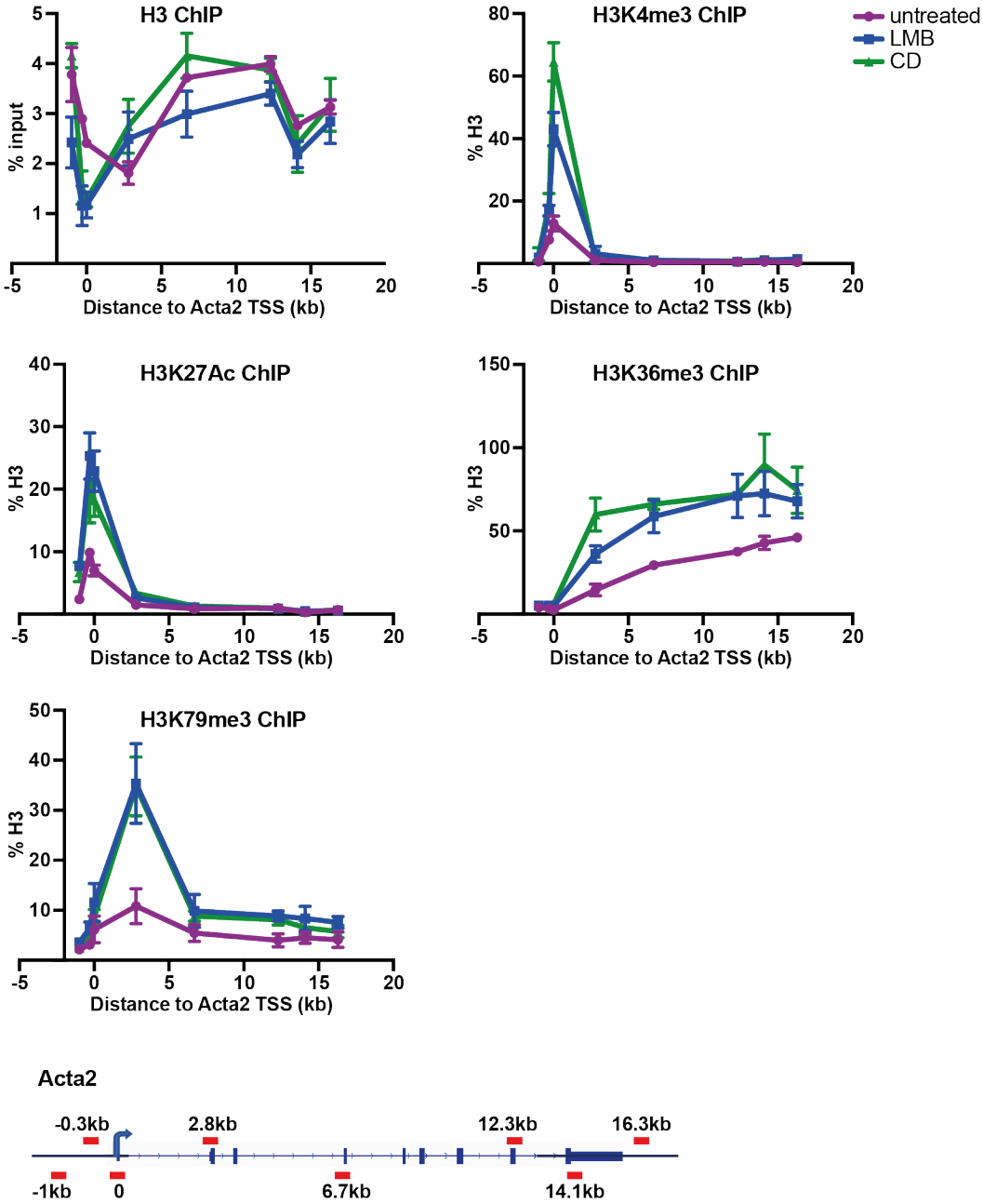
H3 ChIP
% input
Distance to Acta2 TSS (kb)
H3K4me3 ChIP
% H3
Distance to Acta2 TSS (kb)
untreated
LMB
CD
H3K27Ac ChIP
% H3
Distance to Acta2 TSS (kb)
H3K36me3 ChIP
% H3
Distance to Acta2 TSS (kb)
H3K79me3 ChIP
% H3
Distance to Acta2 TSS (kb)
Acta2
-0.3kb
2.8kb
12.3kb
16.3kb
-1kb
0
6.7kb
14.1kb

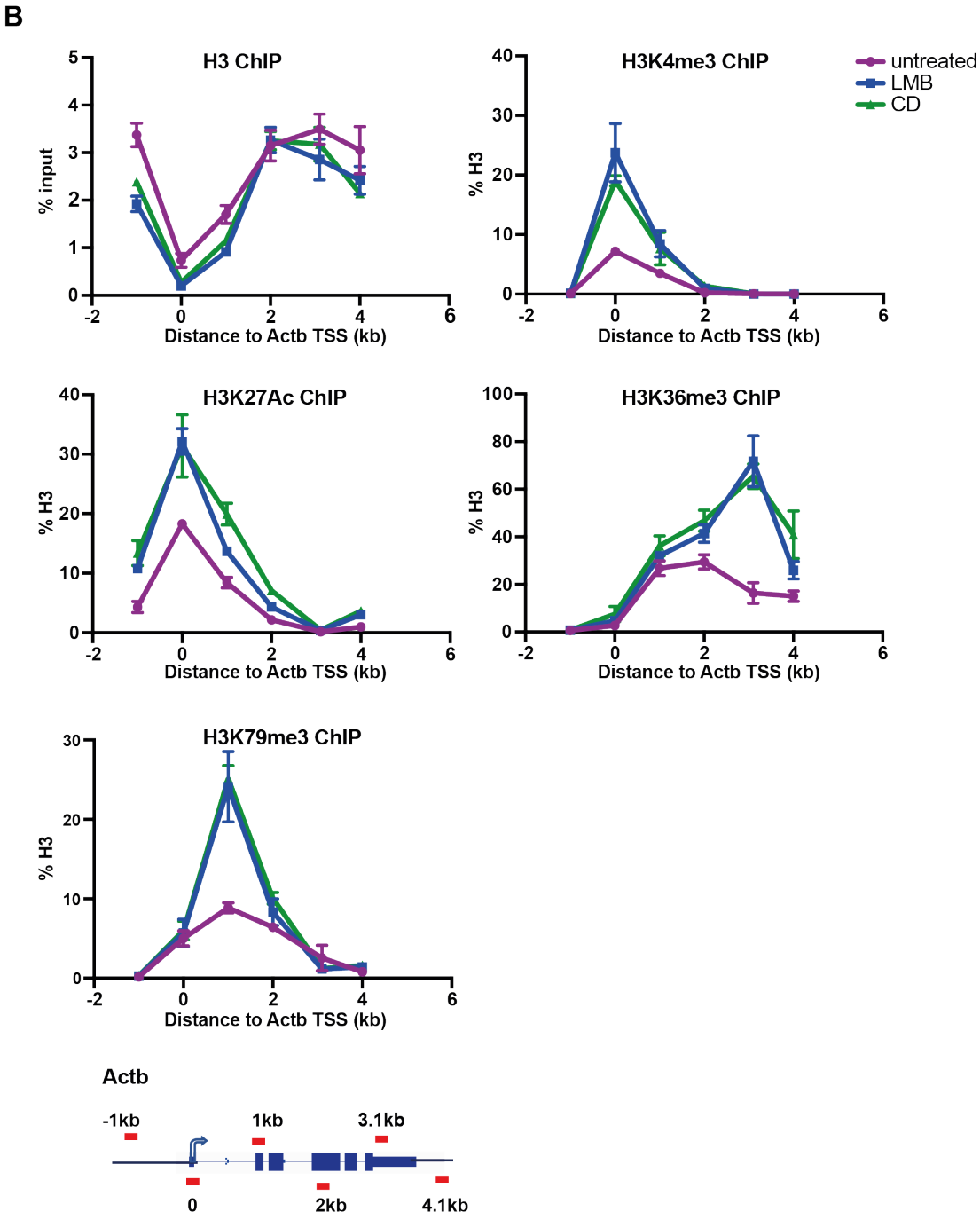

Figure 67 Chromatin remodeling in LMB-treated cells

H3 (ab1791), H3K4me3 (ab8580), H3K27Ac (ab4729), H3K36me3 (ab9050) and H3K79me3 (ab2621) ChIP at the *Acta2* (A) and *Actb* (B) genes. NIH3T3 fibroblasts were serum-starved overnight and stimulated for 30 min with 3μM CD (Cytochalasin D); 50nM LMB (Leptomycin B) or left untreated. Signal was normalized to input or H3, as indicated in the figure. Data is shown as mean ± SEM and is representative of three independent experiments. The lines connecting individual points within data series are not necessarily representative of ChIP levels between data points. The location of the qPCR probes, relative to the TSS (0), is indicated by the red lines in the gene schematics.

In CD-stimulated cells, H3K4me3 and H3K27Ac were upregulated at the TSS of the *Acta2* and *Actb* genes. Within the gene body, H3K79me3 was detected towards the 5' end, whereas H3K36me3 started accumulating within the gene body, reaching maximum towards the 3' end of the gene. Similar results were seen in LMB-treated cells. Both H3K4me3 and H3K27Ac were present at the TSS of the *Acta2* and *Actb* genes, at levels similar to these in CD-stimulated cells. H3K79me3 and H3K36me3 were observed at the 5' and 3' end of the gene body, respectively, at levels comparable to these seen in CD-stimulated cells.

Consistent with the presence of elongating Pol II and active transcription, chromatin remodeling at the promoter region, as well as within the gene body of MRTF target genes appears to occur normally in response to LMB treatement.

7.2 Pol II pause-release occurs in LMB-treated cells

Prior to transitioning into elongation, Pol II undergoes promoter-proximal pausing (Chen et al., 2018). In addition to promoting 5' capping of the nascent transcript, pausing potentially represents a transcriptional checkpoint to ensure that Pol II is competent for elongation. To examine Pol II pausing in the LMB-induced non-productive transcriptional state, the recruitment of CDK9 and the positive and negative elongation factors DSIF and NELF, which regulate the transition of the paused Pol II into elongation (Figure 68A), was analysed at MRTF target genes.

As before, NIH3T3 cells were treated with CD or LMB and the recruitment of NELF and CDK9 to MRTF target gene promoters assessed by ChIP-qPCR. The *Zfp37* gene, which is not regulated by MRTF, was used as a control. To determine whether DSIF was properly associated with the elongating Pol II, ChIP for its Spt5 subunit was performed. Whereas CDK9 and NELF associate with paused Pol II at 5' ends of genes, Spt5 remains associated with the elongating form of the Pol II. Therefore, qPCR probes targeting regions along the whole transcriptional unit of the *Acta2* and *Actb* genes were used. Results are shown in Figure 68.

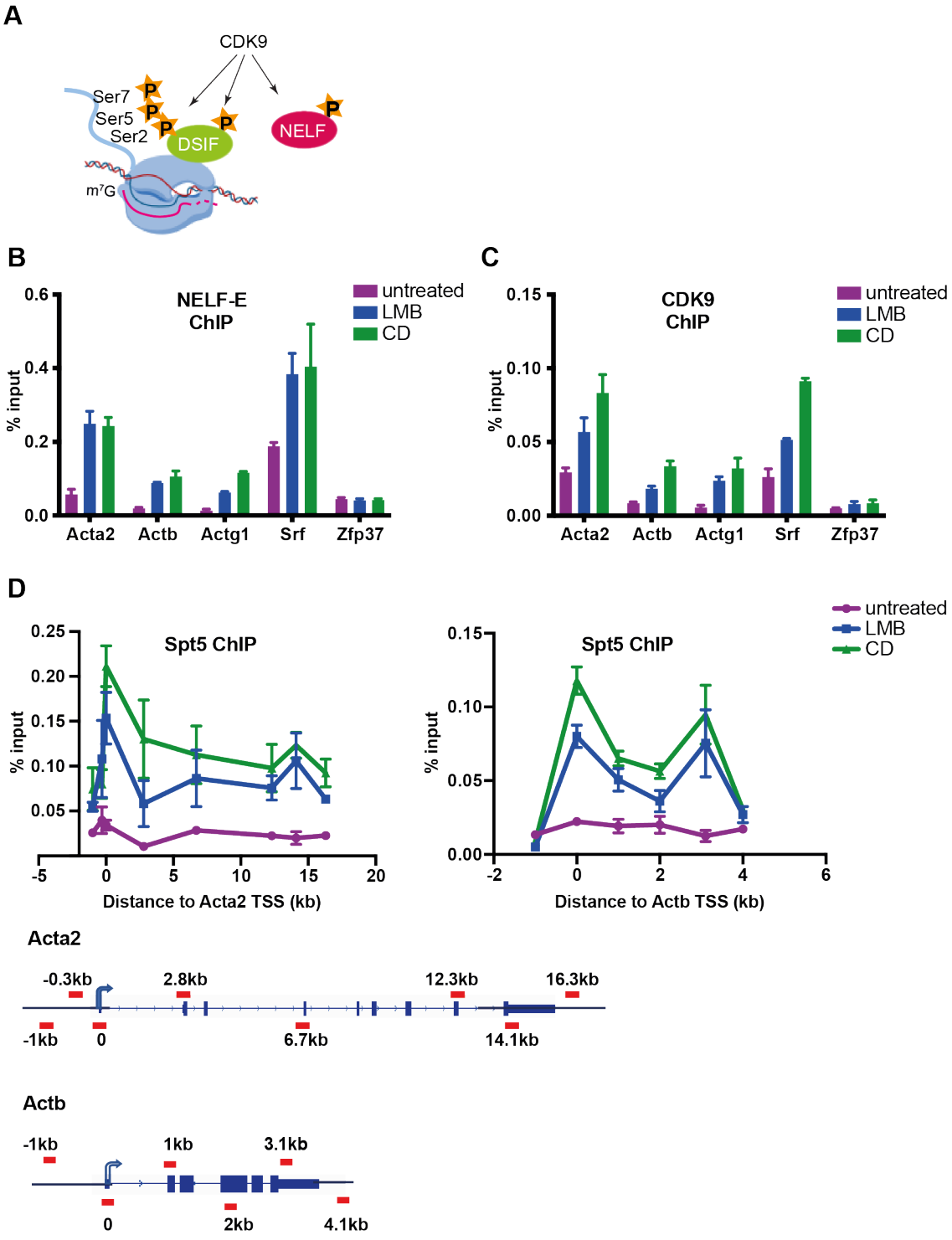
A
CDK9
Ser7
Ser5
Ser2
P
DSIF
NELF
m7G
B
NELF-E ChIP
untreated
LMB
CD
% input
0.6
0.4
0.2
0.0
Acta2
Actb
Actg1
Srf
Zfp37
C
CDK9 ChIP
untreated
LMB
CD
% input
0.15
0.10
0.05
0.00
Acta2
Actb
Actg1
Srf
Zfp37
D
Spt5 ChIP
% input
0.25
0.20
0.15
0.10
0.05
-5
0
5
10
15
20
Distance to Acta2 TSS (kb)
Spt5 ChIP
% input
0.15
0.10
0.05
0.00
-2
0
2
4
6
Distance to Actb TSS (kb)
untreated
LMB
CD
Acta2
-0.3kb
2.8kb
12.3kb
16.3kb
-1kb
0
6.7kb
14.1kb
Actb
-1kb
1kb
3.1kb
0
2kb
4.1kb

Figure 68 Pol II undergoes pause-release in LMB-treated cells

(A) Pol II pause-release is dependent on CDK9. CDK9 phosphorylates NELF, DSIF and Serine 2 of the Pol II CTD, allowing the Pol II to transition into elongation. (B) NELF-E (10705-1-AP), (C) CDK9 (2316) and (D) Spt5 (sc-28678) ChIP at MRTF target genes. NIH3T3 fibroblasts were serum-starved overnight and stimulated for 30 min with 3μM CD (Cytochalasin D); 50nM LMB (Leptomycin B) or left untreated. Signal was normalized to input. Data is shown as mean ± SEM and is representative of three independent experiments. The lines connecting individual points within data series are not necessarily representative of ChIP levels between data points. The location of the qPCR probes, relative to the TSS (0), is indicated by the red lines in the gene schematics.

In response to CD stimulation, CDK9, NELF-E and Spt5 were recruited to MRTF target gene promoters. The Spt5 profile along the gene resembled the one of the Pol II. Spt5 was present along the gene, with a pronounced peak at the TSS. LMB treatment also induced recruitment of NELF, CDK9 and Spt5 at MRTF target genes. Furthermore, the Spt5 ChIP profile was similar to that in CD-stimulated cells. Nevertheless, ChIP levels were somewhat reduced as compared to these in CD-stimulated cells.

These results indicate that promoter-proximal pausing occurs at MRTF targets in LMB-treated cells and that the released Pol II is accompanied by DSIF.

7.3 The non-productive transcriptional state in LMB-treated cells correlates with aberrant phosphorylation of the Pol II CTD

The phosphorylation state of the Pol II CTD orchestrates the recruitment of various factors that mediate transcription and RNA processing throughout the transcriptional cycle (Zaborowska et al., 2016). Therefore, whether the susceptibility of MRTF-dependent transcripts to degradation by the exosome correlates with defective phosphorylation of the Pol II CTD was investigated next.

In mammalian cells, the CTD of the Pol II consists of 52 heptad repeats of the consensus sequence $Y^1S^2P^3T^4S^5P^6S^7$ (Bartolomei et al., 1988; Corden et al., 1985). Dynamic phosphorylation of residues within the Pol II CTD is the best characterized CTD modification in transcription. Distinct CTD phosphorylation patterns correlate with different stages of the transcription cycle. Serine 5 phosphorylation is associated with initiation of transcription, whereas phospho-Ser2 and phospho-Thr4 are involved in elongation and termination (Gomes et al., 2006; Kim et al., 2002; Komarnitsky et al., 2000). Despite being present at all actively transcribed genes, phospho-Ser7 appears to play specific role in the transcription and RNA processing of snRNA genes (Egloff et al., 2007). Tyr1P is involved in the control of transcription directionality (Descostes et al., 2014).

To determine whether the different treatments affect Pol II CTD phosphorylation globally, the phosphorylation status of the Pol II CTD was examined by Western blot using phospho-specific antibodies. NIH3T3 cells were treated with CD, which induces productive RNA synthesis at MRTF target genes; LMB which induces non-productive transcription; or LatB, which inhibits MRTF-dependent transcription. Results are shown in Figure 69.

Rpb1 antibody detected two Pol II species, a higher molecular weight one which corresponds to the phosphorylated form of Pol II (Pol II0), and a lower molecular weight one which corresponds to unphosphorylated Pol II (Pol IIA). As compared to untreated cells, Pol II0 levels remained unchanged in cells treated with CD, LMB or LatB. None of the treatments affected Ser5P, Ser7P, Ser2P, Thr4P or Tyr1P levels, demonstrating that they have no general effect on Pol II phosphorylation.

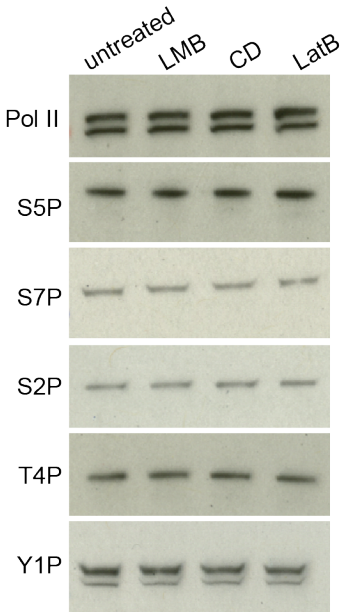

Figure 69 Inhibition of Crm1 does not affect Pol II CTD phosphorylation globally

Western blot analysis of RNA polymerase II C-terminal domain phospho-activating marks. Cells were serum-starved overnight and stimulated for 30 min with 3μM CD (Cytochalasin D); 50nM LMB (Leptomycin B); 0.5μM LatB (Latrunculin B) or left untreated. Samples were probed with antibodies targeting Rpb1 (D8L4Y), RNA Polymerase II C-terminal domain phosphorylated at Serine 5 (S5P, 3E8), Serine 7 (S7P, 4E12), Serine 2 (S2P, 3E10), Tyrosine 1 (Y1P, 3D12) or Threonine 4 (Thr4P, 6D7).

Next, potential differences in Pol II recruitment and phosphorylation status between conditions at MRTF target genes, specifically, were examined by ChIP. NIH3T3 cells were treated with CD or LMB and Pol II recruitment to target genes was assessed using antibodies against the Rpb1 subunit of the Pol II (D8L4Y), to measure total Pol II, and phospho-specific antibodies targeting Ser5P (3E8), Ser7P (4E12), Ser2P (3E10), Thr4P (6D7) and Tyr1P (3D12) of the Rpb1 CTD (Chapman et al., 2007). The model gene *Acta2* was used. As before, qPCR probes targeting regions along the length of the gene were used. Results are shown in Figure 70.

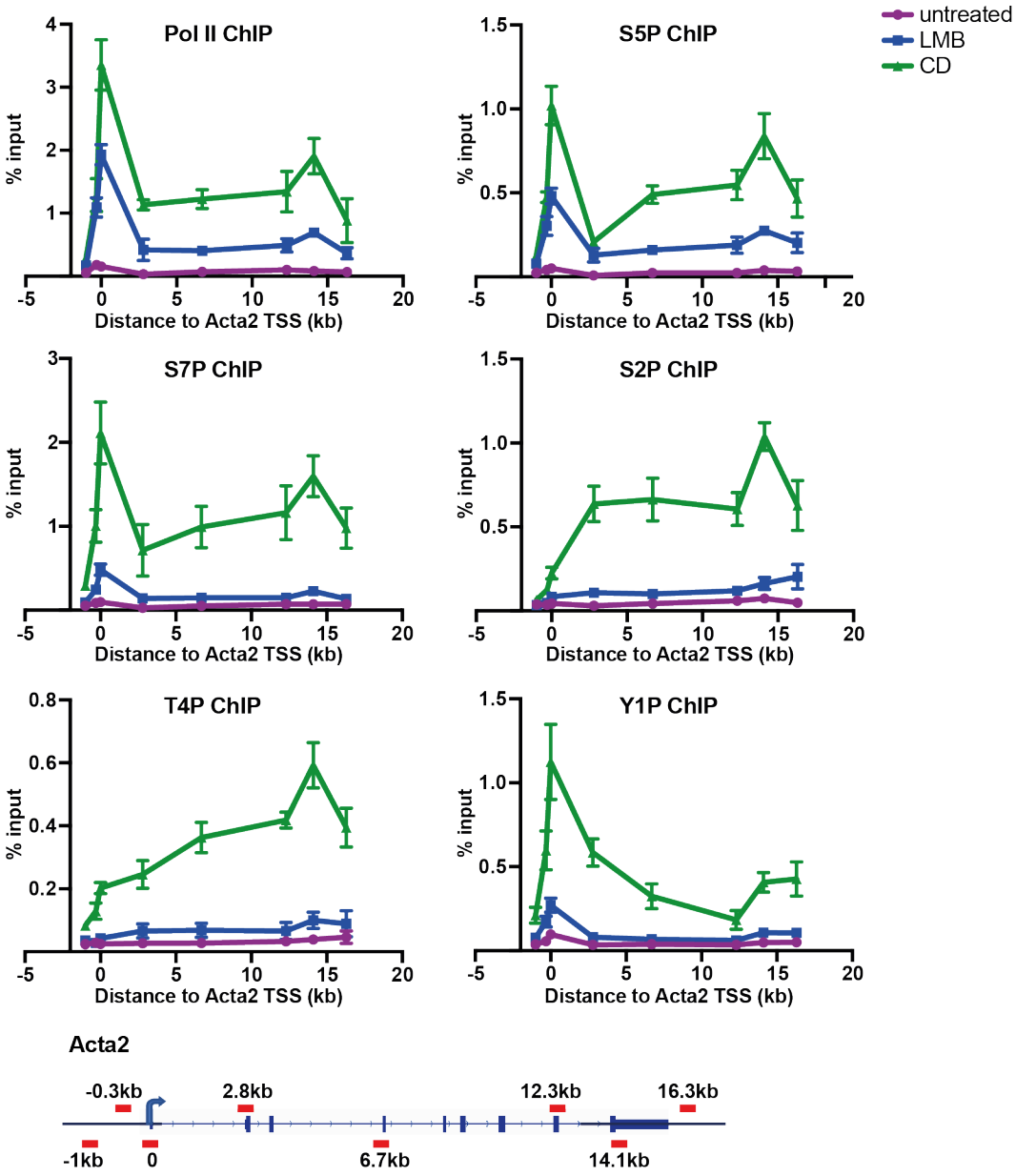

Figure 70 Pol II recruitment and CTD phosphorylation at the *Acta2* gene

Rpb1 (D8L4Y), phospo-Ser5 (S5P, 3E8), phospho-Ser7 (S7P, 4E12), phospho-Ser2 (S2P, 3E10), phospho-Thr4 (T4P, 6D7) and phospho-Tyr1 (Y1P, 3D12) ChIP at the model gene *Acta2*. NIH3T3 fibroblasts were serum-starved overnight and stimulated for 30 min with 3μM CD (Cytochalasin D); 50nM LMB (Leptomycin B); or left untreated. Signal was normalized to input. Data is shown as mean ± SEM and is representative of three independent experiments. The lines connecting individual points within the series and are not necessarily representative of ChIP levels between data points. The location of the qPCR probes, relative to the TSS (0), is indicated by the red lines in the gene schematic.

In response to CD stimulation, Pol II was recruited to the *Acta2* gene. Pol II ChIP signal was present across the *Acta2* gene, with a peak at the TSS. The ChIP profile of Ser5P and Ser7P followed the one of total Pol II, while Ser2P and Thr4P started accumulating within the gene body and reached maximum towards the poly(A) site at the 3' end of the gene. Tyr1P reached maximum near the TSS of the *Acta2* gene.

LMB treatment also induced Pol II recruitment. Pol II distribution along the gene was as in CD-stimulated cells. However, ChIP levels were reduced compared to these in CD-stimulated cells. The same result was observed for phospho-Ser5. LMB treatment did not induce Ser7P, Ser2P, Thr4P or Tyr1P accumulation.

These results suggest that the LMB-induced non-productive transcriptional state correlates with aberrant phosphorylation of the Pol II CTD. To determine whether this was generally true for MRTF target genes, we performed ChIPseq.

NIH3T3 cells were treated with CD or LMB, sequencing libraries were prepared following IPs using antibodies against the Rpb1 subunit of the Pol II (D8L4Y), to measure total Pol II, and phospho-specific antibodies targeting Ser5P (3E8), Ser7P (4E12) and Ser2P (3E10) (Chapman et al., 2007). Pol II recruitment and CTD phosphorylation was analysed at the 312 stringent CD-induced gene set defined in Chapter 3.3. Bioinformatic analysis of ChIPseq data was performed by Francesco Gualdrini. Metaprofiles of total Pol II and Ser5P, Ser7P and Ser2P forms of Pol II are shown in Figure 71A and metaprofiles of Ser5P, Ser7P and Ser2P forms of Pol II normalized to total Pol II signal are shown in Figure 71B, separately covering three gene regions: the TSS of MRTF target genes, defined as the region spanning 500bp upstream to 500bp downstream of the TSS; the gene body, defined as the region 500bp downstream of the TSS to 500bp upstream of the TTS, normalized to 100%; and the TTS- the region 500bp upstream of the TTS to 7000bp downstream of the TTS.

Like at the *Acta2* model gene, in response to CD stimulation, the fully phosphorylated form of Pol II was recruited at MRTF target genes. Pol II ChIP signal was present across the gene, with a peak at the TSS. The ChIP profile of

Ser5P and Ser7P followed the one of total Pol II, while Ser2P reached maximum towards the poly(A) site at the 3' end of genes. In response to LMB treatment, the Pol II was recruited to MRTF target genes, albeit at reduced levels. The Pol II ChIP profile was as in CD-stimulated cells. However, the CTD of the recruited Pol II was aberrantly phosphorylated. Ser5P and Ser7P levels were reduced, with the effect on Ser7P being more pronounced, while Ser2P was virtually absent. In contrast, Pol II recruitment and CTD phosphorylation was unaltered in CD- and LMB-treated cells at a control set of 160 constitutively expressed genes, which are not under the regulation of MRTF (Figure 72).

Overall, stimulation with CD, which activates productive RNA synthesis at MRTF target genes, induces the recruitment of the fully phosphorylated form of the RNA Pol II. On the other hand, the LMB-induced non-productive transcriptional state correlates with defective Pol II CTD phosphorylation. This data suggests that while hypo-phosphorylated Pol II is competent for elongation, additional phosphorylation events are required for productive RNA synthesis.

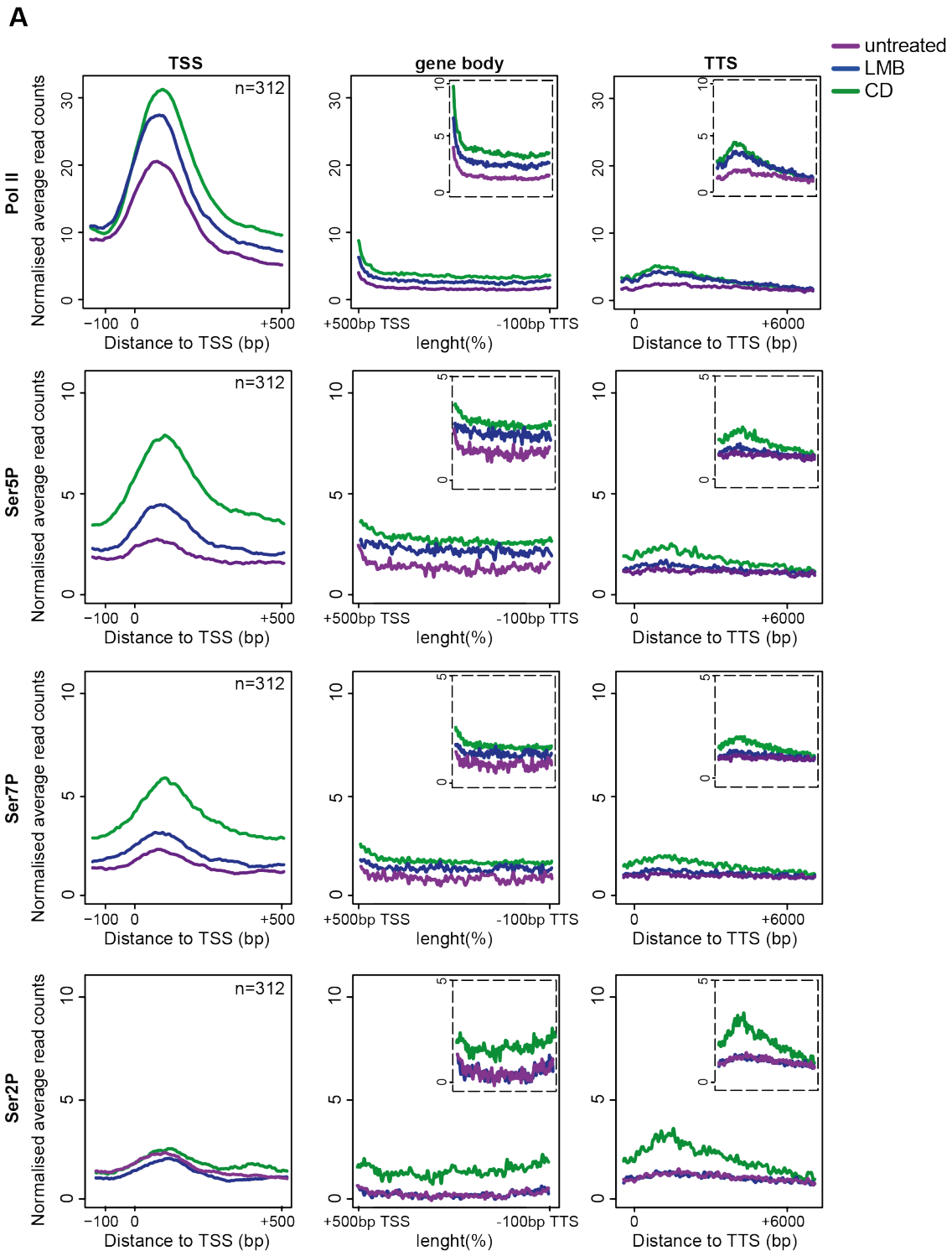
A
TSS
gene body
TTS
untreated
LMB
CD
Pol II
Ser5P
Ser7P
Ser2P
Normalised average read counts
n=312
−100 0 +500
Distance to TSS (bp)
+500bp TSS
-100bp TTS
lenght(%)
0 +6000
Distance to TTS (bp)

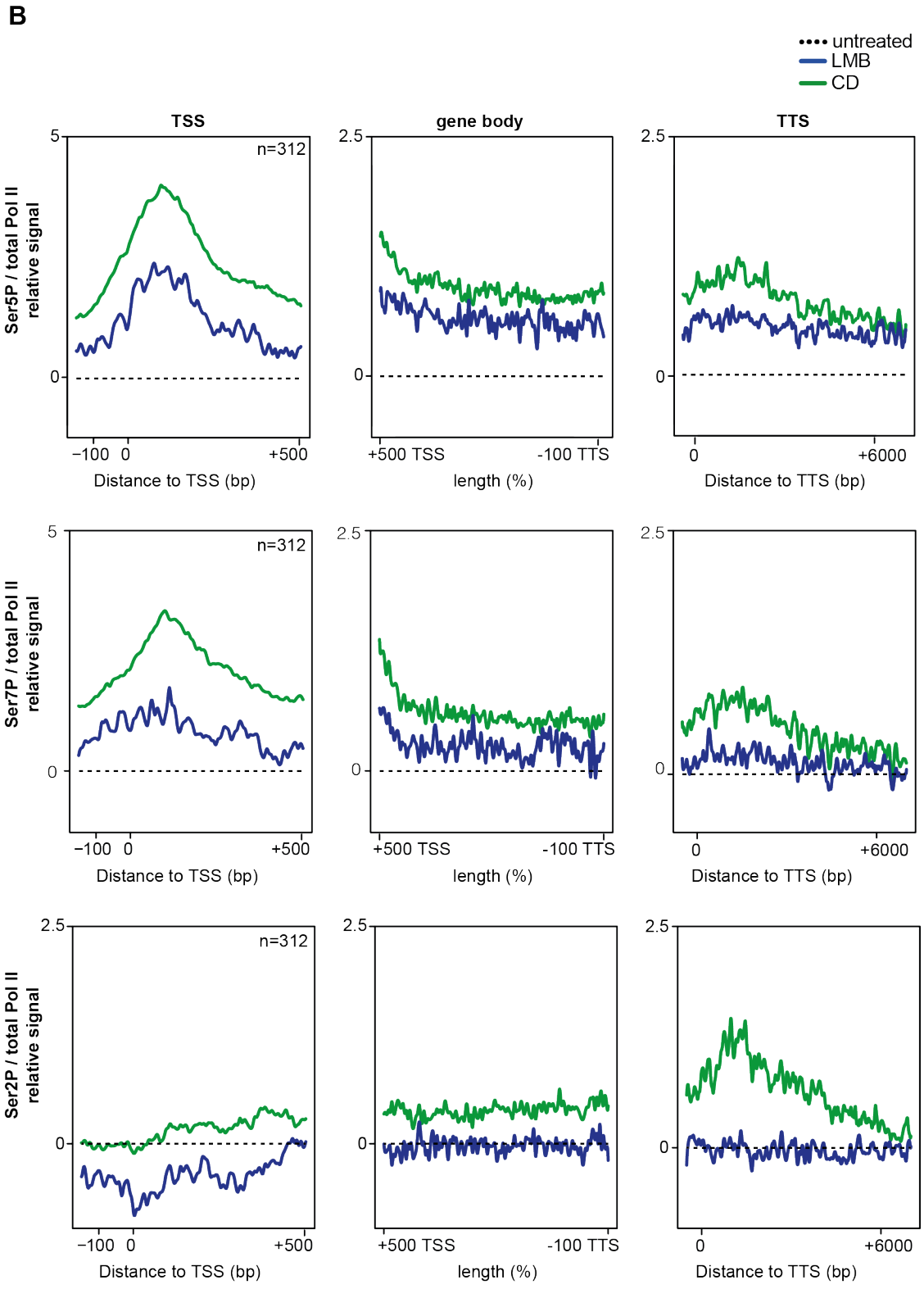
B
untreated
LMB
CD
TSS
gene body
TTS
Ser5P / total Pol II relative signal
Ser7P / total Pol II relative signal
Ser2P / total Pol II relative signal
n=312
5
2.5
0
−100 0
+500
Distance to TSS (bp)
+500 TSS
-100 TTS
length (%)
0
+6000
Distance to TTS (bp)

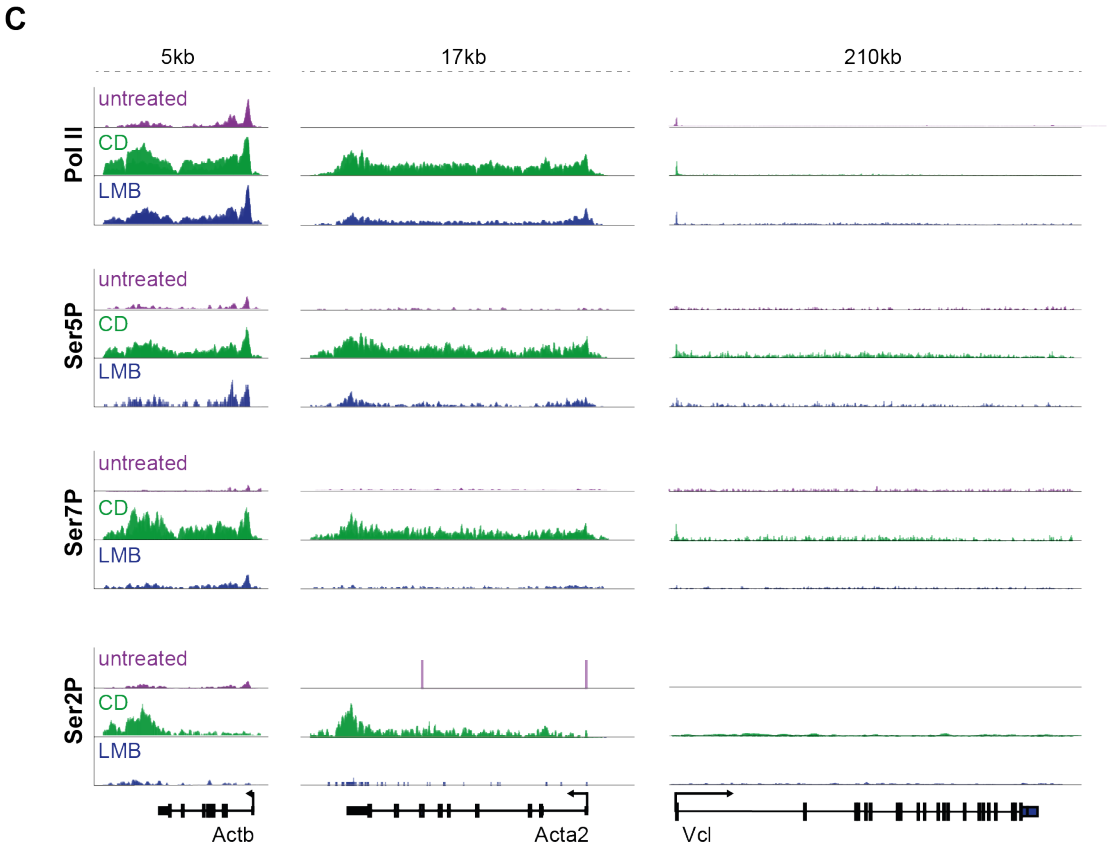

Figure 71 Pol II ChIPseq at the stringent 312 CD-inducible gene set

(A) Metaprofiles of Rpb1 (D8L4Y), phospo-Ser5 (Ser5P, 3E8), phospho-Ser7 (Ser7P, 4E12) and phospho-Ser2 (Ser2P, 3E10) ChIPseq at the 312 CD-inducible gene set defined in Chapter 3.3. NIH3T3 fibroblasts were serum-starved overnight and stimulated for 30 min with 3µM CD (Cytochalasin D); 50nM LMB (Leptomycin B); or left untreated. Normalized average read counts are plotted at the TSS region (500bp upstream to 500bp downstream of the TSS (0)); the gene body (500bp downstream of the TSS to 500bp upstream of the TTS, normalized to 100%); the TTS (500bp upstream to 7000bp downstream of the TTS (0)). (B) Metaprofiles of phospo-Ser5 (Ser5P), phospho-Ser7 (Ser7P) and phospho-Ser2 (Ser2P) ChIPseq relative to total Pol II at the 312 CD-inducible gene set defined in Chapter 3.3. The untreated ChIP profile per base was substracted from each individual ChIP, the per-base ratio between CD/LMB for total Pol II was calculated and the obtained Pol II per-base ratio from CD/LMB was applied on the ChIP of Ser5P, Ser7P and Ser2P. Relative signal is plotted at the TSS region (500bp upstream to 500bp downstream of the TSS (0)); the gene body (500bp downstream of the TSS to 500bp upstream of the TTS, normalized to 100%); the TTS (500bp upstream to 7000bp downstream of the TTS (0)). (C) ChIPseq read plots in untreated, CD-stimulated and LMB-treated cells at the CD-inducible MRTF-SRF target genes *Actb*, *Acta2* and *Vcl*. Bioinformatic analysis of ChIPseq data was performed by Francesco Gualdrini.

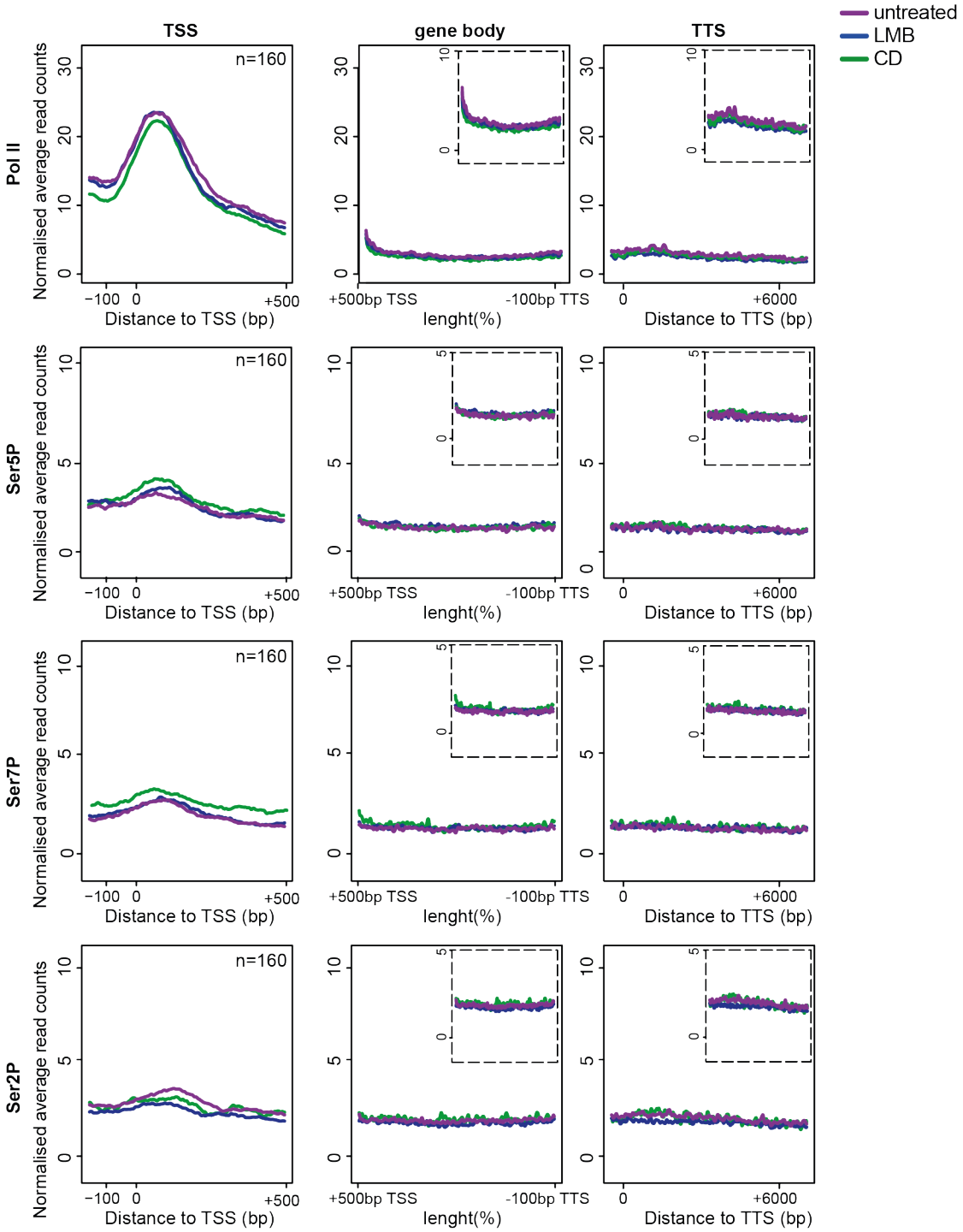

Figure 72 Pol II ChIPseq at constitutively expressed genes

Metaprofiles of Rpb1 (D8L4Y), phospo-Ser5 (Ser5P, 3E8), phospho-Ser7 (Ser7P, 4E12) and phospho-Ser2 (Ser2P, 3E10) ChIPseq at a control set of constitutively expressed genes (n=160). NIH3T3 fibroblasts were serum-starved overnight and stimulated for 30 min with 3μM CD (Cytochalasin D); 50nM LMB (Leptomycin B); or left untreated. Normalized average read counts are plotted at the TSS region (500bp upstream to 500bp downstream of the TSS (0)); the gene body (500bp downstream of the TSS to 500bp upstream of the TTS, normalized to 100%); the TTS (500bp upstream to 7000bp downstream of the TTS (0)). Bioinformatic analysis of ChIPseq data was performed by Francesco Gualdrini.

7.4 Mtr4 and Nrde2 depletion does not affect Pol II recruitment at MRTF target genes

As described in Chapter 5, Mtr4 depletion restores productive RNA synthesis in LMB-treated NIH3T3 cells. Conversely, Nrde2 depletion can inhibit CD-stimulation of MRTF target genes. To exclude the possibility that rather than acting directly at the level of RNA turnover, depletion of Mtr4 and Nrde2 affect Pol II recruitment or CTD phosphorylation at MRTF target genes, ChIP assays in cells depleted of Mtr4 or Nrde2 were performed.

NIH3T3 cells were treated with siRNA against Mtr4, Nrde2 or a non-targeting scrambled siRNA for 48 hours and subsequently stimulated with LMB or CD. As before, Pol II recruitment and CTD phosphorylation at the *Acta2* model gene was assessed by qPCR. qPCR probes targeting regions along the length of the *Acta2* gene were used. Results are shown in Figure 73.

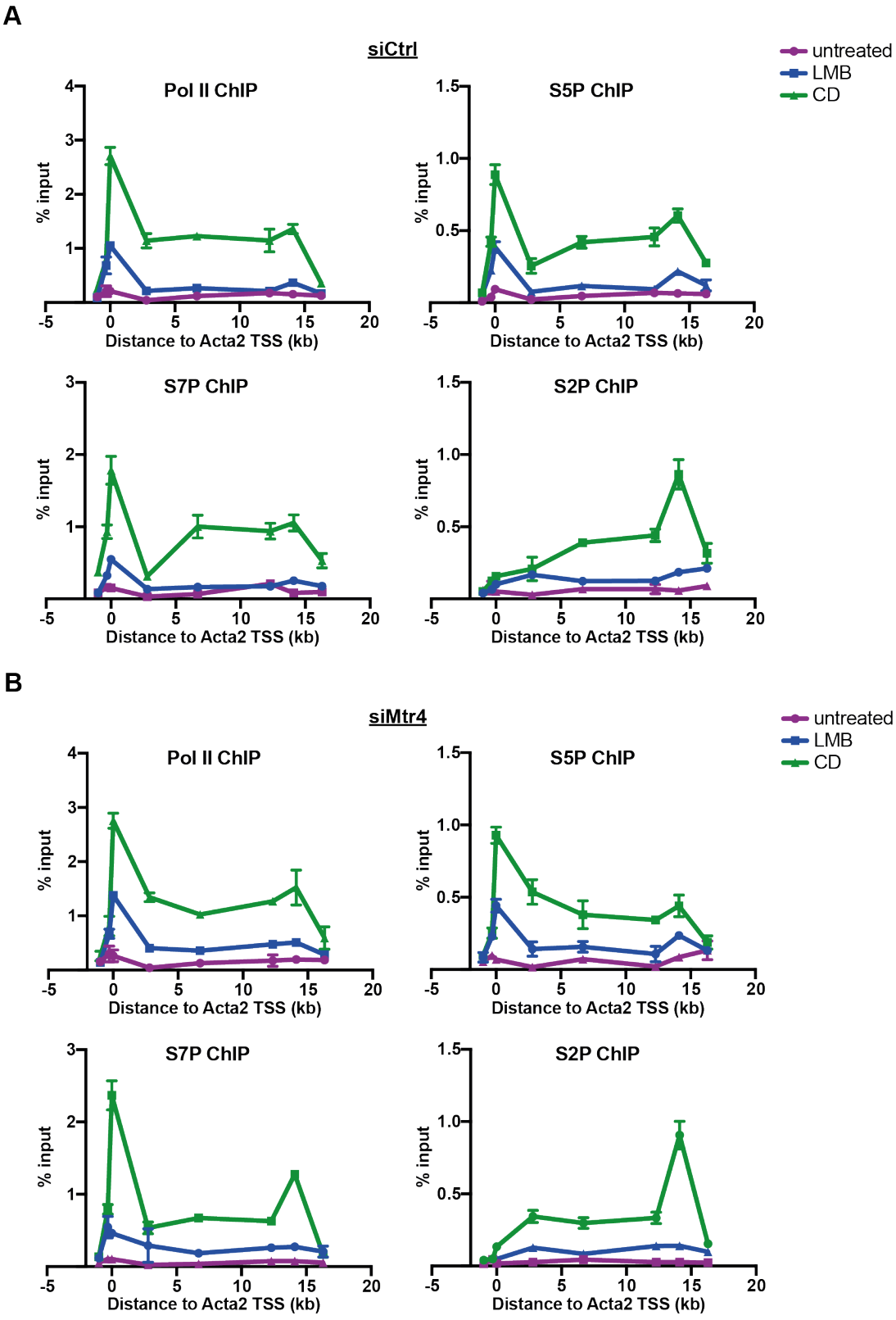
A
siCtrl
untreated
LMB
CD
Pol II ChIP
S5P ChIP
S7P ChIP
S2P ChIP
% input
Distance to Acta2 TSS (kb)
B
siMtr4
untreated
LMB
CD
Pol II ChIP
S5P ChIP
S7P ChIP
S2P ChIP
% input
Distance to Acta2 TSS (kb)

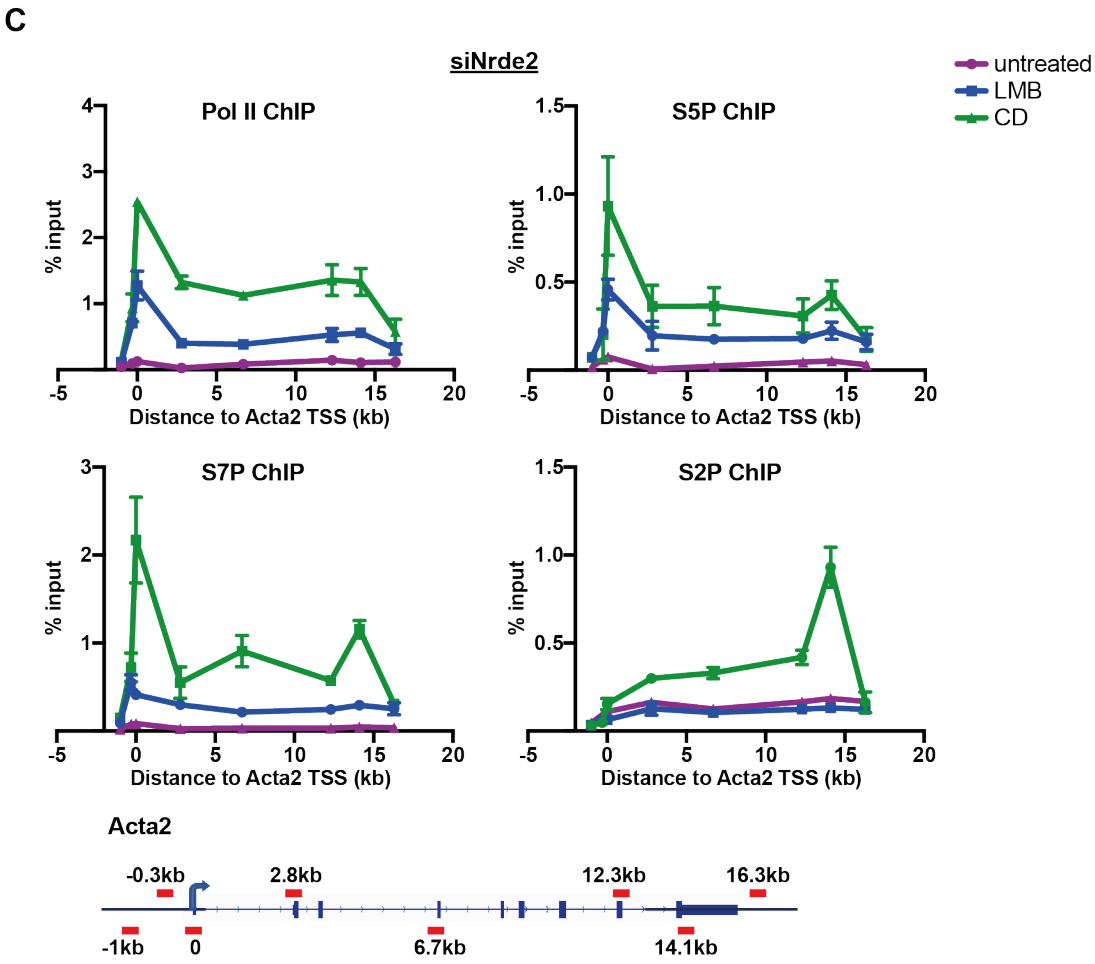

Figure 73 Depletion of Mtr4 and Nrde2 does not affect Pol II recruitment

Total RNA Polymerase (Pol II, D8L4Y), phospho-serine 5 (S5P, 3E8), phospho-serine 7 (S7P, 4E12) and phospho-serine 2 (S2P, 3E10) of the Pol II CTD ChIP at the *Acta2* gene. NIH3T3 fibroblasts were treated with non-targeting siRNA (A), siRNA against Mtr4 (B) or siRNA against Nrde2 (C) for 48h, serum-starved overnight and stimulated for 30 min with 3μM CD (Cytochalasin D) or 50nM LMB (Leptomycin B). Signal was normalized to input. Data is shown as mean ± SEM and is representative of three independent experiments. The lines connecting individual points within data series are not necessarily representative of ChIP levels between data points. The location of the qPCR probes, relative to the TSS (0), is indicated by the red lines in the gene schematic.

In cells treated with siCtrl, CD stimulation induced the recruitment of the fully phosphorylated form of the Pol II to the *Acta2* gene. The ChIP profiles of total Pol II, Ser5P, Ser7P and Ser2P were as in wild-type NIH3T3 cells. LMB treatment also

induced Pol II recruitment. Pol II distribution along the gene and CTD phosphorylation was as in wild-type NIH3T3 cells (Figure 73A).

Next, Pol II recruitment and CTD phosphorylation was examined in cells depleted of Mtr4 (Figure 73B) or Nrde2 (Figure 73C). Mtr4 or Nrde2 depletion did not alter Pol II recruitment or distribution along the gene in response to CD or LMB treatment. Furthermore, levels of phospho-Ser5, phospho-Ser7 and phospho-Ser2 were not affected in cells depleted of Mtr4 or Nrde2.

These results show that depletion of Mtr4 restores productive RNA synthesis at MRTF target genes in LMB-treated cells, without affecting Pol II loading on the gene or Pol II CTD phosphorylation. Moreover, Nrde2 depletion, which inhibits RNA synthesis in response to CD stimulation, does not perturb Pol II recruitment or phosphorylation. This data is consistent with a model in which Mtr4 and its inhibitor Nrde2 act downstream of Pol II, to regulate the turn-over of transcripts of MRTF target genes.

7.5 The non-productive transcriptional state in dKO$^{MRTF\text{-}NLS}$ cells correlates with aberrant phosphorylation of the Pol II CTD

The non-productive transcriptional state observed in LMB-treated NIH3T3 cells also occurs in dKO MEF cells expressing the constitutively nuclear MRTF-NLS derivative. Under resting conditions, the constitutively nuclear MRTF-NLS is recruited to target gene promoters and induces transcription, but not productive RNA synthesis. To test the correlation between the non-productive transcriptional state and the abnormal phosphorylation status of the Pol II CTD, Pol II recruitment and CTD phosphorylation at MRTF target genes in dKO$^{MRTF\text{-}NLS}$ cells were examined.

Pol II recruitment and CTD phosphorylation were examined by ChIP-qPCR at the *Acta2* and *Actb* genes in dKO$^{MRTF\text{-}NLS}$ under resting conditions, as well as in response to CD, which induces productive RNA synthesis, and LatB, which inhibits

transcription at MRTF target genes. As controls, the experiment was repeated in dKO^{MRTF} cells, in which in the absence of stimulation target genes are inactive, and in dKO$^{MRTF\text{-}XXX}$ cells, in which MRTF target genes are constitutively active.

In dKO^{MRTF} cells under resting conditions Pol II was not recruited to the *Acta2* and *Actb* genes (Figure 74). Pol II remained absent from MRTF target genes in LatB-treated cells. In response to stimulation with CD, Pol II was recruited to target genes. Pol II signal was present throughout the gene, with a distinct peak at the TSS. In CD-treated cells, Ser5P, Ser7P and Ser2P were upregulated. Ser5P and Ser7P ChIP profile resembled that of total Pol II, whereas Ser2P started accumulating within the gene body and reached maximum at the 3' end of genes.

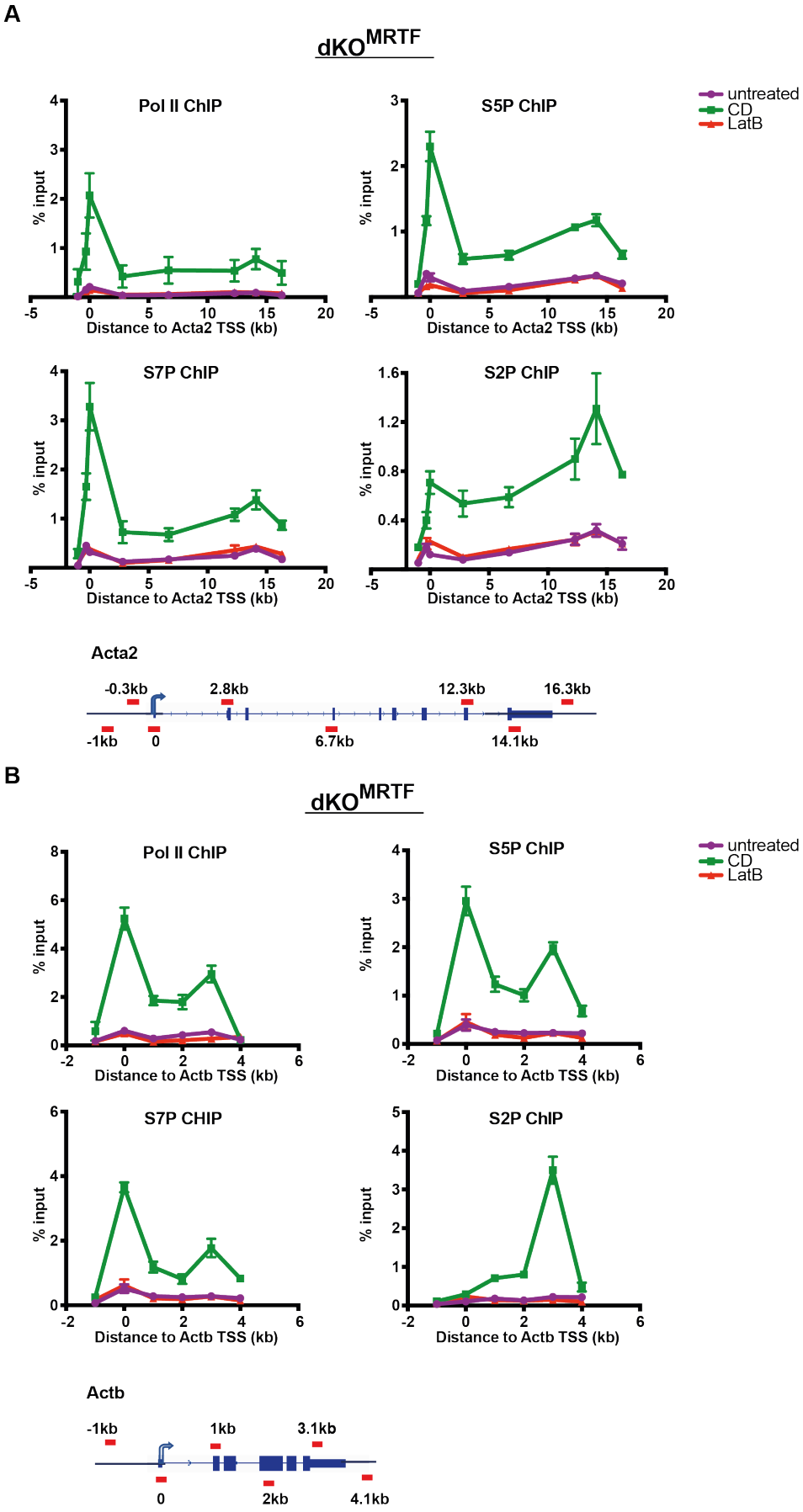
A
dKO MRTF
Pol II ChIP
S5P ChIP
S7P ChIP
S2P ChIP
% input
Distance to Acta2 TSS (kb)
untreated
CD
LatB
Acta2
-0.3kb
2.8kb
12.3kb
16.3kb
-1kb
0
6.7kb
14.1kb
B
dKO MRTF
Pol II ChIP
S5P ChIP
S7P CHIP
S2P ChIP
% input
Distance to Actb TSS (kb)
untreated
CD
LatB
Actb
-1kb
1kb
3.1kb
0
2kb
4.1kb

Figure 74 Pol II recruitment and phosphorylation at MRTF target genes in dKO^{MRTF} cells

Total RNA Polymerase (Pol II, D8L4Y), RNA Polymerase II C-terminal domain phosphorylated at Serine 5 (S5P, 3E8), Serine 7 (S7P, 4E12) or Serine 2 (S2P, 3E10) ChIP in dKO^{MRTF} cells on the model genes *Acta2* (A) and *Actb* (B). Cells were stimulated for 30 min with 3μM CD (Cytochalasin D); 0.5μM LatB (Latrunculin B) or left untreated. Signal was normalized to input. Data is shown as mean ± SEM and is representative of three independent experiments. The lines connecting individual points within data series are not necessarily representative of ChIP levels between data points. The location of the qPCR probes, relative to the TSS (0), is indicated by the red lines in the gene schematics.

In contrast, in dKO$^{MRTF\text{-}NLS}$ cells, Pol II was recruited at the *Acta2* and *Actb* genes under resting conditions, although at reduced levels, relative to these in CD-stimulated cells (Figure 75). Furthermore, Ser5P was present at the 5' end of the gene, albeit at reduced levels. In contrast, Ser7 and Ser2 were not phosphorylated at the 3' end of the genes tested. CD treatment induced Pol II recruitment and phosphorylation at Ser5P, Ser7P and Ser2P. The ChIP profiles of the total and phosphorylated forms of Pol II were as in CD-stimulated dKO^{MRTF} cells. LatB addition abolished Pol II recruitment.

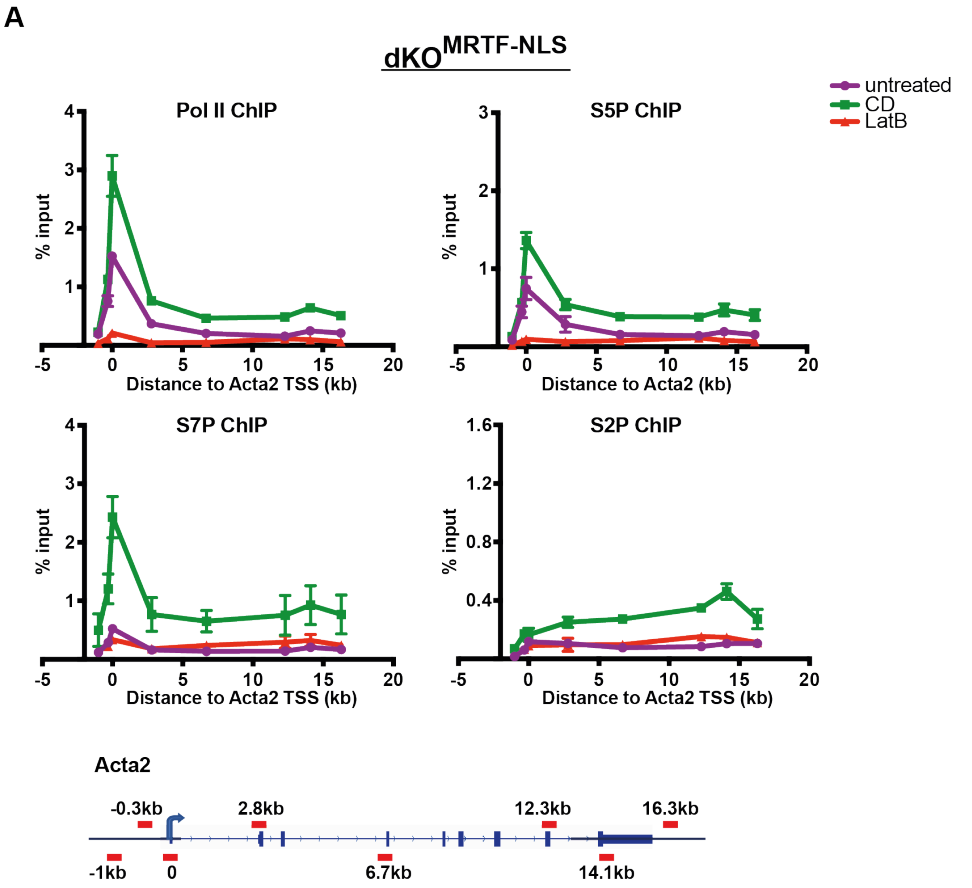
A
dKOMRTF-NLS
untreated
CD
LatB
Pol II ChIP
S5P ChIP
S7P ChIP
S2P ChIP
% input
Distance to Acta2 TSS (kb)
Distance to Acta2 (kb)
Acta2
-0.3kb
2.8kb
12.3kb
16.3kb
-1kb
0
6.7kb
14.1kb

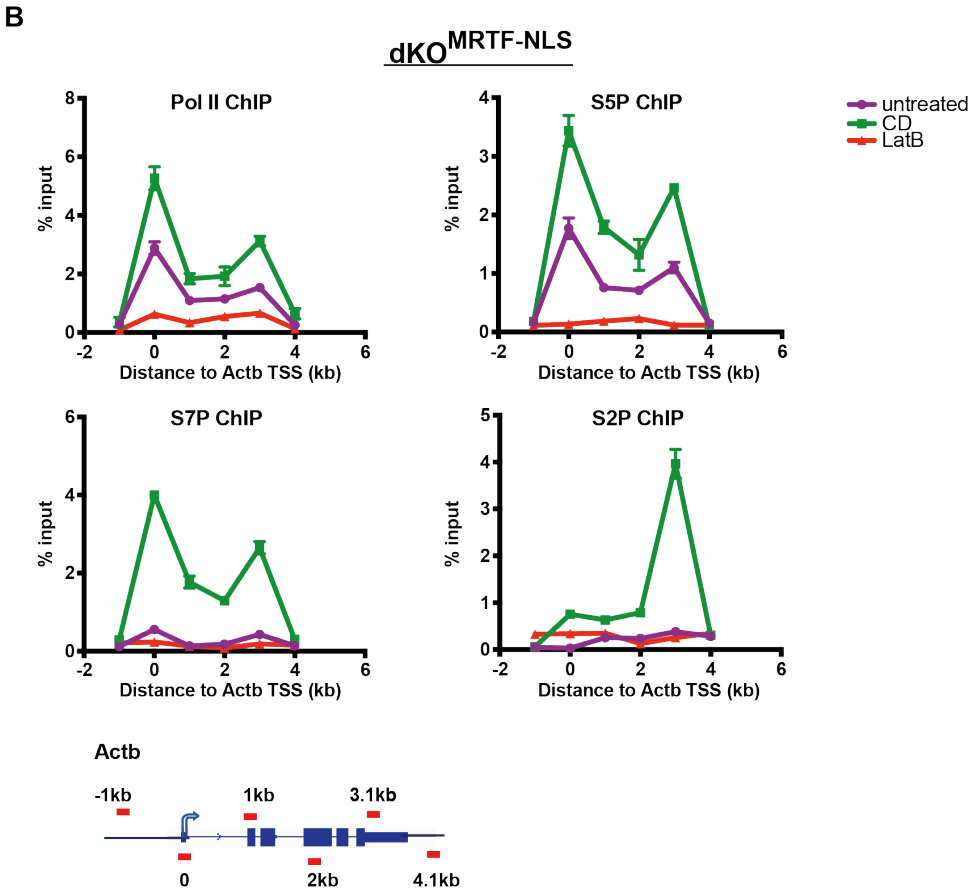
B
dKOMRTF-NLS
untreated
CD
LatB
Pol II ChIP
S5P ChIP
S7P ChIP
S2P ChIP
% input
Distance to Actb TSS (kb)
Actb
-1kb
1kb
3.1kb
0
2kb
4.1kb

Figure 75 Pol II recruitment and phosphorylation at MRTF target genes in dKO$^{MRTF\text{-}NLS}$ cells

Total RNA Polymerase (Pol II, D8L4Y), RNA Polymerase II C-terminal domain phosphorylated at Serine 5 (S5P, 3E8), Serine 7 (S7P, 4E12) or Serine 2 (S2P, 3E10) ChIP in dKO$^{MRTF\text{-}NLS}$ cells on the model genes *Acta2* (A) and *Actb* (B). Cells were stimulated for 30 min with 3μM CD (Cytochalasin D); 0.5μM LatB (Latrunculin B) or left untreated. Signal was normalized to input. Data is shown as mean ± SEM and is representative of three independent experiments. The lines connecting individual points within data series are not necessarily representative of ChIP levels between data points. The location of the qPCR probes, relative to the TSS (0), is indicated by the red lines in the gene schematics.

In dKO$^{MRTF\text{-}XXX}$ cells, where MRTF is constitutively active, Pol II was recruited at MRTF target genes in the absence of treatment (Figure 76). Furthermore, its CTD was phosphorylated at Ser5, Ser7 and Ser2. The ChIP profiles of the total and phosphorylated forms of the Pol II were as in CD-stimulated dKO^{MRTF} cells. Consistent with the inability of MRTF-XXX to interact with G-actin, Pol II recruitment and phosphorylation remained unchanged in response to CD and LatB treatments.

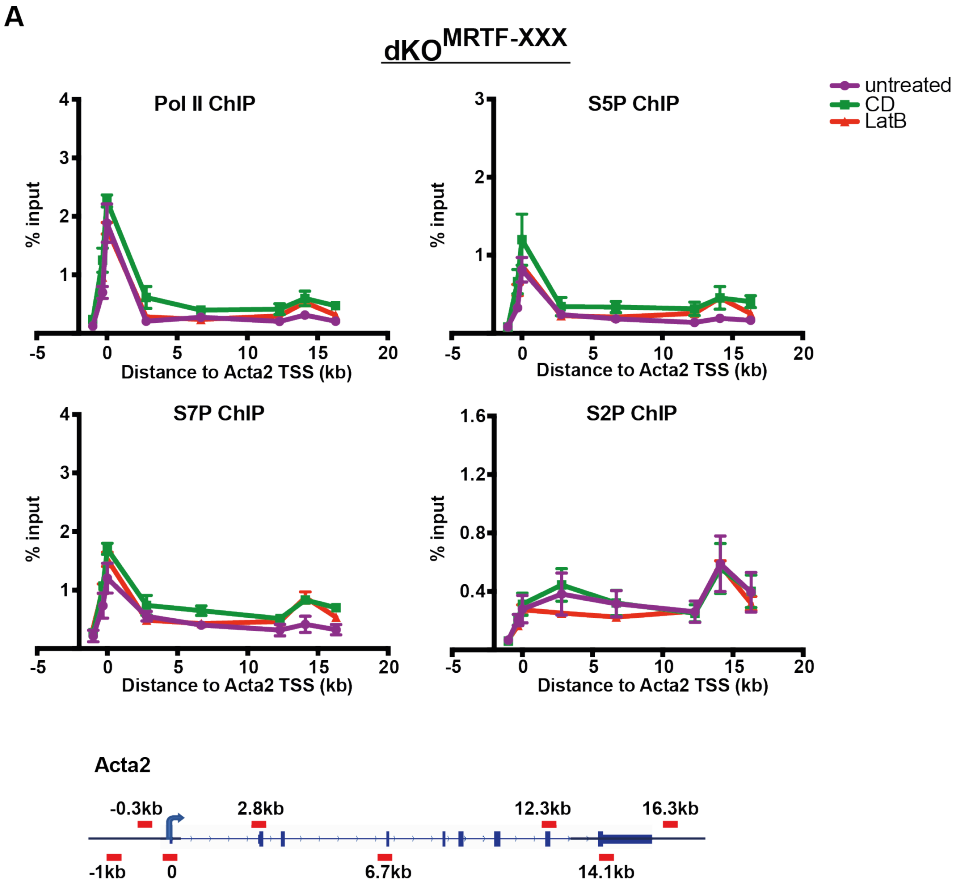
A
dKOMRTF-XXX
untreated
CD
LatB
Pol II ChIP
S5P ChIP
S7P ChIP
S2P ChIP
% input
Distance to Acta2 TSS (kb)
Acta2
-0.3kb
2.8kb
12.3kb
16.3kb
-1kb
0
6.7kb
14.1kb

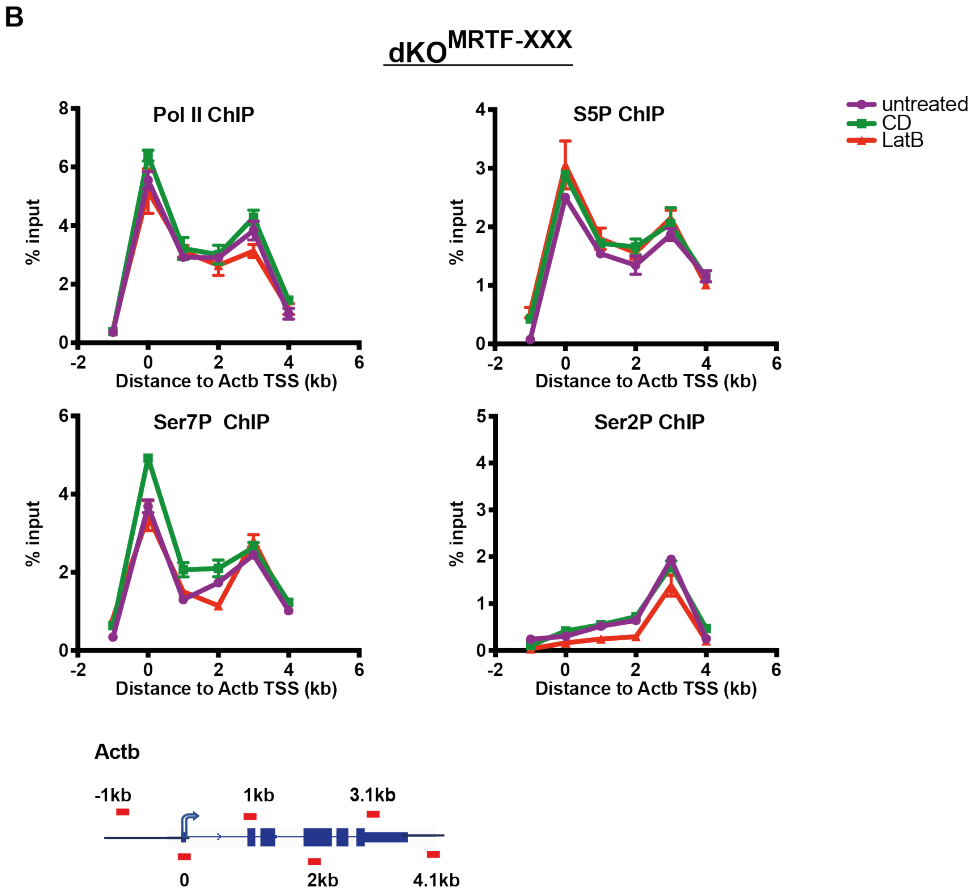
B
dKOMRTF-XXX
untreated
CD
LatB
Pol II ChIP
S5P ChIP
Ser7P ChIP
Ser2P ChIP
% input
Distance to Actb TSS (kb)
Actb
-1kb
1kb
3.1kb
0
2kb
4.1kb

Figure 76 Pol II recruitment and phosphorylation at MRTF target genes in dKO$^{MRTF\text{-}XXX}$ cells

Total RNA Polymerase (Pol II, D8L4Y), RNA Polymerase II C-terminal domain phosphorylated at Serine 5 (S5P, 3E8), Serine 7 (S7P, 4E12) or Serine 2 (S2P, 3E10) ChIP in dKO$^{MRTF\text{-}XXX}$ cells on the model genes *Acta2* (A) and *Actb* (B). Cells were stimulated for 30 min with 3μM CD (Cytochalasin D); 0.5μM LatB (Latrunculin B) or left untreated. Signal was normalized to input. Data is shown as mean ± SEM and is representative of three independent experiments. The lines connecting individual points within data series are not necessarily representative of ChIP levels between data points. The location of the qPCR probes, relative to the TSS (0), is indicated by the red lines in the gene schematics.

The data presented above demonstrates that Pol II recruitment to MRTF target genes is dependent on MRTF binding and that CTD phosphorylation is promoted by disrupting the interaction between MRTF and G-actin. Consistent with data in NIH3T3 cells, these results suggest that in the absence of an activating signal, nuclear MRTF recruits Pol II to targets in a non-productive state associated with aberrant CTD phosphorylation and Mtr4 recruitment.

Chapter 8. Phospho-Ser7 of the Pol II CTD is required for productive RNA synthesis at MRTF target genes

In the absence of an activating signal, nuclear MRTF is recruited to target gene promoters. Its binding induces Pol II recruitment and nascent RNA synthesis, but pre-mRNA does not accumulate. Instead, transcripts of MRTF target genes are bound by Mtr4, which appears to target them for degradation by the nuclear exosome. This non-productive transcriptional state correlates with aberrant phosphorylation of the Pol II CTD. To establish whether the relationship between low Ser5P, Ser7P and Ser2P levels and transcript destabilization is causal or correlative, in this chapter the effect of CTD phospho-marks on productive RNA synthesis at MRTF target genes was examined.

8.1 The effect of CDK inhibitors on MRTF target gene expression

A number of CTD kinases act during the transcription cycle to ensure appropriate regulation of Pol II during transcription. During initiation, CDK7 phosphorylates Ser5 and Ser7 of the Pol II CTD (Glover-Cutter et al., 2009; Ramanathan et al., 2001). During promoter-proximal pausing, CDK9 phosphorylates Ser2 of the Pol II CTD, along with DSIF and NELF, to induce pause release into elongation (Ramanathan et al., 2001). In addition, CDK12 and CDK13 have been shown to target Ser2 (Bartkowiak et al., 2010). Thr4P is deposited by Plk3, whereas the Tyr1P kinase in mouse is unknown (Hintermair et al., 2012; Tybulewicz et al., 1991).

To study the role of different CTD phospho-marks in transcription at MRTF target genes, CDK inhibitors were investigated, aiming to ascertain whether any could block RNA synthesis and recapitulate the defect in Pol II CTD phosphorylation observed in the non-productive transcriptional state. Cells were treated with CD to induce productive transcription and the effect of different CDKs assessed using

specific small molecule inhibitors. Alongside the effect on CD-induced RNA synthesis, recruitment of Pol II to the *Acta2* model gene was examined, together with the distribution of CTD phosphorylations.

NIH3T3 cells were simultaneously treated with CD and THZ1 to inhibit CDK7 (Kwiatkowski et al., 2014); Flavopiridol (FP) to inhibit CDK9 (Biglione et al., 2007; Chao & Price, 2001; Ni et al., 2004); THZ531 to inhibit CDK12 and CDK13 (Zhang et al., 2016); GW843682X to inhibit Plk3 (Pohl et al., 2017). Following treatment pre-mRNA levels at endogenous MRTF target genes were measured by qPCR using probes targeting the first intron of each gene.

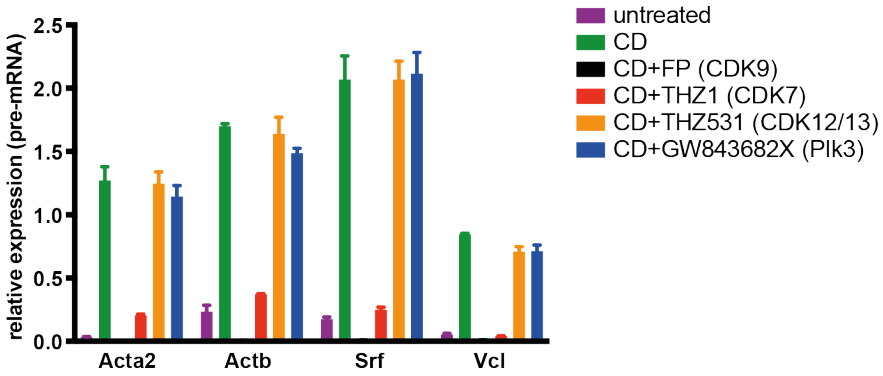

Figure 77 The effect of CDK inhibitors on MRTF target gene expression

Pre-mRNA accumulation in response to stimulation at MRTF target genes. NIH3T3 fibroblasts were serum-starved overnight and stimulated with 3μM CD for 30 min; ; 0.5μM Flavopiridol (FP) for 1h and 3μM CD for 30 min; 0.5μM THZ1 for 1h and 3μM CD for 30 min; 1μM THZ531 for 1h and 3μM CD for 30 min; 10μM GW843682X for 1h and 3μM CD for 30 min; or left untreated. qPCR probes are located within the first intron of each gene. Signal was normalized to *Gapdh*. Data is shown as mean ± SEM and is representative of three independent experiments.

As shown in Figure 77, THZ1 and FP substantially blocked CD induction at all MRTF target genes tested, while THZ531 and GW843682X had no effect.

Next, the effect of the CDK inhibitors on Pol II CTD modifications the model gene *Acta2* was assessed by ChIP-qPCR using antibodies against the Rpb1 subunit of the Pol II (D8L4Y), to measure total Pol II, and phospho-specific antibodies targeting Ser5P (3E8), Ser7P (4E12), Ser2P (3E10), Thr4P (6D7) and Tyr1P (3D12) of the Rpb1 CTD (Chapman et al., 2007). NIH3T3 cells were simultaneously treated with CD and THZ1 to inhibit CDK7; Flavopiridol (FP) to inhibit CDK9; THZ531 to inhibit CDK12 and CDK13; GW843682X to inhibit Plk3. Background ChIP levels were assessed in untreated cells, when MRTF target genes are uninduced. qPCR probes targeting regions along the length of the *Acta2* gene were used.

First, the effect of inhibiting CDK7 was examined. Results are presented in Figure 78. As shown before, CD stimulation induced Pol II recruitment and phosphorylation at Ser5, Ser7, Ser2, Thr4 and Tyr1 of the Pol II CTD. Addition of the CDK7 inhibitor THZ1 to CD-stimulated cells inhibited Pol II loading on the gene.

Next, the effect of inhibiting Ser2 phosphorylation was examined. To this end, Flavopiridol (FP), a CKD9 inhibitor, as well as THZ531, an inhibitor of CDK12 and CDK13, were used. Of these inhibitors only FP inhibited CD-induced RNA synthesis (Figure 77). In CD-stimulated cells treated with FP, a peak of Pol II remained at the TSS of the *Acta2* gene, but no Pol II was detected along the gene body. The paused Pol II was phosphorylated on Ser5, Ser7 and Tyr1 (Figure 79). In contrast, treatment with THZ531 did not affect the profiles of total Pol II, Ser5P, Ser7P or Tyr1P, although levels of Ser2P and Thr4P were reduced at the 3’ end of the gene (Figure 80).

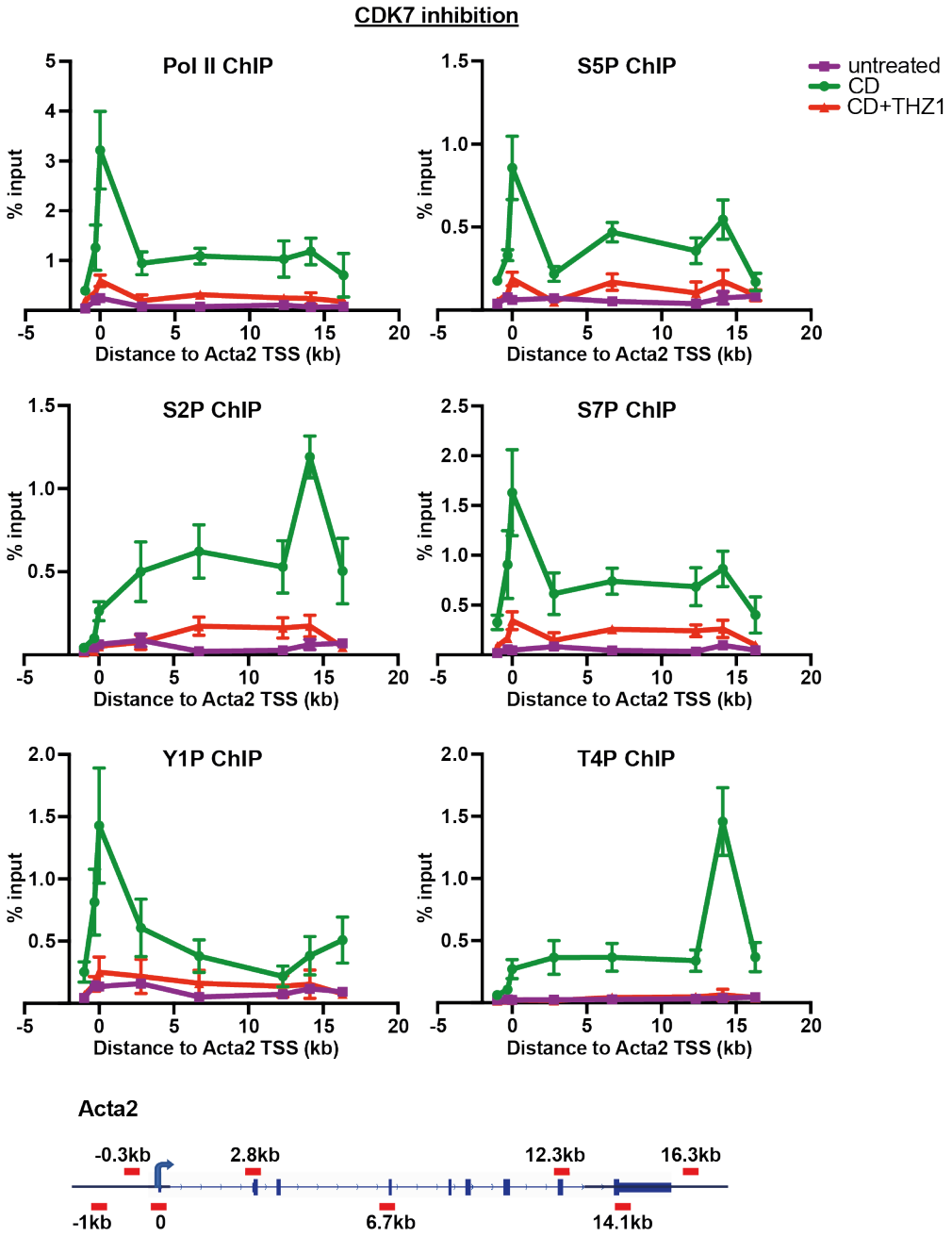

Figure 78 THZ1 inhibits Pol II recruitment at MRTF target genes

(A) Total RNA Polymerase (Pol II, D8L4Y), RNA Polymerase II C-terminal domain phosphorylated at Serine 5 (S5P, 3E8), Serine 7 (S7P, 4E12), Serine 2 (S2P, 3E10), Tyrosine 1 (Y1P, 3D12) or Threonine 4 (T4P, 6D7) ChIP at the *Acta2* gene. NIH3T3 fibroblasts were serum-starved overnight, treated with 0.5μM THZ1 for 1h and stimulated for 30 min with 3μM CD (Cytochalasin D). Signal was normalized to input. Data is shown as mean ± SEM and is representative of three independent experiments. The lines connecting individual points within data series are not necessarily representative of ChIP levels between data points. The location of the qPCR probes, relative to the TSS (0), is indicated by the red lines in the gene schematics.

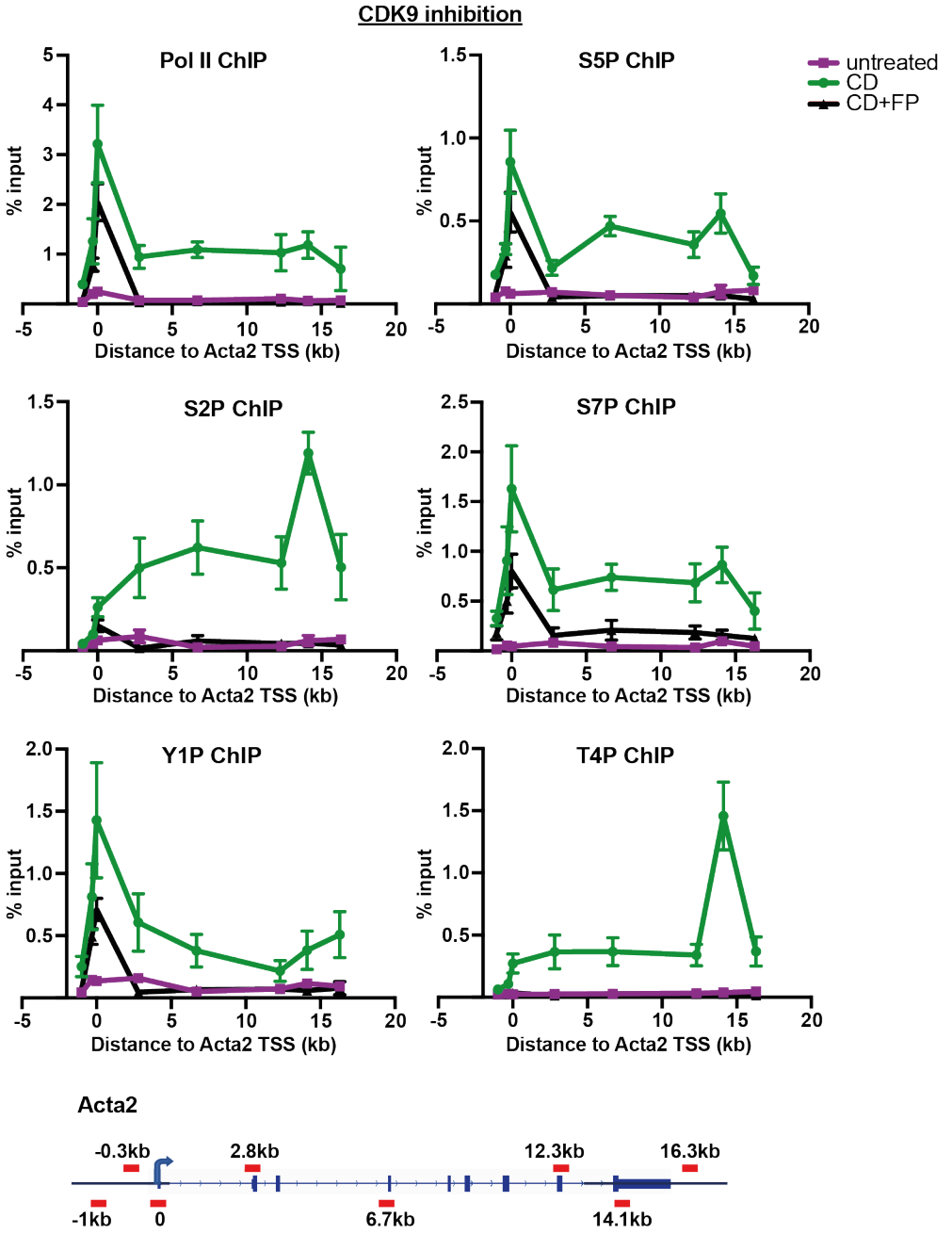

Figure 79 FP inhibits Pol II elongation at MRTF target genes

(A) Total RNA Polymerase (Pol II, D8L4Y), RNA Polymerase II C-terminal domain phosphorylated at Serine 5 (S5P, 3E8), Serine 7 (S7P, 4E12), Serine 2 (S2P, 3E10), Tyrosine 1 (Y1P, 3D12) or Threonine 4 (T4P, 6D7) ChIP at the *Acta2* gene. NIH3T3 fibroblasts were serum-starved overnight, treated with 0.5μM Flavopiridol (FP) for 1h and stimulated for 30 min with 3μM CD (Cytochalasin D). Signal was normalized to input. Data is shown as mean ± SEM and is representative of three independent experiments. The lines connecting individual points within data series are not necessarily representative of ChIP levels between data points. The location of the qPCR probes, relative to the TSS (0), is indicated by the red lines in the gene schematics.

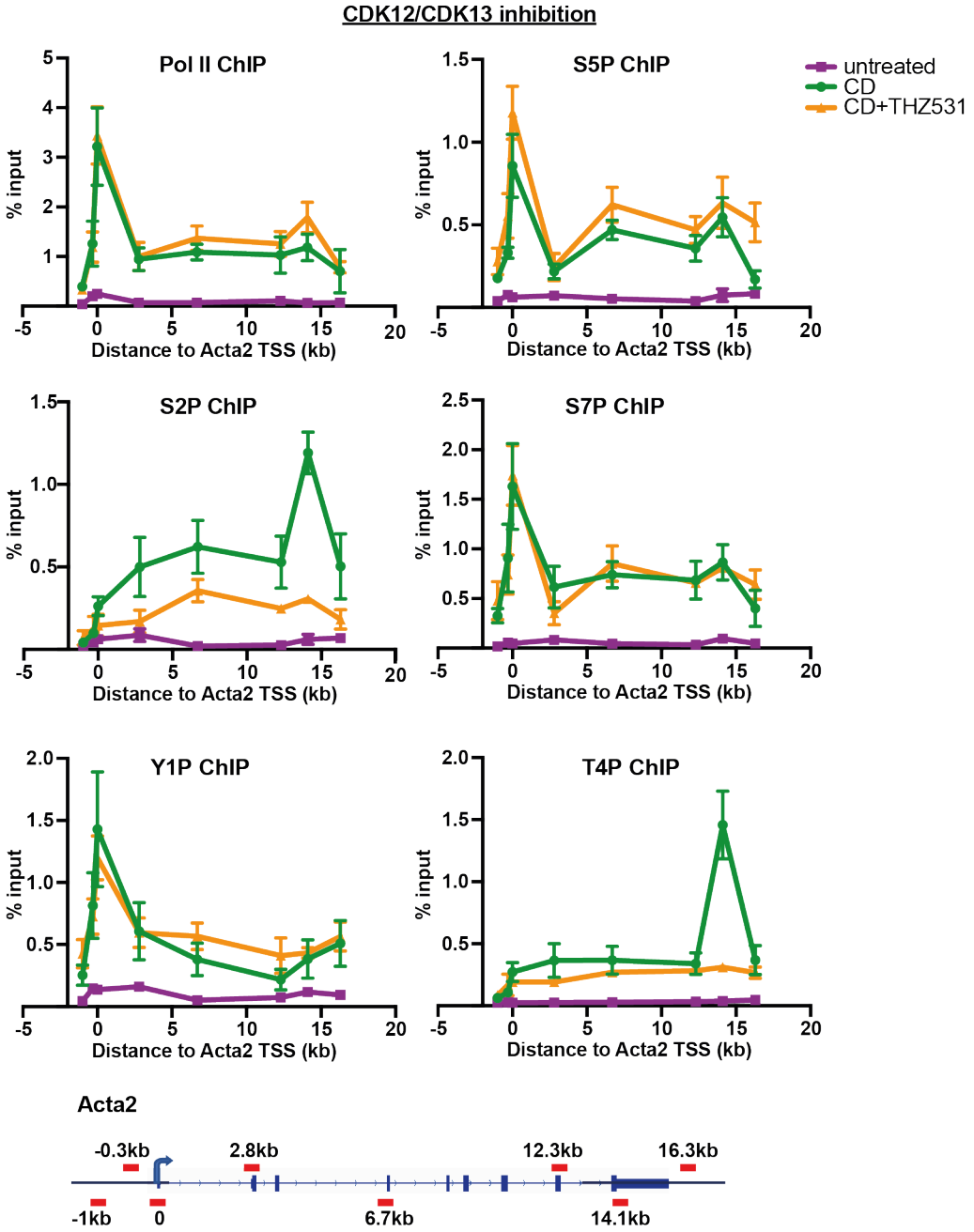

Figure 80 THZ531 does not affect Pol II elongation at MRTF target genes

(A) Total RNA Polymerase (Pol II, D8L4Y), RNA Polymerase II C-terminal domain phosphorylated at Serine 5 (S5P, 3E8), Serine 7 (S7P, 4E12), Serine 2 (S2P, 3E10), Tyrosine 1 (Y1P, 3D12) or Threonine 4 (T4P, 6D7) ChIP at the *Acta2* gene. NIH3T3 fibroblasts were serum-starved overnight, treated with 1μM THZ531 for 1h and stimulated for 30 min with 3μM CD (Cytochalasin D). Signal was normalized to input. Data is shown as mean ± SEM and is representative of three independent experiments. The lines connecting individual points within data series are not necessarily representative of ChIP levels between data points. The location of the qPCR probes, relative to the TSS (0), is indicated by the red lines in the gene schematics.

As shown in Figure 81, addition of the Plk3 inhibitor GW843682X in CD-stimulated cells reduced the accumulation of Thr4P at the 3' end of the gene. Apart from the reduction in Thr4P levels, GW843682X treatment also reduced S2P levels, whereas it did not have an effect on Pol II recruitment and elongation, Ser5P, Ser7P or Tyr1P levels.

We were unable to assess the effect of depleting Tyr1P, as the kinase responsible for depositing this mark in mouse cells remains unidentified (Tybulewicz et al., 1991).

Overall, none of the inhibitors tested reproduced the non-productive state observed in LMB-treated NIH3T3 cells and dKO$^{MRTF\text{-}NLS}$ cells. Although Ser2P and Thr4P levels were reduced by THZ531 or GW843682X treatment, expression of MRTF target genes was unaffected. While inhibiting CDK7 perturbed CD stimulation of MRTF target genes, its effect was due to inhibition of Pol II recruitment, consistent with its role in TFIIH activity. Consistent with the role of CDK9 in pTEFb activity and Pol II pause-release, Flavopiridol addition prevented the transition of the Pol II into elongation. Thus, neither inhibitor that prevents RNA synthesis induces a Pol II CTD phospho-profile similar to that seen in the LMB-induced non-productive transcriptional state.

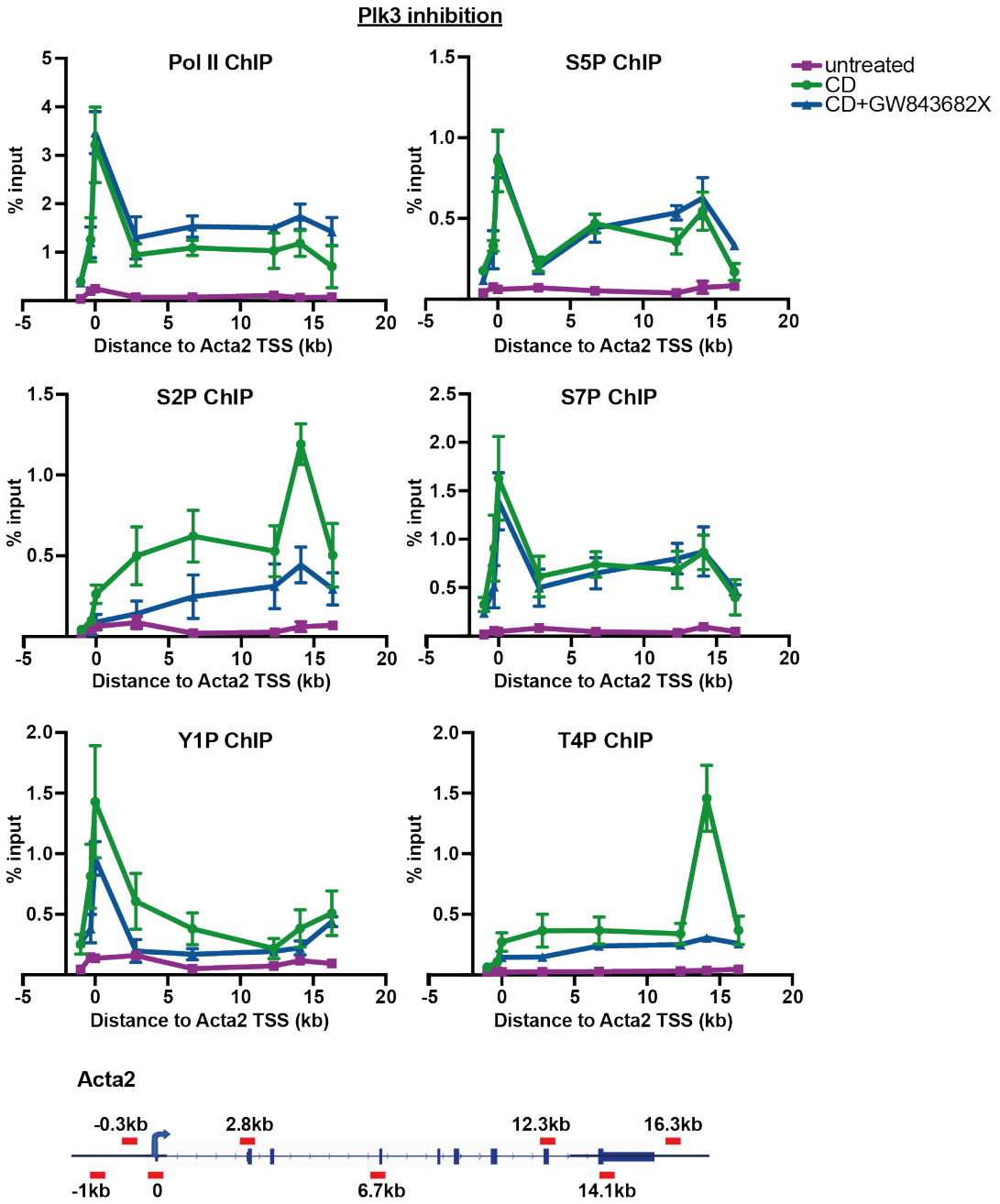

Figure 81 GW843682X does not affect Pol II elongation MRTF target genes

(A) Total RNA Polymerase (Pol II, D8L4Y), RNA Polymerase II C-terminal domain phosphorylated at Serine 5 (S5P, 3E8), Serine 7 (S7P, 4E12), Serine 2 (S2P, 3E10), Tyrosine 1 (Y1P, 3D12) or Threonine 4 (T4P, 6D7) ChIP at the *Acta2* gene. NIH3T3 fibroblasts were serum-starved overnight, treated with 10μM GW843682X for 1h and stimulated for 30 min with 3μM CD (Cytochalasin D). Signal was normalized to input. Data is shown as mean ± SEM and is representative of three independent experiments. The lines connecting individual points within data series are not necessarily representative of ChIP levels between data points. The location of the qPCR probes, relative to the TSS (0), is indicated by the red lines in the gene schematics.

8.2 Generation of NIH3T3 cells expressing Rpb1-S7A mutant

CDK7 phosphorylates both Ser5 and Ser7 of the Pol II CTD. While phosphorylation of Ser5 precedes that of Ser7 and is required for transcription initiation, little is known about the role of Ser7P in transcription at protein-coding genes. We were unable to study the role of Ser7P in transcription of MRTF target genes using CDK7 inhibition, as THZ1 blocked phosphorylation of Ser5 and Pol II recruitment. Therefore, to study the role of Ser7P, a Rpb1 mutant (Rpb1-S7A) was used. The Rpb1 and Rpb1-S7A plasmids were generated by Ana Tufegdzic Vidakovic. Both Rpb1 and Rpb1-S7A plasmids contain point mutations making them siRNA resistant (see Chapter 2.16). Rpb1-S7A harbours serine 7 to alanine substitutions in all 26 Ser7-containing repeats of the Rpb1 CTD (Figure 82A), preventing phosphorylation of the Pol II CTD at this position (Tufegdzic Vidakovic A., unpublished).

To study Rpb1-S7A a conditional depletion-expression strategy was used (Figure 82B). NIH3T3 Flp-In TREx cells were used to generate stable cell lines expressing doxycycline-inducible wild-type Rpb1 (WT) or Rpb1-S7A (S7A). WT and S7A cells were treated with siRNA against Rpb1 for 48 hours, to deplete the endogenous Rpb1 protein, and simultaneously treated with doxycycline, to reconstitute them with either wild-type Rpb1 or Rpb1-S7A, to generate “switch-over” cells expressing exogenous wild-type Rpb1 (WT-ON) or Rpb1-S7A (S7A-ON). WT and S7A cells grown in doxycycline-free medium and treated with scrambled siRNA for 48 hours are referred to as WT-off and S7A-off, respectively. As shown in Figure 82C, Rpb1 protein levels were comparable in WT-ON and S7A-ON cells, while phospho-Ser7 levels were lower in S7A-ON than in WT-ON cells. The remaining Ser7P signal in S7A-ON cells is likely due to incomplete depletion of the endogenous Rpb1 protein.

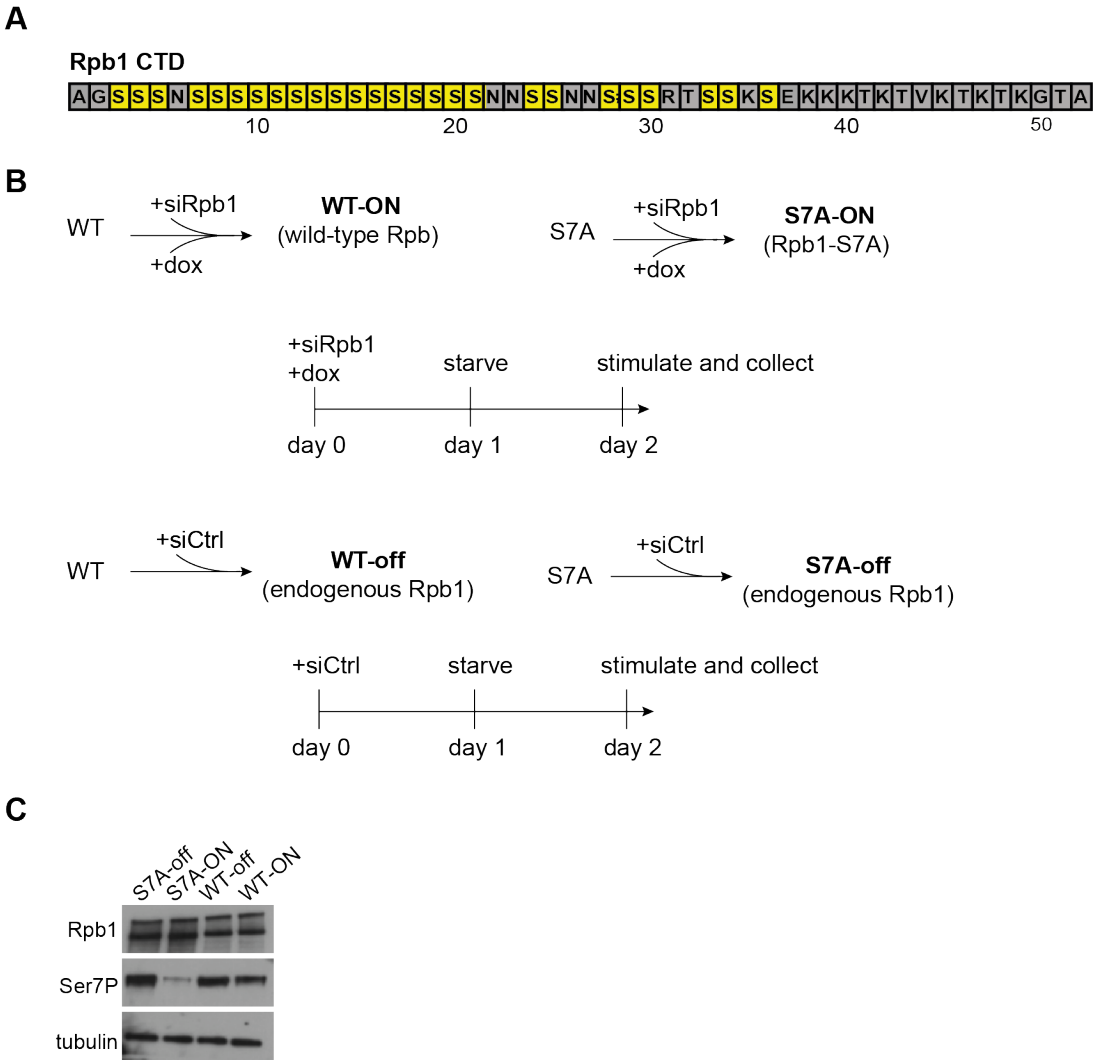

Figure 82 Generation of WT-ON and S7A-ON cells

(A) Human Rpb1 CTD. Ser7-containing repeats are highlighted in yellow. Non-consensus repeats are shown in grey and amino acid substitutions at position 7 of each repeat are indicated. (B) Generation of WT-ON and S7A-ON cells. NIH3T3 Flp-In TREx cells were used to generate stable cell lines expressing doxycycline-inducible wild-type Rpb1 (WT) or Rpb1-S7A (S7A). WT and S7A cells were treated with siRNA against Rpb1 for 48 hours, to deplete the endogenous Rpb1 protein, and simultaneously treated with doxycycline, to reconstitute them with either wild-type Rpb1 or Rpb1-S7A, to generate “switch-over” cells expressing exogenous wild-type Rpb1 (WT-ON) or Rpb1-S7A (S7A-ON). WT and S7A cells grown in Tet-free medium and treated with scrambled siRNA for 48 hours are referred to as WT-off and S7A-off, respectively. For gene expression and ChIP experiments, 24 hours following siRNA treatment, cells were starved overnight and subsequently stimulated with CD or FCS or left untreated. (C) Western blot showing Rpb1 (D8L4Y) and phospho-Ser7 (4E12) levels in WT-off, WT-ON, S7A-off and S7A-ON cells. Tubulin (T5162) was used as loading control.

8.3 Inhibition of phosphorylation at Ser7 of the Pol II CTD perturbs MRTF target gene activation

To examine the effect of inhibition of Ser7P on transcription at MRTF target genes, WT-ON and S7A-ON cells were stimulated with CD or FCS and pre-mRNA levels at endogenous MRTF target genes were measured by qPCR. Probes targeting the first intron of the gene were used. Baseline expression levels were assessed in untreated cells, when MRTF target genes are uninduced. The specificity for MRTF target genes was tested by examining pre-mRNA levels at the *Egr1* and *c-Fos* genes, which are not under the regulation of MRTF, but are serum-inducible TCF-SRF target genes. In addition, pre-mRNA levels at the constitutively active genes *B2m*, *Rps16*, *Pbgd* and *Hprt* were examined. Results are shown in Figure 83.

In WT-ON cells, MRTF target genes were inactive in untreated cells and induced in response to stimulation with CD (Figure 83A). In contrast, CD induction of MRTF target genes was defective in S7A-ON cells. As shown in Figure 83B, despite blocking activation of MRTF target genes, inhibition of phospho-Ser7 did not affect expression of the constitutively active genes *B2m*, *Rps16*, *Pbgd* and *Hprt* (Figure 83B). Inhibition of Ser7P did not affect serum-induced expression of the TCF-SRF target genes *c-Fos* and *Egr1*, which was comparable in WT-ON and S7A-ON cells (Figure 83C). Conversely, Ser7P inhibition blocked FCS stimulation at the MRTF target genes *Acta2* and *Vcl* (Figure 83D).

The same experiment was repeated in WT-off and S7A-off cells. As shown in Figure 84, expression levels in untreated cells or in response to CD or FCS stimulation at MRTF target genes, TCF targets or constitutively induced genes were comparable in WT-off and S7A-off cells.

Taken together, these results suggest that Ser7P of the Pol II CTD is required for productive RNA synthesis at MRTF target genes.

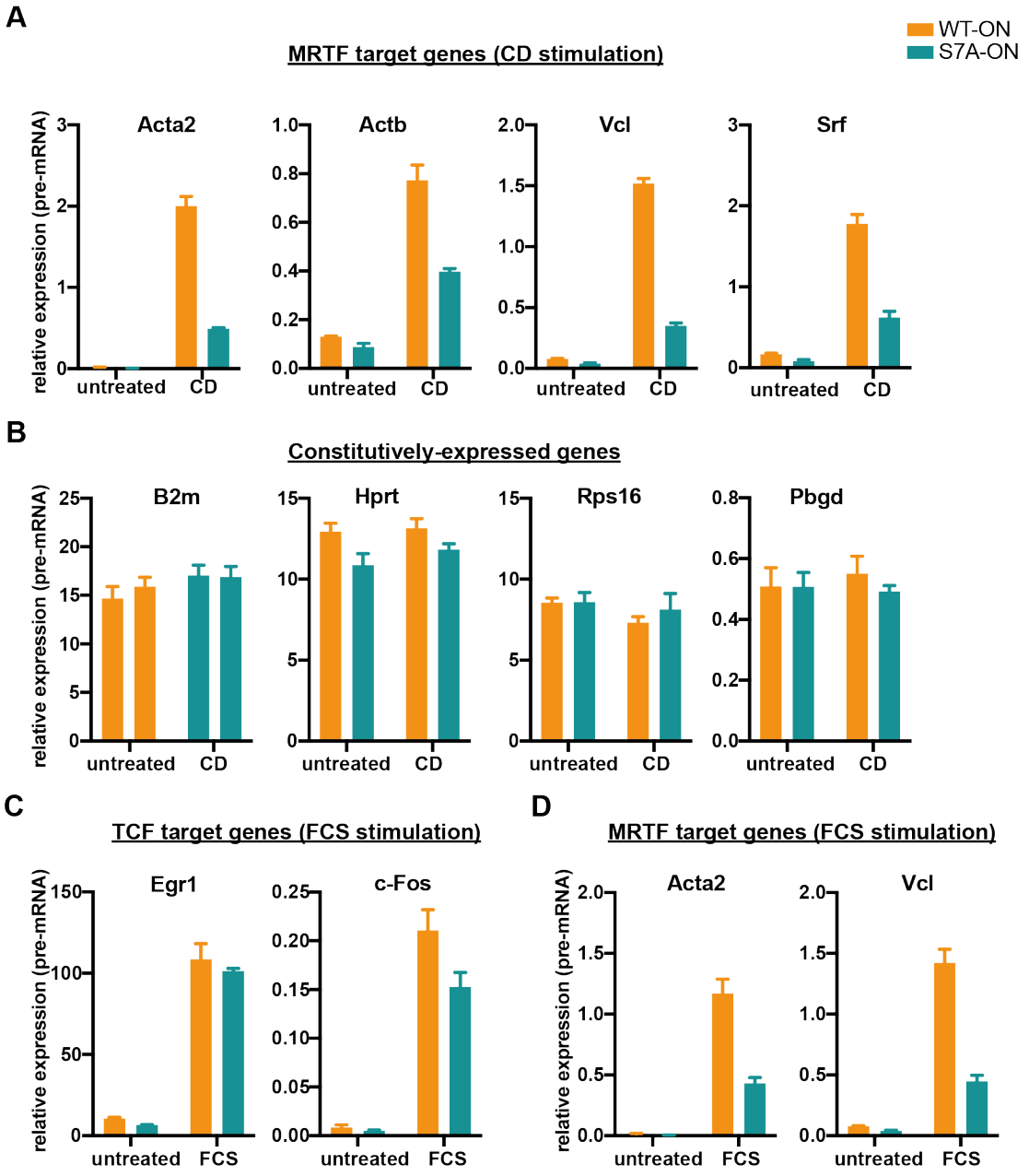

Figure 83 MRTF target gene expression in WT-ON and S7A-ON cells

Pre-mRNA accumulation in response to CD at MRTF target genes (A), constitutively active genes (B) in response to FCS stimulation at TCF target genes (C) and in response to FCS stimulation at MRTF target genes (D). Cells were serum-starved overnight and stimulated for 30 min with 3µM CD (Cytochalasin D), 15% FCS or left untreated. Signal was normalized to *Gapdh*. Data is shown as mean ± SEM and is representative of three independent experiments.

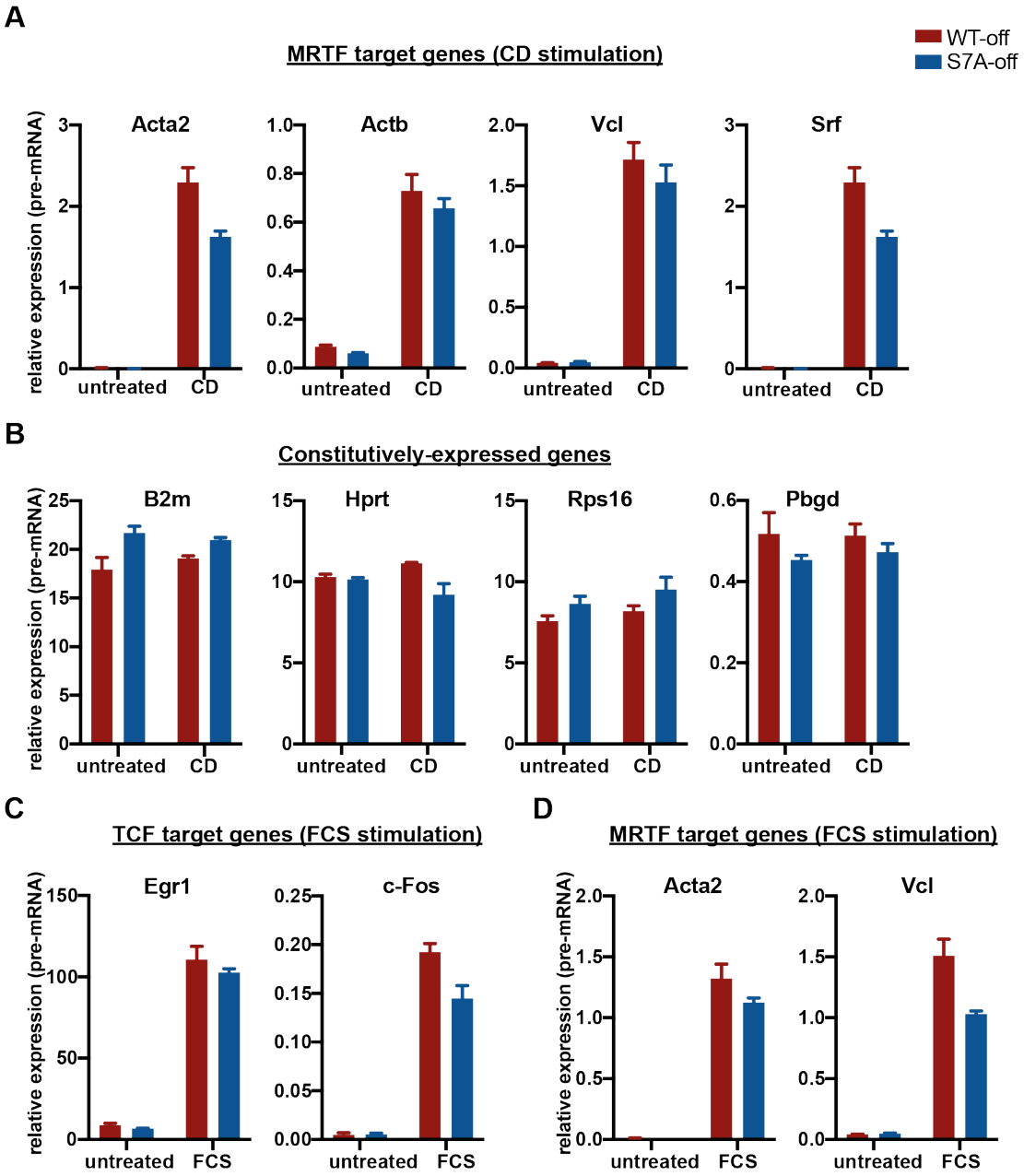

Figure 84 MRTF target gene expression in WT-off and S7A-off cells

Pre-mRNA accumulation in response to CD at MRTF target genes (A), constitutively active genes (B) in response to FCS stimulation at TCF target genes (C) and in response to FCS stimulation at MRTF target genes (D). Cells were serum-starved overnight and stimulated for 30 min with 3µM CD (Cytochalasin D), 15% FCS or left untreated. Signal was normalized to *Gapdh*. Data is shown as mean ± SEM and is representative of three independent experiments.

Next, the effect of Ser7P depletion on Pol II recruitment and CTD phosphorylation at MRTF target genes was examined by ChIP-qPCR. WT-ON and S7A-ON cells were stimulated with CD and Pol II recruitment to target genes was assessed using antibodies against the Rpb1 subunit of the Pol II (D8L4Y), to measure total Pol II, and phospho-specific antibodies targeting Ser5P (3E8), Ser7P (4E12) and Ser2P (3E10) of the Rpb1 CTD (Chapman et al., 2007). qPCR probes targeting regions along the length of the *Acta2*, *Actb* and *Vcl* genes were used. Results are shown in Figure 85.

In WT-ON cells, CD stimulation induced Pol II recruitment and phosphorylation of Ser5, Ser7 and Ser2 of the Pol II CTD. The ChIP profiles of total Pol II and the phosphorylated forms of Pol II were as in wild-type NIH3T3 cells (see Figure 70). In S7A-ON cells, Pol II ChIP levels were reduced in the TSS region, but remained comparable to those in WT-ON cells within the gene body and at the TTS region. Similar results were observed with Ser5P. As expected, Ser7P levels were reduced in S7A-ON cells. In addition, S7A-ON cells also exhibited reduced Ser2P levels at the 3’ end of genes.

These results suggest that inability to induce phosphorylation of Ser7 of the Pol II CTD results in reduced Pol II pausing at MRTF target genes. In addition, depletion of Ser7P is associated with greatly reduced phospho-Ser2 levels, a profile reminiscent of that seen in the non-productive transcriptional state. This data is consistent with phosphorylation of Ser7 preceding that of Ser2 and suggests that Ser7P might be a prerequisite for phosphorylation of Ser2 of the Pol II CTD.

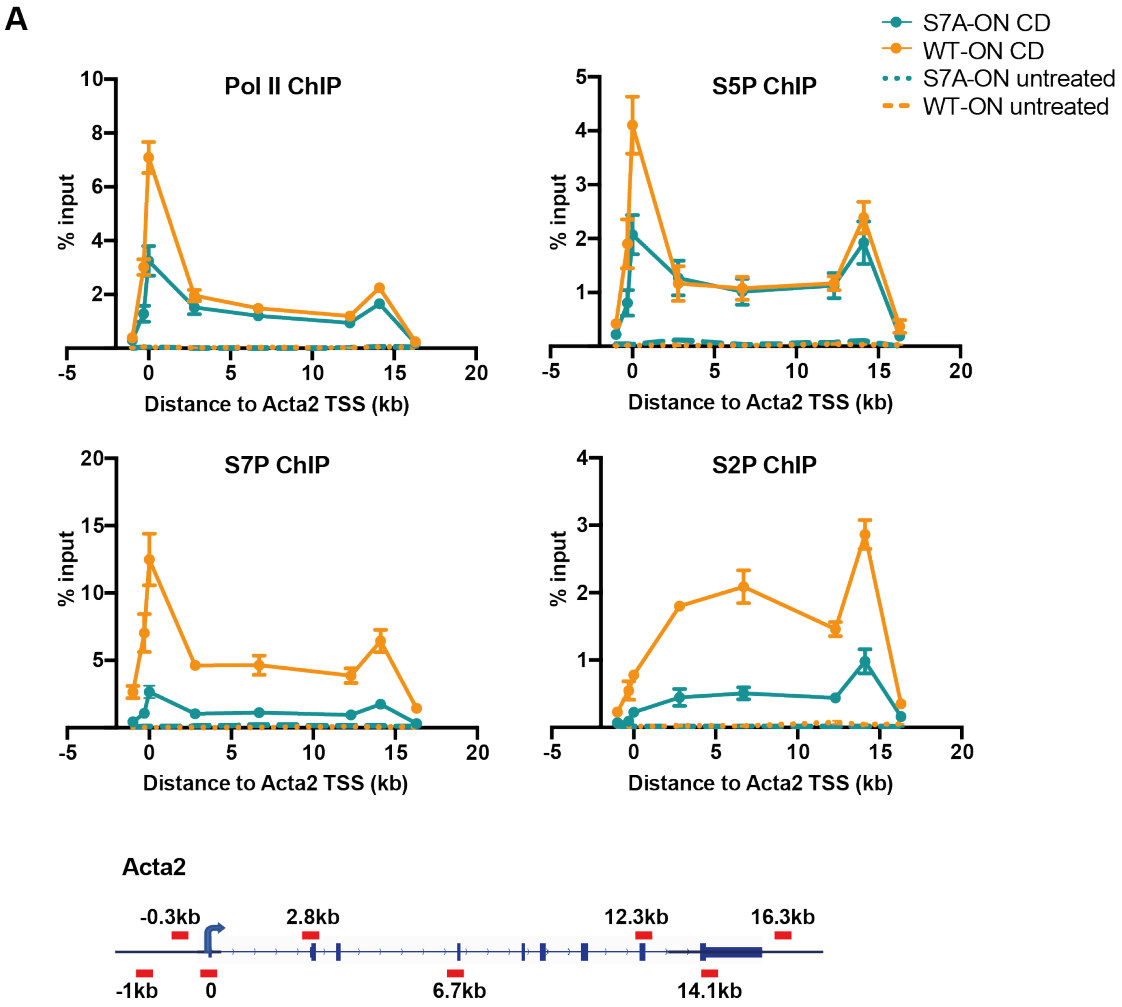
A
S7A-ON CD
WT-ON CD
S7A-ON untreated
WT-ON untreated
Pol II ChIP
S5P ChIP
S7P ChIP
S2P ChIP
% input
Distance to Acta2 TSS (kb)
Acta2
-0.3kb
2.8kb
12.3kb
16.3kb
-1kb
0
6.7kb
14.1kb

B

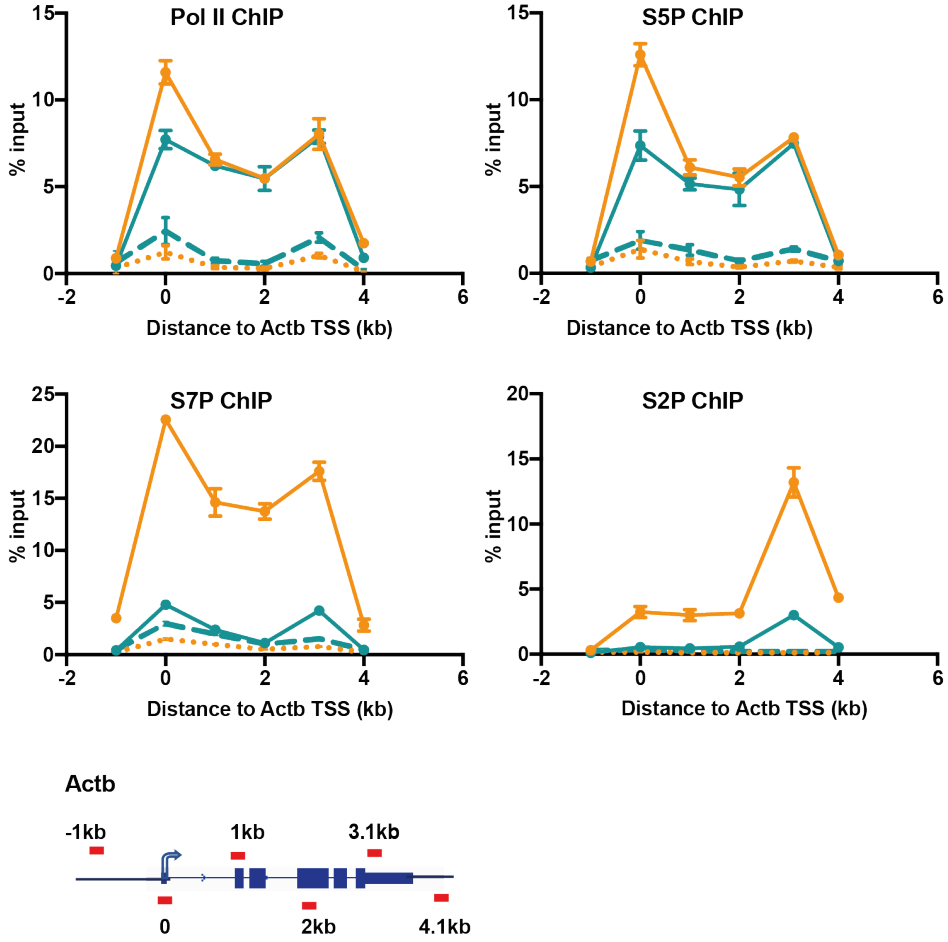
Pol II ChIP
S5P ChIP
S7P ChIP
S2P ChIP
% input
Distance to Actb TSS (kb)
Actb
-1kb
1kb
3.1kb
0
2kb
4.1kb

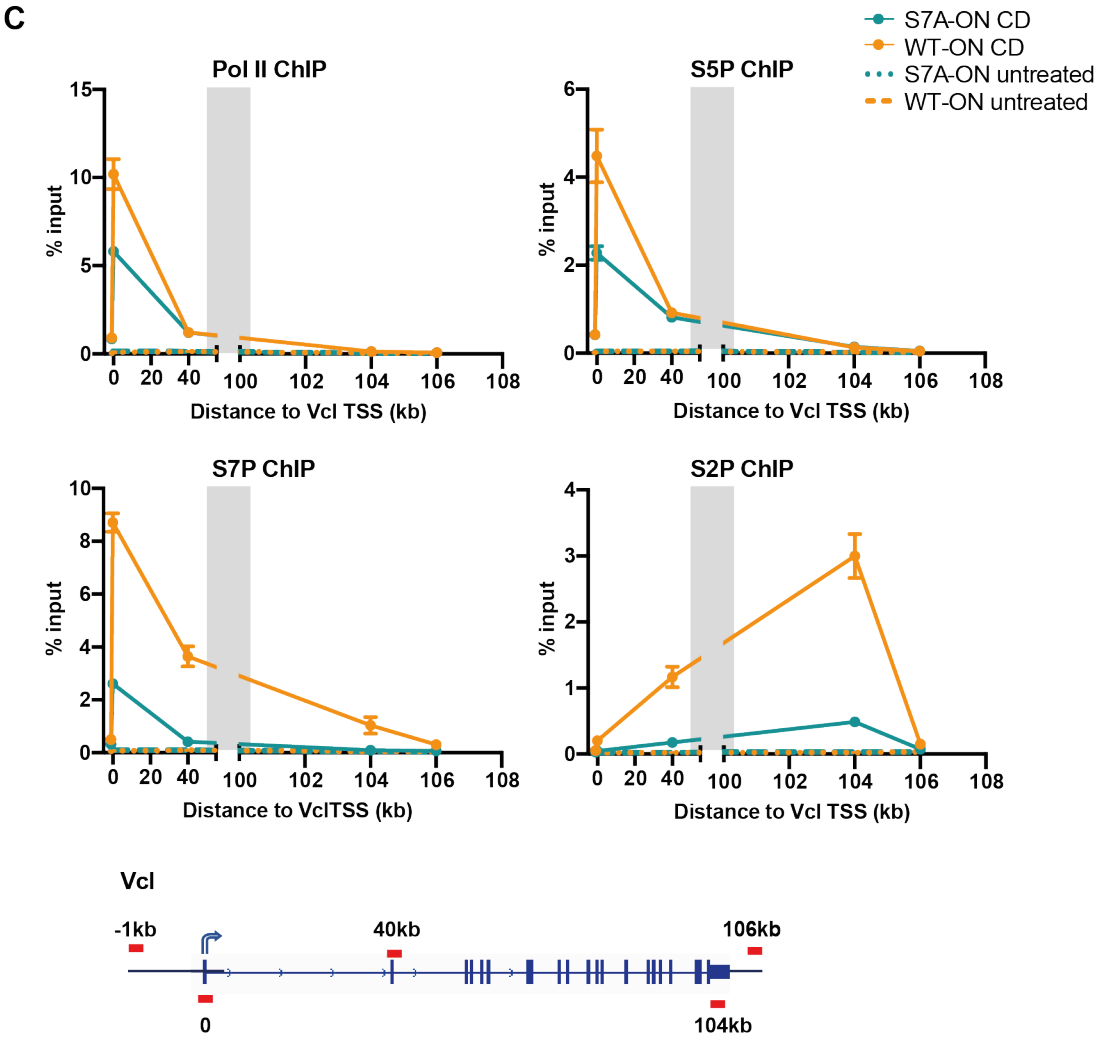

Figure 85 Ser7P inhibition alters the Pol II profile at MRTF target genes

Total RNA Polymerase (Pol II, D8L4Y), RNA Polymerase II C-terminal domain phosphorylated at Serine 5 (S5P, 3E8), Serine 7 (S7P, 4E12) or Serine 2 (S2P, 3E10) ChIP at the *Acta2* (A), *Actb* (B) and *Vcl* (C) genes in WT-ON and S7A-ON cells. Cells were serum-starved overnight and stimulated for 30 min with 3μM CD (Cytochalasin D) or left untreated. Signal was normalized to input. Data is shown as mean ± SEM and is representative of three independent experiments. The lines connecting individual points within data series are not necessarily representative of ChIP levels between data points. The location of the qPCR probes, relative to the TSS (0), is indicated by the red lines in the gene schematics.

8.4 Depletion of Mtr4 restores productive RNA synthesis at MRTF target genes in Ser7P-depleted cells

In cells expressing the Rpb1-S7A mutant, phospho-Ser7 and phospho-Ser2 levels are reduced and expression of MRTF target genes is perturbed, resembling the non-productive transcriptional state observed in LMB-treated NIH3T3 cells and $dKO^{MRTF\text{-}NLS}$ cells. Therefore, whether inactivating the nuclear exosome would restore pre-mRNA synthesis at MRTF target genes in S7A-ON cells was tested next.

To deplete Mtr4 in WT-ON and S7A-ON cells, the parental WT and S7A cells were treated with doxycycline, siRpb1 and siMtr4 for 48 hours. Subsequently cells were stimulated with CD or FCS and pre-mRNA levels at endogenous MRTF target genes were measured by qPCR using probes targeting the first intron of the gene. Baseline expression levels were assessed in untreated cells, when MRTF target genes are uninduced. Results are shown in Figure 86.

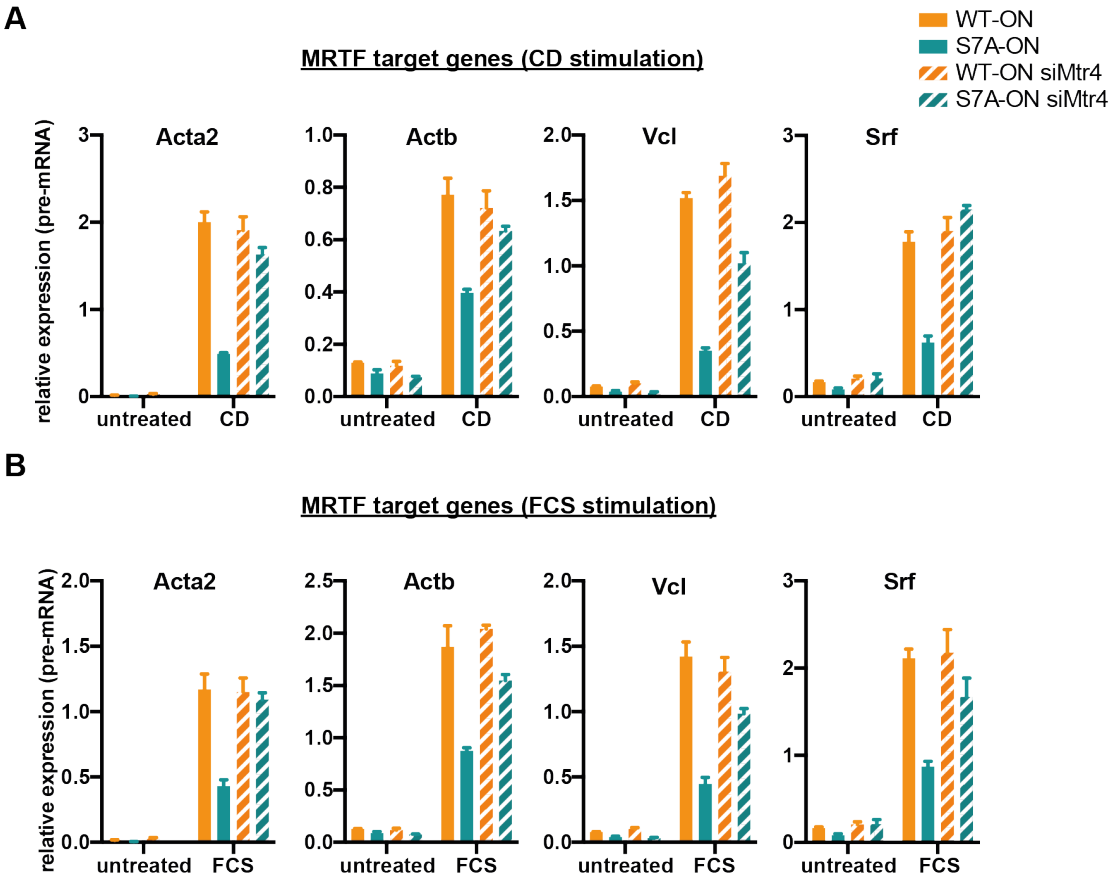

Figure 86 Mtr4 depletion restores MRTF target gene expression in S7A-ON cells

Pre-mRNA accumulation at MRTF target genes in response to CD stimulation (A) or FCS stimulation (B). Cells were treated with siMtr4 for 48 hours, serum-starved overnight and stimulated for 30 min with 3µM CD (Cytochalasin D), 15% FCS or left untreated. Signal was normalized to *Gapdh*. Data is shown as mean ± SEM and is representative of three independent experiments. Data for WT-ON and S7A-ON is from Figure 83.

In WT-ON cells, CD stimulation induced MRTF target genes, while MRTF target gene activation in response to CD was inhibited in S7A-ON cells. Mtr4 depletion restored pre-mRNA synthesis at MRTF target genes in S7A-ON cells, but did not affect expression levels in WT-ON cells (Figure 86A). Similar results were seen upon serum stimulation of MRTF-SRF target genes (Figure 86B).

To confirm that the effect of depleting Mtr4 is specific for the Rpb1-S7A mutant, the experiment was repeated in WT-off and S7A-off cells, where transcription is

controlled by the endogenous Rpb1. As shown in Figure 87, Mtr4 depletion did not affect MRTF target gene expression in cells expressing the endogenous Rpb1 protein.

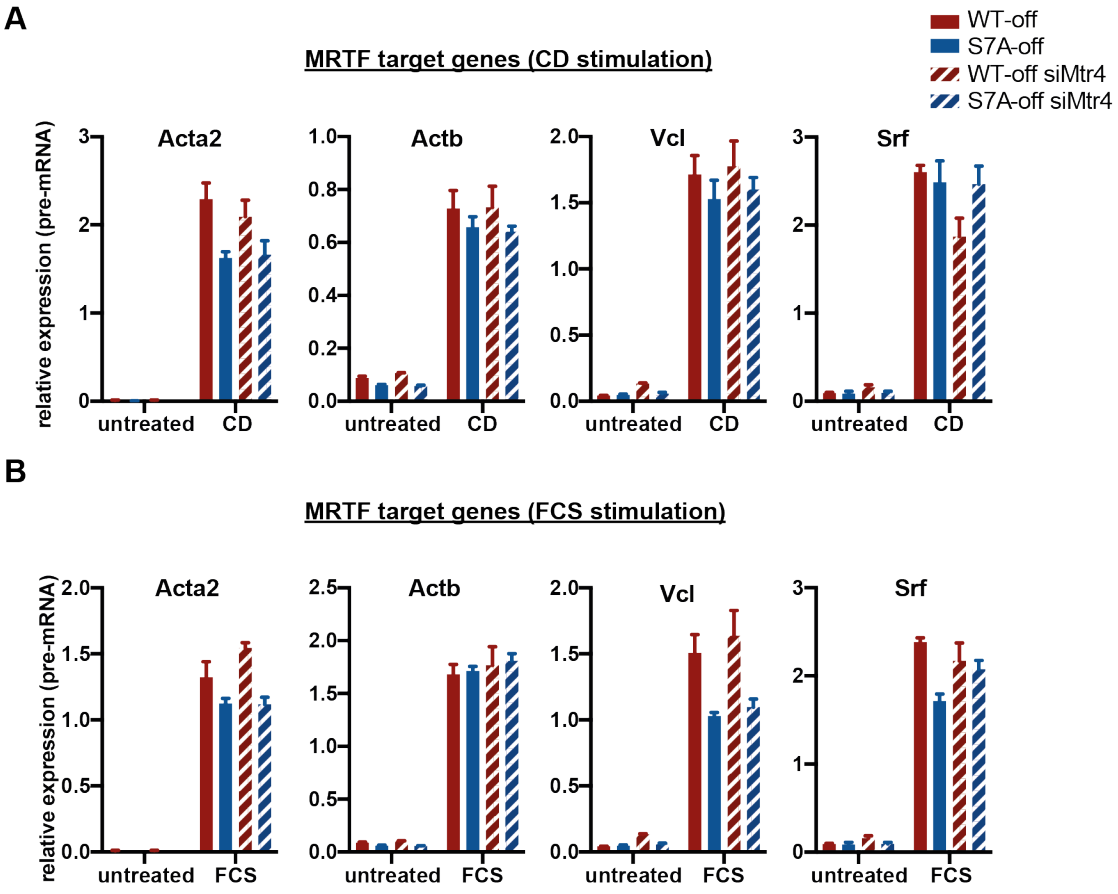

Figure 87 Mtr4 depletion does not affect MRTF target gene expression in WT-off and S7A-off cells

Pre-mRNA accumulation at MRTF target genes in response to CD stimulation (A) or FCS stimulation (B). Cells were treated with siMtr4 for 48 hours, serum-starved overnight and stimulated for 30 min with 3µM CD (Cytochalasin D), 15% FCS or left untreated. Signal was normalized to *Gapdh*. Data is shown as mean ± SEM and is representative of three independent experiments. Data for WT-off and S7A-off cells is from Figure 84.

Taken together these results show that the defective induction of MRTF target genes seen in S7A-ON cells is dependent on Mtr4. This is consistent with a model in which Ser7P protects the nascent RNA from being targeted by the nuclear exosome.

8.5 Depletion of Nrde2 does not exacerbate the transcriptional defect in Ser7P-depleted cells

As presented in Chapter 5.4, depletion of the Mtr4 negative regulator Nrde2 inhibits CD induction of MRTF target genes. Given that Rpb1-S7A exhibits an Mtr4-dependent defect in CD-induced transcription, whether Nrde2 depletion could enhance the transcriptional defect seen in S7A-ON cells was tested next.

WT-ON and S7A-ON cells were treated with siRNA for 48 hours and subsequently stimulated with CD. As before, transcription at MRTF target genes was assessed by qPCR using probes targeting the first intron of the gene. Baseline expression levels were assessed in untreated cells, when MRTF target genes are inactive. To confirm that any effect of Nrde2 depletion reflects the activity of Mtr4, the experiment was repeated in cells depleted of Mtr4. Results are presented in Figure 88.

Consistent with results presented in Chapter 5.4, in WT-ON cells, CD-induced MRTF target gene expression was inhibited by Nrde2 depletion, but not by Mtr4 depletion, and co-depletion of Mtr4 and Nrde2 restored pre-mRNA synthesis, to levels comparable to these in WT-ON cells (Figure 88A).

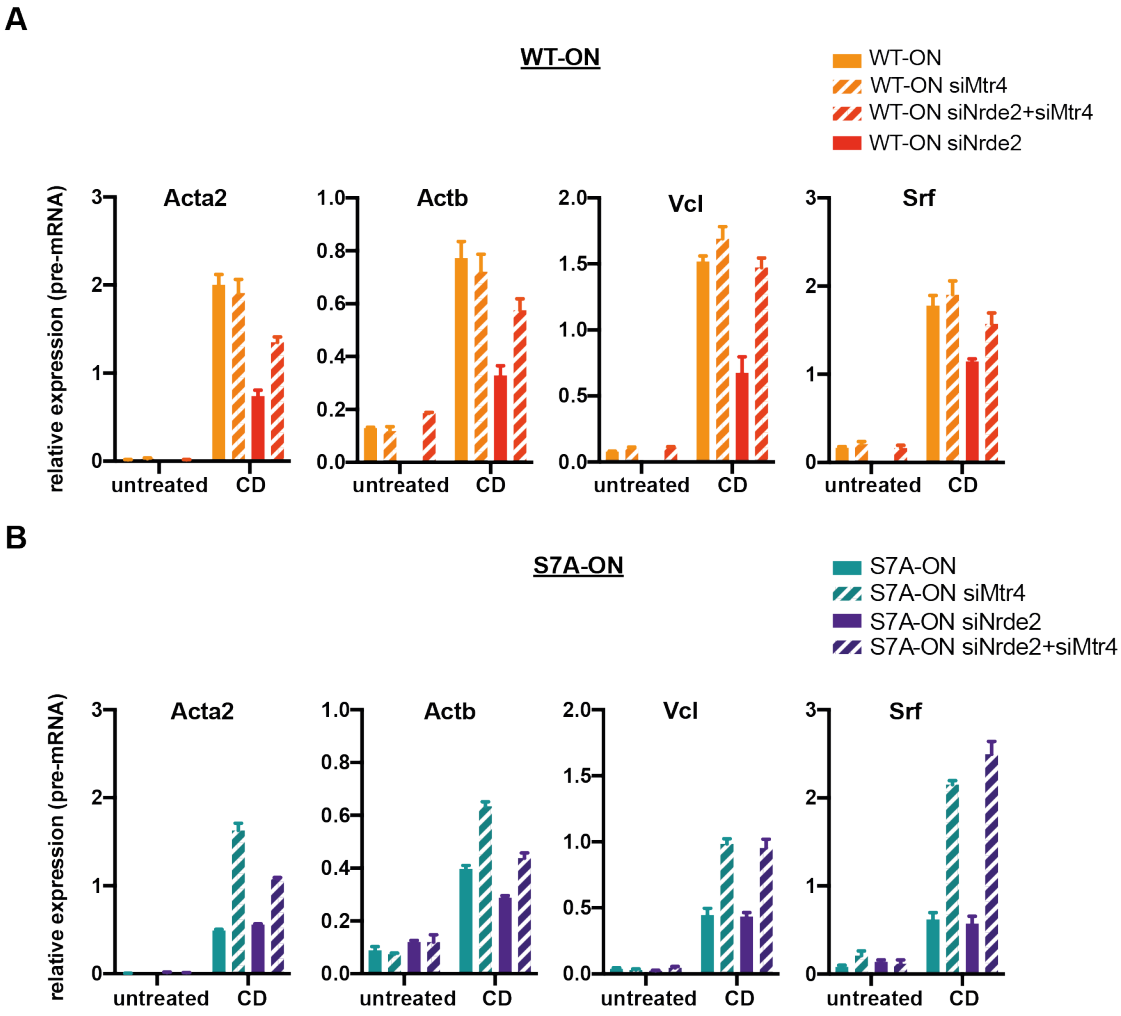

Figure 88 Nrde2 depletion does not affect MRTF target gene expression in S7A-ON cells

Cells were treated with siMtr4, siNrde2 or both for 48 hours, serum-starved overnight and stimulated for 30 min with 3µM CD (Cytochalasin D) or left untreated. Pre-mRNA was measured using qPCR probes targeting the first intron of the gene. Signal was normalized to *Gapdh*. Data is shown as mean ± SEM and is representative of three independent experiments. Data for Mtr4-depleted WT-ON and S7A-ON is from Figure 86.

In S7A-ON cells, CD-stimulation at MRTF target genes was defective and depletion of Mtr4 rescued the pre-mRNA synthesis defect. Depletion of Nrde2 alone did not affect MRTF target gene expression, whereas co-depletion of Mtr4 and Nrde2 upregulated pre-mRNA synthesis (Figure 88B).

As in wild-type NIH3T3 cells, in WT-ON cells Nrde2 depletion inhibits stimulation of MRTF target genes and its effect is dependent on Mtr4. Nrde2 depletion does not exacerbate the transcriptional defect observed in S7A-ON cells, suggesting that it is unlikely that Nrde2 and Ser7P cooperate to regulate exosome recruitment at transcripts of MRTF target genes.

Chapter 9. Discussion

The data presented in this thesis demonstrates that G-actin regulates MRTF activity in the nucleus at two levels. First, G-actin binding to MRTF interferes with ternary complex formation between SRF and MRTF on DNA and inhibits MRTF-dependent transcription. In response to G-actin depletion, MRTF is recruited to target gene promoters and induces the recruitment of the fully phosphorylated form of Pol II, resulting in productive RNA synthesis. In contrast, in high G-actin concentrations, MRTF recruitment to target promoters is impaired. Second, under resting G-actin levels, nuclear MRTF is recruited to target promoters, but at reduced levels, and it induces non-productive transcription. While Pol II is engaged in elongation, no pre-mRNA accumulates. This inhibited transcriptional state correlates with aberrant Pol II CTD phosphorylation, Mtr4 recruitment and degradation of the nascent transcripts by the nuclear exosome. Phosphorylation of Ser7 of the Pol II CTD is required to inhibit Mtr4-mediated degradation of MRTF-dependent transcripts under induced conditions.

9.1 Regulation of MRTF activity in the nucleus

In the nucleus, actin also exists in both monomeric and filamentous form. Nuclear F-actin is formed in response to extracellular stimuli and during cell adhesion and spreading and appears to play a role in maintaining nuclear structure, chromatin organization, as well as in DNA damage repair (Baarlink et al., 2017; Belin et al., 2013; Belin et al., 2015; Bohnsack et al., 2006; Caridi et al., 2018; Kiseleva et al., 2004; Ohkawa & Welch, 2018; Plessner et al., 2015; Schrank et al., 2018; Y. Wang et al., 2019; Yamazaki et al., 2020).

G-actin inhibits ternary complex formation between MRTF and SRF on DNA

Like actin assembly in the cytoplasm, serum stimulation results in a rapid and transient F-actin assembly in the nucleus. Furthermore, nuclear F-actin formation, which is sensitive to treatment with LatB, and subsequent depletion of the nuclear G-actin pool, is sufficient for MRTF activation (Baarlink et al., 2013). Consistent with this data and previous publications from the lab, CD or serum stimulation was required for gene activation by the constitutively nuclear MRTF-NLS and in LMB-

treated cells, when MRTF export from the nucleus is inhibited (Miralles et al., 2003; Vartiainen et al., 2007). In contrast, MRTF-XXX, which is unable to interact with G-actin, was constitutively active, demonstrating that disrupting the interaction between MRTF and G-actin is essential for gene activation.

Crm1 inhibition by LMB or expression of an MRTF-NLS fusion protein, which result in nuclear accumulation of MRTF, without affecting the cellular F- to G-actin ratio or the interaction between MRTF and G-actin, induced MRTF recruitment to target genes, consistent with previous work (Vartiainen et al., 2007). Under these conditions, recruitment of MRTF and SRF to target promoters was sensitive to addition of LatB, which increases G-actin concentration. In contrast, recruitment of MRTF-XXX, which is unable to interact with G-actin, was unaffected by LatB. This data demonstrates that G-actin binding to the MRTF RPEL domain interferes with ternary complex formation between MRTF and SRF on DNA. The exact mechanism by which G-actin inhibits MRTF recruitment is unclear.

Although MRTF contacts DNA in the ternary complex, it is unable to bind to DNA independently of SRF (Miralles et al., 2003; Pellegrini et al., 1995; Zaromytidou et al., 2006). One possibility is that G-actin binding physically inhibits MRTF/SRF complex formation through mediating a conformational change in the protein that occludes the B1 box, through which MRTF/SRF interaction is mediated (Miralles et al., 2003; Zaromytidou et al., 2006). This might occur either by interaction of the actin-bound RPEL domain with the B1 box or through recruitment of additional actin to the B1 box region (Figure 89A). To understand which sequences are required for this inhibition, MRTF mutant proteins lacking the entire N-terminal domain (ΔN-MRTF), with point mutations within the RPEL domain (MRTF-XXX) and B1 box mutants could be used in *in vitro* assays to study the interaction between SRF, MRTF and DNA in the presence of increasing concentrations of G-actin.

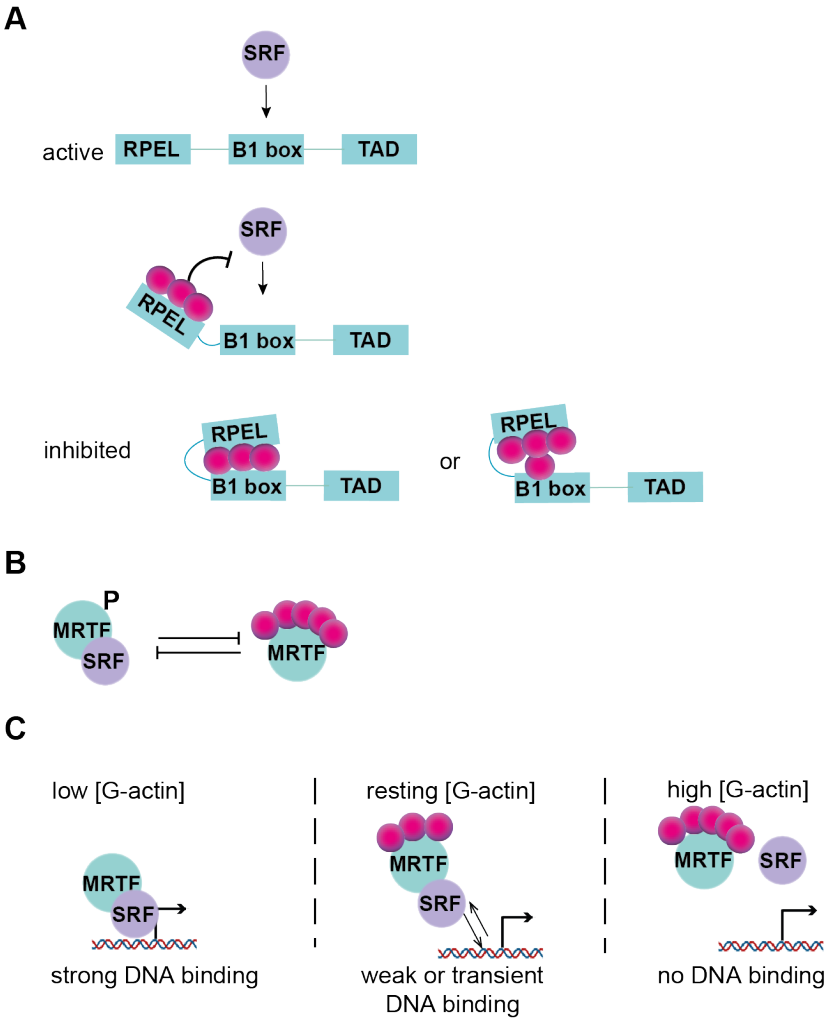

Figure 89 G-actin inhibits the interaction between MRTF and SRF on DNA

(A) G-actin binding to MRTF could inhibit its interaction with SRF directly, through interaction of the RPEL domain with the B1 box or through recruitment of additional actin to the B1 box region. (B) G-actin binding to MRTF could inhibit its interaction with SRF indirectly, by preventing MRTF phosphorylation. G-actin could inhibit the recruitment of the kinase that targets MRTF or it could occlude MRTF phosphorylation sites. (C) Reduced MRTF recruitment to targets under resting G-actin levels could reflect lower efficiency of binding, dependent on how many molecules of G-actin interact with MRTF or more transient interaction of MRTF with target promoters. Under resting G-actin levels, nuclear MRTF would form a trimeric complex with G-actin, which might bind DNA weakly. An increase in the G-actin concentration in the nucleus by treatment with LatB would abolish DNA binding completely by stimulating pentameric complex formation. On the other hand, inhibiting MRTF/G-actin interaction by CD or serum would increase the abundance of free MRTF, which would efficiently associate with DNA.

Alternatively, G-actin might perturb the interaction between MRTF and SRF indirectly, by preventing MRTF phosphorylation (Figure 89B). G-actin binding inhibits MRTF phosphorylation, which normally occurs in response to stimulation with CD or serum and is required for MRTF transcriptional activity (Panayiotou et al., 2016). G-actin might inhibit the recruitment of the kinase that targets MRTF or it could occlude MRTF phosphorylation sites.

It has been shown that phosphorylation of serine 98 of MRTF inhibits G-actin binding (Panayiotou et al., 2016). Apart from Ser98, phosphorylation at Ser231, Ser663 and Ser744 of MRTF also increase substantially in response to serum stimulation (Panayiotou et al., 2016). The role of these phospho-marks on MRTF recruitment to target gene promoters and its ability to activate transcription could be tested by reconstitution of dKO MEFs with S98A, S231A, S663A and S744A MRTF mutants.

Under resting G-actin levels, nuclear MRTF is recruited to target genes at reduced levels

Even though MRTF and SRF were recruited to target gene promoters under resting G-actin levels, their DNA binding was reduced, relative to this in cells stimulated with CD or serum, which deplete free G-actin. One possibility is that any actin binding to MRTF blocks its interaction with SRF and the interaction between MRTF and DNA or G-actin is mutually exclusive. In this case, MRTF recruitment to DNA under resting G-actin levels would reflect the lower effective concentration of free MRTF. Alternatively, reduced recruitment of MRTF to DNA could reflect lower efficiency of binding, dependent on how many molecules of G-actin interact with MRTF (Figure 89C).

The MRTF/G-actin complex exists as a trimer, where each RPEL motif is bound by one actin molecule, or as a pentamer, where in addition to the three RPELs, each of the two spacer regions in between are bound by one actin molecule. It has been proposed that the trimer complex is readily assembled under resting conditions, while the recruitment of additional actin molecules is sensitive to cellular actin concentration (Mouilleron et al., 2008; Mouilleron et al., 2011). According to this

view, the trimer complex is competent for nuclear import, whereas the pentameric complex, in which both of MRTF's NLS elements are occluded, is not. The ability of the different MRTF-actin complexes to interact with SRF and DNA has not been evaluated directly.

Thus, it is conceivable that under resting G-actin levels, nuclear MRTF would form a trimeric complex with G-actin, which might bind DNA weakly. An increase in the G-actin concentration in the nucleus by treatment with LatB would abolish DNA binding completely by stimulating pentameric complex formation. On the other hand, inhibiting MRTF/G-actin interaction by CD or serum would increase the abundance of free MRTF, which would efficiently associate with DNA. Whether actin is at all found with MRTF at target promoters under resting conditions could be studied by ChIP.

Does LMB induce an unstable MRTF-SRF-DNA complex?

ChIP is a global method of studying transcription factor recruitment at target genes, averaging over whole populations of cells. An alternative view of the reduced ChIP signal is that rather than representing weaker binding of the trimeric complex, it reflects a more transient interaction between MRTF and its binding sites. MRTF/G-actin interaction and its effect on MRTF phosphorylation and SRF binding might ultimately impact on the residence time of MRTF at target gene promoters.

In the nucleus many transcription factors exist in three different states, a diffusing state, as transiently bound and as stably bound. Longer residence time of the transcription factor at the target promoter reflects a more stable interaction and correlates with productive output (Gorski et al., 2006; Hager et al., 2009; Misteli, 2001). Slower transcription factor dynamics at a specific promoter have been shown to correlate with more mRNA synthesis for the heat-shock transcription factor (HSF) (Yao et al., 2006), the glucocorticoid receptor and the mineralocorticoid receptor (Stavreva et al., 2004) (Groeneweg et al., 2014) , STAT1 (Tietjen et al., 2010), Sox2 (White et al., 2016), p53 (Morisaki et al., 2014) and SRF (Hipp et al., 2019).

Serum stimulation increases not only the fraction of SRF bound to chromatin, but also the residence time of SRF at promoters, in a LatB-sensitive manner, in both fibroblasts and neuronal cells (Hipp et al., 2019). To determine whether LMB treatment impacts on MRTF residence time at target promoters, an MRTF HaloTag could be used to study MRTF dynamics in response to stimulation. If the decreased ChIP signal in LMB-treated cells reflects a more transient interaction of MRTF with target promoters, MRTF should have short residence time at targets in response to LMB. Addition of LatB, which abolishes MRTF binding by ChIP, should further decrease its residence time, while subsequent re-stimulation of LMB-treated cells with CD should increase MRTF residence time, to reflect stable binding of MRTF to target promoters.

Biological significance of regulated MRTF-SRF interaction

Many transcription factors which regulate inducible genes, such as MRTF, p53, NF-kB and steroid receptors, are controlled via regulating their concentration in the nucleus (Hager et al., 2009; Levine et al., 2013; Stavreva et al., 2004). However, the cellular environment is noisy and stochastic signalling could inadvertently lead to activation of the system which could then have deleterious effects (Aoki et al., 2013; Elowitz et al., 2002; Fang et al., 2013; Hsu et al., 2012; Ozbudak et al., 2002). Hence, additional layers of regulation are needed to modulate transcription factor activity while in the nucleus and discriminate signal from noise.

Residence time at promoters is an example of such a mechanism. In the case of MRTF, since it constantly shuttles between the nucleus and the cytoplasm, it could transiently interact with genomic loci while in the nucleus, even though the system has not been activated. In order to avoid the deleterious effect of overexpressing its target genes, such short-lived interactions would be insufficient to result in engaging a transcriptionally competent form of Pol II.

Under resting G-actin levels, MRTF interacts with actin while in the nucleus (Vartiainen et al., 2007). This interaction results in less DNA binding, which might reflect either decreased residence time at promoters or weaker binding of the actin-bound complex, and is insufficient for target gene activation.

9.2 Nuclear MRTF induces non-productive transcription

RNAseq and TTseq experiments were performed to study the effect of nuclear MRTF on transcription genome-wide, in response to acute stimulation with CD or LMB or chronic stimulation as in dKO$^{MRTF\text{-}NLS}$ cells, when MRTF is constitutively nuclear.

The transcriptional response to CD

Genes significantly upregulated in response to CD by RNAseq and TTseq in NIH3T3 cells were enriched in serum-inducible genes, whose expression is sensitive to an increase in G-actin concentration by LatB, physically associated with SRF and functionally related to MRTF-SRF target genes. These results are consistent with MRTF being the only transcription factor known to be directly activated by CD.

As in NIH3T3 cells, in dKO^{MRTF} and dKO$^{MRTF\text{-}NLS}$ MEF cells CD stimulation induced genes functionally related to MRTF-SRF targets and associated with SRF binding sites. Nevertheless, there was little overlap between these and CD-induced genes in NIH3T3 cells. While this could represent cell-type specific effects, it might also reflect differences arising during the reconstitution of the MRTF-A/B null MEF cells.

The non-productive transcriptional state at MRTF target genes

Under resting G-actin levels, nuclear MRTF was recruited to target gene promoters but did not activate gene expression. There are three potential explanations for this. First, it might be that in the absence of G-actin depletion, MRTF fails to recruit Pol II. Alternatively, this could potentially be due to increased stalling of Pol II at the TSS or co-transcriptional degradation of the nascent transcript.

In NIH3T3 cells, even though no transcriptional changes were detected in response to LMB by RNAseq, more than 90% CD-controlled genes were activated in LMB-treated cells, as assessed by TTseq. TTseq data demonstrated that in response to LMB, Pol II was recruited to MRTF target genes and engaged in elongation. The

TTseq read profiles at MRTF-SRF target genes in response to CD and LMB were very similar. No apparent differences in Pol II processivity and elongation speed or termination were detected.

Genome-wide experiments in dKO$^{MRTF\text{-}NLS}$ MEF cells corroborated these findings, showing that they do not reflect pleiotropic effects of the LMB treatment. As in LMB-treated NIH3T3 cells, in dKO$^{MRTF\text{-}NLS}$ cells, even though no gene activation was detected in the absence of G-actin depletion by RNAseq, CD-regulated genes were induced, as assessed by TTseq. Under resting G-actin levels, Pol II was recruited and engaged in elongation. Gene expression was sensitive to treatement with LatB and subsequent increase in G-actin concentration, indicating this effect is MRTF-dependent.

These results are consistent with a model in which nascent transcripts of MRTF target genes are co-transcriptionally degraded in the non-productive transcriptional state.

9.3 Mtr4 regulates MRTF target gene expression

Inactivation of the NEXT and CBCA complexes restores productive transcription at MRTF target genes

A small-scale RNAi screen identified the RNA helicase Mtr4, as well components of the core nuclear exosome and the NEXT and the CBCA complexes as factors whose depletion can restore productive RNA synthesis in the LMB-induced non-productive transcriptional state. Their depletion also rescued productive transcription under resting conditions in dKO$^{MRTF\text{-}NLS}$ cells.

The RNA exosome consists of a barrel-shaped core of nine subunits and the catalytically active subunit Dis3 (Greimann & Lima, 2008; Lebreton et al., 2008; Schaeffer et al., 2009). To achieve its function, the exosome associates with a variety of co-factors, including the Mtr4 RNA helicase, which is responsible for the threading of the RNA into the exosome (Gerlach et al., 2018; Weick et al., 2018). Mtr4 is part of three nuclear exosome adapter complexes: TRAMP, which is

restricted to the nucleolus, and the nuclear PAXT (Pabpn1, Zfc3h1, Mtr4) and NEXT (Rmb7, Zcchc8, Mtr4) complexes.

Exosomal degradation is mediated in a 3'->5' direction, following cleavage of the transcript by the CPA or the Integrator complex (Kamieniarz-Gdula & Proudfoot, 2019). All exosome adapter complexes are recruited to RNA through the cap-binding complex (CBC) (Andersen et al., 2013; Falk et al., 2016; Giacometti et al., 2017; Hrossova et al., 2015; Meola et al., 2016; Wu et al., 2020). The CBC interacts with the Ars2 adapter protein, forming the CBCA complex (Giacometti et al., 2017; Gruber et al., 2009; Schulze et al., 2018). Subsequently, the CBCA forms higher order complexes with distinct RNA processing factors (Schulze et al., 2018). Recruitment of Zc3h18 to the CBCA marks the transcript for degradation and it is involved in both NEXT and PAXT complex recruitment (Andersen et al., 2013; Falk et al., 2016; Meola et al., 2016).

In addition to rescuing pre-mRNA synthesis in the inhibited transcriptional state at MRTF targets, depletion of Zc3h18 also upregulated the expression of TCF target genes and MRTF targets under induced conditions. This might be due to its more general role in RNA decay. Conversely, CBCA inactivation also attenuated the response to CD stimulation, likely as a result of exposing the 5' cap to de-capping enzymes and 5' exonucleases. Depletion of Zcchc8 and Rmb7 also negatively impacted on CD-induction at some genes. This is perhaps because apart from their role in NEXT-mediated RNA decay, they are also involved in pre-mRNA splicing. The interaction of Rmb7 with components of the spliceosome and the NEXT complex is mutually exclusive (Falk et al., 2016).

Is the NEXT or the PAXT complex involved in MRTF target gene regulation?

Out of the factors tested, Mtr4 showed the strongest effect on MRTF-dependent transcription in the inhibited state, specifically. This could be due to technical issues, such as knock-down efficiency or protein stability, or reflect the involvement of multiple exosome complexes that share Mtr4.

The NEXT complex targets immature RNA such as PROMPTs and eRNAs, while the PAXT complex is recruited to polyadenylated RNA (Meola et al., 2016; Silla et al., 2020; Wu et al., 2020). The preference of PAXT for mature transcripts is consistent with Pabpn1 being a canonical poly(A) binding protein (Banerjee et al., 2013). On the other hand, Rmb7 binds RNA in a promiscuous manner, with some preference for U-rich pyrimidine stretches (Lubas et al., 2015; Vanácová et al., 2005). It is found in association with newly synthesised RNA is general (Andersen et al., 2013; Andersson et al., 2014; Lubas et al., 2015) and preferentially bound to introns (Giacometti et al., 2017; Lubas et al., 2015).

Data presented in Chapter 5.1 suggests that the NEXT and not the PAXT complex is involved in regulating transcription in the LMB-induced non-productive state. First, depletion of Pabpn1 and Zfc3h1 of PAXT did not upregulate pre-mRNA levels at MRTF target genes in response to LMB. Furthermore, simultaneous depletion of the RNA binding proteins Rmb7 and Pabpn1 or the adapter proteins Zcchc8 and Zfc3h1 did not exacerbate the effect of individual depletion of Zcchc8 or Rmb7 of NEXT.

However, interpreting these results is difficult because of the potential involvement of multiple complexes which share Mtr4. The essential functions of exosome components make knock-downs difficult. Furthermore, long siRNA treatments could trigger compensatory mechanisms. Since generating knockouts is not possible, an auxin-based degron system would be useful to study the role of each of these exosome components in regulating RNA turn-over and defining their substrates. RNA IPs with PAXT- and NEXT-specific components could determine which complex is associated with transcripts of MRTF target genes in the non-productive transcriptional state.

Mtr4 is recruited to transcripts of MRTF target genes

Mtr4 depletion did not affect Pol II recruitment or CTD phosphorylation at MRTF target genes, indicating that Mtr4 functions downstream of Pol II, consistent with previous publications (Fan et al., 2017). Furthermore, Mtr4 directly associated with MRTF-dependent transcripts in LMB-treated cells, specifically, demonstrating a

direct effect on RNA turn-over. Others have also observed that apart from its well characterized role in regulating PROMPTs and eRNAs, Mtr4 controls the expression of protein-coding genes (Fan et al., 2017; Ogami et al., 2017; Silla et al., 2018; J. Wang et al., 2019; Yu et al., 2020).

In addition to upregulating pre-mRNA levels, Mtr4 depletion also caused an increase in α-actin and ß-actin messenger RNA and protein levels. This is in line with increased expression of full-length mature RNAs upon exosome inactivation and Mtr4 depletion promoting accumulation of mature RNA in the cytoplasm and its association with polysomes (Ogami et al., 2017; Silla et al., 2018).

Depletion of Mtr4 rescues the defect in the non-productive transcriptional state

To examine the effect of Mtr4 depletion genome-wide, RNAseq was performed. At CD-inducible genes, Mtr4-depetion restored productive RNA synthesis in response to LMB, with a magnitude of induction comparable to that observed by TTseq. In addition, a set of 455 LMB-induced Mtr4-controlled genes was identified, without pre-selecting for CD-inducibility. These were enriched in CD- and FCS-inducible genes, sensitive to an increase in G-actin concentration by LatB, physically associated with SRF and functionally related to MRTF-SRF target genes, strongly suggesting they are MRTF regulated. These results are consistent with a model in which in the non-productive transcriptional state MRTF-dependent transcripts are targeted for exosomal degradation by Mtr4.

In dKO$^{MRTF\text{-}NLS}$ cells, following Mtr4 depletion, no gene expression changes in response to CD or LatB were detected by RNAseq. The prolonged siRNA treatment in combination with the chronic stimulation by the constitutively nuclear MRTF-NLS fusion might lead to elevated basal transcription and decreased sensitivity to signal. Therefore, we attempted to identify genes whose expression under resting conditions was sensitive to LatB, as an indication of MRTF activity, and tested whether these are also induced in the absence of stimulation by TTseq.

Approximately 80% of the 67 genes which were active under resting conditions and sensitive to LatB treatment in Mtr4-depleted dKO$^{MRTF\text{-}NLS}$ cells were also active in resting dKO$^{MRTF\text{-}NLS}$ cells as assessed by TTseq but not detectably upregulated as assessed by RNAseq. This gene set was enriched in genes associated with SRF binding sites and FCS-inducible genes, consistent with regulation by MRTF.

The nuclear MRTF in dKO$^{MRTF\text{-}NLS}$ cells differs from LMB-induced nuclear MRTF, in that the dKO$^{MRTF\text{-}NLS}$ cells are subjected to chronic stimulation, rather than an acute stimulus like the LMB treatment. The chronic state of the dKO$^{MRTF\text{-}NLS}$ cells in combination with the prolonged siRNA treatment impeded the genome-wide analysis of transcriptional changes in Mtr4-depleted cells. Nevertheless, data on the small MRTF-NLS induced Mtr4-controlled gene set and qPCR data on bona-fide MRTF-SRF target genes is consistent with Mtr4 targeting MRTF-dependent transcripts for degradation under uninduced conditions.

Mtr4 regulates DNA repair and cell cycle genes

In NIH3T3 cells under resting conditions Mtr4 depletion alone caused the upregulation of genes associated with cell cycle control and DNA repair. Mtr4 and its negative regulator Nrde2 have been implicated in the response to DNA damage through resolving DNA-RNA hybrids and promoting double-strand break repair (Blasius et al., 2014; Domingo-Prim et al., 2019; Lim et al., 2017; Puno & Lima, 2018; Richard et al., 2018). Data presented in Chapter 5.2 suggests that they might also be involved in the transcriptional regulation of factors involved in the DNA damage response. That Mtr4 depletion upregulated genes involved in cell cycle control is in line with previous publications (Yu et al., 2020).

How is the exosome recruited to its substrates?

How different exosome complexes recognize specific sets of RNA targets remains unclear. It has been proposed that exosome complexes have specificity for a particular structure or sequence within RNAs (Torchet et al., 2002). However, given the wide variety of exosome substrates, a requirement for common structural or sequence features seems unlikely.

Alternatively, RNAs could be recognized based on their functionality. The role of the nuclear exosome in regulating PROMPTs, eRNAs and lincRNAs, aberrantly processed snRNA, snoRNA and histone RNA, as well as CUTs in yeast, has been well-characterized (Giacometti et al., 2017; Lubas et al., 2015; Lubas et al., 2011). Nevertheless, in addition to regulating the expression of non-coding transcripts, exosome complexes are also found at protein-coding genes (Iasillo et al., 2017; Lloret-Llinares et al., 2018; Silla et al., 2018; Wu et al., 2020) and have been found to interact with the elongating Pol II in Drosophila (Andrulis et al., 2002).

Several lines of evidence suggest that whether an RNA molecule is an exosome target is determined by kinetic competition between maturation and degradation processes. The RNA processing factors DROSHA, PHAX, FLASH and Zc3h18 all compete for binding to the CBCA (Giacometti et al., 2017; Gruber et al., 2012; Gruber et al., 2009; Hallais et al., 2013; Schulze & Cusack, 2017; Schulze et al., 2018). Furthermore, the TRAMP, PAXT and NEXT complexes bind to Zc3h18 in a mutually exclusive manner (Giacometti et al., 2017; Meola et al., 2016; Schulze et al., 2018; Silla et al., 2018). Dynamic exchange of RNA processing complexes at the CBC further supports the competition model. While the CBC is stably associated to RNA with the interaction lasting for minutes, recruitment of Zc3h18 and PAXT is very transient, lasting only several seconds (Giacometti et al., 2017).

In addition to exosome complexes, the RNA export machinery is also recruited through the CBCA and competes with the exosome for binding to RNA (Figure 90). Mtr4 and ALYREF are recruited to CBCA in a mutually exclusive manner (Fan et al., 2017). ALYREF is approximately five times more abundant than Mtr4 and it has been proposed that its high concentration is important to prevent promiscuous recruitment of Mtr4 (Fan et al., 2017). On the other hand, ALYREF recruitment to CBCA is stabilized by the recruitment of additional TREX components, efficient splicing and polyadenylation, ensuring appropriate sorting of the RNA substrate for export or degradation (Chi et al., 2013; Luo et al., 2001). Consistently, in RNA export mutants RNAs are targeted for degradation (Fan et al., 2017; Gudipati et al., 2012; Hilleren et al., 2001; Jensen et al., 2001; Libri et al., 2002) and pre-mRNAs

with splicing and polyadenylation defects are also exosome substrates (Bousquet-Antonelli et al., 2000; Milligan et al., 2005)

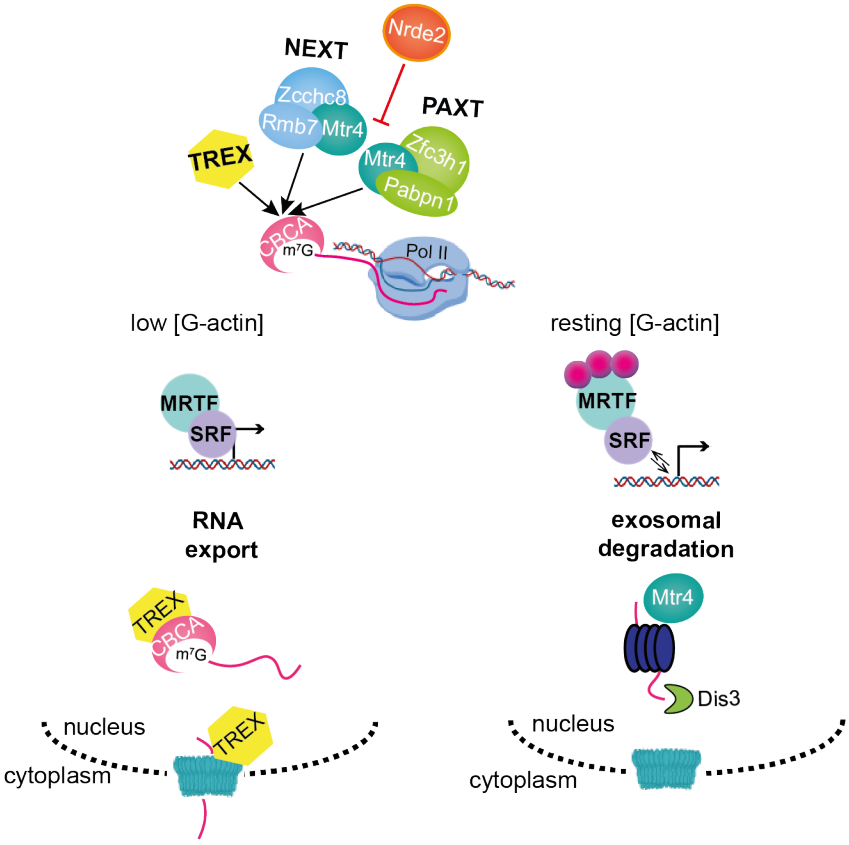

Figure 90 Kinetic competition between the exosome and the export machinery

The TREX RNA export complex and the NEXT and PAXT exosome complexes compete for binding to CBCA. Their recruitment is influenced by additional factors- Nrde2 negatively regulates Mtr4 by preventing its association with transcripts and TREX recruitment is dependent on efficient splicing and polyadenylation. It is conceivable that transcripts unable to efficiently recruit the TREX complex associate with Mtr4 and are degraded by the nuclear exosome. Signal-induced MRTF favours TREX recruitment and nuclear export of transcripts whereas the non-productive transcriptional state at MRTF targets correlates with Mtr4 recruitment and degradation of the nascent transcript by the nuclear exosome.

Consistent with a model of kinetic competition between the exosome and the export machinery, depletion of Nrde2 could potentiate Mtr4 activity on MRTF-dependent transcripts, even under induced conditions, when normally Mtr4 is only weakly associated. This result suggests that Mtr4 association with MRTF target transcripts occurs as part of the normal initiation process, not just in the inhibited state. Nevertheless, Nrde2 depletion did not affect the expression of TCF target genes and control genes, suggesting that regulation by Mtr4 might not be a general feature of Pol II regulated protein-coding genes.

Taken together, these observations suggest that the inhibited transcriptional state reflects an imbalance in the competition between the RNA export machinery and the exosome for the nascent transcripts of MRTF target genes.

9.4 Pol II CTD phosphorylation and transcription at MRTF target genes

The inhibited transcriptional state at MRTF target genes correlates with aberrant Pol II CTD phosphorylation

In response to stimulation, MRTF induced the recruitment of the fully phosphorylated form of Pol II to its target genes, resulting in productive transcription. In contrast, in the inhibited transcriptional state the Pol II CTD lacked phospho-Ser2 and only low levels of Ser5P and Ser7P were detected at MRTF target genes. LMB did not affect the phosphorylation status of the Pol II CTD globally and the defective phosphorylation of the Pol II CTD was also observed in $dKO^{MRTF\text{-}NLS}$ cells, demonstrating that this phenotype is MRTF-dependent.

Subpopulations of Pol II which is differentially phosphorylated have previously been described in the literature. At Toll-like receptor-inducible genes, in the absence of an activating signal, Pol II phosphorylated at Ser5 but not at Ser2 of its CTD is associated with short-lived full-length transcripts, albeit at reduced levels. Stimulation causes phosphorylation of Ser2 of the Pol II CTD and increased levels of mature full-length transcripts (Hargreaves et al., 2009). Pol II phosphorylated at Ser5 but lacking Ser2P has been observed at PRC repressed genes (Brookes et

al., 2012), as well during embryo development (Bellier et al., 1997; Palancade et al., 2001). Generally, high Ser5P to Ser2P ratio correlates with reduced transcription genome-wide (Odawara et al., 2011).

Chromatin remodeling at MRTF target genes is not impaired in the inhibited state

Despite the aberrant phosphorylation of the Pol II CTD, chromatin remodeling at MRTF target genes did not appear to be defective in the non-productive transcriptional state. Presence of H3K4me3 and H3K27Ac at TSSs of MRTF target genes is in line with MRTF binding and Pol II recruitment. In addition, consistent with Pol II elongation, histone marks typically found within the body of actively transcribed genes, including H3K36me3 and H3K79me3, were upregulated at MRTF target genes in response to LMB.

Although chromatin de-condensation within the gene body is thought to be dependent on Ser2P (Kizer et al., 2005; Li et al., 2003; Xiao et al., 2003), others have also observed that Pol II lacking Ser2P is engaged in elongation (Ahn et al., 2004; Blazek et al., 2011; Liang et al., 2015; Zhang et al., 2016). It appears that the necessity for Ser2P might vary between different genes. Genes with stably paused Pol II have more accessible chromatin structure (Gilchrist et al., 2010; Gilchrist et al., 2012; Gilchrist et al., 2008; Muse et al., 2007; Zeitlinger et al., 2007) and chromatin marks associated with active genes are co-dependent (Dover et al., 2002; Lee et al., 2007; Ng, Ciccone, et al., 2003; Sun & Allis, 2002), suggesting that early open-chromatin marks might contribute to the recruitment of additional chromatin remodelers.

Pol II pause-release into elongation is not defective in the inhibited transcriptional state

Pol II enters the pre-initiation complex in an unphosphorylated form and its transition into initiation is dependent on CDK7-mediated phosphorylation of Ser5 of the Pol II CTD (Hengartner et al., 1998; Lu et al., 1992). The Pol II pauses 20-120 nucleotides downstream of the TSS (Plet et al., 1995; Schwartz et al., 2003). The paused Pol II is bound by NELF and DSIF, which function cooperatively to inhibit

Pol II elongation (Muse et al., 2007). In addition to Ser5, CDK7 also phosphorylates Ser7 of the Pol II CTD and Ser7P has been proposed to promote Pol II promoter-proximal pausing (Glover-Cutter et al., 2009).

The transition of the paused Pol II into elongation is mediated by CDK9, which phosphorylates Ser2 of the Pol II CTD, Spt5 of DSIF and NELF. The phosphorylated NELF dissociates from the Pol II, whereas phospho-Spt5 functions as a positive elongation factor associated with the elongating Pol II (Fujinaga et al., 2004; Ping & Rana, 2001; Yamada et al., 2006).

NELF, DSIF and CDK9 were recruited in LMB-treated cells, suggesting pause-release into elongation is not impaired in LMB-treated cells. Furthermore, Spt5, which is known to regulate Pol II transcription rate (Baluapuri et al., 2019; Cortazar et al., 2019), was found associated with the elongating Pol II. This is in line with TTseq data, which did not indicate pre-mature termination or reduced Pol II processivity in the non-productive transcriptional state.

The inhibited transcriptional state does not reflect defective activity of CDK7 or CDK9

In an attempt to recapitulate the non-productive transcriptional state observed in LMB-treated NIH3T3 cells and dKO$^{MRTF\text{-}NLS}$ MEFs, CTD kinase inhibitors were used in combination with CD stimulation and the Pol II profile was assessed by ChIP. Both CDK7 and CDK9 inhibitors blocked induction of MRTF target genes by CD. However, neither inhibitor gave rise to a Pol II profile like the one in the non-productive state.

Inhibition of CDK7 blocked Pol II loading on the *Acta2* model gene upon CD stimulation. Since the Pol II enters the PIC unphosphorylated and Ser5P is required for its transition into initiation, loss of Pol II ChIP signal is probably a result of rapid turn-over of Pol II which is unable to initiate transcription.

Consistent with its role in alleviating Pol II promoter-proximal pausing, CDK9 inhibition in CD-stimulated cells impaired Pol II elongation, but not Pol II

recruitment. A characteristic paused Pol II peak at the TSS of the *Acta2* gene was observed. Unlike the Pol II recruited at MRTF target genes in the non-productive transcriptional state, under this condition, the Pol II CTD was phosphorylated at Ser5, Ser7 and Tyr1.

In addition to CDK9, CDK12 and CDK13 have also been shown to phosphorylate Ser2 of the Pol II CTD. In contrast to CDK9, CDK12 and CDK13 are only found within gene bodies and do not bind near transcription start sites. It has been proposed that they phosphorylate Ser2 only during elongation (Bartkowiak et al., 2010; Blazek et al., 2011; Bowman et al., 2013).

Inhibition of CDK12/13 did not affect MRTF target genes expression, even though levels of Ser2P of the Pol II CTD were reduced at the 3' end of the *Acta2* gene. Although this could be due to incomplete inhibition of phosphorylation, these results suggest that Ser2P is not limiting for activation of MRTF targets.

Similar results were observed when Plk3 was inhibited. While Thr4P levels at the 3' end of the *Acta2* gene were reduced, MRTF target gene expression was unaffected, indicating that Thr4 phosphorylation is not essential for gene expression at MRTF targets.

Pol II lacking Ser2P displays a normal transcriptional profile

While Pol II is phosphorylated on Ser5 and Ser7 along the gene, with a distinct peak at the TSS, Ser2P starts accumulating in the gene body and reaches maximum at the 3' region of the gene. The association of Ser2P with 3' ends of genes has led to the idea that this modification is required for promoter escape and transition into elongation. However, evidence for this stems from experiments done in cells treated with the CDK9 inhibitors DRB and FP, which block not only Ser2 phosphorylation, but also Pol II release into elongation, therefore inhibiting transcription (Biglione et al., 2007; Chao & Price, 2001; Gomes et al., 2006; Komarnitsky et al., 2000; Ni et al., 2004).

Targeting Ser2P and not CDK9, by genetic approaches or by inactivating CDK12 and CDK13 shows that Ser2P is not necessary for Pol II pause-release and elongation. For instance, analysis of a Rpb1-S2A mutant also shows that Ser2P is not necessary for transcription elongation. However, S2P depletion slows down the rate of transcription and the mutant exhibits impaired splicing and 3' end processing (Gu et al., 2013). Furthermore, a reduction in Ser2P levels in cells treated with the CDK12/CDK13 inhibitor THZ531 does not cause global transcriptional shutdown, but affects only a subset of genes involved in DNA replication, recombination and repair (Blazek et al., 2011; Liang et al., 2015; Zhang et al., 2016). In yeast Ctk1 deletion and subsequent depletion of Ser2P does not affect Pol II elongation, but results in inefficient 3' end processing (Ahn et al., 2004).

Ser2P and transcription termination

Despite the aberrant phosphorylation of Ser2 of the Pol II CTD in the non-productive transcriptional state, termination did not appear defective, as no transcription read-through or early termination was detected by TTseq. These observations indicate that loss of Ser2P might not be the main defect underlying the inhibited state.

Previous studies have shown that Ser2P of the Pol II CTD is involved in transcription termination. Pol II becomes competent for termination after transcribing the poly(A) signal, which is then recognised and bound by the 3' processing machinery. Ser2P facilitates recruitment of Pcf11 (Meinhart & Cramer, 2004), a component of the cleavage and polyadenylation complex (CPA), which is involved in poly(A) site recognition (Kamieniarz-Gdula et al., 2019; West & Proudfoot, 2008).

Nevertheless, several lines of evidence suggest that termination can occur in the absence of Ser2P. The CPA complex assembles directly onto the pre-mRNA poly(A) site as it emerges from the exit channel of the Pol II and cap-proximal poly(A) sites terminate transcription of PROMPTs, when Ser2P levels are low (Andersen et al., 2013; Ntini et al., 2013). This data suggests that the presence of

Ser2P increases the efficiency of CPA complex recruitment, but it is not absolutely essential for termination. In addition, phospho-Ser2 is not required for termination in *C.elegans* (Cassart et al., 2020). In yeast, whereas Pcf11 deletion is lethal, cells expressing the Rpb1-S2A mutant are viable (Cassart et al., 2012; Coudreuse et al., 2010).

Ser7P of the Pol II CTD is required for productive transcription at MRTF target genes

In addition to low Ser2P levels, Pol II exhibited severely impaired phosphorylation of Ser7 and reduced phosphorylation of Ser5 in the inhibited transcriptional state. As the only kinase inhibitor that prevents Ser7P also blocked Ser5P and transcription initiation, depletion of endogenous Rpb1 and reconstitution with a Rpb1-S7A mutant was used to study the functional significance of Ser7 phosphorylation.

Expression of Rpb1-S7A was associated with defective MRTF-dependent gene expression. This effect was specific for MRTF targets and dependent on Mtr4. S7A-ON cells exhibited normal regulation of TCF targets and control genes. This result suggests that Ser7P is specifically required for productive transcription of MRTF target genes, consistent with genome-wide analysis of a Rpb1-S7A mutant, whose expression has no global effect on transcription (Chapman et al., 2007; Egloff et al., 2007). Inhibition of the Ser7 targeting kinase CDK7 does not affect transcription globally either (Chapman et al., 2007; Kanin et al., 2007; Lee et al., 2005). However, it perturbs expression of inducible p-53 target genes (Glover-Cutter et al., 2009), snRNA genes (Egloff et al., 2007) and cell-cycle genes (Lee et al., 2005).

In cells reconstituted with the Rpb1-S7A mutant, Pol II levels in the gene body of MRTF targets were normal, although the Pol II peak at the TSS, associated with promoter-proximal pausing, was reduced. Phospho-serine 5 levels at the TSS were also reduced, while occupancy at downstream regions of the gene was unaffected. These results are consistent with a defect in establishment of Pol II promoter-proximal pausing. It has been shown that CDK7 inhibition reduces Pol II occupancy specifically at the TSS, relative to downstream regions of the gene (Glover-Cutter

et al., 2009; Schwartz et al., 2003), a phenotype also observed in NELF-depleted cells (Gilchrist et al., 2012), suggesting that Ser7P is involved in establishing promoter-proximal pausing. Furthermore, the profile of Ser7P along the gene is in line with a role of Ser7P in Pol II pausing. The two peaks of Ser7P correlate with Pol II paused at TSSs and at 3' end pause sites near the poly(A) site of genes (Chapman et al., 2007).

In addition, in S7A-ON cells the recruited Pol II exhibited impaired phosphorylation at Ser2 of its CTD. This is consistent with CTD modifications being deposited in succession: Ser7P primes phosphorylation of Ser2 (Akhtar et al., 2009; Boeing et al., 2010; Bösken et al., 2014; Chapman et al., 2007) , while Ser2P is required for phosphorylation of Thr4 (Hintermair et al., 2012; Krajewska et al., 2019). Thus, lack of Ser7 phosphorylation would impact on downstream phosphorylation events.

These results largely recapitulate the non-productive transcriptional state observed in LMB-treated NIH3T3 cells and dKO$^{MRTF\text{-}NLS}$ MEFs, suggesting that loss of Ser7P of the Pol II CTD might cause the pre-mRNA accumulation defect in the non-productive transcriptional state.

How might defective Ser7P arise in the non-productive transcriptional state?

The reduced levels of Ser5P and Ser7P of the Pol II CTD at MRTF target genes in the non-productive transcriptional state suggest that the defect in Pol II phosphorylation occurs early on in the transcription cycle. One possibility is that under resting G-actin levels, actin directly inhibits the recruitment of CTD kinases at the TSS. It is also possible that reduced residence time of the Pol II complex at promoters might be insufficient for efficient phosphorylation of Ser5 and Ser7 or that the unstable formation of the Pol II complex might lead to their rapid dephosphorylation.

Phosphorylation of Ser5 of the Pol II CTD is required for transcription initiation and capping of the nascent transcript (Komarnitsky et al., 2000). In addition, inhibition of CDK7, the only kinase known to phosphorylate Ser5 and Ser7 of the Pol II CTD *in vivo*, inhibited Pol II loading on genes. Thus, it seems unlikely that the reduced

levels of Ser5P and Ser7P in the non-productive transcriptional state reflect failure to recruit CDK7.

Even though the inhibited transcriptional state does not appear to reflect impaired recruitment CDK7, it is possible that defective phosphorylation at Ser7 of the Pol II CTD might be a result of failure to recruit another kinase. Several lines of evidence suggest that Ser7 might be targeted by other kinases. First, inhibition of CDK7 does not completely abolish Ser7P (Boeing et al., 2010; Tietjen et al., 2010) and at snRNA genes, where Ser7P is essential for transcription, CDK7 is not required (Kuhlman et al., 1999). Moreover, because of its position within the heptad, Ser7 is not a good TFIIH substrate (Songyang et al., 1996). In addition, CDK7 is found in association with the Pol II at gene promoters, but not within gene bodies (Eyboulet et al., 2013; Eyboulet et al., 2015), while Ser7P is present along genes (Chapman et al., 2007). Finally, *in vitro* Ser7 is also a substrate for DNAPK (Egloff et al., 2010; Trigon et al., 1998).

Low Ser5P and Ser7P levels might also arise from de-phosphorylation. The Ssu72 phosphatase targets Ser5P and Ser7P of the Pol II CTD. it is recruited at TSSs and associates with the PIC (Chen et al., 2014; Spector et al., 2019). Ssu72 has been proposed to regulate the transition from initiation into elongation following promoter escape and dissociation of CDK7, possibly by facilitating subsequent phosphorylation of Ser2 of the Pol II CTD and exchange of initiation and elongation factors.

Dephosphorylation would explain how Pol II with low Ser5P and Ser7P levels is able to initiate. Moreover, ChIP experiments in cells reconstituted with the Rpb1-S7A mutant suggest a role of Ser7P in maintaining Pol II promoter-proximal pausing. Yet, unlike S7A-ON cells, LMB-treated NIH3T3 cells and dKO$^{MRTF\text{-}NLS}$ cells do not exhibit a defect in pausing. This observation suggests that Ser5P and Ser7P are likely dephosphorylated.

In addition to its role in early elongation, Ssu72 is also required for efficient transcription termination at snoRNA genes, some protein-coding genes and

promoter-proximal termination of CUTs in yeast (Ansari & Hampsey, 2005; Krishnamurthy et al., 2004; Tan-Wong et al., 2012; Zhang et al., 2012). Analogously to termination of CUTs and PROMPTs, which, like transcripts of MRTF target genes, are associated with aberrantly phosphorylated Pol II and susceptible to degradation by the exosome, it might be that Ssu72-mediated de-phosphorylation of Ser5 and Ser7 is an attempt to terminate transcription prematurely as a result of unstable PIC complex formation (Chiu et al., 2018; Kamieniarz-Gdula et al., 2019). The potential involvement of Ssu72 could be tested by assessing the Pol II CTD phosphorylation status by ChIP in LMB-treated cells depleted of Ssu72.

9.5 A model for the non-productive transcriptional state

Transition into productive elongation might involve exchange of Mtr4 for the RNA export machinery

The non-productive transcriptional state at MRTF target genes correlates with aberrant phosphorylation of Ser5, Ser7 and Ser2 of the Pol II CTD, as well as Mtr4 recruitment to transcripts of MRTF target genes and their degradation by the nuclear exosome. Our data indicates that loss of Ser7P results in Mtr4 recruitment. As discussed in the previous sections, it is conceivable that the weaker or more transient interaction of MRTF with target promoters in the absence of G-actin depletion might impact on the stability of the Pol II complex and result in defective Pol II phosphorylation, possibly reflecting Ssu72 activity.

We favour a “checkpoint” model in which even during the normal initiation process Pol II passes through a state in which it is possible to recruit Mtr4 to the newly capped transcript, potentially targeting it to the NEXT complex (Figure 91). Transition to the productive state would involve exchange of Mtr4 for the nuclear export machinery and this process would be regulated by the phosphorylation status of the Pol II CTD. In this model, MRTF has two functions in target gene activation: recruitment of Pol II, which occurs both in the induced state and in the non-productive transcriptional state, and facilitation of the exchange of exosome and RNA export complexes, a step that is inhibited at resting G-actin levels.

Under induced conditions, G-actin depletion allows stable association of MRTF with target gene promoters. Pol II is recruited and phosphorylation of Ser5 of the Pol II CTD promotes capping of the nascent transcript. At this point, the NEXT complex could be recruited at the CBCA. Subsequent phosphorylation of Ser7 and Ser2 of the Pol II CTD during promoter-proximal pausing and early elongation promote the exchange of the NEXT complex for the TREX complex and nuclear export of the transcript for translation in the cytoplasm. In the non-productive transcriptional state, reduced phosphorylation of Ser7 of the Pol II CTD makes the RNA susceptible to degradation by the nuclear exosome, probably as a result of failure to exchange the NEXT complex for the RNA export machinery, resulting in co-transcriptional degradation of the nascent transcript (Figure 91).

That depletion of Nrde2 could potentiate Mtr4 activity on MRTF-dependent transcripts, even under induced conditions, when Mtr4 is only weakly associated, is consistent with a model of kinetic competition between the exosome and the export machinery. Consistent with an Mtr4 checkpoint prior to release into elongation, low levels of MRTF-dependent transcripts were found associated with Mtr4 in cells stimulated with CD and FCS.

In addition, Mtr4 binding has been observed in a window of 150bp from the TSS where the Pol II solely phosphorylated at Ser5, while Ser7, Ser2, Tyr1 and Thr4 phosphorylations were depleted (Milligan et al., 2016). Moreover, NEXT substrates such as CUTs in yeast lack Ser2, Ser7 and Thr4 phosphorylations of the Pol II CTD (Milligan et al., 2016). In agreement, Mtr4 and Zcchc8 interact specifically with Ser5P of the Pol II CTD (Ebmeier et al., 2017), suggesting that exosome recruitment might be influenced by the phosphorylation status of the Pol II CTD.

Phosphorylation of Ser7 of the Pol II CTD protects MRTF-dependent transcripts from degradation

As in the inhibited transcriptional state, S7A-ON cells exhibited impaired activation of MRTF target genes in response to signal and productive transcription was rescued by Mtr4 depletion, suggesting that Ser7P is important for protecting the transcript from exosomal degradation.

This might be due to Ser7P directly inhibiting exosome recruitment. However, as depletion of the Mtr4 inhibitor Nrde2 perturbs stimulation of MRTF target genes, without affecting Pol II loading or CTD phosphorylation, this seems unlikely. Moreover, the effects of depleting Nrde2 and Ser7P appear to be independent, since Nrde2 depletion does not exacerbate the transcriptional defect in cells reconstituted with Rpb1-S7A.

Because LMB-treated NIH3T3 cells and dKO$^{MRTF\text{-}NLS}$ cells do not exhibit the defect in Pol II promoter-proximal pausing observed in S7A-ON cells, it appears unlikely that exosome recruitment is a consequence of reduced pausing.

Since reduced Ser7P of the Pol II CTD also inhibited phosphorylation of Ser2, it is possible that Mtr4 recruitment is a result of lack of Ser2P. However, inhibiting phosphorylation of Ser2 of the Pol II CTD using the CDK12/13 inhibitor THZ531 did not block gene expression at MRTF target genes.

Alternatively, Ser7 phosphorylation of the Pol II CTD might favour recruitment of the TREX complex, similar to how recruitment of the CPA complex is promoted by Ser2 phosphorylation. The potential interaction of the TREX complex with Pol II CTD phosphorylated at Ser7 could be tested by IP.

It appears that various RNA processing complexes compete for binding to the CBC and continuously exchange during transcription until transcript fate is decided by locking a particular complex at the CBC at a specific stage during the transcription cycle. One such point is the 3’ end processing signal emerging from the Pol II exit channel. It has been shown that cap-proximal poly(A) sites recruit the NEXT complex at the CBCA of PROMPTs (Andersen et al., 2013; Ntini et al., 2013) and 3’ end processing signal at snRNAs recruit the PHAX complex (Hallais et al., 2013).

Another potential checkpoint could be during promoter-proximal pausing. Association with a degradation complex early on during transcription would prevent

the dynamic exchange of factors at the CBC and ensure degradation of the transcript. Aberrant Pol II CTD phosphorylation could be a signal for degradation.

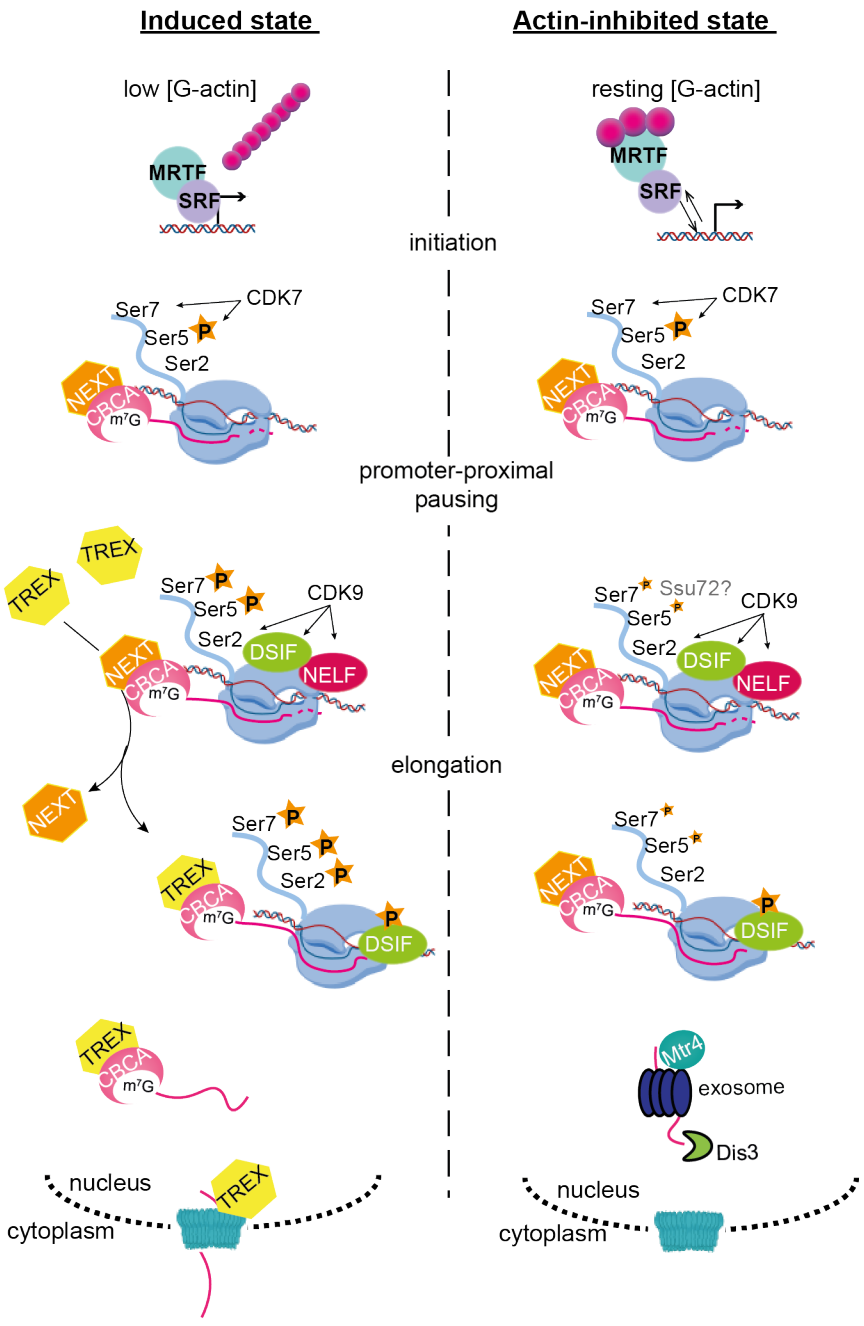

Figure 91 Regulation of transcription at MRTF target genes

G-actin depletion allows stable association of MRTF with target gene promoters. Pol II is recruited and phosphorylation at Ser5 of the Pol II CTD by CDK7 promotes capping of the nascent transcript. At this point, the NEXT complex could be recruited at the CBCA. Subsequent phosphorylation of Ser7 and Ser2 of the Pol II CTD during promoter-proximal pausing and early elongation promotes the exchange of the NEXT complex for the TREX complex and nuclear export of the transcript for translation in the cytoplasm. On the other hand, in the absence of G-actin depletion, G-actin prevents stable association of nuclear MRTF with genomic loci. Pol II is recruited and phosphorylated at Ser5 of the Pol II CTD. The nascent transcript is capped and could be bound by the NEXT complex. The inefficient MRTF recruitment results in a defect in Pol II CTD phosphorylation, possibly due to rapid dephosphorylation of Ser5P and Ser7P, potentially as a result of Ssu72 activity. Reduced phosphorylation of Ser7 of the Pol II CTD makes the RNA susceptible to degradation by the nuclear exosome, probably as a result of failure to exchange the NEXT complex for the RNA export machinery, resulting in co-transcriptional degradation of the nascent transcript.

It is possible that Mtr4 exchange for the export machinery at a checkpoint during transcription occurs at all protein-coding genes. This idea is in line with pre-mRNAs with structural, splicing and polyadenylation defects being exosome substrates (Bousquet-Antonelli et al., 2000; Hilleren et al., 2001; Houseley et al., 2006; Jensen et al., 2001; Lebreton & Séraphin, 2008; Libri et al., 2002; Milligan et al., 2005; Moore et al., 2006; Torchet et al., 2002) and consistent with transcripts being targeted for degradation in RNA export mutants (Fan et al., 2017; Gudipati et al., 2012; Hilleren et al., 2001; Jensen et al., 2001; Libri et al., 2002). Nevertheless, experiments in Nrde2-depleted cells suggest that this checkpoint is not a general feature of Pol II regulated protein-coding genes and might be MRTF-specific. This is line with experiments in S7A-ON cells, which demonstrate that reconstitution with the Rpb1-S7A mutant affected MRTF target gene expression, specifically.

Genome-wide studies in S7A-ON cells in combination with Mtr4 depletion would help understand the potential relationship between phosphorylation of Ser7 of the Pol II CTD and Mtr4 recruitment at additional sets of genes.

Chapter 10. Appendix

GO BIOLOGICAL PROCESS	# Genes	p-value	FDR q-valu
GOBP_CYTOSKELETON_ORGANIZATION	247	2.14E-74	1.62E-70
GOBP_CELL_PROJECTION_ORGANIZATION	256	1.54E-68	5.82E-65
GOBP_POSITIVE_REGULATION_OF_NUCLEOBASE_CONTAINING_COMPOUND_METABOLIC_PROCESS	278	2.96E-67	7.47E-64
GOBP_CELL_MORPHOGENESIS	200	4.19E-66	7.93E-63
GOBP_ACTIN_FILAMENT_BASED_PROCESS	173	1.01E-64	1.54E-61
GOBP_NEUROGENESIS	256	8.58E-64	1.05E-60
GOBP_POSITIVE_REGULATION_OF_CELLULAR_BIOSYNTHETIC_PROCESS	281	9.67E-64	1.05E-60
GOBP_REGULATION_OF_INTRACELLULAR_SIGNAL_TRANSDUCTION	268	3.05E-61	2.89E-58
GOBP_POSITIVE_REGULATION_OF_MOLECULAR_FUNCTION	263	2.35E-60	1.98E-57
GOBP_CELLULAR_MACROMOLECULE_LOCALIZATION	275	2.56E-59	1.94E-56
GOBP_CELL_MIGRATION	237	1.68E-56	9.70E-54
GOBP_REGULATION_OF_ORGANELLE_ORGANIZATION	195	1.01E-54	5.42E-52
GOBP_POSITIVE_REGULATION_OF_CATALYTIC_ACTIVITY	216	2.19E-54	1.09E-51
GOBP_NEURON_DIFFERENTIATION	211	8.90E-54	4.16E-51
GOBP_ESTABLISHMENT_OF_PROTEIN_LOCALIZATION	263	2.09E-53	9.19E-51
GOBP_INTRACELLULAR_TRANSPORT	242	3.59E-53	1.49E-50
GOBP_MACROMOLECULE_CATABOLIC_PROCESS	215	2.27E-52	8.92E-50
GOBP_POSITIVE_REGULATION_OF_CELLULAR_COMPONENT_ORGANIZATION	186	9.20E-52	3.44E-49
GOBP_REGULATION_OF_PROTEIN_MODIFICATION_PROCESS	229	1.05E-50	3.73E-48
GOBP_CELL_CYCLE	249	1.17E-50	3.99E-48
GOBP_NEURON_DEVELOPMENT	182	9.39E-50	3.05E-47
GOBP_REGULATION_OF_CELLULAR_COMPONENT_BIOGENESIS	166	1.13E-48	3.52E-46
GOBP_POSITIVE_REGULATION_OF_PROTEIN_METABOLIC_PROCESS	213	2.06E-46	6.15E-44
GOBP_POSITIVE_REGULATION_OF_SIGNALING	229	2.46E-46	7.09E-44
GOBP_APOPTOTIC_PROCESS	244	1.24E-45	3.44E-43
GOBP_CELL_MORPHOGENESIS_INVOLVED_IN_DIFFERENTIATION	138	2.11E-45	5.63E-43
GOBP_REGULATION_OF_GTPASE_ACTIVITY	112	2.38E-45	6.13E-43
GOBP_SUPRAMOLECULAR_FIBER_ORGANIZATION	136	7.33E-45	1.83E-42
GOBP_BIOLOGICAL_ADHESION	206	1.02E-44	2.46E-42
GOBP_REGULATION_OF_HYDROLASE_ACTIVITY	190	1.76E-44	4.10E-42
GOBP_REGULATION_OF_ANATOMICAL_STRUCTURE_MORPHOGENESIS	164	1.96E-44	4.45E-42
GOBP_PEPTIDYL_AMINO_ACID_MODIFICATION	187	3.79E-44	8.35E-42
GOBP_REGULATION_OF_CELLULAR_COMPONENT_MOVEMENT	172	4.36E-44	9.33E-42
GOBP_CELLULAR_COMPONENT_MORPHOGENESIS	140	8.90E-44	1.85E-41
GOBP_NEGATIVE_REGULATION_OF_BIOSYNTHETIC_PROCESS	220	2.88E-43	5.82E-41
GOBP_CIRCULATORY_SYSTEM_DEVELOPMENT	173	1.47E-42	2.89E-40
GOBP_CELLULAR_MACROMOLECULE_CATABOLIC_PROCESS	178	2.07E-42	3.97E-40
GOBP_REGULATION_OF_CELL_DIFFERENTIATION	211	1.99E-41	3.71E-39
GOBP_CHROMOSOME_ORGANIZATION	180	2.20E-41	4.01E-39
GOBP_REGULATION_OF_PHOSPHORUS_METABOLIC_PROCESS	210	3.04E-41	5.42E-39
GOBP_POSITIVE_REGULATION_OF_TRANSCRIPTION_BY_RNA_POLYMERASE_II	174	4.15E-41	7.22E-39
GOBP_PROTEIN_MODIFICATION_BY_SMALL_PROTEIN_CONJUGATION_OR_REMOVAL	172	5.88E-41	9.99E-39
GOBP_NEGATIVE_REGULATION_OF_NUCLEOBASE_CONTAINING_COMPOUND_METABOLIC_PROCESS	202	6.75E-41	1.12E-38
GOBP_ANIMAL_ORGAN_MORPHOGENESIS	159	2.52E-40	4.11E-38
GOBP_ENZYME_LINKED_RECEPTOR_PROTEIN_SIGNALING_PATHWAY	162	1.25E-39	2.00E-37
GOBP_RESPONSE_TO_ENDOGENOUS_STIMULUS	207	3.80E-39	5.92E-37
GOBP_REGULATION_OF_RESPONSE_TO_STRESS	190	4.40E-39	6.72E-37
GOBP_REGULATION_OF_CATABOLIC_PROCESS	155	5.90E-39	8.83E-37
GOBP_CELL_PART_MORPHOGENESIS	124	8.34E-39	1.22E-36
GOBP_CHROMATIN_ORGANIZATION	136	1.62E-38	2.33E-36
GOBP_ACTIN_FILAMENT_ORGANIZATION	97	4.05E-38	5.72E-36
GOBP_POSITIVE_REGULATION_OF_GTPASE_ACTIVITY	94	4.95E-38	6.86E-36
GOBP_POSITIVE_REGULATION_OF_PROTEIN_MODIFICATION_PROCESS	157	8.50E-38	1.16E-35
GOBP_NEGATIVE_REGULATION_OF_RESPONSE_TO_STIMULUS	208	9.85E-38	1.32E-35
GOBP_CELL_POPULATION_PROLIFERATION	229	1.78E-37	2.34E-35
GOBP_PROTEIN_CONTAINING_COMPLEX_SUBUNIT_ORGANIZATION	229	2.46E-37	3.17E-35
GOBP_POSITIVE_REGULATION_OF_HYDROLASE_ACTIVITY	131	2.52E-37	3.20E-35
GOBP_HEAD_DEVELOPMENT	128	7.20E-37	8.98E-35
GOBP_CELL_CYCLE_PROCESS	185	1.94E-36	2.38E-34
GOBP_REGULATION_OF_PROTEIN_PHOSPHORYLATION	168	2.69E-36	3.25E-34
GOBP_PROTEOLYSIS	214	4.89E-36	5.80E-34
GOBP_PROTEIN_CATABOLIC_PROCESS	144	1.42E-35	1.66E-33
GOBP_REGULATION_OF_CELL_DEATH	202	2.39E-35	2.74E-33
GOBP_REGULATION_OF_CELL_CYCLE	166	3.20E-35	3.63E-33
GOBP_REGULATION_OF_CELLULAR_CATABOLIC_PROCESS	134	6.44E-35	7.19E-33
GOBP_CELL_MORPHOGENESIS_INVOLVED_IN_NEURON_DIFFERENTIATION	108	9.28E-35	1.02E-32
GOBP_TUBE_DEVELOPMENT	154	1.88E-34	2.04E-32
GOBP_CELL_JUNCTION_ORGANIZATION	119	3.17E-34	3.39E-32
GOBP_CENTRAL_NERVOUS_SYSTEM_DEVELOPMENT	144	6.62E-34	6.98E-32
GOBP_POSITIVE_REGULATION_OF_ORGANELLE_ORGANIZATION	107	8.41E-34	8.74E-32
GOBP_EMBRYO_DEVELOPMENT	144	2.55E-33	2.61E-31
GOBP_NEGATIVE_REGULATION_OF_SIGNALING	178	3.73E-33	3.77E-31
GOBP_ORGANONITROGEN_COMPOUND_CATABOLIC_PROCESS	171	1.03E-32	1.03E-30
GOBP_TRANSMEMBRANE_RECEPTOR_PROTEIN_TYROSINE_KINASE_SIGNALING_PATHWAY	120	1.32E-32	1.30E-30
GOBP_POSITIVE_REGULATION_OF_INTRACELLULAR_SIGNAL_TRANSDUCTION	143	3.80E-32	3.69E-30
GOBP_POSITIVE_REGULATION_OF_DEVELOPMENTAL_PROCESS	166	3.95E-32	3.79E-30
GOBP_SMALL_GTPASE_MEDIATED_SIGNAL_TRANSDUCTION	96	5.56E-32	5.26E-30
GOBP_CELLULAR_PROTEIN_CATABOLIC_PROCESS	124	9.34E-32	8.73E-30
GOBP_REGULATION_OF_CELLULAR_RESPONSE_TO_STRESS	115	1.05E-31	9.71E-30
GOBP_HEART_DEVELOPMENT	101	1.20E-31	1.10E-29
GOBP_REGULATION_OF_CELL_PROJECTION_ORGANIZATION	108	1.54E-31	1.38E-29
GOBP_COVALENT_CHROMATIN_MODIFICATION	91	2.12E-31	1.88E-29
GOBP_ANATOMICAL_STRUCTURE_FORMATION_INVOLVED_IN_MORPHOGENESIS	153	2.27E-31	2.00E-29
GOBP_PROTEIN_MODIFICATION_BY_SMALL_PROTEIN_CONJUGATION	137	4.23E-31	3.68E-29
GOBP_REGULATION_OF_TRANSFERASE_ACTIVITY	141	7.94E-31	6.82E-29
GOBP_CELL_CELL_SIGNALING_BY_WNT	95	2.24E-30	1.90E-28
GOBP_CELLULAR_RESPONSE_TO_DNA_DAMAGE_STIMULUS	128	2.55E-30	2.14E-28
GOBP_REGULATION_OF_MULTICELLULAR_ORGANISMAL_DEVELOPMENT	171	3.27E-30	2.72E-28
GOBP_POSITIVE_REGULATION_OF_CELLULAR_COMPONENT_BIOGENESIS	96	4.22E-30	3.47E-28
GOBP_HOMEOSTATIC_PROCESS	209	5.44E-30	4.43E-28
GOBP_REGULATION_OF_CYTOSKELETON_ORGANIZATION	94	5.68E-30	4.57E-28
GOBP_MAPK_CASCADE	131	6.44E-30	5.13E-28
GOBP_CELL_CELL_SIGNALING	191	8.23E-30	6.48E-28
GOBP_MODIFICATION_DEPENDENT_MACROMOLECULE_CATABOLIC_PROCESS	107	2.67E-29	2.08E-27
GOBP_TISSUE_MORPHOGENESIS	105	2.80E-29	2.16E-27
GOBP_GROWTH	129	5.25E-29	4.01E-27
GOBP_MITOTIC_CELL_CYCLE	139	8.57E-29	6.47E-27
GOBP_CELL_SURFACE_RECEPTOR_SIGNALING_PATHWAY_INVOLVED_IN_CELL_CELL_SIGNALING	102	1.21E-28	9.05E-27

Figure 92 Gene ontology analysis of genes upregulated in response to CD in NIH3T3 cells by RNAseq

Gene ontology analysis of genes upregulated by CD treatment in NIH3T3 cells by RNAseq. FDR<0.05. Relates to Figure 33B. Bioinformatic analysis of RNAseq data was performed by Francesco Gualdrini.

GO BIOLOGICAL PROCESS	# Genes	p-value	FDR q-value
GOBP_COTRANSLATIONAL_PROTEIN_TARGETING_TO_MEMBRANE	65	1.30E-85	9.74E-82
GOBP_NUCLEAR_TRANSCRIBED_MRNA_CATABOLIC_PROCESS_NONSENSE_MEDIATED_DECAY	65	6.35E-81	2.38E-77
GOBP_ESTABLISHMENT_OF_PROTEIN_LOCALIZATION_TO_ENDOPLASMIC_RETICULUM	65	1.35E-80	3.37E-77
GOBP_PROTEIN_LOCALIZATION_TO_ENDOPLASMIC_RETICULUM	69	1.50E-79	2.81E-76
GOBP_BIOLOGICAL_PROCESS_INVOLVED_IN_SYMBIOTIC_INTERACTION	135	3.89E-77	5.82E-74
GOBP_VIRAL_GENE_EXPRESSION	73	3.91E-75	4.87E-72
GOBP_TRANSLATIONAL_INITIATION	68	2.07E-68	2.22E-65
GOBP_INTRACELLULAR_TRANSPORT	158	7.01E-66	5.97E-63
GOBP_NUCLEAR_TRANSCRIBED_MRNA_CATABOLIC_PROCESS	68	7.99E-66	5.97E-63
GOBP_PROTEIN_TARGETING_TO_MEMBRANE	68	7.99E-66	5.97E-63
GOBP_CELLULAR_MACROMOLECULE_LOCALIZATION	166	5.48E-64	3.72E-61
GOBP_ESTABLISHMENT_OF_PROTEIN_LOCALIZATION_TO_MEMBRANE	79	2.81E-62	1.75E-59
GOBP_PROTEIN_LOCALIZATION_TO_MEMBRANE	98	1.82E-59	1.05E-56
GOBP_CELLULAR_MACROMOLECULE_CATABOLIC_PROCESS	126	8.63E-59	4.61E-56
GOBP_MACROMOLECULE_CATABOLIC_PROCESS	136	2.07E-58	1.03E-55
GOBP_RNA_CATABOLIC_PROCESS	80	1.53E-57	7.17E-55
GOBP_ORGANONITROGEN_COMPOUND_BIOSYNTHETIC_PROCESS	148	5.16E-56	2.27E-53
GOBP_PEPTIDE_METABOLIC_PROCESS	108	8.39E-56	3.49E-53
GOBP_ESTABLISHMENT_OF_PROTEIN_LOCALIZATION_TO_ORGANELLE	89	2.37E-55	9.35E-53
GOBP_PROTEIN_LOCALIZATION_TO_ORGANELLE	112	4.84E-55	1.81E-52
GOBP_CELLULAR_AMIDE_METABOLIC_PROCESS	120	3.39E-54	1.21E-51
GOBP_MRNA_METABOLIC_PROCESS	105	3.58E-54	1.22E-51
GOBP_PEPTIDE_BIOSYNTHETIC_PROCESS	97	1.13E-53	3.69E-51
GOBP_AMIDE_BIOSYNTHETIC_PROCESS	104	2.43E-53	7.57E-51
GOBP_PROTEIN_TARGETING	78	2.74E-53	8.19E-51
GOBP_ESTABLISHMENT_OF_PROTEIN_LOCALIZATION	152	3.00E-53	8.64E-51
GOBP_INTRACELLULAR_PROTEIN_TRANSPORT	116	9.89E-52	2.74E-49
GOBP_ORGANIC_CYCLIC_COMPOUND_CATABOLIC_PROCESS	88	1.42E-50	3.80E-48
GOBP_NEGATIVE_REGULATION_OF_GENE_EXPRESSION	137	5.86E-50	1.51E-47
GOBP_PROTEIN_CONTAINING_COMPLEX_SUBUNIT_ORGANIZATION	144	4.52E-48	1.13E-45
GOBP_APOPTOTIC_PROCESS	130	3.84E-39	9.27E-37
GOBP_CELLULAR_PROTEIN_CONTAINING_COMPLEX_ASSEMBLY	98	5.23E-39	1.22E-36
GOBP_REGULATION_OF_CELL_DEATH	115	1.13E-35	2.57E-33
GOBP_BIOLOGICAL_ADHESION	107	1.04E-34	2.29E-32
GOBP_CYTOPLASMIC_TRANSLATION	32	7.43E-31	1.59E-28
GOBP_RESPONSE_TO_OXYGEN_CONTAINING_COMPOUND	106	5.81E-30	1.21E-27
GOBP_POSITIVE_REGULATION_OF_PROTEIN_METABOLIC_PROCESS	98	1.02E-27	2.07E-25
GOBP_CELL_POPULATION_PROLIFERATION	109	8.69E-26	1.71E-23
GOBP_NEGATIVE_REGULATION_OF_BIOSYNTHETIC_PROCESS	100	1.15E-25	2.20E-23
GOBP_CELL_MIGRATION	97	1.47E-25	2.74E-23
GOBP_RESPONSE_TO_CYTOKINE	81	1.18E-24	2.15E-22
GOBP_NEGATIVE_REGULATION_OF_PROTEIN_METABOLIC_PROCESS	78	1.41E-24	2.50E-22
GOBP_GENERATION_OF_PRECURSOR_METABOLITES_AND_ENERGY	53	4.49E-24	7.81E-22
GOBP_REGULATION_OF_INTRACELLULAR_SIGNAL_TRANSDUCTION	100	7.61E-24	1.29E-21
GOBP_RESPONSE_TO_ENDOGENOUS_STIMULUS	94	2.20E-23	3.66E-21
GOBP_NEGATIVE_REGULATION_OF_RESPONSE_TO_STIMULUS	94	1.76E-22	2.86E-20
GOBP_TUBE_DEVELOPMENT	73	6.00E-22	9.54E-20
GOBP_CELL_ACTIVATION	86	6.74E-22	1.05E-19
GOBP_CELL_CELL_ADHESION	65	9.59E-22	1.46E-19
GOBP_CELLULAR_RESPONSE_TO_OXYGEN_CONTAINING_COMPOUND	76	1.20E-21	1.79E-19
GOBP_NEGATIVE_REGULATION_OF_NUCLEOBASE_CONTAINING_COMPOUND_METABOLIC_PROC	87	2.25E-21	3.31E-19
GOBP_SECRETION	85	2.87E-21	4.13E-19
GOBP_REGULATION_OF_CELL_DIFFERENTIATION	90	3.00E-21	4.23E-19
GOBP_CELL_CYCLE	98	3.10E-21	4.30E-19
GOBP_LOCOMOTION	101	3.80E-21	5.17E-19
GOBP_REGULATION_OF_PROTEIN_MODIFICATION_PROCESS	90	4.32E-21	5.77E-19
GOBP_REGULATION_OF_HYDROLASE_ACTIVITY	79	4.76E-21	6.25E-19
GOBP_NEGATIVE_REGULATION_OF_CELL_DEATH	68	5.85E-21	7.54E-19
GOBP_SUPRAMOLECULAR_FIBER_ORGANIZATION	57	7.40E-21	9.39E-19
GOBP_REGULATION_OF_PHOSPHORUS_METABOLIC_PROCESS	89	7.66E-21	9.55E-19
GOBP_NEGATIVE_REGULATION_OF_SIGNALING	82	1.34E-20	1.64E-18
GOBP_RESPONSE_TO_NITROGEN_COMPOUND	71	5.33E-20	6.43E-18
GOBP_REGULATION_OF_PROTEOLYSIS	56	1.35E-19	1.61E-17
GOBP_CIRCULATORY_SYSTEM_DEVELOPMENT	71	1.62E-19	1.90E-17
GOBP_CYTOSKELETON_ORGANIZATION	79	1.89E-19	2.18E-17
GOBP_PROTEOLYSIS	92	2.53E-19	2.87E-17
GOBP_TUBE_MORPHOGENESIS	62	2.83E-19	3.15E-17
GOBP_REGULATION_OF_MULTICELLULAR_ORGANISMAL_DEVELOPMENT	79	3.87E-19	4.25E-17
GOBP_POSITIVE_REGULATION_OF_GENE_EXPRESSION	68	4.43E-19	4.80E-17
GOBP_POSITIVE_REGULATION_OF_SIGNALING	89	6.40E-19	6.84E-17
GOBP_RESPONSE_TO_GROWTH_FACTOR	55	6.53E-19	6.88E-17
GOBP_VASCULATURE_DEVELOPMENT	57	8.05E-19	8.37E-17
GOBP_REGULATION_OF_ANATOMICAL_STRUCTURE_MORPHOGENESIS	65	9.65E-19	9.89E-17
GOBP_POSITIVE_REGULATION_OF_MOLECULAR_FUNCTION	89	1.32E-18	1.33E-16
GOBP_ATP_METABOLIC_PROCESS	36	1.50E-18	1.49E-16
GOBP_APOPTOTIC_SIGNALING_PATHWAY	48	2.71E-18	2.66E-16
GOBP_PROTEIN_DNA_COMPLEX_SUBUNIT_ORGANIZATION	34	2.79E-18	2.71E-16
GOBP_EXOCYTOSIS	60	3.23E-18	3.10E-16
GOBP_POSITIVE_REGULATION_OF_CELLULAR_COMPONENT_ORGANIZATION	68	3.40E-18	3.22E-16
GOBP_REGULATION_OF_CELLULAR_COMPONENT_MOVEMENT	67	5.67E-18	5.31E-16
GOBP_GROWTH	60	7.85E-18	7.25E-16
GOBP_MYELOID_LEUKOCYTE_MEDIATED_IMMUNITY	46	9.28E-18	8.47E-16
GOBP_BLOOD_VESSEL_MORPHOGENESIS	51	1.22E-17	1.10E-15
GOBP_REGULATION_OF_CELL_CYCLE	70	1.53E-17	1.36E-15
GOBP_REGULATION_OF_CELLULAR_COMPONENT_BIOGENESIS	61	2.27E-17	2.00E-15
GOBP_RIBONUCLEOPROTEIN_COMPLEX_BIOGENESIS	42	2.58E-17	2.24E-15
GOBP_REGULATION_OF_CELLULAR_RESPONSE_TO_STRESS	51	4.59E-17	3.94E-15
GOBP_NUCLEOSOME_ORGANIZATION	27	5.42E-17	4.61E-15
GOBP_RIBOSOME_ASSEMBLY	18	5.50E-17	4.62E-15
GOBP_REGULATION_OF_CATABOLIC_PROCESS	62	6.05E-17	5.03E-15
GOBP_RESPONSE_TO_ABIOTIC_STIMULUS	69	6.78E-17	5.57E-15
GOBP_REGULATION_OF_TRANSFERASE_ACTIVITY	62	7.30E-17	5.93E-15
GOBP_ACTIN_FILAMENT_BASED_PROCESS	54	8.84E-17	7.11E-15
GOBP_POSITIVE_REGULATION_OF_DEVELOPMENTAL_PROCESS	71	8.93E-17	7.11E-15
GOBP_CELLULAR_COMPONENT_DISASSEMBLY	45	9.58E-17	7.55E-15
GOBP_CELL_ACTIVATION_INVOLVED_IN_IMMUNE_RESPONSE	51	1.73E-16	1.35E-14
GOBP_TISSUE_MIGRATION	36	2.14E-16	1.65E-14
GOBP_PROTEIN_CATABOLIC_PROCESS	59	2.19E-16	1.67E-14
GOBP_POSITIVE_REGULATION_OF_CATALYTIC_ACTIVITY	74	2.27E-16	1.72E-14
GOBP_RIBONUCLEOPROTEIN_COMPLEX_SUBUNIT_ORGANIZATION	29	2.53E-16	1.89E-14

Figure 93 Gene ontology analysis of genes downregulated in response to CD in NIH3T3 cells by RNAseq

Gene ontology analysis of genes downregulated by CD treatment in NIH3T3 cells by RNAseq. FDR<0.05. Relates to Figure 17. Bioinformatic analysis of RNAseq data was performed by Francesco Gualdrini.

GO BIOLOGICAL PROCESS	# Genes	p-value	FDR q-valu
GOBP_ACTIN_FILAMENT_BASED_PROCESS	114	3.39E-56	2.56E-52
GOBP_CYTOSKELETON_ORGANIZATION	145	3.73E-54	1.41E-50
GOBP_CELL_MOTILITY	153	1.68E-45	4.24E-42
GOBP_BIOLOGICAL_ADHESION	134	3.78E-43	7.16E-40
GOBP_APOPTOTIC_PROCESS	156	1.65E-42	2.17E-39
GOBP_SUPRAMOLECULAR_FIBER_ORGANIZATION	93	1.72E-42	2.17E-39
GOBP_REGULATION_OF_INTRACELLULAR_SIGNAL_TRANSDUCTION	150	2.90E-42	3.14E-39
GOBP_REGULATION_OF_CELL_DEATH	140	3.47E-39	3.28E-36
GOBP_REGULATION_OF_CELL_DIFFERENTIATION	147	3.02E-38	2.54E-35
GOBP_REGULATION_OF_CELLULAR_COMPONENT_MOVEMENT	109	4.20E-37	3.18E-34
GOBP_ACTIN_FILAMENT_ORGANIZATION	68	1.61E-36	1.10E-33
GOBP_PROTEIN_PHOSPHORYLATION	126	3.84E-34	2.21E-31
GOBP_POSITIVE_REGULATION_OF_DEVELOPMENTAL_PROCESS	110	2.40E-33	1.28E-30
GOBP_ANATOMICAL_STRUCTURE_FORMATION_INVOLVED_IN_MORPHOGENESIS	103	4.25E-33	2.12E-30
GOBP_CELL_SUBSTRATE_ADHESION	59	5.55E-33	2.59E-30
GOBP_CIRCULATORY_SYSTEM_DEVELOPMENT	101	8.06E-32	3.55E-29
GOBP_POSITIVE_REGULATION_OF_BIOSYNTHETIC_PROCESS	136	1.05E-31	4.36E-29
GOBP_REGULATION_OF_PROTEIN_MODIFICATION_PROCESS	120	2.88E-30	1.13E-27
GOBP_POSITIVE_REGULATION_OF_SIGNALING	124	3.10E-30	1.16E-27
GOBP_RESPONSE_TO_ABIOTIC_STIMULUS	102	3.52E-30	1.25E-27
GOBP_REGULATION_OF_PHOSPHORUS_METABOLIC_PROCESS	119	4.25E-30	1.45E-27
GOBP_ENZYME_LINKED_RECEPTOR_PROTEIN_SIGNALING_PATHWAY	95	5.88E-30	1.91E-27
GOBP_RESPONSE_TO_ENDOGENOUS_STIMULUS	119	9.31E-30	2.90E-27
GOBP_REGULATION_OF_TRANSPORT	122	5.56E-29	1.66E-26
GOBP_POSITIVE_REGULATION_OF_NUCLEOBASE_CONTAINING_COMPOUND_METABOLIC_PROCESS	127	6.37E-29	1.83E-26
GOBP_POSITIVE_REGULATION_OF_MOLECULAR_FUNCTION	122	1.22E-28	3.38E-26
GOBP_MUSCLE_STRUCTURE_DEVELOPMENT	69	2.99E-28	7.99E-26
GOBP_CELL_MORPHOGENESIS	88	1.91E-27	4.92E-25
GOBP_REGULATION_OF_ORGANELLE_ORGANIZATION	95	3.29E-27	8.19E-25
GOBP_REGULATION_OF_PROTEIN_PHOSPHORYLATION	97	3.51E-27	8.47E-25
GOBP_RESPONSE_TO_WOUNDING	70	4.65E-27	1.09E-24
GOBP_WOUND_HEALING	63	9.96E-27	2.26E-24
GOBP_POSITIVE_REGULATION_OF_CELLULAR_COMPONENT_ORGANIZATION	92	1.18E-26	2.60E-24
GOBP_POSITIVE_REGULATION_OF_CELL_DIFFERENTIATION	79	1.50E-26	3.12E-24
GOBP_REGULATION_OF_ACTIN_FILAMENT_BASED_PROCESS	54	1.50E-26	3.12E-24
GOBP_POSITIVE_REGULATION_OF_CATALYTIC_ACTIVITY	104	1.93E-26	3.90E-24
GOBP_RESPONSE_TO_OXYGEN_CONTAINING_COMPOUND	114	3.08E-26	6.06E-24
GOBP_REGULATION_OF_MULTICELLULAR_ORGANISMAL_DEVELOPMENT	103	5.54E-26	1.06E-23
GOBP_CELL_POPULATION_PROLIFERATION	125	8.20E-26	1.53E-23
GOBP_POSITIVE_REGULATION_OF_PROTEIN_METABOLIC_PROCESS	108	9.65E-26	1.76E-23
GOBP_TUBE_DEVELOPMENT	89	1.05E-25	1.87E-23
GOBP_HOMEOSTATIC_PROCESS	123	1.24E-25	2.16E-23
GOBP_REGULATION_OF_CELLULAR_COMPONENT_BIOGENESIS	83	1.28E-25	2.18E-23
GOBP_TUBE_MORPHOGENESIS	80	2.08E-25	3.45E-23
GOBP_VASCULATURE_DEVELOPMENT	74	4.45E-25	7.24E-23
GOBP_REGULATION_OF_CELL_ADHESION	71	7.35E-25	1.17E-22
GOBP_POSITIVE_REGULATION_OF_MULTICELLULAR_ORGANISMAL_PROCESS	101	7.75E-25	1.21E-22
GOBP_NEGATIVE_REGULATION_OF_CELL_DEATH	83	1.30E-24	1.99E-22
GOBP_POSITIVE_REGULATION_OF_LOCOMOTION	63	1.35E-24	2.02E-22
GOBP_POSITIVE_REGULATION_OF_INTRACELLULAR_SIGNAL_TRANSDUCTION	83	3.27E-24	4.79E-22
GOBP_CELL_CELL_ADHESION	76	2.06E-23	2.96E-21
GOBP_CELL_ACTIVATION	101	2.24E-23	3.16E-21
GOBP_REGULATION_OF_RESPONSE_TO_STRESS	99	2.51E-23	3.48E-21
GOBP_RESPONSE_TO_GROWTH_FACTOR	68	7.90E-23	1.08E-20
GOBP_EXTERNAL_ENCAPSULATING_STRUCTURE_ORGANIZATION	50	8.48E-23	1.13E-20
GOBP_CELL_MATRIX_ADHESION	39	1.00E-22	1.31E-20
GOBP_NEGATIVE_REGULATION_OF_NUCLEOBASE_CONTAINING_COMPOUND_METABOLIC_PROCESS	102	1.16E-22	1.49E-20
GOBP_REGULATION_OF_CYTOSKELETON_ORGANIZATION	56	2.15E-22	2.72E-20
GOBP_PROTEOLYSIS	112	2.92E-22	3.63E-20
GOBP_EMBRYO_DEVELOPMENT	79	4.17E-22	5.06E-20
GOBP_REGULATION_OF_HYDROLASE_ACTIVITY	92	4.19E-22	5.06E-20
GOBP_EPITHELIUM_DEVELOPMENT	91	4.72E-22	5.61E-20
GOBP_BLOOD_VESSEL_MORPHOGENESIS	64	6.47E-22	7.56E-20
GOBP_ANIMAL_ORGAN_MORPHOGENESIS	80	7.82E-22	9.00E-20
GOBP_NEGATIVE_REGULATION_OF_SIGNALING	96	8.40E-22	9.52E-20
GOBP_REGULATION_OF_TRANSFERASE_ACTIVITY	79	1.25E-21	1.40E-19
GOBP_NEGATIVE_REGULATION_OF_BIOSYNTHETIC_PROCESS	106	2.27E-21	2.50E-19
GOBP_RESPONSE_TO_CYTOKINE	86	2.83E-21	3.07E-19
GOBP_POSITIVE_REGULATION_OF_PHOSPHORUS_METABOLIC_PROCESS	77	3.41E-21	3.65E-19
GOBP_CELL_JUNCTION_ORGANIZATION	64	3.47E-21	3.66E-19
GOBP_REGULATION_OF_ION_TRANSPORT	91	3.58E-21	3.68E-19
GOBP_SECRETION	97	3.59E-21	3.68E-19
GOBP_NEGATIVE_REGULATION_OF_RESPONSE_TO_STIMULUS	105	4.07E-21	4.11E-19
GOBP_POSITIVE_REGULATION_OF_CELL_DEATH	61	1.03E-20	1.03E-18
GOBP_REGULATION_OF_CELL_SUBSTRATE_ADHESION	36	1.11E-20	1.09E-18
GOBP_CELL_JUNCTION_ASSEMBLY	49	1.19E-20	1.16E-18
GOBP_NEGATIVE_REGULATION_OF_MOLECULAR_FUNCTION	84	1.21E-20	1.16E-18
GOBP_MAPK_CASCADE	73	1.27E-20	1.20E-18
GOBP_NEUROGENESIS	101	2.92E-20	2.73E-18
GOBP_RESPONSE_TO_ORGANIC_CYCLIC_COMPOUND	72	3.76E-20	3.47E-18
GOBP_CELL_PROJECTION_ORGANIZATION	99	3.85E-20	3.52E-18
GOBP_REGULATION_OF_ANATOMICAL_STRUCTURE_MORPHOGENESIS	76	5.80E-20	5.23E-18
GOBP_CELL_CYCLE	110	6.22E-20	5.54E-18
GOBP_POSITIVE_REGULATION_OF_TRANSCRIPTION_BY_RNA_POLYMERASE_II	83	8.62E-20	7.59E-18
GOBP_RESPONSE_TO_HORMONE	70	8.93E-20	7.77E-18
GOBP_CELL_CELL_SIGNALING	102	1.18E-19	1.02E-17
GOBP_REGULATION_OF_PROTEIN_KINASE_ACTIVITY	66	1.37E-19	1.16E-17
GOBP_MUSCLE_SYSTEM_PROCESS	49	1.80E-19	1.51E-17
GOBP_TRANSMEMBRANE_RECEPTOR_PROTEIN_TYROSINE_KINASE_SIGNALING_PATHWAY	63	2.35E-19	1.95E-17
GOBP_NEGATIVE_REGULATION_OF_TRANSCRIPTION_BY_RNA_POLYMERASE_II	69	2.80E-19	2.30E-17
GOBP_CELLULAR_RESPONSE_TO_OXYGEN_CONTAINING_COMPOUND	82	3.35E-19	2.73E-17
GOBP_REGULATION_OF_SUPRAMOLECULAR_FIBER_ORGANIZATION	44	3.41E-19	2.74E-17
GOBP_POSITIVE_REGULATION_OF_CELL_ADHESION	47	4.06E-19	3.23E-17
GOBP_REGULATION_OF_ACTIN_FILAMENT_ORGANIZATION	38	4.21E-19	3.32E-17
GOBP_POSITIVE_REGULATION_OF_TRANSPORT	69	5.13E-19	4.00E-17
GOBP_POSITIVE_REGULATION_OF_PROTEIN_MODIFICATION_PROCESS	76	7.10E-19	5.48E-17
GOBP_NEURON_DIFFERENTIATION	88	1.10E-18	8.39E-17
GOBP_IMMUNE_SYSTEM_DEVELOPMENT	73	1.18E-18	8.89E-17
GOBP_TISSUE_MORPHOGENESIS	57	1.26E-18	9.44E-17

Figure 94 Gene ontology analysis of genes upregulated in response to CD in NIH3T3 cells by TTseq

Gene ontology analysis of genes upregulated by CD treatment in NIH3T3 cells by TTseq. FDR<0.05. Relates to Figure 34B. Bioinformatic analysis of TTseq data was performed by Francesco Gualdrini.

GO BIOLOGICAL PROCESS	# Genes	p-value	FDR q-value
GOBP_SMALL_MOLECULE_METABOLIC_PROCESS	141	1.13E-30	8.48E-27
GOBP_LIPID_METABOLIC_PROCESS	116	2.21E-28	8.28E-25
GOBP_CELL_CYCLE	132	2.73E-26	6.81E-23
GOBP_NEGATIVE_REGULATION_OF_BIOSYNTHETIC_PROCESS	122	2.80E-25	5.23E-22
GOBP_CELLULAR_LIPID_METABOLIC_PROCESS	92	1.28E-24	1.92E-21
GOBP_CELLULAR_MACROMOLECULE_LOCALIZATION	133	1.63E-24	2.04E-21
GOBP_REGULATION_OF_INTRACELLULAR_SIGNAL_TRANSDUCTION	123	1.10E-23	1.18E-20
GOBP_NEGATIVE_REGULATION_OF_NUCLEOBASE_CONTAINING_COMPOUND_METABOLIC_PROCESS	110	7.45E-23	6.97E-20
GOBP_CELL_CYCLE_PROCESS	105	1.23E-22	1.02E-19
GOBP_CARBOHYDRATE_DERIVATIVE_METABOLIC_PROCESS	92	1.54E-22	1.16E-19
GOBP_POSITIVE_REGULATION_OF_NUCLEOBASE_CONTAINING_COMPOUND_METABOLIC_PROCESS	122	1.02E-21	6.41E-19
GOBP_CELL_POPULATION_PROLIFERATION	126	1.03E-21	6.41E-19
GOBP_POSITIVE_REGULATION_OF_BIOSYNTHETIC_PROCESS	126	1.12E-21	6.45E-19
GOBP_ORGANONITROGEN_COMPOUND_BIOSYNTHETIC_PROCESS	115	8.02E-20	4.28E-17
GOBP_HOMEOSTATIC_PROCESS	119	2.46E-19	1.23E-16
GOBP_REGULATION_OF_CELL_CYCLE	89	4.93E-19	2.30E-16
GOBP_REGULATION_OF_MULTICELLULAR_ORGANISMAL_DEVELOPMENT	97	5.51E-19	2.42E-16
GOBP_REGULATION_OF_CELL_DIFFERENTIATION	106	7.50E-19	3.12E-16
GOBP_ORGANOPHOSPHATE_METABOLIC_PROCESS	79	3.32E-18	1.31E-15
GOBP_APOPTOTIC_PROCESS	117	3.89E-18	1.46E-15
GOBP_ORGANONITROGEN_COMPOUND_CATABOLIC_PROCESS	92	6.64E-18	2.37E-15
GOBP_RESPONSE_TO_ENDOGENOUS_STIMULUS	104	8.00E-18	2.72E-15
GOBP_REGULATION_OF_CELL_DEATH	105	1.24E-17	4.02E-15
GOBP_RESPONSE_TO_OXYGEN_CONTAINING_COMPOUND	103	7.73E-17	2.41E-14
GOBP_CARBOHYDRATE_DERIVATIVE_BIOSYNTHETIC_PROCESS	60	9.94E-17	2.97E-14
GOBP_ORGANIC_ACID_METABOLIC_PROCESS	78	1.13E-16	3.25E-14
GOBP_ESTABLISHMENT_OF_PROTEIN_LOCALIZATION	115	1.80E-16	4.99E-14
GOBP_RESPONSE_TO_ABIOTIC_STIMULUS	84	1.97E-16	5.25E-14
GOBP_POSITIVE_REGULATION_OF_SIGNALING	104	4.71E-16	1.21E-13
GOBP_PROTEIN_CONTAINING_COMPLEX_SUBUNIT_ORGANIZATION	112	1.29E-15	3.19E-13
GOBP_CELLULAR_RESPONSE_TO_DNA_DAMAGE_STIMULUS	67	1.35E-15	3.19E-13
GOBP_CIRCULATORY_SYSTEM_DEVELOPMENT	79	1.36E-15	3.19E-13
GOBP_INTRACELLULAR_TRANSPORT	103	1.50E-15	3.39E-13
GOBP_REGULATION_OF_CATABOLIC_PROCESS	73	1.65E-15	3.62E-13
GOBP_ORGANOPHOSPHATE_BIOSYNTHETIC_PROCESS	53	2.29E-15	4.90E-13
GOBP_NEGATIVE_REGULATION_OF_RESPONSE_TO_STIMULUS	100	3.13E-15	6.50E-13
GOBP_REGULATION_OF_PROTEIN_MODIFICATION_PROCESS	98	3.76E-15	7.61E-13
GOBP_NEGATIVE_REGULATION_OF_TRANSCRIPTION_BY_RNA_POLYMERASE_II	66	5.38E-15	1.06E-12
GOBP_NEUROGENESIS	97	5.81E-15	1.11E-12
GOBP_MITOTIC_CELL_CYCLE	73	6.08E-15	1.14E-12
GOBP_POSITIVE_REGULATION_OF_TRANSCRIPTION_BY_RNA_POLYMERASE_II	79	8.76E-15	1.60E-12
GOBP_NEGATIVE_REGULATION_OF_DEVELOPMENTAL_PROCESS	68	9.91E-15	1.76E-12
GOBP_REGULATION_OF_CELL_CYCLE_PROCESS	61	2.33E-14	4.05E-12
GOBP_TUBE_DEVELOPMENT	74	2.53E-14	4.30E-12
GOBP_LIPID_BIOSYNTHETIC_PROCESS	58	2.86E-14	4.76E-12
GOBP_MONOCARBOXYLIC_ACID_METABOLIC_PROCESS	54	3.05E-14	4.96E-12
GOBP_NEGATIVE_REGULATION_OF_MULTICELLULAR_ORGANISMAL_PROCESS	74	6.05E-14	9.63E-12
GOBP_IMMUNE_SYSTEM_DEVELOPMENT	69	6.69E-14	1.04E-11
GOBP_EMBRYO_DEVELOPMENT	69	7.73E-14	1.18E-11
GOBP_MACROMOLECULE_CATABOLIC_PROCESS	87	8.14E-14	1.22E-11
GOBP_RESPONSE_TO_OXIDATIVE_STRESS	43	9.96E-14	1.46E-11
GOBP_PROTEOLYSIS	101	1.05E-13	1.51E-11
GOBP_PROTEIN_PHOSPHORYLATION	94	1.12E-13	1.58E-11
GOBP_CHROMOSOME_ORGANIZATION	79	1.40E-13	1.95E-11
GOBP_REGULATION_OF_ANATOMICAL_STRUCTURE_MORPHOGENESIS	69	1.50E-13	2.04E-11
GOBP_REGULATION_OF_CELLULAR_CATABOLIC_PROCESS	62	1.70E-13	2.27E-11
GOBP_CELLULAR_RESPONSE_TO_OXYGEN_CONTAINING_COMPOUND	76	2.25E-13	2.95E-11
GOBP_PROTEIN_LOCALIZATION_TO_ORGANELLE	68	3.08E-13	3.98E-11
GOBP_REGULATION_OF_RESPONSE_TO_STRESS	85	3.17E-13	4.02E-11
GOBP_NEGATIVE_REGULATION_OF_CELLULAR_COMPONENT_ORGANIZATION	56	3.57E-13	4.46E-11
GOBP_CELL_MIGRATION	92	4.29E-13	5.25E-11
GOBP_POSITIVE_REGULATION_OF_CELL_DIFFERENTIATION	61	4.40E-13	5.25E-11
GOBP_LOCOMOTION	106	4.42E-13	5.25E-11
GOBP_REGULATION_OF_MITOTIC_CELL_CYCLE	50	4.50E-13	5.26E-11
GOBP_REGULATION_OF_PHOSPHORUS_METABOLIC_PROCESS	92	5.68E-13	6.51E-11
GOBP_ALCOHOL_METABOLIC_PROCESS	38	5.75E-13	6.51E-11
GOBP_PROTEIN_MODIFICATION_BY_SMALL_PROTEIN_CONJUGATION_OR_REMOVAL	74	6.92E-13	7.72E-11
GOBP_POSITIVE_REGULATION_OF_DEVELOPMENTAL_PROCESS	79	7.09E-13	7.77E-11
GOBP_VASCULATURE_DEVELOPMENT	58	7.17E-13	7.77E-11
GOBP_REGULATION_OF_CELLULAR_RESPONSE_TO_STRESS	54	7.61E-13	8.13E-11
GOBP_NEGATIVE_REGULATION_OF_CELL_POPULATION_PROLIFERATION	56	1.25E-12	1.32E-10
GOBP_NEGATIVE_REGULATION_OF_CELL_CYCLE	50	1.42E-12	1.48E-10
GOBP_PROTEIN_CATABOLIC_PROCESS	64	2.24E-12	2.29E-10
GOBP_POSITIVE_REGULATION_OF_CELLULAR_COMPONENT_ORGANIZATION	71	2.54E-12	2.57E-10
GOBP_POSITIVE_REGULATION_OF_MULTICELLULAR_ORGANISMAL_PROCESS	82	2.89E-12	2.88E-10
GOBP_ORGANIC_HYDROXY_COMPOUND_METABOLIC_PROCESS	46	3.54E-12	3.48E-10
GOBP_CELL_CYCLE_PHASE_TRANSITION	50	3.82E-12	3.71E-10
GOBP_CELL_PROJECTION_ORGANIZATION	88	4.74E-12	4.53E-10
GOBP_REGULATION_OF_CELL_CYCLE_PHASE_TRANSITION	42	4.78E-12	4.53E-10
GOBP_TUBE_MORPHOGENESIS	61	6.60E-12	6.17E-10
GOBP_ENZYME_LINKED_RECEPTOR_PROTEIN_SIGNALING_PATHWAY	68	7.89E-12	7.29E-10
GOBP_RESPONSE_TO_RADIATION	40	8.17E-12	7.46E-10
GOBP_CELLULAR_MACROMOLECULE_CATABOLIC_PROCESS	73	9.32E-12	8.40E-10
GOBP_POSITIVE_REGULATION_OF_INTRACELLULAR_SIGNAL_TRANSDUCTION	65	1.01E-11	9.01E-10
GOBP_FATTY_ACID_METABOLIC_PROCESS	37	1.12E-11	9.88E-10
GOBP_SMALL_MOLECULE_CATABOLIC_PROCESS	39	1.14E-11	9.88E-10
GOBP_HEAD_DEVELOPMENT	54	1.15E-11	9.88E-10
GOBP_NEGATIVE_REGULATION_OF_CELL_DIFFERENTIATION	50	1.30E-11	1.10E-09
GOBP_INTRACELLULAR_PROTEIN_TRANSPORT	71	1.43E-11	1.20E-09
GOBP_NEGATIVE_REGULATION_OF_CELL_DEATH	64	1.56E-11	1.30E-09
GOBP_REGULATION_OF_ORGANELLE_ORGANIZATION	71	1.67E-11	1.37E-09
GOBP_PHOSPHOLIPID_METABOLIC_PROCESS	38	1.95E-11	1.59E-09
GOBP_POSITIVE_REGULATION_OF_MOLECULAR_FUNCTION	93	1.97E-11	1.59E-09
GOBP_RESPONSE_TO_UV	22	2.37E-11	1.88E-09
GOBP_MODIFICATION_DEPENDENT_MACROMOLECULE_CATABOLIC_PROCESS	49	2.76E-11	2.17E-09
GOBP_EMBRYO_DEVELOPMENT_ENDING_IN_BIRTH_OR_EGG_HATCHING	46	3.18E-11	2.48E-09
GOBP_RESPONSE_TO_LIPID	58	3.35E-11	2.58E-09
GOBP_RESPONSE_TO_NITROGEN_COMPOUND	68	4.77E-11	3.64E-09
GOBP_DNA_METABOLIC_PROCESS	61	5.71E-11	4.32E-09
GOBP_REGULATION_OF_TRANSPORT	91	6.54E-11	4.89E-09

Figure 95 Gene ontology analysis of genes downregulated in response to CD in NIH3T3 cells by TTseq

Gene ontology analysis of genes downregulated by CD treatment in NIH3T3 cells by TTseq. FDR<0.05. Relates to Figure 34. Bioinformatic analysis of TTseq data was performed by Francesco Gualdrini.

GO BIOLOGICAL PROCESS	# Genes	p-value	FDR q-value
GOBP_CYTOSKELETON_ORGANIZATION	203	7.16E-62	5.42E-58
GOBP_ACTIN_FILAMENT_BASED_PROCESS	146	1.57E-56	5.94E-53
GOBP_BIOLOGICAL_ADHESION	201	2.95E-56	7.45E-53
GOBP_CELL_MOTILITY	225	6.15E-56	1.16E-52
GOBP_REGULATION_OF_INTRACELLULAR_SIGNAL_TRANSDUCTION	223	6.69E-53	1.01E-49
GOBP_APOPTOTIC_PROCESS	229	2.89E-51	3.65E-48
GOBP_REGULATION_OF_CELL_DEATH	205	3.29E-47	3.55E-44
GOBP_ANATOMICAL_STRUCTURE_FORMATION_INVOLVED_IN_MORPHOGENESIS	164	4.93E-46	4.67E-43
GOBP_CELL_MORPHOGENESIS	151	1.15E-45	9.69E-43
GOBP_SUPRAMOLECULAR_FIBER_ORGANIZATION	123	6.43E-45	4.87E-42
GOBP_HOMEOSTATIC_PROCESS	211	1.16E-44	8.67E-42
GOBP_PROTEIN_PHOSPHORYLATION	191	1.31E-44	8.88E-42
GOBP_RESPONSE_TO_ENDOGENOUS_STIMULUS	191	2.69E-44	1.67E-41
GOBP_CIRCULATORY_SYSTEM_DEVELOPMENT	155	1.53E-43	8.17E-41
GOBP_ENZYME_LINKED_RECEPTOR_PROTEIN_SIGNALING_PATHWAY	148	2.27E-42	1.13E-39
GOBP_CELL_POPULATION_PROLIFERATION	208	1.39E-41	6.50E-39
GOBP_RESPONSE_TO_WOUNDING	112	4.66E-41	2.05E-38
GOBP_REGULATION_OF_PHOSPHORUS_METABOLIC_PROCESS	184	6.58E-41	2.73E-38
GOBP_POSITIVE_REGULATION_OF_SIGNALING	191	1.56E-40	6.15E-38
GOBP_REGULATION_OF_PROTEIN_MODIFICATION_PROCESS	182	3.43E-39	1.28E-36
GOBP_CELL_SUBSTRATE_ADHESION	81	6.41E-39	2.28E-36
GOBP_TUBE_DEVELOPMENT	143	1.30E-38	4.22E-36
GOBP_WOUND_HEALING	98	1.40E-38	4.37E-36
GOBP_REGULATION_OF_CELL_DIFFERENTIATION	179	6.72E-38	1.94E-35
GOBP_REGULATION_OF_PROTEIN_PHOSPHORYLATION	151	6.74E-38	1.94E-35
GOBP_ACTIN_FILAMENT_ORGANIZATION	87	1.76E-37	4.89E-35
GOBP_REGULATION_OF_CELLULAR_COMPONENT_MOVEMENT	142	2.51E-37	6.70E-35
GOBP_POSITIVE_REGULATION_OF_NUCLEOBASE_CONTAINING_COMPOUND_METABOLIC_PROCESS	193	4.21E-37	1.08E-34
GOBP_REGULATION_OF_TRANSPORT	184	1.13E-36	2.83E-34
GOBP_CELL_PROJECTION_ORGANIZATION	173	1.68E-36	4.05E-34
GOBP_MUSCLE_STRUCTURE_DEVELOPMENT	101	5.48E-36	1.28E-33
GOBP_POSITIVE_REGULATION_OF_BIOSYNTHETIC_PROCESS	197	5.98E-36	1.36E-33
GOBP_RESPONSE_TO_OXYGEN_CONTAINING_COMPOUND	177	1.33E-35	2.93E-33
GOBP_NEGATIVE_REGULATION_OF_SIGNALING	160	3.38E-35	7.23E-33
GOBP_NEGATIVE_REGULATION_OF_RESPONSE_TO_STIMULUS	177	5.73E-35	1.19E-32
GOBP_POSITIVE_REGULATION_OF_MOLECULAR_FUNCTION	180	3.76E-34	7.61E-32
GOBP_EXTERNAL_ENCAPSULATING_STRUCTURE_ORGANIZATION	79	5.62E-34	1.11E-31
GOBP_ANIMAL_ORGAN_MORPHOGENESIS	130	2.04E-33	3.91E-31
GOBP_TUBE_MORPHOGENESIS	120	5.94E-33	1.11E-30
GOBP_REGULATION_OF_MULTICELLULAR_ORGANISMAL_DEVELOPMENT	155	6.09E-33	1.11E-30
GOBP_POSITIVE_REGULATION_OF_DEVELOPMENTAL_PROCESS	147	9.79E-33	1.74E-30
GOBP_POSITIVE_REGULATION_OF_MULTICELLULAR_ORGANISMAL_PROCESS	154	2.06E-32	3.58E-30
GOBP_EPITHELIUM_DEVELOPMENT	144	1.93E-31	3.28E-29
GOBP_NEUROGENESIS	166	2.30E-31	3.82E-29
GOBP_POSITIVE_REGULATION_OF_INTRACELLULAR_SIGNAL_TRANSDUCTION	125	2.51E-31	4.09E-29
GOBP_POSITIVE_REGULATION_OF_PROTEIN_METABOLIC_PROCESS	160	4.36E-31	6.93E-29
GOBP_POSITIVE_REGULATION_OF_LOCOMOTION	92	6.47E-31	1.01E-28
GOBP_POSITIVE_REGULATION_OF_CATALYTIC_ACTIVITY	151	1.13E-30	1.72E-28
GOBP_RESPONSE_TO_GROWTH_FACTOR	103	2.16E-30	3.24E-28
GOBP_CELL_CELL_ADHESION	113	1.32E-29	1.93E-27
GOBP_CELL_CELL_SIGNALING	165	4.45E-29	6.40E-27
GOBP_REGULATION_OF_ORGANELLE_ORGANIZATION	132	5.39E-29	7.61E-27
GOBP_CELL_MORPHOGENESIS_INVOLVED_IN_DIFFERENTIATION	100	7.08E-29	9.82E-27
GOBP_CELL_ACTIVATION	151	9.63E-29	1.31E-26
GOBP_REGULATION_OF_RESPONSE_TO_STRESS	147	2.96E-28	3.96E-26
GOBP_NEURON_DIFFERENTIATION	143	4.28E-28	5.62E-26
GOBP_CELL_CYCLE	175	4.75E-28	6.13E-26
GOBP_POSITIVE_REGULATION_OF_PHOSPHORUS_METABOLIC_PROCESS	117	9.95E-28	1.26E-25
GOBP_TRANSMEMBRANE_RECEPTOR_PROTEIN_TYROSINE_KINASE_SIGNALING_PATHWAY	99	1.39E-27	1.73E-25
GOBP_POSITIVE_REGULATION_OF_CELLULAR_COMPONENT_ORGANIZATION	126	1.73E-27	2.12E-25
GOBP_CELL_MATRIX_ADHESION	54	2.88E-27	3.43E-25
GOBP_TRANSMEMBRANE_TRANSPORT	157	2.89E-27	3.43E-25
GOBP_VASCULATURE_DEVELOPMENT	102	3.55E-27	4.15E-25
GOBP_RESPONSE_TO_HORMONE	108	7.55E-27	8.69E-25
GOBP_EMBRYO_DEVELOPMENT	116	9.52E-27	1.08E-24
GOBP_POSITIVE_REGULATION_OF_PROTEIN_PHOSPHORYLATION	104	1.04E-26	1.17E-24
GOBP_REGULATION_OF_CELLULAR_COMPONENT_BIOGENESIS	113	1.95E-26	2.15E-24
GOBP_SECRETION	146	3.20E-26	3.46E-24
GOBP_REGULATION_OF_CELL_ADHESION	96	5.54E-26	5.92E-24
GOBP_LIPID_METABOLIC_PROCESS	143	6.25E-26	6.59E-24
GOBP_REGULATION_OF_ACTIN_FILAMENT_BASED_PROCESS	68	7.19E-26	7.47E-24
GOBP_CELLULAR_RESPONSE_TO_OXYGEN_CONTAINING_COMPOUND	127	8.80E-26	9.02E-24
GOBP_POSITIVE_REGULATION_OF_PROTEIN_MODIFICATION_PROCESS	118	1.20E-25	1.22E-23
GOBP_PROTEOLYSIS	165	1.33E-25	1.33E-23
GOBP_REGULATION_OF_HYDROLASE_ACTIVITY	134	1.52E-25	1.50E-23
GOBP_REGULATION_OF_ION_TRANSPORT	135	1.68E-25	1.63E-23
GOBP_CELL_JUNCTION_ORGANIZATION	92	4.67E-25	4.46E-23
GOBP_SMALL_MOLECULE_METABOLIC_PROCESS	169	4.71E-25	4.46E-23
GOBP_REGULATION_OF_CELL_SUBSTRATE_ADHESION	50	7.46E-25	6.98E-23
GOBP_SMALL_GTPASE_MEDIATED_SIGNAL_TRANSDUCTION	76	1.00E-24	9.26E-23
GOBP_NEURON_DEVELOPMENT	120	1.15E-24	1.05E-22
GOBP_HEART_DEVELOPMENT	80	1.73E-24	1.56E-22
GOBP_COAGULATION	62	3.17E-24	2.82E-22
GOBP_POSITIVE_REGULATION_OF_CELL_DEATH	87	3.63E-24	3.19E-22
GOBP_MUSCLE_TISSUE_DEVELOPMENT	64	4.25E-24	3.70E-22
GOBP_RESPONSE_TO_CYTOKINE	124	4.45E-24	3.83E-22
GOBP_TISSUE_MORPHOGENESIS	85	8.90E-24	7.57E-22
GOBP_CATION_TRANSPORT	121	1.19E-23	1.00E-21
GOBP_BLOOD_VESSEL_MORPHOGENESIS	88	1.22E-23	1.02E-21
GOBP_REGULATION_OF_TRANSFERASE_ACTIVITY	111	2.01E-23	1.66E-21
GOBP_RESPONSE_TO_NITROGEN_COMPOUND	118	2.18E-23	1.77E-21
GOBP_REGULATION_OF_PROTEIN_KINASE_ACTIVITY	96	2.38E-23	1.90E-21
GOBP_CELLULAR_COMPONENT_MORPHOGENESIS	94	2.38E-23	1.90E-21
GOBP_REGULATION_OF_BODY_FLUID_LEVELS	74	2.77E-23	2.18E-21
GOBP_NEGATIVE_REGULATION_OF_MOLECULAR_FUNCTION	121	2.87E-23	2.24E-21
GOBP_MAPK_CASCADE	104	3.15E-23	2.43E-21
GOBP_RESPONSE_TO_ABIOTIC_STIMULUS	124	3.38E-23	2.58E-21
GOBP_NEGATIVE_REGULATION_OF_CELL_DEATH	109	4.80E-23	3.63E-21
GOBP_NEGATIVE_REGULATION_OF_BIOSYNTHETIC_PROCESS	152	7.92E-23	5.92E-21

Figure 96 Gene ontology analysis of genes upregulated in response to LMB in NIH3T3 cells by TTseq

Gene ontology analysis of genes upregulated by LMB treatment in NIH3T3 cells by TTseq. FDR<0.05. Relates to Figure 37B. Bioinformatic analysis of TTseq data was performed by Francesco Gualdrini.

GO BIOLOGICAL PROCESS	# Genes	p-value	FDR q-value
GOBP_CELLULAR_MACROMOLECULE_LOCALIZATION	300	8.84E-74	6.61E-70
GOBP_INTRACELLULAR_TRANSPORT	264	3.08E-65	1.15E-61
GOBP_MACROMOLECULE_CATABOLIC_PROCESS	231	1.74E-61	4.33E-58
GOBP_ESTABLISHMENT_OF_PROTEIN_LOCALIZATION	275	3.31E-59	6.18E-56
GOBP_PROTEIN_MODIFICATION_BY_SMALL_PROTEIN_CONJUGATION_OR_REMOVAL	198	2.16E-56	3.23E-53
GOBP_CELLULAR_MACROMOLECULE_CATABOLIC_PROCESS	198	5.56E-54	6.93E-51
GOBP_ORGANONITROGEN_COMPOUND_BIOSYNTHETIC_PROCESS	244	4.59E-51	4.57E-48
GOBP_PROTEIN_CONTAINING_COMPLEX_SUBUNIT_ORGANIZATION	258	4.88E-51	4.57E-48
GOBP_PROTEIN_CATABOLIC_PROCESS	165	3.64E-48	3.03E-45
GOBP_CELL_CYCLE	244	2.24E-47	1.68E-44
GOBP_ORGANONITROGEN_COMPOUND_CATABOLIC_PROCESS	196	1.18E-45	8.06E-43
GOBP_REGULATION_OF_CATABOLIC_PROCESS	166	3.26E-45	2.03E-42
GOBP_PROTEIN_MODIFICATION_BY_SMALL_PROTEIN_CONJUGATION	161	5.79E-45	3.33E-42
GOBP_INTRACELLULAR_PROTEIN_TRANSPORT	179	1.64E-44	8.78E-42
GOBP_LIPID_METABOLIC_PROCESS	200	2.10E-43	1.05E-40
GOBP_SMALL_MOLECULE_METABOLIC_PROCESS	237	2.88E-43	1.35E-40
GOBP_CELLULAR_PROTEIN_CATABOLIC_PROCESS	142	1.04E-42	4.59E-40
GOBP_POSITIVE_REGULATION_OF_BIOSYNTHETIC_PROCESS	237	1.38E-40	5.74E-38
GOBP_POSITIVE_REGULATION_OF_NUCLEOBASE_CONTAINING_COMPOUND_METABOLIC_PROCESS	227	1.76E-39	6.94E-37
GOBP_PROTEIN_LOCALIZATION_TO_ORGANELLE	154	2.33E-38	8.60E-36
GOBP_PROTEOLYSIS	220	2.41E-38	8.60E-36
GOBP_REGULATION_OF_CELLULAR_CATABOLIC_PROCESS	140	3.30E-38	1.12E-35
GOBP_NEGATIVE_REGULATION_OF_BIOSYNTHETIC_PROCESS	209	3.39E-37	1.10E-34
GOBP_CHROMOSOME_ORGANIZATION	173	4.78E-37	1.49E-34
GOBP_NEGATIVE_REGULATION_OF_NUCLEOBASE_CONTAINING_COMPOUND_METABOLIC_PROCESS	195	8.63E-37	2.58E-34
GOBP_REGULATION_OF_INTRACELLULAR_SIGNAL_TRANSDUCTION	215	1.78E-36	5.02E-34
GOBP_CELL_CYCLE_PROCESS	186	1.81E-36	5.02E-34
GOBP_REGULATION_OF_ORGANELLE_ORGANIZATION	165	2.50E-36	6.68E-34
GOBP_REGULATION_OF_PROTEIN_MODIFICATION_PROCESS	202	4.90E-36	1.26E-33
GOBP_ORGANOPHOSPHATE_METABOLIC_PROCESS	152	7.28E-36	1.82E-33
GOBP_CELLULAR_LIPID_METABOLIC_PROCESS	155	7.81E-36	1.88E-33
GOBP_MODIFICATION_DEPENDENT_MACROMOLECULE_CATABOLIC_PROCESS	116	1.05E-34	2.45E-32
GOBP_REGULATION_OF_PHOSPHORUS_METABOLIC_PROCESS	197	2.87E-34	6.50E-32
GOBP_POSITIVE_REGULATION_OF_PROTEIN_METABOLIC_PROCESS	189	1.70E-33	3.74E-31
GOBP_APOPTOTIC_PROCESS	219	3.26E-33	6.97E-31
GOBP_PEPTIDYL_AMINO_ACID_MODIFICATION	167	8.04E-33	1.67E-30
GOBP_PROTEIN_PHOSPHORYLATION	194	1.23E-32	2.49E-30
GOBP_REGULATION_OF_PROTEIN_LOCALIZATION	132	5.38E-32	1.06E-29
GOBP_REGULATION_OF_CELLULAR_LOCALIZATION	126	9.74E-32	1.87E-29
GOBP_CELLULAR_RESPONSE_TO_DNA_DAMAGE_STIMULUS	131	1.12E-31	2.10E-29
GOBP_MITOTIC_CELL_CYCLE	145	1.33E-31	2.43E-29
GOBP_REGULATION_OF_CELLULAR_PROTEIN_LOCALIZATION	100	3.21E-31	5.66E-29
GOBP_CELLULAR_AMIDE_METABOLIC_PROCESS	157	3.25E-31	5.66E-29
GOBP_REGULATION_OF_CELL_CYCLE	159	3.74E-31	6.36E-29
GOBP_BIOLOGICAL_PROCESS_INVOLVED_IN_SYMBIOTIC_INTERACTION	141	4.76E-31	7.92E-29
GOBP_CELLULAR_PROTEIN_CONTAINING_COMPLEX_ASSEMBLY	149	2.36E-30	3.83E-28
GOBP_NCRNA_METABOLIC_PROCESS	93	2.88E-30	4.59E-28
GOBP_POSITIVE_REGULATION_OF_MOLECULAR_FUNCTION	198	4.84E-30	7.54E-28
GOBP_PROTEASOMAL_PROTEIN_CATABOLIC_PROCESS	91	1.34E-29	2.04E-27
GOBP_AMIDE_BIOSYNTHETIC_PROCESS	128	1.39E-29	2.08E-27
GOBP_REGULATION_OF_TRANSFERASE_ACTIVITY	139	2.17E-29	3.18E-27
GOBP_CELL_PROJECTION_ORGANIZATION	182	7.45E-29	1.07E-26
GOBP_POSITIVE_REGULATION_OF_CELLULAR_COMPONENT_ORGANIZATION	146	2.09E-28	2.94E-26
GOBP_NEGATIVE_REGULATION_OF_RESPONSE_TO_STIMULUS	188	5.18E-28	7.18E-26
GOBP_LIPID_BIOSYNTHETIC_PROCESS	112	5.51E-28	7.49E-26
GOBP_RESPONSE_TO_ENDOGENOUS_STIMULUS	184	7.47E-28	9.99E-26
GOBP_REGULATION_OF_CELL_DIFFERENTIATION	183	1.30E-27	1.71E-25
GOBP_REGULATION_OF_CELLULAR_COMPONENT_BIOGENESIS	131	1.61E-27	2.08E-25
GOBP_PHOSPHOLIPID_METABOLIC_PROCESS	81	3.36E-27	4.26E-25
GOBP_CHROMATIN_ORGANIZATION	117	7.32E-27	9.13E-25
GOBP_MEMBRANE_ORGANIZATION	129	8.01E-27	9.82E-25
GOBP_ORGANOPHOSPHATE_BIOSYNTHETIC_PROCESS	96	3.15E-26	3.81E-24
GOBP_MITOCHONDRION_ORGANIZATION	92	5.60E-26	6.57E-24
GOBP_REGULATION_OF_RESPONSE_TO_STRESS	164	5.62E-26	6.57E-24
GOBP_REGULATION_OF_CELL_DEATH	182	6.76E-26	7.78E-24
GOBP_REGULATION_OF_PROTEIN_PHOSPHORYLATION	148	8.72E-26	9.88E-24
GOBP_REGULATION_OF_TRANSPORT	186	2.03E-25	2.26E-23
GOBP_CARBOHYDRATE_DERIVATIVE_METABOLIC_PROCESS	141	2.47E-25	2.72E-23
GOBP_NEGATIVE_REGULATION_OF_PROTEIN_METABOLIC_PROCESS	139	2.76E-25	2.99E-23
GOBP_CELL_POPULATION_PROLIFERATION	201	5.10E-25	5.45E-23
GOBP_REGULATION_OF_CELLULAR_RESPONSE_TO_STRESS	104	6.88E-25	7.25E-23
GOBP_MRNA_METABOLIC_PROCESS	119	1.16E-24	1.20E-22
GOBP_NCRNA_PROCESSING	75	2.01E-24	2.06E-22
GOBP_GENERATION_OF_PRECURSOR_METABOLITES_AND_ENERGY	87	2.73E-24	2.76E-22
GOBP_CYTOSKELETON_ORGANIZATION	157	5.03E-24	5.02E-22
GOBP_POSITIVE_REGULATION_OF_CATALYTIC_ACTIVITY	158	9.51E-24	9.36E-22
GOBP_NEGATIVE_REGULATION_OF_SIGNALING	157	4.23E-23	4.11E-21
GOBP_REGULATION_OF_HYDROLASE_ACTIVITY	148	8.13E-23	7.80E-21
GOBP_DNA_METABOLIC_PROCESS	121	8.52E-23	8.07E-21
GOBP_NEUROGENESIS	171	9.40E-23	8.79E-21
GOBP_HOMEOSTATIC_PROCESS	192	1.00E-22	9.27E-21
GOBP_RESPONSE_TO_OXYGEN_CONTAINING_COMPOUND	173	2.20E-22	2.00E-20
GOBP_NEGATIVE_REGULATION_OF_CELLULAR_COMPONENT_ORGANIZATION	102	2.26E-22	2.04E-20
GOBP_REGULATION_OF_CELL_CYCLE_PROCESS	107	2.42E-22	2.16E-20
GOBP_NUCLEAR_TRANSPORT	66	2.71E-22	2.39E-20
GOBP_NEGATIVE_REGULATION_OF_PROTEIN_MODIFICATION_PROCESS	86	5.73E-22	4.99E-20
GOBP_NEGATIVE_REGULATION_OF_TRANSCRIPTION_BY_RNA_POLYMERASE_II	113	6.37E-22	5.48E-20
GOBP_REGULATION_OF_MULTICELLULAR_ORGANISMAL_DEVELOPMENT	153	8.54E-22	7.26E-20
GOBP_REGULATION_OF_CELL_PROJECTION_ORGANIZATION	92	1.12E-21	9.38E-20
GOBP_REGULATION_OF_ANATOMICAL_STRUCTURE_MORPHOGENESIS	123	1.35E-21	1.12E-19
GOBP_RESPONSE_TO_ABIOTIC_STIMULUS	139	1.50E-21	1.23E-19
GOBP_COVALENT_CHROMATIN_MODIFICATION	76	3.41E-21	2.77E-19
GOBP_ORGANELLE_LOCALIZATION	93	3.53E-21	2.84E-19
GOBP_REGULATION_OF_PROTEIN_KINASE_ACTIVITY	105	4.12E-21	3.28E-19
GOBP_RNA_PROCESSING	153	5.45E-21	4.29E-19
GOBP_REGULATION_OF_PROTEIN_CATABOLIC_PROCESS	68	6.63E-21	5.15E-19
GOBP_ALCOHOL_METABOLIC_PROCESS	67	6.68E-21	5.15E-19
GOBP_ORGANELLE_ASSEMBLY	111	7.92E-21	6.04E-19
GOBP_RIBONUCLEOPROTEIN_COMPLEX_BIOGENESIS	76	1.27E-20	9.57E-19
GOBP_CELLULAR_COMPONENT_DISASSEMBLY	84	1.45E-20	1.09E-18

Figure 97 Gene ontology analysis of genes downregulated in response to LMB treatment in NIH3T3 cells by TTseq

Gene ontology analysis of genes downregulated by LMB treatment in NIH3T3 cells by TTseq. FDR<0.05. Relates to Figure 37. Bioinformatic analysis of TTseq data was performed by Francesco Gualdrini.

GO BIOLOGICAL PROCESS	# Genes	p-value	FDR q-value
GOBP_ACTIN_FILAMENT_BASED_PROCESS	50	1.88E-30	1.42E-26
GOBP_CYTOSKELETON_ORGANIZATION	59	5.09E-27	1.93E-23
GOBP_CELL_MOTILITY	66	1.61E-26	4.07E-23
GOBP_RESPONSE_TO_CYTOKINE	54	1.39E-25	2.64E-22
GOBP_ANATOMICAL_STRUCTURE_FORMATION_INVOLVED_IN_MORPHOGENESIS	51	1.99E-23	3.02E-20
GOBP_SUPRAMOLECULAR_FIBER_ORGANIZATION	40	1.03E-22	1.31E-19
GOBP_APOPTOTIC_PROCESS	62	2.00E-21	2.17E-18
GOBP_REGULATION_OF_CELLULAR_COMPONENT_MOVEMENT	47	4.47E-21	4.23E-18
GOBP_BIOLOGICAL_ADHESION	53	5.49E-21	4.62E-18
GOBP_POSITIVE_REGULATION_OF_MULTICELLULAR_ORGANISMAL_PROCESS	58	3.60E-20	2.72E-17
GOBP_REGULATION_OF_CELL_DEATH	54	1.40E-19	8.03E-17
GOBP_CIRCULATORY_SYSTEM_DEVELOPMENT	45	1.53E-19	8.19E-17
GOBP_PROTEIN_PHOSPHORYLATION	53	2.29E-19	1.07E-16
GOBP_REGULATION_OF_RESPONSE_TO_STRESS	49	6.74E-19	2.97E-16
GOBP_POSITIVE_REGULATION_OF_SIGNALING	54	7.78E-19	3.23E-16
GOBP_RESPONSE_TO_ENDOGENOUS_STIMULUS	52	1.46E-18	5.74E-16
GOBP_WOUND_HEALING	31	2.70E-18	1.01E-15
GOBP_VASCULATURE_DEVELOPMENT	36	8.53E-18	3.04E-15
GOBP_BIOLOGICAL_PROCESS_INVOLVED_IN_SYMBIOTIC_INTERACTION	40	1.10E-17	3.74E-15
GOBP_RESPONSE_TO_WOUNDING	33	1.28E-17	4.16E-15
GOBP_REGULATION_OF_ANATOMICAL_STRUCTURE_MORPHOGENESIS	40	1.49E-17	4.66E-15
GOBP_REGULATION_OF_ACTIN_FILAMENT_ORGANIZATION	23	2.25E-17	6.73E-15
GOBP_REGULATION_OF_ACTIN_FILAMENT_BASED_PROCESS	26	5.21E-17	1.50E-14
GOBP_RESPONSE_TO_BIOTIC_STIMULUS	49	1.10E-16	3.05E-14
GOBP_POSITIVE_REGULATION_OF_GENE_EXPRESSION	40	1.42E-16	3.79E-14
GOBP_POSITIVE_REGULATION_OF_BIOSYNTHETIC_PROCESS	54	1.77E-16	4.56E-14
GOBP_POSITIVE_REGULATION_OF_LOCOMOTION	30	2.67E-16	6.52E-14
GOBP_REGULATION_OF_PROTEIN_PHOSPHORYLATION	42	2.70E-16	6.52E-14
GOBP_NEGATIVE_REGULATION_OF_CELL_DEATH	38	3.31E-16	7.74E-14
GOBP_POSITIVE_REGULATION_OF_INTRACELLULAR_SIGNAL_TRANSDUCTION	38	5.20E-16	1.18E-13
GOBP_ACTOMYOSIN_STRUCTURE_ORGANIZATION	19	6.05E-16	1.33E-13
GOBP_MUSCLE_STRUCTURE_DEVELOPMENT	30	7.17E-16	1.53E-13
GOBP_RESPONSE_TO_ORGANIC_CYCLIC_COMPOUND	36	7.38E-16	1.53E-13
GOBP_CYTOKINE_MEDIATED_SIGNALING_PATHWAY	34	7.55E-16	1.53E-13
GOBP_RESPONSE_TO_VIRUS	24	8.05E-16	1.58E-13
GOBP_REGULATION_OF_PROTEIN_MODIFICATION_PROCESS	48	8.54E-16	1.64E-13
GOBP_REGULATION_OF_SUPRAMOLECULAR_FIBER_ORGANIZATION	24	1.68E-15	3.14E-13
GOBP_POSITIVE_REGULATION_OF_PROTEIN_METABOLIC_PROCESS	46	1.75E-15	3.20E-13
GOBP_POSITIVE_REGULATION_OF_CELL_POPULATION_PROLIFERATION	36	2.27E-15	4.05E-13
GOBP_REGULATION_OF_PHOSPHORUS_METABOLIC_PROCESS	47	2.63E-15	4.57E-13
GOBP_REGULATION_OF_CYTOSKELETON_ORGANIZATION	27	4.08E-15	6.94E-13
GOBP_POSITIVE_REGULATION_OF_NUCLEOBASE_CONTAINING_COMPOUND_MET	50	7.08E-15	1.18E-12
GOBP_CELL_SUBSTRATE_ADHESION	23	8.62E-15	1.40E-12
GOBP_REGULATION_OF_ORGANELLE_ORGANIZATION	39	1.08E-14	1.68E-12
GOBP_CELL_CELL_ADHESION	34	1.08E-14	1.68E-12
GOBP_POSITIVE_REGULATION_OF_MOLECULAR_FUNCTION	48	1.20E-14	1.83E-12
GOBP_RESPONSE_TO_GROWTH_FACTOR	31	1.47E-14	2.20E-12
GOBP_CELL_MORPHOGENESIS	36	1.61E-14	2.36E-12
GOBP_TUBE_DEVELOPMENT	37	3.13E-14	4.50E-12
GOBP_CELL_ACTIVATION	43	3.49E-14	4.88E-12
GOBP_REGULATION_OF_TRANSPORT	47	3.68E-14	5.01E-12
GOBP_CELLULAR_COMPONENT_MORPHOGENESIS	31	5.11E-14	6.83E-12
GOBP_PROTEIN_CONTAINING_COMPLEX_SUBUNIT_ORGANIZATION	50	5.47E-14	7.18E-12
GOBP_BLOOD_VESSEL_MORPHOGENESIS	29	8.46E-14	1.09E-11
GOBP_ENZYME_LINKED_RECEPTOR_PROTEIN_SIGNALING_PATHWAY	36	1.13E-13	1.43E-11
GOBP_REGULATION_OF_ANATOMICAL_STRUCTURE_SIZE	25	1.16E-13	1.43E-11
GOBP_TUBE_MORPHOGENESIS	33	1.17E-13	1.43E-11
GOBP_RESPONSE_TO_OXYGEN_CONTAINING_COMPOUND	45	1.31E-13	1.58E-11
GOBP_EPITHELIUM_DEVELOPMENT	39	1.85E-13	2.20E-11
GOBP_NEGATIVE_REGULATION_OF_RESPONSE_TO_STIMULUS	45	1.95E-13	2.28E-11
GOBP_IMMUNE_EFFECTOR_PROCESS	39	3.07E-13	3.53E-11
GOBP_AMEBOIDAL_TYPE_CELL_MIGRATION	24	3.59E-13	4.07E-11
GOBP_CELL_PROJECTION_ORGANIZATION	43	3.68E-13	4.11E-11
GOBP_POSITIVE_REGULATION_OF_TRANSCRIPTION_BY_RNA_POLYMERASE_II	37	3.90E-13	4.29E-11
GOBP_DEFENSE_RESPONSE	46	5.04E-13	5.47E-11
GOBP_REGULATION_OF_CELL_ADHESION	29	5.89E-13	6.30E-11
GOBP_REGULATION_OF_CELLULAR_COMPONENT_BIOGENESIS	33	6.26E-13	6.59E-11
GOBP_TISSUE_MORPHOGENESIS	27	7.24E-13	7.52E-11
GOBP_NEGATIVE_REGULATION_OF_SIGNALING	40	9.28E-13	9.51E-11
GOBP_CELL_JUNCTION_ORGANIZATION	28	1.16E-12	1.17E-10
GOBP_CELLULAR_MACROMOLECULE_LOCALIZATION	48	1.22E-12	1.21E-10
GOBP_REGULATION_OF_CELLULAR_COMPONENT_SIZE	21	1.34E-12	1.32E-10
GOBP_ACTIN_FILAMENT_BUNDLE_ORGANIZATION	15	1.44E-12	1.40E-10
GOBP_POSITIVE_REGULATION_OF_CYTOSKELETON_ORGANIZATION	17	1.46E-12	1.40E-10
GOBP_NEURON_DEVELOPMENT	34	6.95E-12	6.58E-10
GOBP_POSITIVE_REGULATION_OF_CELLULAR_COMPONENT_ORGANIZATION	34	8.64E-12	8.08E-10
GOBP_RESPONSE_TO_HORMONE	30	8.86E-12	8.18E-10
GOBP_CELL_MORPHOGENESIS_INVOLVED_IN_DIFFERENTIATION	27	1.48E-11	1.35E-09
GOBP_NEUROGENESIS	41	1.51E-11	1.36E-09
GOBP_HOMEOSTATIC_PROCESS	45	1.77E-11	1.58E-09
GOBP_RESPONSE_TO_ABIOTIC_STIMULUS	35	1.90E-11	1.67E-09
GOBP_POSITIVE_REGULATION_OF_DEVELOPMENTAL_PROCESS	36	2.00E-11	1.74E-09
GOBP_MAPK_CASCADE	30	2.37E-11	2.04E-09
GOBP_ORGANONITROGEN_COMPOUND_BIOSYNTHETIC_PROCESS	43	2.57E-11	2.19E-09
GOBP_RESPONSE_TO_NITROGEN_COMPOUND	33	3.81E-11	3.20E-09
GOBP_REGULATION_OF_IMMUNE_SYSTEM_PROCESS	40	3.95E-11	3.28E-09
GOBP_PROTEIN_LOCALIZATION_TO_MEMBRANE	25	6.02E-11	4.95E-09
GOBP_REGULATION_OF_CELL_DIFFERENTIATION	40	6.28E-11	5.11E-09
GOBP_TISSUE_MIGRATION	19	7.08E-11	5.69E-09
GOBP_CELL_CELL_JUNCTION_ORGANIZATION	15	8.79E-11	7.00E-09
GOBP_REGULATION_OF_HYDROLASE_ACTIVITY	35	1.09E-10	8.58E-09
GOBP_ACTIN_POLYMERIZATION_OR_DEPOLYMERIZATION	15	1.31E-10	1.02E-08
GOBP_POSITIVE_REGULATION_OF_CELL_ADHESION	20	1.32E-10	1.02E-08
GOBP_REGULATION_OF_CELL_SUBSTRATE_ADHESION	15	1.59E-10	1.21E-08
GOBP_RESPONSE_TO_LIPID	28	1.64E-10	1.24E-08
GOBP_SECRETION	37	1.91E-10	1.43E-08

Figure 98 Gene ontology analysis of genes upregulated in response to CD treatment in dKO^{MRTF} cells by RNAseq

Gene ontology analysis of genes upregulated by CD treatment in dKO^{MRTF} cells by RNAseq. FDR<0.05. Relates to Figure 44. Bioinformatic analysis of RNAseq data was performed by Francesco Gualdrini.

GO BIOLOGICAL PROCESS	# Genes	p-value	FDR q-value
GOBP_LOCOMOTION	120	1.04E-49	7.75E-46
GOBP_CELL_MIGRATION	104	2.42E-45	9.05E-42
GOBP_REGULATION_OF_CELLULAR_COMPONENT_MOVEMENT	82	7.38E-40	1.84E-36
GOBP_NEUROGENESIS	97	2.31E-39	4.32E-36
GOBP_REGULATION_OF_CELL_DIFFERENTIATION	93	4.02E-36	6.02E-33
GOBP_POSITIVE_REGULATION_OF_DEVELOPMENTAL_PROCESS	82	5.54E-35	6.91E-32
GOBP_REGULATION_OF_MULTICELLULAR_ORGANISMAL_DEVELOPMENT	83	3.60E-33	3.85E-30
GOBP_NEURON_DIFFERENTIATION	81	1.69E-32	1.58E-29
GOBP_ANIMAL_ORGAN_MORPHOGENESIS	70	1.29E-31	1.07E-28
GOBP_RESPONSE_TO_ENDOGENOUS_STIMULUS	87	1.71E-31	1.28E-28
GOBP_CELL_POPULATION_PROLIFERATION	95	3.77E-31	2.56E-28
GOBP_CIRCULATORY_SYSTEM_DEVELOPMENT	71	1.36E-29	8.50E-27
GOBP_TUBE_DEVELOPMENT	69	2.66E-29	1.53E-26
GOBP_BIOLOGICAL_ADHESION	80	3.66E-29	1.85E-26
GOBP_CELL_CELL_SIGNALING	85	3.71E-29	1.85E-26
GOBP_ENZYME_LINKED_RECEPTOR_PROTEIN_SIGNALING_PATHWAY	67	5.07E-28	2.37E-25
GOBP_CELL_PROJECTION_ORGANIZATION	80	1.53E-27	6.73E-25
GOBP_POSITIVE_REGULATION_OF_MULTICELLULAR_ORGANISMAL_PROCESS	74	1.91E-26	7.93E-24
GOBP_RESPONSE_TO_GROWTH_FACTOR	54	4.10E-26	1.62E-23
GOBP_NEGATIVE_REGULATION_OF_RESPONSE_TO_STIMULUS	80	1.07E-25	4.02E-23
GOBP_POSITIVE_REGULATION_OF_CELL_DIFFERENTIATION	57	1.44E-25	5.12E-23
GOBP_NEGATIVE_REGULATION_OF_NUCLEOBASE_CONTAINING_COMPOUND_METABOLIC_PROCESS	75	6.28E-25	2.14E-22
GOBP_NEURON_DEVELOPMENT	64	6.82E-25	2.22E-22
GOBP_NEGATIVE_REGULATION_OF_MULTICELLULAR_ORGANISMAL_PROCESS	63	2.98E-24	9.29E-22
GOBP_NEGATIVE_REGULATION_OF_BIOSYNTHETIC_PROCESS	78	3.72E-24	1.11E-21
GOBP_REGULATION_OF_ANATOMICAL_STRUCTURE_MORPHOGENESIS	60	4.30E-24	1.24E-21
GOBP_GROWTH	57	5.31E-24	1.47E-21
GOBP_EMBRYO_DEVELOPMENT	59	1.22E-23	3.25E-21
GOBP_POSITIVE_REGULATION_OF_SIGNALING	78	1.53E-23	3.94E-21
GOBP_CELL_SURFACE_RECEPTOR_SIGNALING_PATHWAY_INVOLVED_IN_CELL_CELL_SIGNALING	47	1.64E-23	4.10E-21
GOBP_TUBE_MORPHOGENESIS	56	2.09E-23	5.04E-21
GOBP_REGULATION_OF_INTRACELLULAR_SIGNAL_TRANSDUCTION	79	2.69E-23	6.29E-21
GOBP_CELL_CELL_SIGNALING_BY_WNT	43	4.61E-23	1.05E-20
GOBP_REGULATION_OF_PHOSPHORUS_METABOLIC_PROCESS	74	9.37E-23	2.06E-20
GOBP_POSITIVE_REGULATION_OF_TRANSCRIPTION_BY_RNA_POLYMERASE_II	63	9.79E-23	2.09E-20
GOBP_HEART_DEVELOPMENT	44	1.21E-22	2.51E-20
GOBP_NEGATIVE_REGULATION_OF_TRANSCRIPTION_BY_RNA_POLYMERASE_II	54	1.68E-22	3.40E-20
GOBP_REGULATION_OF_PROTEIN_MODIFICATION_PROCESS	74	1.73E-22	3.41E-20
GOBP_SKELETAL_SYSTEM_DEVELOPMENT	41	3.31E-22	6.34E-20
GOBP_ACTIN_FILAMENT_BASED_PROCESS	51	4.37E-22	8.17E-20
GOBP_DEVELOPMENTAL_GROWTH	45	5.08E-22	9.27E-20
GOBP_CELL_MORPHOGENESIS	57	6.85E-22	1.22E-19
GOBP_POSITIVE_REGULATION_OF_NUCLEOBASE_CONTAINING_COMPOUND_METABOLIC_PROCESS	78	1.34E-21	2.34E-19
GOBP_POSITIVE_REGULATION_OF_BIOSYNTHETIC_PROCESS	80	1.98E-21	3.36E-19
GOBP_NEGATIVE_REGULATION_OF_LOCOMOTION	36	2.16E-21	3.60E-19
GOBP_REGULATION_OF_CELL_PROJECTION_ORGANIZATION	45	2.25E-21	3.66E-19
GOBP_NEGATIVE_REGULATION_OF_DEVELOPMENTAL_PROCESS	54	2.91E-21	4.64E-19
GOBP_REGULATION_OF_CELLULAR_COMPONENT_BIOGENESIS	54	1.17E-20	1.83E-18
GOBP_VASCULATURE_DEVELOPMENT	49	1.29E-20	1.97E-18
GOBP_CELLULAR_COMPONENT_MORPHOGENESIS	48	2.64E-20	3.95E-18
GOBP_RESPONSE_TO_OXYGEN_CONTAINING_COMPOUND	71	3.40E-20	4.98E-18
GOBP_TAXIS	44	4.02E-20	5.79E-18
GOBP_CELL_PART_MORPHOGENESIS	45	4.87E-20	6.87E-18
GOBP_ANATOMICAL_STRUCTURE_FORMATION_INVOLVED_IN_MORPHOGENESIS	58	5.99E-20	8.29E-18
GOBP_OSSIFICATION	35	1.23E-19	1.68E-17
GOBP_POSITIVE_REGULATION_OF_MOLECULAR_FUNCTION	72	1.58E-19	2.11E-17
GOBP_PROTEIN_PHOSPHORYLATION	69	1.63E-19	2.14E-17
GOBP_TRANSMEMBRANE_RECEPTOR_PROTEIN_SERINE_THREONINE_KINASE_SIGNALING_PATHWAY	33	3.09E-19	3.98E-17
GOBP_CELL_GROWTH	37	4.13E-19	5.23E-17
GOBP_EPITHELIUM_DEVELOPMENT	60	5.09E-19	6.34E-17
GOBP_MORPHOGENESIS_OF_AN_EPITHELIUM	39	5.61E-19	6.88E-17
GOBP_APOPTOTIC_PROCESS	75	7.58E-19	9.02E-17
GOBP_NEGATIVE_REGULATION_OF_CELL_DIFFERENTIATION	43	7.62E-19	9.02E-17
GOBP_NEGATIVE_REGULATION_OF_SIGNALING	63	7.71E-19	9.02E-17
GOBP_APPENDAGE_DEVELOPMENT	24	8.59E-19	9.88E-17
GOBP_TISSUE_MORPHOGENESIS	42	9.16E-19	1.04E-16
GOBP_APPENDAGE_MORPHOGENESIS	22	1.28E-18	1.43E-16
GOBP_CIRCULATORY_SYSTEM_PROCESS	41	1.44E-18	1.59E-16
GOBP_CELL_MORPHOGENESIS_INVOLVED_IN_NEURON_DIFFERENTIATION	40	1.48E-18	1.60E-16
GOBP_POSITIVE_REGULATION_OF_LOCOMOTION	40	2.12E-18	2.26E-16
GOBP_HEAD_DEVELOPMENT	45	2.25E-18	2.37E-16
GOBP_CELL_MORPHOGENESIS_INVOLVED_IN_DIFFERENTIATION	44	3.23E-18	3.35E-16
GOBP_CENTRAL_NERVOUS_SYSTEM_DEVELOPMENT	51	4.46E-18	4.57E-16
GOBP_EMBRYONIC_MORPHOGENESIS	39	5.28E-18	5.33E-16
GOBP_UROGENITAL_SYSTEM_DEVELOPMENT	30	8.36E-18	8.34E-16
GOBP_REGULATION_OF_NEURON_PROJECTION_DEVELOPMENT	34	8.90E-18	8.76E-16
GOBP_BLOOD_VESSEL_MORPHOGENESIS	42	9.79E-18	9.44E-16
GOBP_REGULATION_OF_GROWTH	41	9.84E-18	9.44E-16
GOBP_POSITIVE_REGULATION_OF_CATALYTIC_ACTIVITY	61	1.06E-17	1.00E-15
GOBP_NEGATIVE_REGULATION_OF_CELL_POPULATION_PROLIFERATION	44	1.39E-17	1.30E-15
GOBP_REGULATION_OF_PROTEIN_PHOSPHORYLATION	56	1.82E-17	1.69E-15
GOBP_FOREBRAIN_DEVELOPMENT	31	2.10E-17	1.91E-15
GOBP_AMEBOIDAL_TYPE_CELL_MIGRATION	35	2.67E-17	2.40E-15
GOBP_CELL_JUNCTION_ORGANIZATION	42	3.06E-17	2.73E-15
GOBP_REGULATION_OF_NERVOUS_SYSTEM_DEVELOPMENT	33	4.36E-17	3.84E-15
GOBP_POSITIVE_REGULATION_OF_CELLULAR_COMPONENT_ORGANIZATION	53	5.02E-17	4.37E-15
GOBP_CYTOSKELETON_ORGANIZATION	59	8.47E-17	7.28E-15
GOBP_EMBRYONIC_APPENDAGE_MORPHOGENESIS	19	1.54E-16	1.31E-14
GOBP_MESENCHYMAL_CELL_DIFFERENTIATION	25	1.62E-16	1.36E-14
GOBP_AXON_DEVELOPMENT	35	2.26E-16	1.88E-14
GOBP_POSITIVE_REGULATION_OF_INTRACELLULAR_SIGNAL_TRANSDUCTION	49	2.76E-16	2.27E-14
GOBP_REGULATION_OF_HYDROLASE_ACTIVITY	56	3.62E-16	2.94E-14
GOBP_EXTERNAL_ENCAPSULATING_STRUCTURE_ORGANIZATION	31	3.86E-16	3.11E-14
GOBP_RESPONSE_TO_LIPID	45	4.65E-16	3.70E-14
GOBP_REGULATION_OF_CELL_DEATH	64	5.15E-16	4.05E-14
GOBP_POSITIVE_REGULATION_OF_PROTEIN_METABOLIC_PROCESS	61	5.71E-16	4.45E-14
GOBP_DEVELOPMENTAL_GROWTH_INVOLVED_IN_MORPHOGENESIS	24	9.12E-16	7.03E-14
GOBP_SYNAPSE_ORGANIZATION	31	1.16E-15	8.83E-14
GOBP_NEURON_PROJECTION_GUIDANCE	26	1.41E-15	1.07E-13
GOBP_CANONICAL_WNT_SIGNALING_PATHWAY	28	1.74E-15	1.30E-13

Figure 99 Gene ontology analysis of genes downregulated in response to CD treatment in dKO^{MRTF} cells by RNAseq

Gene ontology analysis of genes downregulated by CD treatment in dKO^{MRTF} cells by RNAseq. FDR<0.05. Relates to Figure 44. Bioinformatic analysis of RNAseq data was performed by Francesco Gualdrini.

GO BIOLOGOCAL PROCESS	# Genes	p-value	FDR q-value
GOBP_REGULATION_OF_CELL_DIFFERENTIATION	366	6.75E-134	5.11E-130
GOBP_CYTOSKELETON_ORGANIZATION	306	1.93E-129	7.32E-126
GOBP_NEUROGENESIS	321	1.02E-118	2.56E-115
GOBP_POSITIVE_REGULATION_OF_NUCLEOBASE_CONTAINING_COMPOUND_METABOLIC_PROCESS	327	6.39E-110	1.21E-106
GOBP_POSITIVE_REGULATION_OF_MULTICELLULAR_ORGANISMAL_PROCESS	321	5.06E-106	7.67E-103
GOBP_NEURON_DIFFERENTIATION	277	1.44E-104	1.82E-101
GOBP_POSITIVE_REGULATION_OF_DEVELOPMENTAL_PROCESS	281	4.31E-103	4.66E-100
GOBP_POSITIVE_REGULATION_OF_BIOSYNTHETIC_PROCESS	325	1.31E-101	1.24E-98
GOBP_CELL_CYCLE	317	2.67E-101	2.25E-98
GOBP_CELL_MOTILITY	311	5.92E-101	4.48E-98
GOBP_CELL_MIGRATION	287	7.91E-98	7.39E-95
GOBP_REGULATION_OF_MULTICELLULAR_ORGANISMAL_DEVELOPMENT	264	4.36E-95	3.26E-92
GOBP_CELL_PROJECTION_ORGANIZATION	276	4.30E-92	2.93E-89
GOBP_NEURON_DEVELOPMENT	230	6.76E-91	4.21E-88
GOBP_BIOLOGICAL_ADHESION	265	7.52E-90	4.02E-87
GOBP_CELL_MORPHOGENESIS	217	2.98E-89	1.49E-86
GOBP_RESPONSE_TO_ENDOGENOUS_STIMULUS	274	6.26E-87	2.93E-84
GOBP_REGULATION_OF_ORGANELLE_ORGANIZATION	229	1.40E-85	6.18E-83
GOBP_POSITIVE_REGULATION_OF_CELLULAR_COMPONENT_ORGANIZATION	221	5.42E-83	2.25E-80
GOBP_TUBE_DEVELOPMENT	214	4.20E-80	1.65E-77
GOBP_NEGATIVE_REGULATION_OF_BIOSYNTHETIC_PROCESS	269	1.09E-79	4.07E-77
GOBP_ENZYME_LINKED_RECEPTOR_PROTEIN_SIGNALING_PATHWAY	211	8.85E-79	3.01E-76
GOBP_REGULATION_OF_PHOSPHORUS_METABOLIC_PROCESS	261	9.71E-79	3.16E-76
GOBP_CELL_CYCLE_PROCESS	243	2.64E-78	8.22E-76
GOBP_CELLULAR_COMPONENT_MORPHOGENESIS	178	3.02E-78	9.05E-76
GOBP_NEGATIVE_REGULATION_OF_NUCLEOBASE_CONTAINING_COMPOUND_METABOLIC_PROCESS	252	4.62E-78	1.33E-75
GOBP_CELL_POPULATION_PROLIFERATION	289	5.91E-78	1.64E-75
GOBP_REGULATION_OF_INTRACELLULAR_SIGNAL_TRANSDUCTION	274	1.68E-77	4.48E-75
GOBP_CIRCULATORY_SYSTEM_DEVELOPMENT	216	1.82E-77	4.71E-75
GOBP_MITOTIC_CELL_CYCLE	205	3.13E-77	7.81E-75
GOBP_POSITIVE_REGULATION_OF_MOLECULAR_FUNCTION	269	2.54E-76	6.13E-74
GOBP_ACTIN_FILAMENT_BASED_PROCESS	178	5.83E-76	1.36E-73
GOBP_REGULATION_OF_CELLULAR_COMPONENT_MOVEMENT	210	7.08E-76	1.60E-73
GOBP_PROTEIN_PHOSPHORYLATION	257	1.13E-75	2.50E-73
GOBP_REGULATION_OF_PROTEIN_MODIFICATION_PROCESS	256	2.29E-74	4.89E-72
GOBP_ANATOMICAL_STRUCTURE_FORMATION_INVOLVED_IN_MORPHOGENESIS	212	2.61E-74	5.42E-72
GOBP_APOPTOTIC_PROCESS	279	7.41E-73	1.50E-70
GOBP_EMBRYO_DEVELOPMENT	194	8.34E-72	1.64E-69
GOBP_TUBE_MORPHOGENESIS	184	2.78E-71	5.34E-69
GOBP_CELL_PART_MORPHOGENESIS	159	2.52E-70	4.72E-68
GOBP_REGULATION_OF_ANATOMICAL_STRUCTURE_MORPHOGENESIS	193	5.62E-70	1.03E-67
GOBP_CELLULAR_MACROMOLECULE_LOCALIZATION	278	9.45E-70	1.68E-67
GOBP_REGULATION_OF_CELL_CYCLE	212	1.48E-69	2.58E-67
GOBP_CELL_MORPHOGENESIS_INVOLVED_IN_DIFFERENTIATION	163	1.56E-69	2.65E-67
GOBP_NEGATIVE_REGULATION_OF_RESPONSE_TO_STIMULUS	251	1.49E-68	2.47E-66
GOBP_REGULATION_OF_CELLULAR_COMPONENT_BIOGENESIS	186	2.43E-68	3.94E-66
GOBP_EPITHELIUM_DEVELOPMENT	212	1.80E-65	2.86E-63
GOBP_GROWTH	177	3.40E-65	5.30E-63
GOBP_RESPONSE_TO_OXYGEN_CONTAINING_COMPOUND	244	4.15E-65	6.33E-63
GOBP_REGULATION_OF_CELL_DEATH	244	7.55E-65	1.13E-62
GOBP_SUPRAMOLECULAR_FIBER_ORGANIZATION	156	8.68E-65	1.27E-62
GOBP_CHROMOSOME_ORGANIZATION	207	6.01E-64	8.65E-62
GOBP_MICROTUBULE_BASED_PROCESS	169	6.32E-64	8.92E-62
GOBP_RESPONSE_TO_GROWTH_FACTOR	157	7.71E-64	1.07E-61
GOBP_POSITIVE_REGULATION_OF_TRANSCRIPTION_BY_RNA_POLYMERASE_II	201	8.43E-64	1.15E-61
GOBP_VASCULATURE_DEVELOPMENT	162	3.39E-63	4.53E-61
GOBP_ANIMAL_ORGAN_MORPHOGENESIS	185	1.14E-62	1.49E-60
GOBP_POSITIVE_REGULATION_OF_PROTEIN_METABOLIC_PROCESS	228	1.30E-61	1.67E-59
GOBP_MICROTUBULE_CYTOSKELETON_ORGANIZATION	138	4.79E-61	6.07E-59
GOBP_REGULATION_OF_CYTOSKELETON_ORGANIZATION	128	2.32E-60	2.89E-58
GOBP_CELL_JUNCTION_ORGANIZATION	149	4.03E-60	4.95E-58
GOBP_NEGATIVE_REGULATION_OF_SIGNALING	215	1.04E-59	1.26E-57
GOBP_NEGATIVE_REGULATION_OF_TRANSCRIPTION_BY_RNA_POLYMERASE_II	165	8.05E-59	9.55E-57
GOBP_DEVELOPMENTAL_GROWTH	137	1.15E-58	1.35E-56
GOBP_CELL_MORPHOGENESIS_INVOLVED_IN_NEURON_DIFFERENTIATION	133	9.58E-58	1.10E-55
GOBP_POSITIVE_REGULATION_OF_CELL_DIFFERENTIATION	160	3.83E-57	4.34E-55
GOBP_CENTRAL_NERVOUS_SYSTEM_DEVELOPMENT	173	4.19E-57	4.68E-55
GOBP_PEPTIDYL_AMINO_ACID_MODIFICATION	198	1.83E-56	2.01E-54
GOBP_POSITIVE_REGULATION_OF_CATALYTIC_ACTIVITY	209	2.84E-56	3.08E-54
GOBP_POSITIVE_REGULATION_OF_SIGNALING	233	5.59E-55	5.97E-53
GOBP_CELL_DIVISION	131	3.80E-54	4.01E-52
GOBP_REGULATION_OF_HYDROLASE_ACTIVITY	196	1.20E-53	1.25E-51
GOBP_AXON_DEVELOPMENT	120	1.24E-53	1.27E-51
GOBP_TISSUE_MORPHOGENESIS	134	1.28E-53	1.30E-51
GOBP_CELLULAR_RESPONSE_TO_OXYGEN_CONTAINING_COMPOUND	186	1.48E-53	1.47E-51
GOBP_NEGATIVE_REGULATION_OF_DEVELOPMENTAL_PROCESS	163	1.80E-53	1.77E-51
GOBP_REGULATION_OF_CELL_ADHESION	143	9.74E-53	9.46E-51
GOBP_REGULATION_OF_PROTEIN_PHOSPHORYLATION	187	1.39E-52	1.34E-50
GOBP_CELL_CELL_SIGNALING	224	3.57E-52	3.38E-50
GOBP_HEAD_DEVELOPMENT	144	3.92E-52	3.67E-50
GOBP_EMBRYONIC_MORPHOGENESIS	125	5.35E-52	4.94E-50
GOBP_MORPHOGENESIS_OF_AN_EPITHELIUM	121	5.59E-52	5.10E-50
GOBP_CELL_CELL_ADHESION	156	1.04E-51	9.38E-50
GOBP_ESTABLISHMENT_OF_PROTEIN_LOCALIZATION	246	2.88E-51	2.56E-49
GOBP_HOMEOSTATIC_PROCESS	240	7.55E-51	6.65E-49
GOBP_INTRACELLULAR_TRANSPORT	226	9.46E-51	8.23E-49
GOBP_RESPONSE_TO_HORMONE	154	1.46E-50	1.26E-48
GOBP_REGULATION_OF_TRANSPORT	225	3.45E-50	2.93E-48
GOBP_BLOOD_VESSEL_MORPHOGENESIS	134	4.03E-50	3.39E-48
GOBP_REGULATION_OF_CELL_CYCLE_PROCESS	145	4.77E-50	3.96E-48
GOBP_PROTEIN_CONTAINING_COMPLEX_SUBUNIT_ORGANIZATION	242	4.93E-50	4.06E-48
GOBP_REGULATION_OF_CELLULAR_LOCALIZATION	147	6.79E-50	5.52E-48
GOBP_POSITIVE_REGULATION_OF_PROTEIN_MODIFICATION_PROCESS	168	2.81E-49	2.26E-47
GOBP_POSITIVE_REGULATION_OF_GENE_EXPRESSION	170	3.29E-49	2.62E-47
GOBP_MACROMOLECULE_CATABOLIC_PROCESS	199	7.93E-49	6.24E-47
GOBP_REGULATION_OF_TRANSFERASE_ACTIVITY	163	2.27E-48	1.77E-46
GOBP_MUSCLE_STRUCTURE_DEVELOPMENT	124	5.86E-48	4.52E-46
GOBP_POSITIVE_REGULATION_OF_PHOSPHORUS_METABOLIC_PROCESS	159	1.98E-47	1.51E-45
GOBP_REGULATION_OF_CATABOLIC_PROCESS	161	2.75E-47	2.08E-45
GOBP_POSITIVE_REGULATION_OF_LOCOMOTION	120	1.26E-46	9.43E-45

Figure 100 Gene ontology analysis of genes upregulated in response to CD in dKO$^{MRTF\text{-}NLS}$ cells by RNAseq

Gene ontology analysis of genes upregulated by CD treatment in dKO$^{MRTF\text{-}NLS}$ cells by RNAseq. FDR<0.05. Relates to Figure 45. Bioinformatic analysis of RNAseq data was performed by Francesco Gualdrini.

GO BIOLOGOCAL PROCESS	# Genes	p-value	FDR q-value
GOBP_NEGATIVE_REGULATION_OF_BIOSYNTHETIC_PROCESS	45	4.02E-17	2.36E-13
GOBP_BIOLOGICAL_ADHESION	42	6.32E-17	2.36E-13
GOBP_RESPONSE_TO_VIRUS	22	6.61E-16	1.65E-12
GOBP_EXTERNAL_ENCAPSULATING_STRUCTURE_ORGANIZATION	22	5.30E-15	9.92E-12
GOBP_RESPONSE_TO_CYTOKINE	35	1.07E-14	1.60E-11
GOBP_NEGATIVE_REGULATION_OF_NUCLEOBASE_CONTAINING_COMPOUND_METABOLIC_PROCESS	39	2.29E-14	2.86E-11
GOBP_RESPONSE_TO_ENDOGENOUS_STIMULUS	40	3.91E-14	4.18E-11
GOBP_REGULATION_OF_MULTICELLULAR_ORGANISMAL_DEVELOPMENT	37	4.50E-14	4.21E-11
GOBP_RESPONSE_TO_TYPE_I_INTERFERON	13	5.13E-14	4.26E-11
GOBP_REGULATION_OF_CELL_ADHESION	27	8.21E-14	6.14E-11
GOBP_CYTOKINE_MEDIATED_SIGNALING_PATHWAY	28	1.09E-13	7.40E-11
GOBP_REGULATION_OF_CELL_DIFFERENTIATION	39	1.67E-13	1.04E-10
GOBP_INTERFERON_GAMMA_MEDIATED_SIGNALING_PATHWAY	12	3.63E-13	2.09E-10
GOBP_CELL_POPULATION_PROLIFERATION	42	7.68E-13	4.10E-10
GOBP_RESPONSE_TO_INTERFERON_GAMMA	15	1.33E-12	6.62E-10
GOBP_RESPONSE_TO_BIOTIC_STIMULUS	37	2.85E-12	1.33E-09
GOBP_ANATOMICAL_STRUCTURE_FORMATION_INVOLVED_IN_MORPHOGENESIS	31	3.35E-12	1.44E-09
GOBP_NEGATIVE_REGULATION_OF_DEVELOPMENTAL_PROCESS	28	3.47E-12	1.44E-09
GOBP_TUBE_DEVELOPMENT	30	4.89E-12	1.93E-09
GOBP_DEFENSE_RESPONSE_TO_VIRUS	16	6.54E-12	2.38E-09
GOBP_RESPONSE_TO_OXYGEN_CONTAINING_COMPOUND	37	6.69E-12	2.38E-09
GOBP_NEGATIVE_REGULATION_OF_VIRAL_PROCESS	11	7.35E-12	2.43E-09
GOBP_REGULATION_OF_VIRAL_LIFE_CYCLE	13	7.47E-12	2.43E-09
GOBP_CELL_SUBSTRATE_ADHESION	18	9.44E-12	2.94E-09
GOBP_POSITIVE_REGULATION_OF_NUCLEOBASE_CONTAINING_COMPOUND_METABOLIC_PROCESS	39	1.12E-11	3.36E-09
GOBP_POSITIVE_REGULATION_OF_BIOSYNTHETIC_PROCESS	40	1.34E-11	3.87E-09
GOBP_DEFENSE_RESPONSE	38	1.56E-11	4.33E-09
GOBP_CIRCULATORY_SYSTEM_DEVELOPMENT	30	1.65E-11	4.41E-09
GOBP_REGULATION_OF_BIOLOGICAL_PROCESS_INVOLVED_IN_SYMBIOTIC_INTERACTION	14	2.05E-11	5.29E-09
GOBP_NEGATIVE_REGULATION_OF_CELL_DIFFERENTIATION	23	2.14E-11	5.33E-09
GOBP_BLOOD_VESSEL_MORPHOGENESIS	23	3.23E-11	7.81E-09
GOBP_NEGATIVE_REGULATION_OF_MULTICELLULAR_ORGANISMAL_PROCESS	29	3.85E-11	9.00E-09
GOBP_POSITIVE_REGULATION_OF_DEVELOPMENTAL_PROCESS	31	6.31E-11	1.43E-08
GOBP_ENZYME_LINKED_RECEPTOR_PROTEIN_SIGNALING_PATHWAY	28	9.77E-11	2.15E-08
GOBP_VASCULATURE_DEVELOPMENT	24	1.05E-10	2.24E-08
GOBP_NEGATIVE_REGULATION_OF_SIGNALING	32	1.41E-10	2.93E-08
GOBP_NEGATIVE_REGULATION_OF_TRANSCRIPTION_BY_RNA_POLYMERASE_II	25	1.56E-10	3.15E-08
GOBP_NEGATIVE_REGULATION_OF_RESPONSE_TO_STIMULUS	35	1.62E-10	3.18E-08
GOBP_CELL_MIGRATION	34	2.09E-10	4.02E-08
GOBP_TUBE_MORPHOGENESIS	25	2.99E-10	5.60E-08
GOBP_POSITIVE_REGULATION_OF_CELL_DIFFERENTIATION	24	4.35E-10	7.95E-08
GOBP_VIRAL_LIFE_CYCLE	16	4.90E-10	8.56E-08
GOBP_POSITIVE_REGULATION_OF_MULTICELLULAR_ORGANISMAL_PROCESS	31	4.92E-10	8.56E-08
GOBP_REGULATION_OF_ANATOMICAL_STRUCTURE_MORPHOGENESIS	26	5.96E-10	1.01E-07
GOBP_REGULATION_OF_CELL_SUBSTRATE_ADHESION	13	9.45E-10	1.57E-07
GOBP_POSITIVE_REGULATION_OF_MOLECULAR_FUNCTION	34	1.87E-09	3.02E-07
GOBP_APOPTOTIC_PROCESS	36	1.90E-09	3.02E-07
GOBP_REGULATION_OF_VIRAL_GENOME_REPLICATION	9	2.02E-09	3.15E-07
GOBP_BIOLOGICAL_PROCESS_INVOLVED_IN_SYMBIOTIC_INTERACTION	25	2.39E-09	3.58E-07
GOBP_INNATE_IMMUNE_RESPONSE	25	2.39E-09	3.58E-07
GOBP_NEGATIVE_REGULATION_OF_MOLECULAR_FUNCTION	27	2.94E-09	4.32E-07
GOBP_LOCOMOTION	36	3.42E-09	4.92E-07
GOBP_RESPONSE_TO_LIPID	23	3.64E-09	5.14E-07
GOBP_CELL_CELL_ADHESION	23	5.02E-09	6.95E-07
GOBP_TRANSMEMBRANE_RECEPTOR_PROTEIN_SERINE_THREONINE_KINASE_SIGNALING_PATHWAY	15	6.06E-09	8.13E-07
GOBP_DEFENSE_RESPONSE_TO_OTHER_ORGANISM	27	6.09E-09	8.13E-07
GOBP_IMMUNE_EFFECTOR_PROCESS	28	6.49E-09	8.51E-07
GOBP_RESPONSE_TO_TRANSFORMING_GROWTH_FACTOR_BETA	13	6.91E-09	8.91E-07
GOBP_CYTOKINE_PRODUCTION	22	7.36E-09	9.33E-07
GOBP_POSITIVE_REGULATION_OF_CELL_ADHESION	16	8.50E-09	1.06E-06
GOBP_REGULATION_OF_PHOSPHORUS_METABOLIC_PROCESS	31	1.37E-08	1.68E-06
GOBP_PROTEIN_PHOSPHORYLATION	31	1.49E-08	1.80E-06
GOBP_POSITIVE_REGULATION_OF_TRANSCRIPTION_BY_RNA_POLYMERASE_II	26	1.58E-08	1.88E-06
GOBP_ANIMAL_ORGAN_MORPHOGENESIS	24	1.88E-08	2.19E-06
GOBP_RESPONSE_TO_NITROGEN_COMPOUND	25	2.25E-08	2.58E-06
GOBP_REGULATION_OF_CELLULAR_COMPONENT_BIOGENESIS	23	2.35E-08	2.66E-06
GOBP_RESPONSE_TO_GROWTH_FACTOR	20	2.49E-08	2.79E-06
GOBP_OSSIFICATION	15	2.56E-08	2.81E-06
GOBP_NEGATIVE_REGULATION_OF_VIRAL_GENOME_REPLICATION	7	3.69E-08	4.00E-06
GOBP_NEGATIVE_REGULATION_OF_CELL_POPULATION_PROLIFERATION	20	3.96E-08	4.23E-06
GOBP_RESPONSE_TO_ORGANIC_CYCLIC_COMPOUND	22	4.10E-08	4.32E-06
GOBP_TRANSFORMING_GROWTH_FACTOR_BETA_RECEPTOR_SIGNALING_PATHWAY	11	4.81E-08	4.99E-06
GOBP_REGULATION_OF_CELL_DEVELOPMENT	16	5.15E-08	5.28E-06
GOBP_NEGATIVE_REGULATION_OF_GENE_EXPRESSION	31	5.26E-08	5.32E-06
GOBP_CELL_MORPHOGENESIS	23	5.59E-08	5.57E-06
GOBP_REGULATION_OF_PROTEIN_MODIFICATION_PROCESS	30	6.18E-08	6.09E-06
GOBP_REGULATION_OF_CELL_CELL_ADHESION	15	8.37E-08	8.13E-06
GOBP_VIRAL_GENOME_REPLICATION	9	9.91E-08	9.50E-06
GOBP_RESPONSE_TO_HORMONE	21	1.03E-07	9.72E-06
GOBP_REGULATION_OF_PROTEIN_PHOSPHORYLATION	25	1.05E-07	9.83E-06
GOBP_ORGANONITROGEN_COMPOUND_CATABOLIC_PROCESS	26	1.70E-07	1.57E-05
GOBP_CELL_MATRIX_ADHESION	11	1.79E-07	1.63E-05
GOBP_MESENCHYME_DEVELOPMENT	12	2.11E-07	1.90E-05
GOBP_AMEBOIDAL_TYPE_CELL_MIGRATION	15	2.31E-07	2.06E-05
GOBP_REGULATION_OF_CELL_DEATH	29	3.16E-07	2.78E-05
GOBP_NEGATIVE_REGULATION_OF_PROTEIN_METABOLIC_PROCESS	23	3.28E-07	2.85E-05
GOBP_REGULATION_OF_HYDROLASE_ACTIVITY	25	3.76E-07	3.24E-05
GOBP_ACTIN_FILAMENT_BASED_PROCESS	19	4.05E-07	3.45E-05
GOBP_REGULATION_OF_INTRACELLULAR_SIGNAL_TRANSDUCTION	30	4.34E-07	3.64E-05
GOBP_POSITIVE_REGULATION_OF_CELL_DEATH	17	5.60E-07	4.66E-05
GOBP_EMBRYO_IMPLANTATION	6	5.74E-07	4.72E-05
GOBP_NEUROGENESIS	28	5.90E-07	4.79E-05
GOBP_UROGENITAL_SYSTEM_DEVELOPMENT	12	6.69E-07	5.38E-05
GOBP_RESPONSE_TO_OXYGEN_LEVELS	13	7.23E-07	5.75E-05
GOBP_IMMUNE_SYSTEM_DEVELOPMENT	21	7.39E-07	5.82E-05
GOBP_POSITIVE_REGULATION_OF_CELL_SUBSTRATE_ADHESION	8	7.78E-07	6.00E-05
GOBP_RESPONSE_TO_PEPTIDE	15	7.78E-07	6.00E-05
GOBP_NEURON_DIFFERENTIATION	25	8.56E-07	6.54E-05
GOBP_RESPONSE_TO_INTERFERON_BETA	5	9.62E-07	7.27E-05
GOBP_REGULATION_OF_TRANSFERASE_ACTIVITY	21	1.03E-06	7.73E-05

Figure 101 Gene ontology analysis of genes downregulated in response to CD in dKO$^{MRTF\text{-}NLS}$ cells by RNAseq

Gene ontology analysis of genes downregulated by CD treatment in dKO$^{MRTF\text{-}NLS}$ cells by RNAseq. FDR<0.05. Relates to Figure 45. Bioinformatic analysis of RNAseq data was performed by Francesco Gualdrini.

GO BIOLOGICAL PROCESS	# Genes	p-value	FDR q-value
GOBP_ACTIN_FILAMENT_BASED_PROCESS	154	1.60E-65	1.21E-61
GOBP_CYTOSKELETON_ORGANIZATION	202	2.00E-64	7.56E-61
GOBP_REGULATION_OF_INTRACELLULAR_SIGNAL_TRANSDUCTION	234	4.55E-63	1.15E-59
GOBP_CELL_MORPHOGENESIS	169	5.69E-61	1.08E-57
GOBP_CELL_MOTILITY	226	5.36E-60	8.12E-57
GOBP_BIOLOGICAL_ADHESION	199	4.46E-58	5.63E-55
GOBP_CELLULAR_MACROMOLECULE_LOCALIZATION	234	8.07E-58	8.73E-55
GOBP_REGULATION_OF_CELL_DIFFERENTIATION	227	2.15E-55	2.04E-52
GOBP_APOPTOTIC_PROCESS	229	1.17E-54	9.84E-52
GOBP_POSITIVE_REGULATION_OF_MOLECULAR_FUNCTION	216	1.05E-53	7.93E-51
GOBP_POSITIVE_REGULATION_OF_BIOSYNTHETIC_PROCESS	222	2.24E-52	1.40E-49
GOBP_MACROMOLECULE_CATABOLIC_PROCESS	182	7.24E-50	4.17E-47
GOBP_POSITIVE_REGULATION_OF_NUCLEOBASE_CONTAINING_COMPOUND_METABOLIC_PROCESS	210	3.21E-49	1.72E-46
GOBP_RESPONSE_TO_ENDOGENOUS_STIMULUS	194	6.13E-49	3.06E-46
GOBP_POSITIVE_REGULATION_OF_SIGNALING	199	6.92E-48	3.24E-45
GOBP_REGULATION_OF_PROTEIN_MODIFICATION_PROCESS	191	4.94E-47	2.17E-44
GOBP_SUPRAMOLECULAR_FIBER_ORGANIZATION	122	8.74E-47	3.63E-44
GOBP_NEUROGENESIS	189	2.08E-46	8.20E-44
GOBP_REGULATION_OF_CELL_DEATH	192	2.31E-46	8.64E-44
GOBP_REGULATION_OF_CELLULAR_COMPONENT_MOVEMENT	152	6.05E-46	2.16E-43
GOBP_ESTABLISHMENT_OF_PROTEIN_LOCALIZATION	212	7.98E-46	2.71E-43
GOBP_CELL_POPULATION_PROLIFERATION	208	1.43E-44	4.64E-42
GOBP_CELL_MORPHOGENESIS_INVOLVED_IN_DIFFERENTIATION	120	1.76E-44	5.50E-42
GOBP_REGULATION_OF_RESPONSE_TO_STRESS	172	2.41E-44	6.95E-42
GOBP_REGULATION_OF_PHOSPHORUS_METABOLIC_PROCESS	185	3.43E-44	9.51E-42
GOBP_ENZYME_LINKED_RECEPTOR_PROTEIN_SIGNALING_PATHWAY	147	5.07E-44	1.35E-41
GOBP_POSITIVE_REGULATION_OF_PROTEIN_METABOLIC_PROCESS	179	6.88E-44	1.77E-41
GOBP_BIOLOGICAL_PROCESS_INVOLVED_IN_SYMBIOTIC_INTERACTION	141	8.59E-44	2.14E-41
GOBP_INTRACELLULAR_TRANSPORT	192	1.09E-43	2.63E-41
GOBP_NEGATIVE_REGULATION_OF_RESPONSE_TO_STIMULUS	187	5.80E-43	1.34E-40
GOBP_CELL_PROJECTION_ORGANIZATION	180	5.92E-43	1.34E-40
GOBP_CIRCULATORY_SYSTEM_DEVELOPMENT	150	1.02E-42	2.25E-40
GOBP_CELLULAR_COMPONENT_MORPHOGENESIS	121	1.45E-42	3.09E-40
GOBP_CELLULAR_MACROMOLECULE_CATABOLIC_PROCESS	154	1.64E-42	3.41E-40
GOBP_CELL_JUNCTION_ORGANIZATION	115	2.95E-42	5.88E-40
GOBP_HOMEOSTATIC_PROCESS	201	2.99E-42	5.88E-40
GOBP_REGULATION_OF_ANATOMICAL_STRUCTURE_MORPHOGENESIS	139	5.29E-42	1.01E-39
GOBP_POSITIVE_REGULATION_OF_CELLULAR_COMPONENT_ORGANIZATION	147	7.99E-42	1.49E-39
GOBP_ORGANONITROGEN_COMPOUND_BIOSYNTHETIC_PROCESS	192	1.08E-41	1.97E-39
GOBP_RESPONSE_TO_WOUNDING	110	2.24E-41	3.99E-39
GOBP_NEURON_DIFFERENTIATION	163	2.69E-41	4.68E-39
GOBP_POSITIVE_REGULATION_OF_CATALYTIC_ACTIVITY	166	2.96E-41	5.04E-39
GOBP_CELL_CYCLE	196	6.43E-41	1.07E-38
GOBP_REGULATION_OF_PROTEIN_PHOSPHORYLATION	152	8.77E-41	1.43E-38
GOBP_POSITIVE_REGULATION_OF_DEVELOPMENTAL_PROCESS	157	1.02E-40	1.62E-38
GOBP_MUSCLE_STRUCTURE_DEVELOPMENT	105	1.15E-40	1.79E-38
GOBP_ACTIN_FILAMENT_ORGANIZATION	89	1.18E-40	1.80E-38
GOBP_NEGATIVE_REGULATION_OF_SIGNALING	165	2.16E-40	3.24E-38
GOBP_TUBE_DEVELOPMENT	142	3.61E-40	5.30E-38
GOBP_ANATOMICAL_STRUCTURE_FORMATION_INVOLVED_IN_MORPHOGENESIS	146	4.20E-40	6.05E-38
GOBP_WOUND_HEALING	97	2.06E-39	2.90E-37
GOBP_PROTEIN_CONTAINING_COMPLEX_SUBUNIT_ORGANIZATION	198	3.89E-39	5.40E-37
GOBP_NEURON_DEVELOPMENT	142	4.42E-39	6.01E-37
GOBP_MRNA_METABOLIC_PROCESS	124	2.00E-38	2.67E-36
GOBP_CELL_SUBSTRATE_ADHESION	78	1.26E-37	1.66E-35
GOBP_POSITIVE_REGULATION_OF_MULTICELLULAR_ORGANISMAL_PROCESS	159	2.11E-37	2.72E-35
GOBP_RESPONSE_TO_CYTOKINE	144	6.51E-37	8.25E-35
GOBP_CELL_PART_MORPHOGENESIS	106	6.89E-37	8.59E-35
GOBP_REGULATION_OF_CELL_ADHESION	110	1.08E-36	1.33E-34
GOBP_REGULATION_OF_TRANSPORT	179	1.25E-36	1.51E-34
GOBP_CELL_CELL_SIGNALING	175	1.94E-36	2.31E-34
GOBP_INTRACELLULAR_PROTEIN_TRANSPORT	141	3.07E-36	3.59E-34
GOBP_CELLULAR_AMIDE_METABOLIC_PROCESS	142	7.51E-36	8.65E-34
GOBP_POSITIVE_REGULATION_OF_INTRACELLULAR_SIGNAL_TRANSDUCTION	129	1.23E-35	1.40E-33
GOBP_NEGATIVE_REGULATION_OF_PROTEIN_METABOLIC_PROCESS	136	2.27E-35	2.53E-33
GOBP_TUBE_MORPHOGENESIS	120	8.80E-35	9.68E-33
GOBP_PEPTIDE_METABOLIC_PROCESS	120	1.22E-34	1.32E-32
GOBP_POSITIVE_REGULATION_OF_LOCOMOTION	95	1.47E-34	1.57E-32
GOBP_RESPONSE_TO_OXYGEN_CONTAINING_COMPOUND	170	2.07E-34	2.18E-32
GOBP_REGULATION_OF_HYDROLASE_ACTIVITY	147	2.25E-34	2.34E-32
GOBP_REGULATION_OF_TRANSFERASE_ACTIVITY	127	3.48E-34	3.57E-32
GOBP_PROTEIN_LOCALIZATION_TO_MEMBRANE	100	7.67E-34	7.76E-32
GOBP_MAPK_CASCADE	119	1.36E-33	1.36E-31
GOBP_REGULATION_OF_MULTICELLULAR_ORGANISMAL_DEVELOPMENT	152	1.62E-33	1.60E-31
GOBP_MUSCLE_SYSTEM_PROCESS	82	2.06E-33	2.01E-31
GOBP_RESPONSE_TO_GROWTH_FACTOR	105	2.56E-33	2.46E-31
GOBP_POSITIVE_REGULATION_OF_GENE_EXPRESSION	129	1.17E-32	1.11E-30
GOBP_VASCULATURE_DEVELOPMENT	108	1.60E-32	1.50E-30
GOBP_NEGATIVE_REGULATION_OF_MOLECULAR_FUNCTION	135	1.68E-32	1.55E-30
GOBP_CELL_JUNCTION_ASSEMBLY	78	2.93E-32	2.67E-30
GOBP_AMIDE_BIOSYNTHETIC_PROCESS	114	4.68E-32	4.22E-30
GOBP_CELL_MORPHOGENESIS_INVOLVED_IN_NEURON_DIFFERENTIATION	91	5.11E-32	4.55E-30
GOBP_RESPONSE_TO_ABIOTIC_STIMULUS	137	8.76E-32	7.71E-30
GOBP_PEPTIDE_BIOSYNTHETIC_PROCESS	103	1.58E-31	1.37E-29
GOBP_REGULATION_OF_CELL_CYCLE	136	2.06E-31	1.77E-29
GOBP_SECRETION	152	3.03E-31	2.58E-29
GOBP_POSITIVE_REGULATION_OF_PHOSPHORUS_METABOLIC_PROCESS	120	3.39E-31	2.85E-29
GOBP_TRANSMEMBRANE_RECEPTOR_PROTEIN_TYROSINE_KINASE_SIGNALING_PATHWAY	102	5.06E-31	4.21E-29
GOBP_REGULATION_OF_ORGANELLE_ORGANIZATION	132	6.96E-31	5.72E-29
GOBP_REGULATION_OF_PROTEIN_KINASE_ACTIVITY	106	7.53E-31	6.12E-29
GOBP_CELL_ACTIVATION	151	7.99E-31	6.42E-29
GOBP_RNA_CATABOLIC_PROCESS	75	1.12E-30	8.91E-29
GOBP_RIBONUCLEOPROTEIN_COMPLEX_BIOGENESIS	80	1.23E-30	9.69E-29
GOBP_REGULATION_OF_CELLULAR_COMPONENT_BIOGENESIS	117	2.07E-30	1.61E-28
GOBP_TRANSLATIONAL_INITIATION	52	2.44E-30	1.88E-28
GOBP_NEGATIVE_REGULATION_OF_CELL_DEATH	119	3.39E-30	2.59E-28
GOBP_BLOOD_VESSEL_MORPHOGENESIS	96	4.35E-30	3.29E-28
GOBP_ANIMAL_ORGAN_MORPHOGENESIS	121	5.33E-30	3.99E-28

Figure 102 Gene ontology analysis of genes upregulated in response to CD in dKO^{MRTF} cells by TTseq

Gene ontology analysis of genes upregulated by CD treatment in dKO^{MRTF} cells by TTseq. FDR<0.05. Relates to Figure 47. Bioinformatic analysis of TTseq data was performed by Francesco Gualdrini.

GO BIOLOGICAL PROCESS	# Genes	p-value	FDR q-value
GOBP_SMALL_MOLECULE_METABOLIC_PROCESS	183	7.44E-35	5.57E-31
GOBP_LIPID_METABOLIC_PROCESS	136	3.33E-25	1.24E-21
GOBP_CELLULAR_RESPONSE_TO_DNA_DAMAGE_STIMULUS	100	1.09E-24	2.72E-21
GOBP_PROTEIN_CONTAINING_COMPLEX_SUBUNIT_ORGANIZATION	158	1.28E-21	2.39E-18
GOBP_CELLULAR_LIPID_METABOLIC_PROCESS	106	2.24E-21	3.35E-18
GOBP_ORGANIC_ACID_CATABOLIC_PROCESS	45	1.42E-18	1.77E-15
GOBP_CELL_CYCLE	144	6.06E-18	6.48E-15
GOBP_ORGANONITROGEN_COMPOUND_CATABOLIC_PROCESS	114	1.17E-17	1.09E-14
GOBP_SMALL_MOLECULE_CATABOLIC_PROCESS	57	2.64E-17	2.20E-14
GOBP_CARBOHYDRATE_DERIVATIVE_METABOLIC_PROCESS	100	1.84E-16	1.38E-13
GOBP_DNA_METABOLIC_PROCESS	89	2.29E-16	1.56E-13
GOBP_SMALL_MOLECULE_BIOSYNTHETIC_PROCESS	73	2.83E-16	1.76E-13
GOBP_NEGATIVE_REGULATION_OF_NUCLEOBASE_CONTAINING_COMPOUND_METABOLIC_PROCESS	120	6.30E-16	3.63E-13
GOBP_CELLULAR_MACROMOLECULE_LOCALIZATION	144	7.02E-16	3.75E-13
GOBP_REGULATION_OF_CELL_DIFFERENTIATION	125	8.02E-16	4.00E-13
GOBP_ORGANONITROGEN_COMPOUND_BIOSYNTHETIC_PROCESS	133	1.57E-15	7.35E-13
GOBP_CELL_PROJECTION_ORGANIZATION	121	2.49E-15	1.10E-12
GOBP_ESTABLISHMENT_OF_PROTEIN_LOCALIZATION	142	3.63E-15	1.51E-12
GOBP_ORGANIC_ACID_METABOLIC_PROCESS	93	4.43E-15	1.74E-12
GOBP_CELL_CYCLE_PROCESS	112	5.47E-15	2.05E-12
GOBP_DNA_REPAIR	62	1.16E-14	4.14E-12
GOBP_MONOCARBOXYLIC_ACID_CATABOLIC_PROCESS	28	2.15E-14	7.32E-12
GOBP_REGULATION_OF_CELL_CYCLE	99	3.15E-14	1.02E-11
GOBP_NEGATIVE_REGULATION_OF_BIOSYNTHETIC_PROCESS	124	3.73E-14	1.16E-11
GOBP_FATTY_ACID_METABOLIC_PROCESS	49	4.12E-14	1.23E-11
GOBP_FATTY_ACID_CATABOLIC_PROCESS	25	4.80E-14	1.37E-11
GOBP_CILIUM_ORGANIZATION	50	4.94E-14	1.37E-11
GOBP_CELLULAR_LIPID_CATABOLIC_PROCESS	36	1.18E-13	3.08E-11
GOBP_NEGATIVE_REGULATION_OF_CELL_DIFFERENTIATION	66	1.19E-13	3.08E-11
GOBP_REGULATION_OF_INTRACELLULAR_SIGNAL_TRANSDUCTION	127	1.77E-13	4.41E-11
GOBP_REPRODUCTION	109	2.56E-13	6.19E-11
GOBP_MONOCARBOXYLIC_ACID_METABOLIC_PROCESS	64	3.26E-13	7.62E-11
GOBP_RESPONSE_TO_ENDOGENOUS_STIMULUS	118	3.63E-13	8.24E-11
GOBP_ORGANIC_HYDROXY_COMPOUND_METABOLIC_PROCESS	58	4.93E-13	1.09E-10
GOBP_SULFUR_COMPOUND_METABOLIC_PROCESS	46	6.50E-13	1.39E-10
GOBP_LIPID_OXIDATION	24	9.51E-13	1.97E-10
GOBP_ORGANOPHOSPHATE_METABOLIC_PROCESS	85	9.76E-13	1.97E-10
GOBP_POSITIVE_REGULATION_OF_NUCLEOBASE_CONTAINING_COMPOUND_METABOLIC_PROCESS	128	1.40E-12	2.75E-10
GOBP_NEGATIVE_REGULATION_OF_DEVELOPMENTAL_PROCESS	79	1.79E-12	3.43E-10
GOBP_MICROTUBULE_BASED_PROCESS	74	2.36E-12	4.42E-10
GOBP_NEGATIVE_REGULATION_OF_RESPONSE_TO_STIMULUS	118	2.56E-12	4.67E-10
GOBP_PROTEIN_DNA_COMPLEX_SUBUNIT_ORGANIZATION	38	2.64E-12	4.70E-10
GOBP_LIPID_BIOSYNTHETIC_PROCESS	67	2.90E-12	5.04E-10
GOBP_ORGANELLE_ASSEMBLY	75	4.74E-12	8.06E-10
GOBP_REGULATION_OF_MULTICELLULAR_ORGANISMAL_DEVELOPMENT	103	5.28E-12	8.78E-10
GOBP_DEVELOPMENTAL_PROCESS_INVOLVED_IN_REPRODUCTION	79	8.28E-12	1.35E-09
GOBP_HOMEOSTATIC_PROCESS	128	1.01E-11	1.61E-09
GOBP_NUCLEOSOME_ASSEMBLY	26	1.28E-11	2.00E-09
GOBP_PEROXISOME_ORGANIZATION	20	1.33E-11	2.03E-09
GOBP_NUCLEOSOME_ORGANIZATION	29	2.05E-11	3.07E-09
GOBP_MITOTIC_CELL_CYCLE	82	2.26E-11	3.31E-09
GOBP_POSITIVE_REGULATION_OF_BIOSYNTHETIC_PROCESS	129	2.34E-11	3.36E-09
GOBP_NEGATIVE_REGULATION_OF_TRANSCRIPTION_BY_RNA_POLYMERASE_II	73	2.74E-11	3.86E-09
GOBP_SKELETAL_SYSTEM_DEVELOPMENT	50	3.25E-11	4.50E-09
GOBP_NUCLEOBASE_CONTAINING_SMALL_MOLECULE_METABOLIC_PROCESS	58	3.68E-11	5.01E-09
GOBP_INTRACELLULAR_TRANSPORT	117	4.46E-11	5.96E-09
GOBP_NEUROGENESIS	111	5.20E-11	6.83E-09
GOBP_CELLULAR_PROTEIN_CONTAINING_COMPLEX_ASSEMBLY	85	5.74E-11	7.40E-09
GOBP_CYTOSKELETON_ORGANIZATION	99	6.39E-11	7.97E-09
GOBP_REGULATION_OF_CELL_DEATH	113	6.40E-11	7.97E-09
GOBP_APOPTOTIC_PROCESS	126	7.78E-11	9.55E-09
GOBP_PROTEOLYSIS	119	1.11E-10	1.34E-08
GOBP_ORGANOPHOSPHATE_BIOSYNTHETIC_PROCESS	55	1.25E-10	1.48E-08
GOBP_PROTEIN_MODIFICATION_BY_SMALL_PROTEIN_CONJUGATION	76	1.26E-10	1.48E-08
GOBP_CHROMOSOME_ORGANIZATION	91	1.44E-10	1.65E-08
GOBP_PROTEIN_LOCALIZATION_TO_ORGANELLE	78	1.52E-10	1.72E-08
GOBP_CELL_POPULATION_PROLIFERATION	126	1.70E-10	1.90E-08
GOBP_DOUBLE_STRAND_BREAK_REPAIR	34	2.11E-10	2.29E-08
GOBP_CARBOHYDRATE_DERIVATIVE_BIOSYNTHETIC_PROCESS	60	2.13E-10	2.29E-08
GOBP_LIPID_CATABOLIC_PROCESS	39	2.15E-10	2.29E-08
GOBP_STEROL_METABOLIC_PROCESS	26	2.51E-10	2.65E-08
GOBP_REGULATION_OF_ORGANELLE_ORGANIZATION	86	2.99E-10	3.11E-08
GOBP_EMBRYONIC_MORPHOGENESIS	53	3.56E-10	3.65E-08
GOBP_REPRODUCTIVE_SYSTEM_DEVELOPMENT	43	3.86E-10	3.90E-08
GOBP_NEGATIVE_REGULATION_OF_CELL_CYCLE	56	4.56E-10	4.43E-08
GOBP_CHROMATIN_ASSEMBLY_OR_DISASSEMBLY	30	4.67E-10	4.43E-08
GOBP_REGULATION_OF_RESPONSE_TO_DNA_DAMAGE_STIMULUS	30	4.67E-10	4.43E-08
GOBP_SEX_DIFFERENTIATION	33	4.68E-10	4.43E-08
GOBP_GAMETE_GENERATION	60	4.71E-10	4.43E-08
GOBP_APPENDAGE_MORPHOGENESIS	23	4.74E-10	4.43E-08
GOBP_PEROXISOMAL_TRANSPORT	17	5.20E-10	4.77E-08
GOBP_EMBRYONIC_ORGAN_DEVELOPMENT	43	5.23E-10	4.77E-08
GOBP_CARTILAGE_DEVELOPMENT	27	5.92E-10	5.34E-08
GOBP_DNA_PACKAGING	31	8.38E-10	7.46E-08
GOBP_ALCOHOL_METABOLIC_PROCESS	40	9.42E-10	8.29E-08
GOBP_FATTY_ACID_BETA_OXIDATION	17	1.03E-09	8.94E-08
GOBP_STEROID_METABOLIC_PROCESS	37	1.07E-09	9.24E-08
GOBP_NUCLEOSIDE_BISPHOSPHATE_METABOLIC_PROCESS	23	1.16E-09	9.84E-08
GOBP_NEGATIVE_REGULATION_OF_CELLULAR_COMPONENT_ORGANIZATION	61	1.20E-09	9.85E-08
GOBP_PROTEIN_MODIFICATION_BY_SMALL_PROTEIN_CONJUGATION_OR_REMOVAL	84	1.20E-09	9.85E-08
GOBP_MULTICELLULAR_ORGANISM_REPRODUCTION	67	1.21E-09	9.85E-08
GOBP_MICROTUBULE_CYTOSKELETON_ORGANIZATION	53	1.21E-09	9.85E-08
GOBP_DEVELOPMENT_OF_PRIMARY_SEXUAL_CHARACTERISTICS	29	1.31E-09	1.05E-07
GOBP_RESPONSE_TO_GROWTH_FACTOR	61	1.33E-09	1.06E-07
GOBP_EMBRYO_DEVELOPMENT	75	1.49E-09	1.17E-07
GOBP_REGULATION_OF_CELL_CYCLE_PROCESS	64	1.62E-09	1.25E-07
GOBP_REGULATION_OF_CELLULAR_RESPONSE_TO_STRESS	59	1.62E-09	1.25E-07
GOBP_DNA_CONFORMATION_CHANGE	38	2.04E-09	1.56E-07
GOBP_SEXUAL_REPRODUCTION	67	2.15E-09	1.63E-07
GOBP_POSITIVE_REGULATION_OF_TRANSCRIPTION_BY_RNA_POLYMERASE_II	84	2.67E-09	2.00E-07

Figure 103 Gene ontology analysis of genes downregulated in response to CD in dKO^{MRTF} cells by TTseq

Gene ontology analysis of genes downregulated by CD treatment in dKO^{MRTF} cells by TTseq. FDR<0.05. Relates to Figure 47. Bioinformatic analysis of TTseq data was performed by Francesco Gualdrini.

GO BIOLOGICAL PROCESS	# Genes	p-value	FDR q-value
GOBP_MRNA_METABOLIC_PROCESS	143	1.48E-98	1.12E-94
GOBP_TRANSLATIONAL_INITIATION	78	1.39E-87	5.28E-84
GOBP_CELLULAR_MACROMOLECULE_CATABOLIC_PROCESS	145	4.09E-82	1.03E-78
GOBP_INTRACELLULAR_TRANSPORT	170	7.44E-82	1.41E-78
GOBP_RNA_CATABOLIC_PROCESS	96	5.77E-81	8.74E-78
GOBP_COTRANSLATIONAL_PROTEIN_TARGETING_TO_MEMBRANE	61	7.93E-81	1.00E-77
GOBP_MACROMOLECULE_CATABOLIC_PROCESS	154	3.10E-80	3.35E-77
GOBP_NUCLEAR_TRANSCRIBED_MRNA_CATABOLIC_PROCESS_NONSENSE_MEDIATED_DECAY	62	4.68E-78	4.43E-75
GOBP_CELLULAR_MACROMOLECULE_LOCALIZATION	175	6.39E-78	5.37E-75
GOBP_ESTABLISHMENT_OF_PROTEIN_LOCALIZATION_TO_ENDOPLASMIC_RETICULUM	62	9.46E-78	7.16E-75
GOBP_BIOLOGICAL_PROCESS_INVOLVED_IN_SYMBIOTIC_INTERACTION	130	1.04E-77	7.10E-75
GOBP_INTRACELLULAR_PROTEIN_TRANSPORT	136	2.19E-75	1.37E-72
GOBP_PROTEIN_LOCALIZATION_TO_ENDOPLASMIC_RETICULUM	64	5.64E-74	3.25E-71
GOBP_ESTABLISHMENT_OF_PROTEIN_LOCALIZATION	167	1.26E-71	6.74E-69
GOBP_VIRAL_GENE_EXPRESSION	68	1.61E-70	8.01E-68
GOBP_NUCLEAR_TRANSCRIBED_MRNA_CATABOLIC_PROCESS	69	2.46E-70	1.15E-67
GOBP_ORGANIC_CYCLIC_COMPOUND_CATABOLIC_PROCESS	100	3.30E-67	1.45E-64
GOBP_PEPTIDE_BIOSYNTHETIC_PROCESS	106	3.77E-67	1.57E-64
GOBP_PROTEIN_TARGETING_TO_MEMBRANE	66	8.25E-66	3.25E-63
GOBP_PEPTIDE_METABOLIC_PROCESS	111	2.93E-63	1.10E-60
GOBP_ESTABLISHMENT_OF_PROTEIN_LOCALIZATION_TO_MEMBRANE	76	7.59E-62	2.70E-59
GOBP_AMIDE_BIOSYNTHETIC_PROCESS	108	1.38E-61	4.69E-59
GOBP_PROTEIN_LOCALIZATION_TO_ORGANELLE	113	1.29E-60	4.20E-58
GOBP_PROTEIN_TARGETING	78	1.33E-56	4.16E-54
GOBP_CELLULAR_AMIDE_METABOLIC_PROCESS	116	1.71E-55	5.13E-53
GOBP_PROTEIN_LOCALIZATION_TO_MEMBRANE	90	4.23E-55	1.22E-52
GOBP_ORGANONITROGEN_COMPOUND_BIOSYNTHETIC_PROCESS	139	1.16E-54	3.22E-52
GOBP_ESTABLISHMENT_OF_PROTEIN_LOCALIZATION_TO_ORGANELLE	79	2.01E-48	5.37E-46
GOBP_NEGATIVE_REGULATION_OF_GENE_EXPRESSION	128	2.76E-48	7.12E-46
GOBP_CYTOPLASMIC_TRANSLATION	35	1.05E-36	2.61E-34
GOBP_RNA_PROCESSING	102	1.57E-36	3.79E-34
GOBP_PROTEIN_CONTAINING_COMPLEX_SUBUNIT_ORGANIZATION	116	7.82E-34	1.83E-31
GOBP_RNA_SPLICING	56	7.98E-31	1.81E-28
GOBP_MRNA_PROCESSING	59	1.22E-30	2.68E-28
GOBP_RIBONUCLEOPROTEIN_COMPLEX_BIOGENESIS	55	3.23E-30	6.91E-28
GOBP_REGULATION_OF_MRNA_METABOLIC_PROCESS	47	1.38E-29	2.86E-27
GOBP_CELL_CYCLE	103	2.11E-27	4.26E-25
GOBP_RNA_SPLICING_VIA_TRANSESTERIFICATION_REACTIONS	46	6.50E-26	1.28E-23
GOBP_POSITIVE_REGULATION_OF_BIOSYNTHETIC_PROCESS	101	9.71E-25	1.86E-22
GOBP_PROTEIN_CATABOLIC_PROCESS	68	1.80E-24	3.31E-22
GOBP_REGULATION_OF_RNA_SPLICING	30	1.82E-24	3.31E-22
GOBP_REGULATION_OF_CATABOLIC_PROCESS	70	2.22E-24	3.95E-22
GOBP_POSITIVE_REGULATION_OF_PROTEIN_METABOLIC_PROCESS	87	3.87E-24	6.73E-22
GOBP_RIBOSOME_BIOGENESIS	40	4.59E-24	7.81E-22
GOBP_POSITIVE_REGULATION_OF_NUCLEOBASE_CONTAINING_COMPOUND_METABOLIC_PROCE	95	5.36E-23	8.84E-21
GOBP_REGULATION_OF_CELLULAR_AMIDE_METABOLIC_PROCESS	48	5.44E-23	8.84E-21
GOBP_CELLULAR_PROTEIN_CATABOLIC_PROCESS	60	9.66E-23	1.54E-20
GOBP_POSTTRANSCRIPTIONAL_REGULATION_OF_GENE_EXPRESSION	73	1.63E-22	2.54E-20
GOBP_PROTEIN_MODIFICATION_BY_SMALL_PROTEIN_CONJUGATION	65	3.94E-22	6.02E-20
GOBP_MODIFICATION_DEPENDENT_MACROMOLECULE_CATABOLIC_PROCESS	53	1.39E-21	2.07E-19
GOBP_PROTEIN_MODIFICATION_BY_SMALL_PROTEIN_CONJUGATION_OR_REMOVAL	71	1.57E-21	2.31E-19
GOBP_REGULATION_OF_CELLULAR_CATABOLIC_PROCESS	60	2.28E-21	3.29E-19
GOBP_CELLULAR_PROTEIN_CONTAINING_COMPLEX_ASSEMBLY	68	1.03E-20	1.46E-18
GOBP_CELL_CYCLE_PROCESS	77	2.96E-20	4.09E-18
GOBP_ESTABLISHMENT_OF_RNA_LOCALIZATION	30	3.86E-20	5.25E-18
GOBP_RNA_EXPORT_FROM_NUCLEUS	26	7.02E-20	9.38E-18
GOBP_ORGANONITROGEN_COMPOUND_CATABOLIC_PROCESS	73	2.08E-19	2.74E-17
GOBP_REGULATION_OF_CELL_CYCLE	69	2.84E-19	3.66E-17
GOBP_RNA_LOCALIZATION	31	3.32E-19	4.21E-17
GOBP_NUCLEOBASE_CONTAINING_COMPOUND_TRANSPORT	32	3.64E-19	4.54E-17
GOBP_NEGATIVE_REGULATION_OF_BIOSYNTHETIC_PROCESS	83	4.09E-19	5.02E-17
GOBP_NEGATIVE_REGULATION_OF_NUCLEOBASE_CONTAINING_COMPOUND_METABOLIC_PROC	78	4.83E-19	5.83E-17
GOBP_NUCLEAR_EXPORT	29	4.91E-19	5.83E-17
GOBP_RRNA_METABOLIC_PROCESS	31	6.23E-19	7.28E-17
GOBP_REGULATION_OF_RESPONSE_TO_STRESS	73	5.44E-18	6.26E-16
GOBP_PROTEOLYSIS	84	5.53E-18	6.26E-16
GOBP_REGULATION_OF_PROTEIN_MODIFICATION_PROCESS	79	7.03E-18	7.85E-16
GOBP_NUCLEAR_TRANSPORT	35	9.23E-18	1.02E-15
GOBP_REGULATION_OF_MRNA_SPLICING_VIA_SPLICEOSOME	21	1.32E-17	1.43E-15
GOBP_ORGANELLE_ASSEMBLY	55	2.22E-17	2.37E-15
GOBP_REGULATION_OF_INTRACELLULAR_SIGNAL_TRANSDUCTION	82	3.68E-17	3.88E-15
GOBP_POSITIVE_REGULATION_OF_MOLECULAR_FUNCTION	80	1.11E-16	1.16E-14
GOBP_REGULATION_OF_MRNA_CATABOLIC_PROCESS	27	1.62E-16	1.66E-14
GOBP_REGULATION_OF_TRANSFERASE_ACTIVITY	58	1.70E-16	1.72E-14
GOBP_POSITIVE_REGULATION_OF_CELLULAR_AMIDE_METABOLIC_PROCESS	24	3.41E-16	3.39E-14
GOBP_PROTEASOMAL_PROTEIN_CATABOLIC_PROCESS	39	3.45E-16	3.39E-14
GOBP_APOPTOTIC_PROCESS	84	3.69E-16	3.58E-14
GOBP_MITOTIC_CELL_CYCLE	58	4.42E-16	4.24E-14
GOBP_POSITIVE_REGULATION_OF_TRANSLATION	22	4.70E-16	4.45E-14
GOBP_REGULATION_OF_PHOSPHORUS_METABOLIC_PROCESS	75	4.78E-16	4.47E-14
GOBP_NCRNA_METABOLIC_PROCESS	39	6.81E-16	6.29E-14
GOBP_POSITIVE_REGULATION_OF_GENE_EXPRESSION	59	7.02E-16	6.40E-14
GOBP_PROTEIN_CONTAINING_COMPLEX_LOCALIZATION	30	7.30E-16	6.58E-14
GOBP_REGULATION_OF_TRANSLATIONAL_INITIATION	18	7.46E-16	6.64E-14
GOBP_NEGATIVE_REGULATION_OF_PROTEIN_METABOLIC_PROCESS	60	7.80E-16	6.87E-14
GOBP_NCRNA_PROCESSING	35	1.10E-15	9.54E-14
GOBP_APOPTOTIC_SIGNALING_PATHWAY	42	1.23E-15	1.05E-13
GOBP_REGULATION_OF_MRNA_PROCESSING	22	1.23E-15	1.05E-13
GOBP_REGULATION_OF_CELLULAR_RESPONSE_TO_STRESS	46	1.88E-15	1.58E-13
GOBP_RIBOSOMAL_SMALL_SUBUNIT_BIOGENESIS	17	4.17E-15	3.46E-13
GOBP_MITOCHONDRION_ORGANIZATION	40	4.58E-15	3.76E-13
GOBP_POSITIVE_REGULATION_OF_SIGNALING	76	5.66E-15	4.60E-13
GOBP_REGULATION_OF_ORGANELLE_ORGANIZATION	60	6.72E-15	5.41E-13
GOBP_MRNA_TRANSPORT	22	7.35E-15	5.85E-13
GOBP_RIBONUCLEOPROTEIN_COMPLEX_SUBUNIT_ORGANIZATION	26	1.22E-14	9.60E-13
GOBP_RESPONSE_TO_CYTOKINE	60	1.58E-14	1.23E-12
GOBP_VIRAL_LIFE_CYCLE	31	2.96E-14	2.28E-12
GOBP_MRNA_EXPORT_FROM_NUCLEUS	19	3.46E-14	2.64E-12
GOBP_INTRINSIC_APOPTOTIC_SIGNALING_PATHWAY	28	3.89E-14	2.94E-12
GOBP_MEMBRANE_ORGANIZATION	52	4.27E-14	3.19E-12

Figure 104 Gene ontology analysis of genes upregulated in response to CD in dKO$^{MRTF\text{-}NLS}$ cells by TTseq

Gene ontology analysis of genes upregulated by CD treatment in dKO$^{MRTF\text{-}NLS}$ cells by TTseq. FDR<0.05. Relates to Figure 48. Bioinformatic analysis of TTseq data was performed by Francesco Gualdrini.

GO BIOLOGICAL PROCESS	# Genes	p-value	FDR q-value
GOBP_CHROMOSOME_ORGANIZATION	69	3.74E-32	2.80E-28
GOBP_CELL_CYCLE	82	4.26E-31	1.59E-27
GOBP_NEGATIVE_REGULATION_OF_NUCLEOBASE_CONTAINING_COMPOUND_METABOLIC_PROCESS	73	4.32E-30	1.08E-26
GOBP_CIRCULATORY_SYSTEM_DEVELOPMENT	63	3.00E-29	5.62E-26
GOBP_CELL_POPULATION_PROLIFERATION	81	4.54E-29	6.79E-26
GOBP_TUBE_DEVELOPMENT	61	1.01E-28	1.26E-25
GOBP_REGULATION_OF_MULTICELLULAR_ORGANISMAL_DEVELOPMENT	68	2.52E-28	2.69E-25
GOBP_NEGATIVE_REGULATION_OF_BIOSYNTHETIC_PROCESS	74	4.87E-28	4.56E-25
GOBP_MITOTIC_CELL_CYCLE	58	2.62E-27	2.18E-24
GOBP_LOCOMOTION	78	1.26E-26	9.43E-24
GOBP_CELL_CYCLE_PROCESS	66	1.92E-26	1.30E-23
GOBP_CELL_MIGRATION	69	1.20E-25	7.27E-23
GOBP_EMBRYO_DEVELOPMENT	55	1.26E-25	7.27E-23
GOBP_CELL_DIVISION	44	2.00E-25	1.07E-22
GOBP_REGULATION_OF_ORGANELLE_ORGANIZATION	58	1.19E-24	5.93E-22
GOBP_POSITIVE_REGULATION_OF_BIOSYNTHETIC_PROCESS	74	4.23E-24	1.98E-21
GOBP_POSITIVE_REGULATION_OF_NUCLEOBASE_CONTAINING_COMPOUND_METABOLIC_PROCESS	72	4.51E-24	1.99E-21
GOBP_REGULATION_OF_CELL_DIFFERENTIATION	67	5.96E-24	2.48E-21
GOBP_REGULATION_OF_CELL_CYCLE	58	8.10E-24	3.19E-21
GOBP_TUBE_MORPHOGENESIS	50	2.23E-23	8.35E-21
GOBP_VASCULATURE_DEVELOPMENT	47	2.44E-23	8.70E-21
GOBP_NEUROGENESIS	65	1.32E-22	4.48E-20
GOBP_POSITIVE_REGULATION_OF_DEVELOPMENTAL_PROCESS	58	1.42E-22	4.63E-20
GOBP_CYTOSKELETON_ORGANIZATION	60	1.64E-22	5.13E-20
GOBP_REGULATION_OF_CELL_DEATH	65	5.81E-22	1.74E-19
GOBP_CHROMATIN_ORGANIZATION	45	3.58E-21	1.03E-18
GOBP_RESPONSE_TO_ENDOGENOUS_STIMULUS	63	4.52E-21	1.25E-18
GOBP_REGULATION_OF_CELL_CYCLE_PROCESS	44	1.01E-20	2.70E-18
GOBP_MITOTIC_NUCLEAR_DIVISION	29	1.54E-20	3.97E-18
GOBP_PROTEIN_PHOSPHORYLATION	62	1.68E-20	4.20E-18
GOBP_APOPTOTIC_PROCESS	68	1.84E-20	4.43E-18
GOBP_ANATOMICAL_STRUCTURE_FORMATION_INVOLVED_IN_MORPHOGENESIS	52	1.95E-20	4.55E-18
GOBP_POSITIVE_REGULATION_OF_CELLULAR_COMPONENT_ORGANIZATION	51	4.33E-20	9.83E-18
GOBP_POSITIVE_REGULATION_OF_MOLECULAR_FUNCTION	63	1.67E-19	3.67E-17
GOBP_REPRODUCTION	56	8.63E-19	1.84E-16
GOBP_ANIMAL_ORGAN_MORPHOGENESIS	47	1.17E-18	2.44E-16
GOBP_RESPONSE_TO_GROWTH_FACTOR	40	1.25E-18	2.52E-16
GOBP_REGULATION_OF_INTRACELLULAR_SIGNAL_TRANSDUCTION	62	2.08E-18	4.10E-16
GOBP_NEGATIVE_REGULATION_OF_CELL_CYCLE_PROCESS	29	3.10E-18	5.94E-16
GOBP_REGULATION_OF_MITOTIC_CELL_CYCLE	36	5.11E-18	9.55E-16
GOBP_NEURON_DIFFERENTIATION	53	6.41E-18	1.17E-15
GOBP_NEGATIVE_REGULATION_OF_CELLULAR_COMPONENT_ORGANIZATION	39	7.40E-18	1.32E-15
GOBP_NEGATIVE_REGULATION_OF_RESPONSE_TO_STIMULUS	59	8.13E-18	1.41E-15
GOBP_NEGATIVE_REGULATION_OF_CELL_CYCLE	36	1.36E-17	2.32E-15
GOBP_NUCLEOSOME_ASSEMBLY	20	1.76E-17	2.91E-15
GOBP_DNA_CONFORMATION_CHANGE	28	1.79E-17	2.91E-15
GOBP_HEART_DEVELOPMENT	34	1.85E-17	2.95E-15
GOBP_DNA_PACKAGING	24	2.05E-17	3.20E-15
GOBP_ORGANELLE_FISSION	32	2.15E-17	3.28E-15
GOBP_POSITIVE_REGULATION_OF_SIGNALING	59	3.30E-17	4.94E-15
GOBP_CHROMATIN_ASSEMBLY_OR_DISASSEMBLY	23	3.98E-17	5.83E-15
GOBP_NUCLEOSOME_ORGANIZATION	21	1.28E-16	1.82E-14
GOBP_EMBRYO_DEVELOPMENT_ENDING_IN_BIRTH_OR_EGG_HATCHING	34	1.29E-16	1.82E-14
GOBP_CELL_PROJECTION_ORGANIZATION	55	1.48E-16	2.05E-14
GOBP_NEGATIVE_REGULATION_OF_MITOTIC_CELL_CYCLE	26	1.67E-16	2.27E-14
GOBP_POSITIVE_REGULATION_OF_CELL_DIFFERENTIATION	40	1.72E-16	2.29E-14
GOBP_BLOOD_VESSEL_MORPHOGENESIS	36	1.76E-16	2.29E-14
GOBP_ENZYME_LINKED_RECEPTOR_PROTEIN_SIGNALING_PATHWAY	45	1.80E-16	2.29E-14
GOBP_PROTEIN_CONTAINING_COMPLEX_SUBUNIT_ORGANIZATION	62	1.81E-16	2.29E-14
GOBP_POSITIVE_REGULATION_OF_PROTEIN_METABOLIC_PROCESS	54	2.16E-16	2.70E-14
GOBP_BIOLOGICAL_ADHESION	53	2.52E-16	3.09E-14
GOBP_NEGATIVE_REGULATION_OF_CELL_CYCLE_PHASE_TRANSITION	24	2.58E-16	3.11E-14
GOBP_EMBRYONIC_MORPHOGENESIS	33	2.77E-16	3.29E-14
GOBP_NUCLEAR_CHROMOSOME_SEGREGATION	24	3.93E-16	4.59E-14
GOBP_POSITIVE_REGULATION_OF_MULTICELLULAR_ORGANISMAL_PROCESS	51	4.42E-16	5.09E-14
GOBP_CHROMOSOME_SEGREGATION	26	5.42E-16	6.14E-14
GOBP_NEURON_DEVELOPMENT	45	6.25E-16	6.98E-14
GOBP_SISTER_CHROMATID_SEGREGATION	21	7.14E-16	7.86E-14
GOBP_PROTEIN_DNA_COMPLEX_SUBUNIT_ORGANIZATION	24	7.55E-16	8.19E-14
GOBP_REGULATION_OF_CELL_CYCLE_PHASE_TRANSITION	30	8.06E-16	8.62E-14
GOBP_CENTRAL_NERVOUS_SYSTEM_DEVELOPMENT	42	9.64E-16	1.02E-13
GOBP_CELLULAR_MACROMOLECULE_LOCALIZATION	61	1.14E-15	1.19E-13
GOBP_APPENDAGE_MORPHOGENESIS	18	1.18E-15	1.21E-13
GOBP_POSITIVE_REGULATION_OF_TRANSCRIPTION_BY_RNA_POLYMERASE_II	46	1.27E-15	1.29E-13
GOBP_IMMUNE_SYSTEM_DEVELOPMENT	42	1.32E-15	1.32E-13
GOBP_CELL_CYCLE_PHASE_TRANSITION	34	1.36E-15	1.34E-13
GOBP_GROWTH	40	1.97E-15	1.91E-13
GOBP_RESPONSE_TO_LIPID	39	2.13E-15	2.04E-13
GOBP_REGULATION_OF_ANATOMICAL_STRUCTURE_MORPHOGENESIS	42	2.37E-15	2.24E-13
GOBP_ESTABLISHMENT_OR_MAINTENANCE_OF_CELL_POLARITY	21	2.58E-15	2.38E-13
GOBP_SKELETAL_SYSTEM_MORPHOGENESIS	21	2.58E-15	2.38E-13
GOBP_MITOTIC_SISTER_CHROMATID_SEGREGATION	19	3.08E-15	2.81E-13
GOBP_EXTERNAL_ENCAPSULATING_STRUCTURE_ORGANIZATION	27	3.12E-15	2.81E-13
GOBP_MICROTUBULE_CYTOSKELETON_ORGANIZATION_INVOLVED_IN_MITOSIS	18	3.79E-15	3.38E-13
GOBP_APPENDAGE_DEVELOPMENT	19	4.31E-15	3.80E-13
GOBP_REGULATION_OF_CYTOSKELETON_ORGANIZATION	30	4.52E-15	3.94E-13
GOBP_EPITHELIUM_DEVELOPMENT	47	4.89E-15	4.21E-13
GOBP_RESPONSE_TO_OXYGEN_CONTAINING_COMPOUND	54	5.78E-15	4.91E-13
GOBP_NEGATIVE_REGULATION_OF_GENE_EXPRESSION_EPIGENETIC	17	5.96E-15	5.01E-13
GOBP_EMBRYONIC_ORGAN_DEVELOPMENT	27	8.19E-15	6.81E-13
GOBP_REGULATION_OF_CELL_ADHESION	35	1.13E-14	9.26E-13
GOBP_REGULATION_OF_PROTEIN_MODIFICATION_PROCESS	53	1.16E-14	9.44E-13
GOBP_CHROMATIN_ORGANIZATION_INVOLVED_IN_REGULATION_OF_TRANSCRIPTION	18	1.42E-14	1.14E-12
GOBP_NEGATIVE_REGULATION_OF_TRANSCRIPTION_BY_RNA_POLYMERASE_II	38	1.45E-14	1.15E-12
GOBP_EMBRYONIC_APPENDAGE_MORPHOGENESIS	16	1.70E-14	1.34E-12
GOBP_NEGATIVE_REGULATION_OF_CELL_POPULATION_PROLIFERATION	35	2.49E-14	1.94E-12
GOBP_NEGATIVE_REGULATION_OF_CELL_DEATH	40	3.42E-14	2.64E-12
GOBP_POSITIVE_REGULATION_OF_CATALYTIC_ACTIVITY	48	3.84E-14	2.93E-12
GOBP_REGULATION_OF_CHROMOSOME_ORGANIZATION	22	4.09E-14	3.09E-12
GOBP_REPRODUCTIVE_SYSTEM_DEVELOPMENT	26	5.00E-14	3.74E-12

Figure 105 Gene ontology analysis of genes downregulated in response to CD in dKO$^{MRTF\text{-}NLS}$ cells by TTseq

Gene ontology analysis of genes downregulated by CD treatment in dKO$^{MRTF\text{-}NLS}$ cells by TTseq. FDR<0.05. Relates to Figure 48. Bioinformatic analysis of TTseq data was performed by Francesco Gualdrini.

GO BIOLOGICAL PROCESS	# Genes	p-value	FDR q-value
GOBP_CELL_CYCLE	152	4.49E-32	3.40E-28
GOBP_CELL_CYCLE_PROCESS	120	5.72E-27	2.17E-23
GOBP_MITOTIC_CELL_CYCLE	96	4.23E-24	1.07E-20
GOBP_CELLULAR_RESPONSE_TO_DNA_DAMAGE_STIMULUS	85	1.43E-23	2.71E-20
GOBP_REGULATION_OF_INTRACELLULAR_SIGNAL_TRANSDUCTION	131	4.21E-22	6.37E-19
GOBP_CYTOSKELETON_ORGANIZATION	107	6.71E-21	8.47E-18
GOBP_PROTEIN_CONTAINING_COMPLEX_SUBUNIT_ORGANIZATION	130	1.80E-19	1.95E-16
GOBP_CELLULAR_MACROMOLECULE_LOCALIZATION	128	1.94E-18	1.84E-15
GOBP_REGULATION_OF_CELL_CYCLE	93	5.53E-18	4.66E-15
GOBP_REGULATION_OF_ORGANELLE_ORGANIZATION	96	1.50E-17	1.14E-14
GOBP_CARBOHYDRATE_DERIVATIVE_METABOLIC_PROCESS	88	5.08E-17	4.22E-15
GOBP_CELL_POPULATION_PROLIFERATION	123	6.00E-17	1.36E-14
GOBP_DNA_METABOLIC_PROCESS	77	6.21E-17	3.57E-14
GOBP_ACTIN_FILAMENT_BASED_PROCESS	69	6.84E-17	3.57E-14
GOBP_SMALL_MOLECULE_METABOLIC_PROCESS	118	1.45E-16	7.29E-14
GOBP_NEGATIVE_REGULATION_OF_RESPONSE_TO_STIMULUS	109	1.46E-16	7.29E-14
GOBP_APOPTOTIC_PROCESS	117	1.95E-15	8.56E-13
GOBP_RESPONSE_TO_ENDOGENOUS_STIMULUS	104	2.38E-15	9.88E-13
GOBP_REGULATION_OF_CELL_DEATH	105	3.73E-15	1.47E-12
GOBP_NEGATIVE_REGULATION_OF_SIGNALING	94	5.03E-15	1.88E-12
GOBP_RESPONSE_TO_ABIOTIC_STIMULUS	85	8.27E-15	2.95E-12
GOBP_REGULATION_OF_PHOSPHORUS_METABOLIC_PROCESS	102	8.93E-15	3.04E-12
GOBP_ORGANELLE_FISSION	49	9.64E-15	3.13E-12
GOBP_ORGANELLE_ASSEMBLY	69	1.04E-14	3.20E-12
GOBP_CHROMOSOME_ORGANIZATION	86	1.07E-14	3.20E-12
GOBP_PEPTIDYL_AMINO_ACID_MODIFICATION	87	1.19E-14	3.43E-12
GOBP_REGULATION_OF_PROTEIN_MODIFICATION_PROCESS	101	4.33E-14	1.20E-11
GOBP_POSITIVE_REGULATION_OF_NUCLEOBASE_CONTAINING_COMPOUND_METABOLIC_PROCESS	110	6.43E-14	1.72E-11
GOBP_DNA_REPAIR	52	7.63E-14	1.97E-11
GOBP_CELL_DIVISION	53	1.70E-13	4.24E-11
GOBP_REGULATION_OF_CELL_DIFFERENTIATION	99	1.88E-13	4.53E-11
GOBP_REGULATION_OF_HYDROLASE_ACTIVITY	85	2.87E-13	6.72E-11
GOBP_INTRACELLULAR_TRANSPORT	103	3.16E-13	7.17E-11
GOBP_ESTABLISHMENT_OF_PROTEIN_LOCALIZATION	113	3.49E-13	7.68E-11
GOBP_REGULATION_OF_CELLULAR_COMPONENT_BIOGENESIS	69	7.36E-13	1.55E-10
GOBP_REGULATION_OF_TRANSPORT	102	7.47E-13	1.55E-10
GOBP_POSITIVE_REGULATION_OF_BIOSYNTHETIC_PROCESS	111	7.98E-13	1.61E-10
GOBP_ORGANONITROGEN_COMPOUND_BIOSYNTHETIC_PROCESS	104	9.30E-13	1.83E-10
GOBP_HOMEOSTATIC_PROCESS	109	9.54E-13	1.83E-10
GOBP_ORGANONITROGEN_COMPOUND_CATABOLIC_PROCESS	85	1.19E-12	2.22E-10
GOBP_POSITIVE_REGULATION_OF_PROTEIN_METABOLIC_PROCESS	93	1.43E-12	2.61E-10
GOBP_BIOLOGICAL_ADHESION	91	1.50E-12	2.67E-10
GOBP_CARBOHYDRATE_DERIVATIVE_BIOSYNTHETIC_PROCESS	55	2.05E-12	3.56E-10
GOBP_PROTEIN_PHOSPHORYLATION	96	2.43E-12	4.12E-10
GOBP_POSITIVE_REGULATION_OF_MOLECULAR_FUNCTION	101	2.89E-12	4.81E-10
GOBP_POSITIVE_REGULATION_OF_SIGNALING	100	3.41E-12	5.55E-10
GOBP_CELL_CYCLE_CHECKPOINT	28	6.62E-12	1.05E-09
GOBP_RESPONSE_TO_OXYGEN_CONTAINING_COMPOUND	96	8.92E-12	1.39E-09
GOBP_REGULATION_OF_MITOTIC_CELL_CYCLE	50	9.58E-12	1.46E-09
GOBP_NEGATIVE_REGULATION_OF_CELL_DEATH	68	1.00E-11	1.50E-09
GOBP_CELL_PROJECTION_ORGANIZATION	92	1.35E-11	1.98E-09
GOBP_RESPONSE_TO_WOUNDING	52	1.55E-11	2.23E-09
GOBP_WOUND_HEALING	46	1.72E-11	2.42E-09
GOBP_NUCLEOBASE_CONTAINING_SMALL_MOLECULE_METABOLIC_PROCESS	50	1.94E-11	2.69E-09
GOBP_CELL_CYCLE_PHASE_TRANSITION	51	2.38E-11	3.23E-09
GOBP_LOCOMOTION	107	3.28E-11	4.38E-09
GOBP_CELL_SUBSTRATE_ADHESION	36	3.93E-11	5.16E-09
GOBP_POSITIVE_REGULATION_OF_CATALYTIC_ACTIVITY	84	4.03E-11	5.19E-09
GOBP_ORGANOPHOSPHATE_METABOLIC_PROCESS	68	4.22E-11	5.31E-09
GOBP_REGULATION_OF_PROTEIN_PHOSPHORYLATION	76	4.26E-11	5.31E-09
GOBP_CELL_MIGRATION	92	4.36E-11	5.34E-09
GOBP_NEGATIVE_REGULATION_OF_MOLECULAR_FUNCTION	74	4.84E-11	5.84E-09
GOBP_REGULATION_OF_ION_TRANSPORT	80	5.58E-11	6.63E-09
GOBP_SECRETION	86	6.32E-11	7.38E-09
GOBP_RESPONSE_TO_HORMONE	61	6.64E-11	7.65E-09
GOBP_REGULATION_OF_APOPTOTIC_SIGNALING_PATHWAY	35	6.75E-11	7.65E-09
GOBP_SIGNAL_TRANSDUCTION_BY_P53_CLASS_MEDIATOR	30	7.18E-11	8.02E-09
GOBP_DNA_REPLICATION	31	7.45E-11	8.20E-09
GOBP_APOPTOTIC_SIGNALING_PATHWAY	47	7.82E-11	8.47E-09
GOBP_REGULATION_OF_CELL_SUBSTRATE_ADHESION	27	9.78E-11	1.05E-08
GOBP_SUPRAMOLECULAR_FIBER_ORGANIZATION	53	1.07E-10	1.12E-08
GOBP_POSITIVE_REGULATION_OF_CELLULAR_COMPONENT_ORGANIZATION	71	1.13E-10	1.18E-08
GOBP_REGULATION_OF_RESPONSE_TO_STRESS	83	1.43E-10	1.47E-08
GOBP_MUSCLE_SYSTEM_PROCESS	40	1.62E-10	1.64E-08
GOBP_ACTIN_FILAMENT_ORGANIZATION	39	1.64E-10	1.64E-08
GOBP_NEGATIVE_REGULATION_OF_CELL_CYCLE	48	2.87E-10	2.82E-08
GOBP_NEUROGENESIS	90	3.10E-10	3.01E-08
GOBP_POSITIVE_REGULATION_OF_APOPTOTIC_SIGNALING_PATHWAY	20	3.14E-10	3.01E-08
GOBP_POSITIVE_REGULATION_OF_INTRACELLULAR_SIGNAL_TRANSDUCTION	65	3.38E-10	3.20E-08
GOBP_DNA_INTEGRITY_CHECKPOINT	22	4.33E-10	4.04E-08
GOBP_POSITIVE_REGULATION_OF_DEVELOPMENTAL_PROCESS	76	6.11E-10	5.64E-08
GOBP_MITOTIC_CELL_CYCLE_CHECKPOINT	22	6.27E-10	5.72E-08
GOBP_CARBOHYDRATE_METABOLIC_PROCESS	47	6.37E-10	5.74E-08
GOBP_POSITIVE_REGULATION_OF_ORGANELLE_ORGANIZATION	45	9.27E-10	8.25E-08
GOBP_SMALL_MOLECULE_BIOSYNTHETIC_PROCESS	50	1.04E-09	9.13E-08
GOBP_MACROMOLECULE_CATABOLIC_PROCESS	81	1.22E-09	1.06E-07
GOBP_NEGATIVE_REGULATION_OF_PROTEIN_METABOLIC_PROCESS	68	1.25E-09	1.08E-07
GOBP_MUSCLE_CONTRACTION	33	1.43E-09	1.22E-07
GOBP_REGULATION_OF_CELL_CYCLE_PROCESS	54	1.54E-09	1.29E-07
GOBP_CELL_MATRIX_ADHESION	26	1.59E-09	1.32E-07
GOBP_RESPONSE_TO_NITROGEN_COMPOUND	68	1.62E-09	1.32E-07
GOBP_PROTEIN_LOCALIZATION_TO_ORGANELLE	63	1.63E-09	1.32E-07
GOBP_PROTEIN_LOCALIZATION_TO_MEMBRANE	48	1.64E-09	1.32E-07
GOBP_INTRINSIC_APOPTOTIC_SIGNALING_PATHWAY	29	1.85E-09	1.47E-07
GOBP_NEGATIVE_REGULATION_OF_CATALYTIC_ACTIVITY	55	1.86E-09	1.47E-07
GOBP_GROWTH	59	1.88E-09	1.47E-07
GOBP_REGULATION_OF_CELLULAR_COMPONENT_MOVEMENT	67	2.10E-09	1.62E-07
GOBP_REGULATION_OF_CATABOLIC_PROCESS	63	2.22E-09	1.70E-07
GOBP_REGULATION_OF_PROTEOLYSIS	51	2.31E-09	1.75E-07
GOBP_DEVELOPMENTAL_GROWTH	45	2.93E-09	2.19E-07

Figure 106 Gene ontology analysis of genes upregulated in response to CD in Mtr4-depeted NIH3T3 cells by RNAseq

Gene ontology analysis of genes upregulated by CD treatment in Mtr4-depleted NIH3T3 cells by RNAseq. FDR<0.05. Relates to Figure 53. Bioinformatic analysis of RNAseq data was performed by Francesco Gualdrini.

GO BIOLOGICAL PROCESS	# Genes	p-value	FDR q-value
GOBP_POSITIVE_REGULATION_OF_NUCLEOBASE_CONTAINING_COMPOUND_METABOLIC_PROCESS	225	2.25E-67	1.68E-63
GOBP_POSITIVE_REGULATION_OF_BIOSYNTHETIC_PROCESS	228	4.01E-65	1.50E-61
GOBP_POSITIVE_REGULATION_OF_MOLECULAR_FUNCTION	213	3.57E-64	8.91E-61
GOBP_REGULATION_OF_INTRACELLULAR_SIGNAL_TRANSDUCTION	215	7.33E-64	1.37E-60
GOBP_POSITIVE_REGULATION_OF_CATALYTIC_ACTIVITY	177	4.07E-55	6.09E-52
GOBP_POSITIVE_REGULATION_OF_TRANSCRIPTION_BY_RNA_POLYMERASE_II	161	1.29E-54	1.61E-51
GOBP_ENZYME_LINKED_RECEPTOR_PROTEIN_SIGNALING_PATHWAY	147	4.50E-50	4.81E-47
GOBP_REGULATION_OF_CELL_DIFFERENTIATION	183	6.90E-50	6.45E-47
GOBP_POSITIVE_REGULATION_OF_SIGNALING	187	2.81E-48	2.33E-45
GOBP_REGULATION_OF_PHOSPHORUS_METABOLIC_PROCESS	179	1.05E-47	7.86E-45
GOBP_NEUROGENESIS	179	1.37E-47	9.31E-45
GOBP_REGULATION_OF_PROTEIN_MODIFICATION_PROCESS	179	4.66E-47	2.91E-44
GOBP_PROTEIN_PHOSPHORYLATION	178	7.35E-47	4.23E-44
GOBP_NEGATIVE_REGULATION_OF_RESPONSE_TO_STIMULUS	179	2.35E-45	1.25E-42
GOBP_REGULATION_OF_HYDROLASE_ACTIVITY	155	4.29E-45	2.14E-42
GOBP_CELL_PROJECTION_ORGANIZATION	171	1.99E-44	9.29E-42
GOBP_NEGATIVE_REGULATION_OF_BIOSYNTHETIC_PROCESS	178	2.71E-44	1.19E-41
GOBP_POSITIVE_REGULATION_OF_DEVELOPMENTAL_PROCESS	152	1.06E-43	4.39E-41
GOBP_APOPTOTIC_PROCESS	191	1.75E-43	6.88E-41
GOBP_NEGATIVE_REGULATION_OF_SIGNALING	159	4.37E-43	1.64E-40
GOBP_SMALL_GTPASE_MEDIATED_SIGNAL_TRANSDUCTION	93	9.63E-43	3.43E-40
GOBP_CELL_POPULATION_PROLIFERATION	191	1.03E-42	3.50E-40
GOBP_NEURON_DIFFERENTIATION	155	1.23E-42	3.85E-40
GOBP_LOCOMOTION	192	1.24E-42	3.85E-40
GOBP_NEGATIVE_REGULATION_OF_NUCLEOBASE_CONTAINING_COMPOUND_METABOLIC_PROCESS	165	1.40E-42	4.19E-40
GOBP_RESPONSE_TO_ENDOGENOUS_STIMULUS	171	2.33E-42	6.71E-40
GOBP_INTRACELLULAR_TRANSPORT	176	1.32E-41	3.66E-39
GOBP_ESTABLISHMENT_OF_PROTEIN_LOCALIZATION	189	9.06E-41	2.42E-38
GOBP_POSITIVE_REGULATION_OF_PROTEIN_METABOLIC_PROCESS	161	7.09E-40	1.83E-37
GOBP_CELLULAR_MACROMOLECULE_LOCALIZATION	187	1.02E-39	2.55E-37
GOBP_MACROMOLECULE_CATABOLIC_PROCESS	153	1.07E-38	2.59E-36
GOBP_NEGATIVE_REGULATION_OF_TRANSCRIPTION_BY_RNA_POLYMERASE_II	115	1.61E-37	3.76E-35
GOBP_CELL_MIGRATION	160	8.65E-37	1.96E-34
GOBP_REGULATION_OF_SMALL_GTPASE_MEDIATED_SIGNAL_TRANSDUCTION	69	2.36E-36	5.19E-34
GOBP_CELL_MORPHOGENESIS	122	3.41E-36	7.30E-34
GOBP_CYTOSKELETON_ORGANIZATION	145	9.58E-36	1.99E-33
GOBP_REGULATION_OF_CATABOLIC_PROCESS	121	1.84E-35	3.71E-33
GOBP_REGULATION_OF_TRANSFERASE_ACTIVITY	121	2.71E-35	5.33E-33
GOBP_CELL_CELL_SIGNALING_BY_WNT	85	3.34E-35	6.40E-33
GOBP_NEURON_DEVELOPMENT	127	4.96E-35	9.27E-33
GOBP_REGULATION_OF_PROTEIN_PHOSPHORYLATION	133	9.02E-35	1.65E-32
GOBP_POSITIVE_REGULATION_OF_HYDROLASE_ACTIVITY	104	1.08E-34	1.93E-32
GOBP_POSITIVE_REGULATION_OF_INTRACELLULAR_SIGNAL_TRANSDUCTION	119	3.15E-34	5.49E-32
GOBP_CIRCULATORY_SYSTEM_DEVELOPMENT	127	7.90E-34	1.34E-31
GOBP_REGULATION_OF_MULTICELLULAR_ORGANISMAL_DEVELOPMENT	142	1.91E-33	3.17E-31
GOBP_REGULATION_OF_CELL_DEATH	157	2.30E-33	3.73E-31
GOBP_HOMEOSTATIC_PROCESS	171	2.41E-33	3.83E-31
GOBP_REGULATION_OF_GTPASE_ACTIVITY	80	4.15E-33	6.46E-31
GOBP_TRANSMEMBRANE_RECEPTOR_PROTEIN_TYROSINE_KINASE_SIGNALING_PATHWAY	99	4.78E-33	7.29E-31
GOBP_CELLULAR_MACROMOLECULE_CATABOLIC_PROCESS	129	8.48E-33	1.27E-30
GOBP_POSITIVE_REGULATION_OF_CELL_DIFFERENTIATION	106	9.37E-33	1.37E-30
GOBP_PEPTIDYL_AMINO_ACID_MODIFICATION	133	1.11E-32	1.60E-30
GOBP_CELL_CELL_SIGNALING	156	1.89E-32	2.66E-30
GOBP_CELL_SURFACE_RECEPTOR_SIGNALING_PATHWAY_INVOLVED_IN_CELL_CELL_SIGNALING	89	2.32E-32	3.21E-30
GOBP_TUBE_DEVELOPMENT	121	2.73E-32	3.71E-30
GOBP_EMBRYO_DEVELOPMENT	115	3.03E-32	4.05E-30
GOBP_PROTEOLYSIS	162	5.74E-32	7.53E-30
GOBP_PROTEIN_MODIFICATION_BY_SMALL_PROTEIN_CONJUGATION_OR_REMOVAL	125	6.83E-32	8.82E-30
GOBP_POSITIVE_REGULATION_OF_CELLULAR_COMPONENT_ORGANIZATION	122	1.18E-31	1.50E-29
GOBP_REGULATION_OF_ORGANELLE_ORGANIZATION	124	3.98E-31	4.96E-29
GOBP_ORGANONITROGEN_COMPOUND_CATABOLIC_PROCESS	134	4.08E-31	5.00E-29
GOBP_PROTEIN_CATABOLIC_PROCESS	110	6.08E-31	7.34E-29
GOBP_SKELETAL_SYSTEM_DEVELOPMENT	77	9.29E-31	1.10E-28
GOBP_REGULATION_OF_CELLULAR_CATABOLIC_PROCESS	103	1.27E-30	1.48E-28
GOBP_ANIMAL_ORGAN_MORPHOGENESIS	114	2.40E-30	2.77E-28
GOBP_POSITIVE_REGULATION_OF_PHOSPHORUS_METABOLIC_PROCESS	111	3.25E-30	3.68E-28
GOBP_SUPRAMOLECULAR_FIBER_ORGANIZATION	93	3.43E-30	3.83E-28
GOBP_POSITIVE_REGULATION_OF_GTPASE_ACTIVITY	70	4.01E-30	4.41E-28
GOBP_POSITIVE_REGULATION_OF_PROTEIN_MODIFICATION_PROCESS	115	5.70E-30	6.18E-28
GOBP_REGULATION_OF_CELLULAR_COMPONENT_MOVEMENT	118	5.96E-30	6.37E-28
GOBP_CELL_MORPHOGENESIS_INVOLVED_IN_DIFFERENTIATION	93	1.25E-29	1.32E-27
GOBP_NEGATIVE_REGULATION_OF_PROTEIN_METABOLIC_PROCESS	118	1.36E-29	1.39E-27
GOBP_POSITIVE_REGULATION_OF_MULTICELLULAR_ORGANISMAL_PROCESS	135	1.36E-29	1.39E-27
GOBP_HEAD_DEVELOPMENT	94	4.60E-29	4.65E-27
GOBP_BIOLOGICAL_ADHESION	138	1.18E-28	1.18E-26
GOBP_RESPONSE_TO_GROWTH_FACTOR	92	1.34E-28	1.32E-26
GOBP_CHROMATIN_ORGANIZATION	97	1.58E-28	1.53E-26
GOBP_ANATOMICAL_STRUCTURE_FORMATION_INVOLVED_IN_MORPHOGENESIS	118	1.75E-28	1.68E-26
GOBP_CELLULAR_COMPONENT_MORPHOGENESIS	94	2.33E-28	2.20E-26
GOBP_RESPONSE_TO_OXYGEN_CONTAINING_COMPOUND	147	2.35E-28	2.20E-26
GOBP_REGULATION_OF_WNT_SIGNALING_PATHWAY	64	2.93E-28	2.71E-26
GOBP_PROTEIN_MODIFICATION_BY_SMALL_PROTEIN_CONJUGATION	106	4.11E-28	3.70E-26
GOBP_REGULATION_OF_CELLULAR_COMPONENT_BIOGENESIS	106	4.11E-28	3.70E-26
GOBP_EMBRYONIC_MORPHOGENESIS	79	1.62E-27	1.44E-25
GOBP_REGULATION_OF_ANATOMICAL_STRUCTURE_MORPHOGENESIS	108	1.71E-27	1.51E-25
GOBP_IMMUNE_SYSTEM_DEVELOPMENT	106	6.13E-27	5.33E-25
GOBP_CELLULAR_RESPONSE_TO_OXYGEN_CONTAINING_COMPOUND	117	1.31E-26	1.13E-24
GOBP_CELL_CYCLE	155	1.34E-26	1.14E-24
GOBP_REGULATION_OF_PROTEIN_KINASE_ACTIVITY	93	1.50E-26	1.26E-24
GOBP_CELLULAR_PROTEIN_CATABOLIC_PROCESS	93	1.81E-26	1.51E-24
GOBP_REGULATION_OF_TRANSPORT	147	2.33E-26	1.92E-24
GOBP_CELL_PART_MORPHOGENESIS	85	2.46E-26	2.00E-24
GOBP_CELL_MORPHOGENESIS_INVOLVED_IN_NEURON_DIFFERENTIATION	78	2.56E-26	2.06E-24
GOBP_TUBE_MORPHOGENESIS	99	4.46E-26	3.55E-24
GOBP_REGULATION_OF_RESPONSE_TO_STRESS	129	5.87E-26	4.62E-24
GOBP_PROTEIN_CONTAINING_COMPLEX_SUBUNIT_ORGANIZATION	158	6.68E-26	5.21E-24
GOBP_CHROMOSOME_ORGANIZATION	119	9.40E-26	7.25E-24
GOBP_POSITIVE_REGULATION_OF_TRANSFERASE_ACTIVITY	84	1.10E-25	8.41E-24
GOBP_MAPK_CASCADE	99	1.23E-25	9.32E-24
GOBP_CENTRAL_NERVOUS_SYSTEM_DEVELOPMENT	103	1.58E-25	1.18E-23

Figure 107 Gene ontology analysis of genes downregulated in response to CD in Mtr4-depeted NIH3T3 cells by RNAseq

Gene ontology analysis of genes downregulated by CD treatment in Mtr4-depleted NIH3T3 cells by RNAseq. FDR<0.05. Relates to Figure 53. Bioinformatic analysis of RNAseq data was performed by Francesco Gualdrini.

Gene Set Name	# Genes	p-value	FDR q-value
GOBP_ACTIN_FILAMENT_BASED_PROCESS	85	3.13E-45	2.37E-41
GOBP_CYTOSKELETON_ORGANIZATION	105	4.22E-42	1.60E-38
GOBP_BIOLOGICAL_ADHESION	104	4.96E-39	1.25E-35
GOBP_REGULATION_OF_INTRACELLULAR_SIGNAL_TRANSDUCTION	115	6.91E-38	1.31E-34
GOBP_REGULATION_OF_PHOSPHORUS_METABOLIC_PROCESS	114	4.19E-37	6.35E-34
GOBP_REGULATION_OF_CELL_DIFFERENTIATION	115	3.74E-36	4.68E-33
GOBP_CELL_MOTILITY	111	4.33E-36	4.68E-33
GOBP_APOPTOTIC_PROCESS	115	3.76E-35	3.56E-32
GOBP_REGULATION_OF_CELL_DEATH	105	1.53E-33	1.29E-30
GOBP_REGULATION_OF_PHOSPHORYLATION	102	3.66E-33	2.77E-30
GOBP_CELL_MIGRATION	102	8.81E-33	1.10E-31
GOBP_POSITIVE_REGULATION_OF_SIGNALING	103	8.84E-33	6.61E-30
GOBP_ACTIN_FILAMENT_ORGANIZATION	54	1.46E-32	9.93E-30
GOBP_RESPONSE_TO_ENDOGENOUS_STIMULUS	98	1.59E-31	9.18E-29
GOBP_POSITIVE_REGULATION_OF_MOLECULAR_FUNCTION	101	4.97E-31	2.65E-28
GOBP_SUPRAMOLECULAR_FIBER_ORGANIZATION	65	5.49E-31	2.74E-28
GOBP_RESPONSE_TO_WOUNDING	62	1.82E-30	8.52E-28
GOBP_REGULATION_OF_CELLULAR_COMPONENT_MOVEMENT	79	2.41E-30	1.06E-27
GOBP_WOUND_HEALING	56	8.64E-30	3.59E-27
GOBP_REGULATION_OF_PROTEIN_MODIFICATION_PROCESS	94	8.60E-29	3.22E-26
GOBP_NEUROGENESIS	93	2.04E-28	7.26E-26
GOBP_CELL_MORPHOGENESIS	72	1.21E-27	4.11E-25
GOBP_RESPONSE_TO_OXYGEN_CONTAINING_COMPOUND	93	1.30E-27	4.23E-25
GOBP_REGULATION_OF_PROTEIN_PHOSPHORYLATION	79	1.39E-27	4.34E-25
GOBP_CELL_SUBSTRATE_ADHESION	45	1.96E-27	5.88E-25
GOBP_REGULATION_OF_CELLULAR_COMPONENT_BIOGENESIS	70	2.12E-27	6.11E-25
GOBP_NEGATIVE_REGULATION_OF_RESPONSE_TO_STIMULUS	93	3.01E-27	8.34E-25
GOBP_REGULATION_OF_CELL_ADHESION	61	6.09E-27	1.63E-24
GOBP_REGULATION_OF_ANATOMICAL_STRUCTURE_MORPHOGENESIS	71	7.51E-27	1.94E-24
GOBP_CELL_POPULATION_PROLIFERATION	100	1.64E-26	4.08E-24
GOBP_POSITIVE_REGULATION_OF_CATALYTIC_ACTIVITY	83	4.02E-26	9.70E-24
GOBP_POSITIVE_REGULATION_OF_DEVELOPMENTAL_PROCESS	79	6.12E-26	1.43E-23
GOBP_ENZYME_LINKED_RECEPTOR_PROTEIN_SIGNALING_PATHWAY	72	6.32E-26	1.43E-23
GOBP_REGULATION_OF_ORGANELLE_ORGANIZATION	75	7.56E-26	1.66E-23
GOBP_RESPONSE_TO_HORMONE	65	7.91E-26	1.69E-23
GOBP_POSITIVE_REGULATION_OF_PROTEIN_METABOLIC_PROCESS	86	1.47E-25	3.05E-23
GOBP_POSITIVE_REGULATION_OF_CELLULAR_COMPONENT_ORGANIZATION	73	1.54E-25	3.11E-23
GOBP_NEGATIVE_REGULATION_OF_SIGNALING	82	2.53E-25	4.98E-23
GOBP_CELL_PROJECTION_ORGANIZATION	86	8.04E-25	1.54E-22
GOBP_CIRCULATORY_SYSTEM_DEVELOPMENT	72	2.42E-24	4.53E-22
GOBP_POSITIVE_REGULATION_OF_PROTEIN_MODIFICATION_PROCESS	69	2.65E-24	4.78E-22
GOBP_ANATOMICAL_STRUCTURE_FORMATION_INVOLVED_IN_MORPHOGENESIS	72	2.68E-24	4.78E-22
GOBP_REGULATION_OF_CELL_SUBSTRATE_ADHESION	34	3.70E-24	6.44E-22
GOBP_MAPK_CASCADE	64	3.95E-24	6.72E-22
GOBP_SMALL_MOLECULE_METABOLIC_PROCESS	94	4.20E-24	6.98E-22
GOBP_POSITIVE_REGULATION_OF_PHOSPHORUS_METABOLIC_PROCESS	66	7.46E-24	1.21E-21
GOBP_REGULATION_OF_MULTICELLULAR_ORGANISMAL_DEVELOPMENT	79	1.26E-23	2.00E-21
GOBP_NEGATIVE_REGULATION_OF_CELL_DEATH	66	1.30E-23	2.03E-21
GOBP_POSITIVE_REGULATION_OF_MULTICELLULAR_ORGANISMAL_PROCESS	78	5.41E-23	8.26E-21
GOBP_REGULATION_OF_MAPK_CASCADE	55	6.05E-23	9.05E-21
GOBP_TUBE_DEVELOPMENT	68	7.75E-23	1.14E-20
GOBP_POSITIVE_REGULATION_OF_PROTEIN_PHOSPHORYLATION	58	5.26E-22	7.56E-20
GOBP_REGULATION_OF_TRANSPORT	86	5.50E-22	7.76E-20
GOBP_POSITIVE_REGULATION_OF_INTRACELLULAR_SIGNAL_TRANSDUCTION	63	3.24E-21	4.49E-19
GOBP_REGULATION_OF_HYDROLASE_ACTIVITY	72	4.02E-21	5.47E-19
GOBP_TUBE_MORPHOGENESIS	59	7.41E-21	9.89E-19
GOBP_REGULATION_OF_RESPONSE_TO_STRESS	75	7.89E-21	1.04E-18
GOBP_CELLULAR_RESPONSE_TO_OXYGEN_CONTAINING_COMPOUND	68	8.22E-21	1.06E-18
GOBP_VASCULATURE_DEVELOPMENT	55	8.51E-21	1.08E-18
GOBP_POSITIVE_REGULATION_OF_BIOSYNTHETIC_PROCESS	90	9.55E-21	1.19E-18
GOBP_BLOOD_VESSEL_MORPHOGENESIS	51	9.78E-21	1.20E-18
GOBP_TRANSMEMBRANE_RECEPTOR_PROTEIN_TYROSINE_KINASE_SIGNALING_PATHWAY	53	1.33E-20	1.60E-18
GOBP_CELLULAR_COMPONENT_MORPHOGENESIS	54	1.40E-20	1.66E-18
GOBP_APOPTOTIC_SIGNALING_PATHWAY	47	1.79E-20	2.09E-18
GOBP_REGULATION_OF_ACTIN_FILAMENT_BASED_PROCESS	39	2.14E-20	2.46E-18
GOBP_POSITIVE_REGULATION_OF_LOCOMOTION	47	2.53E-20	2.87E-18
GOBP_RESPONSE_TO_ABIOTIC_STIMULUS	68	3.74E-20	4.18E-18
GOBP_EXTERNAL_ENCAPSULATING_STRUCTURE_ORGANIZATION	39	4.03E-20	4.43E-18
GOBP_NEURON_DIFFERENTIATION	72	5.00E-20	5.42E-18
GOBP_CELL_JUNCTION_ASSEMBLY	40	6.79E-20	7.25E-18
GOBP_REGULATION_OF_PROTEIN_KINASE_ACTIVITY	54	7.03E-20	7.41E-18
GOBP_POSITIVE_REGULATION_OF_CELLULAR_COMPONENT_BIOGENESIS	44	1.05E-19	1.09E-17
GOBP_MUSCLE_STRUCTURE_DEVELOPMENT	47	1.13E-19	1.16E-17
GOBP_CELL_MORPHOGENESIS_INVOLVED_IN_DIFFERENTIATION	51	1.66E-19	1.68E-17
GOBP_RESPONSE_TO_CYTOKINE	66	1.95E-19	1.95E-17
GOBP_POSITIVE_REGULATION_OF_CELL_DIFFERENTIATION	55	2.18E-19	2.14E-17
GOBP_SECRETION	74	2.21E-19	2.15E-17
GOBP_REGULATION_OF_APOPTOTIC_SIGNALING_PATHWAY	36	2.27E-19	2.18E-17
GOBP_HOMEOSTATIC_PROCESS	86	3.10E-19	2.93E-17
GOBP_CELL_MATRIX_ADHESION	30	3.42E-19	3.20E-17
GOBP_REGULATION_OF_TRANSFERASE_ACTIVITY	60	4.05E-19	3.74E-17
GOBP_POSITIVE_REGULATION_OF_CELL_ADHESION	39	4.82E-19	4.40E-17
GOBP_CELL_SUBSTRATE_JUNCTION_ORGANIZATION	22	6.98E-19	6.30E-17
GOBP_POSITIVE_REGULATION_OF_ORGANELLE_ORGANIZATION	45	7.87E-19	7.01E-17
GOBP_REGULATION_OF_CYTOSKELETON_ORGANIZATION	42	1.13E-18	9.94E-17
GOBP_GROWTH	56	1.23E-18	1.07E-16
GOBP_CELL_CELL_ADHESION	55	1.41E-18	1.21E-16
GOBP_NEURON_DEVELOPMENT	62	1.94E-18	1.65E-16
GOBP_REGULATION_OF_ACTIN_FILAMENT_ORGANIZATION	31	5.09E-18	4.28E-16
GOBP_RESPONSE_TO_ORGANIC_CYCLIC_COMPOUND	55	5.38E-18	4.47E-16
GOBP_CELL_JUNCTION_ORGANIZATION	48	5.93E-18	4.87E-16
GOBP_CELLULAR_RESPONSE_TO_HORMONE_STIMULUS	45	7.80E-18	6.34E-16
GOBP_REGULATION_OF_SUPRAMOLECULAR_FIBER_ORGANIZATION	35	1.24E-17	1.00E-15
GOBP_REGULATION_OF_CELL_MORPHOGENESIS	32	1.54E-17	1.22E-15
GOBP_REGULATION_OF_ION_TRANSPORT	66	3.16E-17	2.49E-15
GOBP_TAXIS	45	3.48E-17	2.71E-15
GOBP_REGULATION_OF_ANATOMICAL_STRUCTURE_SIZE	39	7.78E-17	6.00E-15
GOBP_REGULATION_OF_CELLULAR_COMPONENT_SIZE	34	8.82E-17	6.74E-15
GOBP_POSITIVE_REGULATION_OF_MAPK_CASCADE	40	1.05E-16	7.95E-15
GOBP_REGULATION_OF_ANION_TRANSPORT	51	1.35E-16	1.01E-14

Figure 108 Gene ontology analysis of genes upregulated in response to LMB in Mtr4-depeted NIH3T3 cells by RNAseq

Gene ontology analysis of genes upregulated by LMB treatment in Mtr4-depleted NIH3T3 cells by RNAseq. FDR<0.05. Relates to Figure 53. Bioinformatic analysis of RNAseq data was performed by Francesco Gualdrini.

Gene Set Name	# Genes	p-value	FDR q-value
GOBP_CIRCULATORY_SYSTEM_DEVELOPMENT	18	2.01E-09	1.51E-05
GOBP_TUBE_DEVELOPMENT	17	6.64E-09	1.52E-05
GOBP_REGULATION_OF_MULTICELLULAR_ORGANISMAL_DEVELOPMENT	19	7.72E-09	1.52E-05
GOBP_REGULATION_OF_CELLULAR_COMPONENT_MOVEMENT	17	8.13E-09	1.52E-05
GOBP_EXTERNAL_ENCAPSULATING_STRUCTURE_ORGANIZATION	11	1.28E-08	1.75E-05
GOBP_ANATOMICAL_STRUCTURE_FORMATION_INVOLVED_IN_MORPHOGENESIS	17	1.41E-08	1.75E-05
GOBP_BIOLOGICAL_ADHESION	19	1.96E-08	2.09E-05
GOBP_BLOOD_VESSEL_MORPHOGENESIS	13	4.50E-08	4.21E-05
GOBP_LIPID_METABOLIC_PROCESS	18	6.18E-08	5.14E-05
GOBP_POSITIVE_REGULATION_OF_DEVELOPMENTAL_PROCESS	17	7.62E-08	5.70E-05
GOBP_REGULATION_OF_EPITHELIAL_CELL_MIGRATION	9	1.22E-07	8.32E-05
GOBP_TUBE_MORPHOGENESIS	14	1.75E-07	1.09E-04
GOBP_POSITIVE_REGULATION_OF_SIGNALING	19	2.11E-07	1.18E-04
GOBP_HOMEOSTATIC_PROCESS	20	2.20E-07	1.18E-04
GOBP_VASCULATURE_DEVELOPMENT	13	2.49E-07	1.19E-04
GOBP_REGULATION_OF_ENDOTHELIAL_CELL_MIGRATION	8	2.55E-07	1.19E-04
GOBP_CELL_MIGRATION	18	3.44E-07	1.51E-04
GOBP_TISSUE_MIGRATION	9	7.70E-07	3.20E-04
GOBP_ENDOTHELIAL_CELL_MIGRATION	8	1.03E-06	4.06E-04
GOBP_POSITIVE_REGULATION_OF_MULTICELLULAR_ORGANISMAL_PROCESS	16	1.29E-06	4.84E-04
GOBP_OSSIFICATION	9	1.60E-06	5.44E-04
GOBP_LOCOMOTION	19	1.60E-06	5.44E-04
GOBP_REGULATION_OF_LIPID_METABOLIC_PROCESS	9	1.67E-06	5.44E-04
GOBP_NEGATIVE_REGULATION_OF_MULTICELLULAR_ORGANISMAL_PROCESS	14	1.97E-06	6.13E-04
GOBP_NEGATIVE_REGULATION_OF_RESPONSE_TO_STIMULUS	17	2.95E-06	8.82E-04
GOBP_SMALL_MOLECULE_METABOLIC_PROCESS	18	3.50E-06	1.01E-03
GOBP_POSITIVE_REGULATION_OF_INTRACELLULAR_SIGNAL_TRANSDUCTION	13	3.79E-06	1.05E-03
GOBP_CHEMICAL_HOMEOSTASIS	14	4.53E-06	1.17E-03
GOBP_LIPID_CATABOLIC_PROCESS	8	4.58E-06	1.17E-03
GOBP_REGULATION_OF_VASCULATURE_DEVELOPMENT	8	4.68E-06	1.17E-03
GOBP_POSITIVE_REGULATION_OF_LOCOMOTION	10	4.91E-06	1.18E-03
GOBP_AMEBOIDAL_TYPE_CELL_MIGRATION	9	6.37E-06	1.49E-03
GOBP_SKELETAL_SYSTEM_DEVELOPMENT	9	7.78E-06	1.76E-03
GOBP_REGULATION_OF_CELL_DIFFERENTIATION	16	8.36E-06	1.84E-03
GOBP_POSITIVE_REGULATION_OF_EPITHELIAL_CELL_MIGRATION	6	9.05E-06	1.91E-03
GOBP_NEGATIVE_REGULATION_OF_DEVELOPMENTAL_PROCESS	12	9.20E-06	1.91E-03
GOBP_MONOSACCHARIDE_METABOLIC_PROCESS	7	1.04E-05	2.10E-03
GOBP_POSITIVE_REGULATION_OF_NUCLEOBASE_CONTAINING_COMPOUND_METABOLIC_PROCESS	17	1.16E-05	2.28E-03
GOBP_LIPID_OXIDATION	5	1.35E-05	2.58E-03
GOBP_COLLAGEN_FIBRIL_ORGANIZATION	4	1.49E-05	2.79E-03
GOBP_CELL_POPULATION_PROLIFERATION	17	2.24E-05	4.09E-03
GOBP_SKELETAL_SYSTEM_MORPHOGENESIS	6	2.68E-05	4.77E-03
GOBP_RESPONSE_TO_ABIOTIC_STIMULUS	13	2.84E-05	4.95E-03
GOBP_UROGENITAL_SYSTEM_DEVELOPMENT	7	2.94E-05	5.00E-03
GOBP_NEGATIVE_REGULATION_OF_SIGNALING	14	3.06E-05	5.09E-03
GOBP_HORMONE_METABOLIC_PROCESS	6	3.13E-05	5.09E-03
GOBP_POSITIVE_REGULATION_OF_ENDOTHELIAL_CELL_MIGRATION	5	3.24E-05	5.10E-03
GOBP_REGULATION_OF_PHOSPHORUS_METABOLIC_PROCESS	15	3.27E-05	5.10E-03
GOBP_CELL_AGGREGATION	3	3.36E-05	5.11E-03
GOBP_PROTEIN_PHOSPHORYLATION	15	3.42E-05	5.11E-03
GOBP_STEROID_METABOLIC_PROCESS	7	3.51E-05	5.15E-03
GOBP_ORGANIC_ACID_METABOLIC_PROCESS	12	3.62E-05	5.21E-03
GOBP_CELLULAR_HORMONE_METABOLIC_PROCESS	5	3.74E-05	5.28E-03
GOBP_SENSORY_ORGAN_MORPHOGENESIS	6	5.86E-05	8.11E-03
GOBP_ION_HOMEOSTASIS	10	6.16E-05	8.38E-03
GOBP_REGULATION_OF_HORMONE_LEVELS	8	8.24E-05	1.10E-02
GOBP_NEGATIVE_REGULATION_OF_CELL_DEATH	11	8.74E-05	1.13E-02
GOBP_NEGATIVE_REGULATION_OF_CELL_DIFFERENTIATION	9	8.86E-05	1.13E-02
GOBP_MULTICELLULAR_ORGANISMAL_HOMEOSTASIS	8	8.93E-05	1.13E-02
GOBP_POSITIVE_REGULATION_OF_TRANSCRIPTION_BY_RNA_POLYMERASE_II	12	9.44E-05	1.18E-02
GOBP_REGULATION_OF_ANATOMICAL_STRUCTURE_MORPHOGENESIS	11	9.97E-05	1.22E-02
GOBP_REGULATION_OF_FATTY_ACID_OXIDATION	3	1.02E-04	1.22E-02
GOBP_REGULATION_OF_INTRACELLULAR_SIGNAL_TRANSDUCTION	15	1.03E-04	1.22E-02
GOBP_FATTY_ACID_METABOLIC_PROCESS	7	1.05E-04	1.23E-02
GOBP_REGULATION_OF_MESENCHYMAL_STEM_CELL_DIFFERENTIATION	2	1.10E-04	1.26E-02
GOBP_POSITIVE_REGULATION_OF_PHOSPHATIDYLINOSITOL_3_KINASE_SIGNALING	4	1.12E-04	1.27E-02
GOBP_POSITIVE_REGULATION_OF_VASCULATURE_DEVELOPMENT	5	1.23E-04	1.38E-02
GOBP_CYTOKINE_PRODUCTION_INVOLVED_IN_IMMUNE_RESPONSE	4	1.27E-04	1.40E-02
GOBP_RESPONSE_TO_ENDOGENOUS_STIMULUS	14	1.39E-04	1.50E-02
GOBP_CARTILAGE_DEVELOPMENT	5	1.56E-04	1.64E-02
GOBP_CELLULAR_LIPID_METABOLIC_PROCESS	11	1.56E-04	1.64E-02
GOBP_NOTCH_SIGNALING_PATHWAY	5	1.64E-04	1.70E-02
GOBP_ENZYME_LINKED_RECEPTOR_PROTEIN_SIGNALING_PATHWAY	11	1.73E-04	1.78E-02
GOBP_POSITIVE_REGULATION_OF_GENE_EXPRESSION	11	1.78E-04	1.80E-02
GOBP_TRANSMEMBRANE_RECEPTOR_PROTEIN_TYROSINE_KINASE_SIGNALING_PATHWAY	9	1.95E-04	1.95E-02
GOBP_REGULATION_OF_SMALL_MOLECULE_METABOLIC_PROCESS	7	2.02E-04	1.99E-02
GOBP_INOSITOL_LIPID_MEDIATED_SIGNALING	5	2.09E-04	2.03E-02
GOBP_IMMUNE_EFFECTOR_PROCESS	12	2.25E-04	2.13E-02
GOBP_NEGATIVE_REGULATION_OF_CELL_POPULATION_PROLIFERATION	9	2.27E-04	2.13E-02
GOBP_EMBRYO_DEVELOPMENT_ENDING_IN_BIRTH_OR_EGG_HATCHING	8	2.28E-04	2.13E-02
GOBP_RESPONSE_TO_MECHANICAL_STIMULUS	5	2.40E-04	2.21E-02
GOBP_EAR_MORPHOGENESIS	4	2.43E-04	2.21E-02
GOBP_APOPTOTIC_PROCESS	15	2.45E-04	2.21E-02
GOBP_REGULATION_OF_OSSIFICATION	4	2.51E-04	2.24E-02
GOBP_MESENCHYMAL_STEM_CELL_DIFFERENTIATION	2	2.62E-04	2.31E-02
GOBP_MUSCLE_STRUCTURE_DEVELOPMENT	8	2.69E-04	2.34E-02
GOBP_INFLAMMATORY_RESPONSE	9	2.78E-04	2.37E-02
GOBP_CARBOHYDRATE_DERIVATIVE_METABOLIC_PROCESS	11	2.80E-04	2.37E-02
GOBP_POSITIVE_REGULATION_OF_BIOSYNTHETIC_PROCESS	15	2.82E-04	2.37E-02
GOBP_GLUCOSE_METABOLIC_PROCESS	5	2.87E-04	2.39E-02
GOBP_REGULATION_OF_IMMUNE_EFFECTOR_PROCESS	7	2.94E-04	2.42E-02
GOBP_VASCULAR_ENDOTHELIAL_GROWTH_FACTOR_SIGNALING_PATHWAY	3	3.13E-04	2.54E-02
GOBP_REGULATION_OF_GLUCOSE_METABOLIC_PROCESS	4	3.27E-04	2.63E-02
GOBP_NEGATIVE_REGULATION_OF_EPITHELIAL_CELL_APOPTOTIC_PROCESS	3	3.53E-04	2.81E-02
GOBP_POSITIVE_REGULATION_OF_PHOSPHORUS_METABOLIC_PROCESS	10	3.64E-04	2.85E-02
GOBP_ORGANONITROGEN_COMPOUND_BIOSYNTHETIC_PROCESS	14	3.66E-04	2.85E-02
GOBP_EMBRYO_DEVELOPMENT	10	3.97E-04	3.02E-02
GOBP_CELLULAR_RESPONSE_TO_OXYGEN_CONTAINING_COMPOUND	11	3.98E-04	3.02E-02
GOBP_LIMB_BUD_FORMATION	2	3.99E-04	3.02E-02
GOBP_MONOCARBOXYLIC_ACID_METABOLIC_PROCESS	8	4.03E-04	3.02E-02

Figure 109 Gene ontology analysis of genes downregulated in response to LMB in Mtr4-depeted NIH3T3 cells by RNAseq

Gene ontology analysis of genes downregulated by LMB treatment in Mtr4-depleted NIH3T3 cells by RNAseq. FDR<0.05. Relates to Figure 53. Bioinformatic analysis of RNAseq data was performed by Francesco Gualdrini.

GO BIOLOGICAL PROCESS	# Genes	p-value	FDR q-value
GOBP_CELL_CYCLE	145	4.08E-30	3.09E-26
GOBP_CELLULAR_RESPONSE_TO_DNA_DAMAGE_STIMULUS	88	1.63E-26	6.16E-23
GOBP_CELL_CYCLE_PROCESS	112	4.77E-24	1.20E-20
GOBP_CARBOHYDRATE_DERIVATIVE_METABOLIC_PROCESS	94	5.01E-22	9.48E-19
GOBP_REGULATION_OF_CELL_CYCLE	95	5.09E-20	7.72E-17
GOBP_DNA_METABOLIC_PROCESS	80	2.67E-19	3.37E-16
GOBP_MITOTIC_CELL_CYCLE	82	1.55E-17	1.68E-14
GOBP_DNA_REPAIR	56	7.74E-17	7.33E-14
GOBP_CARBOHYDRATE_DERIVATIVE_BIOSYNTHETIC_PROCESS	60	9.78E-16	7.99E-13
GOBP_POSITIVE_REGULATION_OF_NUCLEOBASE_CONTAINING_COMPOUND_METABOLIC_PROCESS	113	1.05E-15	7.99E-13
GOBP_SMALL_MOLECULE_METABOLIC_PROCESS	116	1.54E-15	1.20E-13
GOBP_ORGANONITROGEN_COMPOUND_BIOSYNTHETIC_PROCESS	108	5.48E-15	3.41E-12
GOBP_CELL_POPULATION_PROLIFERATION	114	1.09E-14	6.03E-12
GOBP_DNA_REPLICATION	36	1.13E-14	6.03E-12
GOBP_PROTEIN_CONTAINING_COMPLEX_SUBUNIT_ORGANIZATION	112	7.06E-14	3.52E-11
GOBP_PROTEIN_PHOSPHORYLATION	98	9.27E-14	4.34E-11
GOBP_CELL_DIVISION	52	2.29E-13	1.01E-10
GOBP_REGULATION_OF_PHOSPHORUS_METABOLIC_PROCESS	96	4.52E-13	1.88E-10
GOBP_APOPTOTIC_PROCESS	108	8.14E-13	3.13E-10
GOBP_POSITIVE_REGULATION_OF_PROTEIN_METABOLIC_PROCESS	92	8.36E-13	3.13E-10
GOBP_REGULATION_OF_INTRACELLULAR_SIGNAL_TRANSDUCTION	102	9.78E-13	3.49E-10
GOBP_CELLULAR_LIPID_METABOLIC_PROCESS	72	1.13E-12	3.85E-10
GOBP_CELLULAR_MACROMOLECULE_LOCALIZATION	108	3.90E-12	1.27E-09
GOBP_REGULATION_OF_PROTEIN_MODIFICATION_PROCESS	94	4.71E-12	1.47E-09
GOBP_ORGANOPHOSPHATE_METABOLIC_PROCESS	69	5.10E-12	1.47E-09
GOBP_ORGANONITROGEN_COMPOUND_CATABOLIC_PROCESS	82	5.14E-12	1.47E-09
GOBP_REGULATION_OF_ORGANELLE_ORGANIZATION	75	5.31E-12	1.47E-09
GOBP_NEGATIVE_REGULATION_OF_BIOSYNTHETIC_PROCESS	96	6.22E-12	1.66E-09
GOBP_DNA_RECOMBINATION	33	6.46E-12	1.67E-09
GOBP_HOMEOSTATIC_PROCESS	104	1.16E-11	2.88E-09
GOBP_CYTOSKELETON_ORGANIZATION	83	1.23E-11	2.97E-09
GOBP_REGULATION_OF_CELL_DEATH	94	1.37E-11	3.20E-09
GOBP_NEUROGENESIS	92	1.61E-11	3.65E-09
GOBP_DNA_DEPENDENT_DNA_REPLICATION	23	4.84E-11	1.07E-08
GOBP_DOUBLE_STRAND_BREAK_REPAIR	30	6.23E-11	1.33E-08
GOBP_MACROMOLECULE_CATABOLIC_PROCESS	83	6.93E-11	1.44E-08
GOBP_CIRCULATORY_SYSTEM_DEVELOPMENT	71	8.72E-11	1.76E-08
GOBP_NEGATIVE_REGULATION_OF_RESPONSE_TO_STIMULUS	92	1.10E-10	2.17E-08
GOBP_REGULATION_OF_CELLULAR_COMPONENT_MOVEMENT	69	1.19E-10	2.29E-08
GOBP_CELL_CYCLE_DNA_REPLICATION	15	1.24E-10	2.32E-08
GOBP_LIPID_METABOLIC_PROCESS	82	1.47E-10	2.68E-08
GOBP_ORGANELLE_ASSEMBLY	59	1.79E-10	3.19E-08
GOBP_NEGATIVE_REGULATION_OF_SIGNALING	81	1.94E-10	3.37E-08
GOBP_POSITIVE_REGULATION_OF_MOLECULAR_FUNCTION	94	2.01E-10	3.42E-08
GOBP_RECOMBINATIONAL_REPAIR	21	2.12E-10	3.53E-08
GOBP_CELL_PROJECTION_ORGANIZATION	87	2.27E-10	3.70E-08
GOBP_NUCLEOBASE_CONTAINING_SMALL_MOLECULE_METABOLIC_PROCESS	47	2.66E-10	4.23E-08
GOBP_POSITIVE_REGULATION_OF_MULTICELLULAR_ORGANISMAL_PROCESS	80	3.02E-10	4.64E-08
GOBP_CELL_CYCLE_PHASE_TRANSITION	48	3.04E-10	4.64E-08
GOBP_NEGATIVE_REGULATION_OF_CELL_CYCLE	47	3.85E-10	5.76E-08
GOBP_REGULATION_OF_MITOTIC_CELL_CYCLE	46	4.37E-10	6.41E-08
GOBP_POSITIVE_REGULATION_OF_SIGNALING	92	5.26E-10	7.56E-08
GOBP_CELL_MIGRATION	87	6.69E-10	9.44E-08
GOBP_POSITIVE_REGULATION_OF_CATALYTIC_ACTIVITY	79	8.17E-10	1.13E-07
GOBP_NEGATIVE_REGULATION_OF_NUCLEOBASE_CONTAINING_COMPOUND_METABOLIC_PROCES	83	1.27E-09	1.73E-07
GOBP_RESPONSE_TO_ABIOTIC_STIMULUS	71	1.39E-09	1.86E-07
GOBP_RESPONSE_TO_OXYGEN_CONTAINING_COMPOUND	88	1.43E-09	1.88E-07
GOBP_PEPTIDYL_AMINO_ACID_MODIFICATION	73	1.53E-09	1.98E-07
GOBP_REGULATION_OF_CELL_CYCLE_PROCESS	53	1.74E-09	2.20E-07
GOBP_POSITIVE_REGULATION_OF_BIOSYNTHETIC_PROCESS	99	1.81E-09	2.25E-07
GOBP_REGULATION_OF_CATABOLIC_PROCESS	62	2.09E-09	2.57E-07
GOBP_POSITIVE_REGULATION_OF_TRANSCRIPTION_BY_RNA_POLYMERASE_II	69	2.25E-09	2.68E-07
GOBP_NEURON_DIFFERENTIATION	76	2.26E-09	2.68E-07
GOBP_MUSCLE_TISSUE_DEVELOPMENT	33	2.87E-09	3.36E-07
GOBP_PROTEIN_LOCALIZATION_TO_ORGANELLE	61	3.85E-09	4.43E-07
GOBP_EXTERNAL_ENCAPSULATING_STRUCTURE_ORGANIZATION	34	4.09E-09	4.64E-07
GOBP_ANIMAL_ORGAN_MORPHOGENESIS	62	4.24E-09	4.74E-07
GOBP_GROWTH	57	4.92E-09	5.41E-07
GOBP_REGULATION_OF_CELLULAR_RESPONSE_TO_STRESS	48	5.08E-09	5.51E-07
GOBP_HOMOLOGOUS_RECOMBINATION	13	5.99E-09	6.41E-07
GOBP_TUBE_DEVELOPMENT	64	6.24E-09	6.57E-07
GOBP_ORGANELLE_FISSION	38	6.73E-09	7.00E-07
GOBP_CARBOHYDRATE_METABOLIC_PROCESS	44	7.63E-09	7.82E-07
GOBP_LOCOMOTION	97	1.15E-08	1.17E-06
GOBP_CELL_CYCLE_G1_S_PHASE_TRANSITION	28	1.37E-08	1.36E-06
GOBP_ORGANOPHOSPHATE_BIOSYNTHETIC_PROCESS	42	1.38E-08	1.36E-06
GOBP_REGULATION_OF_PROTEIN_PHOSPHORYLATION	68	1.46E-08	1.42E-06
GOBP_OSSIFICATION	33	1.71E-08	1.64E-06
GOBP_NUCLEOSIDE_PHOSPHATE_BIOSYNTHETIC_PROCESS	26	2.01E-08	1.90E-06
GOBP_MEMBRANE_ORGANIZATION	57	2.29E-08	2.15E-06
GOBP_INTRACELLULAR_TRANSPORT	87	2.40E-08	2.22E-06
GOBP_ESTABLISHMENT_OF_PROTEIN_LOCALIZATION	96	2.69E-08	2.45E-06
GOBP_POSITIVE_REGULATION_OF_INTRACELLULAR_SIGNAL_TRANSDUCTION	59	2.90E-08	2.62E-06
GOBP_DEVELOPMENTAL_GROWTH	42	3.39E-08	3.02E-06
GOBP_REGULATION_OF_HYDROLASE_ACTIVITY	70	4.22E-08	3.71E-06
GOBP_POSITIVE_REGULATION_OF_CELL_CYCLE	32	4.56E-08	3.96E-06
GOBP_REGULATION_OF_TRANSPORT	86	4.83E-08	4.15E-06
GOBP_REPRODUCTION	75	6.15E-08	5.23E-06
GOBP_ANATOMICAL_STRUCTURE_HOMEOSTASIS	35	7.09E-08	5.96E-06
GOBP_CELLULAR_PROTEIN_CONTAINING_COMPLEX_ASSEMBLY	62	7.22E-08	6.00E-06
GOBP_HEART_DEVELOPMENT	39	7.58E-08	6.23E-06
GOBP_REGULATION_OF_MULTICELLULAR_ORGANISMAL_DEVELOPMENT	73	7.72E-08	6.28E-06
GOBP_CHROMOSOME_ORGANIZATION	67	8.92E-08	7.17E-06
GOBP_REGULATION_OF_CELL_DIFFERENTIATION	81	9.00E-08	7.17E-06
GOBP_TRNA_METABOLIC_PROCESS	20	9.60E-08	7.56E-06
GOBP_RESPONSE_TO_ENDOGENOUS_STIMULUS	81	1.05E-07	8.18E-06
GOBP_POSITIVE_REGULATION_OF_DEVELOPMENTAL_PROCESS	68	1.33E-07	1.03E-05
GOBP_POSITIVE_REGULATION_OF_CYSTEINE_TYPE_ENDOPEPTIDASE_ACTIVITY_INVOLVED_IN_APOP	6	1.57E-07	1.19E-05
GOBP_REGULATION_OF_CYSTEINE_TYPE_ENDOPEPTIDASE_ACTIVITY_INVOLVED_IN_APOPTOTIC_SIG	7	1.57E-07	1.19E-05
GOBP_NEURON_DEVELOPMENT	61	1.66E-07	1.24E-05

Figure 110 Gene ontology analysis of genes upregulated by Mtr4 depletion

Gene ontology analysis of genes upregulated by Mtr4 depletion NIH3T3 cells by RNAseq. FDR<0.05. Relates to Figure 57. Bioinformatic analysis of RNAseq data was performed by Francesco Gualdrini.

GO BIOLOGICAL PROCESS	# Genes	p-value	FDR q-value
GOBP_REGULATION_OF_CELL_POPULATION_PROLIFERATION	65	1.56E-24	1.18E-20
GOBP_POSITIVE_REGULATION_OF_CELL_POPULATION_PROLIFERATION	45	3.79E-24	1.44E-20
GOBP_BIOLOGICAL_ADHESION	55	1.14E-23	2.89E-20
GOBP_RESPONSE_TO_CYTOKINE	47	1.43E-22	2.71E-19
GOBP_POSITIVE_REGULATION_OF_MULTICELLULAR_ORGANISMAL_PROCESS	47	5.68E-22	8.60E-19
GOBP_POSITIVE_REGULATION_OF_DEVELOPMENTAL_PROCESS	28	5.28E-20	6.66E-17
GOBP_POSITIVE_REGULATION_OF_CELL_ADHESION	53	3.58E-19	3.88E-16
GOBP_REGULATION_OF_PHOSPHORUS_METABOLIC_PROCESS	52	2.72E-18	2.57E-15
GOBP_POSITIVE_REGULATION_OF_MOLECULAR_FUNCTION	34	4.47E-18	3.76E-15
GOBP_REGULATION_OF_PHOSPHORYLATION	46	1.18E-17	8.96E-15
GOBP_REGULATION_OF_INTRACELLULAR_SIGNAL_TRANSDUCTION	53	1.40E-17	6.84E-15
GOBP_REGULATION_OF_CELL_ADHESION	34	2.64E-17	2.13E-14
GOBP_REGULATION_OF_MULTICELLULAR_ORGANISMAL_DEVELOPMENT	46	2.85E-17	2.13E-14
GOBP_RESPONSE_TO_ENDOGENOUS_STIMULUS	49	7.51E-17	5.11E-14
GOBP_CIRCULATORY_SYSTEM_DEVELOPMENT	41	9.04E-17	5.56E-14
GOBP_TUBE_DEVELOPMENT	40	9.66E-17	5.56E-14
GOBP_REGULATION_OF_CELLULAR_COMPONENT_MOVEMENT	40	1.53E-16	7.62E-14
GOBP_POSITIVE_REGULATION_OF_CATALYTIC_ACTIVITY	45	1.69E-16	7.62E-14
GOBP_POSITIVE_REGULATION_OF_SIGNALING	50	1.73E-16	7.62E-14
GOBP_VASCULATURE_DEVELOPMENT	34	2.20E-16	9.14E-14
GOBP_REGULATION_OF_HYDROLASE_ACTIVITY	43	2.73E-16	1.07E-13
GOBP_REGULATION_OF_CELL_DIFFERENTIATION	48	3.11E-16	1.16E-13
GOBP_CELL_MIGRATION	47	1.00E-15	3.45E-13
GOBP_NEGATIVE_REGULATION_OF_SIGNALING	44	1.02E-15	3.45E-13
GOBP_TUBE_MORPHOGENESIS	35	1.91E-15	5.95E-13
GOBP_LOCOMOTION	52	1.99E-15	5.95E-13
GOBP_ENZYME_LINKED_RECEPTOR_PROTEIN_SIGNALING_PATHWAY	38	2.11E-15	6.08E-13
GOBP_NEGATIVE_REGULATION_OF_RESPONSE_TO_STIMULUS	47	5.03E-15	1.39E-12
GOBP_REGULATION_OF_RESPONSE_TO_STRESS	43	5.60E-15	1.50E-12
GOBP_BLOOD_VESSEL_MORPHOGENESIS	30	7.52E-15	1.88E-12
GOBP_REGULATION_OF_PROTEIN_MODIFICATION_PROCESS	46	8.10E-15	1.95E-12
GOBP_CELL_CELL_SIGNALING	46	2.17E-14	5.06E-12
GOBP_NEUROGENESIS	45	2.64E-14	5.98E-12
GOBP_RESPONSE_TO_OXYGEN_CONTAINING_COMPOUND	45	6.37E-14	1.40E-11
GOBP_REGULATION_OF_IMMUNE_SYSTEM_PROCESS	44	7.46E-14	1.59E-11
GOBP_GROWTH	33	8.48E-14	1.76E-11
GOBP_ANIMAL_ORGAN_MORPHOGENESIS	35	8.72E-14	1.76E-11
GOBP_REGULATION_OF_PROTEIN_PHOSPHORYLATION	38	9.51E-14	1.83E-11
GOBP_POSITIVE_REGULATION_OF_BIOSYNTHETIC_PROCESS	49	9.53E-14	1.83E-11
GOBP_NEGATIVE_REGULATION_OF_PROTEIN_METABOLIC_PROCESS	36	1.72E-13	3.21E-11
GOBP_POSITIVE_REGULATION_OF_INTRACELLULAR_SIGNAL_TRANSDUCTION	34	2.63E-13	4.79E-11
GOBP_RESPONSE_TO_GROWTH_FACTOR	29	3.45E-13	6.15E-11
GOBP_POSITIVE_REGULATION_OF_CELL_DIFFERENTIATION	31	3.82E-13	6.61E-11
GOBP_ANATOMICAL_STRUCTURE_FORMATION_INVOLVED_IN_MORPHOGENESIS	36	3.94E-13	6.61E-11
GOBP_EXTERNAL_ENCAPSULATING_STRUCTURE_ORGANIZATION	22	3.98E-13	6.61E-11
GOBP_CYTOKINE_MEDIATED_SIGNALING_PATHWAY	30	6.09E-13	9.91E-11
GOBP_REGULATION_OF_ANATOMICAL_STRUCTURE_MORPHOGENESIS	33	1.39E-12	2.21E-10
GOBP_POSITIVE_REGULATION_OF_PROTEIN_METABOLIC_PROCESS	41	1.46E-12	2.27E-10
GOBP_MAPK_CASCADE	31	2.81E-12	4.29E-10
GOBP_NEURON_DIFFERENTIATION	38	2.96E-12	4.43E-10
GOBP_OSSIFICATION	21	3.85E-12	5.65E-10
GOBP_IMMUNE_SYSTEM_DEVELOPMENT	32	4.45E-12	6.40E-10
GOBP_RESPONSE_TO_NITROGEN_COMPOUND	34	4.85E-12	6.84E-10
GOBP_BIOLOGICAL_PROCESS_INVOLVED_IN_SYMBIOTIC_INTERACTION	32	5.48E-12	7.60E-10
GOBP_CELL_CELL_ADHESION	30	6.00E-12	8.17E-10
GOBP_POSITIVE_REGULATION_OF_GENE_EXPRESSION	33	8.17E-12	1.09E-09
GOBP_EPITHELIAL_CELL_PROLIFERATION	21	1.44E-11	1.89E-09
GOBP_NEGATIVE_REGULATION_OF_MOLECULAR_FUNCTION	34	1.58E-11	2.04E-09
GOBP_CELL_CYCLE	44	1.64E-11	2.07E-09
GOBP_CENTRAL_NERVOUS_SYSTEM_DEVELOPMENT	31	1.73E-11	2.16E-09
GOBP_POSITIVE_REGULATION_OF_PHOSPHORUS_METABOLIC_PROCESS	31	1.78E-11	2.18E-09
GOBP_POSITIVE_REGULATION_OF_LOCOMOTION	24	2.05E-11	2.47E-09
GOBP_SKELETAL_SYSTEM_DEVELOPMENT	22	2.13E-11	2.49E-09
GOBP_POSITIVE_REGULATION_OF_PROTEIN_MODIFICATION_PROCESS	32	2.13E-11	2.49E-09
GOBP_NEGATIVE_REGULATION_OF_DEVELOPMENTAL_PROCESS	30	2.21E-11	2.54E-09
GOBP_NEGATIVE_REGULATION_OF_BIOSYNTHETIC_PROCESS	41	3.11E-11	3.52E-09
GOBP_DEVELOPMENTAL_GROWTH	24	4.08E-11	4.56E-09
GOBP_POSITIVE_REGULATION_OF_NUCLEOBASE_CONTAINING_COMPOUND_METABOLIC_PROCESS	43	4.59E-11	5.05E-09
GOBP_REGULATION_OF_TRANSPORT	41	6.80E-11	7.37E-09
GOBP_MESENCHYME_DEVELOPMENT	17	7.28E-11	7.78E-09
GOBP_NEGATIVE_REGULATION_OF_NUCLEOBASE_CONTAINING_COMPOUND_METABOLIC_PROCESS	38	7.90E-11	8.33E-09
GOBP_ESTABLISHMENT_OF_PROTEIN_LOCALIZATION	44	1.02E-10	1.05E-08
GOBP_POSITIVE_REGULATION_OF_CELLULAR_COMPONENT_ORGANIZATION	32	1.02E-10	1.05E-08
GOBP_CARBOHYDRATE_DERIVATIVE_METABOLIC_PROCESS	32	1.46E-10	1.47E-08
GOBP_APOPTOTIC_PROCESS	43	1.55E-10	1.55E-08
GOBP_REGULATION_OF_TRANSFERASE_ACTIVITY	30	1.69E-10	1.67E-08
GOBP_NEGATIVE_REGULATION_OF_MULTICELLULAR_ORGANISMAL_PROCESS	31	3.24E-10	3.15E-08
GOBP_REGULATION_OF_ION_TRANSPORT	34	3.59E-10	3.44E-08
GOBP_RESPONSE_TO_BIOTIC_STIMULUS	38	3.81E-10	3.61E-08
GOBP_HOMEOSTATIC_PROCESS	42	3.92E-10	3.67E-08
GOBP_GLAND_DEVELOPMENT	19	4.05E-10	3.74E-08
GOBP_NEGATIVE_REGULATION_OF_CELL_DEATH	29	4.89E-10	4.46E-08
GOBP_RESPONSE_TO_LIPID	27	5.01E-10	4.51E-08
GOBP_TISSUE_MORPHOGENESIS	23	5.97E-10	5.32E-08
GOBP_ORGANONITROGEN_COMPOUND_BIOSYNTHETIC_PROCESS	40	6.18E-10	5.44E-08
GOBP_REGULATION_OF_CELL_CELL_ADHESION	19	1.03E-09	9.00E-08
GOBP_POSITIVE_REGULATION_OF_HYDROLASE_ACTIVITY	25	1.13E-09	9.74E-08
GOBP_PROTEIN_KINASE_B_SIGNALING	15	2.71E-09	2.30E-07
GOBP_POSITIVE_REGULATION_OF_CELL_CELL_ADHESION	15	3.14E-09	2.61E-07
GOBP_RESPONSE_TO_PEPTIDE	20	3.14E-09	2.61E-07
GOBP_POSITIVE_REGULATION_OF_PROTEIN_PHOSPHORYLATION	25	3.98E-09	3.27E-07
GOBP_REGULATION_OF_GROWTH	22	4.27E-09	3.43E-07
GOBP_TAXIS	22	4.27E-09	3.43E-07
GOBP_NEGATIVE_REGULATION_OF_CELL_DIFFERENTIATION	22	7.20E-09	5.73E-07
GOBP_HEART_DEVELOPMENT	20	9.08E-09	7.11E-07
GOBP_POSITIVE_REGULATION_OF_EPITHELIAL_CELL_MIGRATION	12	9.22E-09	7.11E-07
GOBP_POSITIVE_REGULATION_OF_PROTEIN_KINASE_B_SIGNALING	12	9.22E-09	7.11E-07
GOBP_POSITIVE_REGULATION_OF_TRANSFERASE_ACTIVITY	22	1.10E-08	8.42E-07
GOBP_REGULATION_OF_PEPTIDYL_TYROSINE_PHOSPHORYLATION	14	1.31E-08	9.92E-07
GOBP_HEAD_DEVELOPMENT	23	1.40E-08	1.05E-06

Figure 111 Gene ontology analysis of genes upregulated in response to CD, relative to LatB-treated cells, in Mtr4-depleted dKO$^{MRTF\text{-}NLS}$ cells

Gene ontology analysis of genes upregulated in response to CD, relative to LatB-treated cells, in Mtr4-depleted dKO$^{MRTF\text{-}NLS}$ cells by RNAseq. FDR<0.05. Relates to Figure 62. Bioinformatic analysis of RNAseq data was performed by Francesco Gualdrini.

GO BIOLOGICAL PROCESS	# Genes	p-value	FDR q-value
GOBP_REGULATION_OF_CELL_DEATH	23	4.04E-17	3.02E-13
GOBP_APOPTOTIC_PROCESS	23	1.06E-15	2.76E-12
GOBP_RESPONSE_TO_WOUNDING	16	1.10E-15	2.76E-12
GOBP_LOCOMOTION	23	1.72E-15	3.22E-12
GOBP_MUSCLE_STRUCTURE_DEVELOPMENT	15	8.47E-15	1.27E-11
GOBP_CELL_POPULATION_PROLIFERATION	22	1.72E-14	2.14E-11
GOBP_WOUND_HEALING	14	3.42E-14	3.66E-11
GOBP_PROTEIN_PHOSPHORYLATION	20	6.41E-14	5.99E-11
GOBP_POSITIVE_REGULATION_OF_MOLECULAR_FUNCTION	20	2.66E-13	2.21E-10
GOBP_CIRCULATORY_SYSTEM_DEVELOPMENT	17	3.82E-13	2.67E-10
GOBP_ANATOMICAL_STRUCTURE_FORMATION_INVOLVED_IN_MORPHOGENESIS	17	3.93E-13	2.67E-10
GOBP_CELL_MIGRATION	19	6.70E-13	4.18E-10
GOBP_RESPONSE_TO_ENDOGENOUS_STIMULUS	19	8.51E-13	4.90E-10
GOBP_RESPONSE_TO_OXYGEN_CONTAINING_COMPOUND	19	1.17E-12	6.27E-10
GOBP_RESPONSE_TO_HORMONE	15	1.66E-12	8.27E-10
GOBP_REGULATION_OF_CELLULAR_COMPONENT_MOVEMENT	16	3.10E-12	1.45E-09
GOBP_VASCULATURE_DEVELOPMENT	14	6.05E-12	2.66E-09
GOBP_NEGATIVE_REGULATION_OF_SIGNALING	17	1.09E-11	4.53E-09
GOBP_REGULATION_OF_TRANSFERASE_ACTIVITY	15	1.24E-11	4.88E-09
GOBP_ENZYME_LINKED_RECEPTOR_PROTEIN_SIGNALING_PATHWAY	15	2.86E-11	1.07E-08
GOBP_MUSCLE_ORGAN_DEVELOPMENT	10	3.51E-11	1.25E-08
GOBP_POSITIVE_REGULATION_OF_PROTEIN_METABOLIC_PROCESS	17	3.87E-11	1.31E-08
GOBP_MAPK_CASCADE	14	4.32E-11	1.38E-08
GOBP_REGULATION_OF_INTRACELLULAR_SIGNAL_TRANSDUCTION	18	4.42E-11	1.38E-08
GOBP_POSITIVE_REGULATION_OF_CELL_POPULATION_PROLIFERATION	14	6.51E-11	1.95E-08
GOBP_REGULATION_OF_PHOSPHORUS_METABOLIC_PROCESS	17	8.69E-11	2.50E-08
GOBP_ACTIN_FILAMENT_BASED_PROCESS	13	1.01E-10	2.67E-08
GOBP_POSITIVE_REGULATION_OF_MULTICELLULAR_ORGANISMAL_PROCESS	16	1.07E-10	2.67E-08
GOBP_REGULATION_OF_MULTICELLULAR_ORGANISMAL_DEVELOPMENT	16	1.07E-10	2.67E-08
GOBP_REGULATION_OF_PROTEIN_KINASE_ACTIVITY	13	1.07E-10	2.67E-08
GOBP_REGULATION_OF_RESPONSE_TO_STRESS	16	1.28E-10	2.99E-08
GOBP_NEGATIVE_REGULATION_OF_CELL_DEATH	14	1.28E-10	2.99E-08
GOBP_REGULATION_OF_PROTEIN_PHOSPHORYLATION	15	1.56E-10	3.45E-08
GOBP_NEGATIVE_REGULATION_OF_RESPONSE_TO_STIMULUS	17	1.57E-10	3.45E-08
GOBP_BIOLOGICAL_ADHESION	16	2.51E-10	5.36E-08
GOBP_TUBE_DEVELOPMENT	14	4.15E-10	8.63E-08
GOBP_RESPONSE_TO_GROWTH_FACTOR	12	5.94E-10	1.20E-07
GOBP_REGULATION_OF_CELL_DIFFERENTIATION	16	9.03E-10	1.78E-07
GOBP_REGULATION_OF_WOUND_HEALING	7	9.65E-10	1.83E-07
GOBP_REGULATION_OF_PROTEIN_MODIFICATION_PROCESS	16	9.78E-10	1.83E-07
GOBP_RESPONSE_TO_MINERALOCORTICOID	5	1.10E-09	2.01E-07
GOBP_POSITIVE_REGULATION_OF_CATALYTIC_ACTIVITY	15	1.16E-09	2.06E-07
GOBP_RESPONSE_TO_STEROID_HORMONE	9	1.30E-09	2.26E-07
GOBP_POSITIVE_REGULATION_OF_PHOSPHORUS_METABOLIC_PROCESS	13	1.40E-09	2.37E-07
GOBP_RESPONSE_TO_ABIOTIC_STIMULUS	14	1.80E-09	2.99E-07
GOBP_TAXIS	11	2.22E-09	3.61E-07
GOBP_POSITIVE_REGULATION_OF_PROTEIN_PHOSPHORYLATION	12	2.28E-09	3.63E-07
GOBP_POSITIVE_REGULATION_OF_CELL_DEATH	11	2.52E-09	3.93E-07
GOBP_RESPONSE_TO_CORTICOSTEROID	7	2.73E-09	4.17E-07
GOBP_EPITHELIUM_DEVELOPMENT	14	3.29E-09	4.92E-07
GOBP_MUSCLE_TISSUE_DEVELOPMENT	9	3.60E-09	5.28E-07
GOBP_BLOOD_VESSEL_MORPHOGENESIS	11	3.73E-09	5.36E-07
GOBP_RESPONSE_TO_LIPID	12	3.92E-09	5.54E-07
GOBP_SMOOTH_MUSCLE_CELL_PROLIFERATION	7	4.25E-09	5.78E-07
GOBP_RESPONSE_TO_PEPTIDE	10	4.25E-09	5.78E-07
GOBP_REGULATION_OF_RESPONSE_TO_WOUNDING	7	4.63E-09	6.19E-07
GOBP_SUPRAMOLECULAR_FIBER_ORGANIZATION	11	6.18E-09	8.11E-07
GOBP_RESPONSE_TO_NITROGEN_COMPOUND	13	6.58E-09	8.42E-07
GOBP_RESPONSE_TO_ORGANIC_CYCLIC_COMPOUND	12	6.64E-09	8.42E-07
GOBP_EPITHELIAL_CELL_PROLIFERATION	9	1.24E-08	1.55E-06
GOBP_POSITIVE_REGULATION_OF_LOCOMOTION	10	1.27E-08	1.56E-06
GOBP_POSITIVE_REGULATION_OF_BIOSYNTHETIC_PROCESS	16	1.35E-08	1.63E-06
GOBP_ACTIN_FILAMENT_ORGANIZATION	9	1.40E-08	1.64E-06
GOBP_RESPONSE_TO_PEPTIDE_HORMONE	9	1.42E-08	1.64E-06
GOBP_RESPONSE_TO_KETONE	7	1.43E-08	1.64E-06
GOBP_CELLULAR_RESPONSE_TO_EXTERNAL_STIMULUS	8	1.48E-08	1.67E-06
GOBP_RESPONSE_TO_MECHANICAL_STIMULUS	7	1.96E-08	2.18E-06
GOBP_REGULATION_OF_RESPONSE_TO_EXTERNAL_STIMULUS	12	2.87E-08	3.16E-06
GOBP_POSITIVE_REGULATION_OF_PROTEIN_MODIFICATION_PROCESS	12	3.36E-08	3.64E-06
GOBP_MUSCLE_CELL_PROLIFERATION	7	3.74E-08	3.99E-06
GOBP_SKELETAL_MUSCLE_CELL_DIFFERENTIATION	5	4.03E-08	4.25E-06
GOBP_COAGULATION	8	4.21E-08	4.37E-06
GOBP_REGULATION_OF_BODY_FLUID_LEVELS	9	4.93E-08	5.06E-06
GOBP_POSITIVE_REGULATION_OF_TRANSFERASE_ACTIVITY	10	5.14E-08	5.20E-06
GOBP_NEGATIVE_REGULATION_OF_PROTEIN_METABOLIC_PROCESS	12	6.08E-08	6.07E-06
GOBP_POSITIVE_REGULATION_OF_CELLULAR_COMPONENT_ORGANIZATION	12	6.58E-08	6.47E-06
GOBP_TUBE_MORPHOGENESIS	11	6.81E-08	6.55E-06
GOBP_REGULATION_OF_COAGULATION	5	6.83E-08	6.55E-06
GOBP_NEGATIVE_REGULATION_OF_INTRACELLULAR_SIGNAL_TRANSDUCTION	9	6.98E-08	6.61E-06
GOBP_POSITIVE_REGULATION_OF_PROTEIN_KINASE_ACTIVITY	9	7.45E-08	6.97E-06
GOBP_CYTOSKELETON_ORGANIZATION	13	7.83E-08	7.24E-06
GOBP_RESPONSE_TO_OXYGEN_LEVELS	8	9.15E-08	8.35E-06
GOBP_REGULATION_OF_ACTIN_FILAMENT_BASED_PROCESS	8	1.01E-07	9.09E-06
GOBP_REGULATION_OF_PROTEOLYSIS	10	1.02E-07	9.09E-06
GOBP_TRANSMEMBRANE_RECEPTOR_PROTEIN_TYROSINE_KINASE_SIGNALING_I	10	1.10E-07	9.68E-06
GOBP_POSITIVE_REGULATION_OF_TRANSCRIPTION_BY_RNA_POLYMERASE_II	12	1.18E-07	1.02E-05
GOBP_CELLULAR_RESPONSE_TO_OXYGEN_CONTAINING_COMPOUND	12	1.20E-07	1.02E-05
GOBP_SKELETAL_MUSCLE_ORGAN_DEVELOPMENT	6	1.20E-07	1.02E-05
GOBP_RESPONSE_TO_CYTOKINE	12	1.27E-07	1.06E-05
GOBP_POSITIVE_REGULATION_OF_SIGNALING	14	1.42E-07	1.18E-05
GOBP_APOPTOTIC_SIGNALING_PATHWAY	9	1.65E-07	1.35E-05
GOBP_INFLAMMATORY_RESPONSE	10	1.71E-07	1.39E-05
GOBP_EPITHELIAL_CELL_DIFFERENTIATION	10	1.75E-07	1.41E-05
GOBP_POSITIVE_REGULATION_OF_INTRACELLULAR_SIGNAL_TRANSDUCTION	11	2.05E-07	1.64E-05
GOBP_DEFENSE_RESPONSE	14	2.23E-07	1.76E-05
GOBP_NEGATIVE_REGULATION_OF_TRANSFERASE_ACTIVITY	7	2.64E-07	2.06E-05
GOBP_NEGATIVE_REGULATION_OF_CATALYTIC_ACTIVITY	10	2.81E-07	2.16E-05
GOBP_POSITIVE_REGULATION_OF_DEVELOPMENTAL_PROCESS	12	2.91E-07	2.22E-05
GOBP_POSITIVE_REGULATION_OF_IMMUNE_SYSTEM_PROCESS	11	3.17E-07	2.40E-05
GOBP_CELL_CHEMOTAXIS	7	3.23E-07	2.41E-05

Figure 112 Gene ontology analysis of genes active in untreated cells, relative to LatB-treated cells, in Mtr4-depleted dKO$^{MRTF\text{-}NLS}$ cells

Gene ontology analysis of genes active in untreated cells, relative to LatB-treated cells, in Mtr4-depleted dKO$^{MRTF\text{-}NLS}$ cells by RNAseq. FDR<0.05. Relates to Figure 62. Bioinformatic analysis of RNAseq data was performed by Francesco Gualdrini.

GO BIOLOGICAL PROCESS	# Genes	p-value	FDR q-value
GOBP_MUSCLE_STRUCTURE_DEVELOPMENT	15	4.16E-19	1.64E-15
GOBP_REGULATION_OF_CELL_DEATH	22	4.33E-19	1.64E-15
GOBP_APOPTOTIC_PROCESS	21	8.93E-18	2.26E-14
GOBP_REGULATION_OF_CELL_POPULATION_PROLIFERATION	20	1.63E-16	3.07E-13
GOBP_RESPONSE_TO_ENDOGENOUS_STIMULUS	19	7.40E-16	1.12E-12
GOBP_RESPONSE_TO_HORMONE	15	1.35E-15	1.70E-12
GOBP_CELL_MOTILITY	17	4.40E-15	4.62E-12
GOBP_RESPONSE_TO_WOUNDING	16	4.88E-15	4.62E-12
GOBP_CIRCULATORY_SYSTEM_DEVELOPMENT	16	7.50E-15	6.19E-12
GOBP_ANATOMICAL_STRUCTURE_FORMATION_INVOLVED_IN_MORPHOGENESIS	16	8.17E-15	6.19E-12
GOBP_WOUND_HEALING	14	2.69E-14	4.60E-12
GOBP_LOCOMOTION	21	4.79E-14	5.98E-12
GOBP_RESPONSE_TO_OXYGEN_CONTAINING_COMPOUND	19	3.46E-13	3.40E-11
GOBP_PROTEIN_PHOSPHORYLATION	18	3.63E-13	1.99E-10
GOBP_POSITIVE_REGULATION_OF_MOLECULAR_FUNCTION	18	1.26E-12	6.72E-10
GOBP_POSITIVE_REGULATION_OF_PROTEIN_METABOLIC_PROCESS	17	1.90E-12	9.45E-10
GOBP_MUSCLE_ORGAN_DEVELOPMENT	10	6.10E-12	2.68E-09
GOBP_POSITIVE_REGULATION_OF_MULTICELLULAR_ORGANISMAL_PROCESS	16	6.44E-12	2.68E-09
GOBP_NEGATIVE_REGULATION_OF_SIGNALING	16	7.32E-12	2.88E-09
GOBP_REGULATION_OF_RESPONSE_TO_STRESS	16	7.72E-12	2.89E-09
GOBP_VASCULATURE_DEVELOPMENT	13	9.75E-12	3.47E-09
GOBP_ACTIN_FILAMENT_BASED_PROCESS	13	1.04E-11	3.52E-09
GOBP_REGULATION_OF_PROTEIN_KINASE_ACTIVITY	13	1.11E-11	3.52E-09
GOBP_REGULATION_OF_PROTEIN_PHOSPHORYLATION	15	1.13E-11	3.52E-09
GOBP_REGULATION_OF_TRANSFERASE_ACTIVITY	14	1.43E-11	4.26E-09
GOBP_REGULATION_OF_INTRACELLULAR_SIGNAL_TRANSDUCTION	17	2.16E-11	6.21E-09
GOBP_ENZYME_LINKED_RECEPTOR_PROTEIN_SIGNALING_PATHWAY	14	3.13E-11	8.67E-09
GOBP_REGULATION_OF_CELLULAR_COMPONENT_MOVEMENT	14	4.39E-11	1.17E-08
GOBP_REGULATION_OF_PHOSPHORUS_METABOLIC_PROCESS	16	5.30E-11	1.37E-08
GOBP_REGULATION_OF_CELL_DIFFERENTIATION	16	5.70E-11	1.42E-08
GOBP_MAPK_CASCADE	13	6.12E-11	1.45E-08
GOBP_REGULATION_OF_PROTEIN_MODIFICATION_PROCESS	16	6.19E-11	1.45E-08
GOBP_REGULATION_OF_MULTICELLULAR_ORGANISMAL_DEVELOPMENT	15	8.34E-11	1.89E-08
GOBP_POSITIVE_REGULATION_OF_CELL_POPULATION_PROLIFERATION	13	9.00E-11	1.98E-08
GOBP_NEGATIVE_REGULATION_OF_RESPONSE_TO_STIMULUS	16	9.33E-11	1.99E-08
GOBP_RESPONSE_TO_ABIOTIC_STIMULUS	14	1.63E-10	3.39E-08
GOBP_NEGATIVE_REGULATION_OF_CELL_DEATH	13	1.70E-10	3.43E-08
GOBP_RESPONSE_TO_STEROID_HORMONE	9	2.76E-10	5.44E-08
GOBP_REGULATION_OF_WOUND_HEALING	7	2.89E-10	5.48E-08
GOBP_POSITIVE_REGULATION_OF_PROTEIN_PHOSPHORYLATION	12	2.93E-10	5.48E-08
GOBP_RESPONSE_TO_MINERALOCORTICOID	5	4.69E-10	8.56E-08
GOBP_RESPONSE_TO_LIPID	12	5.08E-10	8.89E-08
GOBP_TUBE_DEVELOPMENT	13	5.11E-10	8.89E-08
GOBP_RESPONSE_TO_NITROGEN_COMPOUND	13	7.27E-10	1.24E-07
GOBP_RESPONSE_TO_PEPTIDE	10	7.72E-10	1.26E-07
GOBP_MUSCLE_TISSUE_DEVELOPMENT	9	7.73E-10	1.26E-07
GOBP_RESPONSE_TO_CORTICOSTEROID	7	8.22E-10	1.31E-07
GOBP_RESPONSE_TO_ORGANIC_CYCLIC_COMPOUND	12	8.67E-10	1.35E-07
GOBP_SUPRAMOLECULAR_FIBER_ORGANIZATION	11	9.52E-10	1.45E-07
GOBP_POSITIVE_REGULATION_OF_CATALYTIC_ACTIVITY	14	1.03E-09	1.54E-07
GOBP_RESPONSE_TO_GROWTH_FACTOR	11	1.27E-09	1.85E-07
GOBP_SMOOTH_MUSCLE_CELL_PROLIFERATION	7	1.28E-09	1.85E-07
GOBP_REGULATION_OF_RESPONSE_TO_WOUNDING	7	1.40E-09	1.97E-07
GOBP_BIOLOGICAL_ADHESION	14	2.08E-09	2.85E-07
GOBP_POSITIVE_REGULATION_OF_PHOSPHORUS_METABOLIC_PROCESS	12	2.09E-09	2.85E-07
GOBP_ACTIN_FILAMENT_ORGANIZATION	9	3.03E-09	4.05E-07
GOBP_RESPONSE_TO_PEPTIDE_HORMONE	9	3.09E-09	4.06E-07
GOBP_CELLULAR_RESPONSE_TO_EXTERNAL_STIMULUS	8	3.79E-09	4.89E-07
GOBP_RESPONSE_TO_KETONE	7	4.34E-09	5.50E-07
GOBP_POSITIVE_REGULATION_OF_PROTEIN_MODIFICATION_PROCESS	12	4.52E-09	5.63E-07
GOBP_RESPONSE_TO_MECHANICAL_STIMULUS	7	5.95E-09	7.29E-07
GOBP_POSITIVE_REGULATION_OF_CELL_DEATH	10	6.57E-09	7.92E-07
GOBP_NEGATIVE_REGULATION_OF_PROTEIN_METABOLIC_PROCESS	12	8.29E-09	9.76E-07
GOBP_POSITIVE_REGULATION_OF_BIOSYNTHETIC_PROCESS	15	8.35E-09	9.76E-07
GOBP_CYTOSKELETON_ORGANIZATION	13	9.15E-09	1.05E-06
GOBP_BLOOD_VESSEL_MORPHOGENESIS	10	9.37E-09	1.06E-06
GOBP_REGULATION_OF_BODY_FLUID_LEVELS	9	1.09E-08	1.20E-06
GOBP_COAGULATION	8	1.09E-08	1.20E-06
GOBP_MUSCLE_CELL_PROLIFERATION	7	1.14E-08	1.24E-06
GOBP_POSITIVE_REGULATION_OF_SIGNALING	14	1.44E-08	1.54E-06
GOBP_POSITIVE_REGULATION_OF_PROTEIN_KINASE_ACTIVITY	9	1.65E-08	1.72E-06
GOBP_CELLULAR_RESPONSE_TO_OXYGEN_CONTAINING_COMPOUND	12	1.66E-08	1.72E-06
GOBP_SKELETAL_MUSCLE_CELL_DIFFERENTIATION	5	1.72E-08	1.77E-06
GOBP_RESPONSE_TO_CYTOKINE	12	1.75E-08	1.77E-06
GOBP_REGULATION_OF_PROTEOLYSIS	10	1.93E-08	1.93E-06
GOBP_RESPONSE_TO_OXYGEN_LEVELS	8	2.39E-08	2.35E-06
GOBP_REGULATION_OF_ACTIN_FILAMENT_BASED_PROCESS	8	2.64E-08	2.56E-06
GOBP_REGULATION_OF_COAGULATION	5	2.93E-08	2.81E-06
GOBP_POSITIVE_REGULATION_OF_INTRACELLULAR_SIGNAL_TRANSDUCTION	11	3.36E-08	3.19E-06
GOBP_EPITHELIUM_DEVELOPMENT	12	3.80E-08	3.56E-06
GOBP_POSITIVE_REGULATION_OF_LOCOMOTION	9	3.96E-08	3.66E-06
GOBP_POSITIVE_REGULATION_OF_DEVELOPMENTAL_PROCESS	12	4.11E-08	3.75E-06
GOBP_SKELETAL_MUSCLE_ORGAN_DEVELOPMENT	6	4.37E-08	3.94E-06
GOBP_REGULATION_OF_RESPONSE_TO_EXTERNAL_STIMULUS	11	4.58E-08	4.08E-06
GOBP_NEGATIVE_REGULATION_OF_CATALYTIC_ACTIVITY	10	5.40E-08	4.76E-06
GOBP_EPITHELIAL_CELL_PROLIFERATION	8	5.50E-08	4.78E-06
GOBP_POSITIVE_REGULATION_OF_CELL_DIFFERENTIATION	10	7.40E-08	6.36E-06
GOBP_NEGATIVE_REGULATION_OF_TRANSFERASE_ACTIVITY	7	8.17E-08	6.95E-06
GOBP_TAXIS	9	8.96E-08	7.53E-06
GOBP_TUBE_MORPHOGENESIS	10	1.34E-07	1.11E-05
GOBP_ACTOMYOSIN_STRUCTURE_ORGANIZATION	6	1.35E-07	1.11E-05
GOBP_POSITIVE_REGULATION_OF_TRANSFERASE_ACTIVITY	9	1.40E-07	1.14E-05
GOBP_CELLULAR_RESPONSE_TO_ABIOTIC_STIMULUS	7	1.67E-07	1.35E-05
GOBP_POSITIVE_REGULATION_OF_TRANSCRIPTION_BY_RNA_POLYMERASE_II	11	1.69E-07	1.35E-05
GOBP_STRIATED_MUSCLE_CELL_DEVELOPMENT	5	1.91E-07	1.50E-05
GOBP_REGULATION_OF_APOPTOTIC_SIGNALING_PATHWAY	7	2.44E-07	1.90E-05
GOBP_NEGATIVE_REGULATION_OF_INTRACELLULAR_SIGNAL_TRANSDUCTION	8	2.57E-07	1.98E-05
GOBP_TRANSMEMBRANE_RECEPTOR_PROTEIN_TYROSINE_KINASE_SIGNALING_PATHWAY	9	2.79E-07	2.13E-05
GOBP_POSITIVE_REGULATION_OF_NUCLEOBASE_CONTAINING_COMPOUND_METABOLIC_PROCESS	13	2.89E-07	2.19E-05
GOBP_RESPONSE_TO_PROGESTERONE	4	3.00E-07	2.25E-05

Figure 113 Gene ontology analysis of the 55 Mtr4-controlled MRTF-NLS-induced genes

Gene ontology analysis of the 55 Mtr4-controlled MRTF-NLS-induced genes by RNAseq. FDR<0.05. Relates to Figure 63. Bioinformatic analysis of RNAseq data was performed by Francesco Gualdrini.

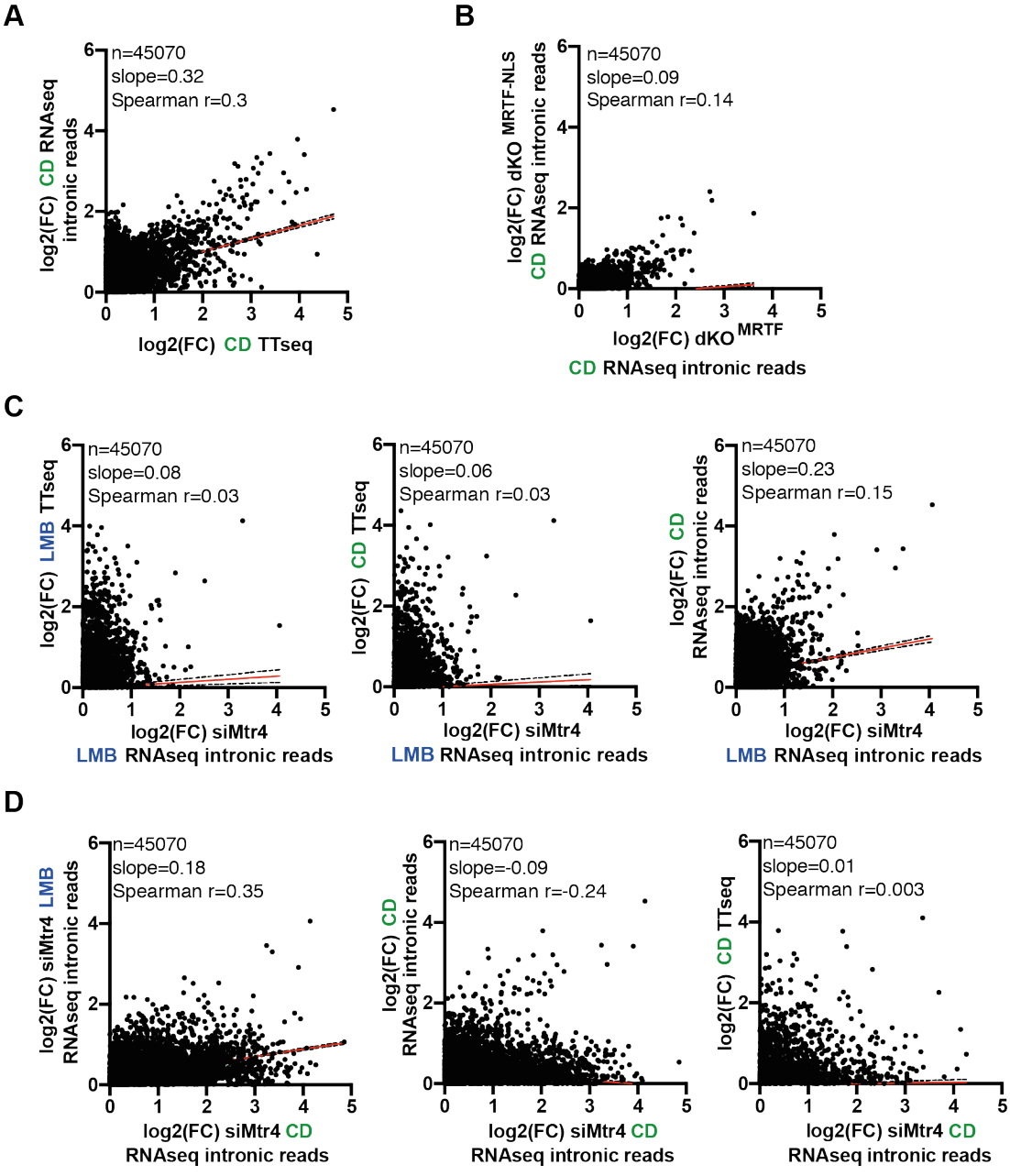

Figure 114 Correlation plots of full datasets

(A) Scatter plot comparing fold change expression at 45070 genes between CD-treated NIH3T3 cells by RNAseq and TTseq. Relates to Figure 35. (B) Scatter plot comparing fold change expression at 45070 genes between CD-treated dKO^{MRTF} and dKO$^{MRTF\text{-}NLS}$ cells by RNAseq. Relates to Figure 46. (C) Scatter plots comparing fold change expression at 45070 genes between Mtr4-depleted LMB-treated NIH3T3 cells by RNAseq and LMB-treated NIH3T3 cells by TTseq; Mtr4-depleted LMB-treated NIH3T3 cells by RNAseq and CD-treated NIH3T3 cells by TTseq; Mtr4-depleted LMB-treated NIH3T3 cells by RNAseq and CD-treated NIH3T3 cells by RNAseq. Relates to Figure 54. (D) Scatter plots comparing fold change expression at 45070 genes between Mtr4-depleted CD-treated and LMB-treated NIH3T3 cells by RNAseq; Mtr4-depleted CD-treated NIH3T3 cells by RNAseq and CD-treated NIH3T3 cells by RNAseq; Mtr4-depleted CD-treated NIH3T3 cells by RNAseq and CD-treated NIH3T3 cells by TTseq. Relates to Figure 55. The black lines represent the 95% confidence bands of the best-fit line (red). Bioinformatic analysis of RNAseq and TTseq data was performed by Francesco Gualdrini.

Chapter 11. Reference List

Adelman, K., Marr, M. T., Werner, J., Saunders, A., Ni, Z., Andrulis, E. D., & Lis, J. T. (2005). Efficient release from promoter-proximal stall sites requires transcript cleavage factor TFIIS. *Mol Cell*, *17*(1), 103-112. https://doi.org/10.1016/j.molcel.2004.11.028

Adelman, K., Wei, W., Ardehali, M. B., Werner, J., Zhu, B., Reinberg, D., & Lis, J. T. (2006). Drosophila Paf1 modulates chromatin structure at actively transcribed genes. *Mol Cell Biol*, *26*(1), 250-260. https://doi.org/10.1128/MCB.26.1.250-260.2006

Ahn, S. H., Kim, M., & Buratowski, S. (2004). Phosphorylation of serine 2 within the RNA polymerase II C-terminal domain couples transcription and 3' end processing. *Mol Cell*, *13*(1), 67-76. https://doi.org/10.1016/s1097-2765(03)00492-1

Akhtar, M. S., Heidemann, M., Tietjen, J. R., Zhang, D. W., Chapman, R. D., Eick, D., & Ansari, A. Z. (2009). TFIIH kinase places bivalent marks on the carboxy-terminal domain of RNA polymerase II. *Mol Cell*, *34*(3), 387-393. https://doi.org/10.1016/j.molcel.2009.04.016

Albert, T., Mautner, J., Funk, J. O., Hörtnagel, K., Pullner, A., & Eick, D. (1997). Nucleosomal structures of c-myc promoters with transcriptionally engaged RNA polymerase II. *Mol Cell Biol*, *17*(8), 4363-4371. https://doi.org/10.1128/mcb.17.8.4363

Alberti, S., Krause, S. M., Kretz, O., Philippar, U., Lemberger, T., Casanova, E., Wiebel, F. F., Schwarz, H., Frotscher, M., Schütz, G., & Nordheim, A. (2005). Neuronal migration in the murine rostral migratory stream requires serum response factor. *Proc Natl Acad Sci U S A*, *102*(17), 6148-6153. https://doi.org/10.1073/pnas.0501191102

Allen, B. L., & Taatjes, D. J. (2015). The Mediator complex: a central integrator of transcription. *Nat Rev Mol Cell Biol*, *16*(3), 155-166. https://doi.org/10.1038/nrm3951

Allison, L. A., Wong, J. K., Fitzpatrick, V. D., Moyle, M., & Ingles, C. J. (1988). The C-terminal domain of the largest subunit of RNA polymerase II of Saccharomyces cerevisiae, Drosophila melanogaster, and mammals: a conserved structure with an essential function. *Mol Cell Biol*, *8*(1), 321-329. https://doi.org/10.1128/mcb.8.1.321

Alpert, T., Herzel, L., & Neugebauer, K. M. (2017). Perfect timing: splicing and transcription rates in living cells. *Wiley Interdiscip Rev RNA*, *8*(2). https://doi.org/10.1002/wrna.1401

Amrani, N., Minet, M., Wyers, F., Dufour, M. E., Aggerbeck, L. P., & Lacroute, F. (1997). PCF11 encodes a third protein component of yeast cleavage and polyadenylation factor I. *Mol Cell Biol*, *17*(3), 1102-1109. https://doi.org/10.1128/mcb.17.3.1102

Anamika, K., Gyenis, À., Poidevin, L., Poch, O., & Tora, L. (2012). RNA polymerase II pausing downstream of core histone genes is different from genes producing polyadenylated transcripts. *PLoS One*, *7*(6), e38769. https://doi.org/10.1371/journal.pone.0038769

Andersen, P. R., Domanski, M., Kristiansen, M. S., Storvall, H., Ntini, E., Verheggen, C., Schein, A., Bunkenborg, J., Poser, I., Hallais, M., Sandberg, R., Hyman, A., LaCava, J., Rout, M. P., Andersen, J. S., Bertrand, E., & Jensen, T. H. (2013). The human cap-binding complex is functionally connected to the nuclear RNA

exosome. *Nat Struct Mol Biol*, *20*(12), 1367-1376. https://doi.org/10.1038/nsmb.2703

Anderson, J. R., Mukherjee, D., Muthukumaraswamy, K., Moraes, K. C., Wilusz, C. J., & Wilusz, J. (2006). Sequence-specific RNA binding mediated by the RNase PH domain of components of the exosome. *RNA*, *12*(10), 1810-1816. https://doi.org/10.1261/rna.144606

Andersson, R., Gebhard, C., Miguel-Escalada, I., Hoof, I., Bornholdt, J., Boyd, M., Chen, Y., Zhao, X., Schmidl, C., Suzuki, T., Ntini, E., Arner, E., Valen, E., Li, K., Schwarzfischer, L., Glatz, D., Raithel, J., Lilje, B., Rapin, N., Bagger, F. O., Jørgensen, M., Andersen, P. R., Bertin, N., Rackham, O., Burroughs, A. M., Baillie, J. K., Ishizu, Y., Shimizu, Y., Furuhata, E., Maeda, S., Negishi, Y., Mungall, C. J., Meehan, T. F., Lassmann, T., Itoh, M., Kawaji, H., Kondo, N., Kawai, J., Lennartsson, A., Daub, C. O., Heutink, P., Hume, D. A., Jensen, T. H., Suzuki, H., Hayashizaki, Y., Müller, F., Forrest, A. R. R., Carninci, P., Rehli, M., & Sandelin, A. (2014). An atlas of active enhancers across human cell types and tissues. *Nature*, *507*(7493), 455-461. https://doi.org/10.1038/nature12787

Andrulis, E. D., Guzmán, E., Döring, P., Werner, J., & Lis, J. T. (2000). High-resolution localization of Drosophila Spt5 and Spt6 at heat shock genes in vivo: roles in promoter proximal pausing and transcription elongation. *Genes Dev*, *14*(20), 2635-2649. https://doi.org/10.1101/gad.844200

Andrulis, E. D., Werner, J., Nazarian, A., Erdjument-Bromage, H., Tempst, P., & Lis, J. T. (2002). The RNA processing exosome is linked to elongating RNA polymerase II in Drosophila. *Nature*, *420*(6917), 837-841. https://doi.org/10.1038/nature01181

Ansari, A., & Hampsey, M. (2005). A role for the CPF 3'-end processing machinery in RNAP II-dependent gene looping. *Genes Dev*, *19*(24), 2969-2978. https://doi.org/10.1101/gad.1362305

Aoki, K., Kumagai, Y., Sakurai, A., Komatsu, N., Fujita, Y., Shionyu, C., & Matsuda, M. (2013). Stochastic ERK activation induced by noise and cell-to-cell propagation regulates cell density-dependent proliferation. *Mol Cell*, *52*(4), 529-540. https://doi.org/10.1016/j.molcel.2013.09.015

Ardehali, M. B., & Lis, J. T. (2009). Tracking rates of transcription and splicing in vivo. *Nat Struct Mol Biol*, *16*(11), 1123-1124. https://doi.org/10.1038/nsmb1109-1123

Baarlink, C., Plessner, M., Sherrard, A., Morita, K., Misu, S., Virant, D., Kleinschnitz, E. M., Harniman, R., Alibhai, D., Baumeister, S., Miyamoto, K., Endesfelder, U., Kaidi, A., & Grosse, R. (2017). A transient pool of nuclear F-actin at mitotic exit controls chromatin organization. *Nat Cell Biol*, *19*(12), 1389-1399. https://doi.org/10.1038/ncb3641

Baarlink, C., Wang, H., & Grosse, R. (2013). Nuclear actin network assembly by formins regulates the SRF coactivator MAL. *Science*, *340*(6134), 864-867. https://doi.org/10.1126/science.1235038

Baluapuri, A., Hofstetter, J., Dudvarski Stankovic, N., Endres, T., Bhandare, P., Vos, S. M., Adhikari, B., Schwarz, J. D., Narain, A., Vogt, M., Wang, S. Y., Düster, R., Jung, L. A., Vanselow, J. T., Wiegering, A., Geyer, M., Maric, H. M., Gallant, P., Walz, S., Schlosser, A., Cramer, P., Eilers, M., & Wolf, E. (2019). MYC Recruits SPT5 to RNA Polymerase II to Promote Processive Transcription Elongation. *Mol Cell*, *74*(4), 674-687.e611. https://doi.org/10.1016/j.molcel.2019.02.031

Banerjee, A., Apponi, L. H., Pavlath, G. K., & Corbett, A. H. (2013). PABPN1: molecular function and muscle disease. *FEBS J*, *280*(17), 4230-4250. https://doi.org/10.1111/febs.12294

Bannister, A. J., Zegerman, P., Partridge, J. F., Miska, E. A., Thomas, J. O., Allshire, R. C., & Kouzarides, T. (2001). Selective recognition of methylated lysine 9 on

histone H3 by the HP1 chromo domain. *Nature*, *410*(6824), 120-124. https://doi.org/10.1038/35065138

Barboric, M., Nissen, R. M., Kanazawa, S., Jabrane-Ferrat, N., & Peterlin, B. M. (2001). NF-kappaB binds P-TEFb to stimulate transcriptional elongation by RNA polymerase II. *Mol Cell*, *8*(2), 327-337. https://doi.org/10.1016/s1097-2765(01)00314-8

Barillà, D., Lee, B. A., & Proudfoot, N. J. (2001). Cleavage/polyadenylation factor IA associates with the carboxyl-terminal domain of RNA polymerase II in Saccharomyces cerevisiae. *Proc Natl Acad Sci U S A*, *98*(2), 445-450. https://doi.org/10.1073/pnas.98.2.445

Bartkowiak, B., Liu, P., Phatnani, H. P., Fuda, N. J., Cooper, J. J., Price, D. H., Adelman, K., Lis, J. T., & Greenleaf, A. L. (2010). CDK12 is a transcription elongation-associated CTD kinase, the metazoan ortholog of yeast Ctk1. *Genes Dev*, *24*(20), 2303-2316. https://doi.org/10.1101/gad.1968210

Bartolomei, M. S., Halden, N. F., Cullen, C. R., & Corden, J. L. (1988). Genetic analysis of the repetitive carboxyl-terminal domain of the largest subunit of mouse RNA polymerase II. *Mol Cell Biol*, *8*(1), 330-339. https://doi.org/10.1128/mcb.8.1.330

Baskaran, R., Dahmus, M. E., & Wang, J. Y. (1993). Tyrosine phosphorylation of mammalian RNA polymerase II carboxyl-terminal domain. *Proc Natl Acad Sci U S A*, *90*(23), 11167-11171. https://doi.org/10.1073/pnas.90.23.11167

Bataille, A. R., Jeronimo, C., Jacques, P., Laramée, L., Fortin, M., Forest, A., Bergeron, M., Hanes, S. D., & Robert, F. (2012). A universal RNA polymerase II CTD cycle is orchestrated by complex interplays between kinase, phosphatase, and isomerase enzymes along genes. *Mol Cell*, *45*(2), 158-170. https://doi.org/10.1016/j.molcel.2011.11.024

Belin, B. J., Cimini, B. A., Blackburn, E. H., & Mullins, R. D. (2013). Visualization of actin filaments and monomers in somatic cell nuclei. *Mol Biol Cell*, *24*(7), 982-994. https://doi.org/10.1091/mbc.E12-09-0685

Belin, B. J., Lee, T., & Mullins, R. D. (2015). DNA damage induces nuclear actin filament assembly by Formin -2 and Spire-½ that promotes efficient DNA repair. [corrected]. *Elife*, *4*, e07735. https://doi.org/10.7554/eLife.07735

Bellier, S., Chastant, S., Adenot, P., Vincent, M., Renard, J. P., & Bensaude, O. (1997). Nuclear translocation and carboxyl-terminal domain phosphorylation of RNA polymerase II delineate the two phases of zygotic gene activation in mammalian embryos. *EMBO J*, *16*(20), 6250-6262. https://doi.org/10.1093/emboj/16.20.6250

Belotserkovskaya, R., Oh, S., Bondarenko, V. A., Orphanides, G., Studitsky, V. M., & Reinberg, D. (2003). FACT facilitates transcription-dependent nucleosome alteration. *Science*, *301*(5636), 1090-1093. https://doi.org/10.1126/science.1085703

Bernecky, C., Plitzko, J. M., & Cramer, P. (2017). Structure of a transcribing RNA polymerase II-DSIF complex reveals a multidentate DNA-RNA clamp. *Nat Struct Mol Biol*, *24*(10), 809-815. https://doi.org/10.1038/nsmb.3465

Bernstein, B. E., Kamal, M., Lindblad-Toh, K., Bekiranov, S., Bailey, D. K., Huebert, D. J., McMahon, S., Karlsson, E. K., Kulbokas, E. J., Gingeras, T. R., Schreiber, S. L., & Lander, E. S. (2005). Genomic maps and comparative analysis of histone modifications in human and mouse. *Cell*, *120*(2), 169-181. https://doi.org/10.1016/j.cell.2005.01.001

Bernstein, B. E., Liu, C. L., Humphrey, E. L., Perlstein, E. O., & Schreiber, S. L. (2004). Global nucleosome occupancy in yeast. *Genome Biol*, *5*(9), R62. https://doi.org/10.1186/gb-2004-5-9-r62

Biglione, S., Byers, S. A., Price, J. P., Nguyen, V. T., Bensaude, O., Price, D. H., & Maury, W. (2007). Inhibition of HIV-1 replication by P-TEFb inhibitors DRB, seliciclib and flavopiridol correlates with release of free P-TEFb from the large, inactive form of the complex. *Retrovirology*, *4*, 47. https://doi.org/10.1186/1742-4690-4-47

Blasius, M., Wagner, S. A., Choudhary, C., Bartek, J., & Jackson, S. P. (2014). A quantitative 14-3-3 interaction screen connects the nuclear exosome targeting complex to the DNA damage response. *Genes Dev*, *28*(18), 1977-1982. https://doi.org/10.1101/gad.246272.114

Blazek, D., Kohoutek, J., Bartholomeeusen, K., Johansen, E., Hulinkova, P., Luo, Z., Cimermancic, P., Ule, J., & Peterlin, B. M. (2011). The Cyclin K/Cdk12 complex maintains genomic stability via regulation of expression of DNA damage response genes. *Genes Dev*, *25*(20), 2158-2172. https://doi.org/10.1101/gad.16962311

Boehm, A. K., Saunders, A., Werner, J., & Lis, J. T. (2003). Transcription factor and polymerase recruitment, modification, and movement on dhsp70 in vivo in the minutes following heat shock. *Mol Cell Biol*, *23*(21), 7628-7637. https://doi.org/10.1128/mcb.23.21.7628-7637.2003

Boeing, S., Rigault, C., Heidemann, M., Eick, D., & Meisterernst, M. (2010). RNA polymerase II C-terminal heptarepeat domain Ser-7 phosphorylation is established in a mediator-dependent fashion. *J Biol Chem*, *285*(1), 188-196. https://doi.org/10.1074/jbc.M109.046565

Bohnsack, M. T., Stüven, T., Kuhn, C., Cordes, V. C., & Görlich, D. (2006). A selective block of nuclear actin export stabilizes the giant nuclei of Xenopus oocytes. *Nat Cell Biol*, *8*(3), 257-263. https://doi.org/10.1038/ncb1357

Boros, J., Donaldson, I. J., O'Donnell, A., Odrowaz, Z. A., Zeef, L., Lupien, M., Meyer, C. A., Liu, X. S., Brown, M., & Sharrocks, A. D. (2009). Elucidation of the ELK1 target gene network reveals a role in the coordinate regulation of core components of the gene regulation machinery. *Genome Res*, *19*(11), 1963-1973. https://doi.org/10.1101/gr.093047.109

Bortvin, A., & Winston, F. (1996). Evidence that Spt6p controls chromatin structure by a direct interaction with histones. *Science*, *272*(5267), 1473-1476. https://doi.org/10.1126/science.272.5267.1473

Boulon, S., Verheggen, C., Jady, B. E., Girard, C., Pescia, C., Paul, C., Ospina, J. K., Kiss, T., Matera, A. G., Bordonné, R., & Bertrand, E. (2004). PHAX and CRM1 are required sequentially to transport U3 snoRNA to nucleoli. *Mol Cell*, *16*(5), 777-787. https://doi.org/10.1016/j.molcel.2004.11.013

Bousquet-Antonelli, C., Presutti, C., & Tollervey, D. (2000). Identification of a regulated pathway for nuclear pre-mRNA turnover. *Cell*, *102*(6), 765-775. https://doi.org/10.1016/s0092-8674(00)00065-9

Bowman, E. A., Bowman, C. R., Ahn, J. H., & Kelly, W. G. (2013). Phosphorylation of RNA polymerase II is independent of P-TEFb in the C. elegans germline. *Development*, *140*(17), 3703-3713. https://doi.org/10.1242/dev.095778

Brannan, K., Kim, H., Erickson, B., Glover-Cutter, K., Kim, S., Fong, N., Kiemele, L., Hansen, K., Davis, R., Lykke-Andersen, J., & Bentley, D. L. (2012). mRNA decapping factors and the exonuclease Xrn2 function in widespread premature termination of RNA polymerase II transcription. *Mol Cell*, *46*(3), 311-324. https://doi.org/10.1016/j.molcel.2012.03.006

Brenner, S. L., & Korn, E. D. (1980). The effects of cytochalasins on actin polymerization and actin ATPase provide insights into the mechanism of polymerization. *J Biol Chem*, *255*(3), 841-844.

Brookes, E., de Santiago, I., Hebenstreit, D., Morris, K. J., Carroll, T., Xie, S. Q., Stock, J. K., Heidemann, M., Eick, D., Nozaki, N., Kimura, H., Ragoussis, J.,

Teichmann, S. A., & Pombo, A. (2012). Polycomb associates genome-wide with a specific RNA polymerase II variant, and regulates metabolic genes in ESCs. *Cell Stem Cell*, *10*(2), 157-170. https://doi.org/10.1016/j.stem.2011.12.017

Brown, S. A., Imbalzano, A. N., & Kingston, R. E. (1996). Activator-dependent regulation of transcriptional pausing on nucleosomal templates. *Genes Dev*, *10*(12), 1479-1490. https://doi.org/10.1101/gad.10.12.1479

Brown, S. A., & Kingston, R. E. (1997). Disruption of downstream chromatin directed by a transcriptional activator. *Genes Dev*, *11*(23), 3116-3121. https://doi.org/10.1101/gad.11.23.3116

Brugiolo, M., Herzel, L., & Neugebauer, K. M. (2013). Counting on co-transcriptional splicing. *F1000Prime Rep*, *5*, 9. https://doi.org/10.12703/P5-9

Brès, V., Gomes, N., Pickle, L., & Jones, K. A. (2005). A human splicing factor, SKIP, associates with P-TEFb and enhances transcription elongation by HIV-1 Tat. *Genes Dev*, *19*(10), 1211-1226. https://doi.org/10.1101/gad.1291705

Buchwalter, G., Gross, C., & Wasylyk, B. (2005). The ternary complex factor Net regulates cell migration through inhibition of PAI-1 expression. *Mol Cell Biol*, *25*(24), 10853-10862. https://doi.org/10.1128/MCB.25.24.10853-10862.2005

Buckley, M. S., Kwak, H., Zipfel, W. R., & Lis, J. T. (2014). Kinetics of promoter Pol II on Hsp70 reveal stable pausing and key insights into its regulation. *Genes Dev*, *28*(1), 14-19. https://doi.org/10.1101/gad.231886.113

Bösken, C. A., Farnung, L., Hintermair, C., Merzel Schachter, M., Vogel-Bachmayr, K., Blazek, D., Anand, K., Fisher, R. P., Eick, D., & Geyer, M. (2014). The structure and substrate specificity of human Cdk12/Cyclin K. *Nat Commun*, *5*, 3505. https://doi.org/10.1038/ncomms4505

Cadena, D. L., & Dahmus, M. E. (1987). Messenger RNA synthesis in mammalian cells is catalyzed by the phosphorylated form of RNA polymerase II. *J Biol Chem*, *262*(26), 12468-12474.

Caridi, C. P., D'Agostino, C., Ryu, T., Zapotoczny, G., Delabaere, L., Li, X., Khodaverdian, V. Y., Amaral, N., Lin, E., Rau, A. R., & Chiolo, I. (2018). Nuclear F-actin and myosins drive relocalization of heterochromatic breaks. *Nature*, *559*(7712), 54-60. https://doi.org/10.1038/s41586-018-0242-8

Carter, R., & Drouin, G. (2009). Structural differentiation of the three eukaryotic RNA polymerases. *Genomics*, *94*(6), 388-396. https://doi.org/10.1016/j.ygeno.2009.08.011

Cassart, C., Drogat, J., Migeot, V., & Hermand, D. (2012). Distinct requirement of RNA polymerase II CTD phosphorylations in budding and fission yeast. *Transcription*, *3*(5), 231-234. https://doi.org/10.4161/trns.21066

Cassart, C., Yague-Sanz, C., Bauer, F., Ponsard, P., Stubbe, F. X., Migeot, V., Wery, M., Morillon, A., Palladino, F., Robert, V., & Hermand, D. (2020). RNA polymerase II CTD S2P is dispensable for embryogenesis but mediates exit from developmental diapause in. *Sci Adv*, *6*(50). https://doi.org/10.1126/sciadv.abc1450

Cen, B., Selvaraj, A., Burgess, R. C., Hitzler, J. K., Ma, Z., Morris, S. W., & Prywes, R. (2003). Megakaryoblastic leukemia 1, a potent transcriptional coactivator for serum response factor (SRF), is required for serum induction of SRF target genes. *Mol Cell Biol*, *23*(18), 6597-6608. https://doi.org/10.1128/mcb.23.18.6597-6608.2003

Chao, S. H., & Price, D. H. (2001). Flavopiridol inactivates P-TEFb and blocks most RNA polymerase II transcription in vivo. *J Biol Chem*, *276*(34), 31793-31799. https://doi.org/10.1074/jbc.M102306200

Chapman, R. D., Heidemann, M., Albert, T. K., Mailhammer, R., Flatley, A., Meisterernst, M., Kremmer, E., & Eick, D. (2007). Transcribing RNA polymerase

II is phosphorylated at CTD residue serine-7. *Science*, *318*(5857), 1780-1782. https://doi.org/10.1126/science.1145977

Charbonney, E., Speight, P., Masszi, A., Nakano, H., & Kapus, A. (2011). β-catenin and Smad3 regulate the activity and stability of myocardin-related transcription factor during epithelial-myofibroblast transition. *Mol Biol Cell*, *22*(23), 4472-4485. https://doi.org/10.1091/mbc.E11-04-0335

Chen, F., Gao, X., & Shilatifard, A. (2015). Stably paused genes revealed through inhibition of transcription initiation by the TFIIH inhibitor triptolide. *Genes Dev*, *29*(1), 39-47. https://doi.org/10.1101/gad.246173.114

Chen, F. X., Smith, E. R., & Shilatifard, A. (2018). Born to run: control of transcription elongation by RNA polymerase II. *Nat Rev Mol Cell Biol*, *19*(7), 464-478. https://doi.org/10.1038/s41580-018-0010-5

Chen, H. H., Wang, Y. C., & Fann, M. J. (2006). Identification and characterization of the CDK12/cyclin L1 complex involved in alternative splicing regulation. *Mol Cell Biol*, *26*(7), 2736-2745. https://doi.org/10.1128/MCB.26.7.2736-2745.2006

Chen, H. H., Wong, Y. H., Geneviere, A. M., & Fann, M. J. (2007). CDK13/CDC2L5 interacts with L-type cyclins and regulates alternative splicing. *Biochem Biophys Res Commun*, *354*(3), 735-740. https://doi.org/10.1016/j.bbrc.2007.01.049

Chen, R., Liu, M., Li, H., Xue, Y., Ramey, W. N., He, N., Ai, N., Luo, H., Zhu, Y., Zhou, N., & Zhou, Q. (2008). PP2B and PP1alpha cooperatively disrupt 7SK snRNP to release P-TEFb for transcription in response to Ca2+ signaling. *Genes Dev*, *22*(10), 1356-1368. https://doi.org/10.1101/gad.1636008

Chen, Y., Zhang, L., Estarás, C., Choi, S. H., Moreno, L., Karn, J., Moresco, J. J., Yates, J. R., & Jones, K. A. (2014). A gene-specific role for the Ssu72 RNAPII CTD phosphatase in HIV-1 Tat transactivation. *Genes Dev*, *28*(20), 2261-2275. https://doi.org/10.1101/gad.250449.114

Cheng, C., & Sharp, P. A. (2003). RNA polymerase II accumulation in the promoter-proximal region of the dihydrofolate reductase and gamma-actin genes. *Mol Cell Biol*, *23*(6), 1961-1967. https://doi.org/10.1128/mcb.23.6.1961-1967.2003

Cheng, H., Dufu, K., Lee, C. S., Hsu, J. L., Dias, A., & Reed, R. (2006). Human mRNA export machinery recruited to the 5' end of mRNA. *Cell*, *127*(7), 1389-1400. https://doi.org/10.1016/j.cell.2006.10.044

Chi, B., Wang, Q., Wu, G., Tan, M., Wang, L., Shi, M., Chang, X., & Cheng, H. (2013). Aly and THO are required for assembly of the human TREX complex and association of TREX components with the spliced mRNA. *Nucleic Acids Res*, *41*(2), 1294-1306. https://doi.org/10.1093/nar/gks1188

Chiu, A. C., Suzuki, H. I., Wu, X., Mahat, D. B., Kriz, A. J., & Sharp, P. A. (2018). Transcriptional Pause Sites Delineate Stable Nucleosome-Associated Premature Polyadenylation Suppressed by U1 snRNP. *Mol Cell*, *69*(4), 648-663.e647. https://doi.org/10.1016/j.molcel.2018.01.006

Chlebowski, A., Tomecki, R., López, M. E., Séraphin, B., & Dziembowski, A. (2010). Catalytic properties of the eukaryotic exosome. *Adv Exp Med Biol*, *702*, 63-78.

Cho, E. J., Kobor, M. S., Kim, M., Greenblatt, J., & Buratowski, S. (2001). Opposing effects of Ctk1 kinase and Fcp1 phosphatase at Ser 2 of the RNA polymerase II C-terminal domain. *Genes Dev*, *15*(24), 3319-3329. https://doi.org/10.1101/gad.935901

Cho, E. J., Takagi, T., Moore, C. R., & Buratowski, S. (1997). mRNA capping enzyme is recruited to the transcription complex by phosphorylation of the RNA polymerase II carboxy-terminal domain. *Genes Dev*, *11*(24), 3319-3326. https://doi.org/10.1101/gad.11.24.3319

Cho, H., Kim, T. K., Mancebo, H., Lane, W. S., Flores, O., & Reinberg, D. (1999). A protein phosphatase functions to recycle RNA polymerase II. *Genes Dev*, *13*(12), 1540-1552. https://doi.org/10.1101/gad.13.12.1540

Chopra, V. S., Cande, J., Hong, J. W., & Levine, M. (2009). Stalled Hox promoters as chromosomal boundaries. *Genes Dev*, *23*(13), 1505-1509. https://doi.org/10.1101/gad.1807309

Chu, C., Zhang, Q. C., da Rocha, S. T., Flynn, R. A., Bharadwaj, M., Calabrese, J. M., Magnuson, T., Heard, E., & Chang, H. Y. (2015). Systematic discovery of Xist RNA binding proteins. *Cell*, *161*(2), 404-416. https://doi.org/10.1016/j.cell.2015.03.025

Chu, Y., Simic, R., Warner, M. H., Arndt, K. M., & Prelich, G. (2007). Regulation of histone modification and cryptic transcription by the Bur1 and Paf1 complexes. *EMBO J*, *26*(22), 4646-4656. https://doi.org/10.1038/sj.emboj.7601887

Col, E., Hoghoughi, N., Dufour, S., Penin, J., Koskas, S., Faure, V., Ouzounova, M., Hernandez-Vargash, H., Reynoird, N., Daujat, S., Folco, E., Vigneron, M., Schneider, R., Verdel, A., Khochbin, S., Herceg, Z., Caron, C., & Vourc'h, C. (2017). Bromodomain factors of BET family are new essential actors of pericentric heterochromatin transcriptional activation in response to heat shock. *Sci Rep*, *7*(1), 5418. https://doi.org/10.1038/s41598-017-05343-8

Colgan, D. F., & Manley, J. L. (1997). Mechanism and regulation of mRNA polyadenylation. *Genes Dev*, *11*(21), 2755-2766. https://doi.org/10.1101/gad.11.21.2755

Conaway, J. W., Bradsher, J. N., Tan, S., & Conaway, R. C. (1993). Transcription factor SIII: a novel component of the RNA polymerase II elongation complex. *Cell Mol Biol Res*, *39*(4), 323-329.

Connelly, S., & Manley, J. L. (1988). A functional mRNA polyadenylation signal is required for transcription termination by RNA polymerase II. *Genes Dev*, *2*(4), 440-452. https://doi.org/10.1101/gad.2.4.440

Copeland, J. W., & Treisman, R. (2002). The diaphanous-related formin mDia1 controls serum response factor activity through its effects on actin polymerization. *Mol Biol Cell*, *13*(11), 4088-4099. https://doi.org/10.1091/mbc.02-06-0092

Corden, J. L., Cadena, D. L., Ahearn, J. M., & Dahmus, M. E. (1985). A unique structure at the carboxyl terminus of the largest subunit of eukaryotic RNA polymerase II. *Proc Natl Acad Sci U S A*, *82*(23), 7934-7938. https://doi.org/10.1073/pnas.82.23.7934

Core, L., & Adelman, K. (2019). Promoter-proximal pausing of RNA polymerase II: a nexus of gene regulation. *Genes Dev*, *33*(15-16), 960-982. https://doi.org/10.1101/gad.325142.119

Core, L. J., & Lis, J. T. (2008). Transcription regulation through promoter-proximal pausing of RNA polymerase II. *Science*, *319*(5871), 1791-1792. https://doi.org/10.1126/science.1150843

Core, L. J., Waterfall, J. J., & Lis, J. T. (2008). Nascent RNA sequencing reveals widespread pausing and divergent initiation at human promoters. *Science*, *322*(5909), 1845-1848. https://doi.org/10.1126/science.1162228

Cortazar, M. A., Sheridan, R. M., Erickson, B., Fong, N., Glover-Cutter, K., Brannan, K., & Bentley, D. L. (2019). Control of RNA Pol II Speed by PNUTS-PP1 and Spt5 Dephosphorylation Facilitates Termination by a "Sitting Duck Torpedo" Mechanism. *Mol Cell*, *76*(6), 896-908.e894. https://doi.org/10.1016/j.molcel.2019.09.031

Costello, P., Nicolas, R., Willoughby, J., Wasylyk, B., Nordheim, A., & Treisman, R. (2010). Ternary complex factors SAP-1 and Elk-1, but not net, are functionally equivalent in thymocyte development. *J Immunol*, *185*(2), 1082-1092. https://doi.org/10.4049/jimmunol.1000472

Costello, P., Sargent, M., Maurice, D., Esnault, C., Foster, K., Anjos-Afonso, F., & Treisman, R. (2015). MRTF-SRF signaling is required for seeding of HSC/Ps in

bone marrow during development. *Blood*, *125*(8), 1244-1255. https://doi.org/10.1182/blood-2014-08-595603

Costello, P. S., Nicolas, R. H., Watanabe, Y., Rosewell, I., & Treisman, R. (2004). Ternary complex factor SAP-1 is required for Erk-mediated thymocyte positive selection. *Nat Immunol*, *5*(3), 289-298. https://doi.org/10.1038/ni1038

Coudreuse, D., van Bakel, H., Dewez, M., Soutourina, J., Parnell, T., Vandenhaute, J., Cairns, B., Werner, M., & Hermand, D. (2010). A gene-specific requirement of RNA polymerase II CTD phosphorylation for sexual differentiation in S. pombe. *Curr Biol*, *20*(12), 1053-1064. https://doi.org/10.1016/j.cub.2010.04.054

Cramer, P. (2019). Organization and regulation of gene transcription. *Nature*, *573*(7772), 45-54. https://doi.org/10.1038/s41586-019-1517-4

Cramer, P., Armache, K. J., Baumli, S., Benkert, S., Brueckner, F., Buchen, C., Damsma, G. E., Dengl, S., Geiger, S. R., Jasiak, A. J., Jawhari, A., Jennebach, S., Kamenski, T., Kettenberger, H., Kuhn, C. D., Lehmann, E., Leike, K., Sydow, J. F., & Vannini, A. (2008). Structure of eukaryotic RNA polymerases. *Annu Rev Biophys*, *37*, 337-352. https://doi.org/10.1146/annurev.biophys.37.032807.130008

Cramer, P., Bushnell, D. A., & Kornberg, R. D. (2001). Structural basis of transcription: RNA polymerase II at 2.8 angstrom resolution. *Science*, *292*(5523), 1863-1876. https://doi.org/10.1126/science.1059493

Czudnochowski, N., Bösken, C. A., & Geyer, M. (2012). Serine-7 but not serine-5 phosphorylation primes RNA polymerase II CTD for P-TEFb recognition. *Nat Commun*, *3*, 842. https://doi.org/10.1038/ncomms1846

Dalton, S., & Treisman, R. (1992). Characterization of SAP-1, a protein recruited by serum response factor to the c-fos serum response element. *Cell*, *68*(3), 597-612. https://doi.org/10.1016/0092-8674(92)90194-h

Danko, C. G., Hah, N., Luo, X., Martins, A. L., Core, L., Lis, J. T., Siepel, A., & Kraus, W. L. (2013). Signaling pathways differentially affect RNA polymerase II initiation, pausing, and elongation rate in cells. *Mol Cell*, *50*(2), 212-222. https://doi.org/10.1016/j.molcel.2013.02.015

Daury, L., Chailleux, C., Bonvallet, J., & Trouche, D. (2006). Histone H3.3 deposition at E2F-regulated genes is linked to transcription. *EMBO Rep*, *7*(1), 66-71. https://doi.org/10.1038/sj.embor.7400561

de la Mata, M., Alonso, C. R., Kadener, S., Fededa, J. P., Blaustein, M., Pelisch, F., Cramer, P., Bentley, D., & Kornblihtt, A. R. (2003). A slow RNA polymerase II affects alternative splicing in vivo. *Mol Cell*, *12*(2), 525-532. https://doi.org/10.1016/j.molcel.2003.08.001

de Vries, H., Rüegsegger, U., Hübner, W., Friedlein, A., Langen, H., & Keller, W. (2000). Human pre-mRNA cleavage factor II(m) contains homologs of yeast proteins and bridges two other cleavage factors. *EMBO J*, *19*(21), 5895-5904. https://doi.org/10.1093/emboj/19.21.5895

Dengl, S., Mayer, A., Sun, M., & Cramer, P. (2009). Structure and in vivo requirement of the yeast Spt6 SH2 domain. *J Mol Biol*, *389*(1), 211-225. https://doi.org/10.1016/j.jmb.2009.04.016

Dermody, J. L., Dreyfuss, J. M., Villén, J., Ogundipe, B., Gygi, S. P., Park, P. J., Ponticelli, A. S., Moore, C. L., Buratowski, S., & Bucheli, M. E. (2008). Unphosphorylated SR-like protein Npl3 stimulates RNA polymerase II elongation. *PLoS One*, *3*(9), e3273. https://doi.org/10.1371/journal.pone.0003273

Descostes, N., Heidemann, M., Spinelli, L., Schüller, R., Maqbool, M. A., Fenouil, R., Koch, F., Innocenti, C., Gut, M., Gut, I., Eick, D., & Andrau, J. C. (2014). Tyrosine phosphorylation of RNA polymerase II CTD is associated with

antisense promoter transcription and active enhancers in mammalian cells. *Elife*, *3*, e02105. https://doi.org/10.7554/eLife.02105

Devaiah, B. N., Lewis, B. A., Cherman, N., Hewitt, M. C., Albrecht, B. K., Robey, P. G., Ozato, K., Sims, R. J., & Singer, D. S. (2012). BRD4 is an atypical kinase that phosphorylates serine2 of the RNA polymerase II carboxy-terminal domain. *Proc Natl Acad Sci U S A*, *109*(18), 6927-6932. https://doi.org/10.1073/pnas.1120422109

Di Vona, C., Bezdan, D., Islam, A. B., Salichs, E., López-Bigas, N., Ossowski, S., & de la Luna, S. (2015). Chromatin-wide profiling of DYRK1A reveals a role as a gene-specific RNA polymerase II CTD kinase. *Mol Cell*, *57*(3), 506-520. https://doi.org/10.1016/j.molcel.2014.12.026

Dias, J. D., Rito, T., Torlai Triglia, E., Kukalev, A., Ferrai, C., Chotalia, M., Brookes, E., Kimura, H., & Pombo, A. (2015). Methylation of RNA polymerase II non-consensus Lysine residues marks early transcription in mammalian cells. *Elife*, *4*. https://doi.org/10.7554/eLife.11215

Diring, J., Mouilleron, S., McDonald, N. Q., & Treisman, R. (2019). RPEL-family rhoGAPs link Rac/Cdc42 GTP loading to G-actin availability. *Nat Cell Biol*, *21*(7), 845-855. https://doi.org/10.1038/s41556-019-0337-y

Domingo-Prim, J., Endara-Coll, M., Bonath, F., Jimeno, S., Prados-Carvajal, R., Friedländer, M. R., Huertas, P., & Visa, N. (2019). EXOSC10 is required for RPA assembly and controlled DNA end resection at DNA double-strand breaks. *Nat Commun*, *10*(1), 2135. https://doi.org/10.1038/s41467-019-10153-9

Donner, A. J., Ebmeier, C. C., Taatjes, D. J., & Espinosa, J. M. (2010). CDK8 is a positive regulator of transcriptional elongation within the serum response network. *Nat Struct Mol Biol*, *17*(2), 194-201. https://doi.org/10.1038/nsmb.1752

Dou, Y., Milne, T. A., Tackett, A. J., Smith, E. R., Fukuda, A., Wysocka, J., Allis, C. D., Chait, B. T., Hess, J. L., & Roeder, R. G. (2005). Physical association and coordinate function of the H3 K4 methyltransferase MLL1 and the H4 K16 acetyltransferase MOF. *Cell*, *121*(6), 873-885. https://doi.org/10.1016/j.cell.2005.04.031

Dover, J., Schneider, J., Tawiah-Boateng, M. A., Wood, A., Dean, K., Johnston, M., & Shilatifard, A. (2002). Methylation of histone H3 by COMPASS requires ubiquitination of histone H2B by Rad6. *J Biol Chem*, *277*(32), 28368-28371. https://doi.org/10.1074/jbc.C200348200

Dowen, J. M., Fan, Z. P., Hnisz, D., Ren, G., Abraham, B. J., Zhang, L. N., Weintraub, A. S., Schujiers, J., Lee, T. I., Zhao, K., & Young, R. A. (2014). Control of cell identity genes occurs in insulated neighborhoods in mammalian chromosomes. *Cell*, *159*(2), 374-387. https://doi.org/10.1016/j.cell.2014.09.030

Du, K. L., Chen, M., Li, J., Lepore, J. J., Mericko, P., & Parmacek, M. S. (2004). Megakaryoblastic leukemia factor-1 transduces cytoskeletal signals and induces smooth muscle cell differentiation from undifferentiated embryonic stem cells. *J Biol Chem*, *279*(17), 17578-17586. https://doi.org/10.1074/jbc.M400961200

Eberhardy, S. R., & Farnham, P. J. (2001). c-Myc mediates activation of the cad promoter via a post-RNA polymerase II recruitment mechanism. *J Biol Chem*, *276*(51), 48562-48571. https://doi.org/10.1074/jbc.M109014200

Eberhardy, S. R., & Farnham, P. J. (2002). Myc recruits P-TEFb to mediate the final step in the transcriptional activation of the cad promoter. *J Biol Chem*, *277*(42), 40156-40162. https://doi.org/10.1074/jbc.M207441200

Egloff, S., O'Reilly, D., Chapman, R. D., Taylor, A., Tanzhaus, K., Pitts, L., Eick, D., & Murphy, S. (2007). Serine-7 of the RNA polymerase II CTD is specifically required for snRNA gene expression. *Science*, *318*(5857), 1777-1779. https://doi.org/10.1126/science.1145989

Egloff, S., O'Reilly, D., & Murphy, S. (2008). Expression of human snRNA genes from beginning to end. *Biochem Soc Trans*, *36*(Pt 4), 590-594. https://doi.org/10.1042/BST0360590

Egloff, S., Szczepaniak, S. A., Dienstbier, M., Taylor, A., Knight, S., & Murphy, S. (2010). The integrator complex recognizes a new double mark on the RNA polymerase II carboxyl-terminal domain. *J Biol Chem*, *285*(27), 20564-20569. https://doi.org/10.1074/jbc.M110.132530

Egloff, S., Zaborowska, J., Laitem, C., Kiss, T., & Murphy, S. (2012). Ser7 phosphorylation of the CTD recruits the RPAP2 Ser5 phosphatase to snRNA genes. *Mol Cell*, *45*(1), 111-122. https://doi.org/10.1016/j.molcel.2011.11.006

Ehara, H., Yokoyama, T., Shigematsu, H., Yokoyama, S., Shirouzu, M., & Sekine, S. I. (2017). Structure of the complete elongation complex of RNA polymerase II with basal factors. *Science*, *357*(6354), 921-924. https://doi.org/10.1126/science.aan8552

Eick, D., & Geyer, M. (2013). The RNA polymerase II carboxy-terminal domain (CTD) code. *Chem Rev*, *113*(11), 8456-8490. https://doi.org/10.1021/cr400071f

Eifler, T. T., Shao, W., Bartholomeeusen, K., Fujinaga, K., Jäger, S., Johnson, J. R., Luo, Z., Krogan, N. J., & Peterlin, B. M. (2015). Cyclin-dependent kinase 12 increases 3' end processing of growth factor-induced c-FOS transcripts. *Mol Cell Biol*, *35*(2), 468-478. https://doi.org/10.1128/MCB.01157-14

Elowitz, M. B., Levine, A. J., Siggia, E. D., & Swain, P. S. (2002). Stochastic gene expression in a single cell. *Science*, *297*(5584), 1183-1186. https://doi.org/10.1126/science.1070919

Esnault, C., Stewart, A., Gualdrini, F., East, P., Horswell, S., Matthews, N., & Treisman, R. (2014). Rho-actin signaling to the MRTF coactivators dominates the immediate transcriptional response to serum in fibroblasts. *Genes Dev*, *28*(9), 943-958. https://doi.org/10.1101/gad.239327.114

Eyboulet, F., Cibot, C., Eychenne, T., Neil, H., Alibert, O., Werner, M., & Soutourina, J. (2013). Mediator links transcription and DNA repair by facilitating Rad2/XPG recruitment. *Genes Dev*, *27*(23), 2549-2562. https://doi.org/10.1101/gad.225813.113

Eyboulet, F., Wydau-Dematteis, S., Eychenne, T., Alibert, O., Neil, H., Boschiero, C., Nevers, M. C., Volland, H., Cornu, D., Redeker, V., Werner, M., & Soutourina, J. (2015). Mediator independently orchestrates multiple steps of preinitiation complex assembly in vivo. *Nucleic Acids Res*, *43*(19), 9214-9231. https://doi.org/10.1093/nar/gkv782

Falk, S., Finogenova, K., Melko, M., Benda, C., Lykke-Andersen, S., Jensen, T. H., & Conti, E. (2016). Structure of the RBM7-ZCCHC8 core of the NEXT complex reveals connections to splicing factors. *Nat Commun*, *7*, 13573. https://doi.org/10.1038/ncomms13573

Fan, J., Kuai, B., Wu, G., Wu, X., Chi, B., Wang, L., Wang, K., Shi, Z., Zhang, H., Chen, S., He, Z., Wang, S., Zhou, Z., Li, G., & Cheng, H. (2017). Exosome cofactor hMTR4 competes with export adaptor ALYREF to ensure balanced nuclear RNA pools for degradation and export. *EMBO J*, *36*(19), 2870-2886. https://doi.org/10.15252/embj.201696139

Fang, M., Xie, H., Dougan, S. K., Ploegh, H., & van Oudenaarden, A. (2013). Stochastic cytokine expression induces mixed T helper cell States. *PLoS Biol*, *11*(7), e1001618. https://doi.org/10.1371/journal.pbio.1001618

Feng, Q., Wang, H., Ng, H. H., Erdjument-Bromage, H., Tempst, P., Struhl, K., & Zhang, Y. (2002). Methylation of H3-lysine 79 is mediated by a new family of HMTases without a SET domain. *Curr Biol*, *12*(12), 1052-1058. https://doi.org/10.1016/s0960-9822(02)00901-6

Fish, R. N., & Kane, C. M. (2002). Promoting elongation with transcript cleavage stimulatory factors. *Biochim Biophys Acta*, *1577*(2), 287-307. https://doi.org/10.1016/s0167-4781(02)00459-1

Fitz, J., Neumann, T., & Pavri, R. (2018). Regulation of RNA polymerase II processivity by Spt5 is restricted to a narrow window during elongation. *EMBO J*, *37*(8). https://doi.org/10.15252/embj.201797965

Flaherty, S. M., Fortes, P., Izaurralde, E., Mattaj, I. W., & Gilmartin, G. M. (1997). Participation of the nuclear cap binding complex in pre-mRNA 3' processing. *Proc Natl Acad Sci U S A*, *94*(22), 11893-11898. https://doi.org/10.1073/pnas.94.22.11893

Flynn, R. A., Almada, A. E., Zamudio, J. R., & Sharp, P. A. (2011). Antisense RNA polymerase II divergent transcripts are P-TEFb dependent and substrates for the RNA exosome. *Proc Natl Acad Sci U S A*, *108*(26), 10460-10465. https://doi.org/10.1073/pnas.1106630108

Fong, N., & Bentley, D. L. (2001). Capping, splicing, and 3' processing are independently stimulated by RNA polymerase II: different functions for different segments of the CTD. *Genes Dev*, *15*(14), 1783-1795. https://doi.org/10.1101/gad.889101

Fong, N., Brannan, K., Erickson, B., Kim, H., Cortazar, M. A., Sheridan, R. M., Nguyen, T., Karp, S., & Bentley, D. L. (2015). Effects of Transcription Elongation Rate and Xrn2 Exonuclease Activity on RNA Polymerase II Termination Suggest Widespread Kinetic Competition. *Mol Cell*, *60*(2), 256-267. https://doi.org/10.1016/j.molcel.2015.09.026

Foster, C. T., Gualdrini, F., & Treisman, R. (2017). Mutual dependence of the MRTF-SRF and YAP-TEAD pathways in cancer-associated fibroblasts is indirect and mediated by cytoskeletal dynamics. *Genes Dev*, *31*(23-24), 2361-2375. https://doi.org/10.1101/gad.304501.117

Franco, C. A., Blanc, J., Parlakian, A., Blanco, R., Aspalter, I. M., Kazakova, N., Diguet, N., Mylonas, E., Gao-Li, J., Vaahtokari, A., Penard-Lacronique, V., Fruttiger, M., Rosewell, I., Mericskay, M., Gerhardt, H., & Li, Z. (2013). SRF selectively controls tip cell invasive behavior in angiogenesis. *Development*, *140*(11), 2321-2333. https://doi.org/10.1242/dev.091074

Fresco, L. D., & Buratowski, S. (1996). Conditional mutants of the yeast mRNA capping enzyme show that the cap enhances, but is not required for, mRNA splicing. *RNA*, *2*(6), 584-596.

Fuchs, G., Hollander, D., Voichek, Y., Ast, G., & Oren, M. (2014). Cotranscriptional histone H2B monoubiquitylation is tightly coupled with RNA polymerase II elongation rate. *Genome Res*, *24*(10), 1572-1583. https://doi.org/10.1101/gr.176487.114

Fujinaga, K., Irwin, D., Huang, Y., Taube, R., Kurosu, T., & Peterlin, B. M. (2004). Dynamics of human immunodeficiency virus transcription: P-TEFb phosphorylates RD and dissociates negative effectors from the transactivation response element. *Mol Cell Biol*, *24*(2), 787-795. https://doi.org/10.1128/mcb.24.2.787-795.2004

Galbraith, M. D., Bender, H., & Espinosa, J. M. (2019). Therapeutic targeting of transcriptional cyclin-dependent kinases. *Transcription*, *10*(2), 118-136. https://doi.org/10.1080/21541264.2018.1539615

Gates, L. A., Foulds, C. E., & O'Malley, B. W. (2017). Histone Marks in the 'Driver's Seat': Functional Roles in Steering the Transcription Cycle. *Trends Biochem Sci*, *42*(12), 977-989. https://doi.org/10.1016/j.tibs.2017.10.004

Gau, D., Veon, W., Capasso, T. L., Bottcher, R., Shroff, S., Roman, B. L., & Roy, P. (2017). Pharmacological intervention of MKL/SRF signaling by CCG-1423

impedes endothelial cell migration and angiogenesis. *Angiogenesis*, *20*(4), 663-672. https://doi.org/10.1007/s10456-017-9560-y

Gelbart, M. E., Larschan, E., Peng, S., Park, P. J., & Kuroda, M. I. (2009). Drosophila MSL complex globally acetylates H4K16 on the male X chromosome for dosage compensation. *Nat Struct Mol Biol*, *16*(8), 825-832. https://doi.org/10.1038/nsmb.1644

Geneste, O., Copeland, J. W., & Treisman, R. (2002). LIM kinase and Diaphanous cooperate to regulate serum response factor and actin dynamics. *J Cell Biol*, *157*(5), 831-838. https://doi.org/10.1083/jcb.200203126

Gerlach, P., Schuller, J. M., Bonneau, F., Basquin, J., Reichelt, P., Falk, S., & Conti, E. (2018). Distinct and evolutionary conserved structural features of the human nuclear exosome complex. *Elife*, *7*. https://doi.org/10.7554/eLife.38686

Ghosh, A., Shuman, S., & Lima, C. D. (2008). The structure of Fcp1, an essential RNA polymerase II CTD phosphatase. *Mol Cell*, *32*(4), 478-490. https://doi.org/10.1016/j.molcel.2008.09.021

Giacometti, S., Benbahouche, N. E. H., Domanski, M., Robert, M. C., Meola, N., Lubas, M., Bukenborg, J., Andersen, J. S., Schulze, W. M., Verheggen, C., Kudla, G., Jensen, T. H., & Bertrand, E. (2017). Mutually Exclusive CBC-Containing Complexes Contribute to RNA Fate. *Cell Rep*, *18*(11), 2635-2650. https://doi.org/10.1016/j.celrep.2017.02.046

Gibson, B. A., Zhang, Y., Jiang, H., Hussey, K. M., Shrimp, J. H., Lin, H., Schwede, F., Yu, Y., & Kraus, W. L. (2016). Chemical genetic discovery of PARP targets reveals a role for PARP-1 in transcription elongation. *Science*, *353*(6294), 45-50. https://doi.org/10.1126/science.aaf7865

Gilchrist, D. A., Dos Santos, G., Fargo, D. C., Xie, B., Gao, Y., Li, L., & Adelman, K. (2010). Pausing of RNA polymerase II disrupts DNA-specified nucleosome organization to enable precise gene regulation. *Cell*, *143*(4), 540-551. https://doi.org/10.1016/j.cell.2010.10.004

Gilchrist, D. A., Fromm, G., dos Santos, G., Pham, L. N., McDaniel, I. E., Burkholder, A., Fargo, D. C., & Adelman, K. (2012). Regulating the regulators: the pervasive effects of Pol II pausing on stimulus-responsive gene networks. *Genes Dev*, *26*(9), 933-944. https://doi.org/10.1101/gad.187781.112

Gilchrist, D. A., Nechaev, S., Lee, C., Ghosh, S. K., Collins, J. B., Li, L., Gilmour, D. S., & Adelman, K. (2008). NELF-mediated stalling of Pol II can enhance gene expression by blocking promoter-proximal nucleosome assembly. *Genes Dev*, *22*(14), 1921-1933. https://doi.org/10.1101/gad.1643208

Gilman, M. Z., Wilson, R. N., & Weinberg, R. A. (1986). Multiple protein-binding sites in the 5'-flanking region regulate c-fos expression. *Mol Cell Biol*, *6*(12), 4305-4316. https://doi.org/10.1128/mcb.6.12.4305

Gineitis, D., & Treisman, R. (2001). Differential usage of signal transduction pathways defines two types of serum response factor target gene. *J Biol Chem*, *276*(27), 24531-24539. https://doi.org/10.1074/jbc.M102678200

Glover-Cutter, K., Kim, S., Espinosa, J., & Bentley, D. L. (2008). RNA polymerase II pauses and associates with pre-mRNA processing factors at both ends of genes. *Nat Struct Mol Biol*, *15*(1), 71-78. https://doi.org/10.1038/nsmb1352

Glover-Cutter, K., Larochelle, S., Erickson, B., Zhang, C., Shokat, K., Fisher, R. P., & Bentley, D. L. (2009). TFIIH-associated Cdk7 kinase functions in phosphorylation of C-terminal domain Ser7 residues, promoter-proximal pausing, and termination by RNA polymerase II. *Mol Cell Biol*, *29*(20), 5455-5464. https://doi.org/10.1128/MCB.00637-09

Gomes, N. P., Bjerke, G., Llorente, B., Szostek, S. A., Emerson, B. M., & Espinosa, J. M. (2006). Gene-specific requirement for P-TEFb activity and RNA polymerase

II phosphorylation within the p53 transcriptional program. *Genes Dev*, *20*(5), 601-612. https://doi.org/10.1101/gad.1398206

Goodrich, J. A., & Tjian, R. (1994). Transcription factors IIE and IIH and ATP hydrolysis direct promoter clearance by RNA polymerase II. *Cell*, *77*(1), 145-156. https://doi.org/10.1016/0092-8674(94)90242-9

Gorski, S. A., Dundr, M., & Misteli, T. (2006). The road much traveled: trafficking in the cell nucleus. *Curr Opin Cell Biol*, *18*(3), 284-290. https://doi.org/10.1016/j.ceb.2006.03.002

Graham, R., & Gilman, M. (1991). Distinct protein targets for signals acting at the c-fos serum response element. *Science*, *251*(4990), 189-192. https://doi.org/10.1126/science.1898992

Greenberg, M. E., Siegfried, Z., & Ziff, E. B. (1987). Mutation of the c-fos gene dyad symmetry element inhibits serum inducibility of transcription in vivo and the nuclear regulatory factor binding in vitro. *Mol Cell Biol*, *7*(3), 1217-1225. https://doi.org/10.1128/mcb.7.3.1217

Greenleaf, A. L. (2019). Human CDK12 and CDK13, multi-tasking CTD kinases for the new millenium. *Transcription*, *10*(2), 91-110. https://doi.org/10.1080/21541264.2018.1535211

Greger, I. H., Demarchi, F., Giacca, M., & Proudfoot, N. J. (1998). Transcriptional interference perturbs the binding of Sp1 to the HIV-1 promoter. *Nucleic Acids Res*, *26*(5), 1294-1301. https://doi.org/10.1093/nar/26.5.1294

Greger, I. H., & Proudfoot, N. J. (1998). Poly(A) signals control both transcriptional termination and initiation between the tandem GAL10 and GAL7 genes of Saccharomyces cerevisiae. *EMBO J*, *17*(16), 4771-4779. https://doi.org/10.1093/emboj/17.16.4771

Gregersen, L. H., Mitter, R., & Svejstrup, J. Q. (2020). Using TT. *Nat Protoc*, *15*(2), 604-627. https://doi.org/10.1038/s41596-019-0262-3

Gregersen, L. H., Mitter, R., Ugalde, A. P., Nojima, T., Proudfoot, N. J., Agami, R., Stewart, A., & Svejstrup, J. Q. (2019). SCAF4 and SCAF8, mRNA Anti-Terminator Proteins. *Cell*, *177*(7), 1797-1813.e1718. https://doi.org/10.1016/j.cell.2019.04.038

Greimann, J. C., & Lima, C. D. (2008). Reconstitution of RNA exosomes from human and Saccharomyces cerevisiae cloning, expression, purification, and activity assays. *Methods Enzymol*, *448*, 185-210. https://doi.org/10.1016/S0076-6879(08)02610-4

Groeneweg, F. L., van Royen, M. E., Fenz, S., Keizer, V. I., Geverts, B., Prins, J., de Kloet, E. R., Houtsmuller, A. B., Schmidt, T. S., & Schaaf, M. J. (2014). Quantitation of glucocorticoid receptor DNA-binding dynamics by single-molecule microscopy and FRAP. *PLoS One*, *9*(3), e90532. https://doi.org/10.1371/journal.pone.0090532

Gromak, N., West, S., & Proudfoot, N. J. (2006). Pause sites promote transcriptional termination of mammalian RNA polymerase II. *Mol Cell Biol*, *26*(10), 3986-3996. https://doi.org/10.1128/MCB.26.10.3986-3996.2006

Gross, S., & Moore, C. (2001). Five subunits are required for reconstitution of the cleavage and polyadenylation activities of Saccharomyces cerevisiae cleavage factor I. *Proc Natl Acad Sci U S A*, *98*(11), 6080-6085. https://doi.org/10.1073/pnas.101046598

Gruber, J. J., Olejniczak, S. H., Yong, J., La Rocca, G., Dreyfuss, G., & Thompson, C. B. (2012). Ars2 promotes proper replication-dependent histone mRNA 3' end formation. *Mol Cell*, *45*(1), 87-98. https://doi.org/10.1016/j.molcel.2011.12.020

Gruber, J. J., Zatechka, D. S., Sabin, L. R., Yong, J., Lum, J. J., Kong, M., Zong, W. X., Zhang, Z., Lau, C. K., Rawlings, J., Cherry, S., Ihle, J. N., Dreyfuss, G., & Thompson, C. B. (2009). Ars2 links the nuclear cap-binding complex to RNA

interference and cell proliferation. *Cell*, *138*(2), 328-339. https://doi.org/10.1016/j.cell.2009.04.046

Gu, B., Eick, D., & Bensaude, O. (2013). CTD serine-2 plays a critical role in splicing and termination factor recruitment to RNA polymerase II in vivo. *Nucleic Acids Res*, *41*(3), 1591-1603. https://doi.org/10.1093/nar/gks1327

Gualdrini, F., Esnault, C., Horswell, S., Stewart, A., Matthews, N., & Treisman, R. (2016). SRF Co-factors Control the Balance between Cell Proliferation and Contractility. *Mol Cell*, *64*(6), 1048-1061. https://doi.org/10.1016/j.molcel.2016.10.016

Gudipati, R. K., Xu, Z., Lebreton, A., Séraphin, B., Steinmetz, L. M., Jacquier, A., & Libri, D. (2012). Extensive degradation of RNA precursors by the exosome in wild-type cells. *Mol Cell*, *48*(3), 409-421. https://doi.org/10.1016/j.molcel.2012.08.018

Guenther, M. G., Levine, S. S., Boyer, L. A., Jaenisch, R., & Young, R. A. (2007). A chromatin landmark and transcription initiation at most promoters in human cells. *Cell*, *130*(1), 77-88. https://doi.org/10.1016/j.cell.2007.05.042

Guettler, S., Vartiainen, M. K., Miralles, F., Larijani, B., & Treisman, R. (2008). RPEL motifs link the serum response factor cofactor MAL but not myocardin to Rho signaling via actin binding. *Mol Cell Biol*, *28*(2), 732-742. https://doi.org/10.1128/mcb.01623-07

Guo, R., Zheng, L., Park, J. W., Lv, R., Chen, H., Jiao, F., Xu, W., Mu, S., Wen, H., Qiu, J., Wang, Z., Yang, P., Wu, F., Hui, J., Fu, X., Shi, X., Shi, Y. G., Xing, Y., Lan, F., & Shi, Y. (2014). BS69/ZMYND11 reads and connects histone H3.3 lysine 36 trimethylation-decorated chromatin to regulated pre-mRNA processing. *Mol Cell*, *56*(2), 298-310. https://doi.org/10.1016/j.molcel.2014.08.022

Haak, A. J., Appleton, K. M., Lisabeth, E. M., Misek, S. A., Ji, Y., Wade, S. M., Bell, J. L., Rockwell, C. E., Airik, M., Krook, M. A., Larsen, S. D., Verhaegen, M., Lawlor, E. R., & Neubig, R. R. (2017). Pharmacological Inhibition of Myocardin-related Transcription Factor Pathway Blocks Lung Metastases of RhoC-Overexpressing Melanoma. *Mol Cancer Ther*, *16*(1), 193-204. https://doi.org/10.1158/1535-7163.MCT-16-0482

Hager, G. L., McNally, J. G., & Misteli, T. (2009). Transcription dynamics. *Mol Cell*, *35*(6), 741-753. https://doi.org/10.1016/j.molcel.2009.09.005

Hallais, M., Pontvianne, F., Andersen, P. R., Clerici, M., Lener, D., Benbahouche, N. I. H., Gostan, T., Vandermoere, F., Robert, M. C., Cusack, S., Verheggen, C., Jensen, T. H., & Bertrand, E. (2013). CBC-ARS2 stimulates 3'-end maturation of multiple RNA families and favors cap-proximal processing. *Nat Struct Mol Biol*, *20*(12), 1358-1366. https://doi.org/10.1038/nsmb.2720

Hargreaves, D. C., Horng, T., & Medzhitov, R. (2009). Control of inducible gene expression by signal-dependent transcriptional elongation. *Cell*, *138*(1), 129-145. https://doi.org/10.1016/j.cell.2009.05.047

Harlen, K. M., Trotta, K. L., Smith, E. E., Mosaheb, M. M., Fuchs, S. M., & Churchman, L. S. (2016). Comprehensive RNA Polymerase II Interactomes Reveal Distinct and Varied Roles for Each Phospho-CTD Residue. *Cell Rep*, *15*(10), 2147-2158. https://doi.org/10.1016/j.celrep.2016.05.010

Hartzog, G. A., Wada, T., Handa, H., & Winston, F. (1998). Evidence that Spt4, Spt5, and Spt6 control transcription elongation by RNA polymerase II in Saccharomyces cerevisiae. *Genes Dev*, *12*(3), 357-369. https://doi.org/10.1101/gad.12.3.357

Hassler, M., & Richmond, T. J. (2001). The B-box dominates SAP-1-SRF interactions in the structure of the ternary complex. *EMBO J*, *20*(12), 3018-3028. https://doi.org/10.1093/emboj/20.12.3018

Hausmann, S., & Shuman, S. (2002). Characterization of the CTD phosphatase Fcp1 from fission yeast. Preferential dephosphorylation of serine 2 versus serine 5. *J Biol Chem*, *277*(24), 21213-21220. https://doi.org/10.1074/jbc.M202056200

Hazelbaker, D. Z., Marquardt, S., Wlotzka, W., & Buratowski, S. (2013). Kinetic competition between RNA Polymerase II and Sen1-dependent transcription termination. *Mol Cell*, *49*(1), 55-66. https://doi.org/10.1016/j.molcel.2012.10.014

He, N., Chan, C. K., Sobhian, B., Chou, S., Xue, Y., Liu, M., Alber, T., Benkirane, M., & Zhou, Q. (2011). Human Polymerase-Associated Factor complex (PAFc) connects the Super Elongation Complex (SEC) to RNA polymerase II on chromatin. *Proc Natl Acad Sci U S A*, *108*(36), E636-645. https://doi.org/10.1073/pnas.1107107108

Heidemann, M., Hintermair, C., Voß, K., & Eick, D. (2013). Dynamic phosphorylation patterns of RNA polymerase II CTD during transcription. *Biochim Biophys Acta*, *1829*(1), 55-62. https://doi.org/10.1016/j.bbagrm.2012.08.013

Hengartner, C. J., Myer, V. E., Liao, S. M., Wilson, C. J., Koh, S. S., & Young, R. A. (1998). Temporal regulation of RNA polymerase II by Srb10 and Kin28 cyclin-dependent kinases. *Mol Cell*, *2*(1), 43-53. https://doi.org/10.1016/s1097-2765(00)80112-4

Henriques, T., Scruggs, B. S., Inouye, M. O., Muse, G. W., Williams, L. H., Burkholder, A. B., Lavender, C. A., Fargo, D. C., & Adelman, K. (2018). Widespread transcriptional pausing and elongation control at enhancers. *Genes Dev*, *32*(1), 26-41. https://doi.org/10.1101/gad.309351.117

Herzel, L., Ottoz, D. S. M., Alpert, T., & Neugebauer, K. M. (2017). Splicing and transcription touch base: co-transcriptional spliceosome assembly and function. *Nat Rev Mol Cell Biol*, *18*(10), 637-650. https://doi.org/10.1038/nrm.2017.63

Hill, C. S., Marais, R., John, S., Wynne, J., Dalton, S., & Treisman, R. (1993). Functional analysis of a growth factor-responsive transcription factor complex. *Cell*, *73*(2), 395-406.

Hill, C. S., Wynne, J., & Treisman, R. (1994). Serum-regulated transcription by serum response factor (SRF): a novel role for the DNA binding domain. *EMBO J*, *13*(22), 5421-5432.

Hill, C. S., Wynne, J., & Treisman, R. (1995). The Rho family GTPases RhoA, Rac1, and CDC42Hs regulate transcriptional activation by SRF. *Cell*, *81*(7), 1159-1170.

Hilleren, P., McCarthy, T., Rosbash, M., Parker, R., & Jensen, T. H. (2001). Quality control of mRNA 3'-end processing is linked to the nuclear exosome. *Nature*, *413*(6855), 538-542. https://doi.org/10.1038/35097110

Hinojosa, L. S., Holst, M., Baarlink, C., & Grosse, R. (2017). MRTF transcription and Ezrin-dependent plasma membrane blebbing are required for entotic invasion. *J Cell Biol*, *216*(10), 3087-3095. https://doi.org/10.1083/jcb.201702010

Hintermair, C., Heidemann, M., Koch, F., Descostes, N., Gut, M., Gut, I., Fenouil, R., Ferrier, P., Flatley, A., Kremmer, E., Chapman, R. D., Andrau, J. C., & Eick, D. (2012). Threonine-4 of mammalian RNA polymerase II CTD is targeted by Polo-like kinase 3 and required for transcriptional elongation. *EMBO J*, *31*(12), 2784-2797. https://doi.org/10.1038/emboj.2012.123

Hintermair, C., Voß, K., Forné, I., Heidemann, M., Flatley, A., Kremmer, E., Imhof, A., & Eick, D. (2016). Specific threonine-4 phosphorylation and function of RNA polymerase II CTD during M phase progression. *Sci Rep*, *6*, 27401. https://doi.org/10.1038/srep27401

Hipp, L., Beer, J., Kuchler, O., Reisser, M., Sinske, D., Michaelis, J., Gebhardt, J. C. M., & Knöll, B. (2019). Single-molecule imaging of the transcription factor SRF reveals prolonged chromatin-binding kinetics upon cell stimulation. *Proc Natl Acad Sci U S A*, *116*(3), 880-889. https://doi.org/10.1073/pnas.1812734116

Hipskind, R. A., Rao, V. N., Mueller, C. G., Reddy, E. S., & Nordheim, A. (1991). Ets-related protein Elk-1 is homologous to the c-fos regulatory factor p62TCF. *Nature*, *354*(6354), 531-534. https://doi.org/10.1038/354531a0

Hirano, H., & Matsuura, Y. (2011). Sensing actin dynamics: structural basis for G-actin-sensitive nuclear import of MAL. *Biochem Biophys Res Commun*, *414*(2), 373-378. https://doi.org/10.1016/j.bbrc.2011.09.079

Hirose, Y., & Manley, J. L. (1998). RNA polymerase II is an essential mRNA polyadenylation factor. *Nature*, *395*(6697), 93-96. https://doi.org/10.1038/25786

Hirose, Y., & Manley, J. L. (2000). RNA polymerase II and the integration of nuclear events. *Genes Dev*, *14*(12), 1415-1429.

Hirose, Y., Tacke, R., & Manley, J. L. (1999). Phosphorylated RNA polymerase II stimulates pre-mRNA splicing. *Genes Dev*, *13*(10), 1234-1239. https://doi.org/10.1101/gad.13.10.1234

Ho, C. K., & Shuman, S. (1999). Distinct roles for CTD Ser-2 and Ser-5 phosphorylation in the recruitment and allosteric activation of mammalian mRNA capping enzyme. *Mol Cell*, *3*(3), 405-411. https://doi.org/10.1016/s1097-2765(00)80468-2

Hobson, D. J., Wei, W., Steinmetz, L. M., & Svejstrup, J. Q. (2012). RNA polymerase II collision interrupts convergent transcription. *Mol Cell*, *48*(3), 365-374. https://doi.org/10.1016/j.molcel.2012.08.027

Holz-Schietinger, C., Matje, D. M., & Reich, N. O. (2012). Mutations in DNA methyltransferase (DNMT3A) observed in acute myeloid leukemia patients disrupt processive methylation. *J Biol Chem*, *287*(37), 30941-30951. https://doi.org/10.1074/jbc.M112.366625

Hosoda, N., Kim, Y. K., Lejeune, F., & Maquat, L. E. (2005). CBP80 promotes interaction of Upf1 with Upf2 during nonsense-mediated mRNA decay in mammalian cells. *Nat Struct Mol Biol*, *12*(10), 893-901. https://doi.org/10.1038/nsmb995

Hottiger, M. O. (2015). Nuclear ADP-Ribosylation and Its Role in Chromatin Plasticity, Cell Differentiation, and Epigenetics. *Annu Rev Biochem*, *84*, 227-263. https://doi.org/10.1146/annurev-biochem-060614-034506

Howe, K. J., Kane, C. M., & Ares, M. (2003). Perturbation of transcription elongation influences the fidelity of internal exon inclusion in Saccharomyces cerevisiae. *RNA*, *9*(8), 993-1006. https://doi.org/10.1261/rna.5390803

Hrossova, D., Sikorsky, T., Potesil, D., Bartosovic, M., Pasulka, J., Zdrahal, Z., Stefl, R., & Vanacova, S. (2015). RBM7 subunit of the NEXT complex binds U-rich sequences and targets 3'-end extended forms of snRNAs. *Nucleic Acids Res*, *43*(8), 4236-4248. https://doi.org/10.1093/nar/gkv240

Hsin, J. P., Li, W., Hoque, M., Tian, B., & Manley, J. L. (2014). RNAP II CTD tyrosine 1 performs diverse functions in vertebrate cells. *Elife*, *3*, e02112. https://doi.org/10.7554/eLife.02112

Hsin, J. P., Sheth, A., & Manley, J. L. (2011). RNAP II CTD phosphorylated on threonine-4 is required for histone mRNA 3' end processing. *Science*, *334*(6056), 683-686. https://doi.org/10.1126/science.1206034

Hsin, J. P., Xiang, K., & Manley, J. L. (2014). Function and control of RNA polymerase II C-terminal domain phosphorylation in vertebrate transcription and RNA processing. *Mol Cell Biol*, *34*(13), 2488-2498. https://doi.org/10.1128/MCB.00181-14

Hsu, C., Scherrer, S., Buetti-Dinh, A., Ratna, P., Pizzolato, J., Jaquet, V., & Becskei, A. (2012). Stochastic signalling rewires the interaction map of a multiple feedback network during yeast evolution. *Nat Commun*, *3*, 682. https://doi.org/10.1038/ncomms1687

Huang, B., Yang, X. D., Zhou, M. M., Ozato, K., & Chen, L. F. (2009). Brd4 coactivates transcriptional activation of NF-kappaB via specific binding to acetylated RelA. *Mol Cell Biol*, *29*(5), 1375-1387. https://doi.org/10.1128/MCB.01365-08

Huertas, P., & Aguilera, A. (2003). Cotranscriptionally formed DNA:RNA hybrids mediate transcription elongation impairment and transcription-associated recombination. *Mol Cell*, *12*(3), 711-721. https://doi.org/10.1016/j.molcel.2003.08.010

Huet, G., Rajakylä, E. K., Viita, T., Skarp, K. P., Crivaro, M., Dopie, J., & Vartiainen, M. K. (2013). Actin-regulated feedback loop based on Phactr4, PP1 and cofilin maintains the actin monomer pool. *J Cell Sci*, *126*(Pt 2), 497-507. https://doi.org/10.1242/jcs.113241

Iasillo, C., Schmid, M., Yahia, Y., Maqbool, M. A., Descostes, N., Karadoulama, E., Bertrand, E., Andrau, J. C., & Jensen, T. H. (2017). ARS2 is a general suppressor of pervasive transcription. *Nucleic Acids Res*, *45*(17), 10229-10241. https://doi.org/10.1093/nar/gkx647

Inoue, K., Ohno, M., Sakamoto, H., & Shimura, Y. (1989). Effect of the cap structure on pre-mRNA splicing in Xenopus oocyte nuclei. *Genes Dev*, *3*(9), 1472-1479. https://doi.org/10.1101/gad.3.9.1472

Ivanov, D., Kwak, Y. T., Guo, J., & Gaynor, R. B. (2000). Domains in the SPT5 protein that modulate its transcriptional regulatory properties. *Mol Cell Biol*, *20*(9), 2970-2983. https://doi.org/10.1128/mcb.20.9.2970-2983.2000

Izaurralde, E., Lewis, J., McGuigan, C., Jankowska, M., Darzynkiewicz, E., & Mattaj, I. W. (1994). A nuclear cap binding protein complex involved in pre-mRNA splicing. *Cell*, *78*(4), 657-668. https://doi.org/10.1016/0092-8674(94)90530-4

Jarmolowski, A., Boelens, W. C., Izaurralde, E., & Mattaj, I. W. (1994). Nuclear export of different classes of RNA is mediated by specific factors. *J Cell Biol*, *124*(5), 627-635. https://doi.org/10.1083/jcb.124.5.627

Jasiak, A. J., Armache, K. J., Martens, B., Jansen, R. P., & Cramer, P. (2006). Structural biology of RNA polymerase III: subcomplex C17/25 X-ray structure and 11 subunit enzyme model. *Mol Cell*, *23*(1), 71-81. https://doi.org/10.1016/j.molcel.2006.05.013

Jelinic, P., Pellegrino, J., & David, G. (2011). A novel mammalian complex containing Sin3B mitigates histone acetylation and RNA polymerase II progression within transcribed loci. *Mol Cell Biol*, *31*(1), 54-62. https://doi.org/10.1128/MCB.00840-10

Jensen, T. H., Boulay, J., Rosbash, M., & Libri, D. (2001). The DECD box putative ATPase Sub2p is an early mRNA export factor. *Curr Biol*, *11*(21), 1711-1715. https://doi.org/10.1016/s0960-9822(01)00529-2

Jeronimo, C., & Robert, F. (2017). The Mediator Complex: At the Nexus of RNA Polymerase II Transcription. *Trends Cell Biol*, *27*(10), 765-783. https://doi.org/10.1016/j.tcb.2017.07.001

Jin, C., Zang, C., Wei, G., Cui, K., Peng, W., Zhao, K., & Felsenfeld, G. (2009). H3.3/H2A.Z double variant-containing nucleosomes mark 'nucleosome-free regions' of active promoters and other regulatory regions. *Nat Genet*, *41*(8), 941-945. https://doi.org/10.1038/ng.409

Johnson, S. A., Cubberley, G., & Bentley, D. L. (2009). Cotranscriptional recruitment of the mRNA export factor Yra1 by direct interaction with the 3' end processing factor Pcf11. *Mol Cell*, *33*(2), 215-226. https://doi.org/10.1016/j.molcel.2008.12.007

Johnson, S. J., & Jackson, R. N. (2013). Ski2-like RNA helicase structures: common themes and complex assemblies. *RNA Biol*, *10*(1), 33-43. https://doi.org/10.4161/rna.22101

Jonkers, I., Kwak, H., & Lis, J. T. (2014). Genome-wide dynamics of Pol II elongation and its interplay with promoter proximal pausing, chromatin, and exons. *Elife*, *3*, e02407. https://doi.org/10.7554/eLife.02407

Jove, R., & Manley, J. L. (1984). In vitro transcription from the adenovirus 2 major late promoter utilizing templates truncated at promoter-proximal sites. *J Biol Chem*, *259*(13), 8513-8521.

Kagey, M. H., Newman, J. J., Bilodeau, S., Zhan, Y., Orlando, D. A., van Berkum, N. L., Ebmeier, C. C., Goossens, J., Rahl, P. B., Levine, S. S., Taatjes, D. J., Dekker, J., & Young, R. A. (2010). Mediator and cohesin connect gene expression and chromatin architecture. *Nature*, *467*(7314), 430-435. https://doi.org/10.1038/nature09380

Kamenski, T., Heilmeier, S., Meinhart, A., & Cramer, P. (2004). Structure and mechanism of RNA polymerase II CTD phosphatases. *Mol Cell*, *15*(3), 399-407. https://doi.org/10.1016/j.molcel.2004.06.035

Kamieniarz-Gdula, K., Gdula, M. R., Panser, K., Nojima, T., Monks, J., Wiśniewski, J. R., Riepsaame, J., Brockdorff, N., Pauli, A., & Proudfoot, N. J. (2019). Selective Roles of Vertebrate PCF11 in Premature and Full-Length Transcript Termination. *Mol Cell*, *74*(1), 158-172.e159. https://doi.org/10.1016/j.molcel.2019.01.027

Kamieniarz-Gdula, K., & Proudfoot, N. J. (2019). Transcriptional Control by Premature Termination: A Forgotten Mechanism. *Trends Genet*, *35*(8), 553-564. https://doi.org/10.1016/j.tig.2019.05.005

Kanin, E. I., Kipp, R. T., Kung, C., Slattery, M., Viale, A., Hahn, S., Shokat, K. M., & Ansari, A. Z. (2007). Chemical inhibition of the TFIIH-associated kinase Cdk7/Kin28 does not impair global mRNA synthesis. *Proc Natl Acad Sci U S A*, *104*(14), 5812-5817. https://doi.org/10.1073/pnas.0611505104

Kao, C. F., Hillyer, C., Tsukuda, T., Henry, K., Berger, S., & Osley, M. A. (2004). Rad6 plays a role in transcriptional activation through ubiquitylation of histone H2B. *Genes Dev*, *18*(2), 184-195. https://doi.org/10.1101/gad.1149604

Katan-Khaykovich, Y., & Struhl, K. (2002). Dynamics of global histone acetylation and deacetylation in vivo: rapid restoration of normal histone acetylation status upon removal of activators and repressors. *Genes Dev*, *16*(6), 743-752. https://doi.org/10.1101/gad.967302

Kettenberger, H., Armache, K. J., & Cramer, P. (2004). Complete RNA polymerase II elongation complex structure and its interactions with NTP and TFIIS. *Mol Cell*, *16*(6), 955-965. https://doi.org/10.1016/j.molcel.2004.11.040

Khodor, Y. L., Rodriguez, J., Abruzzi, K. C., Tang, C. H., Marr, M. T., & Rosbash, M. (2011). Nascent-seq indicates widespread cotranscriptional pre-mRNA splicing in Drosophila. *Genes Dev*, *25*(23), 2502-2512. https://doi.org/10.1101/gad.178962.111

Kilchert, C., Wittmann, S., & Vasiljeva, L. (2016). The regulation and functions of the nuclear RNA exosome complex. *Nat Rev Mol Cell Biol*, *17*(4), 227-239. https://doi.org/10.1038/nrm.2015.15

Kim, J., Guermah, M., McGinty, R. K., Lee, J. S., Tang, Z., Milne, T. A., Shilatifard, A., Muir, T. W., & Roeder, R. G. (2009). RAD6-Mediated transcription-coupled H2B ubiquitylation directly stimulates H3K4 methylation in human cells. *Cell*, *137*(3), 459-471. https://doi.org/10.1016/j.cell.2009.02.027

Kim, J., Guermah, M., & Roeder, R. G. (2010). The human PAF1 complex acts in chromatin transcription elongation both independently and cooperatively with SII/TFIIS. *Cell*, *140*(4), 491-503. https://doi.org/10.1016/j.cell.2009.12.050

Kim, J. B., & Sharp, P. A. (2001). Positive transcription elongation factor B phosphorylates hSPT5 and RNA polymerase II carboxyl-terminal domain

independently of cyclin-dependent kinase-activating kinase. *J Biol Chem*, *276*(15), 12317-12323. https://doi.org/10.1074/jbc.M010908200

Kim, K. M., Cho, H., Choi, K., Kim, J., Kim, B. W., Ko, Y. G., Jang, S. K., & Kim, Y. K. (2009). A new MIF4G domain-containing protein, CTIF, directs nuclear cap-binding protein CBP80/20-dependent translation. *Genes Dev*, *23*(17), 2033-2045. https://doi.org/10.1101/gad.1823409

Kim, M., Krogan, N. J., Vasiljeva, L., Rando, O. J., Nedea, E., Greenblatt, J. F., & Buratowski, S. (2004). The yeast Rat1 exonuclease promotes transcription termination by RNA polymerase II. *Nature*, *432*(7016), 517-522. https://doi.org/10.1038/nature03041

Kim, T. K., Ebright, R. H., & Reinberg, D. (2000). Mechanism of ATP-dependent promoter melting by transcription factor IIH. *Science*, *288*(5470), 1418-1422. https://doi.org/10.1126/science.288.5470.1418

Kim, W. Y., & Dahmus, M. E. (1986). Immunochemical analysis of mammalian RNA polymerase II subspecies. Stability and relative in vivo concentration. *J Biol Chem*, *261*(30), 14219-14225.

Kim, Y. K., Bourgeois, C. F., Isel, C., Churcher, M. J., & Karn, J. (2002). Phosphorylation of the RNA polymerase II carboxyl-terminal domain by CDK9 is directly responsible for human immunodeficiency virus type 1 Tat-activated transcriptional elongation. *Mol Cell Biol*, *22*(13), 4622-4637. https://doi.org/10.1128/mcb.22.13.4622-4637.2002

Kiriyama, M., Kobayashi, Y., Saito, M., Ishikawa, F., & Yonehara, S. (2009). Interaction of FLASH with arsenite resistance protein 2 is involved in cell cycle progression at S phase. *Mol Cell Biol*, *29*(17), 4729-4741. https://doi.org/10.1128/MCB.00289-09

Kiseleva, E., Drummond, S. P., Goldberg, M. W., Rutherford, S. A., Allen, T. D., & Wilson, K. L. (2004). Actin- and protein-4.1-containing filaments link nuclear pore complexes to subnuclear organelles in Xenopus oocyte nuclei. *J Cell Sci*, *117*(Pt 12), 2481-2490. https://doi.org/10.1242/jcs.01098

Kizer, K. O., Phatnani, H. P., Shibata, Y., Hall, H., Greenleaf, A. L., & Strahl, B. D. (2005). A novel domain in Set2 mediates RNA polymerase II interaction and couples histone H3 K36 methylation with transcript elongation. *Mol Cell Biol*, *25*(8), 3305-3316. https://doi.org/10.1128/MCB.25.8.3305-3316.2005

Knöll, B., Kretz, O., Fiedler, C., Alberti, S., Schütz, G., Frotscher, M., & Nordheim, A. (2006). Serum response factor controls neuronal circuit assembly in the hippocampus. *Nat Neurosci*, *9*(2), 195-204. https://doi.org/10.1038/nn1627

Kobor, M. S., Venkatasubrahmanyam, S., Meneghini, M. D., Gin, J. W., Jennings, J. L., Link, A. J., Madhani, H. D., & Rine, J. (2004). A protein complex containing the conserved Swi2/Snf2-related ATPase Swr1p deposits histone variant H2A.Z into euchromatin. *PLoS Biol*, *2*(5), E131. https://doi.org/10.1371/journal.pbio.0020131

Kokai, E., Beck, H., Weissbach, J., Arnold, F., Sinske, D., Sebert, U., Gaiselmann, G., Schmidt, V., Walther, P., Münch, J., Posern, G., & Knöll, B. (2014). Analysis of nuclear actin by overexpression of wild-type and actin mutant proteins. *Histochem Cell Biol*, *141*(2), 123-135. https://doi.org/10.1007/s00418-013-1151-4

Komarnitsky, P., Cho, E. J., & Buratowski, S. (2000). Different phosphorylated forms of RNA polymerase II and associated mRNA processing factors during transcription. *Genes Dev*, *14*(19), 2452-2460. https://doi.org/10.1101/gad.824700

Konarska, M. M., Padgett, R. A., & Sharp, P. A. (1984). Recognition of cap structure in splicing in vitro of mRNA precursors. *Cell*, *38*(3), 731-736. https://doi.org/10.1016/0092-8674(84)90268-x

Kortenjann, M., Thomae, O., & Shaw, P. E. (1994). Inhibition of v-raf-dependent c-fos expression and transformation by a kinase-defective mutant of the mitogen-activated protein kinase Erk2. *Mol Cell Biol*, *14*(7), 4815-4824. https://doi.org/10.1128/mcb.14.7.4815

Krajewska, M., Dries, R., Grassetti, A. V., Dust, S., Gao, Y., Huang, H., Sharma, B., Day, D. S., Kwiatkowski, N., Pomaville, M., Dodd, O., Chipumuro, E., Zhang, T., Greenleaf, A. L., Yuan, G. C., Gray, N. S., Young, R. A., Geyer, M., Gerber, S. A., & George, R. E. (2019). CDK12 loss in cancer cells affects DNA damage response genes through premature cleavage and polyadenylation. *Nat Commun*, *10*(1), 1757. https://doi.org/10.1038/s41467-019-09703-y

Krishnamurthy, S., Ghazy, M. A., Moore, C., & Hampsey, M. (2009). Functional interaction of the Ess1 prolyl isomerase with components of the RNA polymerase II initiation and termination machineries. *Mol Cell Biol*, *29*(11), 2925-2934. https://doi.org/10.1128/MCB.01655-08

Krishnamurthy, S., He, X., Reyes-Reyes, M., Moore, C., & Hampsey, M. (2004). Ssu72 Is an RNA polymerase II CTD phosphatase. *Mol Cell*, *14*(3), 387-394. https://doi.org/10.1016/s1097-2765(04)00235-7

Krogan, N. J., Dover, J., Wood, A., Schneider, J., Heidt, J., Boateng, M. A., Dean, K., Ryan, O. W., Golshani, A., Johnston, M., Greenblatt, J. F., & Shilatifard, A. (2003). The Paf1 complex is required for histone H3 methylation by COMPASS and Dot1p: linking transcriptional elongation to histone methylation. *Mol Cell*, *11*(3), 721-729. https://doi.org/10.1016/s1097-2765(03)00091-1

Krumm, A., Meulia, T., Brunvand, M., & Groudine, M. (1992). The block to transcriptional elongation within the human c-myc gene is determined in the promoter-proximal region. *Genes Dev*, *6*(11), 2201-2213. https://doi.org/10.1101/gad.6.11.2201

Kudo, N., Matsumori, N., Taoka, H., Fujiwara, D., Schreiner, E. P., Wolff, B., Yoshida, M., & Horinouchi, S. (1999). Leptomycin B inactivates CRM1/exportin 1 by covalent modification at a cysteine residue in the central conserved region. *Proc Natl Acad Sci U S A*, *96*(16), 9112-9117.

Kuhlman, T. C., Cho, H., Reinberg, D., & Hernandez, N. (1999). The general transcription factors IIA, IIB, IIF, and IIE are required for RNA polymerase II transcription from the human U1 small nuclear RNA promoter. *Mol Cell Biol*, *19*(3), 2130-2141. https://doi.org/10.1128/mcb.19.3.2130

Kuhn, C. D., Geiger, S. R., Baumli, S., Gartmann, M., Gerber, J., Jennebach, S., Mielke, T., Tschochner, H., Beckmann, R., & Cramer, P. (2007). Functional architecture of RNA polymerase I. *Cell*, *131*(7), 1260-1272. https://doi.org/10.1016/j.cell.2007.10.051

Kumar, G. S., Chang, W., Xie, T., Patel, A., Zhang, Y., Wang, G. G., David, G., & Radhakrishnan, I. (2012). Sequence requirements for combinatorial recognition of histone H3 by the MRG15 and Pf1 subunits of the Rpd3S/Sin3S corepressor complex. *J Mol Biol*, *422*(4), 519-531. https://doi.org/10.1016/j.jmb.2012.06.013

Kuzmichev, A., Nishioka, K., Erdjument-Bromage, H., Tempst, P., & Reinberg, D. (2002). Histone methyltransferase activity associated with a human multiprotein complex containing the Enhancer of Zeste protein. *Genes Dev*, *16*(22), 2893-2905. https://doi.org/10.1101/gad.1035902

Kwak, H., Fuda, N. J., Core, L. J., & Lis, J. T. (2013). Precise maps of RNA polymerase reveal how promoters direct initiation and pausing. *Science*, *339*(6122), 950-953. https://doi.org/10.1126/science.1229386

Kwiatkowski, N., Zhang, T., Rahl, P. B., Abraham, B. J., Reddy, J., Ficarro, S. B., Dastur, A., Amzallag, A., Ramaswamy, S., Tesar, B., Jenkins, C. E., Hannett, N. M., McMillin, D., Sanda, T., Sim, T., Kim, N. D., Look, T., Mitsiades, C. S., Weng, A. P., Brown, J. R., Benes, C. H., Marto, J. A., Young, R. A., & Gray, N.

S. (2014). Targeting transcription regulation in cancer with a covalent CDK7 inhibitor. *Nature*, *511*(7511), 616-620. https://doi.org/10.1038/nature13393

Kyburz, A., Friedlein, A., Langen, H., & Keller, W. (2006). Direct interactions between subunits of CPSF and the U2 snRNP contribute to the coupling of pre-mRNA 3' end processing and splicing. *Mol Cell*, *23*(2), 195-205. https://doi.org/10.1016/j.molcel.2006.05.037

LaCava, J., Houseley, J., Saveanu, C., Petfalski, E., Thompson, E., Jacquier, A., & Tollervey, D. (2005). RNA degradation by the exosome is promoted by a nuclear polyadenylation complex. *Cell*, *121*(5), 713-724. https://doi.org/10.1016/j.cell.2005.04.029

Lachner, M., O'Carroll, D., Rea, S., Mechtler, K., & Jenuwein, T. (2001). Methylation of histone H3 lysine 9 creates a binding site for HP1 proteins. *Nature*, *410*(6824), 116-120. https://doi.org/10.1038/35065132

Lagha, M., Bothma, J. P., Esposito, E., Ng, S., Stefanik, L., Tsui, C., Johnston, J., Chen, K., Gilmour, D. S., Zeitlinger, J., & Levine, M. S. (2013). Paused Pol II coordinates tissue morphogenesis in the Drosophila embryo. *Cell*, *153*(5), 976-987. https://doi.org/10.1016/j.cell.2013.04.045

Laribee, R. N., Krogan, N. J., Xiao, T., Shibata, Y., Hughes, T. R., Greenblatt, J. F., & Strahl, B. D. (2005). BUR kinase selectively regulates H3 K4 trimethylation and H2B ubiquitylation through recruitment of the PAF elongation complex. *Curr Biol*, *15*(16), 1487-1493. https://doi.org/10.1016/j.cub.2005.07.028

Latos, P. A., Pauler, F. M., Koerner, M. V., Şenergin, H. B., Hudson, Q. J., Stocsits, R. R., Allhoff, W., Stricker, S. H., Klement, R. M., Warczok, K. E., Aumayr, K., Pasierbek, P., & Barlow, D. P. (2012). Airn transcriptional overlap, but not its lncRNA products, induces imprinted Igf2r silencing. *Science*, *338*(6113), 1469-1472. https://doi.org/10.1126/science.1228110

Lebreton, A., Tomecki, R., Dziembowski, A., & Séraphin, B. (2008). Endonucleolytic RNA cleavage by a eukaryotic exosome. *Nature*, *456*(7224), 993-996. https://doi.org/10.1038/nature07480

Lee, C. K., Shibata, Y., Rao, B., Strahl, B. D., & Lieb, J. D. (2004). Evidence for nucleosome depletion at active regulatory regions genome-wide. *Nat Genet*, *36*(8), 900-905. https://doi.org/10.1038/ng1400

Lee, D. Y., Hayes, J. J., Pruss, D., & Wolffe, A. P. (1993). A positive role for histone acetylation in transcription factor access to nucleosomal DNA. *Cell*, *72*(1), 73-84. https://doi.org/10.1016/0092-8674(93)90051-q

Lee, J. S., Garrett, A. S., Yen, K., Takahashi, Y. H., Hu, D., Jackson, J., Seidel, C., Pugh, B. F., & Shilatifard, A. (2012). Codependency of H2B monoubiquitination and nucleosome reassembly on Chd1. *Genes Dev*, *26*(9), 914-919. https://doi.org/10.1101/gad.186841.112

Lee, J. S., Shukla, A., Schneider, J., Swanson, S. K., Washburn, M. P., Florens, L., Bhaumik, S. R., & Shilatifard, A. (2007). Histone crosstalk between H2B monoubiquitination and H3 methylation mediated by COMPASS. *Cell*, *131*(6), 1084-1096. https://doi.org/10.1016/j.cell.2007.09.046

Lee, K. M., Miklos, I., Du, H., Watt, S., Szilagyi, Z., Saiz, J. E., Madabhushi, R., Penkett, C. J., Sipiczki, M., Bähler, J., & Fisher, R. P. (2005). Impairment of the TFIIH-associated CDK-activating kinase selectively affects cell cycle-regulated gene expression in fission yeast. *Mol Biol Cell*, *16*(6), 2734-2745. https://doi.org/10.1091/mbc.e04-11-0982

Lei, H., Wu, D., Wang, J. Y., Li, L., Zhang, C. L., Feng, H., Fu, F. Y., & Wu, L. L. (2015). C1q/tumor necrosis factor-related protein-6 attenuates post-infarct cardiac fibrosis by targeting RhoA/MRTF-A pathway and inhibiting myofibroblast differentiation. *Basic Res Cardiol*, *110*(4), 35. https://doi.org/10.1007/s00395-015-0492-7

Levine, J. H., Lin, Y., & Elowitz, M. B. (2013). Functional roles of pulsing in genetic circuits. *Science*, *342*(6163), 1193-1200. https://doi.org/10.1126/science.1239999

Li, B., Carey, M., & Workman, J. L. (2007). The role of chromatin during transcription. *Cell*, *128*(4), 707-719. https://doi.org/10.1016/j.cell.2007.01.015

Li, B., Howe, L., Anderson, S., Yates, J. R., & Workman, J. L. (2003). The Set2 histone methyltransferase functions through the phosphorylated carboxyl-terminal domain of RNA polymerase II. *J Biol Chem*, *278*(11), 8897-8903. https://doi.org/10.1074/jbc.M212134200

Li, H., Zhang, Z., Wang, B., Zhang, J., Zhao, Y., & Jin, Y. (2007). Wwp2-mediated ubiquitination of the RNA polymerase II large subunit in mouse embryonic pluripotent stem cells. *Mol Cell Biol*, *27*(15), 5296-5305. https://doi.org/10.1128/MCB.01667-06

Li, J., Zhu, X., Chen, M., Cheng, L., Zhou, D., Lu, M. M., Du, K., Epstein, J. A., & Parmacek, M. S. (2005). Myocardin-related transcription factor B is required in cardiac neural crest for smooth muscle differentiation and cardiovascular development. *Proc Natl Acad Sci U S A*, *102*(25), 8916-8921. https://doi.org/10.1073/pnas.0503741102

Li, S., Chang, S., Qi, X., Richardson, J. A., & Olson, E. N. (2006). Requirement of a myocardin-related transcription factor for development of mammary myoepithelial cells. *Mol Cell Biol*, *26*(15), 5797-5808. https://doi.org/10.1128/MCB.00211-06

Liang, G., Lin, J. C., Wei, V., Yoo, C., Cheng, J. C., Nguyen, C. T., Weisenberger, D. J., Egger, G., Takai, D., Gonzales, F. A., & Jones, P. A. (2004). Distinct localization of histone H3 acetylation and H3-K4 methylation to the transcription start sites in the human genome. *Proc Natl Acad Sci U S A*, *101*(19), 7357-7362. https://doi.org/10.1073/pnas.0401866101

Liang, K., Gao, X., Gilmore, J. M., Florens, L., Washburn, M. P., Smith, E., & Shilatifard, A. (2015). Characterization of human cyclin-dependent kinase 12 (CDK12) and CDK13 complexes in C-terminal domain phosphorylation, gene transcription, and RNA processing. *Mol Cell Biol*, *35*(6), 928-938. https://doi.org/10.1128/MCB.01426-14

Liao, S. M., Zhang, J., Jeffery, D. A., Koleske, A. J., Thompson, C. M., Chao, D. M., Viljoen, M., van Vuuren, H. J., & Young, R. A. (1995). A kinase-cyclin pair in the RNA polymerase II holoenzyme. *Nature*, *374*(6518), 193-196. https://doi.org/10.1038/374193a0

Liberzon, A., Subramanian, A., Pinchback, R., Thorvaldsdóttir, H., Tamayo, P., & Mesirov, J. P. (2011). Molecular signatures database (MSigDB) 3.0. *Bioinformatics*, *27*(12), 1739-1740. https://doi.org/10.1093/bioinformatics/btr260

Libri, D., Dower, K., Boulay, J., Thomsen, R., Rosbash, M., & Jensen, T. H. (2002). Interactions between mRNA export commitment, 3'-end quality control, and nuclear degradation. *Mol Cell Biol*, *22*(23), 8254-8266. https://doi.org/10.1128/mcb.22.23.8254-8266.2002

Licatalosi, D. D., Geiger, G., Minet, M., Schroeder, S., Cilli, K., McNeil, J. B., & Bentley, D. L. (2002). Functional interaction of yeast pre-mRNA 3' end processing factors with RNA polymerase II. *Mol Cell*, *9*(5), 1101-1111. https://doi.org/10.1016/s1097-2765(02)00518-x

Lim, J., Giri, P. K., Kazadi, D., Laffleur, B., Zhang, W., Grinstein, V., Pefanis, E., Brown, L. M., Ladewig, E., Martin, O., Chen, Y., Rabadan, R., Boyer, F., Rothschild, G., Cogné, M., Pinaud, E., Deng, H., & Basu, U. (2017). Nuclear Proximity of Mtr4 to RNA Exosome Restricts DNA Mutational Asymmetry. *Cell*, *169*(3), 523-537.e515. https://doi.org/10.1016/j.cell.2017.03.043

Lin, C., Smith, E. R., Takahashi, H., Lai, K. C., Martin-Brown, S., Florens, L., Washburn, M. P., Conaway, J. W., Conaway, R. C., & Shilatifard, A. (2010). AFF4, a component of the ELL/P-TEFb elongation complex and a shared subunit of MLL chimeras, can link transcription elongation to leukemia. *Mol Cell*, *37*(3), 429-437. https://doi.org/10.1016/j.molcel.2010.01.026

Lin, P. S., Dubois, M. F., & Dahmus, M. E. (2002). TFIIF-associating carboxyl-terminal domain phosphatase dephosphorylates phosphoserines 2 and 5 of RNA polymerase II. *J Biol Chem*, *277*(48), 45949-45956. https://doi.org/10.1074/jbc.M208588200

Lin, S., Coutinho-Mansfield, G., Wang, D., Pandit, S., & Fu, X. D. (2008). The splicing factor SC35 has an active role in transcriptional elongation. *Nat Struct Mol Biol*, *15*(8), 819-826. https://doi.org/10.1038/nsmb.1461

Lis, J. T., Mason, P., Peng, J., Price, D. H., & Werner, J. (2000). P-TEFb kinase recruitment and function at heat shock loci. *Genes Dev*, *14*(7), 792-803.

Liu, L. F., & Wang, J. C. (1987). Supercoiling of the DNA template during transcription. *Proc Natl Acad Sci U S A*, *84*(20), 7024-7027. https://doi.org/10.1073/pnas.84.20.7024

Ljungman, M., & Hanawalt, P. C. (1996). The anti-cancer drug camptothecin inhibits elongation but stimulates initiation of RNA polymerase II transcription. *Carcinogenesis*, *17*(1), 31-35. https://doi.org/10.1093/carcin/17.1.31

Lloret-Llinares, M., Karadoulama, E., Chen, Y., Wojenski, L. A., Villafano, G. J., Bornholdt, J., Andersson, R., Core, L., Sandelin, A., & Jensen, T. H. (2018). The RNA exosome contributes to gene expression regulation during stem cell differentiation. *Nucleic Acids Res*, *46*(21), 11502-11513. https://doi.org/10.1093/nar/gky817

Logan, J., Falck-Pedersen, E., Darnell, J. E., & Shenk, T. (1987). A poly(A) addition site and a downstream termination region are required for efficient cessation of transcription by RNA polymerase II in the mouse beta maj-globin gene. *Proc Natl Acad Sci U S A*, *84*(23), 8306-8310. https://doi.org/10.1073/pnas.84.23.8306

Lu, H., Flores, O., Weinmann, R., & Reinberg, D. (1991). The nonphosphorylated form of RNA polymerase II preferentially associates with the preinitiation complex. *Proc Natl Acad Sci U S A*, *88*(22), 10004-10008. https://doi.org/10.1073/pnas.88.22.10004

Lu, H., Zawel, L., Fisher, L., Egly, J. M., & Reinberg, D. (1992). Human general transcription factor IIH phosphorylates the C-terminal domain of RNA polymerase II. *Nature*, *358*(6388), 641-645. https://doi.org/10.1038/358641a0

Lubas, M., Andersen, P. R., Schein, A., Dziembowski, A., Kudla, G., & Jensen, T. H. (2015). The human nuclear exosome targeting complex is loaded onto newly synthesized RNA to direct early ribonucleolysis. *Cell Rep*, *10*(2), 178-192. https://doi.org/10.1016/j.celrep.2014.12.026

Lubas, M., Christensen, M. S., Kristiansen, M. S., Domanski, M., Falkenby, L. G., Lykke-Andersen, S., Andersen, J. S., Dziembowski, A., & Jensen, T. H. (2011). Interaction profiling identifies the human nuclear exosome targeting complex. *Mol Cell*, *43*(4), 624-637. https://doi.org/10.1016/j.molcel.2011.06.028

Lubas, M., Damgaard, C. K., Tomecki, R., Cysewski, D., Jensen, T. H., & Dziembowski, A. (2013). Exonuclease hDIS3L2 specifies an exosome-independent 3'-5' degradation pathway of human cytoplasmic mRNA. *EMBO J*, *32*(13), 1855-1868. https://doi.org/10.1038/emboj.2013.135

Luco, R. F., Pan, Q., Tominaga, K., Blencowe, B. J., Pereira-Smith, O. M., & Misteli, T. (2010). Regulation of alternative splicing by histone modifications. *Science*, *327*(5968), 996-1000. https://doi.org/10.1126/science.1184208

Lundquist, M. R., Storaska, A. J., Liu, T. C., Larsen, S. D., Evans, T., Neubig, R. R., & Jaffrey, S. R. (2014). Redox modification of nuclear actin by MICAL-2 regulates SRF signaling. *Cell*, *156*(3), 563-576. https://doi.org/10.1016/j.cell.2013.12.035

Luo, M. L., Zhou, Z., Magni, K., Christoforides, C., Rappsilber, J., Mann, M., & Reed, R. (2001). Pre-mRNA splicing and mRNA export linked by direct interactions between UAP56 and Aly. *Nature*, *413*(6856), 644-647. https://doi.org/10.1038/35098106

Luo, Z., Lin, C., & Shilatifard, A. (2012). The super elongation complex (SEC) family in transcriptional control. *Nat Rev Mol Cell Biol*, *13*(9), 543-547. https://doi.org/10.1038/nrm3417

Lynch, C. J., Bernad, R., Calvo, I., Nóbrega-Pereira, S., Ruiz, S., Ibarz, N., Martinez-Val, A., Graña-Castro, O., Gómez-López, G., Andrés-León, E., Espinosa Angarica, V., Del Sol, A., Ortega, S., Fernandez-Capetillo, O., Rojo, E., Munoz, J., & Serrano, M. (2018). The RNA Polymerase II Factor RPAP1 Is Critical for Mediator-Driven Transcription and Cell Identity. *Cell Rep*, *22*(2), 396-410. https://doi.org/10.1016/j.celrep.2017.12.062

Malik, S., & Roeder, R. G. (2010). The metazoan Mediator co-activator complex as an integrative hub for transcriptional regulation. *Nat Rev Genet*, *11*(11), 761-772. https://doi.org/10.1038/nrg2901

Mandel, C. R., Kaneko, S., Zhang, H., Gebauer, D., Vethantham, V., Manley, J. L., & Tong, L. (2006). Polyadenylation factor CPSF-73 is the pre-mRNA 3'-end-processing endonuclease. *Nature*, *444*(7121), 953-956. https://doi.org/10.1038/nature05363

Marais, R., Wynne, J., & Treisman, R. (1993). The SRF accessory protein Elk-1 contains a growth factor-regulated transcriptional activation domain. *Cell*, *73*(2), 381-393. https://doi.org/10.1016/0092-8674(93)90237-k

Margueron, R., & Reinberg, D. (2011). The Polycomb complex PRC2 and its mark in life. *Nature*, *469*(7330), 343-349. https://doi.org/10.1038/nature09784

Marshall, N. F., Peng, J., Xie, Z., & Price, D. H. (1996). Control of RNA polymerase II elongation potential by a novel carboxyl-terminal domain kinase. *J Biol Chem*, *271*(43), 27176-27183. https://doi.org/10.1074/jbc.271.43.27176

Marzluff, W. F., Wagner, E. J., & Duronio, R. J. (2008). Metabolism and regulation of canonical histone mRNAs: life without a poly(A) tail. *Nat Rev Genet*, *9*(11), 843-854. https://doi.org/10.1038/nrg2438

Mason, P. B., & Struhl, K. (2005). Distinction and relationship between elongation rate and processivity of RNA polymerase II in vivo. *Mol Cell*, *17*(6), 831-840. https://doi.org/10.1016/j.molcel.2005.02.017

Maurice, D., Costello, P., Sargent, M., & Treisman, R. (2018). ERK Signaling Controls Innate-like CD8. *J Immunol*, *201*(6), 1681-1691. https://doi.org/10.4049/jimmunol.1800704

Mayer, A., Heidemann, M., Lidschreiber, M., Schreieck, A., Sun, M., Hintermair, C., Kremmer, E., Eick, D., & Cramer, P. (2012). CTD tyrosine phosphorylation impairs termination factor recruitment to RNA polymerase II. *Science*, *336*(6089), 1723-1725. https://doi.org/10.1126/science.1219651

McCracken, S., Fong, N., Rosonina, E., Yankulov, K., Brothers, G., Siderovski, D., Hessel, A., Foster, S., Shuman, S., & Bentley, D. L. (1997). 5'-Capping enzymes are targeted to pre-mRNA by binding to the phosphorylated carboxy-terminal domain of RNA polymerase II. *Genes Dev*, *11*(24), 3306-3318. https://doi.org/10.1101/gad.11.24.3306

McHugh, C. A., Chen, C. K., Chow, A., Surka, C. F., Tran, C., McDonel, P., Pandya-Jones, A., Blanco, M., Burghard, C., Moradian, A., Sweredoski, M. J., Shishkin, A. A., Su, J., Lander, E. S., Hess, S., Plath, K., & Guttman, M. (2015). The Xist

lncRNA interacts directly with SHARP to silence transcription through HDAC3. *Nature*, *521*(7551), 232-236. https://doi.org/10.1038/nature14443

Medjkane, S., Perez-Sanchez, C., Gaggioli, C., Sahai, E., & Treisman, R. (2009). Myocardin-related transcription factors and SRF are required for cytoskeletal dynamics and experimental metastasis. *Nat Cell Biol*, *11*(3), 257-268. https://doi.org/10.1038/ncb1833

Meinhart, A., & Cramer, P. (2004). Recognition of RNA polymerase II carboxy-terminal domain by 3'-RNA-processing factors. *Nature*, *430*(6996), 223-226. https://doi.org/10.1038/nature02679

Meneghini, M. D., Wu, M., & Madhani, H. D. (2003). Conserved histone variant H2A.Z protects euchromatin from the ectopic spread of silent heterochromatin. *Cell*, *112*(5), 725-736. https://doi.org/10.1016/s0092-8674(03)00123-5

Meola, N., Domanski, M., Karadoulama, E., Chen, Y., Gentil, C., Pultz, D., Vitting-Seerup, K., Lykke-Andersen, S., Andersen, J. S., Sandelin, A., & Jensen, T. H. (2016). Identification of a Nuclear Exosome Decay Pathway for Processed Transcripts. *Mol Cell*, *64*(3), 520-533. https://doi.org/10.1016/j.molcel.2016.09.025

Michels, A. A., Fraldi, A., Li, Q., Adamson, T. E., Bonnet, F., Nguyen, V. T., Sedore, S. C., Price, J. P., Price, D. H., Lania, L., & Bensaude, O. (2004). Binding of the 7SK snRNA turns the HEXIM1 protein into a P-TEFb (CDK9/cyclin T) inhibitor. *EMBO J*, *23*(13), 2608-2619. https://doi.org/10.1038/sj.emboj.7600275

Milligan, L., Torchet, C., Allmang, C., Shipman, T., & Tollervey, D. (2005). A nuclear surveillance pathway for mRNAs with defective polyadenylation. *Mol Cell Biol*, *25*(22), 9996-10004. https://doi.org/10.1128/MCB.25.22.9996-10004.2005

Milne, T. A., Briggs, S. D., Brock, H. W., Martin, M. E., Gibbs, D., Allis, C. D., & Hess, J. L. (2002). MLL targets SET domain methyltransferase activity to Hox gene promoters. *Mol Cell*, *10*(5), 1107-1117. https://doi.org/10.1016/s1097-2765(02)00741-4

Miralles, F., Posern, G., Zaromytidou, A. I., & Treisman, R. (2003). Actin dynamics control SRF activity by regulation of its coactivator MAL. *Cell*, *113*(3), 329-342.

Misteli, T. (2001). Protein dynamics: implications for nuclear architecture and gene expression. *Science*, *291*(5505), 843-847. https://doi.org/10.1126/science.291.5505.843

Mitchell, P., Petfalski, E., Shevchenko, A., Mann, M., & Tollervey, D. (1997). The exosome: a conserved eukaryotic RNA processing complex containing multiple 3'-->5' exoribonucleases. *Cell*, *91*(4), 457-466. https://doi.org/10.1016/s0092-8674(00)80432-8

Mito, Y., Henikoff, J. G., & Henikoff, S. (2005). Genome-scale profiling of histone H3.3 replacement patterns. *Nat Genet*, *37*(10), 1090-1097. https://doi.org/10.1038/ng1637

Mizuguchi, G., Shen, X., Landry, J., Wu, W. H., Sen, S., & Wu, C. (2004). ATP-driven exchange of histone H2AZ variant catalyzed by SWR1 chromatin remodeling complex. *Science*, *303*(5656), 343-348. https://doi.org/10.1126/science.1090701

Mohan, M., Herz, H. M., Takahashi, Y. H., Lin, C., Lai, K. C., Zhang, Y., Washburn, M. P., Florens, L., & Shilatifard, A. (2010). Linking H3K79 trimethylation to Wnt signaling through a novel Dot1-containing complex (DotCom). *Genes Dev*, *24*(6), 574-589. https://doi.org/10.1101/gad.1898410

Mohun, T., Garrett, N., & Treisman, R. (1987). Xenopus cytoskeletal actin and human c-fos gene promoters share a conserved protein-binding site. *EMBO J*, *6*(3), 667-673.

Mokalled, M. H., Johnson, A., Kim, Y., Oh, J., & Olson, E. N. (2010). Myocardin-related transcription factors regulate the Cdk5/Pctaire1 kinase cascade to control

neurite outgrowth, neuronal migration and brain development. *Development*, *137*(14), 2365-2374. https://doi.org/10.1242/dev.047605

Morisaki, T., Müller, W. G., Golob, N., Mazza, D., & McNally, J. G. (2014). Single-molecule analysis of transcription factor binding at transcription sites in live cells. *Nat Commun*, *5*, 4456. https://doi.org/10.1038/ncomms5456

Morris, D. P., Phatnani, H. P., & Greenleaf, A. L. (1999). Phospho-carboxyl-terminal domain binding and the role of a prolyl isomerase in pre-mRNA 3'-End formation. *J Biol Chem*, *274*(44), 31583-31587. https://doi.org/10.1074/jbc.274.44.31583

Morton, W. M., Ayscough, K. R., & McLaughlin, P. J. (2000). Latrunculin alters the actin-monomer subunit interface to prevent polymerization. *Nat Cell Biol*, *2*(6), 376-378. https://doi.org/10.1038/35014075

Mosley, A. L., Pattenden, S. G., Carey, M., Venkatesh, S., Gilmore, J. M., Florens, L., Workman, J. L., & Washburn, M. P. (2009). Rtr1 is a CTD phosphatase that regulates RNA polymerase II during the transition from serine 5 to serine 2 phosphorylation. *Mol Cell*, *34*(2), 168-178. https://doi.org/10.1016/j.molcel.2009.02.025

Mouilleron, S., Guettler, S., Langer, C. A., Treisman, R., & McDonald, N. Q. (2008). Molecular basis for G-actin binding to RPEL motifs from the serum response factor coactivator MAL. *EMBO J*, *27*(23), 3198-3208. https://doi.org/10.1038/emboj.2008.235

Mouilleron, S., Langer, C. A., Guettler, S., McDonald, N. Q., & Treisman, R. (2011). Structure of a pentavalent G-actin*MRTF-A complex reveals how G-actin controls nucleocytoplasmic shuttling of a transcriptional coactivator. *Sci Signal*, *4*(177), ra40. https://doi.org/10.1126/scisignal.2001750

Muehlich, S., Wang, R., Lee, S. M., Lewis, T. C., Dai, C., & Prywes, R. (2008). Serum-induced phosphorylation of the serum response factor coactivator MKL1 by the extracellular signal-regulated kinase 1/2 pathway inhibits its nuclear localization. *Mol Cell Biol*, *28*(20), 6302-6313. https://doi.org/10.1128/MCB.00427-08

Muse, G. W., Gilchrist, D. A., Nechaev, S., Shah, R., Parker, J. S., Grissom, S. F., Zeitlinger, J., & Adelman, K. (2007). RNA polymerase is poised for activation across the genome. *Nat Genet*, *39*(12), 1507-1511. https://doi.org/10.1038/ng.2007.21

Muthukrishnan, S., Both, G. W., Furuichi, Y., & Shatkin, A. J. (1975). 5'-Terminal 7-methylguanosine in eukaryotic mRNA is required for translation. *Nature*, *255*(5503), 33-37. https://doi.org/10.1038/255033a0

Nag, A., Narsinh, K., & Martinson, H. G. (2007). The poly(A)-dependent transcriptional pause is mediated by CPSF acting on the body of the polymerase. *Nat Struct Mol Biol*, *14*(7), 662-669. https://doi.org/10.1038/nsmb1253

Nakajima, N., Horikoshi, M., & Roeder, R. G. (1988). Factors involved in specific transcription by mammalian RNA polymerase II: purification, genetic specificity, and TATA box-promoter interactions of TFIID. *Mol Cell Biol*, *8*(10), 4028-4040. https://doi.org/10.1128/mcb.8.10.4028

Nakamura, T., Mori, T., Tada, S., Krajewski, W., Rozovskaia, T., Wassell, R., Dubois, G., Mazo, A., Croce, C. M., & Canaani, E. (2002). ALL-1 is a histone methyltransferase that assembles a supercomplex of proteins involved in transcriptional regulation. *Mol Cell*, *10*(5), 1119-1128. https://doi.org/10.1016/s1097-2765(02)00740-2

Narita, T., Yung, T. M., Yamamoto, J., Tsuboi, Y., Tanabe, H., Tanaka, K., Yamaguchi, Y., & Handa, H. (2007). NELF interacts with CBC and participates in 3' end processing of replication-dependent histone mRNAs. *Mol Cell*, *26*(3), 349-365. https://doi.org/10.1016/j.molcel.2007.04.011

Neil, H., Malabat, C., d'Aubenton-Carafa, Y., Xu, Z., Steinmetz, L. M., & Jacquier, A. (2009). Widespread bidirectional promoters are the major source of cryptic transcripts in yeast. *Nature*, *457*(7232), 1038-1042. https://doi.org/10.1038/nature07747

Nemec, C. M., Yang, F., Gilmore, J. M., Hintermair, C., Ho, Y. H., Tseng, S. C., Heidemann, M., Zhang, Y., Florens, L., Gasch, A. P., Eick, D., Washburn, M. P., Varani, G., & Ansari, A. Z. (2017). Different phosphoisoforms of RNA polymerase II engage the Rtt103 termination factor in a structurally analogous manner. *Proc Natl Acad Sci U S A*, *114*(20), E3944-E3953. https://doi.org/10.1073/pnas.1700128114

Ng, H. H., Ciccone, D. N., Morshead, K. B., Oettinger, M. A., & Struhl, K. (2003). Lysine-79 of histone H3 is hypomethylated at silenced loci in yeast and mammalian cells: a potential mechanism for position-effect variegation. *Proc Natl Acad Sci U S A*, *100*(4), 1820-1825. https://doi.org/10.1073/pnas.0437846100

Ng, H. H., Robert, F., Young, R. A., & Struhl, K. (2003). Targeted recruitment of Set1 histone methylase by elongating Pol II provides a localized mark and memory of recent transcriptional activity. *Mol Cell*, *11*(3), 709-719. https://doi.org/10.1016/s1097-2765(03)00092-3

Nguyen, V. T., Kiss, T., Michels, A. A., & Bensaude, O. (2001). 7SK small nuclear RNA binds to and inhibits the activity of CDK9/cyclin T complexes. *Nature*, *414*(6861), 322-325. https://doi.org/10.1038/35104581

Ni, Z., Olsen, J. B., Guo, X., Zhong, G., Ruan, E. D., Marcon, E., Young, P., Guo, H., Li, J., Moffat, J., Emili, A., & Greenblatt, J. F. (2011). Control of the RNA polymerase II phosphorylation state in promoter regions by CTD interaction domain-containing proteins RPRD1A and RPRD1B. *Transcription*, *2*(5), 237-242. https://doi.org/10.4161/trns.2.5.17803

Ni, Z., Saunders, A., Fuda, N. J., Yao, J., Suarez, J. R., Webb, W. W., & Lis, J. T. (2008). P-TEFb is critical for the maturation of RNA polymerase II into productive elongation in vivo. *Mol Cell Biol*, *28*(3), 1161-1170. https://doi.org/10.1128/MCB.01859-07

Ni, Z., Schwartz, B. E., Werner, J., Suarez, J. R., & Lis, J. T. (2004). Coordination of transcription, RNA processing, and surveillance by P-TEFb kinase on heat shock genes. *Mol Cell*, *13*(1), 55-65. https://doi.org/10.1016/s1097-2765(03)00526-4

Ni, Z., Xu, C., Guo, X., Hunter, G. O., Kuznetsova, O. V., Tempel, W., Marcon, E., Zhong, G., Guo, H., Kuo, W. W., Li, J., Young, P., Olsen, J. B., Wan, C., Loppnau, P., El Bakkouri, M., Senisterra, G. A., He, H., Huang, H., Sidhu, S. S., Emili, A., Murphy, S., Mosley, A. L., Arrowsmith, C. H., Min, J., & Greenblatt, J. F. (2014). RPRD1A and RPRD1B are human RNA polymerase II C-terminal domain scaffolds for Ser5 dephosphorylation. *Nat Struct Mol Biol*, *21*(8), 686-695. https://doi.org/10.1038/nsmb.2853

Nojima, T., Dienstbier, M., Murphy, S., Proudfoot, N. J., & Dye, M. J. (2013). Definition of RNA polymerase II CoTC terminator elements in the human genome. *Cell Rep*, *3*(4), 1080-1092. https://doi.org/10.1016/j.celrep.2013.03.012

Nojima, T., Gomes, T., Grosso, A. R. F., Kimura, H., Dye, M. J., Dhir, S., Carmo-Fonseca, M., & Proudfoot, N. J. (2015). Mammalian NET-Seq Reveals Genome-wide Nascent Transcription Coupled to RNA Processing. *Cell*, *161*(3), 526-540. https://doi.org/10.1016/j.cell.2015.03.027

Norman, C., Runswick, M., Pollock, R., & Treisman, R. (1988). Isolation and properties of cDNA clones encoding SRF, a transcription factor that binds to the c-fos serum response element. *Cell*, *55*(6), 989-1003. https://doi.org/10.1016/0092-8674(88)90244-9

Ntini, E., Järvelin, A. I., Bornholdt, J., Chen, Y., Boyd, M., Jørgensen, M., Andersson, R., Hoof, I., Schein, A., Andersen, P. R., Andersen, P. K., Preker, P., Valen, E., Zhao, X., Pelechano, V., Steinmetz, L. M., Sandelin, A., & Jensen, T. H. (2013). Polyadenylation site-induced decay of upstream transcripts enforces promoter directionality. *Nat Struct Mol Biol*, *20*(8), 923-928. https://doi.org/10.1038/nsmb.2640

O'Reilly, D., & Greaves, D. R. (2007). Cell-type-specific expression of the human CD68 gene is associated with changes in Pol II phosphorylation and short-range intrachromosomal gene looping. *Genomics*, *90*(3), 407-415. https://doi.org/10.1016/j.ygeno.2007.04.010

O'Sullivan, C., Christie, J., Pienaar, M., Gambling, J., Nickerson, P. E., Alford, S. C., Chow, R. L., & Howard, P. L. (2015). Mutagenesis of ARS2 Domains To Assess Possible Roles in Cell Cycle Progression and MicroRNA and Replication-Dependent Histone mRNA Biogenesis. *Mol Cell Biol*, *35*(21), 3753-3767. https://doi.org/10.1128/MCB.00272-15

Odawara, J., Harada, A., Yoshimi, T., Maehara, K., Tachibana, T., Okada, S., Akashi, K., & Ohkawa, Y. (2011). The classification of mRNA expression levels by the phosphorylation state of RNAPII CTD based on a combined genome-wide approach. *BMC Genomics*, *12*, 516. https://doi.org/10.1186/1471-2164-12-516

Ogami, K., Chen, Y., & Manley, J. L. (2018). RNA surveillance by the nuclear RNA exosome: mechanisms and significance. *Noncoding RNA*, *4*(1). https://doi.org/10.3390/ncrna4010008

Ogami, K., Richard, P., Chen, Y., Hoque, M., Li, W., Moresco, J. J., Yates, J. R., Tian, B., & Manley, J. L. (2017). An Mtr4/ZFC3H1 complex facilitates turnover of unstable nuclear RNAs to prevent their cytoplasmic transport and global translational repression. *Genes Dev*, *31*(12), 1257-1271. https://doi.org/10.1101/gad.302604.117

Oh, J., Richardson, J. A., & Olson, E. N. (2005). Requirement of myocardin-related transcription factor-B for remodeling of branchial arch arteries and smooth muscle differentiation. *Proc Natl Acad Sci U S A*, *102*(42), 15122-15127. https://doi.org/10.1073/pnas.0507346102

Ohkawa, T., & Welch, M. D. (2018). Baculovirus Actin-Based Motility Drives Nuclear Envelope Disruption and Nuclear Egress. *Curr Biol*, *28*(13), 2153-2159.e2154. https://doi.org/10.1016/j.cub.2018.05.027

Ohno, M., Sakamoto, H., & Shimura, Y. (1987). Preferential excision of the 5' proximal intron from mRNA precursors with two introns as mediated by the cap structure. *Proc Natl Acad Sci U S A*, *84*(15), 5187-5191. https://doi.org/10.1073/pnas.84.15.5187

Ohno, M., Segref, A., Bachi, A., Wilm, M., & Mattaj, I. W. (2000). PHAX, a mediator of U snRNA nuclear export whose activity is regulated by phosphorylation. *Cell*, *101*(2), 187-198. https://doi.org/10.1016/S0092-8674(00)80829-6

Olson, E. N., & Nordheim, A. (2010). Linking actin dynamics and gene transcription to drive cellular motile functions. *Nat Rev Mol Cell Biol*, *11*(5), 353-365. https://doi.org/10.1038/nrm2890

Osman, S., & Cramer, P. (2020a). Structural Biology of RNA Polymerase II Transcription: 20 Years On. *Annu Rev Cell Dev Biol*, *36*, 1-34. https://doi.org/10.1146/annurev-cellbio-042020-021954

Osman, S., & Cramer, P. (2020b). Structural Biology of RNA Polymerase II Transcription: 20 Years On. *Annu Rev Cell Dev Biol*. https://doi.org/10.1146/annurev-cellbio-042020-021954

Ozbudak, E. M., Thattai, M., Kurtser, I., Grossman, A. D., & van Oudenaarden, A. (2002). Regulation of noise in the expression of a single gene. *Nat Genet*, *31*(1), 69-73. https://doi.org/10.1038/ng869

Pabis, M., Neufeld, N., Steiner, M. C., Bojic, T., Shav-Tal, Y., & Neugebauer, K. M. (2013). The nuclear cap-binding complex interacts with the U4/U6·U5 tri-snRNP and promotes spliceosome assembly in mammalian cells. *RNA*, *19*(8), 1054-1063. https://doi.org/10.1261/rna.037069.112

Palancade, B., Bellier, S., Almouzni, G., & Bensaude, O. (2001). Incomplete RNA polymerase II phosphorylation in Xenopus laevis early embryos. *J Cell Sci*, *114*(Pt 13), 2483-2489.

Panayiotou, R., Miralles, F., Pawlowski, R., Diring, J., Flynn, H. R., Skehel, M., & Treisman, R. (2016). Phosphorylation acts positively and negatively to regulate MRTF-A subcellular localisation and activity. *Elife*, *5*. https://doi.org/10.7554/eLife.15460

Papamichos-Chronakis, M., Watanabe, S., Rando, O. J., & Peterson, C. L. (2011). Global regulation of H2A.Z localization by the INO80 chromatin-remodeling enzyme is essential for genome integrity. *Cell*, *144*(2), 200-213. https://doi.org/10.1016/j.cell.2010.12.021

Parker, C. S., & Topol, J. (1984). A Drosophila RNA polymerase II transcription factor contains a promoter-region-specific DNA-binding activity. *Cell*, *36*(2), 357-369. https://doi.org/10.1016/0092-8674(84)90229-0

Pavri, R., Zhu, B., Li, G., Trojer, P., Mandal, S., Shilatifard, A., & Reinberg, D. (2006). Histone H2B monoubiquitination functions cooperatively with FACT to regulate elongation by RNA polymerase II. *Cell*, *125*(4), 703-717. https://doi.org/10.1016/j.cell.2006.04.029

Pawłowski, R., Rajakylä, E. K., Vartiainen, M. K., & Treisman, R. (2010). An actin-regulated importin α/β-dependent extended bipartite NLS directs nuclear import of MRTF-A. *EMBO J*, *29*(20), 3448-3458. https://doi.org/10.1038/emboj.2010.216

Payne, J. M., Laybourn, P. J., & Dahmus, M. E. (1989). The transition of RNA polymerase II from initiation to elongation is associated with phosphorylation of the carboxyl-terminal domain of subunit IIa. *J Biol Chem*, *264*(33), 19621-19629.

Pei, Y., Schwer, B., & Shuman, S. (2003). Interactions between fission yeast Cdk9, its cyclin partner Pch1, and mRNA capping enzyme Pct1 suggest an elongation checkpoint for mRNA quality control. *J Biol Chem*, *278*(9), 7180-7188. https://doi.org/10.1074/jbc.M211713200

Pellegrini, L., Tan, S., & Richmond, T. J. (1995). Structure of serum response factor core bound to DNA. *Nature*, *376*(6540), 490-498. https://doi.org/10.1038/376490a0

Pengelly, A. R., Copur, Ö., Jäckle, H., Herzig, A., & Müller, J. (2013). A histone mutant reproduces the phenotype caused by loss of histone-modifying factor Polycomb. *Science*, *339*(6120), 698-699. https://doi.org/10.1126/science.1231382

Phillips-Cremins, J. E., Sauria, M. E., Sanyal, A., Gerasimova, T. I., Lajoie, B. R., Bell, J. S., Ong, C. T., Hookway, T. A., Guo, C., Sun, Y., Bland, M. J., Wagstaff, W., Dalton, S., McDevitt, T. C., Sen, R., Dekker, J., Taylor, J., & Corces, V. G. (2013). Architectural protein subclasses shape 3D organization of genomes during lineage commitment. *Cell*, *153*(6), 1281-1295. https://doi.org/10.1016/j.cell.2013.04.053

Ping, Y. H., & Rana, T. M. (2001). DSIF and NELF interact with RNA polymerase II elongation complex and HIV-1 Tat stimulates P-TEFb-mediated phosphorylation of RNA polymerase II and DSIF during transcription elongation. *J Biol Chem*, *276*(16), 12951-12958. https://doi.org/10.1074/jbc.M006130200

Pirngruber, J., Shchebet, A., Schreiber, L., Shema, E., Minsky, N., Chapman, R. D., Eick, D., Aylon, Y., Oren, M., & Johnsen, S. A. (2009). CDK9 directs H2B

monoubiquitination and controls replication-dependent histone mRNA 3'-end processing. *EMBO Rep*, *10*(8), 894-900. https://doi.org/10.1038/embor.2009.108

Plessner, M., Melak, M., Chinchilla, P., Baarlink, C., & Grosse, R. (2015). Nuclear F-actin formation and reorganization upon cell spreading. *J Biol Chem*, *290*(18), 11209-11216. https://doi.org/10.1074/jbc.M114.627166

Plet, A., Eick, D., & Blanchard, J. M. (1995). Elongation and premature termination of transcripts initiated from c-fos and c-myc promoters show dissimilar patterns. *Oncogene*, *10*(2), 319-328.

Pohl, M. O., von Recum-Knepper, J., Rodriguez-Frandsen, A., Lanz, C., Yángüez, E., Soonthornvacharin, S., Wolff, T., Chanda, S. K., & Stertz, S. (2017). Identification of Polo-like kinases as potential novel drug targets for influenza A virus. *Sci Rep*, *7*(1), 8629. https://doi.org/10.1038/s41598-017-08942-7

Pokholok, D. K., Hannett, N. M., & Young, R. A. (2002). Exchange of RNA polymerase II initiation and elongation factors during gene expression in vivo. *Mol Cell*, *9*(4), 799-809. https://doi.org/10.1016/s1097-2765(02)00502-6

Pokholok, D. K., Harbison, C. T., Levine, S., Cole, M., Hannett, N. M., Lee, T. I., Bell, G. W., Walker, K., Rolfe, P. A., Herbolsheimer, E., Zeitlinger, J., Lewitter, F., Gifford, D. K., & Young, R. A. (2005). Genome-wide map of nucleosome acetylation and methylation in yeast. *Cell*, *122*(4), 517-527. https://doi.org/10.1016/j.cell.2005.06.026

Pollock, R., & Treisman, R. (1991). Human SRF-related proteins: DNA-binding properties and potential regulatory targets. *Genes Dev*, *5*(12A), 2327-2341.

Posern, G., Miralles, F., Guettler, S., & Treisman, R. (2004). Mutant actins that stabilise F-actin use distinct mechanisms to activate the SRF coactivator MAL. *EMBO J*, *23*(20), 3973-3983. https://doi.org/10.1038/sj.emboj.7600404

Posern, G., Sotiropoulos, A., & Treisman, R. (2002). Mutant actins demonstrate a role for unpolymerized actin in control of transcription by serum response factor. *Mol Biol Cell*, *13*(12), 4167-4178. https://doi.org/10.1091/mbc.02-05-0068

Posern, G., & Treisman, R. (2006). Actin' together: serum response factor, its cofactors and the link to signal transduction. *Trends Cell Biol*, *16*(11), 588-596. https://doi.org/10.1016/j.tcb.2006.09.008

Preker, P., Almvig, K., Christensen, M. S., Valen, E., Mapendano, C. K., Sandelin, A., & Jensen, T. H. (2011). PROMoter uPstream Transcripts share characteristics with mRNAs and are produced upstream of all three major types of mammalian promoters. *Nucleic Acids Res*, *39*(16), 7179-7193. https://doi.org/10.1093/nar/gkr370

Preker, P., Nielsen, J., Kammler, S., Lykke-Andersen, S., Christensen, M. S., Mapendano, C. K., Schierup, M. H., & Jensen, T. H. (2008). RNA exosome depletion reveals transcription upstream of active human promoters. *Science*, *322*(5909), 1851-1854. https://doi.org/10.1126/science.1164096

Prescott, E. M., & Proudfoot, N. J. (2002). Transcriptional collision between convergent genes in budding yeast. *Proc Natl Acad Sci U S A*, *99*(13), 8796-8801. https://doi.org/10.1073/pnas.132270899

Price, M. A., Cruzalegui, F. H., & Treisman, R. (1996). The p38 and ERK MAP kinase pathways cooperate to activate Ternary Complex Factors and c-fos transcription in response to UV light. *EMBO J*, *15*(23), 6552-6563.

Protacio, R. U., Li, G., Lowary, P. T., & Widom, J. (2000). Effects of histone tail domains on the rate of transcriptional elongation through a nucleosome. *Mol Cell Biol*, *20*(23), 8866-8878. https://doi.org/10.1128/mcb.20.23.8866-8878.2000

Proudfoot, N. (1996). Ending the message is not so simple. *Cell*, *87*(5), 779-781. https://doi.org/10.1016/s0092-8674(00)81982-0

Puno, M. R., & Lima, C. D. (2018). Structural basis for MTR4-ZCCHC8 interactions that stimulate the MTR4 helicase in the nuclear exosome-targeting complex. *Proc Natl Acad Sci U S A*, *115*(24), E5506-E5515. https://doi.org/10.1073/pnas.1803530115

Rahl, P. B., Lin, C. Y., Seila, A. C., Flynn, R. A., McCuine, S., Burge, C. B., Sharp, P. A., & Young, R. A. (2010). c-Myc regulates transcriptional pause release. *Cell*, *141*(3), 432-445. https://doi.org/10.1016/j.cell.2010.03.030

Raingeaud, J., Whitmarsh, A. J., Barrett, T., Dérijard, B., & Davis, R. J. (1996). MKK3- and MKK6-regulated gene expression is mediated by the p38 mitogen-activated protein kinase signal transduction pathway. *Mol Cell Biol*, *16*(3), 1247-1255. https://doi.org/10.1128/mcb.16.3.1247

Rajakylä, E. K., Viita, T., Kyheröinen, S., Huet, G., Treisman, R., & Vartiainen, M. K. (2015). RNA export factor Ddx19 is required for nuclear import of the SRF coactivator MKL1. *Nat Commun*, *6*, 5978. https://doi.org/10.1038/ncomms6978

Ramanathan, A., Robb, G. B., & Chan, S. H. (2016). mRNA capping: biological functions and applications. *Nucleic Acids Res*, *44*(16), 7511-7526. https://doi.org/10.1093/nar/gkw551

Ramanathan, Y., Rajpara, S. M., Reza, S. M., Lees, E., Shuman, S., Mathews, M. B., & Pe'ery, T. (2001). Three RNA polymerase II carboxyl-terminal domain kinases display distinct substrate preferences. *J Biol Chem*, *276*(14), 10913-10920. https://doi.org/10.1074/jbc.M010975200

Rando, O. J., & Chang, H. Y. (2009). Genome-wide views of chromatin structure. *Annu Rev Biochem*, *78*, 245-271. https://doi.org/10.1146/annurev.biochem.78.071107.134639

Ranuncolo, S. M., Ghosh, S., Hanover, J. A., Hart, G. W., & Lewis, B. A. (2012). Evidence of the involvement of O-GlcNAc-modified human RNA polymerase II CTD in transcription in vitro and in vivo. *J Biol Chem*, *287*(28), 23549-23561. https://doi.org/10.1074/jbc.M111.330910

Rasmussen, E. B., & Lis, J. T. (1993). In vivo transcriptional pausing and cap formation on three Drosophila heat shock genes. *Proc Natl Acad Sci U S A*, *90*(17), 7923-7927. https://doi.org/10.1073/pnas.90.17.7923

Rea, S., Eisenhaber, F., O'Carroll, D., Strahl, B. D., Sun, Z. W., Schmid, M., Opravil, S., Mechtler, K., Ponting, C. P., Allis, C. D., & Jenuwein, T. (2000). Regulation of chromatin structure by site-specific histone H3 methyltransferases. *Nature*, *406*(6796), 593-599. https://doi.org/10.1038/35020506

Reinberg, D., & Sims, R. J. (2006). de FACTo nucleosome dynamics. *J Biol Chem*, *281*(33), 23297-23301. https://doi.org/10.1074/jbc.R600007200

Reines, D., Chamberlin, M. J., & Kane, C. M. (1989). Transcription elongation factor SII (TFIIS) enables RNA polymerase II to elongate through a block to transcription in a human gene in vitro. *J Biol Chem*, *264*(18), 10799-10809.

Richard, P., Ogami, K., Chen, Y., Feng, S., Moresco, J. J., Yates, J. R., & Manley, J. L. (2018). NRDE-2, the human homolog of fission yeast Nrl1, prevents DNA damage accumulation in human cells. *RNA Biol*, *15*(7), 868-876. https://doi.org/10.1080/15476286.2018.1467180

Rickert, P., Corden, J. L., & Lees, E. (1999). Cyclin C/CDK8 and cyclin H/CDK7/p36 are biochemically distinct CTD kinases. *Oncogene*, *18*(4), 1093-1102. https://doi.org/10.1038/sj.onc.1202399

Rodriguez, C. R., Cho, E. J., Keogh, M. C., Moore, C. L., Greenleaf, A. L., & Buratowski, S. (2000). Kin28, the TFIIH-associated carboxy-terminal domain kinase, facilitates the recruitment of mRNA processing machinery to RNA polymerase II. *Mol Cell Biol*, *20*(1), 104-112. https://doi.org/10.1128/mcb.20.1.104-112.2000

Roeder, R. G. (2019). 50+ years of eukaryotic transcription: an expanding universe of factors and mechanisms. *Nat Struct Mol Biol*, *26*(9), 783-791. https://doi.org/10.1038/s41594-019-0287-x

Rollins, R. A., Korom, M., Aulner, N., Martens, A., & Dorsett, D. (2004). Drosophila nipped-B protein supports sister chromatid cohesion and opposes the stromalin/Scc3 cohesion factor to facilitate long-range activation of the cut gene. *Mol Cell Biol*, *24*(8), 3100-3111. https://doi.org/10.1128/mcb.24.8.3100-3111.2004

Rougvie, A. E., & Lis, J. T. (1988). The RNA polymerase II molecule at the 5' end of the uninduced hsp70 gene of D. melanogaster is transcriptionally engaged. *Cell*, *54*(6), 795-804. https://doi.org/10.1016/s0092-8674(88)91087-2

Sainsbury, S., Bernecky, C., & Cramer, P. (2015). Structural basis of transcription initiation by RNA polymerase II. *Nat Rev Mol Cell Biol*, *16*(3), 129-143. https://doi.org/10.1038/nrm3952

Saldi, T., Cortazar, M. A., Sheridan, R. M., & Bentley, D. L. (2016). Coupling of RNA Polymerase II Transcription Elongation with Pre-mRNA Splicing. *J Mol Biol*, *428*(12), 2623-2635. https://doi.org/10.1016/j.jmb.2016.04.017

Santos-Rosa, H., Schneider, R., Bannister, A. J., Sherriff, J., Bernstein, B. E., Emre, N. C., Schreiber, S. L., Mellor, J., & Kouzarides, T. (2002). Active genes are tri-methylated at K4 of histone H3. *Nature*, *419*(6905), 407-411. https://doi.org/10.1038/nature01080

Saunders, A., Werner, J., Andrulis, E. D., Nakayama, T., Hirose, S., Reinberg, D., & Lis, J. T. (2003). Tracking FACT and the RNA polymerase II elongation complex through chromatin in vivo. *Science*, *301*(5636), 1094-1096. https://doi.org/10.1126/science.1085712

Schaeffer, D., Tsanova, B., Barbas, A., Reis, F. P., Dastidar, E. G., Sanchez-Rotunno, M., Arraiano, C. M., & van Hoof, A. (2009). The exosome contains domains with specific endoribonuclease, exoribonuclease and cytoplasmic mRNA decay activities. *Nat Struct Mol Biol*, *16*(1), 56-62. https://doi.org/10.1038/nsmb.1528

Schlackow, M., Nojima, T., Gomes, T., Dhir, A., Carmo-Fonseca, M., & Proudfoot, N. J. (2017). Distinctive Patterns of Transcription and RNA Processing for Human lincRNAs. *Mol Cell*, *65*(1), 25-38. https://doi.org/10.1016/j.molcel.2016.11.029

Schmid, M., & Jensen, T. H. (2018). Controlling nuclear RNA levels. *Nat Rev Genet*, *19*(8), 518-529. https://doi.org/10.1038/s41576-018-0013-2

Schmidt, D., Wilson, M. D., Spyrou, C., Brown, G. D., Hadfield, J., & Odom, D. T. (2009). ChIP-seq: using high-throughput sequencing to discover protein-DNA interactions. *Methods*, *48*(3), 240-248. https://doi.org/10.1016/j.ymeth.2009.03.001

Schneider, C., Leung, E., Brown, J., & Tollervey, D. (2009). The N-terminal PIN domain of the exosome subunit Rrp44 harbors endonuclease activity and tethers Rrp44 to the yeast core exosome. *Nucleic Acids Res*, *37*(4), 1127-1140. https://doi.org/10.1093/nar/gkn1020

Schneider, C., & Tollervey, D. (2014). Looking into the barrel of the RNA exosome. *Nat Struct Mol Biol*, *21*(1), 17-18. https://doi.org/10.1038/nsmb.2750

Schneider, J., Bajwa, P., Johnson, F. C., Bhaumik, S. R., & Shilatifard, A. (2006). Rtt109 is required for proper H3K56 acetylation: a chromatin mark associated with the elongating RNA polymerase II. *J Biol Chem*, *281*(49), 37270-37274. https://doi.org/10.1074/jbc.C600265200

Schrank, B. R., Aparicio, T., Li, Y., Chang, W., Chait, B. T., Gundersen, G. G., Gottesman, M. E., & Gautier, J. (2018). Nuclear ARP2/3 drives DNA break clustering for homology-directed repair. *Nature*, *559*(7712), 61-66. https://doi.org/10.1038/s41586-018-0237-5

Schratt, G., Philippar, U., Berger, J., Schwarz, H., Heidenreich, O., & Nordheim, A. (2002). Serum response factor is crucial for actin cytoskeletal organization and focal adhesion assembly in embryonic stem cells. *J Cell Biol*, *156*(4), 737-750. https://doi.org/10.1083/jcb.200106008

Schroeder, S. C., Schwer, B., Shuman, S., & Bentley, D. (2000). Dynamic association of capping enzymes with transcribing RNA polymerase II. *Genes Dev*, *14*(19), 2435-2440. https://doi.org/10.1101/gad.836300

Schröder, S., Herker, E., Itzen, F., He, D., Thomas, S., Gilchrist, D. A., Kaehlcke, K., Cho, S., Pollard, K. S., Capra, J. A., Schnölzer, M., Cole, P. A., Geyer, M., Bruneau, B. G., Adelman, K., & Ott, M. (2013). Acetylation of RNA polymerase II regulates growth-factor-induced gene transcription in mammalian cells. *Mol Cell*, *52*(3), 314-324. https://doi.org/10.1016/j.molcel.2013.10.009

Schulze, W. M., & Cusack, S. (2017). Structural basis for mutually exclusive co-transcriptional nuclear cap-binding complexes with either NELF-E or ARS2. *Nat Commun*, *8*(1), 1302. https://doi.org/10.1038/s41467-017-01402-w

Schulze, W. M., Stein, F., Rettel, M., Nanao, M., & Cusack, S. (2018). Structural analysis of human ARS2 as a platform for co-transcriptional RNA sorting. *Nat Commun*, *9*(1), 1701. https://doi.org/10.1038/s41467-018-04142-7

Schwalb, B., Michel, M., Zacher, B., Frühauf, K., Demel, C., Tresch, A., Gagneur, J., & Cramer, P. (2016). TT-seq maps the human transient transcriptome. *Science*, *352*(6290), 1225-1228. https://doi.org/10.1126/science.aad9841

Schwartz, B. E., Larochelle, S., Suter, B., & Lis, J. T. (2003). Cdk7 is required for full activation of Drosophila heat shock genes and RNA polymerase II phosphorylation in vivo. *Mol Cell Biol*, *23*(19), 6876-6886. https://doi.org/10.1128/mcb.23.19.6876-6886.2003

Schübeler, D., MacAlpine, D. M., Scalzo, D., Wirbelauer, C., Kooperberg, C., van Leeuwen, F., Gottschling, D. E., O'Neill, L. P., Turner, B. M., Delrow, J., Bell, S. P., & Groudine, M. (2004). The histone modification pattern of active genes revealed through genome-wide chromatin analysis of a higher eukaryote. *Genes Dev*, *18*(11), 1263-1271. https://doi.org/10.1101/gad.1198204

Schüller, R., Forné, I., Straub, T., Schreieck, A., Texier, Y., Shah, N., Decker, T. M., Cramer, P., Imhof, A., & Eick, D. (2016). Heptad-Specific Phosphorylation of RNA Polymerase II CTD. *Mol Cell*, *61*(2), 305-314. https://doi.org/10.1016/j.molcel.2015.12.003

Seila, A. C., Calabrese, J. M., Levine, S. S., Yeo, G. W., Rahl, P. B., Flynn, R. A., Young, R. A., & Sharp, P. A. (2008). Divergent transcription from active promoters. *Science*, *322*(5909), 1849-1851. https://doi.org/10.1126/science.1162253

Sharili, A. S., Kenny, F. N., Vartiainen, M. K., & Connelly, J. T. (2016). Nuclear actin modulates cell motility via transcriptional regulation of adhesive and cytoskeletal genes. *Sci Rep*, *6*, 33893. https://doi.org/10.1038/srep33893

Shatkin, A. J., & Manley, J. L. (2000). The ends of the affair: capping and polyadenylation. *Nat Struct Biol*, *7*(10), 838-842. https://doi.org/10.1038/79583

Shaw, P. E., Frasch, S., & Nordheim, A. (1989). Repression of c-fos transcription is mediated through p67SRF bound to the SRE. *EMBO J*, *8*(9), 2567-2574.

Shcherbik, N., Wang, M., Lapik, Y. R., Srivastava, L., & Pestov, D. G. (2010). Polyadenylation and degradation of incomplete RNA polymerase I transcripts in mammalian cells. *EMBO Rep*, *11*(2), 106-111. https://doi.org/10.1038/embor.2009.271

Shearwin, K. E., Callen, B. P., & Egan, J. B. (2005). Transcriptional interference--a crash course. *Trends Genet*, *21*(6), 339-345. https://doi.org/10.1016/j.tig.2005.04.009

Shetty, A., Kallgren, S. P., Demel, C., Maier, K. C., Spatt, D., Alver, B. H., Cramer, P., Park, P. J., & Winston, F. (2017). Spt5 Plays Vital Roles in the Control of Sense and Antisense Transcription Elongation. *Mol Cell*, *66*(1), 77-88.e75. https://doi.org/10.1016/j.molcel.2017.02.023

Shim, E. Y., Walker, A. K., Shi, Y., & Blackwell, T. K. (2002). CDK-9/cyclin T (P-TEFb) is required in two postinitiation pathways for transcription in the C. elegans embryo. *Genes Dev*, *16*(16), 2135-2146. https://doi.org/10.1101/gad.999002

Shore, P., & Sharrocks, A. D. (1995). The MADS-box family of transcription factors. *Eur J Biochem*, *229*(1), 1-13. https://doi.org/10.1111/j.1432-1033.1995.tb20430.x

Shukla, S., & Oberdoerffer, S. (2012). Co-transcriptional regulation of alternative pre-mRNA splicing. *Biochim Biophys Acta*, *1819*(7), 673-683. https://doi.org/10.1016/j.bbagrm.2012.01.014

Sigova, A. A., Abraham, B. J., Ji, X., Molinie, B., Hannett, N. M., Guo, Y. E., Jangi, M., Giallourakis, C. C., Sharp, P. A., & Young, R. A. (2015). Transcription factor trapping by RNA in gene regulatory elements. *Science*, *350*(6263), 978-981. https://doi.org/10.1126/science.aad3346

Sigova, A. A., Mullen, A. C., Molinie, B., Gupta, S., Orlando, D. A., Guenther, M. G., Almada, A. E., Lin, C., Sharp, P. A., Giallourakis, C. C., & Young, R. A. (2013). Divergent transcription of long noncoding RNA/mRNA gene pairs in embryonic stem cells. *Proc Natl Acad Sci U S A*, *110*(8), 2876-2881. https://doi.org/10.1073/pnas.1221904110

Silla, T., Karadoulama, E., Mąkosa, D., Lubas, M., & Jensen, T. H. (2018). The RNA Exosome Adaptor ZFC3H1 Functionally Competes with Nuclear Export Activity to Retain Target Transcripts. *Cell Rep*, *23*(7), 2199-2210. https://doi.org/10.1016/j.celrep.2018.04.061

Silla, T., Schmid, M., Dou, Y., Garland, W., Milek, M., Imami, K., Johnsen, D., Polak, P., Andersen, J. S., Selbach, M., Landthaler, M., & Jensen, T. H. (2020). The human ZC3H3 and RBM26/27 proteins are critical for PAXT-mediated nuclear RNA decay. *Nucleic Acids Res*, *48*(5), 2518-2530. https://doi.org/10.1093/nar/gkz1238

Simic, R., Lindstrom, D. L., Tran, H. G., Roinick, K. L., Costa, P. J., Johnson, A. D., Hartzog, G. A., & Arndt, K. M. (2003). Chromatin remodeling protein Chd1 interacts with transcription elongation factors and localizes to transcribed genes. *EMBO J*, *22*(8), 1846-1856. https://doi.org/10.1093/emboj/cdg179

Sims, R. J., Rojas, L. A., Beck, D. B., Bonasio, R., Schüller, R., Drury, W. J., Eick, D., & Reinberg, D. (2011). The C-terminal domain of RNA polymerase II is modified by site-specific methylation. *Science*, *332*(6025), 99-103. https://doi.org/10.1126/science.1202663

Skaar, D. A., & Greenleaf, A. L. (2002). The RNA polymerase II CTD kinase CTDK-I affects pre-mRNA 3' cleavage/polyadenylation through the processing component Pti1p. *Mol Cell*, *10*(6), 1429-1439. https://doi.org/10.1016/s1097-2765(02)00731-1

Solier, S., Ryan, M. C., Martin, S. E., Varma, S., Kohn, K. W., Liu, H., Zeeberg, B. R., & Pommier, Y. (2013). Transcription poisoning by Topoisomerase I is controlled by gene length, splice sites, and miR-142-3p. *Cancer Res*, *73*(15), 4830-4839. https://doi.org/10.1158/0008-5472.CAN-12-3504

Songyang, Z., Lu, K. P., Kwon, Y. T., Tsai, L. H., Filhol, O., Cochet, C., Brickey, D. A., Soderling, T. R., Bartleson, C., Graves, D. J., DeMaggio, A. J., Hoekstra, M. F., Blenis, J., Hunter, T., & Cantley, L. C. (1996). A structural basis for substrate specificities of protein Ser/Thr kinases: primary sequence preference of casein kinases I and II, NIMA, phosphorylase kinase, calmodulin-dependent kinase II,

CDK5, and Erk1. *Mol Cell Biol*, *16*(11), 6486-6493. https://doi.org/10.1128/mcb.16.11.6486

Sotiropoulos, A., Gineitis, D., Copeland, J., & Treisman, R. (1999). Signal-regulated activation of serum response factor is mediated by changes in actin dynamics. *Cell*, *98*(2), 159-169.

Spector, B. M., Turek, M. E., & Price, D. H. (2019). Functional interaction of human Ssu72 with RNA polymerase II complexes. *PLoS One*, *14*(3), e0213598. https://doi.org/10.1371/journal.pone.0213598

Spector, I., Shochet, N. R., Blasberger, D., & Kashman, Y. (1989). Latrunculins--novel marine macrolides that disrupt microfilament organization and affect cell growth: I. Comparison with cytochalasin D. *Cell Motil Cytoskeleton*, *13*(3), 127-144. https://doi.org/10.1002/cm.970130302

Spector, I., Shochet, N. R., Kashman, Y., & Groweiss, A. (1983). Latrunculins: novel marine toxins that disrupt microfilament organization in cultured cells. *Science*, *219*(4584), 493-495. https://doi.org/10.1126/science.6681676

Srivastava, R., & Ahn, S. H. (2015). Modifications of RNA polymerase II CTD: Connections to the histone code and cellular function. *Biotechnol Adv*, *33*(6 Pt 1), 856-872. https://doi.org/10.1016/j.biotechadv.2015.07.008

Staals, R. H., Bronkhorst, A. W., Schilders, G., Slomovic, S., Schuster, G., Heck, A. J., Raijmakers, R., & Pruijn, G. J. (2010). Dis3-like 1: a novel exoribonuclease associated with the human exosome. *EMBO J*, *29*(14), 2358-2367. https://doi.org/10.1038/emboj.2010.122

Stavreva, D. A., Müller, W. G., Hager, G. L., Smith, C. L., & McNally, J. G. (2004). Rapid glucocorticoid receptor exchange at a promoter is coupled to transcription and regulated by chaperones and proteasomes. *Mol Cell Biol*, *24*(7), 2682-2697. https://doi.org/10.1128/mcb.24.7.2682-2697.2004

Steger, D. J., Lefterova, M. I., Ying, L., Stonestrom, A. J., Schupp, M., Zhuo, D., Vakoc, A. L., Kim, J. E., Chen, J., Lazar, M. A., Blobel, G. A., & Vakoc, C. R. (2008). DOT1L/KMT4 recruitment and H3K79 methylation are ubiquitously coupled with gene transcription in mammalian cells. *Mol Cell Biol*, *28*(8), 2825-2839. https://doi.org/10.1128/MCB.02076-07

Stern, S., Debre, E., Stritt, C., Berger, J., Posern, G., & Knöll, B. (2009). A nuclear actin function regulates neuronal motility by serum response factor-dependent gene transcription. *J Neurosci*, *29*(14), 4512-4518. https://doi.org/10.1523/JNEUROSCI.0333-09.2009

Sterner, D. E., & Berger, S. L. (2000). Acetylation of histones and transcription-related factors. *Microbiol Mol Biol Rev*, *64*(2), 435-459. https://doi.org/10.1128/mmbr.64.2.435-459.2000

Strahl, B. D., & Allis, C. D. (2000). The language of covalent histone modifications. *Nature*, *403*(6765), 41-45. https://doi.org/10.1038/47412

Strahl, B. D., Grant, P. A., Briggs, S. D., Sun, Z. W., Bone, J. R., Caldwell, J. A., Mollah, S., Cook, R. G., Shabanowitz, J., Hunt, D. F., & Allis, C. D. (2002). Set2 is a nucleosomal histone H3-selective methyltransferase that mediates transcriptional repression. *Mol Cell Biol*, *22*(5), 1298-1306. https://doi.org/10.1128/mcb.22.5.1298-1306.2002

Strässer, K., & Hurt, E. (2000). Yra1p, a conserved nuclear RNA-binding protein, interacts directly with Mex67p and is required for mRNA export. *EMBO J*, *19*(3), 410-420. https://doi.org/10.1093/emboj/19.3.410

Subramanian, A., Tamayo, P., Mootha, V. K., Mukherjee, S., Ebert, B. L., Gillette, M. A., Paulovich, A., Pomeroy, S. L., Golub, T. R., Lander, E. S., & Mesirov, J. P. (2005). Gene set enrichment analysis: a knowledge-based approach for interpreting genome-wide expression profiles. *Proc Natl Acad Sci U S A*, *102*(43), 15545-15550. https://doi.org/10.1073/pnas.0506580102

Suh, H., Ficarro, S. B., Kang, U. B., Chun, Y., Marto, J. A., & Buratowski, S. (2016). Direct Analysis of Phosphorylation Sites on the Rpb1 C-Terminal Domain of RNA Polymerase II. *Mol Cell*, *61*(2), 297-304. https://doi.org/10.1016/j.molcel.2015.12.021

Sun, M., Larivière, L., Dengl, S., Mayer, A., & Cramer, P. (2010). A tandem SH2 domain in transcription elongation factor Spt6 binds the phosphorylated RNA polymerase II C-terminal repeat domain (CTD). *J Biol Chem*, *285*(53), 41597-41603. https://doi.org/10.1074/jbc.M110.144568

Sun, X., Zhang, Y., Cho, H., Rickert, P., Lees, E., Lane, W., & Reinberg, D. (1998). NAT, a human complex containing Srb polypeptides that functions as a negative regulator of activated transcription. *Mol Cell*, *2*(2), 213-222. https://doi.org/10.1016/s1097-2765(00)80131-8

Sun, Y., Boyd, K., Xu, W., Ma, J., Jackson, C. W., Fu, A., Shillingford, J. M., Robinson, G. W., Hennighausen, L., Hitzler, J. K., Ma, Z., & Morris, S. W. (2006). Acute myeloid leukemia-associated Mkl1 (Mrtf-a) is a key regulator of mammary gland function. *Mol Cell Biol*, *26*(15), 5809-5826. https://doi.org/10.1128/MCB.00024-06

Sun, Z. W., & Allis, C. D. (2002). Ubiquitination of histone H2B regulates H3 methylation and gene silencing in yeast. *Nature*, *418*(6893), 104-108. https://doi.org/10.1038/nature00883

Taatjes, D. J. (2010). The human Mediator complex: a versatile, genome-wide regulator of transcription. *Trends Biochem Sci*, *35*(6), 315-322. https://doi.org/10.1016/j.tibs.2010.02.004

Takagaki, Y., Ryner, L. C., & Manley, J. L. (1989). Four factors are required for 3'-end cleavage of pre-mRNAs. *Genes Dev*, *3*(11), 1711-1724. https://doi.org/10.1101/gad.3.11.1711

Takahashi, H., Parmely, T. J., Sato, S., Tomomori-Sato, C., Banks, C. A., Kong, S. E., Szutorisz, H., Swanson, S. K., Martin-Brown, S., Washburn, M. P., Florens, L., Seidel, C. W., Lin, C., Smith, E. R., Shilatifard, A., Conaway, R. C., & Conaway, J. W. (2011). Human mediator subunit MED26 functions as a docking site for transcription elongation factors. *Cell*, *146*(1), 92-104. https://doi.org/10.1016/j.cell.2011.06.005

Talbert, P. B., & Henikoff, S. (2010). Histone variants--ancient wrap artists of the epigenome. *Nat Rev Mol Cell Biol*, *11*(4), 264-275. https://doi.org/10.1038/nrm2861

Tan-Wong, S. M., French, J. D., Proudfoot, N. J., & Brown, M. A. (2008). Dynamic interactions between the promoter and terminator regions of the mammalian BRCA1 gene. *Proc Natl Acad Sci U S A*, *105*(13), 5160-5165. https://doi.org/10.1073/pnas.0801048105

Tan-Wong, S. M., Wijayatilake, H. D., & Proudfoot, N. J. (2009). Gene loops function to maintain transcriptional memory through interaction with the nuclear pore complex. *Genes Dev*, *23*(22), 2610-2624. https://doi.org/10.1101/gad.1823209

Tan-Wong, S. M., Zaugg, J. B., Camblong, J., Xu, Z., Zhang, D. W., Mischo, H. E., Ansari, A. Z., Luscombe, N. M., Steinmetz, L. M., & Proudfoot, N. J. (2012). Gene loops enhance transcriptional directionality. *Science*, *338*(6107), 671-675. https://doi.org/10.1126/science.1224350

Tellam, R., & Frieden, C. (1982). Cytochalasin D and platelet gelsolin accelerate actin polymer formation. A model for regulation of the extent of actin polymer formation in vivo. *Biochemistry*, *21*(13), 3207-3214.

Tian, B., Yang, J., & Brasier, A. R. (2012). Two-step cross-linking for analysis of protein-chromatin interactions. *Methods Mol Biol*, *809*, 105-120. https://doi.org/10.1007/978-1-61779-376-9_7

Tie, F., Banerjee, R., Stratton, C. A., Prasad-Sinha, J., Stepanik, V., Zlobin, A., Diaz, M. O., Scacheri, P. C., & Harte, P. J. (2009). CBP-mediated acetylation of histone H3 lysine 27 antagonizes Drosophila Polycomb silencing. *Development*, *136*(18), 3131-3141. https://doi.org/10.1242/dev.037127

Tietjen, J. R., Zhang, D. W., Rodríguez-Molina, J. B., White, B. E., Akhtar, M. S., Heidemann, M., Li, X., Chapman, R. D., Shokat, K., Keles, S., Eick, D., & Ansari, A. Z. (2010). Chemical-genomic dissection of the CTD code. *Nat Struct Mol Biol*, *17*(9), 1154-1161. https://doi.org/10.1038/nsmb.1900

Tomecki, R., Kristiansen, M. S., Lykke-Andersen, S., Chlebowski, A., Larsen, K. M., Szczesny, R. J., Drazkowska, K., Pastula, A., Andersen, J. S., Stepien, P. P., Dziembowski, A., & Jensen, T. H. (2010). The human core exosome interacts with differentially localized processive RNases: hDIS3 and hDIS3L. *EMBO J*, *29*(14), 2342-2357. https://doi.org/10.1038/emboj.2010.121

Tominaga, T., Sahai, E., Chardin, P., McCormick, F., Courtneidge, S. A., & Alberts, A. S. (2000). Diaphanous-related formins bridge Rho GTPase and Src tyrosine kinase signaling. *Mol Cell*, *5*(1), 13-25. https://doi.org/10.1016/s1097-2765(00)80399-8

Topisirovic, I., Svitkin, Y. V., Sonenberg, N., & Shatkin, A. J. (2011). Cap and cap-binding proteins in the control of gene expression. *Wiley Interdiscip Rev RNA*, *2*(2), 277-298. https://doi.org/10.1002/wrna.52

Torchet, C., Bousquet-Antonelli, C., Milligan, L., Thompson, E., Kufel, J., & Tollervey, D. (2002). Processing of 3'-extended read-through transcripts by the exosome can generate functional mRNAs. *Mol Cell*, *9*(6), 1285-1296. https://doi.org/10.1016/s1097-2765(02)00544-0

Treisman, R. (1985). Transient accumulation of c-fos RNA following serum stimulation requires a conserved 5' element and c-fos 3' sequences. *Cell*, *42*(3), 889-902. https://doi.org/10.1016/0092-8674(85)90285-5

Treisman, R. (1986). Identification of a protein-binding site that mediates transcriptional response of the c-fos gene to serum factors. *Cell*, *46*(4), 567-574. https://doi.org/10.1016/0092-8674(86)90882-2

Treisman, R. (1990). The SRE: a growth factor responsive transcriptional regulator. *Semin Cancer Biol*, *1*(1), 47-58.

Treisman, R. (1994). Ternary complex factors: growth factor regulated transcriptional activators. *Curr Opin Genet Dev*, *4*(1), 96-101.

Trigon, S., Serizawa, H., Conaway, J. W., Conaway, R. C., Jackson, S. P., & Morange, M. (1998). Characterization of the residues phosphorylated in vitro by different C-terminal domain kinases. *J Biol Chem*, *273*(12), 6769-6775. https://doi.org/10.1074/jbc.273.12.6769

Tropberger, P., Pott, S., Keller, C., Kamieniarz-Gdula, K., Caron, M., Richter, F., Li, G., Mittler, G., Liu, E. T., Bühler, M., Margueron, R., & Schneider, R. (2013). Regulation of transcription through acetylation of H3K122 on the lateral surface of the histone octamer. *Cell*, *152*(4), 859-872. https://doi.org/10.1016/j.cell.2013.01.032

Tufegdžić Vidaković, A., Mitter, R., Kelly, G. P., Neumann, M., Harreman, M., Rodríguez-Martínez, M., Herlihy, A., Weems, J. C., Boeing, S., Encheva, V., Gaul, L., Milligan, L., Tollervey, D., Conaway, R. C., Conaway, J. W., Snijders, A. P., Stewart, A., & Svejstrup, J. Q. (2020). Regulation of the RNAPII Pool Is Integral to the DNA Damage Response. *Cell*, *180*(6), 1245-1261.e1221. https://doi.org/10.1016/j.cell.2020.02.009

Tybulewicz, V. L., Crawford, C. E., Jackson, P. K., Bronson, R. T., & Mulligan, R. C. (1991). Neonatal lethality and lymphopenia in mice with a homozygous disruption of the c-abl proto-oncogene. *Cell*, *65*(7), 1153-1163. https://doi.org/10.1016/0092-8674(91)90011-m

Ule, J., Jensen, K., Mele, A., & Darnell, R. B. (2005). CLIP: a method for identifying protein-RNA interaction sites in living cells. *Methods*, *37*(4), 376-386. https://doi.org/10.1016/j.ymeth.2005.07.018

Vakoc, C. R., Sachdeva, M. M., Wang, H., & Blobel, G. A. (2006). Profile of histone lysine methylation across transcribed mammalian chromatin. *Mol Cell Biol*, *26*(24), 9185-9195. https://doi.org/10.1128/MCB.01529-06

Valen, E., Preker, P., Andersen, P. R., Zhao, X., Chen, Y., Ender, C., Dueck, A., Meister, G., Sandelin, A., & Jensen, T. H. (2011). Biogenic mechanisms and utilization of small RNAs derived from human protein-coding genes. *Nat Struct Mol Biol*, *18*(9), 1075-1082. https://doi.org/10.1038/nsmb.2091

Vanácová, S., Wolf, J., Martin, G., Blank, D., Dettwiler, S., Friedlein, A., Langen, H., Keith, G., & Keller, W. (2005). A new yeast poly(A) polymerase complex involved in RNA quality control. *PLoS Biol*, *3*(6), e189. https://doi.org/10.1371/journal.pbio.0030189

Vartiainen, M. K., Guettler, S., Larijani, B., & Treisman, R. (2007). Nuclear actin regulates dynamic subcellular localization and activity of the SRF cofactor MAL. *Science*, *316*(5832), 1749-1752. https://doi.org/10.1126/science.1141084

Vitaliano-Prunier, A., Babour, A., Hérissant, L., Apponi, L., Margaritis, T., Holstege, F. C., Corbett, A. H., Gwizdek, C., & Dargemont, C. (2012). H2B ubiquitylation controls the formation of export-competent mRNP. *Mol Cell*, *45*(1), 132-139. https://doi.org/10.1016/j.molcel.2011.12.011

Vogelauer, M., Wu, J., Suka, N., & Grunstein, M. (2000). Global histone acetylation and deacetylation in yeast. *Nature*, *408*(6811), 495-498. https://doi.org/10.1038/35044127

Volanakis, A., Kamieniarz-Gdula, K., Schlackow, M., & Proudfoot, N. J. (2017). WNK1 kinase and the termination factor PCF11 connect nuclear mRNA export with transcription. *Genes Dev*, *31*(21), 2175-2185. https://doi.org/10.1101/gad.303677.117

Voss, K., Forné, I., Descostes, N., Hintermair, C., Schüller, R., Maqbool, M. A., Heidemann, M., Flatley, A., Imhof, A., Gut, M., Gut, I., Kremmer, E., Andrau, J. C., & Eick, D. (2015). Site-specific methylation and acetylation of lysine residues in the C-terminal domain (CTD) of RNA polymerase II. *Transcription*, *6*(5), 91-101. https://doi.org/10.1080/21541264.2015.1114983

Wada, T., Takagi, T., Yamaguchi, Y., Ferdous, A., Imai, T., Hirose, S., Sugimoto, S., Yano, K., Hartzog, G. A., Winston, F., Buratowski, S., & Handa, H. (1998). DSIF, a novel transcription elongation factor that regulates RNA polymerase II processivity, is composed of human Spt4 and Spt5 homologs. *Genes Dev*, *12*(3), 343-356. https://doi.org/10.1101/gad.12.3.343

Wagschal, A., Rousset, E., Basavarajaiah, P., Contreras, X., Harwig, A., Laurent-Chabalier, S., Nakamura, M., Chen, X., Zhang, K., Meziane, O., Boyer, F., Parrinello, H., Berkhout, B., Terzian, C., Benkirane, M., & Kiernan, R. (2012). Microprocessor, Setx, Xrn2, and Rrp6 co-operate to induce premature termination of transcription by RNAPII. *Cell*, *150*(6), 1147-1157. https://doi.org/10.1016/j.cell.2012.08.004

Wang, D. Z., Li, S., Hockemeyer, D., Sutherland, L., Wang, Z., Schratt, G., Richardson, J. A., Nordheim, A., & Olson, E. N. (2002). Potentiation of serum response factor activity by a family of myocardin-related transcription factors. *Proc Natl Acad Sci U S A*, *99*(23), 14855-14860. https://doi.org/10.1073/pnas.222561499

Wang, D. Z., & Olson, E. N. (2004). Control of smooth muscle development by the myocardin family of transcriptional coactivators. *Curr Opin Genet Dev*, *14*(5), 558-566. https://doi.org/10.1016/j.gde.2004.08.003

Wang, J., Chen, J., Wu, G., Zhang, H., Du, X., Chen, S., Zhang, L., Wang, K., Fan, J., Gao, S., Wu, X., Zhang, S., Kuai, B., Zhao, P., Chi, B., Wang, L., Li, G., Wong,

C. C. L., Zhou, Y., Li, J., Yun, C., & Cheng, H. (2019). NRDE2 negatively regulates exosome functions by inhibiting MTR4 recruitment and exosome interaction. *Genes Dev*, *33*(9-10), 536-549. https://doi.org/10.1101/gad.322602.118

Wang, Y., Fairley, J. A., & Roberts, S. G. (2010). Phosphorylation of TFIIB links transcription initiation and termination. *Curr Biol*, *20*(6), 548-553. https://doi.org/10.1016/j.cub.2010.01.052

Wang, Y., Sherrard, A., Zhao, B., Melak, M., Trautwein, J., Kleinschnitz, E. M., Tsopoulidis, N., Fackler, O. T., Schwan, C., & Grosse, R. (2019). GPCR-induced calcium transients trigger nuclear actin assembly for chromatin dynamics. *Nat Commun*, *10*(1), 5271. https://doi.org/10.1038/s41467-019-13322-y

Wang, Z., Zang, C., Rosenfeld, J. A., Schones, D. E., Barski, A., Cuddapah, S., Cui, K., Roh, T. Y., Peng, W., Zhang, M. Q., & Zhao, K. (2008). Combinatorial patterns of histone acetylations and methylations in the human genome. *Nat Genet*, *40*(7), 897-903. https://doi.org/10.1038/ng.154

Wani, S., Yuda, M., Fujiwara, Y., Yamamoto, M., Harada, F., Ohkuma, Y., & Hirose, Y. (2014). Vertebrate Ssu72 regulates and coordinates 3'-end formation of RNAs transcribed by RNA polymerase II. *PLoS One*, *9*(8), e106040. https://doi.org/10.1371/journal.pone.0106040

Wasylyk, B., & Chambon, P. (1979). Transcription by eukaryotic RNA polymerases A and B of chromatin assembled in vitro. *Eur J Biochem*, *98*(2), 317-327. https://doi.org/10.1111/j.1432-1033.1979.tb13191.x

Weick, E. M., Puno, M. R., Januszyk, K., Zinder, J. C., DiMattia, M. A., & Lima, C. D. (2018). Helicase-Dependent RNA Decay Illuminated by a Cryo-EM Structure of a Human Nuclear RNA Exosome-MTR4 Complex. *Cell*, *173*(7), 1663-1677.e1621. https://doi.org/10.1016/j.cell.2018.05.041

Weil, P. A., Luse, D. S., Segall, J., & Roeder, R. G. (1979). Selective and accurate initiation of transcription at the Ad2 major late promotor in a soluble system dependent on purified RNA polymerase II and DNA. *Cell*, *18*(2), 469-484. https://doi.org/10.1016/0092-8674(79)90065-5

Weinl, C., Riehle, H., Park, D., Stritt, C., Beck, S., Huber, G., Wolburg, H., Olson, E. N., Seeliger, M. W., Adams, R. H., & Nordheim, A. (2013). Endothelial SRF/MRTF ablation causes vascular disease phenotypes in murine retinae. *J Clin Invest*, *123*(5), 2193-2206. https://doi.org/10.1172/JCI64201

Weinl, C., Wasylyk, C., Garcia Garrido, M., Sothilingam, V., Beck, S. C., Riehle, H., Stritt, C., Roux, M. J., Seeliger, M. W., Wasylyk, B., & Nordheim, A. (2014). Elk3 deficiency causes transient impairment in post-natal retinal vascular development and formation of tortuous arteries in adult murine retinae. *PLoS One*, *9*(9), e107048. https://doi.org/10.1371/journal.pone.0107048

Weissbach, J., Schikora, F., Weber, A., Kessels, M., & Posern, G. (2016). Myocardin-Related Transcription Factor A Activation by Competition with WH2 Domain Proteins for Actin Binding. *Mol Cell Biol*, *36*(10), 1526-1539. https://doi.org/10.1128/MCB.01097-15

West, M. L., & Corden, J. L. (1995). Construction and analysis of yeast RNA polymerase II CTD deletion and substitution mutations. *Genetics*, *140*(4), 1223-1233.

West, S., Gromak, N., & Proudfoot, N. J. (2004). Human 5' --> 3' exonuclease Xrn2 promotes transcription termination at co-transcriptional cleavage sites. *Nature*, *432*(7016), 522-525. https://doi.org/10.1038/nature03035

West, S., & Proudfoot, N. J. (2008). Human Pcf11 enhances degradation of RNA polymerase II-associated nascent RNA and transcriptional termination. *Nucleic Acids Res*, *36*(3), 905-914. https://doi.org/10.1093/nar/gkm1112

White, E., Kamieniarz-Gdula, K., Dye, M. J., & Proudfoot, N. J. (2013). AT-rich sequence elements promote nascent transcript cleavage leading to RNA polymerase II termination. *Nucleic Acids Res*, *41*(3), 1797-1806. https://doi.org/10.1093/nar/gks1335

White, M. D., Angiolini, J. F., Alvarez, Y. D., Kaur, G., Zhao, Z. W., Mocskos, E., Bruno, L., Bissiere, S., Levi, V., & Plachta, N. (2016). Long-Lived Binding of Sox2 to DNA Predicts Cell Fate in the Four-Cell Mouse Embryo. *Cell*, *165*(1), 75-87. https://doi.org/10.1016/j.cell.2016.02.032

Whittaker, S. R., Mallinger, A., Workman, P., & Clarke, P. A. (2017). Inhibitors of cyclin-dependent kinases as cancer therapeutics. *Pharmacol Ther*, *173*, 83-105. https://doi.org/10.1016/j.pharmthera.2017.02.008

Wiezlak, M., Diring, J., Abella, J., Mouilleron, S., Way, M., McDonald, N. Q., & Treisman, R. (2012). G-actin regulates the shuttling and PP1 binding of the RPEL protein Phactr1 to control actomyosin assembly. *J Cell Sci*, *125*(Pt 23), 5860-5872. https://doi.org/10.1242/jcs.112078

Williams, S. K., Truong, D., & Tyler, J. K. (2008). Acetylation in the globular core of histone H3 on lysine-56 promotes chromatin disassembly during transcriptional activation. *Proc Natl Acad Sci U S A*, *105*(26), 9000-9005. https://doi.org/10.1073/pnas.0800057105

Wirbelauer, C., Bell, O., & Schübeler, D. (2005). Variant histone H3.3 is deposited at sites of nucleosomal displacement throughout transcribed genes while active histone modifications show a promoter-proximal bias. *Genes Dev*, *19*(15), 1761-1766. https://doi.org/10.1101/gad.347705

Wong, K. H., Jin, Y., & Struhl, K. (2014). TFIIH phosphorylation of the Pol II CTD stimulates mediator dissociation from the preinitiation complex and promoter escape. *Mol Cell*, *54*(4), 601-612. https://doi.org/10.1016/j.molcel.2014.03.024

Wood, A., Schneider, J., Dover, J., Johnston, M., & Shilatifard, A. (2005). The Bur1/Bur2 complex is required for histone H2B monoubiquitination by Rad6/Bre1 and histone methylation by COMPASS. *Mol Cell*, *20*(4), 589-599. https://doi.org/10.1016/j.molcel.2005.09.010

Wright, R. H., Lioutas, A., Le Dily, F., Soronellas, D., Pohl, A., Bonet, J., Nacht, A. S., Samino, S., Font-Mateu, J., Vicent, G. P., Wierer, M., Trabado, M. A., Schelhorn, C., Carolis, C., Macias, M. J., Yanes, O., Oliva, B., & Beato, M. (2016). ADP-ribose-derived nuclear ATP synthesis by NUDIX5 is required for chromatin remodeling. *Science*, *352*(6290), 1221-1225. https://doi.org/10.1126/science.aad9335

Wu, C. H., Yamaguchi, Y., Benjamin, L. R., Horvat-Gordon, M., Washinsky, J., Enerly, E., Larsson, J., Lambertsson, A., Handa, H., & Gilmour, D. (2003). NELF and DSIF cause promoter proximal pausing on the hsp70 promoter in Drosophila. *Genes Dev*, *17*(11), 1402-1414. https://doi.org/10.1101/gad.1091403

Wu, G., Schmid, M., Rib, L., Polak, P., Meola, N., Sandelin, A., & Jensen, T. H. (2020). A Two-Layered Targeting Mechanism Underlies Nuclear RNA Sorting by the Human Exosome. *Cell Rep*, *30*(7), 2387-2401.e2385. https://doi.org/10.1016/j.celrep.2020.01.068

Wu, T., Pinto, H. B., Kamikawa, Y. F., & Donohoe, M. E. (2015). The BET family member BRD4 interacts with OCT4 and regulates pluripotency gene expression. *Stem Cell Reports*, *4*(3), 390-403. https://doi.org/10.1016/j.stemcr.2015.01.012

Wu, X., Wilcox, C. B., Devasahayam, G., Hackett, R. L., Arévalo-Rodríguez, M., Cardenas, M. E., Heitman, J., & Hanes, S. D. (2000). The Ess1 prolyl isomerase is linked to chromatin remodeling complexes and the general transcription machinery. *EMBO J*, *19*(14), 3727-3738. https://doi.org/10.1093/emboj/19.14.3727

Wyers, F., Rougemaille, M., Badis, G., Rousselle, J. C., Dufour, M. E., Boulay, J., Régnault, B., Devaux, F., Namane, A., Séraphin, B., Libri, D., & Jacquier, A. (2005). Cryptic pol II transcripts are degraded by a nuclear quality control pathway involving a new poly(A) polymerase. *Cell*, *121*(5), 725-737. https://doi.org/10.1016/j.cell.2005.04.030

Xiang, K., Manley, J. L., & Tong, L. (2012). An unexpected binding mode for a Pol II CTD peptide phosphorylated at Ser7 in the active site of the CTD phosphatase Ssu72. *Genes Dev*, *26*(20), 2265-2270. https://doi.org/10.1101/gad.198853.112

Xiao, T., Hall, H., Kizer, K. O., Shibata, Y., Hall, M. C., Borchers, C. H., & Strahl, B. D. (2003). Phosphorylation of RNA polymerase II CTD regulates H3 methylation in yeast. *Genes Dev*, *17*(5), 654-663. https://doi.org/10.1101/gad.1055503

Xiao, T., Kao, C. F., Krogan, N. J., Sun, Z. W., Greenblatt, J. F., Osley, M. A., & Strahl, B. D. (2005). Histone H2B ubiquitylation is associated with elongating RNA polymerase II. *Mol Cell Biol*, *25*(2), 637-651. https://doi.org/10.1128/MCB.25.2.637-651.2005

Xu, F., Zhang, K., & Grunstein, M. (2005). Acetylation in histone H3 globular domain regulates gene expression in yeast. *Cell*, *121*(3), 375-385. https://doi.org/10.1016/j.cell.2005.03.011

Xu, Y. X., Hirose, Y., Zhou, X. Z., Lu, K. P., & Manley, J. L. (2003). Pin1 modulates the structure and function of human RNA polymerase II. *Genes Dev*, *17*(22), 2765-2776. https://doi.org/10.1101/gad.1135503

Xu, Y. X., & Manley, J. L. (2007). Pin1 modulates RNA polymerase II activity during the transcription cycle. *Genes Dev*, *21*(22), 2950-2962. https://doi.org/10.1101/gad.1592807

Xu, Z., Wei, W., Gagneur, J., Perocchi, F., Clauder-Münster, S., Camblong, J., Guffanti, E., Stutz, F., Huber, W., & Steinmetz, L. M. (2009). Bidirectional promoters generate pervasive transcription in yeast. *Nature*, *457*(7232), 1033-1037. https://doi.org/10.1038/nature07728

Yamada, T., Yamaguchi, Y., Inukai, N., Okamoto, S., Mura, T., & Handa, H. (2006). P-TEFb-mediated phosphorylation of hSpt5 C-terminal repeats is critical for processive transcription elongation. *Mol Cell*, *21*(2), 227-237. https://doi.org/10.1016/j.molcel.2005.11.024

Yamaguchi, Y., Takagi, T., Wada, T., Yano, K., Furuya, A., Sugimoto, S., Hasegawa, J., & Handa, H. (1999). NELF, a multisubunit complex containing RD, cooperates with DSIF to repress RNA polymerase II elongation. *Cell*, *97*(1), 41-51. https://doi.org/10.1016/s0092-8674(00)80713-8

Yamaguchi, Y., Wada, T., Watanabe, D., Takagi, T., Hasegawa, J., & Handa, H. (1999). Structure and function of the human transcription elongation factor DSIF. *J Biol Chem*, *274*(12), 8085-8092. https://doi.org/10.1074/jbc.274.12.8085

Yamazaki, S., Gerhold, C., Yamamoto, K., Ueno, Y., Grosse, R., Miyamoto, K., & Harata, M. (2020). The Actin-Family Protein Arp4 Is a Novel Suppressor for the Formation and Functions of Nuclear F-Actin. *Cells*, *9*(3). https://doi.org/10.3390/cells9030758

Yang, X. C., Burch, B. D., Yan, Y., Marzluff, W. F., & Dominski, Z. (2009). FLASH, a proapoptotic protein involved in activation of caspase-8, is essential for 3' end processing of histone pre-mRNAs. *Mol Cell*, *36*(2), 267-278. https://doi.org/10.1016/j.molcel.2009.08.016

Yang, Z., Zhu, Q., Luo, K., & Zhou, Q. (2001). The 7SK small nuclear RNA inhibits the CDK9/cyclin T1 kinase to control transcription. *Nature*, *414*(6861), 317-322. https://doi.org/10.1038/35104575

Yao, J., Munson, K. M., Webb, W. W., & Lis, J. T. (2006). Dynamics of heat shock factor association with native gene loci in living cells. *Nature*, *442*(7106), 1050-1053. https://doi.org/10.1038/nature05025

Yeo, M., Lin, P. S., Dahmus, M. E., & Gill, G. N. (2003). A novel RNA polymerase II C-terminal domain phosphatase that preferentially dephosphorylates serine 5. *J Biol Chem*, *278*(28), 26078-26085. https://doi.org/10.1074/jbc.M301791200

Yik, J. H., Chen, R., Nishimura, R., Jennings, J. L., Link, A. J., & Zhou, Q. (2003). Inhibition of P-TEFb (CDK9/Cyclin T) kinase and RNA polymerase II transcription by the coordinated actions of HEXIM1 and 7SK snRNA. *Mol Cell*, *12*(4), 971-982. https://doi.org/10.1016/s1097-2765(03)00388-5

Yoh, S. M., Cho, H., Pickle, L., Evans, R. M., & Jones, K. A. (2007). The Spt6 SH2 domain binds Ser2-P RNAPII to direct Iws1-dependent mRNA splicing and export. *Genes Dev*, *21*(2), 160-174. https://doi.org/10.1101/gad.1503107

Yu, L., Kim, J., Jiang, L., Feng, B., Ying, Y., Ji, K. Y., Tang, Q., Chen, W., Mai, T., Dou, W., Zhou, J., Xiang, L. Y., He, Y. F., Yang, D., Li, Q., Fu, X., & Xu, Y. (2020). MTR4 drives liver tumorigenesis by promoting cancer metabolic switch through alternative splicing. *Nat Commun*, *11*(1), 708. https://doi.org/10.1038/s41467-020-14437-3

Yue, Z., Maldonado, E., Pillutla, R., Cho, H., Reinberg, D., & Shatkin, A. J. (1997). Mammalian capping enzyme complements mutant Saccharomyces cerevisiae lacking mRNA guanylyltransferase and selectively binds the elongating form of RNA polymerase II. *Proc Natl Acad Sci U S A*, *94*(24), 12898-12903. https://doi.org/10.1073/pnas.94.24.12898

Zaborowska, J., Egloff, S., & Murphy, S. (2016). The pol II CTD: new twists in the tail. *Nat Struct Mol Biol*, *23*(9), 771-777. https://doi.org/10.1038/nsmb.3285

Zaromytidou, A. I., Miralles, F., & Treisman, R. (2006). MAL and ternary complex factor use different mechanisms to contact a common surface on the serum response factor DNA-binding domain. *Mol Cell Biol*, *26*(11), 4134-4148. https://doi.org/10.1128/MCB.01902-05

Zeitlinger, J., Stark, A., Kellis, M., Hong, J. W., Nechaev, S., Adelman, K., Levine, M., & Young, R. A. (2007). RNA polymerase stalling at developmental control genes in the Drosophila melanogaster embryo. *Nat Genet*, *39*(12), 1512-1516. https://doi.org/10.1038/ng.2007.26

Zhang, D. W., Mosley, A. L., Ramisetty, S. R., Rodríguez-Molina, J. B., Washburn, M. P., & Ansari, A. Z. (2012). Ssu72 phosphatase-dependent erasure of phospho-Ser7 marks on the RNA polymerase II C-terminal domain is essential for viability and transcription termination. *J Biol Chem*, *287*(11), 8541-8551. https://doi.org/10.1074/jbc.M111.335687

Zhang, H., Rigo, F., & Martinson, H. G. (2015). Poly(A) Signal-Dependent Transcription Termination Occurs through a Conformational Change Mechanism that Does Not Require Cleavage at the Poly(A) Site. *Mol Cell*, *59*(3), 437-448. https://doi.org/10.1016/j.molcel.2015.06.008

Zhang, J., & Corden, J. L. (1991). Identification of phosphorylation sites in the repetitive carboxyl-terminal domain of the mouse RNA polymerase II largest subunit. *J Biol Chem*, *266*(4), 2290-2296.

Zhang, T., Kwiatkowski, N., Olson, C. M., Dixon-Clarke, S. E., Abraham, B. J., Greifenberg, A. K., Ficarro, S. B., Elkins, J. M., Liang, Y., Hannett, N. M., Manz, T., Hao, M., Bartkowiak, B., Greenleaf, A. L., Marto, J. A., Geyer, M., Bullock, A. N., Young, R. A., & Gray, N. S. (2016). Covalent targeting of remote cysteine residues to develop CDK12 and CDK13 inhibitors. *Nat Chem Biol*, *12*(10), 876-884. https://doi.org/10.1038/nchembio.2166

Zhang, Z., Fu, J., & Gilmour, D. S. (2005). CTD-dependent dismantling of the RNA polymerase II elongation complex by the pre-mRNA 3'-end processing factor, Pcf11. *Genes Dev*, *19*(13), 1572-1580. https://doi.org/10.1101/gad.1296305

Zhang, Z., & Gilmour, D. S. (2006). Pcf11 is a termination factor in Drosophila that dismantles the elongation complex by bridging the CTD of RNA polymerase II to the nascent transcript. *Mol Cell*, *21*(1), 65-74. https://doi.org/10.1016/j.molcel.2005.11.002

Zhao, J., Hyman, L., & Moore, C. (1999). Formation of mRNA 3' ends in eukaryotes: mechanism, regulation, and interrelationships with other steps in mRNA synthesis. *Microbiol Mol Biol Rev*, *63*(2), 405-445.

Zhu, B., Mandal, S. S., Pham, A. D., Zheng, Y., Erdjument-Bromage, H., Batra, S. K., Tempst, P., & Reinberg, D. (2005). The human PAF complex coordinates transcription with events downstream of RNA synthesis. *Genes Dev*, *19*(14), 1668-1673. https://doi.org/10.1101/gad.1292105

Zhu, B., Zheng, Y., Pham, A. D., Mandal, S. S., Erdjument-Bromage, H., Tempst, P., & Reinberg, D. (2005). Monoubiquitination of human histone H2B: the factors involved and their roles in HOX gene regulation. *Mol Cell*, *20*(4), 601-611. https://doi.org/10.1016/j.molcel.2005.09.025

Zippo, A., Serafini, R., Rocchigiani, M., Pennacchini, S., Krepelova, A., & Oliviero, S. (2009). Histone crosstalk between H3S10ph and H4K16ac generates a histone code that mediates transcription elongation. *Cell*, *138*(6), 1122-1136. https://doi.org/10.1016/j.cell.2009.07.031